Université d'Ottawa · University of Ottawa

BEARING CAPACITY OF PILES FROM CONE PENETRATION TEST DATA

: Abolfazl Eslami, B. Sc. Eng., M. Sc.

A Thesis
Submitted to the School of Graduate Studies and Research
Under the Supervision of

Dr. Bengt H. Fellenius

in partial fulfillment of the requirements for the degree of
Doctor of Philosophy in Civil Engineering

Department of Civil Engineering
Faculty of Engineering
University of Ottawa
Ottawa, Ontario

October 1996

The Doctor of Philosophy in Civil Engineering is a joint program between Carleton University and the University of Ottawa administrated by the Ottawa-Carleton Institute of Civil Engineering

0-612-21000-6

UNIVERSITY OF OTTAWA - SCHOOL OF GRADUATE STUDIES

CERTIFICATE OF EXAMINATION

The Thesis by

Abolfazl Eslami, B. Sc. Eng., M. Sc.

Entitled

BEARING CAPACITY OF PILES FROM CONE PENETRATION TEST DATA

is accepted in partial fulfillment of
the requirements for the degree of
Doctor of Philosophy in
Civil Engineering

Examination Board

Dr. ROBERT D. HOLTZ	Dr. K. TIM LAW
Dr. VINOD GARGA	Dr. ERMAN EVGIN

Supervising Professor

Dr. BENGT H. FELLENIUS

ACKNOWLEDGMENTS

My experience at Ottawa was very rewarding thanks to several teachers, colleagues, and friends. Professor Bengt H. Fellenius, the Thesis supervisor, provided me with a unique research opportunity beyond my expectations. His guidance, invaluable suggestions and comments, great interest for this research work, and the continuous support are gratefully acknowledged and will never be forgotten.

My stay in Vancouver, where part of my research was done, was productive and pleasant. Special thanks are due to Dr. Richard G. Campanella for all that I learned from him during courses and technical discussions, and also for providing a part of the database.

Thanks are due to M. Tumay, L. Briaud, A. Altaee, T. L. Yen, M. O'Neill, P. Mayne, K. Gwizdala, J. Long, K. Davidson, T. Matsumoto, L. Weber, and others who generously supplied database records.

A word of Thanks are also extended to Dr. K. T. Law, Dr. V. Garga, and Dr. E. Evgin for having served on my advisory committee during this research work, and to Dr. Robert D. Holtz of the University of Washington who served as External Examiner.

My doctoral studies at Ottawa were made more effective and pleasing, thanks to Noella Simard, Dick Moore, A. Ghie, J. A. Infante Sedano, M. Rezaii and family, and Zavosh and Chris Rabieian. Particular thanks and sincere appreciation are extended to my parents, parents in-law, sisters, and brothers for their companion, continuous support, and warm encouragement.

Last but not least, thanks to my family, my wife Zoya, for her love, perseverance, and patience, as well as to my son, Mandro, for his emotional support and understanding. Their support made this work possible.

The financial supports provided by the Ministry of Culture and Higher Education of Iran, University of Ottawa, the National Sciences and Engineering Council of Canada (NSERC) are gratefully acknowledged.

To the holy spirit and memory of my beloved mother

and to my family: Zoya, Mandro, and Makan.

SUMMARY

In recent years, the CPT is becoming the preferred type of penetration test for pile analysis. Because it is simple, fast, relatively economical, supplies continuous records with depth, and a variety of sensors can be incorporated with cone penetrometer. Also, with regard to pile analysis, the cone penetrometer can be realized as a model pile. Because of similarities between CPT and pile, and advantages of CPT as a useful geotecnical investigation tool, the estimation of pile capacity from CPT data was one of the first applications of cone penetrometer.

It has been realized that, by analogy of cone penetrometer as a model pile, the measured cone resistance and sleeve friction can be employed for estimation of unit toe and shaft resistances, respectively. It is possible to develop almost a continuous resistance profile by CPT measurement with depth.

The main advantages of using CPT data for pile design are that the problems of providing representative undisturbed samples, and also determining correct values of required soil parameters by conventional laboratory testing, will be eliminated. Furthermore, there is no need for estimating intermediate parameters such as K_s and N_q for pile capacity estimation. The main advantages of using CPT data for pile design are that dynamic analysis requires input assumptions that can significantly bias the results and a considerable limitation for dynamic methods is that the capacity estimation is not available until the pile is driven.

The direct CPT methods currently used in North American practice were investigated. Consequently, it was found that considerable uncertainty exists regarding strain softening, resistance degradation due to pile installation, filtering, smoothing and averaging cone data to relate to pile resistances, failure (influence) zone around pile toe, soil interpreting, using total stress approaches, effects of sensitivity and dilatancy during pile driving, and capacity of piles with limited toe penetration in dense strata.

A direct CPTu method is proposed for determining the capacity of an axially loaded pile. The method employs all of the CPTu data with the cone point resistance, q_c, as the primary measurement. The sleeve friction, f_s, which is an imprecise measurement, is limited to use in combination with the effective cone resistance, q_E (cone point resistance adjusted to effective stress by the deducting the measured pore pressure) to interpret the soil according to a classification chart, developed as a part of this dissertation. Both the pile unit toe and shaft resistances are functions of the CPTu effective cone resistance, with the toe and shaft correlation coefficients, C_t and C_s, respectively.

Calibration chamber tests are often used to calibrate and validate the methods and approaches in geotechnical engineering that are applied to CPT data. However, the test procedure and interpreting soil parameters from CPT data involve problems and limitations. Most of the calibration chamber tests have been performed on uniform, clean, mostly silica sands, whereas natural sand deposits are rarely uniform. For practical reasons, the employed calibration chambers have limited size. This fact together with the lack of knowledge of the field conditions in terms of stress and strain, are involved for the so-called chamber size effects. Therefore, difficulties and limitations exist to extrapolate the results of model-scale tests of CPT and piles performed in the conventional calibration chamber to the full-scale piles for determining pile capacity from CPT data.

Hence, for determining pile capacity from CPT data, only the results of full-scale pile loading tests with CPT soundings performed close to the pile locations are considered useful for this research programme.

An extensive search of published and unpublished literature was conducted to collect axially loaded piles and CPT soundings, and a large number of cases were found. Many of the cases involved limitations, such as CPT results by mechanical cone which cannot produce as accurate measurements as those achievable by the piezocone, manually smoothed and filtered cone data, incomplete results of pile loading tests, etc. Therefore, selection criteria were established to compile a database of case histories pile tests and CPT soundings performed close to the pile locations. The established selection criteria are: CPT soundings (preferably the piezocone, CPTu) must be performed close to the pile locations, CPT data must be measured in short distance, e.g., 300 mm depth intervals— preferably every 25 mm, sites must include sediments of clay, silt, and sand soil layers, and pile loading tests must have reached failure.

A database consisting of 142 case histories was compiled to calibrate and develop an improved CPT direct method, and to reference to the current CPT direct methods for pile capacity calculation. The case histories contain results of full-scale pile loading tests, soil characteristics, and CPT soundings which were performed close to the pile locations. The cases were obtained from 37 sources reporting data from 53 sites in 13 countries.

According to extent of how the selection criteria are satisfied, the collected cases are categorized in three types; I (56 cases), II (40 cases), III (40 cases), indicating a decreasing degree of satisfaction all of selection criteria.

The cases are from sites with soft clay and clay, silt, mixture of clay and silt, mixture of silt and sand, and sand. The embedment lengths for the steel and concrete piles with different shapes range from 6 m through 67 m and the diameters range from 200 mm through 915 mm. The pile capacities range from 80 KN through 8,000 KN.

The proposed method relates both the pile unit toe resistance and the unit shaft resistance to the effective cone point resistance, q_E. The hypothesis for the study was explored that both toe and shaft resistances are proportional to the effective cone resistance and can be determined by assigning a correlation factor to q_E. Twenty-four pile case histories have been compiled including static loading tests performed in uplift, or in push with separation of shaft and toe resistances at sites which comprise CPT soundings. These case histories are used to calibrate the two formulae for estimation of pile toe and shaft resistances from CPTu data.

As a result of the calibration based on 24 pile case histories with separate measurement of pile toe and shaft capacities, for pile unit toe resistance, a simple mathematical rule is used to relate the cone resistance to the pile unit toe resistance in a one-to-one relationship. The geometric average of effective cone resistance is determined as the unit toe resistance of pile in an influence zone depending on the soil situations in the vicinity of pile toe. The influence zone extends 4b below to 8b above pile toe when a pile is installed through a weak soil into a dense soil, 4b below to 2b above pile toe when a pile is installed through a dense soil into a weak soil, and the length of the influence zone is not critical for homogeneous soil.

For pile unit shaft resistance, a routine soil interpreting procedure is introduced based on CPTu data. The pile unit shaft resistance is determined from effective cone resistance by using a correlation coefficient that depends on the soil type interpreted from the CPTu data based on the soil classification chart developed in this dissertation.

A plot of CPTu data was developed with strict separation of the variables, similar to that used by Begemann (1965), effective cone resistance ($q_E = q_t - u_2$) versus sleeve friction. A representative number of cone values were selected from each soil layer from about 20 sites included with the database. A detailed study of the plots made it possible to separate out five main soil categories: very soft sensitive soil, soft clay, silty clay and stiff clay, silty sand, and sand and gravel. Boundaries were obtained by enveloping about 90 % of all points of each main soil type.

For comparison, all data points were also plotted in the diagram format of Robertson et al. (1986), and Campanella and Robertson (1988). The comparison shows a good agreement between the soil types of the database and the soil interpretation obtained by means of the Robertson and Campanella classification chart. However, the delineation—separation of the soil types—is much simpler and also more distinct in the Begemann type chart. Moreover, the developed soil classification chart has the advantage that it does not require manipulation of the data before making an interpretation.

Five CPT direct methods which currently used in North American practice have been investigated to reference the proposed method. The five CPT direct methods are: The Schmertmann method, the European Method, the French method, the Meyerhof method, and the Tumay method.

The results of estimated pile capacity from the proposed method and the other methods were compared to the measured pile capacity for 142 case records compiled in the database.

The statistical approach for validation of the predictive methods was used based on relative difference between the estimated and measured pile capacity. The two basic statistical parameters are used for quantification of estimation error, the mean and the standard deviation. The relative error is determined as the difference between the estimated and measured pile capacities dived by the measured pile capacity. Negative values of relative error indicate that the method underestimated the measured pile capacity.

Also, to provide additional comparison of the predictive methods, the current set of data was studied based on ascending order of the ratio of calculated to tested pile capacities versus cumulative probability.

It was verified that the main factors that cause significant error in pile capacity estimation by the current methods are: smoothing the CPT data, development based on mechanical cone data, employing undrained shear strength, S_u, imposing an upper limit to the pile unit toe and shaft resistances, not including all CPT measurement, considerable difference between the correlation factors for steel and concrete piles, considerable difference between the correlation factors for tension and compression piles, disregard of factors such as soil sensitivity, dilatancy effects, effective stress.

The results of comparison have shown that for the current methods for 46 cases (10 tension tests used for the calibration of the proposed method were excluded) classified as Type I, the average absolute error is 28 % with the standard deviation of 21 %, for 46 cases of Type II, the average absolute error is 25 % with the standard deviation of 17 %, for 40 cases of Type III, the average absolute error is 31 % with the standard deviation of 23 %. For 67 cases of the Type I and Type II for which the piles reached failure, the methods involve absolute error of 29 % with the standard deviation of 21 %.

In contrast, the proposed method shows for Type I cases the absolute error of 11 % and the standard deviation of 8 %, for Type II cases the absolute error of 19 % and the standard deviation of 14 %, for Type III cases the absolute error of 24 % and the standard deviation of 18 %. For 67 cases of the Type I and Type II for which the piles reached failure, the proposed method shows absolute error of 11 % with the standard deviation of 8 %.

According to the probability approach, the estimated pile capacities estimated by the proposed method exhibit less dispersion and agree better with the tested pile capacity than those analyzed by the current methods.

The proposed direct CPTu method for determining pile capacity has been tested on 142 piles of different size and lengths installed in different type of soils and compared to the results of five current methods. The results of comparison are favorable to the proposed method, demonstrating a remarkably higher accuracy and lower scatter for the proposed method than the current methods. The proposed method is simple, easy to apply, independent of the operator subjective influence which affects the other current methods. Therefore, it is suitable to apply in engineering practice.

TABLE OF CONTENTS

Page

ACKNOWLEDGMENTS iii

SUMMARY v

TABLE OF CONTENTS xi

NOTATIONS xv

LIST OF TABLES xviii

LIST OF FIGURES xx

CHAPTER 1. INTRODUCTION 1

CHAPTER 2. PILE LOAD TRANSFER 8

CHAPTER 3. BACKGROUND TO THE CONE PENETRATION TEST (CPT) 22

CHAPTER 4. CALIBRATION CHAMBER (CC) STUDIES AND TESTING SMALL-SCALE MODELS 38

CHAPTER 5. CURRENT METHODS OF PILE CAPACITY ESTIMATION USING CPT DATA 47

CHAPTER 6. DATABASE AND CASE RECORDS 58

CHAPTER 7. THE PROPOSED DIRECT CPT METHOD FOR DETERMINING PILE TOE AND SHAFT CAPACITIES 64

CHAPTER 8. CALIBRATION OF THE PROPOSED METHOD 76

CHAPTER 9. VALIDATION OF THE PROPOSED METHOD 83

CHAPTER 10. SUMMARY OF RESULTS AND CONCLUSIONS 97

REFERENCES 107

APPENDIX 237

LIST OF CHAPTERS

1. INTRODUCTION 1
1.1 General 1
1.2 Statement of the Problem 1
1.3 Objectives of the Investigation 4
1.4 Hypothesy Investigated 5
1.5 Scope of Research 5
1.6 Outline of Thesis 6

2. PILE LOAD TRANSFER 8
2.1 Introduction 8
2.2 Pile Design 9
2.3 Pile Capacity 9
2.3.1 Capacity from full-scale pile loading tests 10
2.3.2 Capacity from dynamic methods 11
2.3.3 Capacity from static analysis 12
2.3.3.1 Toe resistance 13
2.3.3.2 Shaft resistance 17
2.3.3.4 Limiting unit toe and unit shaft resistances 19
2.4 Concluding Remarks 20

3. BACKGROUND TO THE CONE PENETRATION TEST (CPT) 22
3.1 Historical Background and the Role of CPT 22
3.2 Equipment 23
3.3 Standardization 25
3.4 Piezocone 26
3.5 Recording and Presentation of CPT Results 27
3.6 Other Development of CPT 27
3.6.1 Dual range penetrometer, Brecone 27
3.6.2 Acoustic cone 28
3.6.3 Lateral stress cone (LSCPT) 28
3.6.4 Resistivity cone (RCPTu) 28
3.6.5 Seismic cone (SCPTu) 29
3.6.6 Cone pressuremeter 29
3.6.7 Mini-Cone (MCPT) 29
3.7 Factors Influencing CPT Measurements and Interpretation 30
3.7.1 Equipment design 30
3.7.2 Rate of penetration 31
3.7.3 In-Situ stress 31
3.7.4 Compressibility 31
3.8 Correlation of CPT data with Soil Characteristics 32
3.8.1 Soil classification 32

3.8.2 Undrained shear strength of clay....33
3.8.3 Drained friction angle....36
3.9 Other Applications....36

4. CALIBRATION CHAMBER (CC) STUDIES AND TESTING SMALL-SCALE MODELS....38
4.1 Introduction....38
4.2 Brief History....39
4.3 Operating of the Calibration Chamber Test....39
4.4 Calibration Chamber Studies in Noncohesive Soils....41
4.4.1 CPT data combined with state relationships....42
4.4.2 CPT data combined with density index relationships....44
4.5 Testing Small-Scale Models....45
4.6 Concluding Comments....45

5. CURRENT METHODS OF PILE CAPACITY ESTIMATION USING CPT DATA....47
5.1 Introduction....47
5.2 Using CPT Data for Pile Design....50
5.3 Current CPT Direct Methods....51
5.4 Concluding Comments....55

6. DATABASE AND CASE RECORDS....58
6.1 Introduction....58
6.2 Selection Criteria....58
6.3 Case Records....60
6.4 Case Details....60
6.4.1 Location....60
6.4.2 Pile characteristics....61
6.4.3 Pile loading tests....61
6.4.4 Soil information....62
6.4.5 Cone penetration tests....62
6.4.6 Back-calculated β and N_t coefficients....63
6.5 Concluding Remarks....63

7. THE PROPOSED DIRECT CPT METHOD FOR DETERMINING PILE TOE AND SHAFT CAPACITIES....64
7.1 General....64
A. PILE UNIT TOE RESISTANCE....65
7.2 Cone Resistance Average....65
7.3 Failure (Influence) Zone....68
7.4 Effective Cone Resistance, Conclusions....71
7.5 Determining Pile Unit Toe Resistance, Conclusions....72

B. PILE UNIT SHAFT RESISTANCE.....73
7.6 Background.....73
7.7 Interpreting Soil Profile from CPTu data.....74

8. CALIBRATION OF THE PROPOSED METHOD.....76
8.1 Introduction.....76
8.2 Calibration of the Proposed Method.....76
8.2.1 Calibration of the toe correlation coefficient. C_t.....77
8.2.1 Calibration of the shaft correlation coefficient. C_s.....78
8.3 Implementation of the proposed method.....80
8.4 Concluding Remarks.....81

9. VALIDATION OF THE PROPOSED METHOD.....83
9.1 General.....83
9.2 Divisions of Case Records for Comparison of the Methods.....84
9.3 Presentation and Evaluation of the Results.....85
9.4 Comparison, Discussion, and Validation.....87
A. Relative Difference Approach.....87
9.4.1 Twenty-four cases used for calibration.....87
9.4.2 Type I cases.....90
9.4.3 Type II cases.....91
9.4.4 Type III cases.....92
B. Probability Approach.....93
9.6 Concluding comments.....94

10. SUMMARY OF RESULTS AND CONCLUSIONS.....97
10.1 Results.....97
10.2 Conclusions.....103
10.3 Limitations.....104
10.4 Recommendation for Further Research.....105

NOTATIONS

α	Adhesion factor
α	Pore pressure factor
β	Bjerrum-Burland beta coefficient
δ	Pile-soil interface friction angle
Δu	Excess pore pressure = $u-u_0$
ϵ_v	Volume change parameter
λ	Slope of steady state line
ν	Poisson's ratio
σ_i	Initial total stress = in-situ total octahedral stress
σ_{v0}	Total overburden stress
σ'_m	Mean effective normal stress = $(1+2K_0)/3*\sigma'_{z=D}$
σ'_r	In-Situ radial effective stress
σ'_{v0}	Effective overburden stress
σ'_z	Effective overburden stress at depth z
$\sigma'_{z=D}$	Effective overburden stress at pile toe level
ϕ	Internal friction angle of soil
ϕ_{cv}	Friction angle at constant volume
ϕ'	Drained friction angle
ψ	State parameter
a	Net area ratio of cone
A_N	Load transfer area behind the cone point
A_s	Pile unit circumferential area
A_t	Pile toe cross-sectional area
A_T	Cross-sectional area at base of cone point
b	Pile diameter
B_q	Pore pressure parameter ratio = $\Delta u/(q_t-\sigma_{v0})$
c	Cohesion of soil
C_t	Toe correlation factor
C_s	Shaft correlation factor
D	Pile embedment length
e	Void ratio
E	Modulus of elasticity
e_{max}	Maximum void ratio
e_{min}	Minimum void ratio
F	Overall soil-cone parameter
f_s	Sleeve friction
G	Shear Modulus of soil = $E/2(1+\nu)$
G_{max}	Maximum shear Modulus at small strains
i	the number of value considered for probability
I	Inclination

I_D	Density Index (relative density)
I_r	Rigidity index or stiffness ratio = $G/(c+\sigma'_v \tan\phi)$
I_{rr}	Reduced rigidity index $= I_r/(1+\epsilon_v I_r)$
K_s	Empirical coefficient
K_0	Coefficient of earth pressure at rest
K_a	Coefficient of earth pressure at active condition
K_c	Bearing capacity factor
K_p	Coefficient of earth pressure at passive condition
K_s	Coefficient of lateral earth pressure
m	Mean of relative errors, $\bar{x}$
M	Friction factor for the soil acting on the cone surface
M	Quotient of wall friction = $\tan\delta/\tan\phi$
N	Standard penetration value; blow count
$N_{\Delta u}$	Pore pressure factor = $\Delta u/S_u$
N_σ	Bearing capacity factor
N_c	Bearing capacity factor
N_K	Cone factor
N_q	Bearing capacity factor
OCR	Overconsolidation ratio
p	Mean stress
P	Cumulative probability
p'	Mean effective stress
q	Deviator stress
q_c	Measured total cone resistance
q_{ca}	Arithmetic average of cone resistance
q_{cg}	Geometric average of cone resistance
q_{Eg}	Geometric average of effective cone resistance over influence (failure) zone
q_E	Effective cone resistance
q_t	Corrected total cone resistance for pore pressure
Q_u	Bearing capacity of pile
r_0	Radius of logarithmic spiral at $\theta = 0$
r_c	Radius of logarithmic spiral at $\theta = 180$
R_f	Friction ratio = f_s/q_c*100 or f_s/q_t*100
r_s	Unit shaft resistance of pile
R_e	Estimated pile capacity
R_m	Mstimated pile capacity
R_s	Shaft resistance of pile
r_t	Unit toe resistance of pile
R_t	Toe resistance of pile
R_u	Total pile capacity
SD	standard deviation
S_u	Undrained shear strength

S_{uc} Undrained shear strength mobilized by the cone
θ Angle between the radius at each point and r_o for rupture surface
T Temperature
u Pore pressure
u_0 Equilibrium pore pressure, in-situ
u_1 Measured pore pressure at cone face
u_2 Measured pore pressure behind of cone point
u_3 Measured pore pressure behind of friction sleeve
x Relative error
x_i Relative error for case i

LIST OF TABLES

TABLE TITLE Page

2.1 Pile classification considering different aspects (CFEM, 1992)....131

2.2 Ranges of β-coefficients and N_t-coefficients (after Fellenius, 1989).... 132

4.1 Principal calibration chambers used in geotechnical investigations (after Ghionna and Jamiolkowski, 1991).... 133

4.2 Boundary conditions imposed in flexible-wall calibration chambers (after Veismanis, 1974)....134

5.1 Methods of pile capacity calculation using CPT data (Direct Methods)....135

5.2 Empirical coefficients of the French method for piles (after Bustamante and Gianeslli, 1982)....136

6.1 Case records summary....137

6.2 Summary of case histories site locations....152

6.3 Back-calculated β and N_t coefficients....153

6.4 Summary of case histories information....155

8.1 Comparison of pile unit toe resistance and effective cone resistance....156

8.2 Comparison of pile unit shaft resistance and effective cone resistance....157

8.3 Proposed shaft correlation coefficients, Cs, for different soil types....158

8.4 Measured and estimated pile capacity (KN) for 24 cases including 14 compression and 10 tension tests by the proposed method....159

8.5 Relative error (%) in pile capacity estimation for 24 cases including 14 compression and 10 tension tests by the proposed method....160

9.1 Measured and estimated pile capacity (KN) for Type I cases by methods....161

9.2 Measured and estimated pile capacity (KN) for Type II cases by methods....162

9.3 Measured and estimated pile capacity (KN) for Type III cases by methods....................163

9.4 Measured and estimated pile capacity (KN) for 24 cases including 14 compression and 10 tension tests....................164

9.5 Relative error in pile capacity estimation by different methods....................165

9.6 Relative error for Type II cases (25 cases), not failed....................166

LIST OF FIGURES

FIGURE TITLE Page

2.1 Situation in which piles may be driven (after Vesic, 1977)....167

2.2 Failure pattern under pile toe in soft clay and dense sand (after Rourk, 1961; and Ladanyi, 1961)....168

2.3 Load-displacement diagram of a test pile drawn in two different scales (data from Vanderveen, 1953)....169

2.4 Discrete-elements of the pile-soil system (after Smith, 1960)....170

2.5 Assumed failure mechanism under pile foundations (after Vesic, 1967)....171

2.6 Bearing capacity factor for deep circular foundations (after Vesic, 1964)....172

2.7 Variation of bearing capacity factor with rigidity index and friction angle (after Vesic, 1977)....173

3.1 Mechanical friction-cone penetrometer (after Begemann, 1953)....174

3.2 Electrical friction-cone penetrometer (after Holden, 1971)....175

3.3 Comparison of curved and vertical CPT (after de Ruiter, 1981)....176

3.4 Conceptual pore pressure distribution in saturated soil during CPT based on field measurements (after Robertson, 1986)....177

3.5 Typical piezocone profile and interpreted soil profile using CPTu data (data from Yen et al., 1989)....178

3.6 Relationship between cone resistance, sleeve friction, and soil type (after Begemann, 1965)....179

3.7 Soil classification chart based on normalized CPTU data (after Robertson, 1990)....180

3.8 Simplified soil classification chart based on CPT data (after Robertson et al., 1986; from CPTINT program, Campanella, 1993)....181

3.9 Fissure patterns in OC clays related to scale of cone penetrometer (from Marsland and Quaterman, 1982)....182

3.10 Proposed model for calculating undrained shear strength from cone resistance (from Konrad and Law, 1987)....183

3.11 Relationship between friction angle, cone resistance, and vertical effective stress in uncemented NC quartz sand (after Durgunoglu and Mitchell, 1975)....184

4.1 The flexible-wall calibration chamber developed at the University of Florida (after Reese, 1975)....185

4.2 Different boundary condition for CPT in calibration chamber (after Veismanis, 1974)....186

4.3 Different types of cone resistance profile of CPT in calibration chamber test (after Salgado, 1993)....187

4.4 Typical CPT results in NGI chamber for dense and loose samples (after Parkin and Lunne, 1982)....188

4.5 (a) Typical state diagram (b) steady state lines for different noncohesive soils (after Been and Jefferies, 1985)....189

4.6 Comparison of different relationships between density index, cone resistance, and vertical effective stress (modified after Robertson and Campanella, 1983)....190

5.1 Begemann procedure for determining pile toe capacity from cone resistance (after Nottingham, 1975)....191

5.2a Application of CPT data to pile design (after Schmertmann, 1978)

5.2b Application of CPT data to pile design (after de Ruiter and Beringen, 1979)....192

5.3 Design curves for pile shaft resistance in sand (after Schmertmann, 1978)....193

5.4 Design curves for pile shaft resistance in clay (after Schmertmann, 1978)....194

5.5 Procedure to determine equivalent cone resistance at pile toe (after Bustamante and Gianeslli)....195

6.1 Frequency distribution of pile diameter in the compiled database....196

6.2 Frequency distribution of pile embedment length in the compiled database........................197

6.3 Frequency distribution of pile sections in the compiled database....................................198

6.4 Frequency distribution of pile capacity in the compiled database....................................199

7.1 Comparison of qc-average for different CPT direct methods
for Case #11, POLA2..200

7.2 Rupture surface around cone point and pile toe...201

7.3 Rupture surface around pile toe for different soils..202

7.4 Comparison of pile unit toe resistance for different zones
(a) Homogeneous (b) non-homogeneous..203

7.5 Comparison of cone resistance and calculated geometric average as
pile unit toe resistance in non-homogeneous for different zones..204

7.6 Soil classification chart based on database-clay soils...205

7.7 Soil classification chart based on database-silt soils...206

7.8 Soil classification chart based on database-sand soils...207

7.9 Combination of different soils in soil classification chart...208

7.10 Soil classification chart based on delineation of database...209

7.11 Distribution of database soils (clay) in soil classification chart
proposed by Robertson et al., 1986)...210

7.12 Distribution of database soils (silt) in soil classification chart
proposed by Robertson et al., 1986)...211

7.13 Distribution of database soils (sand) in soil classification chart
proposed by Robertson et al., 1986)...212

7.14 Distribution of database soils in soil classification chart
proposed by Robertson et al., 1986)...213

8.1 Comparison of measured and estimated pile toe capacity
by the proposed method...214

8.2 Comparison of measured and estimated pile shaft capacity by the proposed method....215

8.3 Comparison of measured and estimated pile capacity by the proposed method....216

8.4 Relative error (%) in pile capacity as determined by the proposed method....217

9.1 Measured and estimated pile capacity for 24 cases by the Schmertmann method....218

9.2 Measured and estimated pile capacity for 24 cases by the European method....219

9.3 Measured and estimated pile capacity for 24 cases by the French method....220

9.4 Measured and estimated pile capacity for 17 cases by the Meyerhof....221

9.5 Measured and estimated pile capacity for 6 cases by the Tumay method....222

9.6 Measured and estimated pile capacity for 24 cases by the proposed method....223

9.7 Comparison of measured and estimated pile capacity by the Schmertmann method....224

9.8 Comparison of measured and estimated pile capacity by the European method....225

9.9 Comparison of measured and estimated pile capacity by the French method....226

9.10 Comparison of measured and estimated pile capacity by the Meyerhof method....227

9.11 Comparison of measured and estimated pile capacity by the Tumay method....228

9.12 Comparison of measured and estimated pile capacity by the proposed method..........229

9.13 Relative error (%) in pile capacity as determined by the Schmertmann method..........230

9.14 Relative error (%) in pile capacity as determined by the European method..........231

9.15 Relative error (%) in pile capacity as determined by the French method..........232

9.16 Relative error (%) in pile capacity as determined by the Meyerhof method..........233

9.17 Relative error (%) in pile capacity as determined by the Tumay method..........234

9.18 Relative error (%) in pile capacity as determined by the proposed method..........235

9.19 Comparison of the methods estimation using probability approach..........236

CHAPTER 1

INTRODUCTION

1.1 General

The prediction of axial capacity of piles has been a challenge since the beginning of the geotechnical engineering profession. Several methods and approaches have been developed to overcome the uncertainty in the prediction. The methods include some simplifying assumptions and/or empirical approaches regarding soil stratigraphy, soil-pile structure interaction, and distribution of soil resistance along a pile. Therefore, they provide qualitative results and solutions, rather than truly quantitative values directly useful in foundation design. Because of this situation, pile design often appears to be somewhat of a guessing game and a rather subjective exercise. The work presented in this dissertation aims toward ameliorating the situation in the area of static analysis of load transfer based on in-situ testing using the cone penetrometer, the CPTu.

1.2 Statement of the Problem

Bearing capacity of piles can be determined by five approaches as follows:

1. Interpretation of data from full-scale pile loading tests
2. Dynamic analysis methods based on wave equation analysis
3. Dynamic testing by means of the Pile Driving Analyzer (PDA)
4. Static analysis by applying soil parameters in effective stress or total stress approaches
5. Methods using the results of in-situ investigation tests—directly or indirectly

1. In view of the uncertainties involved in analysis and design of pile foundation, it has become customary, and in many cases mandatory, to perform full-scale pile loading tests. Such tests are expensive, time-consuming, and the costs are often difficult to justify for ordinary or small projects.

2. Dynamic analysis methods apply to driven piles and are based on wave mechanics for the hammer-pile-soil system. The uncertainty of the hammer impact effect, as well as changes in soil strength between conditions at time of pile driving and time of loading from the structure, causes uncertainties in bearing capacity determination. Moreover, a wave equation analysis requires input assumptions that can significantly bias the results.

3. Dynamic testing methods are based on monitoring acceleration and strain near the pile head during driving. From these measurements, the pile capacity can be estimated by means of the Pile Driving Analyzer (PDA) and numerical analysis of the data. However, the PDA can only be used by especially experienced person and the test results apply essentially to the field-testing situation. A considerable limitation is that the capacity estimation is not available until the pile is driven.

4. Static analysis methods approach shaft and toe resistances differently. For shaft resistance, in cohesive as well as noncohesive soils, considerable uncertainty and debate exist over the appropriate choice of the horizontal stress coefficient, K_s. For estimating toe resistance in noncohesive soils, bearing capacity theory is normally applied. However, the theory involves a rather approximate ϕ -N_q relationship coupled with the difficulty of determining a reliable and representative in-situ value of the ϕ angle. This creates doubts about relying on the bearing capacity theory in pile foundation design.

   In cohesive soils pile capacity is usually estimated by direct correlation between the undrained shear strength, S_u, and shaft resistance, r_s. However, S_u is not a unique parameter and depends significantly on the type of test used, the strain rate, and the orientation of failure plane. Besides, drained soil characteristics govern long-term pile capacity also in cohesive soils. Hence, the use of undrained shear strength for long-term capacity is not justified.

Design guidelines based on static analysis often recommend using the critical depth concept. However, the critical depth is an idealization that has neither theoretical nor reliable experimental support, and contradicts physical laws.

5. In recent years, the use of in-situ testing techniques has increased for geotechnical design. This is due to rapid development of in-situ testing instruments, an improved understanding of the behavior of soils, and subsequent realization of some limitations and inadequacies of conventional laboratory testing.

The Standard Penetration Test, SPT, is still the most commonly used in-situ test. However, many problems and limitations exist for the SPT with respect to interpretation and repeatability. These are due to uncertainty of the energy delivered by various SPT hammers to the anvil system and also with the test procedure.

In contrast to the SPT, the Cone Penetration test, CPT, is simple, fast, relatively economical, and it supplies continuous records with depth. The results are interpretable on both empirical and analytical basis, and a variety of sensors can be incorporated with cone penetrometer. With regard to pile analysis, the cone penetrometer can be realized as a model pile. Determination of pile capacity from CPT is one of the earliest applications of the CPT and includes two main approaches for the application of cone data to pile design: direct methods and indirect methods. Therefore, the cone penetration test, CPT is becoming the preferred type of penetration test for pile analysis and design.

Direct CPT methods apply the measured values of cone bearing for toe resistance and sleeve friction for shaft resistance with some modification regarding scale effects (the influence of the ratio of pile diameter to the cone diameter). The direct methods which incorporate scaling effects apply the analogy of the cone penetrometer as a model pile. However, considerable uncertainty exists regarding strain softening, resistance degradation due to pile installation, filtering, smoothing and averaging cone data to relate to pile resistances, failure zone around pile toe, soil interpreting, use of total stress approaches, effects of sensitivity and dilatancy during pile driving, and capacity of piles with limited toe penetration in dense strata.

Indirect CPT methods employ friction angle and undrained shear strength values estimated from CPT data based on bearing capacity and/or cavity expansion theories. Soil parameters estimated from the CPT data include errors due to disregard of horizontal stress, assumption of plane strain failure mechanism for axisymmetric nature of deep penetration, soil compressibility, rate of penetration, and strain softening.

1.3 Objectives

The main objectives of the research work are:

1. Evaluate the accuracy and consistency of current methods for estimating pile capacity from CPT data

2. Develop an improved method for determining pile shaft and toe resistances from CPTu data.

3. Determine how the effects of strain softening, resistance degradation, and associated pore pressures caused by cone penetration on the CPT sleeve friction can be overcome in determining the long-term pile shaft resistance.

4. The new method must be simple to use in engineering practice and the resulting pile capacity value must be independent any subjective influence—originally with the operator.

1.4 Hypothesy Investigated

The hypothesy investigated in this dissertation is that the pile unit toe and shaft resistances can be obtained as directly proportional to the cone resistance adjusted for pore pressure and soil type.

1.5 Scope of Research

The scope of this research has proceeded as follows:

1. Organize a database consisting of full-scale pile loading test results as well as CPT data and develop selection criteria for reducing the database to a reliable set of case histories.

2. Establish a procedure in correlating and averaging the cone point resistance.

3. Develop a theoretical method for calculating pile toe resistance from cone point resistance.

4. Compile the CPTu data in the database to a classification chart useful for reference in determining pile unit shaft resistance.

5. Compile existing methods for determining pile capacity from CPT data.

6. Develop a computer program for determining pile capacity according to the proposed new method and the current methods.

7. Correlate and validate the results of the proposed new method and the current methods to pile case histories in the database.

1.6 Outline of the Thesis

Chapter 2 presents a review of literature on the general theories for determining pile capacity and load transfer. The advantages and disadvantages of different approaches are presented.

Chapter 3 details the background and application of cone penetration test, CPT, and piezocone CPTu. Different approaches for interpreting and determining soil parameters from CPT data are presented.

Chapter 4 describes the history, characteristics, and capabilities of calibration chambers and small-scale tests. The limitations of interpreting parameters and model pile behavior from calibration chamber tests are demonstrated.

Chapter 5 reviews different approaches for relating pile capacity to CPT data. The direct CPT methods used in current North American practice are explained, and their limitations and shortcomings are addressed.

Chapter 6 details the database established for the research and lists the selection criteria as well as characteristics of case histories. The cases are characterized in terms of site location, pile details, loading test results, soil characteristics, and CPT information.

Chapter 7 details the proposed new method for determining the toe and shaft resistances of piles from CPTu data.

Chapter 8 demonstrates the calibration of the proposed method. The procedure for pile capacity calculation is applied to different pile case histories in which the pile unit toe and shaft resistances were measured separately.

Chapter 9 elaborates on a validation the proposed method and comparison to the five current methods for pile capacity estimation. Also, the accuracy and precision of the CPT methods are quantified.

Chapter 10 presents the conclusions and provides some suggestions for further research and development.

Early results of this study have been published in two conference papers, Eslami and Fellenius (1995; 1996).

CHAPTER 2

PILE LOAD TRANSFER

2.1 Introduction

Piles are structural members that are made of steel, concrete, and/or wood installed to transfer superstructure loads to competent soils. Fig. 2.1 illustrates some pile foundation applications. A pile subjected to axial load will carry the load partly by shear resistance generated along the shaft and partly by pile toe resistance. Piles are used where:

1. Upper soil strata are compressible, expansive, collapsive, or weak.
2. Conventional shallow foundations cannot transmit inclined, horizontal, or uplift forces.
3. Scour is likely to occur.
4. Future excavation may be carried out adjacent to the structure.
5. Loose, cohesionless deposits are densified through a combination of pile displacement and driving vibration.
6. The soils beneath machine foundations need to be stiffened to control vibration amplitude and frequency.

Piles can be classified in by a number of factors and aspects as outlined in Table 2.1. The choice of pile installation method as well as pile material type is influenced by surface conditions, location and topography of site, and structural and also geometric characteristics of the structure to be supported. Moreover, practical and economical aspects play an essential role in choosing the type and relative size of pile and installation method for a given application.

2.2 Pile Design

The designer of pile foundation must possess a variety of skills, experience, and considerable knowledge of foundation engineering. No single set of simple rules and procedures can cover the variety of conditions that affect a deep foundation. The main three aspects to be considered are: structural strength, settlement, and bearing capacity.

The structural strength of the pile is governed by the strength of materials making up the pile. The pile material must have the ability to safely resist all loads imposed during installation and service conditions. If the applied load is properly determined from the applicable codes, structural failure is seldom a concern, however, unless the pile is very long.

Many factors affect the settlement of a pile and it is difficult to make accurate estimates of settlement of single pile or pile groups. Generally, the actual load-movement response of a pile is a function of the relative contribution of shaft and toe resistance, the soil conditions, and method of pile installation. Hence, a number of empirical and theoretical approaches have been developed to estimate reasonably the settlement of pile. In this study, only the bearing capacity of piles will be addressed. However, it is important to note that the aspects of capacity and settlement constantly interact and cannot be separated in design (Fellenius, 1989).

The bearing capacity of a pile is the load that fails the soil around the pile. Usually, the soil failure occurs as punching shear failure under the pile toe, accompanied or preceded by direct-shear failure along the pile shaft, as shown in Fig. 2.2.

2.3 Pile Capacity

Several methods exist to determine the bearing capacity of piles, using different approaches, empirically or analytically. These methods can be organized in five categories as follows:

- Interpretation of data from full-scale pile loading tests
- Dynamic analysis methods based on wave equation analysis
- Dynamic testing by means of the Pile Driving Analyzer (PDA) and analysis of the measurements
- Static analysis by applying soil parameters in effective stress or total stress approaches
- Methods using the results of in-situ investigation tests—directly or indirectly

The first four approaches are briefly discussed in this chapter and the fifth will be discussed in more detail in Chapter 5.

2.3.1 Capacity from full-scale pile loading tests

In view of the many uncertainties involved in analysis and design of pile foundations, it has become customary, and in many cases mandatory, to perform full-scale pile loading tests at the site of more important projects. The main purpose of these tests is to verify experimentally that the actual pile capacity, as reflected in load-displacement relationships, is not smaller than the capacity assumed by designer, used as a basis for foundation design. Such conventional tests include the axial compressive and axial tensile loading tests standardized in ASTM D-1143-81 and D-3689-83, respectively.

For a pile, failure load by plunging is reached when a rapid movement occurs under sustained or following slight increase of the load. However, this definition is inadequate, because plunging may require impractically large movements. An early definition of failure load is the load for which the pile head movement exceeds a certain value, for example, 10 % of the diameter of pile head. This definition does not consider the elastic shortening of the pile, which can be substantial for long piles and negligible for short piles. In reality, a movement limit relates only the permissible movement allowed by the superstructure to be supported by the pile, and not to the capacity of pile. Furthermore, in case of large diameter piles, this definition may lead to an irrational acceptance of excessive settlement.

Sometimes, the failure load is defined as load value at the intersection of two straight lines, approximately an initial pseudo-elastic portion of load-settlement curve and a final pseudo-plastic portion. This definition results in interpreted loads which depend greatly on judgement, and /or on the scale effect of the load-movement graph as shown in Fig. 2.3.

Without a proper definition, interpretation of failure load from loading test data becomes meaningless. To be useful, a definition of ultimate load must be based on some mathematical rule and generate a repeatable value that is independent of scale relations and the individual judgement (Fellenius, 1975).

No unique criterion exists for defining the failure load of pile from loading test data and several methods for determining capacity based on pile loading test observations are used in pile foundation industry. Moreover, full-scale pile loading tests are expensive and time-consuming. Therefore, it is often difficult to justify the cost of a pile loading test programme for small or ordinary projects.

2.3.2. Capacity from dynamic methods

There are two main approaches for pile capacity prediction based on dynamic analysis; dynamic formulae and wave equation analysis. A couple of hundred formulae have been derived by equating the nominally delivered energy by the pile driving system with work performed by the pile, calculated as the bearing capacity of pile times the pile penetration per blow. Although in a particular case of local experience consistent results can be obtained, this approach is fundamentally incorrect and unreliable (CFEM, 1992). Dynamic formula cannot yield an accurate quantitative capacity estimation because such formulae fail to model the wave mechanics behavior of the hammer-pile-soil system.

Smith (1960) applied wave equation theory to pile design. In his approach, the pile and the driving system are presented by a series of discrete masses connected by springs, and the shaft and toe resistances are represented by a series of springs and dashpots, as shown in Fig. 2.4. At present, wave equation analysis can be implemented by using commercially available programs, such as GRLWEAP (GRL, 1995).

A wave equation analysis requires input assumptions that can significantly affect the program results. Potential error sources include assumption on hammer performance, hammer and pile cushion parameters, the soil resistance distribution, as well as the soil quake and damping characteristics. Therefore, without actual input data, the results are only useful for qualitative assessment, not for quantitative (Fellenius, 1983).

Most of the shortcomings are overcome by monitoring of acceleration and strain near the pile head during driving by means of the Pile Driving Analyzer (PDA). The PDA uses these measurements to estimate pile capacity, monitor hammer performance and energy transfer, calculate pile driving stresses, and evaluate pile integrity. Also, the PDA provides representative input parameters for a wave equation analysis. Calculation of pile capacity based on numerical analysis of PDA data is accomplished by the CAPWAP program (Rausche et al., 1985). The CAPWAP analysis is in all essential based on the same mathematical model for pile and soil as applied in wave equation analysis.

Normally, performing dynamic testing or dynamic analysis requires experienced persons. It is important to note that a considerable limitation exists that the capacity estimation is not available until the pile is driven.

2.3.3 Capacity from static analysis

The bearing capacity, also termed ultimate resistance or ultimate load, of a pile consists of fully developed shaft resistance (shear resistance generated along the shaft) and toe resistance (resistance generated at the base of the pile) in response to axial load, as follows:

$$Q_u = R_t + R_s = r_t A_t + r_s A_s \tag{2.1}$$

where

Q_u = bearing capacity of pile

R_t = toe resistance

R_s = shaft resistance

r_t = unit toe resistance

r_s = unit shaft resistance

A_t = pile toe cross sectional area

A_s = pile unit circumferential area

The relative magnitude of the shaft and the toe resistances will depend on the geometry of the pile and soil profile. In cohesive soils, the shaft resistance generally dominates, while in noncohesive soils, toe resistance is the main portion of capacity.

2.3.3.1 Toe resistance

It is often assumed that the failure mechanism for bearing capacity is shear failure in the soil supporting the foundation. For shallow foundations, three types of failure can be distinguished: general, local, and punching shear failure, which depend on depth, geometry of footing, and soil compressibility. For deep foundations, no specific evaluation exists for failure mechanism. Fig. 2.5 presents four assumed pile toe failure patterns, suggested by some researchers (Vesic, 1967).

In the conventional bearing capacity theory, the unit toe resistance is calculated as follows:

$$r_t = N_q \sigma'_{z=D} \tag{2.2a}$$

where

N_q = bearing capacity factor

$\sigma'_{z=D}$ = effective vertical stress at pile toe level

D = pile embedment length

Many theoretical solutions are available for determining the bearing capacity factor, N_q. Most are based on the bearing capacity theory. However, the bearing capacity theory does not account the effects of soil compressibility, volume changes associated with shearing, and the dependency of ϕ angle on the mean pressure. As shown in Fig. 2.6, the various theories result in very different values of the bearing capacity factor, N_q. The customary logarithmic plot of N_q hides the fact that a very wide range of N_q -values are obtained when ϕ angle exceeds 35^0 (Berezantzew, 1961).

The rather approximate relationship between N_q, and the ϕ angle, coupled with the difficulty of determining a reliable and representative in-situ value of ϕ angle from laboratory tests, creates doubts about the applicability of the conventional bearing capacity theory in pile foundation analysis and design.

Basically, $\sigma'_{z=D}$ is the effective vertical stress at the pile toe level when failure occurs. However, no method is available to determine this stress, the effective overburden stress is used instead.

Al-Awkati (1975) applied cavity expansion theory to the calculation of unit toe resistance and found that instead of vertical effective stress, the in-situ radial effective stress, σ_r', governs the unit toe resistance. Vesic (1977) included soil compressibility and volume changes and developed a revised set of bearing capacity factor. The soil was realized as an elastic-plastic solid, characterized by the strength parameters (c and ϕ) and the stiffness parameters (E and ν).

$$r_t = N_o \sigma'_m \tag{2.3}$$

where

σ'_m = mean normal effective stress at pile toe = $\dfrac{1+2K_0}{3}\sigma'_{V0}$

K_0 = coefficient of earth pressure at rest

N_o = a bearing capacity factor

σ'_{V0} = effective overburden stress

The conventional bearing capacity factor, N_q, is often related to N_σ, by the following equation:

$$N_q = \frac{\sigma'_m}{\sigma'_{z=D}} N_\sigma \tag{2.4}$$

The effect of soil compressibility on the bearing capacity factor was expressed as rigidity index (ratio of stiffness to strength) as follows:

$$I_r = \frac{G}{(c+\sigma'_V \tan\phi)} \tag{2.5}$$

where

I_r = rigidity index

G = shear modulus of soil = $\dfrac{E}{2(1+\nu)}$

E = modulus of elasticity

ν = Poisson's ratio

Also, Vesic (1977) incorporated the simultaneous effect of a volume change of soil on toe bearing capacity by introducing a volume-change parameter (which is related to the average volumetric strain at failure in the plastic zone), and reduced the rigidity index by the following expression;

$$I_{rr} = \frac{I_r}{(1+\epsilon_v)} \tag{2.6}$$

where

I_{rr} = reduced rigidity index

ϵ_v = volume change parameter

Vesic recommended that for the condition of no volume change (undrained condition) or little volume change (dense strata), I_{rr} can be taken as I_r. As shown in Fig 2.7, the rigidity index is as significant for bearing capacity as the friction angle.

By applying cavity expansion theory, some of the shortcomings involved for the bearing capacity approach are eliminated. However, the method ignores soil dilatancy (for $\epsilon_v = < 0$, the expansion theory unable to formulate the dilating behavior and assumes $\epsilon_v = 0$). Also, providing accurate input data regarding rigidity index and volumetric strain can be difficult. Furthermore, methods based on bearing capacity or cavity expansion theories ignore the effect of pile installation in estimating N_q. In addition to the friction angle, other aspects need to be considered to provide a more realistic unit toe resistance. Such as soil dilatancy, soil compressibility, soil stiffness, and dependency of ϕ-angle on the mean effective stress.

Normally, in geotechnical design, capacity and settlement are treated separately from each other and one of them will control the final design. However, especially in case of pile design, the aspects of capacity and settlement, based on stress-strain response, constantly interact and cannot be realized separately. Considering the capacity-settlement interaction, realizing effective stress, as well as regarding negative skin friction, a unified method for design of piles and pile groups was developed by Fellenius (1984; 1989; 1995). The unit toe resistance, r_t, is presented as the following equation:

$$r_t = N_t \sigma'_{z=D} \tag{2.2b}$$

where

N_t = toe bearing capacity coefficient

A suggested range of the N_t-coefficient is presented in Table 2.2 (Fellenius, 1989; 1995; 1996). The contribution and effects of soil compressibility, soil stiffness, and changes of ϕ angle with effective stress level have not been accounted in the proposed N_t values. Furthermore, due to the wide range of the N_t-coefficients, the domain of changes for calculated unit toe resistance is relatively large. Hence, without relevant experience, the estimated capacity may be erroneous.

In a total stress approach for cohesive soils, the unit toe resistance may be calculated on the following equation:

$$r_t = S_u N_c \tag{2.7}$$

where

S_u = undrained shear strength of soil at pile toe

N_c = bearing capacity factor

S_u is not a unique parameter and depends significantly on the type of test used, the applied strain rate, and the orientation of failure plane. Normally, the value of N_c is considered to range between 6 to 9. Therefore, r_t will vary considerably when determined by Eq. 2.8. However, it is important to note that the toe resistance has only a minor contribution to the pile capacity in cohesive soil. For this reason, the accuracy of toe resistance in cohesive soils, does not significantly affect the accuracy of the pile capacity estimation.

2.3.3.2 Shaft resistance

The theoretical approach for calculation of unit shaft resistance considers soil resistance against sliding of pile as a rigid body. The full relation for unit shaft resistance is (Bozozuk, 1972):

$$r_s = M K_s \sigma'_z \tan\phi \tag{2.8}$$

which can be changed to the basic equation proposed by Bjerrum et al. (1965), and Burland (1973) as follows:

$$r_s = \beta \sigma'_z \tag{2.9}$$

where

r_s = unit shaft resistance

K_s = coefficient of lateral earth pressure

M = quotient of wall friction = $\tan\delta/\tan\phi$

δ = pile-soil interface friction angle

σ'_z = effective overburden stress at depth z

β = Bjerrum-Burland beta coefficient, shown in Table 2.2

There are uncertainties and debate over the appropriate choice of coefficient of horizontal stress condition and imposing limiting values of shaft resistance. The K_s -coefficient depends on the initial in-situ stress conditions, pile installation method, and pile shape. It can be stated that K_s ranges from the coefficient of earth pressure at rest, K_0, in its lower bound, to the coefficient of earth pressure at passive condition, K_p, in its upper bound. Values of K_s reported in the literature range from 0.1 to 5 (Kulhawy, 1984). Pile installation affects the stress state in the existing soil in the vicinity of the pile. For driven piles, the horizontal stresses increase depending on the initial magnitude of stresses and soil displacement. Instead, for bored piles, the horizontal stresses may decrease as compared with initial values.

For evaluating the unit shaft resistance, the soil is considered as a rigid-plastic solid. No attention is paid to soil compressibility, strain softening, and nonlinearity in the failure envelope. Therefore, significant influence of the above factors for the development of the shaft resistance along pile is ignored.

There can be a wide range of beta-coefficient from the combination of K_s values, ϕ angles, and wall friction quotients, however, the variation of β is smaller than the variation of its parts.

Also, some methods have been developed for calculating unit shaft resistance in total stress approaches. According to these methods, the undrained shear strength, S_u, have been used for estimation of unit shaft resistance (Tomlinson, 1957; Vijayvergiya and Focht, 1972).

Drained soil characteristics govern long-term pile capacity also in cohesive soils. Therefore, the use of undrained strength characteristics for long-term capacity estimation is not justified.

2.3.4 Limiting unit toe and unit shaft resistances

The estimated unit toe resistance and unit shaft resistance according to Eqs. 2.2 and 2.9, indicate that both resistances increase with depth and are proportional to effective overburden stress. However, early work by some researchers such as Kerisel (1964), Vesic (1964; 1970), and Tavenas (1971) indicated that above a certain depth, called "critical depth", both shaft and toe resistances follow the effective stress principle. Below the critical depth, the resistances would be constant and equal to the respective value at the critical depth.

Some design guidelines, for example American Petroleum Institute, API, (1984; 1991) and Canadian Foundation Engineering Manual, CFEM, (1992), recommend the concept of critical depth in pile capacity design.

The experimental observation of a gradual reduction in the rate of the increase of pile capacity with depth is modeled by imposing limiting values for both toe and shaft resistances beyond the critical depth.

de Beer (1963) found a reduction in unit shaft resistance with depth and attributed it to the arching that takes place close to the pile toe. This arching phenomenon would result in a decreased vertical stress at the pile toe level that would lead to a reduced unit shaft resistance close to the pile toe.

Kulhawy (1984) argued that the experimental observation of limiting unit shaft resistances arises from a combination of decreasing values of friction angle and K_s with depth (stress level). He stated that most natural soils are overconsolidated rather than normally consolidated, besides, the OCR is larger at shallow depths (i.e., K_0 decreases with depth). Therefore, K_s or β is larger for shallow depth with the maximum value close to the ground surface. Because of these effects, the distribution of the average shows approximately constant with depth. However, Kulhawy (1984) argument does not explain the limiting unit shaft resistance claimed to exist in normally consolidated soils.

According to Randolph et al. (1994), the critical depth for estimating pile capacity is not consistent with the physical process that indicates actual pile capacity. He attributed the gradual reduction in the rate of the increase of unit toe resistance with the increase of stress level to two effects. Decreasing values of friction angle and rigidity index with increasing mean effective stress, results in reducing N_q values. Ultimately, the unit toe resistance will be reduced.

According to Fellenius and Altaee (1995), the critical depth is a fallacy which originates in the failure to interpret the results of full-scale and model-scale pile tests properly. In full-scale tests, neglecting the presence of residual loads makes a measured load distribution appear linear below the critical depth. In model-scale piles, which are tested at shallow depths (small confining stress), the neglect of stress-scale effects results in a similar interpretation error.

2.5 Concluding Comments

The dynamic analysis and dynamic methods as well as the static pile loading tests cannot replace the static analysis. For determining pile capacity, it is always necessary to apply static analysis methods. The main reasons for this necessity are summarized (Nottingham, 1975) as follows:

1. It is often difficult to justify the costs of a pile loading test programmes on ordinary or small projects.

2. Dynamic methods usually do not provide any better results than static analysis, besides, the capacity is not available until the pile is driven.

3. Even pile loading tests can be justified, it is desirable to evaluate the probable performance of different pile types, sizes, and lengths during the design stage of a project in order to intelligently plan the field-testing programme.

Moreover, the static analysis is an integral part of all other methods. All in-situ tests, such as SPT, PMT, and CPT need to be referenced to the static analysis.

As complementary of static analysis for pile capacity determination, in-situ test methods can be realized. In recent years, in-situ testing techniques have shown an increase in use for geotechnical design. This is due to rapid development of in-situ testing instruments, an improved evaluation of the real behavior of soils, and subsequent realization of some limitations and inadequacies of conventional laboratory testing (Wroth, 1984; 1988).

Among many in-situ test techniques for site investigation, the Standard Penetration Test (SPT) and the Cone Penetration Test (CPT) are more common than others for pile design. The SPT is still the most commonly used in-situ test during geotechnical investigation. However, many problems and limitations exist for the SPT with respect to interpretation and repeatability. These are due to uncertainty with the energy delivered from various SPT hammers to the anvil system and as well as with the test procedure. In contrast, the Cone Penetration test (CPT), is simple, fast, relatively economical, and provides continuous records with depth. The results are interpretable on both empirical and analytical basis. Therefore, the CPT is becoming the preferred type of penetration test for pile analysis.

By analogy of cone penetrometer as a model pile, the measured cone resistance and sleeve friction can be employed for estimation of unit toe and shaft resistances, respectively. It is possible to develop almost a continuous resistance profile by CPT measurement with depth. The problems of providing representative undisturbed samples, and also determining correct values of required soil parameters by conventional laboratory testing, will be eliminated. Furthermore, there is no need for estimating intermediate parameters such as K_s and N_q for pile capacity estimation.

Because of similarities between CPT and pile, and advantages of CPT as a useful geotecnical investigation tool, the estimation of pile capacity from CPT data has been one of the earliest applications of cone penetrometer.

CHAPTER 3

BACKGROUND TO THE CONE PENETRATION TEST (CPT)

3.1 Historical Background of the CPT

Penetration testing involves pushing or driving a system of a steel cone and rods into the ground and recording the mobilized resistance to penetration in the soil. Probing with rods through weak soils to locate a firmer stratum was originally developed by Collin in France in mid-nineteenth century. Early versions of soundings were developed in the 1920's by the Swedish and Danish State Railways. Significant improvements of penetration techniques were made around 1930 with the development of the dynamic penetration test methods in the United States and the static penetration test methods in Europe.

The first cone penetration tests were made in the Netherlands in 1934 in a form recognizable today (Barentsen, 1936). The method has been referred to as the Static Penetration Test, Quasi-static Penetration test, Dutch Cone penetration, Dutch Static Cone Penetration Test, and Dutch Deep Sounding Test. The term quasi-static is used, because this type of penetrometer is forced into the ground at a constant speed rather than being subjected to truly static loading condition Sanglerat (1972), and Broms (1988).

Initially, the apparatus consisted of a cone and was followed by a design of a mantle to prevent entrance of soil particles between the cone and the push rods (Vermeiden, 1948). A friction sleeve to measure local side friction over a short length near the cone point, was introduced later by Begemann, (1953; 1965).

The use of CPT is increasing widely as a result of the influence of electronics which has been greatly enhanced the accuracy of measurements. The static cone penetration test is becoming the preferred type of penetration test for site investigation. Reasons for the dominance of CPT among other in-situ tests are according to Mitchell (1988), as follows:

- The CPT is simple and relatively economical.
- Continuous records with depth are obtained.
- The results are interpretable on both empirical and analytical bases.
- Variety of different sensors can be incorporated with penetrometer point and friction sleeve.
- A large experience base is now available.

3.2 Equipment

The CPT apparatus consists of a thrust machine and reaction system, a penetrometer, and equipment for measurement and recording. The penetrometer is in most cases attached to 1-m-long rods which are hydraulically pushed into the ground. The thrust machine for pushing down the penetrometer consists of a hydraulic jacking system. The thrust capacity for performing cone penetration test on land ranges from 50 KN through 200 KN. A thrust capacity of 100 KN is sufficient for about 95% of cone penetration testing to 30 m in normally consolidated soils, provided that they do not contain coarse gravels and boulders. A 200 KN thrust will often allow penetration to depths of 50 m to 60 m in medium dense to dense sands and stiff clays (Robertson and Campanella, 1989).

The common two CPT measurements are: cone point resistance, q_c, and sleeve friction, f_s. The cone point resistance is the ratio of the vertical force on the projected area of conical point. The sleeve friction is the shear stress acting on a lateral friction sleeve.

Penetrometers are divided in two main categories, mechanical and electrical. A mechanical cone is operated using inner and outer rods. When operating with the mechanical cone penetrometer, the cone advanced ahead of the outer rods to activate the cone bearing. Then, the cone and the outer rods are advanced together to measure the total load (combination of bearing and friction resistances). The sleeve friction value is determined by subtracting the previously recorded cone resistance from the total load. The Begemann type of mechanical cone is illustrated in Fig. 3.1.

In the electrical friction-cone penetrometer, the cone and the friction sleeve do not move relative to each other. The cone resistance and sleeve friction are monitored continuously during penetration via separate strain-gage load cells mounted on the cone and friction sleeve. Appropriate load cell selection is important in order to maximize sensitivity and prevent over stressing damage. The signals from the strain gages are transmitted to the surface to the data acquisition system via cables which passed through the center of hollow push rods, see Fig. 3.2.

The mechanical cone offers the advantage of an initial low cost for equipment and simplicity of operation. However, it involves a rather slow incremental procedure (usually every 200 mm), is less effective in soft soils, and requires moving parts. Moreover, the quality of data is poor and operator dependent, and the depth is limited.

In contrast, the electric cone offers more rapid procedure, continuous recording, higher accuracy and repeatability, the possibility of incorporating of other additional sensors in the cone, and automatic data logging, reduction, and plotting (Robertson and Campanella, 1989). However, the electrical cones have an initial high cost for equipment and require skilled operators and adequate back up for technical facilities, calibration, and maintenance.

For monitoring changes of temperature during operation and controlling potential zero shift in cone point measurements, the CPT apparatus incorporates a temperature probe in the penetrometer.

The electronic cones can be equipped with a simple sensor, the inclinometer, to measure the deviation from the vertical of the sounding which greatly increases the reliability of the CPT (de Ruiter, 1982). The deviation from the vertical can be due to the cone being deflected by boulders, the effect of sloping soil layers and/or improper alignment of the rods and pushing system at the start of the test.

This change of inclination during penetration may not only cause significant error in depth records as illustrated in Fig. 3.3, but also damage to the cone and rods. The error and damage might not be immediately apparent to the operator.

3.3 Standardization

International attempts to standardize methods of penetration testing started at the 4th ICSMFE in London in 1957. The ISSMFE technical committee on Penetration Testing prepared an international procedure, which was described at the ESOPT-2, conference in Amsterdam, 1982, ISOPT-1, conference in Florida, 1988, and at the 12th ICSMFE 1989. The ASTM standard D3441-86 also provides procedures and guidelines for CPT.

A cone of 10 cm^2 base area with an apex angle of 60^0 is generally accepted as standard and has been specified in the European and American practice. The friction sleeve located above conical point has a standard area of 150 cm^2. The cone penetrometer is pushed at the standard rate of 20 mm/s. Standard 1 m long rods are used to push the cone penetrometer into the soil. The standard rods have the same outside diameter as the cone, i.e., 35.7 mm.

3.4 Piezocone

The measurement of pore water pressure during the penetration of a probe into soil (dynamic pore pressure) was introduced in the mid-1970's (Torstensson, 1975 and 1982; Wissa et al., 1975). By incorporating piezometer elements into standard electric cone penetrometers, the piezocone (CPTu) was introduced in the early 1980's. The piezocone measures the cone resistance, sleeve friction, and the pore pressure mobilized during penetrating. Also, if required, the rate of dissipation of pore pressure can be measured during any pause in the cone penetrating.

According to Campanella and Robertson (1988), the main advantages of the CPTu over the conventional CPT are:

- ability to distinguish between drained, partially drained, and undrained parameters
- ability to correct measured cone data to account for unbalanced water forces due to unequal end areas in cone design
- improved soil profiling and interpretation
- ability to evaluate consolidation characteristics
- ability to assess pore pressure gradients
- improved evaluation of geotechnical parameters
- assistance in the assessment of stress history and OCR for cohesive soils

Soil properties, cone geometry, and location of the pore pressure filter influence the pore pressures measured during penetration. In normally consolidated soft clays and silts, pore pressures measured on the face of the cone, u_1, are generally 10 percent to 20 percent larger than those measured immediately behind the cone, u_2 (Campanella, et al., 1982; Robertson et al., 1986; Mayne and Kulhawy, 1990; and Mayne et al., 1995; Jacobs and Couts, 1992). In overconsolidated clays, silts, and fine sands, the pore pressure on the face of the cone tends to be large and positive whereas that of the measured behind the cone may be considerably smaller and possibly negative. These phenomena can be attributed the stress conditions around the cone. The measured pore pressures are affected by normal stress at the face and shear stress at the behind of the cone. Fig. 3.4 presents the conceptual pore pressure distribution in saturated soil during CPT.

Measuring pore pressure behind the cone has the main advantages such as that a porous filter is less susceptible to damage, measurements are less influenced by filter compressibility, and the position is appropriate for correction due to unequal end areas (Campanella, 1988). No single location can provide information for all applications of pore pressure interpretation. Therefore, more advanced cones must have been developed which are able to measure the pore pressure at different locations simultaneously, in addition to measuring the cone resistance and sleeve friction.

3.5 Recording and Presentation of Cone Penetration Test Results

Recent advances in data acquisition systems and low cost of electronic components have made it possible to digitize the data in the cone and, hence, transmit a clear signal.

Normally, in CPT sounding, the cone resistance , q_c, sleeve friction , f_s, and pore pressure response, u, at one of these three locations, either at the face of the cone, behind the cone, or behind the friction sleeve, (the values are referred to u_1, u_2, and u_3) are measured. Temperature, T, and inclination, I, are also measured simultaneously as the cone penetrometer is advanced in the ground. All channels are continuously monitored and reported digitally at 25 mm intervals.

After processing the obtained data, they are usually presented graphically, including q_c, f_s, R_f (ratio of sleeve friction to cone resistance), and u versus depth as shown in Fig. 3.5. The graphical presentation of CPT result provides an accurate and useful indication of subsurface condition at the site of the test. Also, graphical presentation provides a quick and convenient way for defining the bearing strata, and estimate the likely type and depth of the required foundation.

3.6 Other Developments of CPT

Some of significant recent developments in CPT apparatus and testing are described in the following sections.

3.6.1 Dual range penetrometer, Brecone

When performing CPT in clays, the values of cone resistance are relatively low, maximum 5 MPa, however, the cone resistance in sands may be 40 MPa and more. Therefore, the highly sensitive load cell designed for use in clays is likely be overloaded when used in sands. On the other hand, a load cell designed for use in sands may not be sensitive enough when used in clays. A dual range cone called Brecone is designed to measure on a high-sensitivity, low-capacity load cell up to a certain limit of cone resistance, and then on a high-capacity, low-sensitivity load cell for higher cone resistance. More details are given by Rigden rt al. (1982).

3.6.2 Acoustic cone

Cones have been equipped with a microphone and data acquisition system to monitor acoustic response of the soil during cone penetrating (Muromachi, 1973; Tringle and Mitchell, 1982; Massarsch, 1986). Noise level, spectrum, and frequency are a function of soil type and density. It was also determined by visual inspections that sand and silt layers as thin as 1 mm could be identified using this apparatus, whereas such thin layers cannot be detectible by conventional CPT (Mitchell, 1988).

3.6.3 Lateral stress cone (LSSCP)

The in-situ horizontal stress is one of the important parameters required for many geotechnical analyses. However, its accurate determination involves difficulty. Several attempts were made for measuring normal stress at the location of the friction sleeve in order to estimate the in-situ lateral stress prior to penetration (Huntsman, 1985; Mitchell, 1986). Masood and Mitchell (1993) proposed a correlation between sleeve friction, overconsolidation ratio, and coefficient of earth pressure at rest. Also, a lateral stress sensing cone penetrometer (LSSCP) was developed at the University of Berkeley (Huntsman and Mitchell, 1986). The simultaneous measurement of lateral stress and the other CPT data can lead to an improved analysis of cone penetrometer data for determining of soil parameters.

3.6.4 Resistivity cone (RCPTu)

The resistivity piezocone is a relatively recent development in CPT technology. The RCPTu consists of a resistivity module which is added to a standard piezocone. The incorporation of the resistivity module enables continuous measuring of bulk resistivity of soil and pore fluid, in addition to all other CPTu measurements. One of the main applications of the RCPTu measurements is evaluation groundwater contamination and contaminant transportation (Campanella and Weemees., 1990). Also, a new approach for dilatancy assessment is developed in the saturated sand based on RCPTU measurements (Campanella and Kokan, 1993). The interpretation is based on resistivity contrast between remolded sand (at the vicinity of the interface) and undisturbed sand (relatively far away from the interface) induced during cone penetration.

3.6.5 Seismic cone (SCPTu)

A seismic cone or SCPTu has been developed by incorporating small velocity seismometers and accelerometers into the conventional electric cone (Campanella et al., 1986). The introduction of seismic measurements into the CPT procedure permits the specific determination of shear wave velocity and therefore dynamic shear modulus (G_{max}). Downhole shear wave velocity measurements can be made during brief pauses in the penetrating of the cone. The seismic cone offers an advantage relative to the crosshole method for shear wave velocity measurement that only one hole is needed, and the test can be performed during the course of a regular cone penetration test.

3.6.6 Cone pressuremeter

The cone pressuremeter is an in-situ testing device which combines the electric piezocone with the pressuremeter (Withers et al., 1989). The cone pressuremeter is a particular form of the full-displacement type, which a self-boring pressuremeter mounted behind a solid conical point with diameter of 43.7 mm. The combination of the profiling ability of piezocone together with stress-strain measurements from the pressuremeter, in the form of cone pressuremeter, provides an appropriate in-situ measurements for geotechnical design.

3.6.7 Mini-Cone (MCPT)

A miniature CPT system, is commonly used for laboratory studies of CPT sounding particularly, in calibration chambers, where the full size penetration tests are not practical (Mitchell, 1988). Two sizes of mini-cone have been developed; 12.5 mm cone diameter with friction sleeve area of 28.51 cm^2, and 19 mm cone diameter with friction sleeve area of 43.22 cm^2. Cone resistance in excess of 40 MPa can be sustained without damage to the instruments.

3.7 Factors Influencing CPT Measurements and Interpretation

The factors that can affect significantly the CPT measurement and interpretation are as follows:

1. Equipment design
2. Rate of penetration
3. In-situ stress
4. Compressibility

3.7.1 Equipment design

The three major areas of cone design that influence the acquired data, and subsequent interpretations, are the piezometer locations, accuracy of measurements, and unequal end area effects. The first is explained in the Section 3.4, description of piezocone. The accuracy of load measurements mainly depends on the design of the load cells that may be involved a calibration error and/or zero shift error.

Due to action of water pressure on the unequal areas of the exposed surface behind the cone, the measured q_c does not represent the true total stress. To overcome the difficulty, particularly in soft clays, q_c must be corrected using the following relationship (Baligh et al., 1981; Campanella et al., 1982):

$$q_t = q_c + u\,(1-a) \qquad (3.1)$$

where

q_t = corrected total cone resistance

q_c = measured total cone resistance

u = measured pore pressure behind the cone point

a = net area ratio = A_N / A_T

A_N = load transfer area behind the cone point

A_T = cross-sectional area at the base of cone point

3.7.2 Rate of penetration

According to Baligh et al. (1980), and Campanella et al. (1982), small variations in rate of penetration relative to the standard rate of 20 mm/s have no significant influence on the cone resistance, q_c. Therefore, the rate variation of ± 25% allowed by the ASTM standard, appears acceptable. The mobilized pore pressures during cone penetration (u_1 and u_2) are more depend on the rate of penetration than q_c and f_s (Robertson and Campanella, 1989).

3.7.3 In-situ stress

Theoretical approaches and calibration chamber studies have shown that the in-situ radial stress, σ_r', has a dominant effect on the q_c and f_s (Houlsby and Hitchmann, 1988; Schmertmann, 1972). Baldi et al. (1982) have shown that for a given density of sand, the q_c depends on the in-situ horizontal effective stress rather than by vertical effective stress. Also, the resulting increase of the q_c and particularly f_s after soil improvement techniques such as dynamic compaction and vibrio flotation is due to the increase of σ_r'. Therefore, the in-situ stress history is important in CPT interpretation.

3.7.4 Compressibility

The compressibility of sand can significantly influence q_c and f_s (Schmertmann, 1978a; Villet and Mitchell 1981; Baldi et al., 1982). Highly compressible sands tend to have low q_c and high friction ratio values. The compressibility of sand is a function of uniformity of grading, angularity of grains, as well as mineralogical type, such as mica, and feldspar as opposed to quartz.

3.8 Correlation of CPT Data with Soil Characteristics

During a cone penetration test, complex changes occur in stresses, strains, and pore pressures, making comprehensive theoretical analysis difficult. Many theoretical and experimental methods have been developed to correlate soil characteristics to CPT and CPTU data. It is important to note that cone bearing is a function of several variables of which the density, pore pressure, and the stress level of the soil are the most important ones. Among wide ranges of correlations, only soil profiling and shear strength parameters derived from cone data are discussed in the following sections.

3.8.1 Soil classification

One of the primary applications of CPT is stratigraphic profiling. This can be done with greater accuracy than that achieved from conventional boring and sampling. A procedure was formulated by Begemann (1965b) for classification of soils using CPT data. Begemann (1965b) was the first to point out that the friction ratio, R_f, increases in general with decreasing particle size (see Fig. 3.6). The sleeve friction, f_s, and the cone resistance, q_c, can be used to classify the different soil layers. Also, work on soil classification regarding soil behavior, using CPT data, was presented by Douglas and Olsen (1981), Olsen and Farr (1986), and Campanella and Robertson (1988). Robertson (1990) proposed a classification system by considering pore pressure in addition to q_c and f_s. Due to the fact that q_c, f_s, and u tend to increase with increasing overburden stress, Robertson (1990) used the "normalized" CPT data as suggested by Wroth (1988) as follows:

Normalized cone resistance = $(q_t - \sigma_{vo}) / \sigma'_{vo}$

Normalized sleeve friction = $f_s / (q_t - \sigma_{vo})$

Normalized pore pressure = $(u-u_0) / (q_t - \sigma_{vo})$

Based on these normalized parameters and using extensive CPTU data, modified soil classification charts have been developed by Robertson (1990), as illustrated in Fig. 3.7. Several rules exist for classifying soils directly from CPT measurements, as developed by Campanella and co-workers. The rules are compiled in a computer program called CPTINT (Campanella, 1993). Fig. 3.8 shows one of soil classification charts based on q_t and R_f which used in CPTINT program.

Normally, clayey soils have q_c smaller than 4 MPa with R_f greater than 3%, whereas for sandy soils q_c is greater than 4 MPa and R_f smaller than 1%. Care has to be taken in case of compressible sands and sensitive clays.

3.8.2 Undrained shear strength of clay, S_u

Methods for estimating of S_u from CPT data have been presented by Baligh et al. (1980); Lunne and Kleven (1981); Jamilokowski et al. (1982). Normally, cone resistance varies directly with the undrained shear strength, S_u, and the formula generally used to equate the two is

$$S_u = \frac{q_c - \sigma_{vo}}{N_k} \tag{3.2}$$

where

S_u = undrained shear strength

σ_{vo} = the in-situ overburden stress

N_k = cone factor

The contribution of q_t instead of q_c, as well as σ_{ho} (in-situ horizontal stress) or σ_m (in-situ mean stress) instead of σ_{vo} in Eq. 3.2. has been considered for calculating S_u from cone resistance.

Theoretical solutions for N_k have been based on bearing capacity theory (Meyerhof, 1961), cavity expansion theory (Ladanyi, 1971; Vesic, 1972), and combination of these two theories (Baligh, 1975).

Some of the main factors that can affect the cone factor, N_k are:

1. geometry and design of the penetrometer
2. plasticity index of the clay
3. stress history
4. macro fabric of the soil
5. soil sensitivity

Typical values for N_k are 10 to 20 for NC clays and 20 to 30 for OC clays.

In stiff OC clays, it is difficult to establish similar correlations, because fissures have a marked effect on the cone factor. This effect varies with the spacing of fissures and other discontinuities. This is illustrated in Fig. 3.9, where three fissure patterns are shown. For the closest spacing (a), cone resistance reflects fully the effect of the fissures, in the case of intermediate (b) only partly reflects, whereas, for widely spaced (c), the strength governing the cone resistance represents the intact strength of clay.

Due to increased accuracy in the measurement of Δu, especially in soft clays where Δu can be very large, S_u can be estimated from Δu. The following relationship is proposed by Campanella et al. (1985):

$$S_u = \frac{\Delta u}{N_{\Delta u}} \tag{3.3}$$

where

$N_{\Delta u}$ = pore pressure factor, varies between 2 and 20

Δu = excess pore pressure

In order to estimate the undrained shear strength from cone resistance, many assumptions are necessary, and thus any approach results in an approximate value of S_u. According to Konrad and

Law (1987), the assumption regarding the slip surfaces when the cone is advanced into the soil media is the most significant with respect to the theoretical bearing capacity factor and, therefore, for calculated soil strength. Konrad and Law (1987) considered the soil-cone interface to be a slip surface in soft clay for obtaining S_u from cone resistance. The analysis is based on spherical cavity expansion in an elasto-plastic medium, see Fig. 3.10. The calculation is based on effective friction parameters and measured pore pressures during penetration. The authors proposed the following equation is proposed to obtain undrained shear strength from cone data.

$$S_{uc} = \frac{q_t - (1+F)\sigma_i + F\alpha u_2}{1.33(1+F)(\ln I_r + 1)} \tag{3.4}$$

where

S_{uc} = undrained shear strength mobilized by the cone

F = overall soil-cone parameter = 1.73 M tan ϕ'

σ_i = initial total stress = in-situ total octahedral stress

α = pore pressure factor which relates the pore pressure at failure zone to the u_2

M = friction factor for the soil acting on the cone surface

ϕ' = drained friction angle

Among the several parameters involved in the above equation for determining undrained shear strength, only cone resistance and pore pressure are obtained from CPT, while the other parameters such as ϕ', M, σ_i, α, and I_r must be evaluated independently. For general applications, Konrad and Law (1987) recommended: $\phi' = 27^0$ for clay, M = 1.0 for usual roughness, $\sigma_i = \sigma_{v0}$, α = 1.0 to1.1, and I_r can be obtained from stress-strain curve of CKU tests based on secant modulus approach.

Experience has shown that no simple unique relationship exists between CPTU data and undrained shear strength for all clay type soils. Also, it has been recognized for many years that the remolded undrained shear strength is about 20% smaller than the sleeve friction (Drenvich et al., 1974; Robertson and Campanella, 1989).

3.8.3 Drained friction angle

For interpretation of drained shear strength of sand from cone resistance different approaches, such as theoretical, experimental, and semi-experimental are used. The main two theories that used are bearing capacity (Janbu and Senesset, 1974; Durgunoglu and Mitchell, 1975) and cavity expansion (Vesic, 1972). Most of the available bearing capacity theories on deep penetration neglect both the curvature of the shear strength envelope and the compressibility of soil. Therefore, they cannot provide reliable estimation of ϕ angle. Work by Vesic (1963) has shown that since soil compressibility influences the cone resistance, no unique relation exists between friction angle and cone resistance for all sands. Studies by Mitchell and Keavney (1986) indicated that the correlation developed by Durgunoglu and Mitchell (1975) based on bearing capacity theory provided reasonable estimates for a variety of sands, but poor agreement for highly compressible sands (see Fig. 3.11).

Based on cavity expansion theory, Vesic (1972) took into account the soil compressibility and volume change and Baligh (1976) incorporated the curvature of the shear strength envelope. Calibration chamber studies by Baldi et al. (1982) and also by Mitchell and Keavney (1986) indicate that the cavity expansion theory appeared to model well the measured response. However, the cavity expansion analysis is complex and requires considerable input data regarding the shear modulus, the shear strength, and the compressibility of the soil.

Calibration chamber results show that a simple closed-form solution to derive the shear strength for all sands is not possible. (Robertson and Campanella, 1983). However, calibration chamber tests provide useful insight for relative importance of various factors which affect cone resistance in sands.

3.9 Other Applications of CPT

In addition to stratigraphy, and estimation of undrained shear strength and drained friction angle from cone data, the following outlines the major application of CPT:

1. Assistance in the assessment of stress history and OCR.
2. Control of compaction and ground improvement.
3. Estimating deformation characteristics of soil.
4. Ability to evaluate consolidation characteristics.
5. Assessment of liquefaction potential.
6. Checking the adequacy and uniformity of a fill.
7. Locating cavities in very soft rocks, e.g., chalk.
8. Locating the boundary of permafrost.
9. Sampling and monitoring of ground water.

CHAPTER 4

CALIBRATION CHAMBER STUDIES AND TESTING SMALL-SCALE MODELS

4.1 Introduction

Interpretation of the cone penetration test (CPT) results is based on empirical correlations between the measured cone data and soil parameters. In cohesive soils, it is common to relate the cone resistance, and/or friction sleeve resistance to the undrained shear strength determined by in-situ vane shear strength and laboratory shear strength tests. Empirical correlations have been proposed between cone data and sensitivity, stress history, overconsolidation ratio, and other consolidation characteristics.

For noncohesive soils, CPT data are difficult to correlate to the soil parameters. No other type of field test exists to determine strength parameters directly in noncohesive soils, and undisturbed samples of sand are only possible to obtain in very special cases. Therefore, correlation or calibration tests in laboratory stress cells or calibration chambers (CC) have become common. Furthermore, the disadvantage of calibration in-situ testing equipment in the field with regard to cost and execution is overcome by calibrating under reproducible conditions in the laboratory.

Laboratory chamber testing of sand follows a well-established technique of preparing a sample of known material to a desired density. Laboratory tests, usually triaxial tests, are carried out to determine the geotechnical parameters of the sample in the chamber. Thereafter, CPT soundings are performed and the CPT data are related either directly or indirectly to the known geotechnical parameters of the soil, such as friction angle and density.

4.2 Brief History

Tcheng (1966), Melzer (1967), and de Beer (1963) performed laboratory calibration testing in rigid-wall test chambers. Rigid wall condition imposes a boundary condition of zero lateral strain on the soil in the chamber. To eliminate the boundary effect, the test chambers must be much larger than the cone penetrometer being tested. A figure of 200 times the diameter of the cone has been mentioned (Chapman, 1974). This criterion leads to a large chamber which would not be feasible in economical as well as practical aspects, and makes the testing time-consuming.

In contrast, the walls of a flexible-wall chamber have much smaller influence on the stresses in the chamber than the rigid walls, and the chamber, therefore, can be made much smaller. The use of flexible-wall calibration chambers started in 1969 at the Country Roads Board (CRB), Melbourne, Australia (Holden, 1971). In 1970, under supervision of Holden and guidance of Schmertmann, as shown in Fig. 4.1, a flexible-wall calibration chamber, cylindrical 1,220 mm diameter and 1,220 mm high, was constructed and installed at The University of Florida (Reese, 1975).

Since the development of the first two flexible calibration chambers, various apparatuses, increasingly sophisticated and automated, have been developed around the world. Ghionna and Jamiolkowski (1991) presented an extensive list of the calibration chambers most actively used in the validation of in-situ techniques in sands, which is reproduced in Table 4.1.

4.3 Operating of the Chamber

The procedure for conducting a test in the calibration chamber involves three major steps as follows:

- Forming the sand in the chamber
- Applying the desired boundary conditions
- Performing CPT or small-scale pile loading tests

The sand specimens, is usually prepared by means of pluvial deposition in air from a hopper through a perforated plate and appropriate diffuser meshes. Sand falls into a rubber membrane with the function of isolating the sample from the environment and allowing the application of the stresses at the lateral surface of the sample. The resulting sample in the chamber is homogeneous, and the density can be controlled by the size of the hole in the perforated plate, i.e., larger holes result in faster pouring rates and looser soil. The most recent calibration chambers offer the possibility of saturating the specimens. This can be achieved by employing de-aired water and CO_2, or a vacuum inside the soil (Bellotti et al., 1982). After soil deposition in the chamber, the soil is consolidated to the desired stress state.

After preparing the soil, the desired boundary condition is implemented. The boundary provided by the test chamber should have a negligible influence on the measured penetration resistance. The magnitude of this effect will depend on: the size of the chamber relative to the cone diameter, and the stress and strain conditions at the boundary. The smaller the chamber, the more pronounced the difference of the results obtained in the chamber and in the field. For the chambers currently used, the correction for chamber size effect must be considered.

Veismanis (1974) defined four different types of boundary conditions named BC1 to BC4, which apply to the flexible-wall calibration chambers, as listed in Table 4.2 and illustrated in Fig. 4.2. Most of the performed tests found in the published literature, used BC1 or BC3 conditions, which more closely simulate field conditions (Baldi et al., 1982). However, none of the indicated boundary conditions in Table 4.2 perfectly produces the boundary conditions encountered in the field.

In the testing stage, the cone penetrometer is driven hydraulically through a hole in the chamber lid, usually with a constant standard speed of 20 mm/s. During penetration, automatic chart records or digitized data from data acquisition system are obtained for cone and friction sleeve resistances. In most tests, the resistance is measured at mid height, the point where theoretically it is affected least by the end boundaries. According to Salgado (1993), six types of cone resistance profile from CPT in the calibration chamber can be identified as illustrated in Fig. 4.3. The type A is the most common case. The degree of uncertainty for interpreting the test results increases when the resistance profile changes from type A to type F. The more typical obtained profile of q_c and f_s from calibration chamber tests are presented in Fig. 4.4, for which the following general characteristics may be noted (Parkin and Lunne, 1982):

1. Initial section, in which penetration resistance is affected by the top plate.
2. Central section, where penetration resistance is constant or slowly varying with local vertical stress.
3. Final section, in which readings are affected by the bottom plate, where an increase or decrease can occur due to the relative stiffness of the sample and the bottom plate.

4.4 Calibration Chamber Studies in Noncohesive Soils

For noncohesive soils, two approaches are used to obtain soil parameters from the results of CPT: empirical correlations or theoretical solutions by using an appropriate constitutive model, a numerical and/or analytical approach. Vesic (1972), Janbu and Senneset (1974), Durgunoglu and Mitchell (1975), and Baligh (1976) developed relationships between CPT data and soil parameters based on bearing capacity and/or cavity expansion theories. Currently, however, no satisfactory general solution exists for interpreting CPT data in noncohesive soils. Therefore, empirical correlations are normally used to derive geotechnical soil parameters from the CPT data.

Two main empirical approaches are used for interpreting sand properties based on CPT data, obtained from calibration chamber tests: CPT data combined with state conditions, and CPT data combined with density index (relative density), I_D, values.

4.4.1 CPT data combined with state condition

The word "state" is used as a description of the physical conditions under which a material exists; the material behavior is controlled by these conditions (i.e., its state). Void ratio and stress level are the most important physical conditions which define the state of the soil.

Roscoe et al. (1958) developed the "critical void ratio" concept introduced by Casagrande (1936). Casagrande (1936) called the ultimate void ratio "critical void ratio", at which continuous deformation occurs with no change in principal stress difference. Ttheoretically, at least it is possible to set up a sample at an initial void ratio such that the volume change at failure would be zero. This void ratio would, of course, be the critical void ratio (Holtz and Kovacs, 1981).

Roscoe and Poorooshasb (1963) applied critical state principles to model testing of clay soil and indicated that for correct relation of scale between model and prototype, the void ratio proximity to the critical state line at the initial mean stress must be the same for the model and the prototype. The critical state line, also called steady state line, is defined as the locus of all points in the void ratio-mean stress plane, a line, at which a soil mass deforms under conditions of constant effective stress, void ratio, and velocity. A single point on the void ratio-mean effective stress plane can be determined by conducting a consolidated undrained triaxial test on a soil sample. By combining the results of a series of consolidated undrained triaxial tests, the critical state line can be defined, see Fig. 4.5.

The critical or steady state line is a reference state that reflects a combination of many physical parameters of sands including compressibility, limiting void ratios (e_{max} ; e_{min}) and friction angle at constant volume. Steady state concepts and steady state line determination have been described by Castro and Polous (1977), Casagrande (1975), and Polous (1981).

The steady state satisfies the conditions for use as a reference state for physical modeling: the state is unique for soil and it is relatively easily established experimentally. The behavior of noncohesive soil is a function of its location in the e-ln (p) plane and its vertical distance to the steady state line, called "e-prime" by Roscoe and Poorooshasb (1963), "the state parameter" by Been and Jefferies (1985), and "upsilon distance" by Altaee and Fellenius (1994).

The upsilon distance is positive above the steady state line and negative below it. Sand in an initial contractible condition (positive upsilons) is loose and can easily liquefy—collapse. Also, sand with small negative upsilon distance may liquefy during shear or shearing disturbance. Sand with a void ratio well below the steady state line (appreciable negative upsilons) is dense and will dilate when sheared.

Because of the importance of upsilon distance for interpreting sand behavior, the possibility of correlating it directly to the cone resistance is of considerable interest. Been et al. (1986) proposed that for given sand, "normalized" cone resistance $(q_c-p)/p'$ is a unique function of upsilon distance (p is the mean total stress and p' is mean effective stress). Been et al. (1987) obtained samples of various sands for which calibration chamber tests data were available and carried out triaxial tests on the samples to determine the steady state parameters. By applying the corrections for the size and boundary effects of calibration chamber and using regression analysis, they suggested that a unique relationship exist between the logarithm of normalized cone resistance and the upsilon distance to the steady state line.

The steady state approach provides a rational procedure for interpreting CPT data obtained for any sand from calibration chamber tests. However, this approach requires independent measurement of steady state line, and the in-situ horizontal stress, which values are difficult to determine.

At present, however, any correlation between cone resistance and the steady state of sand state must be treated with caution. This is because, the CPT interpretation in sands is based on a limited size database from calibration chamber tests which in addition were performed on clean sands of a limited range of grain size, and intrinsic properties (Sladen, 1989). In contrast, a wide spectrum of sands with variety of gradations and properties are encountered in practice. Besides, the problem of the influence of the finite dimensions of the calibration chamber on tests results have been recognized as one of the most important in this type of research (Parkin and Lunne, 1982; Jamiolkowski et al., 1985). Therefore, care must be taken before extrapolating from the limited database.

4.4.2 CPT data combined with density index relationships

Conventional methods of CPT interpretation in sands, consider the soil density or, more commonly, density index, I_D, (Schmertmann, 1978b; Villet and Mitchell, 1981; Baldi et al., 1982; Bellotti et al., 1982). In spite of numerous proposed correlations of cone resistance and soil density index, no single relationship exists between cone resistance, the density index, and vertical effective stress for all sands (Parkin et al., 1980; Villet and Mitchell, 1981). The inconsistency is due to the fact that these correlations require that all sands behave in a similar manner at the same I_D and stress level.

Robertson and Campanella (1983) compiled the relationship between q_c, I_D, and σ'_{v0}, as proposed by different researchers. As illustrated in Fig. 4.6, no single relationship based on density index exists for sands.

According to Been and Jefferies (1985), the triaxial tests performed on sands with identical grain size distribution at different values of initial mean stress, but with the same initial void ratio (i.e., same density index) showed results that are very different in terms of stress-strain and strength behavior. In contrast, triaxial tests performed at different initial mean stress, but with the samples tested at an initial void ratio that had the same upsilon distance, showed similar behavior.

The density index approach assumes the existence of reference densities (i.e., e_{max}, e_{min}) and attempts to normalize behavior in terms of these reference densities. However, there are significant difficulties associated with determination of maximum, minimum, and in-situ densities (void ratios), and hence, for density index. Moreover, works by Lee and Seed (1967), Lade (1977), and Altaee and Fellenius (1994) indicate that the effective consolidation stress modifies material behavior of sands to the point that even dense sand, if tested at high confining stress, will behave similarly to loose sands.

In fact, sand parameters cannot be expressed in terms of density index, I_D, and a description of stress-state must also be included. Therefore, the use of density index for interpretation of CPT data on sands is illogical and unfounded.

4.5 Testing Small-Scale Models

Results from testing models under conditions of normal gravity differ from field conditions, not only because of the difference in the geometric size, but also because of the difference in the magnitude of stress in the soil at which the model test is performed as opposed to the stress in the prototype soil (Altaee and Fellenius, 1994).

To overcome the stress difference, model tests can be performed in the centrifuge. However, centrifuge tests are expensive. As an alternative, the vertical gradient of effective stress can also be increased by imposing a powerful downward gradient of pore fluid. Such increased-stress-gradient methods are cheaper than centrifuge tests, but limited to certain type of soils and situations.

However, neither the results from centrifuge tests nor the increased-stress-gradient tests in the calibration chamber are directly transferable to a prototype unless the tests are performed with the stress in the model equal to the stress in the prototype at homologous points. Besides, modeling in soil requires a scaling relation between stress and strain that builds on an understanding of how the void ratio (density) of the soil changes when stress is imposed (Altaee and Fellenius, 1994). Moreover, at present, constructing the centrifugal and/or increased-stress-gradient type of chamber useful for CPT and pile loading tests studies would be very costly and time-consuming.

4.6 Concluding Comments

Use of the calibration chamber has the advantage over field testing that the sand type and density as well as both vertical and lateral stresses are known. On the other hand, the test procedure and interpreting soil parameters from CPT data in calibration chambers involve problems and limitations.

With few exceptions, the calibration chamber experience is limited to tests on specimens which are freshly reconstituted sands including the fabric may be very different from that of natural soil deposits. Besides, most of the calibration chamber tests have been performed on uniform, clean, mostly silica sands, whereas natural sand deposits are rarely uniform, and almost always contain a non-negligible percentage of fines content. In addition, many relevant engineering problems are linked to more crushable and compressible, usually slightly cemented materials.

The boundary conditions applied in calibration chamber studies cannot realistically simulate conditions. Due to the practical reasons, the employed calibration chambers have finite dimensions. This fact together with the lack of knowledge of the real conditions in terms of stress and strain imposed to the sample boundaries, are involved for the so-called chamber size effects. Therefore, the established engineering correlations from calibration chamber studies to the field situations include uncertainty (Ghionna and Jamiolkowski, 1991).

No unique relationship exists between the density index, cone resistance, and overburden effective stress for all sands. This is because other factors such as soil compressibility and horizontal effective stress influence cone resistance. Although, the steady state approach presents a rational procedure for interpreting CPT data from calibration chamber tests, the necessity associated for measurement of the in-situ horizontal stress for steady state line is difficult.

Transferring the CPT data to the pile design requires also pile loading tests in the chamber, in which the scale effect would be more pronounced for different size of piles. Therefore, difficulties and limitations exist to extrapolate the results of model-scale tests of CPT and piles performed in the conventional calibration chamber to the full-scale piles for determining pile capacity from CPT data.

Hence, for determining pile capacity from CPT data, only the results of full-scale pile loading tests with CPT soundings performed close to the pile locations are considered useful for this research programme.

CHAPTER 5

CURRENT METHODS OF PILE CAPACITY ESTIMATION USING CPT DATA

5.1 General

Determining pile capacity from CPT was one of the first applications of cone penetration test. Early efforts were directed toward estimating the depth to which a pile should be driven to achieve a particular capacity. It was realized that the cone penetrometer can be considered as small-scale model pile and there must be some relationship between the cone point resistance and the unit toe resistance of pile. However, there was considerable disagreement about the failure mechanism and the relationship between the unit cone point resistance and unit toe resistance of pile (Nottingham, 1975).

Meyerhof (1956) performed theoretical and experimental studies of pile loading capacity by comparing results from CPT soundings and static loading tests. He concluded that for deep foundations bearing in sand, the CPT method provides a better correlation than does the bearing capacity formula.

Van der Veen and Boersma (1957) correlated cone data to the results of loading tests on concrete piles in which the pile toe resistance was determined. The scale effect (the difference in diameters of pile and cone) was accounted for by averaging cone resistance values over a depth interval of "4b" above the pile toe level to "1b" below the pile toe level, where b is the equivalent pile diameter.

de Beer (1963) found that below a certain depth in sands, penetrometers of different diameters attained the same value of unit resistance. Vesic (1964) and Kerisel (1964) found one-to-one agreement between the cone resistance and the pile unit toe resistance in sand.

Begemann (1963) suggested a refined averaging procedure of the total cone point resistance used to estimate pile unit toe resistance, which was later adopted by others (Nottingham, 1975; Schmertmann 1978a; de Ruiter and Beringen, 1979). He assumed that the failure pattern at the pile toe follows the classic logarithmic spiral shape in an extension zone of 3.75b below pile toe and 8b above pile toe. Based on his suggestion, the unit toe resistance of pile is:

$$r_t = \frac{q_{c1} + q_{c2}}{2} \tag{5.1}$$

where

r_t = unit toe resistance of pile

q_{c1} = arithmetic average of q_c below pile the toe over a depth (varies from 0.7b through 3.75b)

q_{c2} = arithmetic average of q_c above pile toe over a length of 8b

To account for effect of thin layers and zones of weak soil, which can influence the shape and position of rupture surface at the pile toe, a minimum path rule was recommended by Begemann for calculating q_{c1} and q_{c2} values. The approach is illustrated in Fig. 5.1.

Although the Begemann procedure for estimating unit toe resistance has met with general acceptance, disagreement exists for the assumed rupture surface for pile toe and cone point, and the details of the procedure for relating the cone resistance to the unit toe resistance of pile.

Almost all of the proposed procedures suggest averaging the total cone resistance to obtain the pile unit toe resistance. However, the average total q_c may be higher than the pile unit toe resistance, which gave some concern for a pile design (Nottingham, 1975).

Prior to development of adhesion jacket cone (friction sleeve penetrometer), it was common to relate the cone point resistance results also to unit shaft resistance of pile. This was done either by assuming the unit shaft resistance of pile as a percentage of cone resistance or by estimating the shear strength of the penetrated soil from cone resistance.

Meyerhof (1956) proposed the following simple relationship between cone resistance and unit shaft resistance of pile in sand:

$$r_s = \frac{q_c}{200} \tag{5.2}$$

where

r_s = unit shaft resistance of pile

q_c = cone point resistance

Mohan et al., (1963) performed a number of static loading tests on cast-in-place concrete piles and indicated that in cohesionless soil with average q_c ranging from 1 MPa through 10 MPa, the value of unit shaft resistance of a pile is approximately 2 % of the cone resistance, that is:

$$r_s = \frac{q_c}{50} \tag{5.3}$$

To provide a reliable means for estimate pile unit shaft resistance, Begemann (1953) developed the adhesion jacket (friction sleeve) to measure local friction during cone penetration. The invention of the adhesion jacket cone opened the door to more direct measurement of the unit shaft resistance of pile. Later, Begemann (1965a) analyzed the results of a large number of pile tension tests (uplift tests) to develop a correlation between unit shaft resistance of pile and sleeve friction. CPT methods for estimating pile shaft resistance are almost exclusively based on the result of Begemann's work on pullout tests of piles (Nottingham, 1975).

Begemann (1965a) also suggested that the sleeve friction, f_s, could be set equal to the undrained shear strength of cohesive soil. Therefore, it is also possible to relate the unit shaft resistance of a pile to the sleeve friction by applying static analysis methods based on total stress approach (α-method).

5.2 Using CPT Data for Pile Design

Two main approaches for application of cone data to pile design are used in current practice as follows:

1. Direct use of cone data, i.e., cone resistance for unit toe resistance and sleeve friction for unit shaft resistance by some modification—direct method.
2. Estimate of shear strength parameters such as S_u and ϕ angle from cone data—indirect method.

Direct CPT methods apply cone bearing for unit toe resistance and sleeve friction for unit shaft resistance with some modification regarding to scale effects. By incorporating the scale effects, the analogy of cone penetrometer as a model pile is realized. Essentially, the influence of mean effective stress, soil compressibility, and rigidity index affect the pile and the cone in equal measure, eliminating the need for laboratory testing and calculating intermediate values such as K_s and N_q.

Indirect CPT methods employ soil parameters such as friction angle and undrained shear strength estimated from the cone data as based on bearing capacity and/or cavity expansion theories. These soil parameters include errors due to disregard of horizontal stress, assumption of plane strain failure mechanism for axisymetric nature of deep penetration, soil compressibility, and strain softening. Indirect methods will not be discussed in this dissertation.

The current CPT direct methods, which apply no modification factors, usually overestimate pile toe and shaft resistances. This has been considered due to the combination of the following effects; scale effect, rate of penetration, and difference in insertion technique. Modification factors are required in order to obtain an appropriate relation to the sleeve friction, f_s, and cone resistance, q_c, to the pile unit shaft and unit toe resistances, respectively.

5.3 Current CPT Direct Methods

Normally, the direct methods which incorporate CPT data for pile design provide relatively good agreement for the capacity of different piles in comparison with indirect methods (Meyerhof, 1956; Nottingham, 1975; Tumay and Fakhroo, 1981; Davies, 1987; Briaud and Tucker, 1988). A summary of current CPT methods for estimating the capacity of axially loaded pile is presented in Table 5.1. Of these, the following are of particular interest as they are used in current North American practice:

1. The Schmertmann and Nottingham method (1978, 1975)
2. The de Ruiter and Beringen method (1979), also called European method
3. The LCPC method (Bustamante and Gianeselli, 1982), also called French method
4. The Meyerhof method (1956, 1976 and 1983)
5. The Tumay and Fakhroo method (1981)

1. The **Schmertmann and Nottingham** method is based on a summary of the work on model and full-scale piles presented by Nottingham (1975). The unit toe resistance of a pile, r_t, in sand and in clay is taken as equal to the average of the cone resistance. The average q_c value is determined from the graphical representation of the CPT measurement in a zone ranging from 8b above (b is pile diameter) and from 0.7b through 4b below pile toe (the actual value depends on the trend of q_c values), see Figs. 5.1 and 5.2a. This zone is defined by the failure pattern for the pile toe which is assumed to follow a logarithmic spiral, as originally introduced by Begemann (1963). An upper limit of 15 MPa is imposed for the unit toe resistance.

   The unit shaft resistance of a pile, r_s is determined from either sleeve friction or cone resistance:

$$r_s = K f_s \tag{5.4}$$

where

K = a dimensionless coefficient

f_s = sleeve friction

Depending on pile shape and material, cone type, and embedment ratio, in sand, the K-coefficient ranges from 0.8 through 2.0, and in clay, it ranges from 0.2 through 1.25, see Figs. 5.3 and 5.4. Above an embedment depth of eight pile diameters, the unit shaft resistance is linearly interpolated from zero at the ground surface to the value of Eq. 5.4. In sand, but not in clay, the shaft resistance may be determined from the cone resistance instead:

$$r_s = C q_c \tag{5.5}$$

where

C = a dimensionless coefficient

q_c = cone resistance (total; uncorrected for pore pressure)

The C-coefficient is a function of the pile type and ranges from 0.8 % through 1.8 %. An upper limit of 120 KPa is imposed on the unit shaft resistance, r_s, regardless whether it is determined from Eq. 5.4 or from Eq. 5.5. For tension capacity, the shaft resistance is reduced to 70 % of that determined by Eqs. 5.4 or 5.5.

2. The **de Ruiter and Beringen** method (also called the European method) is based on experience gained from offshore construction in the North Sea. In sand, this method is very similar to the Schmertmann method. Indeed, for unit toe resistance of a pile in sand, the method is the same as the Schmertmann method (both build on Begemann procedure for calculating toe resistance from cone resistance). In clay, the following equation is used:

$$r_t = N_c S_u \tag{5.6}$$

$$S_u = \frac{q_c}{N_k} \tag{5.7}$$

where

N_c = conventional bearing capacity factor

S_u = undrained shear strength

N_k = a dimensionless coefficient, ranges from 15 through 20, reflecting local experience

An upper limit of 15 MPa is imposed for the unit toe resistance which is further governed by the overconsolidation ratio, OCR, as shown in Fig. 5.2b.

The unit shaft resistance of pile, in sand is determined by either Eq. 5.4 with K=1 or Eq. 5.5 with C=0.3 %. In clay, the unit shaft resistance is determined from the undrained shear strength, S_u, which was obtained by Eq. 5.7, as follows:

$$r_s = \alpha S_u \tag{5.8}$$

where

α = adhesion factor of unity for normally consolidated clays and 0.5 to overconsolidted clays

An upper limit of 120 KPa is imposed on the unit shaft resistance. For tension capacity, the shaft resistance is reduced to 75 % of that determined by Eq. 5.5.

3. The LCPC (Laboratoire Central des Ponts et Chausees) method (also called the French method), is based on experimental work of Bustamante and Gianeselli (1982) for the French Highway Department. Both the unit toe and unit shaft resistances are determined from the cone resistance, q_c. The sleeve friction, f_s, is not used. The unit toe resistance is determined as a range of 40 %

through 55 % of the q_c, averaged within a zone of 1.5b above and 1.5b below the pile toe, see Table 5.2 and Fig. 5.5.

The unit shaft resistance is determined from Eq. 5.5 with the C-coefficient ranging from 0.5 % through 3.0 % as governed by rules for the magnitude of the cone resistance, type of soil, and type of pile. Upper limits of the unit shaft resistance are imposed, ranging from 15 KPa through 120 KPa depending on soil type, pile type, and pile installation method, see Table 5.2.

4. The **Meyerhof method** is based on theoretical and experimental studies of deep foundations in sand. For unit toe resistance the influence of scale effect of piles and shallow penetration in dense sand strata have been considered. The unit toe resistance in sand is determined from cone resistance in an empirical relation as follows:

$$r_t = q_{c,a} C_1 C_2 \tag{5.9}$$

where

$q_{c,a}$ = arithmetic average of q_c values in a zone ranging from "1b" below through "4b" above pile toe

C_1 = $[(b + 0.5)/2b]^n$; modification factor for scale effect when b>0.5, otherwise $C_1 = 1$

C_2 = D_b / 10b; modification factor for penetration into dense strata when Db<10b, otherwise $C_2 = 1$

b = pile diameter (m)

n = an index = 1 for loose sand, =2 for medium dense sand, = 3 for dense sand

D_b = embedment of pile (m) in dense sand strata

The unit toe resistance of a bored pile is reduced to 30 % of that determined from Eq. 5.9. The unit shaft of pile resistance is determined from either Eq. 5.4 with K = 1, or Eq. 5.5 with C = 0.5 %. For bored piles, reduction factors of 70 % and 50 % respectively, are applied to the calculated values

5. The **Tumay and Fakhroo** method is based on an experimental study on a number of different piles in clay soils in Louisiana, USA. The unit toe resistance is determined as the same procedure recommended by Schmertmann. The unit shaft resistance is determined according to Eq. 5.5 with the K-coefficient determined from the following relation, in which the coefficient is no longer dimensionless.

$$K = 0.5 + 9.5\, e^{-90 f_s} \qquad (5.10)$$

where

f_s = sleeve friction in MPa

For a sleeve friction ranging from 10 KPa through 50 KPa, Eq. 5.10 results in a K-coefficient ranging from about 4.5 through 0.6.

5.4 Concluding Comments

When using any of the five methods, difficulties arise in applying some of the recommendations of the methods. For example:

1. The methods were developed more than a decade ago, before the piezocone was generally available, therefore, they do not consider the more accurate measurements achievable with the piezocone.

2. While the recommendations are specified to soil type (clay and sand), neither includes a means for identifying the soil type from CPT data. Instead, the soil profile governing the coefficients relies on information from conventional boring and sampling, and laboratory testing, which may not be fully relevant to the CPT data. The soil type is also only very cursorily characterized.

3. All methods include random smoothing and filtering of the CPT data, that is, elimination of peaks and troughs that exposes the results to considerable subjective operator influence.

4. The cone resistance (total resistance) has not been corrected for the pore pressure on the cone shoulder and, therefore, the data behind the methods include errors—smaller in sand, larger in clay.

5. The methods employ total stress values, whereas for long term, effective stress governs pile capacity.

6. All of the methods are locally developed, that is, they are based on limited types of piles and soils.

7. The upper limit of 15 MPa, which is imposed on the unit toe resistance in the Schmertmann, European, and Tumay methods, is not reasonable in very dense sands where values of pile unit toe resistance, r_t, higher than 15 MPa frequently occur. All methods except Meyerhof method impose an upper limit also to the unit shaft resistance, which cannot be justified by effective stress approach. Values higher than those recommended occur frequently.

8. All methods involve a judgment in selecting the coefficient to apply to the average cone resistance to arrive at the unit toe resistance.

9. None of the current CPT direct methods specify any method for evaluating the pile capacity from static loading test results that can be used as reference to the pile capacity estimated from CPT data. Yet, the capacity of a pile is determined from the results of static loading tests, varies considerably with the method used to evaluate the test (Fellenius, 1975).

10. None of the methods consider sensitivity and dilatancy effects from advancing the cone and pile driving.

11. In the European method, the overconsolidation ratio, OCR, is used to relate q_c to the r_t. However, while the OCR is normally known in clay, it is rarely known for sand.

12. In the European method, considerable uncertainty results when converting cone data to undrained shear strength, S_u, and then, in using S_u to estimate the pile toe capacity. S_u is not a unique parameter and depends significantly on the type of test used, strain rate, and the orientation of the failure plane. Furthermore, drained soil characteristics govern long-term pile capacity also in cohesive soils. The use of undrained strength characteristics for long-term capacity is therefore not justified. Moreover, applying S_u for determining pile capacity cannot be considered as a direct CPT method.

13. In the French method, the extent of the zone above and below the pile toe in which the cone resistance is averaged, appears to be too limited. As considered in the Schmertmann method, particularly if the soil strength decreases below the pile toe, the soil average must include the conditions over a depth larger than 1.5b distance below the pile toe.

14. The French method makes no use of sleeve friction in determining unit shaft resistance, which disregards an important aspect of the CPT results and soil characterization.

CHAPTER 6

DATABASE AND CASE RECORDS

6.1 Introduction

An extensive search of published and unpublished literature was conducted to collect axially loaded piles and CPT soundings, resulted in a large number of cases. A database was established from case histories comprising CPT data, soil characteristics, and results of full-scale pile loading tests. The cases were obtained from all over the world.

Many of the cases involved limitations, such as CPT results by mechanical cone which cannot produce as accurate measurements as those achievable by the piezocone, manually smoothed and filtered cone data, incomplete results of pile loading tests, etc. Therefore, selection criteria are necessary to establish a database of case histories pile tests and CPT soundings performed close to the pile locations.

6.2 Selection Criteria

The following selection criteria were applied to the case histories:

- CPT soundings must be performed close to the pile locations, and preferably be using the piezocone, CPTu
- CPT data must be available along the pile and at least four pile diameters beneath the pile toe

- CPT data must be measured in short distance, e.g., within 300 mm depth intervals, preferably every 25 mm
- Sites must include sediments of clay, silt, and sand soil layers
- Pile loading tests must be reached failure
- Pile shafts must have constant cross sectional area
- Piles must be subjected to the axial loads

A large number of case records were reviewed. Many were found not useful because important information was missing. The effort resulted in total of 142 pile case histories from 53 sites and 37 sources. The cases were titled according to location or the name of main authors or sponsoring universities. The following were the main references of the compiled database: Nottingham (1975), Tumay and Fakhroo (1981), O'Neill (1986), Briaud and Tucker (1988), Tucker and Briaud (1988), Campanella et al. (1989), Alsamman (1995), and Almeida et al. (1996). A summary of the case information is presented in Table 6.1, and includes source, location, shape, material, geometry, and pile capacity, available CPT data, type of cone used, and soil profiles.

According to extent of how the criteria are satisfied, the collected cases are categorized in three types; I, II, III, indicating a decreasing degree of satisfaction all of selection criteria.

Type I; 56 cases, which consist of CPT data mostly from electrical cones measured within 300 mm (1 ft) depth intervals. A few cases do not include pore pressure measurements. All pile loading tests indicate a well-defined failure load.

Type II; 46 cases for which some of the CPT information is lacking. However, all cases involve cone resistance measurements at 300 mm (1 ft) depth interval. The failure load in the static loading tests is not always clearly found, which had necessitated a theoretical procedure to obtain the failure load. Some cases did not include a load-movement diagram and for these reasons have been considered as Type II. For these, the failure load given in the source was accepted.

Type III; 40 cases include CPT data of cone resistance and sleeve friction from mechanical cones within depth intervals ranging from 500 mm through 1000 mm. For most of these cases, the CPT data have been filtered and averaged over several measurements. The pile loading tests indicate a well-defined failure load.

6.3 Case Records

The detailed information of the case histories is presented in the Appendix A. Each case information involves two separate sheets; Sheet a and Sheet b. Sheet a presents the CPT profiles which include cone point resistance, q_c, sleeve friction, f_s, measured pore pressure behind cone point, u_2, equilibrium pore pressure, u_0, and friction ratio, R_f. A summary of soil stratigraphy is also shown graphically as determined by the boring, sampling, laboratory testing results, and CPT soil interpretation. Sheet b presents the pile characteristics including pile shape and material, pile geometry, installation method, types of pile loading test, loading procedure, closed or open toe, as well as measured pile toe, shaft, and total capacities. A longitudinal cross section of pile with a schematic soil profile along and beneath the pile is also presented. Moreover, a load-movement diagram is provided indicating the Offset Limit Load and 80 %- Criterion (CFEM, 1992) as well as the range of interpreted pile capacity.

6.4 Case Details

6.4.1 Location

The compiled database includes 53 sites which are from sites obtained from all over the world. Seventy percent of the cases are from USA, sixteen percent are from Europe, and remaining fourteen percent are from different parts of the world. The countries with at least three cases are: USA, UK, Canada, Japan, Taiwan, Norway, Australia, Italy, Belgium, and Brazil. Table 6.2 summarizes the case histories location characteristics including country, site, and number of cases.

6.4.2 Pile characteristics

The 142 steel and concrete piles collected for the database, range in diameter from 200 mm through 915 mm and range in embedment length from 5m through 67 m. Fig. 6.1 shows the frequency distribution of piles in terms of magnitude of pile diameters. As indicated in the Fig. 6.1, about 80 % of piles have a diameter within the range 200 mm to 500 mm, and the more dominant diameter lies between 300 mm to 400 mm. Fig. 6.2 presents the frequency distribution of piles in terms of magnitude of embedment length. As indicated in Fig. 6.2, about 80 % of the piles have the embedment length ranging from 5 m through 20 m, with the dominant embedment length ranging between 10 m through 15 m.

Different pile shapes are collected for this database. Fig. 6.3 presents the frequency distribution of pile shapes. Ninety eight percent of cases are pipe, square, round, and H sections. The majority shapes of pile are round and square. Ninety percent of pile case histories are driven piles.

6.4.3 Pile loading tests

Axial compression and tension tests were performed on almost all of the piles in the database. About 80 % of the tests are compression tests and the rest are tension tests. The piles were loaded incremently either in slow-maintained loads or quick-maintained load procedures. Since the cone test is a high strain test and the CPT data are used for pile capacity estimation, plunging failure was taken as the capacity of the piles. However, the Davisson (1972) Offset Limit Load is indicated for reference. Also, the Brinch Hansen (1963) 80 %- Criterion is accepted as failure load for the cases that the failure load is not clearly defined. Because, normally, the 80 %-Criterion agrees well with the intuitively perceived plunging failure of the pile (Fellenius, 1995).

Fig. 6.4 presents the frequency distribution of piles in terms of magnitude of measured capacity. As indicated in Fig. 6.4, about 75 % of piles have a capacity smaller than 2,000 KN, where the more dominant capacity ranges from 1,000 KN through 1,500 KN.

For 40 % of the cases, the pile shaft and toe capacities in the static loading test were determined separately, because the tests were performed either on instrumented piles or by tension tests.

6.4.4 Soil information

The main sources for soil interpretation were the boring, sampling, laboratory testing results, and/or in-situ testing results particularly the CPT. The major soil layers for the cases along and beneath the pile are listed in Table 6.1, and also illustrated graphically in Sheet a and Sheet b.

The case histories involve sites with soils varying from soft sensitive clay to gravelly dense sand. About 40 % of the sites comprise layered soil of clay, silt, and sand, while 32 % consist of clay soils and 32% consist of silt and sand soils.

6.4.5 Cone penetration tests

The measured cone data represent total stress. For a study based on effective stress, it is necessary to measure the pore pressure. The detailed soil profiles must be based on CPT measurements at short spacing, i.e., 25 mm, standard measurement spacing for piezocone. Both of these two main objectives can be achieved by piezocone but not by mechanical cone. In spite of this, in case of well-documented case histories, and/or for comparison to the similar work done by others, a number of mechanical cone data have been included in the database.

About 60 % of data are from electrical cones and the rest are from mechanical cones. The cases can be categorized based on the CPT measurements as follows:

68 % including q_c, and f_s

20 % including q_c, f_s, and u

12 % including q_c and u

8 % including only q_c

But for the A&M cases, Cases #103 to #142, almost all of the cases include CPT data measured at a spacing within 300 mm (1 ft). Also, the spacing for all of the CPTu data was smaller than 50 mm.

6.4.6 Back-calculated β and N_t coefficients

Table 6.3 presents the back-calculated β and N_t coefficients according to Eqs. 2.8 and 2.9 for 45 pile case histories in the database including separate measurements of the toe and shaft resistances from compression or tension tests. The β and N_t coefficients lie within the range as indicated in Table 2.2, and the ratio of β to N_t shows close agreement with the values recommended in the literature.

6.3 Concluding Remarks

A database consisting of 142 case histories was compiled as reference to the current CPT direct methods for pile capacity estimation and to develop an improved CPT direct method. The case histories contain results of full-scale pile loading tests, soil characteristics, and CPT soundings which were performed close to the pile locations. The cases were obtained from 37 sources reporting data from 53 sites in 13 countries. The general information of the cases is presented in Table 6.1. The detailed information is presented in Appendix A. Table 6.4 summarizes the general case information including piles, soil profile, and CPT soundings.

The majority of the case records are from the USA. The majority of piles have the shapes of pipe, square, round, and H-section. The pile materials are steel and concrete (no wood pile). The pile loading tests are mainly axially compression tests and ninety percent of the piles were installed by driving. The more dominant pile diameters lie within the range of 200 mm through 400 mm and the more dominant range of pile embedment lengths lie within the range of 5 m through 25 m. Most of the piles have the capacity smaller than 2,000 KN. The soils at sites mainly consist of sediments of clay, silt, and sand. The CPT data were measured by the electrical cone are more than those by mechanical cone. About one third of the cases include the pore pressure measurements. Most of the CPT data are from spacings smaller than 300 mm.

CHAPTER 7

THE PROPOSED DIRECT CPTu METHOD FOR DETERMINING PILE TOE AND SHAFT CAPACITIES

7.1 General

A direct CPTu method (developed in this dissertation) is proposed for determining the capacity of an axially loaded pile. The method employs the CPTu data combining the cone point resistance, q_c, the sleeve friction, and the measured pore pressure, u_2. The sleeve friction, f_s, which is an imprecise measurement, is limited to use in combination with the effective cone resistance, q_E (cone point resistance adjusted to effective stress by deducting the measured pore pressure) to interpret the soil according to a classification chart, also developed as a step in this dissertation. Both the pile unit toe and shaft resistances are functions of the CPTu cone resistance.

For the unit toe resistance, the method equates the unit toe resistance to the effective cone resistance taken as the geometric average in the considered failure zone around the pile toe. Also the unit shaft resistance is proportional (correlated) to the effective cone resistance. The correlation coefficient is determined from the interpreted soil type according to the new soil classification chart which has been developed based on all of the CPTu data available in the database. The correlation coefficient considers the effects of resistance degradation and sensitivity, as well as whether the soil is dilating or contracting.

A. PILE UNIT TOE RESISTANCE

7.2 Cone Resistance Average

It is important to note that the variation of soil characteristics must be taken into account by averaging over a sufficient distance above and below the pile toe. The variation of soil characteristics is reflected in the variation of the cone resistance. For most natural soil deposits, a range of cone resistance exists from soft or loose layers into hard or dense layers and vice versa. In particular, natural sand deposits produce q_c profiles with many sharp peaks and troughs.

Along a specific well-defined rupture surface, when the unit force exerted by the pile toe approaches the ultimate unit toe resistance, no single friction angle and/or single fraction of mobilized q_c-value applies to the whole rupture surface. Points at the rupture surface, located at different depths, may have different friction angle and/or mobilized q_c-value due to the soil variation and confining stress. To obtain cone data for pile design especially for unit toe resistance, a representative cone resistance value (friction angle in an indirect method) must be sought. It is important to note that the larger the pile diameter, the greater the extent of rupture surface below and above the pile toe. Therefore, a procedure must be established to find the representative q_c-value to relate to the unit toe resistance of a pile, and the value must be a function of the pile diameter.

To determine the pile unit toe resistance, all current direct CPT methods apply a correlation factor to the cone resistance after filtering the q_c-values, "purging" the peak and trough values from the data. The mean of the resulting smoothened curve, the q_c-average, is then determined over a certain zone, which differs in extent for the methods used in current practice. The correlation factor to apply to the q_c-average differs between the methods.

Filtering the cone data is necessary, because were a true mean produced from the data, the high and low values would have a disproportionate influence on the average. The filtering approach was developed when the CPT data were obtained in hard-copy diagrams only and it brings about a considerable judgment leeway in finding the average cone resistance. However, the subjective filtering is now not necessary, because current tests produce digitized results in the form of tables of data, easily accessible for determining the average by direct computer manipulation, making working with hard-copy diagrams redundant.

Two types of averaging the cone resistance can be considered: arithmetic average and geometric average. The arithmetic average is defined as:

$$q_{ca} = \frac{q_{c1} + q_{c2} + \ldots + q_{cn}}{n} \tag{7.1}$$

where

q_{ca} = arithmetic average of values which range from q_{c1} through q_{cn}

n = number of considered values

Having the CPT data in the computer, the average q_c according to Eq. 7.1 can be obtained automatically. However, without first excluding peaks and troughs, this average is only useful in very homogenous soils where the values are uniform.

In contrast, the natural variability of many sand deposits produces q_c profiles with many sharp peaks and troughs. Filtering is therefore necessary in most cases and, if done manually, it offsets the advantage of the computer. A filter effect can be achieved directly, however, by instead calculating the geometric average of the q_c-values, which is defined as:

$$q_{cg} = \sqrt[n]{q_{c1} \cdot q_{c2} \cdot \ldots \cdot q_{cn}} \qquad (7.2)$$

where

q_{cg} = geometric average of values which range from q_{c1} to q_{cn}

The bias in the arithmetic mean arises from the influence of the absolute magnitude instead of ratios of variations (Kennedy and Neville., 1986). For example, the arithmetic average of the numbers 0.5 and 2.0 is 1.25, and the geometric average is 1.00. If the numbers are 0.33 and 3.00 instead, the arithmetic average becomes 1.65 while the geometric average is still 1.00. For a set of data made up of the numbers 0.33, 0.50, 2.00, and 3.00, the arithmetic and geometric averages are 1.46 and 1.00, respectively.

Assume that a set of values is as follows: 5, 5, 2, 5, 25, 5, 6, 1, 6, 6, 30, and 6, where the dominant values lie between 5 and 6. The arithmetic and geometric averages are 8.50 and 5.71, respectively. The result shows that the geometric average is closer to the dominant values, as opposed to the arithmetic average which is not representative for the dominant range. Thus, by taking the geometric average of q_c-values in a zone at the vicinity of pile toe, a filtered representative value is obtained that is unaffected by operator's judgment and, therefore, repeatable.

As an example of pile case history (Case # 11, POLA2, pile toe located in sand), is given in Fig. 7.1. The arithmetic q_c-average by the Schmertmann and the European methods (applying minimum path rule) is 15.0 MPa, the average by the French method (eliminating peaks and troughs) is 24.7 MPa, and by the Meyerhof method is 17.5 MPa. The geometric q_c-average (over a zone which extends 4b below to 8b above pile toe) is 11.5 MPa. These values and the specified zones recommended by methods for taking the average are indicated in Fig. 7.1. It is important to note that all methods relate the obtained arithmetic average of q_c to the unit toe resistance of pile by using correlation factors.

7.3 Failure (Influence) Zone

To estimate the unit toe resistance of a pile (large-scale), from the average cone point resistance (a small-scale model pile) to it is necessary to identify the failure zone around the pile toe. That is, the problem is to define the extent of the influence zone for averaging the cone resistance. However, no specific evidence exists to support whether the failure is local punching or general shear failure.

Experimental studies by Meyerhof (1956; 1976) indicate that a penetration distance into a soil layer of about 10 times of pile diameter is required to fully mobilize the ultimate unit toe resistance of a bearing layer. A similar depth was found by de Beer (1963) to be needed for developing resistance for penetrometers in sand. Experimental and numerical work by Altaee et al. (1992) on two concrete piles in medium dense sand show that the zone influencing the toe resistance extends from 5b below to 5b above the pile toe.

Ghionna et al. (1993) show that both displacement and non-displacement piles reach a value of ultimate unit penetration resistance that is approximately equal to the cone point unit resistance value. A small difference was found to be due to the slight difference in apex angles between the soil cone that forms beneath a pile and apex angle of the cone penetrometer. However, the ultimate resistance is reached for non-displacement piles at a higher ratio of penetrating than for displacement piles.

According to Salgado (1995), performing tests on dry sand in calibration chambers, the penetration resistance for a penetrometer with a certain apex angle, is independent of the penetrometer diameter. They also found that the difference between the penetration resistance for a flat-ended and for the standard cone penetrometer (with the apex angle of 60^0) is about 15 % for dense sands at moderately low confining stress, and is much smaller for loose sands under high confining stress.

In homogeneous soil, a logarithmic spiral can be assumed to define the failure zone, see Fig. 7.2. The failure pattern is general shear failure type, in which the rupture surfaces reach to the body of pile or penetrometer, similar those proposed by Meyerhof (1951), and de Beer (1963).

As illustrated in Fig. 7.2, for the rupture surface, the radius of logarithmic spiral is determined as follows:

$$r = r_0 \, e^{\theta \tan(\phi)} \tag{7.3}$$

where

r = radius of logarithmic spiral

θ = angle between the radius at each point and r_0, as shown in the Fig. 7.2

ϕ = angle between the radius at each point and normal at that point to the logarithmic spiral curve (assumed equal to the friction angle of the soil)

r_0 = radius of logarithmic spiral for $\theta = 0$ (assumed equal to penetrometer diameter)

For finding the height of the failure zone above the pile toe, the θ is substituted by 180^0 ($\theta = \pi$) in Eq. 7.3 as follows:

$$r_c = b \, e^{\pi \tan(\phi)} \tag{7.4}$$

The value of r_c, in units of penetrometer diameter, can be realized as a criterion to evaluate the depth of penetration of pile to fully mobilize the ultimate toe resistance of the bearing layer.

The deepest point of the rupture surface below the pile toe, is determined by maximizing the projection of the radius of the logarithmic spiral on the vertical-axis as follows:

$$y = r\cos(\theta) = be^{\theta\tan(\phi)}\cos(\theta) \tag{7.5}$$

$$\frac{dy}{d\theta} = 0 \Rightarrow \theta = \phi \tag{7.6}$$

Fig. 7.3 presents different rupture surfaces which obtained from Eq. 7.3, by substituting ϕ angles from 25^0 to 40^0. However, in practice, piles are installed into the soil strata in which the ϕ angles usually range from 25^0 through 35^0. In these types of soils, the failure zone includes a height above pile toe ranging from 4b through 9b, depth below pile toe ranging from 1.1b through 1.5b, and a horizontal extent ranging from 2b through 5b, see Fig. 7.3. For example, for $\phi = 30^0$ and $\theta = 180^0$, the value of r_e is about 6b and the total height of the rupture surface is about 7.5b.

The cone resistance needs to be averaged to a representative value within the failure (influence) zone, and the logarithmic spiral is but one way to determine the zone. However, as mentioned, such rupture surfaces apply only to homogeneous soil and the height of the zone is not critical for averaging cone resistance. To illustrate, the variation of the geometric average can be studied as a function of the extent of the failure zone above and below the pile toe. For the CPT result shown in Fig. 7.4, different zones for averaging cone resistance are considered. Fig. 7.4a presents CPT data from homogeneous soil and Fig. 7.4b shows the records for a two-layered soil with a distinct increase of cone resistance in the lower layer (non-homogeneous soil). A 350 mm diameter pile (10 times the standard cone diameter) is assumed to have been installed a small distance into the lower layer, and is used to illustrate the geometric average of q_c-values in different height failure zones. For homogeneous soil, the geometric q_c-values are insensitive to the height of the zone, see Fig. 7.4a. In contrast, for a pile in non-homogeneous soil when the pile toe is located in the vicinity of the boundary between two layers, significant difference exists between the geometric averages of cone resistance determined in zones of different heights.

With regard to non-homogeneous soil, Fig.7.5 presents CPT profile for a layer with high cone resistance sandwiched between two layers with low cone resistance. A pile of 350 mm diameter is again used to illustrate the effect of three different heights of failure zone on the q_c-average values. The three heights are 4b below to 2b above pile toe, 4b below to 4b above pile toe, and 4b below to 8b above the pile toe. Fig. 7.5 illustrates the results of the q_c-average values which can be considered as pile unit toe resistance. The q_c profile and average q_c distribution, shown in Fig. 7.5, indicate the average q_c value is sensitive to the variation in a non-homogeneous soil.

As a result, in homogeneous soil, the extent of the influence zone for determining the average cone resistance to apply to pile unit toe resistance is not critical. In case of non-homogeneous soil, detailed theoretical analysis does not apply. To calculate the cone resistance average, the distances to be 4b below to 8b above pile toe which is used by current practice, when a pile is installed through a weak soil into a dense soil. When a pile is installed through a dense soil into a weak soil, decreasing the upper limit height from 8b to 2b appears appropriate.

The extent of 4b for influence zone below pile toe is due to fact that the dominant extension of rupture surface below pile toe is horizontal in contrast to the above pile toe which it is vertical. Although, in theory the expansion of a rupture surface in a homogeneous soil below pile toe does not exceed about 1.5b (see Fig. 7.3), it is necessary to take into account the cone resistance in a zone somewhat deeper than 1.5b for two main reasons. First, because of the horizontal extension of the rupture surface which ranges from 2b through 5b, the failure path is longer than 1.5b. Second, to include the effect of weakening of the soil due to tension developing in the boundary to the weak soil—punching effect.

7.4 Effective Cone Resistance

Effective stress governs pile capacity not total stress. Therefore, the effective cone resistance values must be used in determining pile capacity. However, the measured total cone resistance includes the pore water pressure which is mobilized during cone penetration. Subsequently, the corrected cone point resistance, q_t, which is still a total stress value, and it must be reduced to the effective stress value by subtracting the pore pressure. As discussed in Chapter 3, the most useful and reliable pore pressure measurement is from a piezometer located immediately behind the cone, the u_2 measurement. Hence, for this dissertation, the u_2 pore pressure measurement is used for determining the effective cone resistance, q_E.

The pore pressure effect is negligible in pervious soils such as sands, where the excess pore pressures are small and dissipate quickly. However, in clays and silts, the excess pore pressure can be significant.

A method for determining pile capacity in particularly silts and clays, therefore, necessitates the CPTu sounding. In sand, the pore pressures can be assumed to be essentially unchanged during the cone penetration or pile driving. Therefore, CPT data from older types of CPT equipment not recording the pore pressure, are still useful for design of piles in sand soils.

7.5 Determining Pile Unit Toe Resistance, Conclusions

The proposed direct CPTu method applies the geometric average of all effective cone resistance values in the vicinity of the pile toe—zone of influence. In homogeneous soil, the exact height of the influence zone in not important, however, as a criterion in this dissertation it is proposed to use 4b below to 4b above pile toe. In non-homogeneous soil, when the pile toe is located in dense soil with a weak layer above, the influence zone extends 4b below to 8b above pile toe, similar the zone used by some of the current methods. Also, in non-homogeneous soil, when the pile toe is located in weak soil with a dense layer above, in this dissertation it is suggested, the influence zone extends 4b below to 2b above pile toe. Rather than obtaining the unit pile toe resistance as an arbitrary percentage of the average total cone resistance, the proposed method determines the toe resistance as the geometric average of the effective cone resistance. The unit toe resistance of a pile is determined as follows:

$$r_t = C_t \sqrt[n]{q_{E1} \cdot q_{E2} \cdot \ldots \cdot q_{En}} \tag{7.7a}$$

$$r_t = C_t q_{Eg} \tag{7.7b}$$

where

q_E = q_t - u, effective cone resistance

q_{Eg} = geometric average of effective cone resistance values over the influence zone

C_t = toe correlation coefficient

u = pore pressure, usually u_2

n = number of values in the considered zone

B. Pile Unit Shaft Resistance

7.6 Background

Many different aspects affect the use of CPT data to determine pile unit shaft resistance. In soft clay, large excess pore pressures are generated in the vicinity of the cone which do not exist in long-term condition for the pile. In sensitive clay, remolding due to the cone penetration causes significant temporary loss of strength. In stiff clay, the pile installation may cause a gap between the soil and the pile. In fissured clay, because of the relatively small size of the cone penetrometer in comparison to a pile, it is likely that the effects of the fissures will be different for the CPT and the pile. In silty sand, pore pressure induced by the cone shear makes weak soils appear weaker (contractancy effect) and strong soils appear stronger (dilatancy effect) than for the fully drained conditions. Moreover, soil density may be different in coarse-grained soils before and after pile driving due to compaction effects.

Recent studies have shown that the measurement of sleeve friction is often less accurate and reliable than measurement of cone resistance (Lunne et al, 1986; Robertson and Campanella, 1989). Cones of different designs will often produce different sleeve friction. This is due to small variations in mechanical and electrical design features as well as small variations in tolerances. For these reasons, to determine unit shaft resistance of pile, r_s, from CPTu, it is better to combine the sleeve friction with the cone resistance and measured pore pressure to classify the soil, and use this classification to determine a correlation coefficient to be applied to the effective cone resistance, as follows:

$$r_s = C_s q_E \tag{7.8}$$

where

C_s = shaft resistance correlation coefficient, depending on soil type

7.7 Interpreting Soil Profile from CPTu Data

One primary purpose of the CPT is stratigraphic profiling and soil classification. Begemann (1965b) pioneered soil classification based on mechanical cone data and pointed out that the soil type in terms of the grain size can be related to the CPT friction ratio (ratio of sleeve friction to cone resistance). Begemann introduced a soil classification chart (an example is shown in Fig. 3.6), using cone resistance and sleeve friction from the mechanical cone.

Of particular importance, later measurements with the piezocone showed that the cone resistance is affected by the pore pressure generated at the cone shoulder. The advent of the piezocone enabled soil classification that includes cone resistance, sleeve friction, and pore pressure measurements.

Robertson et al. (1986), Campanella and Robertson (1988), and Robertson (1990) proposed soil classification charts based on piezocone data, as shown in Figs. 3.7 and 3.8. That is, the charts plot a y-variable versus its own inverse value. In principle, this does not normally produce good representation of data. Furthermore, the classification charts require manipulation that is not easy to perform. Therefore, it was found necessary to develop a new classification method that is easily and directly "checkable" by hand with the computer serving as a tool for speeding up the process.

This dissertation prefers to plot of data with strict separation of the variables. The preferred plot of cone data is similar to that used by Begemann (1965b), with the difference that the effective cone resistance ($q_E = q_t - u_2$) is used instead of the cone resistance, q_c. Figs. 7.6 through 7.8 show the data base records plotted in a Begemann type diagram— the effective cone resistance, q_E, versus sleeve friction. A representative number of cone values have been selected from each soil layer from about 20 sites included with the database. The figures indicate the three main soil categories: clay (soft clay, stiff clay, silty clay, sandy clay), silt (clayey silt, sandy silt), and sand (clayey sand, silty sand, gravelly sand). The number of data points exceeds 1,000 for each category. Fig. 7.9 combines the data points from all soil categories.

A detailed study of the plot made it possible to separate out five main soil categories: very soft sensitive soil, soft clay, silty clay and stiff clay, silty sand, and sand and gravel. Boundaries were obtained by enveloping about 90 % of all points of each main soil type, as indicated in Fig. 7.10.

For comparison, all data points are also plotted in the diagram format of Robertson et al. (1986) as illustrated in Figs. 7.11 through 7.14. The comparison shows a good agreement between the soil types of the database and the soil interpretation obtained by means of the Robertson classification chart (Figs. 3.7 and 7.14). However, the delineation—separation of the soil types—is much simpler and also more distinct in the Begemann type chart, Figs 7.9 and 7.10. The chart presented in Fig. 7.10 has the advantage that it does not require manipulation of the data before making an interpretation. Moreover, plotting of the data to the latter chart is also much faster than the plotting of the data in the modified two complementary charts proposed by Robertson (1990).

CHAPTER 8

CALIBRATION OF THE PROPOSED METHOD

8.1 Introduction

The proposed method relates both the pile unit toe resistance and the unit shaft resistance to the effective cone point resistance, q_E. The hypotheses, to be explored in this chapter, are that both toe and shaft resistances are proportional to the effective cone resistance and can be determined by assigning a correlation factor to q_E. The same correlation factor will apply to any particular soil type classified by the CPTu data as developed in Chapter 7. Several pile case histories have been compiled including static loading tests performed in uplift, or in push with separation of shaft and toe resistances at sites which comprise CPT soundings. These case histories are used to calibrate the two formulae for estimation of pile toe and shaft resistances from CPTu data.

8.2 Calibrations of the Proposed Method

As explained in the Chapter 7, the pile unit toe and shaft resistances can be determined from the effective cone resistance, q_E, as follows:

$$r_t = C_t \, q_{E_g} \qquad (7.7)$$

$$r_s = C_s \, q_E \qquad (7.8)$$

For the purpose of determining the two correlation coefficients, C_t and C_s, the instrumented pile case histories are implemented from the database. A total of 24 cases contained with the database includes separation of the capacity on toe and shaft resistances. Of these, 14 cases are compression tests with separating measured pile toe and shaft capacities, and 10 cases are tension (uplift) tests. The cases are from sites with soft clay, mixture of clay and silt, mixture of silt and sand, and sand. The embedment lengths for the pile case histories range from 7 m through 34 m and the pile diameters range from 200 mm through 625 mm. The pile capacities range from 80 KN through 5,700 KN. The pile toe capacities range from 9 KN through 4,050 KN and the pile shaft capacities range from 74 KN through 2,730 KN.

8.2.1 Calibration of the toe correlation coefficient, C_t

Table 8.1 presents the measured unit toe resistance, r_t, and geometric average of effective cone resistance, q_E, at the vicinity of pile toe for 14 pile case histories. Also, Table 8.1 shows the ratio of r_t and q_E. The results for this ratio indicate that the r_t values are very close to the q_E values, that is, for 14 pile case histories the average of the ratio of r_t and q_E is 0.98 with the standard deviation of 0.09. As a result, the ratio of r_t and q_E, that is, the toe correlation coefficient, C_t, can be taken as equal to unity.

Results reported in the literature confirm this finding. According to the studies by de Beer (1963), Kerisel (1964), Vesic (1964), Ghionna et al. (1993), and Salgado (1995), there is a one-to-one relationship between the cone resistance and pile unit toe resistance. The explained theoretical approach in Chapter 7 confirms the foregoing finding. Although to reach to ultimate point resistance, the embedment depth in the bearing layer is a function of the penetrometer diameter. That is, the larger the diameter, the deeper to reach the ultimate point resistance which is approximately equal to the cone point resistance.

Therefore, with the toe correlation coefficient, C_t, equal to unity, the Eq. 7.7 becomes:

$$r_t = q_{Eg} \tag{8.1}$$

The effective cone resistance in sensitive or soft clays could obviously be very small resulting in an uncertain value of pile toe resistance. However, for pile in cohesive soils, the major source of the pile capacity is the shaft resistance not the toe resistance. Therefore, the likely underestimation does not result in a significant error.

8.2.2 Calibration of the shaft correlation coefficient, C_s

Table 8.2 presents the results of measured pile unit shaft resistance, r_s, for 13 compression and 10 tension tests. Table 8.2 also presents the average of effective cone resistance, q_E, for these 23 cases for different soil layers along piles, and the ratio of pile unit shaft resistance, r_s, and the average of effective cone resistance, q_E. The results of comparison of measured pile unit shaft resistance and average effective resistance indicate the following ranges for the shaft correlation coefficient, C_s for the different soil types.

Soil Type	C_s Range
Soft sensitive soils	7.37 % through 8.64 %
Clay	4.62 % through 5.56 %
Stiff clay, and mixture of clay and silt	2.06 % through 2.80 %
Mixture of silt and sand	0.87 % through 1.34 %
Sand	0.34 % through 0.60 %

The foregoing five main soil categories were obtained from the proposed soil interpretation procedure explained in the Chapter 7, and shown in Fig. 7.10.

The principle of effective stress was used in determining the correlation coefficient between pile unit shaft resistance and effective cone resistance. As mentioned in Chapter 2, the effective stress analysis of pile unit toe and shaft resistances is as follows:

$$r_s = \beta \sigma'_z \tag{2.9}$$

$$r_t = N_t \sigma'_{z=D} \tag{2.8}$$

Dividing the first parts of Eqs. 2.8 and 2.9 for conditions at the pile toe, results in:

$$\frac{r_s}{r_t} = \frac{\beta \sigma'_z}{N_t \sigma'_z} = \frac{\beta}{N_t} \tag{8.2}$$

The following equations were proposed to determine the pile unit shaft and toe resistances using the CPTu:

$$r_s = C_s q_E \tag{7.7}$$

$$r_t = C_t q_E \tag{7.8}$$

Dividing the first parts of Eqs. 7.7 and 7.8, and combining with Eq. 8.1 in which C_t equals to unity, results in:

$$\frac{r_s}{r_t} = \frac{C_s q_E}{C_t q_E} = \frac{C_s}{C_t} = C_s \tag{8.3}$$

Since the first parts of Eqs. 8.2 and 8.3 are identical, the following equation is obtained.

$$\frac{\beta}{N_t} = C_s \tag{8.4}$$

Therefore, the ratio of β to N_t coefficients, can be used to find out the approximation correlation between pile unit shaft resistance and effective cone resistance. The ratio of β to N_t coefficients proposed by Fellenius (1986; 1995) ranges from 1.2 % through 8 % in clays, 1.2 % through 1.4 % in silts, and 0.4 % through 1 % in sands, which values lie within the ranges of C_s shown in the table given above.

Table 8.3 shows the average values of C_s resulting from the calibration of C_s to the case histories and these values are proposed for determining pile resistance using CPTu data.

8.3 Implementation of the Proposed Method

The estimated pile capacities from the proposed method are compared to the measured pile capacities in compression or tension tests. Fig. 8.1 shows the estimated against measured pile toe capacity for 14 cases. Fig. 8.2 shows the estimated against measured pile shaft capacity for pile shaft capacity of 13 cases, and 10 tension tests. Fig. 8.3 shows the estimated against measured pile capacity for 24 cases. The comparison of estimated pile capacity from the proposed method and measured pile toe, shaft, and total capacity indicate close agreement and good consistency.

To quantify the accuracy of the proposed method, the relative error is determined for the estimated pile capacities. The relative error is the difference between the estimated and measured values divided by the measured values. A negative value indicates an underestimation of the pile capacity.

Table 8.4 presents the estimated pile capacity by the proposed method and also the measured pile toe, shaft, and total capacities for the 24 cases. Table 8.5 presents the relative error in pile capacity estimation by the proposed method for 24 cases. The results indicate that, the mean of relative errors is 3 % with standard deviation of 12 %, for pile toe capacity estimation of 14 cases. And, the mean of relative errors is -1 % with standard deviation of 11 %, for pile shaft capacity estimation of 23 cases. The results for pile total capacity give the mean of relative errors is -1 % with standard deviation of 9 %, for 24 cases. Fig. 8.4 illustrates the frequency distribution of relative errors for the 24 cases. The results indicate that the high frequency of relative error lies between -10 % to 10 % for the proposed method.

8.4 Concluding Remarks

A direct CPTu method has been proposed for determining pile capacity. For pile unit toe resistance, a simple mathematical rule is used to relate the effective cone resistance to the pile unit toe resistance in a one-to-one relationship. The geometric average of effective cone resistance is determined as the unit toe resistance of the pile in an influence zone depending on the soil layering situations in the vicinity of pile toe. The influence zone extends 4b below to 8b above pile toe when a pile is installed through a weak soil into a dense soil, 4b below to 2b above pile toe when a pile is installed through a dense soil into a weak soil, and 4b below to 4b above pile toe for homogeneous soil.

For pile unit shaft resistance, a routine soil interpreting procedure is introduced based on CPTu data. The pile unit shaft resistance is determined from effective cone resistance by using a correlation coefficient that depends on the soil type interpreted from the CPTu data based on the soil classification chart developed in this dissertation.

The proposed direct CPTu method for determining pile toe and shaft resistances has been calibrated on twenty-four piles of different size and lengths installed in different type of soils. The proposed method is simple, easy to apply, and independent of operator influence in filtering and choosing correlation factors. The proposed method shows a good agreement with the measured values, and more important, the agreement is consistent for all the 24 cases.

The following summarizes the step by step procedure of the proposed method for pile capacity estimation using the CPTu data.

1. Determining the influence zone in the vicinity of pile toe. The influence zone extends 4b below to 8b above pile toe when a pile is installed through a weak soil into a dense soil, 4b below to 2b above pile toe when a pile is installed through a dense soil into a weak soil, and 4b below to 4b above pile toe for homogeneous soil.

2. Calculating the effective cone resistance, q_E, which is the subtraction of the measured total corrected cone resistance, q_t, and the measured pore pressure behind the cone point, u_2.

3. Determining the pile unit toe resistance, which is the geometric average of effective cone resistance in the influence zone.

4. Interpreting the soil profile based on CPTu data, including the cone resistance, sleeve friction, and measured pore pressure, according to the developed soil classification chart as shown in Fig. 3.10.

5. Determining the pile unit shaft resistance as a function of effective cone resistance by using a correlation coefficient as proposed in Table 8.3.

CHAPTER 9

VALIDATION OF THE PROPOSED METHOD

9.1 General

As presented in the Chapter 6, a database has been established including 142 pile case histories and CPT soundings to validate the proposed method. In addition to the proposed method, five CPT direct methods currently employed in North American practice are applied to the cases in the database to reference the proposed method.

The five CPT direct methods which were investigated in Chapter 5 in details are: the Schmertmann method, the European Method, the French method, the Meyerhof method, and the Tumay method. The first three methods can be used for piles installed in cohesive and noncohesive soils. The Meyerhof method is recommended for use in noncohesive soils and the Tumay method is recommended for use in cohesive soils. These two cases were extended to use in case of mixed soils. That is, for noncohesive soils including sublayers of cohesive soils, the Meyerhof method was applied, whereas for cohesive soils including sublayers of noncohesive soils, the Tumay method was applied.

Explained in Chapter 7, for pile shaft resistance calculation by the proposed method the soil interpretation is required. The proposed soil interpretation in this dissertation is a function of CPTu data, that is, cone resistance, sleeve friction, and pore pressure. However, some cases in the database do not include the CPTu data such as sleeve friction and the pore pressure, and/or the data were obtained from the mechanical cone. For these cases the pile shaft resistance was calculated based on soil classification provided by laboratory and/or other in-situ testing.

Computer programs were coded in QUICK BASIC to determine the pile capacity using the new proposed method as well as for interpreting the soil profile, based on the CPTu data. The current CPT methods for pile capacity estimation are relatively difficult and time-consuming to implement without the aid of a computer. This is particularly true when the CPT data are measured in very close spacing, that is, 25 mm. Therefore, computer programs were developed for each method. The input information for pile capacity calculation includes CPTu or CPT data provided in the spreadsheet as an ASCII file, pile characteristics, extent of influence zone, and few other parameters specified from different methods. The output information includes the detailed calculation of the pile toe and shaft resistances, interpreted soil type based on CPTu data, and pile toe and shaft capacities.

9.2 Divisions of Case Records for Comparison of the Methods

The results of estimated pile capacity by different CPT direct methods are discussed in two divisions:

First, the discussions are based on the results of estimated pile capacity for 24 selected pile case histories including 14 compression and 10 tension tests, which used for calibrating the proposed method. The comparison of the predictive methods is mainly based on estimated pile toe, and shaft capacities.

Subsequently, the discussions are based on the results of calculated pile capacities for all of 142 cases compiled in the database. The validation of the predictive methods is mainly based on estimated total pile capacity. As mentioned in Chapter 6, in accordance with the selection criteria for the case records, 142 pile case histories were categorized in three types: Type I, Type II, and Type III. The quality of the data was good not only for CPT but also for pile loading tests for 56 cases in Type I, and most of the CPT data are from electrical cones. In order to validate the predictive methods without any bias based on total capacity, the 10 tension cases used for the calibration of the proposed method were excluded from the Type I cases. Therefore, the rest of Type I cases, that is, 46 cases, are considered for comparison. The 46 cases categorized in Type II may lack certain CPTu measurements, such as sleeve friction and pore pressure. For half of the cases, the piles did not fail during the pile loading tests. The quality of data particularly for CPT data for 40 cases classified as Type III, was not good (filtered and smoothed in 1 m depth interval). All of CPT data for Type III cases was from a mechanical cone, which does not provide data as accurate as provided by piezocones.

Tables 9.1 through 9.4 summarizes results of estimated pile capacity from six CPT direct methods and the measured (test) pile capacity for all 24 cases used for the calibration of the proposed method as well as for all cases as categorized in Type I, Type II, and Type III.

9.3 Presentation and Evaluation of the Results

The results of the pile capacity calculation are presented graphically and numerically. The graphical approach presents the plot of the estimated against measured pile capacity. The numerical approach employs a statistical procedure to quantify the comparisons.

Figs. 9.1 through 9.12 illustrate the comparison of estimated and measured pile capacity for all of the case records in a linear plot. Since the capacities in the database range from about 100 KN through 8,000 KN, a "break-out" plot is used to show the results of capacities smaller than 2, 000 KN. For reference, a solid diagonal line is presented in each diagrams indicating a perfect agreement between calculated and measured pile capacity. A deviation of ± 20 % is illustrated by the dashed lines.

The statistical approach for validation of the predictive methods used in this dissertation, is based on relative difference between the estimated and measured pile capacity. The two basic statistical parameters are used for quantification of estimation error, the mean and the standard deviation.

The variable "x" is determined as the difference between the estimated and measured pile capacities divided by the measured pile capacity " relative error" or "relative difference" as follows:

$$x = \frac{R_e - R_m}{R_m} \tag{9.1}$$

where

x = relative error

R_e = estimated pile capacity

R_m = measured pile capacity

Negative values of relative error, x, indicate that the method underestimated the measured pile capacity.

The mean of the relative errors is determined by:

$$\bar{x} = \frac{1}{n}\sum_{i=1}^{n} x_i \tag{9.2}$$

where

$\bar{x}$ = mean of relative error

x_i = relative error for case i

n = number of variables

The standard deviation for relative errors is determined:

$$SD = \sqrt{\frac{1}{n-1}\sum_{i=1}^{n}(x_i - \bar{x})^2} \tag{9.3}$$

where

SD = standard deviation of the average relative error

The mean of relative error $\bar{x}$, represents the accuracy of the estimated pile capacity, that is, the mean can be realized as an indication of bias, and shows how well the measured capacity is estimated on the average. The standard deviation, SD, represents the precision of the estimated values in comparison to the measured values, that is, the scatter around the mean.

A strict average of relative errors in pile capacity estimation does not provide meaningful results. In contrast, the absolute average of errors is more representative. Therefore, in addition to the mean and related standard deviation, the absolute average of errors and the related standard deviation are calculated to refer better the accuracy and precision of the methods in pile capacity estimation.

Table 9.5 summarizes the mean and standard deviation for average and absolute error for case records compiled in the database, including the 24 cases used for the calibration of the proposed method and Types I, II, and III. Figs. 9.12 through 9.18 illustrate the graphical presentation of relative error in pile capacity estimation for Type I and Type II cases, for six predictive methods.

9.4 Comparison, Discussion, and Validation

A. Relative Difference Approach

9.4.1 Twenty-four cases used for the calibration

A total of 24 cases contained with the database includes separation of the capacity on toe and shaft resistances which used for the calibration of the proposed method. Of these, 14 cases are compression tests with separating measured pile toe and shaft capacities, and 10 uplift (tension) tests. The cases are from sites with soft clay, mixture of clay and silt, mixture of silt and sand, and sand.

The embedment lengths for the case histories range from 7 m through 34 m and the diameters range from 200 mm through 625 mm. The pile capacities range from 80 KN through 5,700 KN. The pile toe capacities range from 9 KN through 4,050 KN and the pile shaft capacities range from 74 KN through 2,730 KN. Figs. 9.1 through 9.6 presents the comparison of estimated and measured pile toe, shaft, and total capacities for each method.

For the pile toe capacity, all methods underestimate the pile toe resistance, with the exception of the Meyerhof method. The Schmertmann, European, and the Tumay methods follow the same procedure for determining pile unit toe resistance. The underestimation for these methods is due to smoothing the cone resistance data based on a minimum path rule, and imposing upper limit of 15 MPa to the pile unit toe resistance. The high underestimation by the European method (-23 % error) can be attributed to the fact that the method applies the undrained shear strength, S_u, obtained from cone resistance. The method uses a reduction factor for overconsolidated soils which causes further underestimation of the pile capacity.

The French method is highly biased toward the underestimation (-33 % error). This is because the influence zone recommended by this method for cone resistance averaging is too limited (1.5 b below and above pile toe) which cannot fully include the variation of soil affecting the pile unit toe resistance. Besides, applying correlation factors about 50 % to the average cone resistance to use as pile unit toe resistance is an additional source of the underestimation.

The Meyerhof method shows slight overestimation (13 % error). This is because no filtering of cone data is proposed by this method.

For the pile shaft resistance (13 cases with measured shaft resistance and 10 tension tests), all methods biased highly underestimation. The underestimation for the Schmertmann method (-34 % error) can be attributed to the following effects. First, the method was developed based on the mechanical cone data which provided sleeve friction values higher than those provided by the piezocone, but most of the CPT data for these 24 cases are from piezocone. Second, the significant difference exists between the coefficients recommended for pile shaft capacity calculation in case of concrete piles and steel piles (up to 100 %). Third, using the broad reduction factor of 30 % for the capacity of tension piles in compare to the shaft capacity of compression piles. In addition, imposing an upper limit of 120 KPa is another source of the underestimation.

For the European method with -31 % error, the sources of the underestimation of pile capacity are: use the reduction factor of 33 % for tension piles in contrast to compression piles, the method is based on mechanical cone data, and the imposing 120 KPa upper limits. Besides, the recommendation of using the smallest of the two values: 0.3 % of cone resistance or sleeve friction, as pile unit shaft resistance in sand, could be the source of error. Moreover, the use of the undrained shear strength involves uncertainties for pile shaft resistance calculation in clay.

For the French method, the underestimation (-17 % error) is because the method differentiates between concrete and steel piles for shaft capacity estimation up to an in amount of 100 %. Moreover, the upper limits imposed for pile unit shaft resistances which ranging from 35 KPa through 120 KPa which can cause significant underestimation pile capacity. The excluded sleeve friction, f_s, can be another source of error in pile capacity estimation by this method.

The Meyerhof method highly underestimates the pile shaft capacity (-29 % error). Because the method was developed based on mechanical cone data, which produce higher sleeve friction values than the electrical cone. Besides, the recommendation of using the smallest of the two values: 0.5 % of cone point resistance or sleeve friction, as pile unit shaft resistance in sand, appears low for different noncohesive soils. The recommendation for using the half of the foregoing values for pile unit shaft resistance in case of bored piles can cause underestimation for pile capacity.

The Tumay method applied only for five cases and shows a slight underestimation. The method considers only the sleeve friction, f_s, for pile shaft resistance. However, the sleeve friction is not a precise measurement.

For the total capacity of 24 cases, the Schmertmann, the European, and the Tumay method show high absolute error of about 30 % and the standard deviation of 15 %, while the French method gives the absolute error of 23 % with the standard deviation of 13 % and the Meyerhof method gives the absolute error of 19 % with the standard deviation of 12 %. In contrast of the other methods, the proposed method shows the absolute error of 7 % and the standard deviation of 6 %.

9.4.2 Type I cases

Fifty-six pile case histories are categorized in Type I, including good quality of data mostly from electrical cone, and well-defined failure load for piles. The cases are from sites with clay, silt, mixture of clay and silt, mixture of silt and sand, and sand. The embedment lengths for the steel and concrete piles with different shapes range from 7 m through 67 m and the diameters range from 200 mm through 915 mm. The pile capacities range from 80 KN through 7,500 KN. Figs. 9.7 through 9.12 present a comparison of measured and estimated pile capacities by different methods. Figs. 9.13 through 9.18 illustrates the relative error in pile capacity estimation by different methods.

All methods underestimate pile capacity between about 20 %. The absolute error is about 30 % for all methods with the standard deviation is about 20 %. The main reasons for the high prediction error by the five predictive methods can be attributed to the factors which were discussed for the 24 cases used for the calibration, and the important is that the methods were developed based on mechanical cone data, whereas most of the cases in Type I are from an electrical cone. In contrast to the five current methods, the performance of the proposed method is very good and demonstrates a very slight overestimation of 2 %. As shown in Fig. 9.18, the high frequency of the relative error in pile capacity estimation lies between -10 % to +10 %. The absolute error for the proposed method is 11 % with the standard deviation of 8%. The proposed method not only shows good agreement with measured pile capacity but also it includes consistent agreement for all of 46 cases.

9.4.3 Type II cases

Forty-six pile case histories are categorized in Type II, which do not include some of CPT data such as f_s and u_2, and also the well-defined failure load for piles. Among 46 cases, plunging failure was reached only for 5 cases. For 16 cases, load-movement diagram was not available. The 46 cases are from sites with soft clay, mixture of clay-silt-sand, and sand. The embedment lengths for the steel and concrete piles with different shapes range from 8 m through 43 m and the diameters range from 200 mm through 810 mm. The pile capacities range from 80 KN through 8,000 KN. Figs. 9.7 through 9.12 presents the comparison of measured and estimated pile capacities by different methods. Figs. 9.13 through 9.18 illustrates relative error in pile capacity estimation by current methods.

As presented in Table 9.5, all current methods with the exceptions of the Tumay method, underestimate the pile capacities. The absolute error for the Schmertmann, French, and Meyerhof methods is about 30 % with the standard deviation ranging from 20 % through 30 %. The absolute error for the European is less than the abovementioned methods, which is about 23 % with the standard deviation of 16 %. The Tumay method is applied to only for 5 cases with absolute error of 17 % and the standard deviation of 10 %.

The proposed method biased toward an overestimation (11 % error). However, the errors are less than those for the Schmertmann, French, and Meyerhof method, and close to that of European and Tumay methods. The absolute error is 19 % with the standard deviation of 14 %. Of 46 cases in Type II, 25 cases include load-movement diagrams in which the failure load did not reach after pile loading tests. That is, the failure must be higher than the maximum load which was reported at the end of pile loading test procedure. Table 9.6 summarizes the foregoing 25 cases including the relative error in pile capacity estimation by the proposed method. It is interesting to note that, the proposed method overestimates the pile capacity (27 % on average) for 23 cases out of 25 cases. As a result, the slight overestimation is reasonable and it can be concluded that the calculated pile capacity by the proposed method is consistent to the failure load of piles for which the plunging occurs. The results of pile capacity estimation by the proposed method for Type I cases confirm this, because the failure load for Type I cases was well-defined.

As presented in Table 9.5, the relative errors are also calculated for 67 cases in Type I and Type II (46 cases from Type I and 21 cases from Type II), which failed during the pile loading tests. The results of comparison indicate 29 % average absolute error with standard deviation of 21 % for current methods. In contrast, the proposed method includes the average absolute error of 11 % with standard deviation of 8 %.

9.4.4 Type III cases

Forty pile case histories are categorized in Type III, in which all data are from a mechanical cone. The cases are from sites with clay, and sand. The embedment lengths of the steel and concrete piles with different shapes range from 5.5 m through 21 m, and the pile diameters range from 250 mm through 450 mm. The pile capacities range from 470 KN through 1,780 KN. Figs. 9.7 through 9.12 presents the comparison of measured and estimated pile capacities by different methods.

All methods including the proposed method involve relatively high errors in pile capacity estimation. For the current methods the absolute error is about 38 % with the standard deviation of 26 %. However, for the proposed method the absolute error is about 24 % with the standard deviation of 15 %, indicating better performance of the proposed method than the current methods.

For two main reasons, the slight overestimation of the proposed method can be explained. First, all of the data for Type III cases are from a mechanical cone which does not produce as accurate data as the electrical cone, and the proposed method was developed based on the piezocone data. Second, usually the mechanical cone measurements are obtained in 200 mm spacing, however, the CPT data in Type III presented in 1000 mm spacing, resulting the smoothed or even damaged data. This type of data significantly affects and biases the estimated pile capacity by the proposed method which developed based on very close CPT measurement within 25 mm to 50 mm spacings.

B. Probability Approach

Long and Shimel (1989) and Alsamman (1995) suggest that a comparison will provide more insight when the values are plotted versus a cumulative average, called "cumulative probability". For the current set of data, the ratio of calculated to tested pile capacities, R_c / R_m, is arranged in ascending order (numbered 1, 2, 3, . . i, . . .n) and a cumulative probability, P, is determined for each capacity value, as:

$$P = \frac{i}{(n+1)} \tag{9.4}$$

where

P = cumulative probability

i = the number of the value considered in P

n = total numbers of values

According to Long and Shimel (1989) and Alsamman (1995), to assess the bias and dispersion associated with a particular predictive method the following is useful:

i. The value of R_c / R_m at P = 50 % probability is measure of the tendency to overestimate or underestimate the pile capacity. The closer to a ratio of unity, the better the agreement.

ii. Log-normally distributed data will plot on a straight line.

iii. The slope of the line through the data points is a measure of the dispersion or standard deviation. The flatter the line, the better general agreement.

Fig. 9.19 shows the plot of R_c / R_m values versus cumulative probability for Type I and Type II cases (the 24 cases used for calibration were excluded). For the probability of 50 %, the R_c / R_m value for the CPTu method is close to unity whereas the ratios for the current methods are in the range of 70 % through 80 %, demonstrating a trend toward underestimation. The CPT methods exhibit a higher dispersion than the CPTu method as indicated by the flatter slope of the line through the CPTu data. It is obvious that the results for the CPTu method are closer to log-normal distribution than the CPT methods.

9.5 Concluding Comments

The proposed method and five current CPT direct methods with method have been tested to 142 pile case histories including CPT soundings were performed close to the pile locations, as compiled in the database. The errors for pile capacity estimation of 142 cases in the database are relatively high for the five current methods in compare to the errors for the proposed method.

For the Schmertmann method, the following factors can cause error: smoothing the cone resistance data based on minimum path rule for pile unit toe resistance, relatively low reduction factors for tension and steel piles in contrast to compression and concrete piles respectively, imposing an upper limit of 15 MPa to the pile unit toe resistance, and imposing an upper limit of 120 KPa to the pile unit shaft resistance.

For the European method, the following factors can cause error: smoothing the cone resistance data based on minimum path rule for pile unit toe resistance, relatively low reduction factors for tension piles in contrast to compression piles, imposing an upper limit of 15 MPa to the pile unit toe resistance, imposing an upper limit of 120 KPa to the pile unit shaft resistance, applying reduction factor for pile unit toe resistance in overconsolidated soils, using relatively low values for pile unit shaft resistance, particularly for piezocone data, and converting cone data to the undrained shear strength, S_u, which is used for pile capacity estimation in cohesive soils.

For the French method, the following factors can cause error: smoothing the cone resistance data for pile unit toe resistance, employing a too limited influence zone (1.5b at the vicinity of pile toe) for averaging cone resistance around pile toe, relatively low reduction factors for steel piles in contrast to concrete piles, imposing an upper limit to the pile unit toe resistance, imposing upper limit ranging from 35 KPa through 120 KPa to the pile unit shaft resistance, applying reduction factors to the cone resistance average to obtain pile unit toe resistance which is about 50 %, and excluding sleeve friction in pile unit shaft resistance calculation.

For the Meyerhof method, the following factors can cause error: no filtering of the cone resistance data for pile unit toe resistance calculation, relatively low reduction factors for bored piles in contrast to driven piles, using relatively low values for unit shaft resistance, particularly for piezocone data.

For the Tumay method, the following factors can cause error: smoothing the cone resistance data based on minimum path rule for pile unit toe resistance, imposing an upper limit of 15 MPa to the pile unit toe resistance, imposing an upper limit of 60 KPa to the pile unit shaft resistance, considering only the sleeve friction in pile unit shaft resistance calculation.

The following shows the average of absolute error and standard deviation for five methods as well as for the proposed method in different categories of cases:

Category	Five current methods		Proposed method	
	Error, %	*standard deviation*	*Error, %*	*standard deviation*
Type I, 46 cases	28	21	11	8
Type II, 46 cases	25	17	19	14
Type III, 40 cases	31	23	17	14
Types I and II, 67 cases (failed cases)	29	21	11	8

Comparison indicates that, in contrast to the current methods, the proposed method shows the better agreement and consistency to the measured pile capacity for all the different categories of case records. The results of comparison based on probability approach demonstrate better agreement of the estimated pile capacity using the proposed method to the measured pile capacity than those of the current methods.

The proposed direct CPTu method for determining pile capacity has been validated on 142 piles of different size and lengths installed in different type of soils and compared to the results of five current methods. The proposed method is based on simple mathematical rule for filtering the CPT data, relies on more accurate CPTu data for soil interpretation, and employs the effective stress approach. The proposed method is independent of the operator subjective influence in filtering data and in choosing correlation factors, which are affecting all the current methods. The result of comparison is favorable to the proposed method.

CHAPTER 10

SUMMARY OF RESULTS AND CONCLUSIONS

10.1 Results

Many ideas, suggestions, results, and conclusions appeared, or were implied throughout the thesis. They can be summarized as follows.

1. A direct CPTu method has been proposed for determining the capacity of an axially loaded pile. The method employs the CPTu data combining the cone point resistance, q_c, the sleeve friction, f_s, and the pore pressure, u_2. The sleeve friction, f_s, which is an imprecise measurement, is limited to use in combination with the effective cone resistance, q_E (cone point resistance adjusted to effective stress by the deducting the measured pore pressure) to interpret the soil according to a classification chart. Both the pile unit toe and shaft resistances are functions of the CPTu cone resistance.

2. Filtering the cone data is necessary, because were a true mean produced from the data, the high and low values would have a disproportionate influence on the average. The filtering approach was developed when the CPT data were obtained in hard-copy diagrams only and it brings about a considerable judgment leeway in finding the average cone resistance. However, the subjective filtering is now not necessary, because current tests produce quantified results in the form of tables of data, easily accessible for determining the average by direct computer manipulation, making working with hard-copy diagrams redundant.

3. Having the CPT data in the computer, the arithmetic average of q_c, can be obtained automatically. However, without first excluding peaks and troughs, this average is only useful in very homogenous soils where the values are uniform. In contrast, the natural variability of many sand deposits produces q_c profiles with many sharp peaks and troughs. Filtering is therefore necessary in most cases and, if done manually, it offsets the advantage of the computer. A filter effect can be achieved directly, however, by instead calculating the geometric average of the q_c-values.

4. A procedure must be established to find the representative q_c-value to relate to the unit toe resistance of a pile, and the value must be a function of the pile diameter. That is, the problem is to define the extent of an influence zone for averaging the cone resistance. However, no specific evidence exists to support whether the failure is local punching or general shear failure. The logarithmic spiral is but one way to determine the zone and such rupture surfaces apply only to homogeneous soil and the height of the zone is not critical for averaging cone resistance. In contrast, for a pile in non-homogeneous soil when the pile toe is located in the vicinity of the boundary between two layers, significant difference exists between the geometric averages of cone resistance determined in zones of different heights. As a consequence, in homogeneous soil, the influence zone length to use for determining the pile unit toe resistance is not critical. In case of non-homogeneous soil, detailed theoretical analysis does not apply. To calculate the cone resistance average, the distances are from 4b below to 8b above pile toe which is used by current practice, when a pile is installed through a weak soil into a dense soil. When a pile is installed through a dense soil into a weak soil, decreasing the upper limit height from 8b to 2b appears appropriate.

5. The β and N_t coefficients, which are effective stress parameters for determining pile capacity, were back-calculated for 45 pile case histories in which the pile toe and shaft resistances had been measured separately. A comparison indicates that the β and N_t coefficients lie within the

range as indicated in Table 2.2, and the ratio of β to N_t shows close agreement with the values recommended in the literature. The average back-calculated β-coefficient is lowest in clay and largest in sand with the values in silt in between. However, the ranges are wide and overlapping. The ranges can of course be narrowed in a specific case with more soil information (from sampling and laboratory testing) coupled with local experience. The cone penetrometer, the piezocone in particular, would be quite useful in this process. However, as demonstrated in this study, using the piezocone cone directly and the CPTu method to determine the pile capacity is a more reliable approach than using generally referenced β and N_t coefficients. However, the effective stress analysis using β and N_t coefficients will never be disastrously off. Furthermore, it is not in conflict with the use of the cone penetrometer methods nor with any other method. In fact, it is good practice, whatever the method used to estimate the capacity of a pile, always to check the results by comparing them to the results of an effective stress analysis.

6. Effective stress governs pile capacity not total stress. Therefore, the effective cone resistance values must be used in determining pile capacity. However, the major part of total cone resistance includes the pore water pressure which is mobilized during cone penetration. Subsequently, the measured cone point resistance, q_t, which is a total stress value, must be reduced to the effective stress value by subtracting the pore pressure. The most useful and reliable pore pressure measurement is from a piezometer located immediately behind the cone, the u_2 measurement. Hence, for this dissertation, this measured pore pressure is used for determining the effective cone resistance, q_E. The pore pressure effect is negligible in pervious soils such as sands, where the excess pore pressures are small and dissipate quickly. However, in clays and silts, the excess pore pressure can be significant. A method for determining pile capacity in particularly silts and clays, therefore, necessitates the CPTu sounding. In sand, the pore pressures can be assumed to be essentially unchanged during the cone penetration or pile driving. Therefore, CPT data from older types of CPT equipment not recording the pore pressure, are still useful for design of piles in sand soils.

7. One primary purpose of the CPT is stratigraphic profiling and soil classification. The soil classification proposed by Robertson et al. (1986), Campanella and Robertson (1988), and Robertson (1990), apply a y-variable plotted versus its own inverse value. This approach does not normally constitute a good representation of data. Furthermore, the classification charts require manipulation that is not easy to perform. Therefore, it was found necessary to develop a new classification method that is easily and directly "checkable" by hand with the computer serving as a tool for speeding up the process. A plot of CPTu data was developed with strict separation of the variables, similar to that used by Begemann (1965b), effective cone resistance ($q_E = q_t - u_2$) versus sleeve friction. A representative number of cone values have been selected from each soil layer from about 20 sites included with the database. A detailed study of the plots made it possible to separate out five main soil categories: very soft sensitive soil, soft clay, silty clay and stiff clay, silty sand, and sand and gravel. Boundaries were obtained by enveloping about 90 % of all points of each main soil type.

8. For comparison, all data points were also plotted in the diagram format which used by Robertson et al. (1986) and Campanella and Robertson (1988). The comparison shows a good agreement between the soil types of the database and the soil interpretation obtained by means of the Robertson and Campanella classification chart. However, the delineation—separation of the soil types—is not as simple and it is less distinct. Moreover, the developed soil classification chart has the advantage that it does not require manipulation of the data before making an interpretation. Moreover, plotting of the data to the latter chart is also much faster than the plotting of the data as per the charts proposed by Robertson (1990).

9. Since the proposed method relates both the pile unit toe resistance and the unit shaft resistance to the effective cone point resistance, q_E, the hypothesis was explored that both toe and shaft resistances are proportional to the effective cone resistance and can be determined by assigning a correlation factor to q_E. The same correlation factor will apply to any particular soil type

classified by the CPTu data as developed in this dissertation. Twenty-four special pile case histories were selected from 142 pile case histories to calibrate the two formulae for estimation of pile toe and shaft resistances from CPTu data. The 24 cases included static loading tests performed in uplift, or in push with separation of shaft and toe resistances at sites which comprise CPT soundings. The calibration indicated that there is a one-to-one relationship between the pile unit toe resistance and the geometric average of effective cone resistance, q_{Eg}. That is, the toe correlation coefficient is equal to unity. Also, it was shown that, the shaft correlation coefficient depends on interpreted soil type according to the new soil classification chart which has been developed based on all of the CPTu data available in the database.

10. According to the statistical analysis, the following shows the average absolute error and standard deviation for five methods as well as for the proposed method in different categories of cases:

Category	**Five current methods**		**Proposed method**	
	Error, %	*standard deviation*	*Error, %*	*standard deviation*
Type I, 46 cases	28	21	11	8.0
Type II, 46 cases	25	17	19	14
Type III, 40 cases	31	23	24	18
Types I and II, 67 cases (failed cases)	29	21	11	8.0

The results of comparison based on probability approach demonstrate lower dispersion and better agreement and consistency of the estimated pile capacity using the proposed method to the measured pile capacity than those estimated by the current methods.

11. It was verified that the main factors that cause significant error in pile capacity estimation by the current methods are: smoothing the CPT data, development based on mechanical cone data, employing undrained shear strength, S_u, imposing an upper limit to the pile unit toe and shaft resistances, not including all CPT measurement, considerable difference between the correlation factors for steel and concrete piles, considerable difference between the correlation factors for tension and compression piles, disregard of factors such as soil sensitivity, dilatancy effects, effective stress.

12. The proposed direct CPTu method for determining pile capacity has been tested on 142 piles of different size and lengths installed in different type of soils and compared to the results of five current methods. The results of comparison are favorable to the proposed method, demonstrating a remarkably higher accuracy and lower scatter for the proposed method than the current methods. The proposed method is simple, easy to apply, independent of the operator subjective influence which affects the other current methods. Therefore, it is suitable to apply in engineering practice.

13. The procedure developed during this study for determining pile capacity from CPTu data can be summarized as follows:

    i. Determining the influence zone in the vicinity of pile toe. The influence zone extends 4b below to 8b above pile toe when a pile is installed through a weak soil into a dense soil, 4b below to 2b above pile toe when a pile is installed through a dense soil into a weak soil. The length of the influence zone is not critical for a homogeneous soil.

    ii. Calculating the effective cone resistance, q_E, which is the subtraction of the measured total corrected cone resistance, q_t, and the measured pore pressure behind the cone point, u_2.

iii. Taking as the pile unit toe resistance, the value equals to the smallest of the two geometric averages of effective cone resistance in the influence zone.

iv. Interpreting the soil profile based on CPTu data, including the cone resistance, sleeve friction, and measured pore pressure, according to the developed soil classification chart as shown in Fig. 3.10.

v. Determining the pile unit shaft resistance as a function of point-by-point effective cone resistance by using a correlation coefficient as proposed in Table 8.3.

10.2 Conclusions

Significant contributions of this research are:

1. A procedure has been developed for determining pile unit toe resistance from effective cone resistance. The procedure for filtering the CPT data includes a simple mathematical rule for filtering and averaging the cone resistance.

2. Evidence has been produced for that the influence zone for cone resistance average which is a function of soil conditions in the vicinity of pile toe.

3. A new and simple soil classification was produced in a chart. The classification considers all of the CPTu data.

4. The pile unit shaft resistance has been shown to be a function of effective cone resistance, q_E, and the soil type as classified based on CPTu data.

5. The correlation between toe and shaft resistances determined from the CPTu data has been developed in a proposed method that is simple, easy to apply, independent of the operator subjective influence, and suitable to apply in engineering practice.

6. A database of 142 pile case histories has been compiled that contains pile loading tests and CPT soundings performed close to the pile locations. The compiled database is available in this dissertation.

7. Computer programs have been developed that calculate the capacity of pile and interpret soil profiles from CPTu data for the proposed method and also for five CPT direct methods currently used in North American practice.

8. The various methods for determining pile capacity from CPT data are compiled for comparison of accuracy relevance and scatter.

9. It has been verified that the pile capacity determined by the proposed method is consistent with the measured plunging failure load of the piles.

10. The evidence has been provided indicating that the piezocone data are more useful than the mechanical cone data for pile capacity estimation.

10.3 Limitations

The proposed CPTu method is particularly suitable in non-cohesive soils. However, in dense soils, because of limiting capacity of the cone penetrometer, piles are often taken deeper than the cone penetrometer. Site investigations to be used in pile design often require cone penetrometers with 500-KN capacity. In cohesive soils, the pore pressure measurements become crucial and although the u_2 measurement has shown to provide reasonable correlations in this study, this may not be the governing measurement of pore water pressure particularly for overconsolidated clays. The effect of the uncertainty is to a large extent included in the calibration and validation of the CPTu method. However, the number of cases used are limited and, doubtlessly, further correlation experience will result in adjustment of the coefficients, in particular, the shaft coefficient.

Furthermore, the cone test is a short-term test and pile capacity is a long-term condition. Short-term versus long-term behavior involves soil set-up (capacity gain with time) phenomena, amongst others. For driven piles, further research should correlate measurements from dynamic testing of piles with CPTu data. It is conceivable that such studies will produce insights also in dynamic parameters to use when analyzing drivability of piles from CPTu measurements.

10.4 Recommendation for Further Research

Further research is suggested as follows:

1. Expand the database with more CPTu data including pile case histories for verification of the proposed effective stress approach for pile capacity estimation, particularly for soft sensitive soils.

2. The current CPTu equipment provides the sleeve friction, f_s, data which is not as precise as the other CPTu data. The continued development of the CPTu equipment is necessary to lead increased accuracy and reliability of f_s data, useful for pile unit shaft capacity calculation and soil interpretation.

3. Development a systematic procedure to assess the penetrability and driveability of piles from cone resistance profiles.

4. The CPT sounding has the potential to produce information such as damping and pile shaft resistance distribution to use in determining pile capacity in a dynamic analysis.

5. The CPTu excess pore pressure dissipation tests data can be used to analysis the time required for dissipation of excess pore pressures around the driven piles.

6. Comparison of the CPT data after and before pile driving for evaluating the effective stress changes due to pile driving, to improve the pile design procedure.

REFERENCES

AL-AWKATI, Z., 1975. On problems of soil bearing capacity at depth. Ph. D. Thesis, Duke University, Durham, 203 p.

ALBIERO, J. H., SACILOTTO, A. C., MANTILLA, J. N., TELXEIRA, J., and CARVALHO, D., 1995. Successive load tests on bored piles. Proceedings of 10th Pan-American Conference on Soil Mechanics and Foundation Engineering, Vol. 2, Mexico City, October 29 - November 3, pp. 992 - 1002.

ALMEIDA, M. S. S., DANZIGER, F. A. B., and LUNNE, T., 1996. Use of the piezocone test to predict the axial capacity of driven and jacked piles in clay. Canadian Geotechnical Journal, Vol. 33, No. 1, pp. 23 - 41.

ALSAMMAN, O. M, 1995. The use of CPT for calculating axial capacity of drilled shafts. Ph. D. Thesis, University of Illinois at Urbana, Champaign, 300 p.

ALTAEE, A., FELLENIUS, B. H., and EVGIN, E., 1992. Axial load transfer for piles in sand. 1- Tests on an instrumented precast pile; and Axial load transfer for piles in sand. 2- Numerical analysis. Canadian Geotechnical Journal, Vol. 29, No. 1, pp. 11 - 20, and Vol. 29, No. 1, pp. 21 - 30.

ALTAEE, A., FELLENIUS, B. H., and EVGIN, E., 1993. Load transfer for piles in sand and the critical depth. Canadian Geotechnical Journal, Vol. 30, pp 455 - 463.

ALTAEE, A., FELLENIUS, B. H., 1994. Physical modeling in sand. Canadian Geotechnical Journal, Vol. 31, No. 3, pp. 420-431.

AMERICAN PETROLEUM INSTITUTE, API, 1984. Recommended Practice for Planning, Designing, and Constructing Fixed Offshore Platforms, 15th Edition, Washington.

AMERICAN PETROLEUM INSTITUTE, API, 1990. Recommended Practice for Planning, Designing, and Constructing Fixed Offshore Platforms, 19th Edition, Washington.

APPENDINO, M.,1981. Interpretation of axial load tests on long piles. Proceedings of the 10th International Conference on Soil Mechanics and Foundation Engineering, Stockholm, June 15 - 19, Vol. 2, pp. 593 - 598.

AVASARALA, S. K. V., DAVIDSON, J. L., and MCVAY, A. M., 1994. An evaluation of predicted ultimate capacity of single piles from SPILE and UNIPILE programs. Proceedings of the FHWA International Conference on Design and Construction of Deep Foundations, Orlando, December 7 - 9, Vol.2, pp. 712 - 723.

BALDI, G., BELLOTTI, R., GHIONNA, V., JAMIOLKOWSKI, M., and PASQUALINI, E., 1982. Design parameters for sands from CPT. Proceedings of the 2nd European Symposium on Penetration Testing, ESOPT-2, Amsterdam, Vol.2, pp. 425-436.

BALIGH, M. M., 1975. Theory of deep site static cone penetration resistance. Report No. R.75-76, Massachusetts Institute of Technology, Cambridge, Massachusetts.

BALIGH, M. M., 1976. Cavity expansion in sands with curved envelope. American Society of Civil Engineers, ASCE, Journal of Geotechnical Engineering, Vol. 102, GT11, pp. 1131-1146.

BALIGH, M. M., VIVATRAT, V., and LADD, C. C., 1980. Cone penetration in soil profiling. ASCE, Journal of Geotechnical Engineering, Vol. 106, GT4, pp.447-461.

BALIGH, M. M., AZZOUZ, A. S., WISSA, A. Z. E., MARTIN, R. T., and MORRISON, M. J., 1981. The piezocone penetrometer. Symposium on Cone Penetration Testing and Experience, ASCE, Geotechnical Engineering Division, St. Louis, pp. 247-263.

BARENTSEN, P., 1936. Short description of a field testing method with a cone shaped sounding apparatus. Proceedings of 1st International Conference on Soil Mechanics and Foundation Engineering, ICSMFE, Boston, Vol. 2, 10.

BEEN, K., and JEFFERIES, M. G., 1985. A state parameter for sands. Geotechnique, Vol. 35, No.2, pp. 99-110.

BEEN, K., CROOKS, J. H. A., BECKER, D. E., and JEFFERIES, G., 1986. The cone penetration test in sand: part I, state parameter interpretation. Geotechnique, Vol. 36, No.2, pp.239-249.

BEEN, K., JEFFERIES, M. G., CROOKS, J. H. A., and ROTHENBURG, D., 1987. The cone penetration test in sand: part II, general inference of state. Geotechnique, Vol. 37, No.3, pp. 285-299.

BEGEMANN, H. K., 1953. Improved method of determining resistance to adhesion by sounding through a loose sleeve placed behind the cone. Proceedings of 3rd International Conference on Soil Mechanics and Foundation Engineering, ICSMFE, Zurich, Vol. 1, pp. 213-217.

BEGEMANN, H. K. S., 1963. The use of the static penetrometer in Holland. New Zealand Engineering, Vol. 18, No. 2, p. 41 (as referenced by Nottingham, 1975).

BEGEMANN, H. K. S., 1965a. The maximum pulling force on a single tension pile calculated on the basis of results of adhesion jacket cone. Proceedings of 6th International Conference on Soil Mechanics and Foundation Engineering, ICSMFE, Montreal, Vol. 2 pp. 229-232.

BEGEMANN, H. K. S., 1965b. The friction jacket cone as an aid in determining the soil profile. Proceedings of 6th International Conference on Soil Mechanics and Foundation Engineering, ICSMFE, Montreal, September 8 - 15, pp. 17-20.

BELLOTTI, R., BIZZI, G. And GHIONNA, V. 1982. Design, construction and use of a calibration chamber. Proceedings of the 2nd European Symposium on Penetration Testing, ESOPT-2, Amsterdam, Vol.2, pp. 439-446.

BEREZANTZEW, V. G., 1961. Load bearing capacity and deformation of pile foundations. Proceedings of 5th ICSMFE, Paris, Vol.2, pp. 11-15.

BJERRUM, L., JOHANNESSON, I. J., EIDE, O., 1969. Reduction of skin friction on steel piles to rock. Proceedings of 7th ICSMFE, Vol. 2, pp. 27-34.

BOZOZUK, M., 1972. Downdrag measurements on a 160 ft floating pipe test pile in marine clay. Canadian Geotechnical Journal, Vol. 9, No. 2, pp. 127-136.

BRIAUD, J. L., and TUCKER, L. M., 1988. Measured and predicted axial capacity of 98 piles. American Society of Civil Engineers, ASCE, Journal of Geotechnical Engineering, Vol. 114, No. 9, pp. 984-1001.

BRINCH HANSEN, J., 1963. Discussion on hyperbolic stress-strain response, cohesive soils. American Society of Civil Engineers, ASCE, Journal of Soil Mechanics and Foundation Engineering, Vol. 89, SM4, pp. 241-242.

BROMS, B. B., 1988. History of soil penetration testing. Proceedings of the 1st International Symposium on Penetration Testing, ISOPT-1, Disney world, Vol.1, pp 157-220.

BURLAND, J. B., 1973. Shaft friction of piles in clay—a simple fundamental approach. Ground Engineering, Vol. 6, No. 3, pp. 30-42.

BUSTAMANTE, M. and GIANEESELLI, L., 1982. Pile bearing capacity predictions by means of static penetrometer CPT. Proceedings of the Second European Symposium on Penetration Testing ESOPT-2, Amsterdam, May 24 - 27, A. A. Balkema, Vol. 2, pp 493 - 500.

CAMPANELLA, R. G., GILLESPIE, D., and ROBERTSON, P. K. 1982. Pore pressures during cone penetration testing, Proceedings of the 2nd European Symposium on Penetration Testing, ESOPT-2, Amsterdam, Vol. 2, pp. 507-512.

CAMPANELLA, R. G., ROBERTSON, P. K., GILLESPIE, D, and GREIG, J, 1985. Recent developments in in-situ testing of soils. Proceedings of 11th International Conference on Soil Mechanics and Foundation Engineering, ICSMFE, San Francisco, Vol. 2, pp. 849-854.

CAMPANELLA, R. G., ROBERTSON, P. K., and GILLESPIE, D., 1986. Seismic cone penetration test. Proceedings of In-Situ 86, ASCE Specialty Conference, Blacksburg, Virginia, pp. 116-130.

CAMPANELLA, R. G., and ROBERTSON, P. K., 1988. Current status of the piezocone test. Proceedings of the 1st International Symposium on Penetration Testing, ISOPT-1, Orlando, March 22 - 24, Vol.1, pp 93-116.

CAMPANELLA, R. G., ROBERTSON, P. K., DAVIES, M. P., and SY, A., 1989. Use of in-situ tests in pile design. Proceedings of 12th International Conference on Soil Mechanics and Foundation Engineering, ICSMFE, Rio de Janeiro, Vol. 1, pp.199-203.

CAMPANELLA, R. G., and WEEMEES, I., 1990. Development and use of an electrical resistivity cone for groundwater contamination studies. Canadian Geotechnical Journal, 27, pp. 557-567.

CAMPANELLA, R. G., and KOKAN, M. J., 1993. A new approach to measuring dilatancy in saturated sands. ASTM, Geotechnical Testing Journal, Vol. 6, No. 4, pp. 485-495.

CAMPANELLA, R. G., 1993. Interpreting CPT data, CPTINT. Department of Civil Engineering, University of British Columbia, Vancouver.

CANADIAN FOUNDATION ENGINEERING MANUAL, CFEM, 1992. Third edition, Canadian Geotechnical Society, BiTech. Publishers, Vancouver, 512 p.

CASAGRANDE, A., 1936. Characteristics of cohesionless soils affecting the stability of slopes and earth fills. Journal of the Boston Society of Civil Engineers. Reprinted in Contribution to Soil Mechanics 1925-1940. Boston Society of Civil Engineers, pp. 257-276.

CASAGRANDE, A., 1975. Liquefaction and cyclic deformation of sands, a critical review, Proceedings of 5th Pan American Conference on Soil Mechanics and Foundations Engineering, Buenos Aires, Vol. 5, pp. 80-133 (as referenced by Been et al., 1986).

CASTRO, G., and POLOUS, S. J., 1977. Factors affecting liquefaction and cyclic mobility. American Society of Civil Engineers, ASCE, Journal of Geotechnical Engineering, Vol. 103, GT6, pp. 501-516.

CHAPMAN, G. A., 1974. Calibration chamber for field test equipment. Proceedings of the 1st European Symposium on Penetration Testing, ESOPT-1, Stockholm, Vol.2, pp. 59-64.

CH2M HILL, 1987. Geotechnical report on indicator pile testing and static pile testing, Berths 225 - 229 at Port of Los Angeles. CH2M Hill, Los Angeles.

DAVIES, M. P., 1987. Predicted axially and laterally loaded pile behavior using in-situ testing methods. M. A. Sc. Thesis, Department of Civil Engineering, UBC, Vancouver, 305 p.

DAVISSON, M. T., 1972. High capacity piles. Proceedings, Soil Mechanics Series on Innovation in Foundation Construction, ASCE, Illinois Section, Chicago, pp. 81-112.

DeBEER, E. E., 1963. The scale effect in the transposition of the results of deep sounding tests on the ultimate bearing capacity of piles and caisson foundations.Geotechnique Vol. 13, No. 1, pp.39-75.

DECOURT, L., and NIYAMA, S., 1994. Predicted and measured behavior of displacement piles in residual soils. Proceedings of the 13th International Conference on Soil Mechanics and Foundation Engineering, ICSMFE, New Delhi, January, pp. 477 - 486.

DENIS , N. D., and OLSEN, R. E., 1983a. Axial capacity of steel pipe piles in clay. ASCE, Geotechnical Practice in Offshore Engineering, Austin, pp. 370-387.

DENIS , N. D., and OLSEN, R. E., 1983b. Axial capacity of steel pipe piles in sand. ASCE, Geotechnical Practice in Offshore Engineering, Austin, pp. 389-402.

DeRUITER, J. and BERINGEN, F. L., 1979. Pile foundation for large North Sea structures. Marine Geotechnology, Vol. 3, No. 3 pp. 267 - 314.

DeRUITER, J., 1981. Cone penetration testing and experience. Symposium on Cone Penetration Testing and Experience, ASCE, Geotechnical Engineering Division, St. Louis, pp. 1-48.

DeRUITER, J., 1982. The static cone penetration test state-of-the-art report. Proceedings of the 2nd European Symposium on Penetration Testing, ESOPT-2, Amsterdam, Vol. 2, pp. 389-405.

DOUGLAS, B. J., and OLSEN, R. S., 1981. Soil classification using electric cone penetrometer. Symposium on Cone Penetration Testing and Experience, ASCE, Geotechnical Engineering Division, St. Louis, pp. 209-227.

DRENVICH, V. P., GORMAN, C. T., and HOPKINS, T. C., 1974. Shear strength of cohesive soils and friction sleeve resistance. Proceedings of the 1st European Symposium on Penetration Testing, ESOPT-1, Stockholm, Vol.2, pp. 129-132.

DURGUNOGLU, H. T., and MITCHELL, J. K., 1975. Static penetration of soils: 1-analysis, 2-evaluation of theory implications for practice. Proceedings of ASCE Specialty Conference on In-Situ measurement of Soil Properties, Raleigh, Vol. 1, pp. 172-189.

ESLAMI, A., and FELLENIUS, B. H., 1995. Toe bearing capacity of piles from cone penetration test (CPT) data. Proceedings of International Symposium on Cone Penetration Testing, CPT'95, Linkoping, Sweden, October 4 - 5, Swedish Geotechnical Institute, SGI, Report No. 3:95, Vol. 2, pp. 453-460.

ESLAMI, A., and FELLENIUS, B. H., 1996. Pile shaft capacity determined by piezocone (CPTu) data. Proceedings of 49th Canadian Geotecnical Conference, St. John's, Newfoundland, September 23 - 25, Vol. 2 pp. 859-867.

FELLENIUS, B. H., 1975. Test loading of piles. Methods, interpretation, and new proof testing procedure. American Society of Civil Engineers, ASCE, Journal of Geotechnical Engineering, Vol. 101, GT9, pp. 855-869.

FELLENIUS, B. H., 1983. Wave equation analysis and dynamic monitoring. Deep Foundations Journal, Springfield, Vol. 1, No. 1, pp. 49-55.

FELLENIUS, B. H., 1984. Negative skin friction and settlement of piles. Proceedings of the Second International Seminar of Pile Foundations, Nonyang Technical Institute, Singapore, 18 p.

FELLENIUS, B. H., 1986. The FHWA static testing of a single pile and a pile group—Report on the analysis of soil and installation data plus Addendum Report. The Federal Highway Administration, FHWA, Washington, Prediction Symposium, June 1986, 36 p.

FELLENIUS, B. H., 1989. Unified design of piles and pile groups. Transportation Research Board, TRB Record 1169, Washington, pp. 75-82.

FELLENIUS, B. H., 1991. Summary of pile capacity predictions and comparison with observed behavior. American Society of Civil Engineers, ASCE, Journal of Geotechnical Engineering, Vol. 117, No. 1, pp. 192 - 195.

FELLENIUS, B. H. , and ALTAEE, A. A., 1995. Critical depth: how it came into being and why it does not exist. Proceedings of the Institution of Civil Engineering, Geotechnical Engineering, April, 1995, pp. 107-111.

FELLENIUS, B. H., 1995 Foundations. Ch. 22 in Geotechnical Engineering Handbook. Edited by W. F. Chen, CRC Press New York, pp. 817 - 853.

FELLENIUS, B. H., 1996. Basics of foundation design and background to the UniSoft programs. BiTech Publishers, Vancouver, 140 p.

FINNO, R. J., 1989. Subsurface conditions and pile installation data. American Society of Civil Engineers, Proceedings of Symposium on Predicted and Observed Behavior of Piles, Evanston, June 30, ASCE Geotechnical Special Publication, GSP23, pp. 1 - 74.

FRANK, R., 1994. The new EuroCode and the new French code for the design of deep foundations. Proceedings of the FHWA International Conference on Design and Construction of Deep Foundations, Orlando, December 1994, Vol. 1, pp. 279 - 304.

GAMBINI, F., 1985. Experience in Italy with centricast concrete piles. Proceedings of the International Symposium on Penetrability and Drivability of Piles, San Francisco, Vol. 1, pp. 97-100.

GHIONNA, V. N., and JAMIOLKOWSKI, M., 1991. A critical appraisal of calibration chamber testing of sands. Proceedings of First International Symposium on Calibration Chamber testing, ISOCCT-1, Potsdam, New York, pp. 13-39.

GHIONNA, V. N., and JAMIOLKOWSKI, M., and PEDRONI, R., 1993. Base capacity of bored piles in sands from in-situ tests. Deep Foundations on Bored and Augured Pile, Van Impe, Ed., Balkema, Rotterdam.

GRL, 1995. Wave equation analysis of pile driving. User's Manual, Vols. I through IV, Goble, Rausche, and Likins Inc., Cleveland, 355 p.

GWIZDALA, K., 1984. Large diameter bored piles in non-cohesive soils. Swedish Geotechnical Institute, SGI Report No. 26, 129p.

HAUSTOEFER, I. J., and PLESIOTIS, S., 1988. Instrumented dynamic and static pile load testing at two bridges. Proceedings of the 5th Australia-New Zealand Conference on Geomechanics, Prediction versus Performance, Sydney, August 22 - 28, pp. 514-420.

HOLDEN, J. C., 1971. Research on performance of soil penetrometers. Country Roads Board of Victoria Internal Report, CE-SM-71-1 (as referenced by Chapman, 1974).

HOLTZ, R. D., and KOVACS, W. D., 1981. An introduction to geotechnical Engineering. Prentice-Hall Inc., New York, 780 p.

HORVITZ, G. E., STETTLER, D. R., and CROWSER, J. C., 1986. Comparison of predicted and observed pile capacity. American Society of Civil Engineers, Proceedings of ASCE Symposium on Cone Penetration Testing, St. Louis, pp. 413 - 433.

HOULSBY, G. T., AND HITCHMANN, R., 1988. Calibration chamber tests of a cone penetrometer in sand. Geotechnique Vol. 38, No. 1, pp. 39-44.

HUNT, S. W., 1993. Piles for Marquette University Math Building. Design and Performance of Deep Foundations, American Society of Civil Engineers, ASCE, GSP, No. 38, pp. 91-108.

HUNTSMANN, S. R., 1985. Determination of in-situ lateral pressure of cohesionless soils by cone penetrometer. Ph. D. Thesis, University of California, Berkeley (as referenced by Mitchell, 1988).

HUNTSMANN, S. R., and MITCHELL, J. K., 1986. Lateral stress measurement during cone penetration. Proceedings of In-Situ 86, ASCE Specialty Conference, Blacksburg, pp. 617-634.

JACOBS, P. A., and COUTS, J. S., 1992. A comparison of electric piezocone tips at the Bothkennar test site. Geotechnique Vol. 42, No. 2, pp. 369-375.

JAMILOKOWSKI, M., LANCELLOTTA, R., TORDELLA, L., and BATTAGLIO, M., 1982. Undrained strength from CPT. Proceedings of the 2nd European Symposium on Penetration Testing, ESOPT-2, Amsterdam, Vol.2, pp. 599-606.

JAMIOLKOWSKI, M., LADD. C. C., GERMANIE, J. T., and LANCELLOTTA, R., 1985. New developments in field and laboratory testing of soils. Theme Lecture, 11th International Conference on Soil Mechanics and Foundation Engineering, ICSMFE, San Francisco, Vol. 1, pp. 57-155.

JANBU, N., and SENESSET, J. K., 1974. Effective stress interpretation of in-situ static penetration tests. Proceedings of the 1st European Symposium on Penetration Testing, ESOPT-1, Stockholm, Vol.2:2, pp. 181-193.

JANBU, N., 1976. Static bearing capacity of friction piles. Proceedings of the European Conference on Soil Mechanics and Foundation Engineering, Vol. 1.2, pp.479-488.

KENNEDY, J. B. and NEVILLE, A. M., 1986. Basic statistical methods for engineering and scientists, Harper and Row, New York, 519 p.

KERISEL, J., 1964. Deep foundation —Basic experimental facts. Proceedings of North American Conference on Deep Foundations, Mexico City, pp. 1-31.

KONRAD, J. M., and LAW, K. T., 1987. Undrained shear strength from piezocone tests. Canadian Geotechnical Journal, Vol. 24, pp. 392-405.

KONRAD, J. M., and ROY, M., 1987. Bearing capacity of friction piles in marine clay. Geotechnique, Vol. 37, No. 2, pp. 163-175.

KULHAWY, F. H., 1984. Limiting tip or side resistance: fact or fallacy? Proceedings of the ASCE Symposium on Analysis and Design of Pile Foundations, San Francisco, California, pp. 80-98.

LADANYI, B., 1961. Etude theorique er experimentate de l'expansion dansun sol pulverulent d'une cavite presentant unesymetric spherique ou cylindeigue. Annales des Travaux Publics de Belique, Vol. 62, pp. 365-406.

LADANYI, B., 1967. Expansion of cavities in brittle media. International Journal of Rock Mechanics, Vol. 4, pp. 301-328.

LADE, P. V., 1977. The stress-strain and strength characteristics of cohesionless soils. Ph. D. Thesis, University of California, Berkeley (as referenced by Been, 1986).

LAIER, J. E., 1994. Predicting the ultimate compressive capacity of long 12-H-74 steel pile. Proceedings of the FHWA International Conference on Design and Construction of Deep Foundations, Orlando, December 7-9, Vol. 2, pp. 1804-1818.

LEE, K. L., and SEED, H. B., 1967. Drained characteristics of sands. American Society of Civil Engineers, ASCE, Journal of Soil Mechanics and Foundations Division, Vol. 93, SM6, pp. 117-141.

LONG, J. H., and SHIMEL, I. S., 1989. Drilled shafts, a data-base approach. American Society of Civil Engineers, Proceedings of Foundation Engineering Congress: Current Principles and Practices, ASCE Geotechnical Special Publication, June 25 - 29, GSP 22, Vol. 2, pp. 1091 - 1108.

LUNNE, T., and KLEVEN, A., 1981. Role of CPT in North Sea foundation engineering. Symposium on Cone Penetration Testing and Experience, ASCE Geotechnical Engineering Division, St. Louis, pp. 49-75.

LUNNE, T., EIDSMOEN, D., and HOWLAND, J. D., 1986. Laboratory and field evaluation of cone penetrometers. Proceedings of In-Situ 86, ASCE Specialty Conference, Blacksburg, pp. 714.729.

MARSLAND, A., and QUARTERMAN, R., 1982. Factors affecting the measurement and interpretation of quasi-static penetration tests in clay. Proceedings of the 2nd European Symposium on Penetration Testing, ESOPT-2, Amsterdam, Vol.2, pp. 697-702.

MASOOD, T., and MITCHELL, J. K., 1993. Estimation of in-situ lateral stresses in soil by CPT. ASCE, Journal of Geotechnical Engineering, Vol. 119, No. 10, pp. 1624-1639.

MASSARSCH, K. R., 1986. Acoustic penetration tests. Proceedings of 4th International Geotechnical Seminar, Field Instrumentation and In-Situ Measurements, Nanyang (as referenced by Mitchell, 1988).

MATSUMOTO, T., MICHI, Y, and HIRONO, T., 1995. Performance of axially loaded steel pipe piles driven in a soft rock. American Society of Civil Engineers, ASCE, Journal of Geotechnical Engineering, Vol. 121, No. 4, pp. 305-315.

MAYNE, P. W., and KULHAWY, F. H., 1990. Observations on the development of pore water stresses during piezocone penetration in clays. Canadian Geotechnical Journal, Vol. 27, pp. 418-428.

MAYNE, P. W., 1993. Axial load-displacement behavior of drilled shaft foundations in Piedmont Residuum. Research Report, FHWA-41-30-2175, Federal Highway Administration, Virginia, 162p.

MAYNE, P. W., and MITCHELL, J., K., AUXT, J. A., and YILMAZ, R., 1995. US national report on CPT. Proceedings of International Symposium on Cone Penetration Testing, CPT'95, Linkoping, Sweden, SGI Report 3:95, Vol. 2, pp. 263-276.

MELZER, K. J., 1968. Sondenunterschungen in sand. Dissertation D82, Technichen-Hochschule Aachen.

MEYERHOF, G. G., 1951. The ultimate bearing capacity of foundations. Geotechnique, vol. 2, No.4 pp. 301-332.

MEYERHOF, G. G., 1956. Penetration tests and bearing capacity of cohesionless soils. American Society of Civil Engineers, ASCE, Journal of Soil Mechanics and Foundations Division, Vol. 82, No. SM1, pp. 1-12.

MEYERHOF, G. G., 1961. The ultimate bearing capacity of wedge shaped foundations. Proceedings of 5th International Conference on Soil Mechanics and Foundation Engineering, ICSMFE, Paris, Vol. 2, pp.105-109.

MEYERHOF, G. G., 1976. Bearing capacity of settlement of pile foundations. The Eleventh Terzaghi Lecture, November 5, 1975, American Society of Civil Engineers, ASCE, Journal of Geotechnical Engineering, Vol. 102, GT3, pp. 195 - 228.

MEYERHOF, G. G., 1983. Scale effects of ultimate pile capacity. American Society of Civil Engineers, ASCE, Journal of Geotechnical Engineering, Vol. 108, No. GT3, pp. 195-228.

MILOVIC, D., and STEVANOVIC, S., 1982. Some soil parameters determined by cone penetration tests. Proceedings of the 2nd European Symposium on Penetration Testing, ESOPT-2, Amsterdam, May 24 - 27, Vol.2, pp. 709-714.

MITCHELL, J. K., and KEAVENY, J. M., 1986. Determining sand strength by cone penetrometer. Proceedings of In-Situ 86, ASCE Specialty Conference, Blacksburg, Virginia, pp. 823-869.

MITCHELL, J. K., 1988. New developments in penetration tests and equipment. Proceedings of the 1st International Symposium on Penetration Testing, ISOPT-1, Disney world, Vol.1, pp 245-261.

MOHAN, D., JAIN, G. S., and KUMAR, V., 1963. Load bearing capacity of piles. Geotechnique, vol.13, No. 1, p. 76.

MUROMACHI, T., 1974. Phono-sounding apparatus. Proceedings of the 1st European Symposium on Penetration Testing, ESOPT-1, Stockholm, Vol. 2:1, pp. 110-112.

NEVELES, J. B., and DONALD, R. S., 1994. Comparison of settlement predictions for single piles in sand based on penetration test results. Proceedings of Settlement-94, Vertical and Horizontal Deformations of Foundations and Embankments, ASCE Geotechnical Special Publication,, GSP 40, College Station, June 16 - 18, pp. 1028-1039.

NOTTINGHAM, L. C., 1975. Use of quasi-static friction cone penetrometer data to predict load capacity of displacement piles. Ph. D. Thesis, Dept. of Civil Engineering., University of Florida, 553p.

OLSEN, R. S., AND FARR,V., 1986. Site characterization using the cone penetration test. Proceedings of In-Situ 86, ASCE Specialty Conference, Blacksburg, Virginia, pp. 854-868.

O'NEILL, M. W., 1981. Field study of pile group action. Federal Highway Administration, FHWA Report No. RD-81/002, 217p.

O'NEILL, M. W., 1986. Reliability of pile capacity assessment by CPT in overconsolidated clay. Proceedings of In-Situ 86, ASCE Specialty Conference, Blacksburg, Virginia, pp. 237-256.

O'NEILL, M. W., 1988. Pile group prediction symposium. Summary of prediction results. Federal Highway Administration, FHWA, Draft Report, 51 p.

PARKIN, A. K., HOLDEN, J., AAMOT, K., LAST, N., and LUNNE, T., 1980. Laboratory investigations of CPT's in sand. Norwegian Geotechnical Institute, Oslo, Report 52108-9 (as referenced by Robertson and Campanella, 1989).

PARKIN, A. K., and LUNNE, T., 1982. Boundary effects in the laboratory calibration of a cone penetrometer in sand. Proceedings of the 2nd European Symposium on Penetration Testing, ESOPT-2, Amsterdam, Vol.2, pp. 761-768.

POLOUS, S. J., 1981. The steady state deformation. American Society of Civil Engineers, ASCE, Journal of Geotechnical Engineering, Vol. 107, GT7, pp. 553-562.

RANDOLPH, M. F., DOLWIN, J., and BECK, R., 1994. Design of driven piles in sand. Geotechnique Vol. 44, No. 3, pp. 427-448.

RAUSCHE, F., GOBLE, G. G., and LIKINS, G. E., 1985. Dynamic determining of pile capacity. ASCE, Journal of Geotechnical Engineering, Vol. 111, No. 3, pp. 367-383.

REESE, J. D., 1975. An experimental study on the effects of saturation on the q_c and f_s values from cone penetration tests in the University of Florida chamber. M. Sc. Thesis, University of Florida.

REESE, J. D., O'NEILL, M. W., AND WANG, S. T., 1988. Drilled shaft tests, Interchange of West Belt Roll Road and US290 Highway, Texas. Final Report. Lymon C. Reese and Associates, Austin.

RICHMANN, R., and SPEER, D., 1989. Comparison of measured pile capacity to pile capacity predictions made using electronic cone penetration test data. Report, FHWA/CA/TL-89/16, California State Department of Transportation, Sacramento.

RIGDEN, W. J., THORBURN, S., MARSLAND, A., and QUARTERMAIN, A., 1982. A dual range cone penetrometer. Proceedings of the 2nd European Symposium on Penetration Testing, ESOPT-2, Amsterdam, Vol.2, pp. 787-796.

ROBERTSON, P. K., and CAMPANELLA, R. G., 1983a. Interpretation of cone penetration tests: part I, sand. Canadian Geotechnical Journal, Vol. 20, No. 4, pp. 718-733.

ROBERTSON, P. K., and CAMPANELLA, R. G., 1983b. Interpretation of cone penetration tests: part II, clay. Canadian Geotechnical Journal, Vol. 20, No. 4, pp. 734-745.

ROBERTSON, P. K., CAMPANELLA, R. G., BROWN, P. T., GROF, I., and HUGHES, J. M. K., 1985. Design of axially and laterally loaded piles using in-situ tests: a case history. Canadian Geotechnical Journal, Vol. 22, pp. 518-527.

ROBERTSON, P. K., CAMPANELLA, R. G., GILLESPIE, D., and GRIEG, J., 1986. Use of piezometer cone data. Proceedings of American Society of Civil Engineers, ASCE, In-Situ 86 Specialty Conference, Blacksburg, June 23 - 25, Geotechnical Special Publication GSP 6, pp. 1263 - 1280.

ROBERTSON, P. K., and CAMPANELLA, R. G, 1989. Guidelines for geotechnical design using the cone penetrometer test and CPT with pore pressure measurement. Soil Mechanics Series, No.105, UBC, Dept. of Civil Engineering and Hogentogler and Company, Inc., fourth edition, 193 p.

ROBERTSON, P. K., 1990. Soil classification using the cone penetration test. Canadian Geotechnical Journal, Vol. 27, No. 1, pp. 151-158.

RODIN, S., CORBETT, B., SHERWOOD, D., and THORBURN, S., 1974. Penetration testing in the United Kingdom, state-of-the-art Report. Proceedings of the 1st European Symposium on Penetration Testing, ESOPT-1, Stockholm, Vol. 1, pp. 139-146.

ROSCOE, K. H., SCHOFIELD, A. N., and WROTH, C. P., 1958. On the yielding of soils. Geotechnique, Vol. 8, pp. 22-53.

ROSCOE, K. H., and POOROOSHASB, H., 1963. A fundamental principle of similarity in model test for earth pressure problems. Proceedings of 2nd Asian Regional Conference on Soil Mechanics, Bangkok, Vol. 1, pp. 134-140.

ROURK, T. L., 1961. Model studies of a pile failure surface in a cohesive soil. Master's thesis, Georgia Institute of technology, Atlanta.

SALGADO, R., 1993. Analysis of penetration resistance in sands. Ph. D. Thesis, Civil Engineering Department, University of California, Berkeley, 357p.

SALGADO, R., 1995. Design of piles in sands based on CPT results. Proceedings of 10th Panamerican CSMFE, Vol. 3, pp. 1261-1274.

SANGLERAT, G., 1972. The penetrometer and soil exploration. Elsevier, Amsterdam, 464 p.

SCHMERTMANN, J. H., 1972. Effects of in-situ lateral stress on friction-cone penetrometer data in sands. Proceedings of Fugro Sondeer Symposium, Holland, pp. 37-39.

SCHMERTMANN, J. H., 1978a. Guidelines for cone test, performance and design. Federal Highway Administration, Report FHWA-TS-78209, Washington, 145 p.

SCHMERTMANN, J. H., 1978b. Study of feasibility of using Wissa-type piezometer probe to identify liquefaction potential of saturated sands. U. S. Army Engineer Waterways Experiment Station, Report S-78-2.

SENNESET, K., 1974. Penetration testing in Norway. Proceedings of the 1st European Symposium on Penetration Testing, ESOPT-1, Stockholm, Vol.1, pp. 85-95.

SLADEN, J. A., 1989. Problems with interpretation of sand state from cone penetration test. Geotechnique, Vol. 39, No. 2, pp. 323-332.

SMITH, E. A. L., 1960. Pile driving analysis by the wave equation. American Society of Civil Engineers, ASCE, Journal of Soil Mechanics and Foundations Division, Vol. 86, SM4, pp. 35-60.

TAVENAS, F. A., 1971. Load test results on friction piles in sand . Canadian Geotechnical Journal, Vol. 8, No. 1, pp. 7-22.

TCHENG, Y., 1966. Fondations profonds en milieu pulverulent du batiment et des travaux publics, sols et fondations 54, Nos. 219-220.

TOMLINSON, M. J., 1957. The adhesion of piles driven in clay soils. Proceedings of 4th ICSMFE, London, Vol. 1, pp. 66-71.

TORSTENSSON, B. A., 1975. Pore pressure sounding instrument. Proceedings of ASCE Specialty Conference on In-Situ measurement of Soil Properties, Raleigh, Vol. 2, pp. 48-54.

TORSTENSSON, B. A., 1982. A combined pore pressure and point resistance probe. Proceedings of the 2nd European Symposium on Penetration Testing, ESOPT-2, Amsterdam, Vol. 2, pp. 903-908.

TRINGLE, P. T., and MITCHELL, J. K., 1982. An acoustic cone penetrometer for site investigation. Proceedings of the 2nd European Symposium on Penetration Testing, ESOPT-2, Amsterdam, Vol.2, pp. 909-914.

TUCKER, K. D., 1986. Uplift capacity of pile foundations using CPT data. American Society of Civil Engineers, Proceedings of In-Situ 86 Specialty Conference, Blacksburg, June 23 - 25, Geotechnical Special Publication GSP 6, pp. 1077 - 1093.

TUCKER, L. M., and BRIAUD, J. L., 1986. Analysis of pile load test program at the Lock and Dam 26 replacement project. Final report, US Army Corps of Engineers, 63 p.

TUMAY, M. Y., and FAKHROO, M., 1981. Pile capacity in soft clays using electric QCPT data. American Society of Civil Engineers, ASCE, Proceedings of Conference on Cone Penetration Testing and Experience, St. Louis, October 26 - 30, pp. 434 - 455.

URKKADA TECHNOLOGY LTD., 1995. Dynamic testing of piles and analysis, Puerto Rico. Final Report, Project 9509DH17.

URKKADA TECHNOLOGY LTD., 1996. Geotechnical report on pile foundation testing and analysis. Berths 302-305 at Los Angeles, Project No. 94/3DHO1.

VAN DER VEEN, C., 1953. The bearing capacity of a pile. Proceedings of 3rd International Conference on Soil Mechanics and Foundation Engineering, ICSMFE, Zurich, Vol. 2, pp. 84-90.

VANIMPE, W., 1986. Evaluation and deformation of bearing capacity parameters of foundations from static CPT results. Proceedings of International Geotechnical Seminar on Field Instrumentation and In-situ Measurements, Singapore, pp.51-70.

VANIMPE, W., DEBEER, E., and LOUISBERG, E., 1988. Prediction of single pile bearing capacity in granular soils out of CPT results. First International Symposium on Penetration Testing, ISOPT-1, Specialty Session, Orlando, March 20 - 24, 34 p.

VAN MIERLO, W. C., and KOPPEJAN, A. W., 1952. Lengte en draagvermogen van heipalen. Bouw, January (as referenced by Davies, M., 1987).

VEEN, C. V. D., 1989. Dutch cone penetration test and its use in determining the pile bearing capacity. Proceedings of International Conference on Piling and Deep Foundations, London, Vol. 1, pp. 397-405.

VEEN, C. V. D., and BOERSMA, L., 1957. The bearing capacity of piles predetermined by a cone penetration test. Proceedings of 4th ICSMFE, London, Vol. 2, pp. 72-75.

VEISMANIS, A., 1974. Laboratory investigation of electrical friction cone penetrometers in sand. Proceedings of the 1st European Symposium on Penetration Testing, ESOPT-1, Vol.2, pp. 407-419.

VERMEIDEN, J., 1948. Improved soundings apparatus, as developed in Holland since 1936. Proceedings of 2nd International Conference on Soil Mechanics and Foundation Engineering, ICSMFE, Amsterdam, Vol. 1, pp. 280-287.

VESIC, A. S., 1963. Bearing capacity of deep foundations in sand. Highway Research Report, No. 39, pp. 112-153.

VESIC, A. S., 1964. Model testing of deep foundations in sand and scaling laws. Proceedings of the North American Conference on Deep Foundations, Mexico City, Vol. 2, pp. 525-533.

VESIC, A. S., 1967. A study of bearing capacity of deep foundations. Final Report, Project B-189, Georgia Institute of Technology, Atlanta, 254 p.

VESIC, A. S., 1970. Tests on instrumented piles, Ogeechee River Site. American Society of Civil Engineers, ASCE, Journal of Soil Mechanics and Foundations Division, Vol. 96, SM2, pp. 561-584.

VESIC, A. S., 1972. Expansion of cavities in infinite soil masses. American Society of Civil Engineers, ASCE, Journal of Soil Mechanics and Foundations Division, Vol. 96, SM3, pp. 265-290.

VESIC, A. S., 1977. Design of pile foundation. Transportation Research Board, TRB, National Cooperation Highway Research Program, Washington, Synthesis of Highway Practice No. 42, 68p.

VIERGEVER, M. A., 1982. Relation between cone penetration and static loading of piles on locally strongly varying sand layers. Proceedings of the 2nd European Symposium on Penetration Testing, ESOPT-2, Amsterdam, Vol. 2, pp. 927-932.

VIJAYVERGIYA, V. A., and FOCHT, J. A., 1972. A new way to predict capacity of piles in clays. Proceedings of the Fourth Offshore Technology Conference, Houston, Vol. 2, pp. 865-874.

VILLET, W. C. B., and MITCHELL, J. K., 1981. Cone resistance, relative density, and friction angle. Proceedings of ASCE Specialty Conference on In-Situ measurement of Soil Properties, Raleigh, pp. 178-208.

WEBER, L. 1987. Efficiency improvement of steel H-bearing piles. Areed Recherches, Final Report, No. 7210.SA/503.

WISSA, A. E. Z., MARTIN, R. T., and GARLANGER, J. E., 1975. The piezometer probe. Proceedings of ASCE Specialty Conference on In-Situ measurement of Soil Properties, Raleigh, Vol.2, pp. 536-545.

WITHERS, N. J., HOWIE, J., HUGHES, J. M., and ROBERTSON, P. K., 1989. Performance and analysis of cone pressuremeter tests in sands. Geotechnique, Vol. 39, No. 3, pp. 433-454.

WROTH, C. P., 1984. The interpretation of in-situ soil tests. Geotechnique, Vol. 34, No. 4, pp. 433-454.

WROTH, C. P., 1988. Penetration testing—a more rigorous approach to interpretation. Proceedings of the 1st International Symposium on Penetration Testing, ISOPT-1, Disney world, Vol.1, pp. 303-311.

YEN, T. L., LIN, H., CHIN, C. T., and WANG, R. F., 1989. Interpretation of instrumented driven steel pipe piles. American Society of Civil Engineers, Proceedings of Foundation Engineering Congress: Current Principles and Practices, ASCE Geotechnical Special Publication, June 25 - 29, GSP 22, GSP 22, pp. 1293 - 1308.

ZHOU, J., XIE, Y., ZOU, Z. S., LUO, M. Y., and TANG, X. J., 1982. Prediction of limit load of driven pile by CPT. Proceedings of the 2nd European Symposium on Penetration Testing, ESOPT-2, Amsterdam, Vol.2, pp. 957-961.

Table 2.1 Pile classification considering different aspects (CFEM, 1992)

No.	FACTOR	SUBGROUP
1	Installation	Driven; bored; cast in situ; jetted; excavated; augured.
2	Displacement	Displacement; low-displacement; non-displacement.
3	Material	Concrete; steel; wood.
4	Function	Shaft bearing; toe bearing.
5	Capacity	High; moderate; low.
6	Shape	Square; round; hexagonal; octagonal; H-section.
7	Environment	Land; marine; off-shore.
8	Inclination	Vertical; inclined.
9	Length	Long; short.
10	Structure	Bridges; buildings; platforms; towers; machinery; etc.

Table 2.2 Ranges of β and N_t-Coefficients (Fellenius, 1995)

No.	Soil Type	φ-Angle	β	N_t	β/N_t, %
1	Clay	25 - 30	0.25 - 0.35	3 - 30	1% - 8%
2	Silt	28 - 34	0.27 - 0.50	20 - 40	1.25% -1.35%
3	Sand	32 - 40	0.30 - 0.60	30 - 150	0.4% - 1%
4	Gravel	35 - 45	0.35 - 0.80	60 - 300	0.3% - 0.6%

Table 4.1 Principal calibration chambers used in geotechnical investigations (after Ghionna and Jamiolkowski, 1991)

Test cell, Owner/Location	Specimen diameter (m)	Specimen height (m)	Boundary conditions		
			Radial	Bottom	Top
Country Roads Bureau, Australia	0.76	0.91	Flexible	Cushion	Rigid
Univ. of Florida, USA	1.20	1.20	Flexible	Cushion	Rigid
Monash University, Australia	1.20	1.80	Flexible	Cushion	Rigid
Norwegian Geotecnical Institute	1.20	1.50	Flexible	Cushion	Rigid
ENEL-CRIS, Milano, Italy	1.20	1.50	Flexible	Cushion	Rigid
ISMES, Bergamo, Italy	1.20	1.50	Flexible	Cushion	Rigid
Univ. of California, Berkeley, USA	0.76	0.80	Flexible	Rigid	Rigid
Univ. Of Texas, Austin, USA	Cube 2.10*2.10*2.10			All flexible	
Univ. Of Houston, USA	0.76	2.54	Flexible	Cushion	Cushion
North Carolina State Univ., USA	0.94	1.00	Flexible	Rigid	Rigid
Louisiana State Univ., USA	0.55	0.80	Flexible	Flexible	Rigid
Golder Associates, Calgary, Canada	1.40	1.00	Flexible	Rigid	Cushion
Virginia Polytechnic Institute and State Univ., USA	1.50	1.50	Flexible	Rigid	Rigid
Univ. of Grenoble, France	1.20	1.50	Flexible	Cushion	Cushion
Oxford Univ., UK	0.90	1.10	Flexible	Cushion	Rigid
Univ. of Tokyo, Japan	0.90	1.10	Flexible	Rigid	Rigid
Univ. of Clarkson, USA	0.51	0.76	Flexible	Rigid	Rigid
Univ. of Sheffield, UK	0.79	1.00	Flexible	Rigid	Flexible
Cornell Univ., USA	2.10	2.90	Flexible	Rigid	Rigid

Table 4.2 Boundary conditions imposed in flexible wall calibration chambers (after Veismanis, 1974)

Type	Vertical	Horizontal
BC1	Stress constant	Stress constant
BC2	Change in strain is zero	Change in strain is zero
BC3	Stress constant	Change in strain is zero
BC4	Change in strain is zero	Stress constant

Table 5.1 Methods for pile capacity calculation using CPT data (Direct Methods)

No.	Method	Reference
1	"Dutch" CPT	Van Mierlo and Koppejan, 1952
2	Begemann	Begemann, 1963
3	Mohan and Kumar.	Mohan and Kumar, 1963
4	Senneset	Senneset, 1974
5	Rodin et al.	Rodin, Cobett, Sherwood, and Thorburn, 1974
6	Meyerhof	Meyerhof, 1956; 1976; 1983
7	Schmertmann and Nottingham	Nottingham, 1975; Schmertmann, 1978
8	European	de Ruiter and Beringen (1979)
9	Tumay and Fakhroo.	Tumay and Fakhroo, 1981
10	French; LCPC (Laboratoire Central des Ponts et Chausees)	Bustamante and Gianeselli, 1982
11	Zhou et al.	Zhou et al, 1982
12	Gwizdala	Gwizdala, 1984
13	Van Impe	Van Impe, 1988
14	The New EuroCode	"Eurocode 7-part 1" (ENV 1997-1993) and French Highway Administration (MELT,1993) Frank, 1994

Table 5.2 **Empirical coefficients for French method for pile capacity calculation using CPT (modified after Bustamante and Gianeselli, 1982)**

Nature of Soil	q_c (MPa)	K_c *	Driven Piles				Bored Piles			
			K_s **		Upper limit of r_s (KPa)		K_s		Upper limit of r_s (KPa)	
			A	B	A	B	A	B	A	B
Soft clay and mud	<1	o.5	30	30	15	15	30	30	15	15
Moderately compact clay	1 to 5	0.45	40	80	35 (80)	35 (80)	40	80	35 (80)	35 (80)
Compact to stiff clay and compact silt	>5	0.55	60	120	35 (80)	35 (80)	60	120	35 (80)	35 (80)
Silt and loose sand	<5	0.5	60	120	35	35	60	150	35	35
Moderately compact sand and gravel	5 to 12	0.5	100	200	80 (120)	80	100	200	80	35 (80)
Compact to very compact sand and gravel	>12	0.4	150	200	120 (150)	120	150	300	120 (150)	80 (120)

CATEGORY:

A- Driven precast piles, Prestressed tubular piles, and Jacked concrete piles
B- Driven metal piles, and Jacked metal piles
* $r_t = K_c\, q_{c,a}$
($q_{c,a}$ = average q_c values, see Fig. 5.5)
**$r_s = q_c/K_s$
Note:
Bracket values for r_s: apply to careful execution and minimum disturbance of soil due to disturbance.

Table 6.1 Case Records Summary

No.	Case	Site Identification		Pile Data (1)			Loading Test Data (2)				CPT (3)		Soil Profile
		Reference	Location	Shape Mate-rial	Geometry b, mm	Geometry D, m	Type of Test	R_t KN	R_s KN	R_u KN	Data	Type of Cone	
1	UBC2	Campanella et al. 1989	Vancouver BC, Canada	P, St.	324	13.7	C, QML	*	*	290	q_c, f_s, u	E	2m fill, 13m clay, 13m sand, and silt > 7m
2	UBC3	Campanella et al. 1989	Vancouver BC, Canada	P, St.	324	16.8	C, QML	315	315	630	q_c, f_s, u	E	2m fill, 13m clay, 13m sand, and silt > 7m
3	UBC5	Campanella et al. 1989	Vancouver BC, Canada	P, St.	324	31	C, QML	180	920	1,100	q_c, f_s, u	E	2m fill, 13m clay, 13m sand, and silt > 7m
4	UBCA	Robertson et al. 1985	Vancouver BC, Canada	P, St.	915	67	C, QML	*	*	7,500	q_c, f_s, u	E	2m fill, 13m clay, 13m sand, and silt > 40m
5	NWUP	Finno, 1989	Evanston IL, USA	P, St.	450 t = 9.4	15.2	C, SML	62	958	1,020	q_c, f_s, u	E	7m sand, and clay > 10m
6	NWUH	Finno, 1989	Evanston IL, USA	HP, St.	346 × 371	15.2	C, SML	50	950	1,010	q_c, f_s, u	E	7m sand, and clay > 10m
7	FHWASF	Fellenius, 1986 O'Neill, 1988	S. Francisco CA, USA	P, St.	273 t = 9.3	9.1	C, SML	355	155	490	q_c, f_s, u	E	2m fill, 11m hydraulic sand
8	BGHD1	Altaee et al., 1992 and 1993	Baghdad Iraq	Sq., Conc.	285	11	C, SML	360	640	1,000	q_c, f_s	M	3m silty sand, and uniform sand > 10m
9	BGHD2	Altaee et al., 1992 and 1993	Baghdad Iraq	Sq., Conc.	285	15	C, SML	480	1,120	1,600	q_c, f_s	M	6m silty sand, and uniform sand > 12m
10	POLA1	CH2M Hill, 1987	Los Angeles CA, USA	Oct., Conc.	625	25.8	C	4,050	1,735	5,785	q_c, f_s	E	6m clay, 15m silty sand, and dense sand

(1) P = Pipe; Sq. = Square; Oct. = Octagonal; HP = H-Section; Rd. = Round; Conc. = Concrete; St. = Steel; b = Diameter; t = Wall Thickness; D = Embedment Length
(2) T = Tension; C = Compression; SML = Slow-Maintained Load; QML = Quick-Maintained Load; R_t = Toe Capacity; R_s = Shaft Capacity; R_u = Total Capacity
(3) q_c = Cone Resistance; f_s = Sleeve Friction; u = Measured Pore Pressure; E = Electrical; M = Mechanical
* Not Measured

Table 6.1 Case Records Summary (cont'd)

No.	Case	Site Identification		Pile Data (1)			Loading Test Data (2)				CPT (3)		Soil Profile
		Reference	Location	Shape Material	Geometry		Type of Test	R_t KN	R_s KN	R_u KN	Data	Type of Cone	
					b, mm	D, m							
11	POLA2	Urkkada Ltd. 1995	Los Angeles CA, USA	Oct., Conc.	625	32.6	C	3,560			q_c, f_s	E	10m silty sand, 20m sand, and dense sand
12	JPNOT1	Matsumoto et al. 1995	Noto Island Japan	P, St.	800 * t = 12	8.2	C	1,200	3,500	4,700	q_c, f_s, u	E	stiff clay (soft rock)
13	JPNOT2	Matsumoto et al. 1995	Noto Island Japan	P, St.	800 * t = 12	8.2	C			3190	q_c, f_s, u	E	stiff clay (soft rock)
14	JPNOT3	Matsumoto et al. 1995	Noto Island Japan	P, St.	800 * t = 12	8.2	T	*		3250	q_c, f_s, u	E	stiff clay (soft rock)
15	TWNTP4	Yen et al., 1989	Taiwan	P, St.	609 t = 12	34.2	C, QML	1,450	2,880	4,330	q_c, f_s, u	E	6m sand, 13m clay, and sand
16	TWNTP5	Yen et al., 1989	Taiwan	P, St.	609 t = 12	34.2	T, SML	*	2,500	*	q_c, f_s, u	E	6m sand, 14m clay, and sand
17	TWNTP6	Yen et al., 1989	Taiwan	P, St.	609 t = 12	34.2	C, QML	1650	2,810	4,460	q_c, f_s, u	E	6m sand, 14m clay, and sand
18	LSUA1	Tumay and Fakhroo, 1981	Louisiana USA	Sq., Conc.	350	9.5	C	*	*	900	q_c, f_s	E	9m sand, and clay> 10m
19	LSUB12	Tumay and Fakhroo, 1981	Louisiana USA	Rd., Conc.	900	37.8	C	*	*	3,960	q_c, f_s	E	17m silt, 5m silty clay, 8m sand, andsilty clay
20	LSUN11	Tumay and Fakhroo, 1981	Louisiana USA	Sq., Conc.	450	36.5	C	*	*	2,950	q_c, f_s	E	37m silty clay, and silty sand

(1) P = Pipe; Sq. = Square; Oct. = Octagonal; HP = H-Section; Rd. = Round; Conc. = Concrete; St. = Steel; b = Diameter; t = Wall Thickness; D = Embedment Length
(2) T = Tension; C = Compression; SML = Slow-Maintained Load; QML = Quick-Maintained Load; R_t = Toe Capacity; R_s = Shaft Capacity; R_u = Total Capacity
(3) q_c = Cone Resistance; f_s = Sleeve Friction; u = Measured Pore Pressure; E = Electrical; M = Mechanical
* Not Measured

Table 6.1 Case Records Summary (cont'd)

No.	Case	Site Identification		Pile Data (1)			Loading Test Data (2)				CPT (3)		Soil Profile
		Reference	Location	Shape Material	Geometry		Type of Test	R_t KN	R_s KN	R_u KN	Data	Type of Cone	
					b, mm	D, m							
21	LSUN15	Tumay and Fakhroo, 1981	Louisiana USA	P, St.	400	37.5	C	*	*	2,800	q_c, f_s	E	37m silty clay, and silty sand
22	LSUN28	Tumay and Fakhroo, 1981	Louisiana USA	Tr. Conc.	500	30.5	C	*	*	2,160	q_c, f_s	E	24m clay, 11m silty sand, and clay
23	LSUN2-15	Tumay and Fakhroo, 1981	Louisiana USA	P, St.	350	31.1	C	*	*	1,710	q_c, f_s	E	24m clay, 11m silty sand, and clay
24	LSUN2-16	Tumay and Fakhroo, 1981	Louisiana USA	P, St.	400	41.8	C	*	*	1,890	q_c, f_s	E	24m clay, 11m silty sand, and clay
25	LSUH1	Tumay and Fakhroo, 1981	Louisiana USA	Sq., Conc.	450	29	C	*	*	1,935	q_c, f_s	E	4m clay, 2m sand, and clay
26	LSUR24	Tumay and Fakhroo, 1981	Louisiana USA	Sq., Conc.	600	19.8	C	*	*	2,025	q_c, f_s	E	3m fill, and sandy clay
27	LSUR30	Tumay and Fakhroo, 1981	Louisiana USA	Sq., Conc.	750	19.8	C	*	*	2,610	q_c, f_s	E	3m fill, and sandy clay
28	UFL22	Avasarala et al. 1994	Florida USA	Sq., Conc.	350	16	C	*	*	1,350	q_c, f_s	E	sand
29	UFL52	Avasarala et al. 1994	Florida USA	Sq., Conc.	500	11	C	*	*	2,070	q_c, f_s	E	sand
30	UFL53	Avasarala et al. 1994	Florida USA	Sq., Conc.	350	20.4	C	*	*	1,260	q_c, f_s	E	10m sand, and silt > 10m

(1) P = Pipe; Sq. = Square; Oct. = Octagonal; HP = H-Section; Rd. = Round; Tr. = Triangle; Conc. = Concrete; St. = Steel; b = Diameter; t = Wall Thickness; D = Embedment
(2) T = Tension; C = Compression; SML = Slow-Maintained Load; QML = Quick-Maintained Load; R_t = Toe Capacity; R_s = Shaft Capacity; R_u = Total Capacity
(3) q_c = Cone Resistance; f_s = Sleeve Friction; u = Measured Pore Pressure; E = Electrical; M = Mechanical
* Not Measured

Table 6.1 Case Records Summary (cont'd)

No.	Case	Site Identification		Pile Data (1)			Loading Test Data (2)				CPT (3)		Soil Profile
		Reference	Location	Shape Material	Geometry		Type of Test	R_t KN	R_s KN	R_u KN	Data	Type of Cone	
					b, mm	D, m							
31	LTN741	Reese et al., 1988	Houston, TX USA	Rd., Conc.	810	24.1	C	*	*	7,830	q_c, f_s	M	4m stiff clay, and sand
32	LTN484	Tucker, 1986	California USA	Rd., Conc.	450	7.6	C	*	*	750	q_c, f_s	E	5m silty sand, 2m clay, and silty sand
33	LTN742	Reese et al., 1988	Houston, TX USA	Rd., Conc.	810	24.1	C	*	*	5,850	q_c, f_s	E	4m stiff clay, and sand
34	MUMB	Hunt, 1993	Milwaukee USA	P, St.	273 t =5.6	12.2	C, QML	534	1,152	1,680	q_c, f_s	E	4m fill, and till
35	NETH2	Viergever, 1982	Almere Netherlands	Sq., Conc.	256	9.25	C	*	*	700	q_c, f_s	M	1m fill, 5m clay, and silty sand
36	MILANO	Gambini, 1985	Milano Italy	P, St.	330	10	C	*	*	625	q_c, f_s	E	4m clay, 6m silty sand, and clay
37	OKLA-CO	Neveles and Donald, 1994	Oklahama USA	P, Conc.	660	18.2	C	*	*	3,600	q_c, f_s	E	20 m sand, and silty clay shale
38	OKLA-ST	Neveles and Donald, 1994	Oklahama USA	P, St.	610	18.2	C	*	*	3,650	q_c, f_s	E	20 m sand, and silty clay shale
39	ALABA	Laier, 1994	Alabama USA	HP, St.	310	36.3	C, SML	*	*	2,130	q_c, f_s	E	4m sand, 4m silty clay, and sand
40	SPB	Decourt and Niayama, 1994	Sao Poulo Brazil	Rd., Conc.	500	8.7	C, SML	2,000	1,000	3,000	q_c	E	silty sand

(1) P = Pipe; Sq. = Square; Oct. = Octagonal; HP = H-Section; Rd. = Round; Conc. = Concrete; St. = Steel; b = Diameter; t = Wall Thickness; D = Embedment Length
(2) T = Tension; C = Compression; SML = Slow-Maintained Load; QML = Quick-Maintained Load; R_t = Toe Capacity; R_s = Shaft Capacity; R_u = Total Capacity
(3) q_c = Cone Resistance; f_s = Sleeve Friction; u = Measured Pore Pressure; E = Electrical; M = Mechanical
* Not Measured

Table6.1 Case Records Summary (cont'd)

No.	Case	Site Identification		Pile Data (1)			Loading Test Data (2)				CPT (3)		Soil Profile
		Reference	Location	Shape Mate-rial	Geometry		Type of Test	R_t KN	R_s KN	R_u KN	Data	Type of Cone	
					b, mm	D, m							
41	L&D13A	Tucker and Briaud, 1988	Lock and Dam 26 USA	HP, St.	360	16.5	C, SML	*	*	2,900	q_c, f_s, u	E	sand
42	L&D16	Tucker and Briaud, 1988	Lock and Dam 26 USA	HP, St.	360	16.2	C, SML	*	*	3,600	q_c, f_s, u	E	sand
43	L&D31	Tucker and Briaud, 1988	Lock and Dam 26 USA	P, St.	300	14.2	C, SML	*	*	1,310	q_c, f_s, u	E	sand
44	L&D34	Tucker and Briaud, 1988	Lock and Dam 26 USA	P, St.	350	14.4	C, SML	*	*	1,300	q_c, f_s, u	E	sand
45	L&D37	Tucker and Briaud, 1988	Lock and Dam 26 USA	P, St.	400	14.6	C, SML	*	*	1,800	q_c, f_s, u	E	sand
46	L&D12	Tucker and Briaud, 1988	Lock and Dam 26 USA	HP, St.	360	16.5	T, SML	*	1,170	*	q_c, f_s, u	E	sand
47	L&D314	Tucker and Briaud, 1988	Lock and Dam 26 USA	HP, St.	360	12	T, SML	*	1,170	*	q_c, f_s, u	E	sand
48	L&D21	Tucker and Briaud, 1988	Lock and Dam 26 USA	HP, St.	360	16.8	T, SML	*	1,260	*	q_c, f_s, u	E	sand
49	L&D35	Tucker and Briaud, 1988	Lock and Dam 26 USA	P, St.	350	12.2	T, SML	*	630	*	q_c, f_s, u	E	sand
50	L&D316	Tucker and Briaud, 1988	Lock and Dam 26 USA	HP, St.	360	11.3	T, QML	*	870	*	q_c, f_s, u	E	sand

(1) P = Pipe; Sq. = Square; Oct. = Octagonal; HP = H-Section; Rd. = Round; Conc. = Concrete; St. = Steel; b = Diameter; t = Wall Thickness; D = Embedment Length
(2) T = Tension; C = Compression; SML = Slow-Maintained Load; QML = Quick-Maintained Load; R_t = Toe Capacity; R_s = Shaft Capacity; R_u = Total Capacity
(3) q_c = Cone Resistance; f_s = Sleeve Friction; u = Measured Pore Pressure; E = Electrical; M = Mechanical
* Not Measured

Table 6.1 Case Records Summary (cont'd)

No.	Case	Site Identification		Pile Data (1)			Loading Test Data (2)				CPT (3)		Soil Profile
		Reference	Location	Shape Mate-rial	Geometry		Type of Test	R_t KN	R_s KN	R_u KN	Data	Type of Cone	
					b, mm	D, m							
51	L&D32	Tucker and Briaud, 1988	Lock and Dam 26 USA	P, St.	300	11	T, SML	*	560	*	q_c, f_s, u	E	sand
52	L&D38	Tucker and Briaud, 1988	Lock and Dam 26 USA	P, St.	400	11.1	T, SML	*	945	*	q_c, f_s, u	E	sand
53	L&D315	Tucker and Briaud, 1988	Lock and Dam 26 USA	HP, St.	360	11.3	T, QML	*	817	*	q_c, f_s, u	E	sand
54	SEATW	Horvitz et al. 1986	Seattle USA	Rd., * Conc	350	15.8	C, SML	*	*	900	q_c, f_s, u	E	sand
55	GIT1	Mayne, 1993	Georgia USA	P, ** Conc.	750	16.8	C	*	*	4,500	q_c, f_s	E	2m fill, 17m silty sand, bedrock
56	YOG1	Milovic and Stevanovic, 1982	Yugoslavia	Rd.	520	12	C	*	*	430	q_c	M	clay
57	YOG2	Milovic and Stevanovic, 1982	Yugoslavia	Rd.	520	14.5	C	*	*	700	q_c	M	clay
58	KP1	Weber, 1987	Kallo Belgium	HP, St.	368* 400	14	C, SML	1,000	2,500	3,500	q_c, f_s	E	5m soft soil, and 12 m dense sand
59	MP1	Weber, 1987	Merville France	HP, St.	368* 400	14	C, SML	260	1,925	2,125	q_c, f_s	E	2m soft clay, and stiff clay
60	KLO14A	Van Impe et al. 1988	Kallo Belgium	Rd., Conc.	600	12	C, SML	*	*	5,000	q_c	M	2m peat, 3m clay, and 12m sand

(1) P = Pipe; Sq. = Square; Oct. = Octagonal; HP = H-Section; Rd. = Round; Conc. = Concrete; St. = Steel; b = Diameter; t = Wall Thickness; D = Embedment Length
(2) T = Tension; C = Compression; SML = Slow-Maintained Load; QML = Quick-Maintained Load; R_t = Toe Capacity; R_s = Shaft Capacity; R_u = Total Capacity
(3) q_c = Cone Resistance; f_s = Sleeve Friction; u = Measured Pore Pressure; E = Electrical; M = Mechanical
* Not Measured

Table 6.1 Case Records Summary (cont'd)

No.	Case	Site Identification		Pile Data (1)			Loading Test Data (2)				CPT (3)		Soil Profile
		Reference	Location	Shape Mate-rial	Geometry b, mm	Geometry D, m	Type of Test	R_t KN	R_s KN	R_u KN	Data	Type of Cone	
61	KLO14B	Van Impe et al. 1988	Kallo Belgium	Rd., Conc.	600	11.8	C, SML	*	*	6,100	q_c	M	2m peat, 3m clay, and 12m sand
62	A&N1	Haustorfer and Plesiotis, 1988	Victoria Australia	Sq., Conc.	450	14	C, SML	1,500	2,350	3,850	q_c, f_s	E	5m sand, 7m dense sand, and lime stone
63	A&N2	Haustorfer and Plesiotis, 1988	Victoria Australia	Sq., Conc.	450	13.7	C, SML	1,900	2,350	4,250	q_c, f_s	E	5m sand, 7m dense sand, and lime stone
64	A&N3	Haustorfer and Plesiotis, 1988	Victoria Australia	Sq., Conc.	355	10.2	C, SML	*	*	1,300	q_c, f_s	E	2m silt, 4m sand, and dense sand
65	LTN930	Richmann and Speer, 1988	California USA	Rd., Conc.	400	6.5	C	*	*	1,385	q_c	E	9m silty sand, and sand
66	LTN938	Richmann and Speer, 1988	California USA	Rd., Conc.	400	9.3	C	*	*	1,370	q_c	E	7m silt, and gravelly sand
67	USPB1	Albiero et al. 1995	Sao Poulo Brazil	Rd., * Conc	350	9.4	C, SML	240	405	645	q_c, f_s	E	7m clay and silt, and silty sand
68	USPB2	Albiero et al. 1995	Sao Poulo Brazil	Rd., * Conc.	400	9.4	C, SML	310	415	725	q_c, f_s	E	7m clay and silt, and silty sand
69	PTSER	Apendino, 1981	Porto Tole Italy	Rd., Conc.	508	35.8	C, SML	3,000	2,500	5,500	q_c, f_s	E	30m sandy silt, and dense sand
70	PT361	Apendino, 1981	Porto Tole Italy	Rd., Conc.	508	42	C, SML	2,600	3,400	6,000	q_c, f_s	E	8m silty sand, 23m silty clay, and sand

(1) P = Pipe; Sq. = Square; Oct. = Octagonal; HP = H-Section; Rd. = Round; Conc. = Concrete; St. = Steel; b = Diameter; t = Wall Thickness; D = Embedment Length
(2) T = Tension; C = Compression; SML = Slow-Maintained Load; QML = Quick-Maintained Load; R_t = Toe Capacity; R_s = Shaft Capacity; R_u = Total Capacity
(3) q_c = Cone Resistance; f_s = Sleeve Friction; u = Measured Pore Pressure; E = Electrical; M = Mechanical
* Not Measured

Table 6.1 Case Records Summary (cont'd)

No.	Case	Site Identification		Pile Data (1)			Loading Test Data (2)				CPT (3)		Soil Profile
		Reference	Location	Shape Material	Geometry		Type of Test	R_t KN	R_s KN	R_u KN	Data	Type of Cone	
					b, mm	D, m							
71	N&SWP-B1	Nottingham, 1975	West P. Beach, USA	Sq., Conc.	450	8	C, SML			1,140	q_c, f_s	M	silty sand
72	N&SWP-B2	Nottingham, 1975	West P. Beach, USA	Sq., Conc.	450	11.3	C, SML			830	q_c, f_s	M	silty sand
73	N&SJC1	Nottingham, 1975	Jefferson County, USA	Sq., Conc.	450	9.15	C, SML			1,845	q_c, f_s	M	10m sand, and clay
74	N&SBI-215	Nottingham, 1975	Blount Island, USA	Sq., Conc.	250	21.3	C, SML			810	q_c, f_s	M	13m sand, 5m silty sand
75	N&SBI-316	Nottingham, 1975	Blount Island, USA	Sq., Conc.	350	15.9	C, SML			1,485	q_c, f_s	M	3m fill, 21m silty sand
76	N&SBI-42	Nottingham, 1975	Blount Island, USA	P, St.	270	15.2	C, SML			675	q_c, f_s	M	4m fill, 11m sand, and dense sand
77	N&SBI-43	Nottingham, 1975	Blount Island, USA	P, St.	270	22.5	C, SML			1,620	q_c, f_s	M	4m fill, 14m sand, and dense sand
78	N&SBI-44	Nottingham, 1975	Blount Island, USA	P, St.	270	22.5	T, SML	*	765	*	q_c, f_s	M	4m fill, 14m sand, and dense sand
79	N&SBI-348	Nottingham, 1975	Blount Island, USA	Sq., Conc.	450	14.9	C, SML			1,755	q_c, f_s	M	8m sand, 5m loose sand, and dense sand
80	QBSA	Konrad and Roy, 1987	Quebec Canada	P, St.	220	7.5	C, SML	9	74	83	q_c, u	E	sensitive clay

(1) P = Pipe; Sq. = Square; Oct. = Octagonal; HP = H-Section; Rd. = Round; Conc. = Concrete; St. = Steel; b = Diameter; t = Wall Thickness; D = Embedment Length
(2) T = Tension; C = Compression; SML = Slow-Maintained Load; QML = Quick-Maintained Load; R_t = Toe Capacity; R_s = Shaft Capacity; R_u = Total Capacity
(3) q_c = Cone Resistance; f_s = Sleeve Friction; u = Measured Pore Pressure; E = Electrical; M = Mechanical
* Not Measured

Table 6.1 Case Records Summary (cont'd)

No.	Case	Site Identification		Pile Data (1)			Loading Test Data (2)				CPT (3)		Soil Profile
		Reference	Location	Shape Material	Geometry		Type of Test	R_t KN	R_s KN	R_u KN	Data	Type of Cone	
					b, mm	D, m							
81	UHUC1	O'Neill, 1981 and 1986	Houston, TX USA	P, St.	273	13	C, SML	240	540	780	q_c, f_s	E	8m clay (CL, CH), 6m sandy clay, 4m silt
82	UHUT1	O'Neill, 1981 and 1986	Houston, TX USA	P, St.	273	13	T, SML	*	485	*	q_c, f_s	E	8m clay (CL, CH), 6m sandy clay, 4m silt
83	UHUC11	O'Neill, 1981 and 1986	Houston, TX USA	P, St.	273	13	C, SML	245	555	800	q_c, f_s	E	8m clay (CL, CH), 6m sandy clay, 4m silt
84	UHUT11	O'Neill, 1981 and 1986	Houston, TX USA	P, St.	273	13	T, SML	*	520	*	q_c, f_s	E	8m clay (CL, CH), 6m sandy clay, 4m silt
85	PNTRA5	Almeida et al. 1996	Pentre UK	P, St.	219	25	T, SML	*	190	*	q_c, u	E	4m stiff clay, 21m clayey silt, and clay
86	PNTRA6	Almeida et al. 1996	Pentre UK	P, St.	219	32.5	T, SML	*	460	*	q_c, u	E	4m stiff clay, 21m clayey silt, and clay
87	CWDNC	Almeida et al. 1996	Cowden UK	P, St.	305	10	T, SML	*	400	*	q_c, u	E	5m stiff clay, 5m till, and silty sand
88	CWDND	Almeida et al. 1996	Cowden UK	P, St.	305	10	T, SML	*	404	*	q_c, u	E	5m stiff clay, 5m till, and silty sand
89	CWDNE	Almeida et al. 1996	Cowden UK	P, St.	305	10	T, SML	*	380	*	q_c, u	E	5m stiff clay, 5m till, and silty sand
90	CWDNF	Almeida et al. 1996	Cowden UK	P, St.	305	10	T, SML	*	390	*	q_c, u	E	5m stiff clay, 5m till, and silty sand

(1) P = Pipe; Sq. = Square; Oct. = Octagonal; HP = H-Section; Rd. = Round; Conc. = Concrete; St. = Steel; b = Diameter; t = Wall Thickness; D = Embedment Length
(2) T = Tension; C = Compression; SML = Slow-Maintained Load; QML = Quick-Maintained Load; R_t = Toe Capacity; R_s = Shaft Capacity; R_u = Total Capacity
(3) q_c = Cone Resistance; f_s = Sleeve Friction; u = Measured Pore Pressure; E = Electrical; M = Mechanical
* Not Measured

Table 6.1 Case Records Summary (cont'd)

No.	Case	Site Identification		Pile Data (1)			Loading Test Data (2)				CPT (3)		Soil Profile
		Reference	Location	Shape Material	Geometry		Type of Test	R_t KN	R_s KN	R_u KN	Data	Type of Cone	
					b, mm	D, m							
91	CWDNG	Almeida et al. 1996	Cowden UK	P, St.	203	10	T, SML	*	311	*	q_c, u	E	5m stiff clay, 5m till, and silty sand
92	CWDNH	Almeida et al. 1996	Cowden UK	P, St.	203	10	T, SML	*	350	*	q_c, u	E	5m stiff clay, 5m till, and silty sand
93	CWDNI	Almeida et al. 1996	Cowden UK	P, St.	203	10	T, SML	*	290	*	q_c, u	E	5m stiff clay, 5m till, and silty sand
94	CWDNJ	Almeida et al. 1996	Cowden UK	P, St.	203	10	T, SML	*	280	*	q_c, u	E	5m stiff clay, 5m till, and silty sand
95	CWDNK	Almeida et al. 1996	Cowden UK	P, St.	203	10	T, SML	*	350	*	q_c, u	E	5m stiff clay, 5m till, and silty sand
96	ONSYA1	Almeida et al. 1996	Onsoy Norway	P, St.	219	15	T, SML	*	105	*	q_c, u	E	soft clay
97	ONSYB1	Almeida et al. 1996	Onsoy Norway	P, St.	812	15	T, SML	*	374	*	q_c, u	E	soft clay
98	LSTDA7	Almeida et al. 1996	Lierstranda Norway	P, St.	219	15	T, SML	*	78	*	q_c, u	E	soft clay
99	LSTDA8	Almeida et al. 1996	Lierstranda Norway	P, St.	219	22.5	T, SML	*	86	*	q_c, u	E	soft clay
100	LSTDB2	Almeida et al. 1996	Lierstranda Norway	P, St.	812	15	T, SML	*	444	*	q_c, u	E	soft clay

(1) P = Pipe; Sq. = Square; Oct. = Octagonal; HP = H-Section; Rd. = Round; Conc. = Concrete; St. = Steel; b = Diameter; t = Wall Thickness; D = Embedment Length
(2) T = Tension; C = Compression; SML = Slow-Maintained Load; QML = Quick-Maintained Load; R_t = Toe Capacity; R_s = Shaft Capacity; R_u = Total Capacity
(3) q_c = Cone Resistance; f_s = Sleeve Friction; u = Measured Pore Pressure; E = Electrical; M = Mechanical
* Not Measured

Table 6.1 Case Records Summary (cont'd)

No.	Case	Site Identification		Pile Data (1)			Loading Test Data (2)				CPT (3)		Soil Profile
		Reference	Location	Shape Material	Geometry		Type of Test	R_t KN	R_s KN	R_u KN	Data	Type of Cone	
					b, mm	D, m							
101	PRICOS	Urkkada Ltd., 1996	Puerto Rico USA	P, St.	300	28.4	C			1,240	q_c, f_s, u	E	7m peat, 12m sand, and soft clay
102	PRICOL	Urkkada Ltd., 1996	Puerto Rico USA	P, St.	300	31.4	C			1,690	q_c, f_s, u	E	7m peat, 12m sand, 4m soft clay, and sand
103	A&M5	Briaud and Tucker 1988	Hinds, MS USA	Sq., Conc.	450	8.5	C	*	*	1,330	q_c, f_s	M	clay (CH)
104	A&M6	Briaud and Tucker 1988	Hinds, MS USA	Sq., Conc.	350	6.5	C	*	*	800	q_c, f_s	M	clay (CH)
105	A&M7	Briaud and Tucker 1988	Hinds, MS USA	Sq., Conc.	350	6.7	C	*	*	1,470	q_c, f_s	M	clay (CH)
106	A&M8	Briaud and Tucker 1988	Hinds, MS USA	Sq., Conc.	450	7.6	C	*	*	1,070	q_c, f_s	M	4m clay (CL), and clay (CH)
107	A&M11	Briaud and Tucker 1988	Neshoba, MS USA	Sq., Conc.	350	5.5	C	*	*	1,050	q_c, f_s	M	4.5m clay (CL), and clay (CH)
108	A&M14	Briaud and Tucker 1988	Launderdale, MS, USA	HP, ST.	246* 256	8.5	C	*	*	590	q_c, f_s	M	1.5m clay (CL), and sand
109	A&M16	Briaud and Tucker 1988	Launderdale, MS, USA	HP, ST.	246* 256	9.7	C	*	*	1,070	q_c, f_s	M	5m clay, sand (SM)
110	A&M19	Briaud and Tucker 1988	Neshoba, MS USA	Sq., Conc.	400	8.4	C	*	*	1,240	q_c, f_s	M	6m clay (CL), and clay (CH)

(1) P = Pipe; Sq. = Square; Oct. = Octagonal; HP = H-Section; Rd. = Round; Conc. = Concrete; St. = Steel; b = Diameter; t = Wall Thickness; D = Embedment Length
(2) T = Tension; C = Compression; SML = Slow-Maintained Load; QML = Quick-Maintained Load; R_t = Toe Capacity; R_s = Shaft Capacity; R_u = Total Capacity
(3) q_c = Cone Resistance; f_s = Sleeve Friction; u = Measured Pore Pressure; E = Electrical; M = Mechanical
* Not Measured

Table 6.1 Case Records Summary (cont'd)

No.	Case	Site Identification		Pile Data (1)			Loading Test Data (2)				CPT (3)		Soil Profile
		Reference	Location	Shape Mate-rial	Geometry		Type of Test	R_t KN	R_s KN	R_u KN	Data	Type of Cone	
					b, mm	D, m							
111	A&M20	Briaud and Tucker 1988	Issaquena, MS, USA	Sq., Conc.	400	21	C	*	*	1,330	q_c, f_s	M	2.5m clay (CL), and clay (CH)
112	A&M21	Briaud and Tucker 1988	Launderdale, MS, USA	HP, St.	299* 306	8	C	*	*	470	q_c, f_s	M	2m clay (CH), 5m sand , and clay (CH)
113	A&M22	Briaud and Tucker 1988	Wathhall, MS USA	Sq., Conc.	450	10.3	C	*	*	1,250	q_c, f_s	M	8m sand (SP), and clay (CH)
114	A&M24	Briaud and Tucker 1988	Yazoo, MS USA	Sq., Conc.	400	13.4	C	*	*	1,174	q_c, f_s	M	6m clay (CH), and sand
115	A&M26	Briaud and Tucker 1988	Perry, MS USA	Sq., Conc.	350	8.6	C	*	*	600	q_c, f_s	M	2m sand (SM), 6m sand (SP), and clay
116	A&M30	Briaud and Tucker 1988	Harrison, MS USA	Sq., Conc.	450	15	C	*	*	1,420	q_c, f_s	M	sand (SM)
117	A&M31	Briaud and Tucker 1988	Harrison, MS USA	Sq., Conc.	450	10.4	C	*	*	1,070	q_c, f_s	M	10m silty clay (ML), and clay (CH)
118	A&M32	Briaud and Tucker 1988	Hinds, MS USA	Rd., Conc.	350	10.6	C	*	*	1,160	q_c, f_s	M	clay (CH)
119	A&M33	Briaud and Tucker 1988	Hinds, MS USA	Rd., Conc.	350	8.9	C	*	*	1,170	q_c, f_s	M	clay (CH)
120	A&M34	Briaud and Tucker 1988	Hinds, MS USA	Rd., Conc.	350	6.5	C	*	*	880	q_c, f_s	M	5m clay (CH), and sand

(1) P = Pipe; Sq. = Square; Oct. = Octagonal; HP = H-Section; Rd. = Round; Conc. = Concrete; St. = Steel; b = Diameter; t = Wall Thickness; D = Embedment Length
(2) T = Tension; C = Compression; SML = Slow-Maintained Load; QML = Quick-Maintained Load; R_t = Toe Capacity; R_s = Shaft Capacity; R_u = Total Capacity
(3) q_c = Cone Resistance; f_s = Sleeve Friction; u = Measured Pore Pressure; E = Electrical; M = Mechanical
* Not Measured

Table 6.1 Case Records Summary (cont'd)

No.	Case	Site Identification		Pile Data (1)			Loading Test Data (2)				CPT (3)		Soil Profile
		Reference	Location	Shape Material	Geometry		Type of Test	R_t KN	R_s KN	R_u KN	Data	Type of Cone	
					b, mm	D, m							
121	A&M35	Briaud and Tucker 1988	Hinds, MS USA	Sq., Conc.	400	10.4	C	*	*	1,170	q_c, f_s	M	clay (CH)
122	A&M36	Briaud and Tucker 1988	Hinds, MS USA	Rd., Conc.	350	8.5	C	*	*	720	q_c, f_s	M	clay (CH)
123	A&M38	Briaud and Tucker 1988	Washington, MS, USA	Sq., Conc.	400	11.3	C	*	*	870	q_c, f_s	M	2m clay, and sand (SP)
124	A&M39	Briaud and Tucker 1988	Washington, MS, USA	HP, St.	310* 297	19	C	*	*	1,370	q_c, f_s	M	3m clay, and sand (SP)
125	A&M40	Briaud and Tucker 1988	Washington, MS, USA	Sq., Conc.	350	16	C	*	*	1,070	q_c, f_s	M	3m clay, and sand (SP)
126	A&M41	Briaud and Tucker 1988	Washington, MS, USA	HP, St.	310* 297	12.4	C	*	*	520	q_c, f_s	M	3m clay, and sand (SP)
127	A&M46	Briaud and Tucker 1988	Madison, MS USA	Sq., Conc.	400	11.4	C	*	*	1,140	q_c, f_s	M	5m clay (CH), and sand
128	A&M47	Briaud and Tucker 1988	Hinds, MS USA	Sq., Conc.	400	11.2	C	*	*	1,020	q_c, f_s	M	sand
129	A&M48	Briaud and Tucker 1988	Hinds, MS USA	Sq., Conc.	400	12.5	C	*	*	620	q_c, f_s	M	sand
130	A&M49	Briaud and Tucker 1988	Hinds, MS USA	Sq., Conc.	400	14.7	C	*	*	1,170	q_c, f_s	M	sand

(1) P = Pipe; Sq. = Square; Oct. = Octagonal; HP = H-Section; Rd. = Round; Conc. = Concrete; St. = Steel; b = Diameter; t = Wall Thickness; D = Embedment Length
(2) T = Tension; C = Compression; SML = Slow-Maintained Load; QML = Quick-Maintained Load; R_t = Toe Capacity; R_s = Shaft Capacity; R_u = Total Capacity
(3) q_c = Cone Resistance; f_s = Sleeve Friction; u = Measured Pore Pressure; E = Electrical; M = Mechanical
* Not Measured

Table 6.1 Case Records Summary (cont'd)

No.	Case	Site Identification		Pile Data (1)			Loading Test Data (2)				CPT (3)		Soil Profile
		Reference	Location	Shape Material	Geometry		Type of Test	R_t KN	R_s KN	R_u KN	Data	Type of Cone	
					b, mm	D, m							
131	A&M66	Briaud and Tucker 1988	Jackson, MS USA	Sq., Conc.	350	25	C	*	*	1,560	q_c, f_s	M	5m clay (CH), 11m sand (SM), and clay
132	A&M69	Briaud and Tucker 1988	Jackson, MS USA	Sq., Conc.	400	19.2	C	*	*	1,780	q_c, f_s	M	2m clay, 5m sand, and clay
133	A&M79	Briaud and Tucker 1988	Scott, MS USA	Rd., Conc.	300	11.5	C	*	*	1,320	q_c, f_s	M	clay (CH)
134	A&M81	Briaud and Tucker 1988	Launderdale, MS, USA	HP, St.	299* 306	9	C	*	*	2,100	q_c, f_s	M	5m clay (CL), and silt
135	A&M86	Briaud and Tucker 1988	Hinds, MS USA	Rd., Conc.	355	10.7	C	*	*	1,390	q_c, f_s	M	clay (CH)
136	A&M87	Briaud and Tucker 1988	Hinds, MS USA	Sq., Conc.	400	7.4	C	*	*	640	q_c, f_s	M	clay (CH)
137	A&M90	Briaud and Tucker 1988	Yazoo, MS USA	Sq., Conc.	450	10.7	C	*	*	1,500	q_c, f_s	M	7m clay (CL), and clay (CH)
138	A&M93	Briaud and Tucker 1988	Hinds, MS USA	HP, St.	246* 256	14.5	C	*	*	1,240	q_c, f_s	M	clay (CH)
139	A&M95	Briaud and Tucker 1988	Hinds, MS USA	HP, St.	246* 256	14.7	C	*	*	1,260	q_c, f_s	M	clay (CH)
140	A&M97	Briaud and Tucker 1988	Hinds, MS USA	HP, St.	246* 256	14.7	C	*	*	1,201	q_c, f_s	M	clay (CH)

(1) P = Pipe; Sq. = Square; Oct. = Octagonal; HP = H-Section; Rd. = Round; Conc. = Concrete; St. = Steel; b = Diameter; t = Wall Thickness; D = Embedment Length
(2) T = Tension; C = Compression; SML = Slow-Maintained Load; QML = Quick-Maintained Load; R_t = Toe Capacity; R_s = Shaft Capacity; R_u = Total Capacity
(3) q_c = Cone Resistance; f_s = Sleeve Friction; u = Measured Pore Pressure; E = Electrical; M = Mechanical
* Not Measured

Table 6.1 Case Records Summary (cont'd)

No.	Case	Site Identification		Pile Data (1)			Loading Test Data (2)				CPT (3)		Soil Profile
		Reference	Location	Shape Material	Geometry		Type of Test	R_t KN	R_s KN	R_u KN	Data	Type of Cone	
					b, mm	D, m							
141	A&M1	Briaud and Tucker 1988	Smith, MS USA	Sq., Conc.	400	8.8	C	*	*	1,140	q_c, f_s	M	4m clay (CL), and sand
142	A&M4	Briaud and Tucker 1988	Hinds, MS USA	Rd., Conc.	350	12.5	C	*	*	1,100	q_c, f_s	M	clay (CH)

(1) P = Pipe; Sq. = Square; Oct. = Octagonal; HP = H-Section; Rd. = Round; Conc. = Concrete; St. = Steel; b = Diameter; t = Wall Thickness; D = Embedment Length
(2) T = Tension; C = Compression; SML = Slow-Maintained Load; QML = Quick-Maintained Load; R_t = Toe Capacity; R_s = Shaft Capacity; R_u = Total Capacity
(3) q_c = Cone Resistance; f_s = Sleeve Friction; u = Measured Pore Pressure; E = Electrical; M = Mechanical
* Not Measured

Table 6.2 Summary of case histories site locations

No.	Country	Site Location	Sources	No. of Cases	Total No. of Cases
1	USA	Mississippi (13 sites)	1	40	
		St. Louis	1	13	
		Florida (4 sites)	2	12	
		Louisiana (5 sites)	1	10	
		California (3 sites)	3	6	
		Texas (2 sites)	2	5	
		Puerto Rico	1	2	
		Oklahoma	1	2	
		Evanston	1	2	
		Georgia	1	1	
		Alabama	1	1	
		Washington	1	1	
		Milwaukee	1	1	96
2	UK	Pentre	1	2	
		Cowden	1	9	11
3	Canada	British Columbia	1	4	
		Quebec	1	1	5
4	Norway	Onsoy	1	2	
		Lierstranda	1	3	5
5	Japan	Noto Island	1	3	3
6	Taiwan	* (Not specified)	1	3	3
7	Belgium	Kallo	2	3	3
8	Australia	Barwon, Broken River	1	3	3
9	Brazil	Sao Paulo	2	3	3
10	Italy	Milano	1	1	
		Porto Tole	1	2	3
11	Yugoslavia	* (Not specified)	1	2	2
12	Iraq	Baghdad	1	2	2
13	Netherlands	Holland	2	2	2
14	France	Merville	1	1	1
$\sum$Countries = 14		$\sum$Sites = 53	$\sum$Sources = 37	$\sum$Cases = 142	

Table 6.3 Back-calculated β and N_t coefficients

No.	Case #	Name	Soil Layers	β	N_t	β/N_t %
1	2	UBC3	soft clay	0.25		
			sand	0.43	34	1.26
2	3	UBC5	soft clay	0.25		
			sand	0.30		
			silt	0.25	10	2.50
3	5	NWUP	sand	0.70		
			clay	0.14-0.35	2.3	10.00
4	6	NWUH	sand	0.70		
			clay	0.14-0.35	2.3	10.00
5	7	FHWASF	sand	0.35	75	0.47
6	8	BGHD1	silty sand	0.40		
			sand	0.65	31	2.10
7	9	BGHD2	silty sand	0.50		
			sand	0.70	35	2.00
8	10	POLA1	silt	0.30		
			sand	0.30	55	0.55
9	11	POLA2	sand		40	
10	15	TWNTP4	silt	0.35		
			clay	0.25		
			sand	0.40	20	2.00
11	16	TWNTP5	silt	0.30		
			clay	0.20		
			sand	0.35		*
12	17	TWNTP6	silt	0.30		
			clay	0.20		
			sand	0.40	22	1.82
13	40	SPB	sand	0.85	60	1.42
14	47	L&D314	sand	0.54		*
15	49	L&D35	sand	0.44		*
16	50	L&D316	sand	0.45		*
17	51	L&D32	sand	0.47		*
18	52	L&D38	sand	0.34		*
19	53	L&D315	sand	0.42		*
20	63	A&N2	loose sand	0.70		
			dense sand	0.90		
			lime stone	1.00	60	1.67
21	67	USPB1	sand	0.28	25	1.12
22	68	USPB2	sand	0.31	20	1.55
23	69	PTSER	silt	0.35		
			sand	0.40	40	1.00
24	70	PT361	silty sand	0.30		
			silty clay	0.25		
			silty sand	0.35		
			sand	0.40	41	0.98
25	78	N&SBI44	sand	0.40		

Table 6.3 Back-calculated β and N_t coefficients (Cnt'd)

No.	Case #	Name	Soil Layers	β	N_t	β/N_t %
26	80	QBSA	soft clay	0.40	4	10.00
27	81	UHUC1	stiff clay	0.50		
			sand	0.60	27	2.22
28	82	UHUT1	stiff clay	0.50		
			sand	0.60		*
29	83	UHUC11	stiff clay	0.50		
			sand	0.65	27	2.41
30	84	UHUT11	stiff clay	0.50		
			sand	0.55		*
31	85	PNTRA5	clayey silt	0.15		*
32	86	PNTRA6	clay	0.27		*
33	87	CWDNC	stiff clay	0.40		
			silty sand	0.40		*
34	89	CWDNE	stiff clay	0.38		
			silty sand	0.38		*
35	90	CWDNF	stiff clay	0.39		
			silty sand	0.39		*
36	91	CWDNG	stiff clay	0.46		
			silty sand	0.46		*
37	92	CWDNH	stiff clay	0.51		
			silty sand	0.51		*
38	93	CWDNI	stiff clay	0.43		
			silty sand	0.43		*
39	94	CWDNJ	stiff clay	0.42		
			silty sand	0.42		*
40	95	CWDNK	stiff clay	0.51		
			silty sand	0.51		*
41	96	ONSYA1	soft clay	0.25		*
42	97	ONSYB1	soft clay	0.29		*
43	98	LSTDA7	soft clay	0.15		*
44	99	LSTDA8	soft clay	0.09		*
45	100	LSTDB2	soft clay	0.20		*

* Tension Tests

Table 6.4 Summary of case histories information

No.	Criteria	Category	Number of Cases	Total Number
1	Type of pile loading test	Compression	113	
		Tension	29	142
2	Pile Construction	Driven	125	
		Bored	17	142
3	Pile shape	Pipe	52	
		Square	44	
		Round	23	
		H-Section	20	
		Octagonal	2	
		Triangle	1	142
4	Pile material	Steel	72	
		Concrete	70	142
5	Soil type along pile	Silt and Sand	40	
		Clay	44	
		Layers of clay, silt, and sand	58	142
6	Cone type	Electrical	81	
		Mechanical	61	
7	CPT measurements	q_c, f_s, u	28	
		q_c, u	17	
		q_c, f_s	96	
		q_c	11	142

Table 8.1 Comparison of pile unit toe resistance and effective cone resistance

No.	Case #	Name	Measured Unit Toe Resistance, r_t, MPa	Geometric Average of Effective Cone Resistance, q_E, MPa	Ratio of r_t to q_E, $C_t = r_t/q_E$
1	2	UBC3	3.84	3.53	1.09
2	3	UBC5	2.20	2.56	0.86
3	5	NWUP	0.39	0.36	1.08
4	7	FHWASF.	6.02	6.06	0.99
5	8	BGHD1	4.44	4.10	1.08
6	9	BGHD2	5.93	6.45	0.92
7	10	POLA1	13.15	14.70	0.89
8	11	POLA2	11.85	11.55	1.03
9	15	TWNTP4	5.50	7.26	0.76
10	17	TWNTP6	5.67	5.67	1.00
11	63	A&N2	9.36	10.05	0.93
12	80	QBSA	0.24	0.24	0.99
13	81	UHUC1	4.07	3.95	1.03
14	83	UHUC11	4.15	3.89	1.07
					13.72
					Average = 0.98
					Standard
					Deviation = 0.09

Table 8.2 Comparison of measured pile unit shaft resistance and effective cone resistance

No.	Case #	Name	Soil Layers Along Pile	Measured Unit Shaft Resistance r_s, MPa	Effective Cone Resistance Average q_E, MPa	Ratio of r_s to q_E, $C_s = r_s/q_E$, %
1	2	UBC3	sensitive clay	0.019	0.22	8.64
			sand	0.042	8.18	0.51
2	3	UBC5	sensitive clay	0.019	0.24	7.92
			sand	0.037	10.80	0.34
3	5	NWUP	sand	0.062	15.49	0.40
			clay	0.020	0.36	5.56
4	7	FHWASF	sand	0.025	5.18	0.48
5	8	BGHD1	silty sand	0.051	3.80	1.34
6	9	BGHD2	silty sand	0.065	5.27	1.23
7	10	POLA1	silt	0.040	3.44	1.16
			sand	0.080	14.80	0.54
8	15	TWNTP4	silty sand	0.045	5.17	0.87
			clay	0.027	0.50	5.40
			sand	0.060	10.50	0.57
9	17	TWNTP6	silt	0.045	5.40	0.83
			clay	0.025	0.45	5.56
			sand	0.060	13.00	0.46
10	63	A&N2	sand	0.075	21.00	0.36
11	80	QBSA	sensetive clay	0.014	0.19	7.37
12	81	UHUC1	stiff clay	0.048	2.09	2.30
13	83	UHUC11	stiff clay	0.050	2.21	2.25
14	16	TWNTP5	silt	0.045	4.70	0.96
			clay	0.024	0.52	4.62
			sand	0.052	13.20	0.39
15	47	L&D314	sand	0.066	10.97	0.60
16	49	L&D35	sand	0.051	10.80	0.47
17	50	L&D316	sand	0.053	10.88	0.49
18	51	L&D32	sand	0.054	10.80	0.50
19	52	L&D38	sand	0.051	11.20	0.46
20	53	L&D315	sand	0.050	10.88	0.46
21	78	N&SBI44	silt-sand	0.037	7.60	0.49
22	82	UHUT1	stiff clay	0.043	2.09	2.06
23	84	UHUT11	stiff clay	0.047	2.21	2.13

Table 8.3 Proposed shaft correlation coefficients, C_s, for different soil types

Soil Type	**C_s Approximation**
Very soft clay and soft sensitive soils	8.0 %
Soft clay	5.0 %
Stiff clay, and mixture of clay and silt	2.5 %
Mixture of silt and sand	1.0 %
Sand, Gravelly sand	0.4 %

Table 8.4 Measured and estimated pile capacity (KN) for 24 cases including 14 compression and 10 tension tests by the proposed method

No.	Case #	Name	Proposed Method			Test		
			Toe	Shaft	Total	Toe	Shaft	Total
Compression Tests								
1	2	UBC3	291	339	630	315	315	630
2	3	UBC5	186	950	1136	180	920	1100
3	5	NWUP	57	877	934	62	958	1020
4	7	FHWASF	355	148	503	355	135	490
5	8	BGHD1	334	710	1044	360	640	1000
6	9	BGHD2	524	1015	1539	480	1120	1600
7	10	POLA1	4521	1449	5970	4050	1405	5455
8	11	POLA2	3542			3650		
9	15	TWNTP4	2112	2678	4790	1600	2730	4330
10	17	TWNTP6	1652	2691	4343	1650	2810	4460
11	63	A&N2	2305	1958	4263	1900	2356	4256
12	80	QBSA	9	78	87	9	74	83
13	81	UHUC1	232	418	650	240	540	780
14	83	UHUC11	227	532	759	245	555	800
Tension Tests								
15	16	TWNTP5		2516			2500	
16	47	L&D314		958			1170	
17	49	L&D35		686			630	
18	50	L&D316		922			870	
19	51	L&D32		568			560	
20	52	L&D38		784			945	
21	53	L&D315		921			817	
22	78	N&SBI44		878			765	
23	82	UHUT1		418			485	
24	84	UHUT11		532			520	

Table 8.5 Relative error (%) in pile capacity estimation for 24 cases including 14 compression and 10 tension tests by the proposed method

No.	Case #	Name	Capacity		
			Toe	Shaft	Total
Compression Tests					
1	2	UBC3	-8	8	0
2	3	UBC5	3	3	3
3	5	NWUP	-8	-8	-8
4	7	FHWASF	0	10	3
5	8	BGHD1	-7	11	4
6	9	BGHD2	9	-9	-4
7	10	POLA1	12	3	9
8	11	POLA2	-3		
9	15	TWNTP4	32	-2	11
10	17	TWNTP6	0	-4	-3
11	63	A&N2	21	-17	0
12	80	QBSA	0	5	5
13	81	UHUC1	-3	-23	-17
14	83	UHUC11	-7	-4	-5
Tension Tests					
15	16	TWNTP5			1
16	47	L&D314			-18
17	49	L&D35			9
18	50	L&D316			6
19	51	L&D32			1
20	52	L&D38			-17
21	53	L&D315			13
22	78	N&SBI44			15
23	82	UHUT1			-14
24	84	UHUT11			2

Table.9.1 Measured and estimated pile capacity (KN) for Type I Cases by methods

No.	Case #	Name	Schmertmann	de Ruiter	French	Meyerhof	Tumay	Proposed	TEST
1	1	UBC2	141	253	217		651	244	290
2	2	UBC3	431	562	633		997	630	630
3	3	UBC5	825	871	1053	1001		1136	1100
4	4	UBCA	6714	5015	6902	6741		9510	7500
5	5	NWUP	933	1207	902		835	934	1020
6	6	NWUH	971	1212	903		825	933	1010
7	7	FHWASF	326	337	421	535		503	490
8	8	BGHD1	549	376	665	593		1044	1000
9	9	BGHD2	1039	730	1226	1066		1539	1600
10	10	POLA1	5260	4570	4342	4918		5970	5455
11	11	POLA2	4600	4600	3038	3917		3542	3650
12	12	JPNOT1	3318	3625	4475	4007		5145	4700
13	15	TWNTP4	3612	3680	3152	3805		4790	4330
14	17	TWNTP6	3410	3694	3402	4184		4343	4460
15	18	LSUA1	1116	556	1030	1050		880	900
16	20	LSUN11	1474	3117	2063		3287	3046	2950
17	21	LSUN15	1053	2267	1177		2365	2201	2800
18	22	LSUN28	974	1795	1187		2246	1832	2160
19	23	LSUN215	834	1390	858		1729	1469	1710
20	27	LSUR30	2384	2592	2187		2765	2943	2610
21	31	LTN741	9144	6688	9396	3185		8115	7830
22	32	LTN484	234	384	407	210		678	750
23	33	LTN742	6124	6725	5639	3327		7145	5850
24	35	NETH2	272	513	398		438	794	700
25	36	MILANO	504	677	538		449	700	625
26	37	OKLACO	2774	2649	4211	4378		4183	3600
27	43	L&D31	1545	1300	1054	1523		1635	1310
28	54	SEATW	1027	621	1011	349		1153	900
29	55	GIT1	4104	2551	3057	1257		4753	4500
30	58	KP1	1546	3438	2654	1923		2717	3500
31	59	MP1	1280	2237	1106		1345	1743	2125
32	60	KALO14A	5798	5948	3086	1955		6237	5500
33	61	KALO14B	5798	5948	3578	5305		6237	6100
34	63	A&N2	2887	2229	2802	3289		3993	4250
35	64	A&N3	1334	1106	1241	1410		1596	1300
36	67	USPB1	401	274	405	398		689	645
37	68	USPB2	488	345	478	491		817	725
38	71	N&SWPB1	1036	977	883	901		1021	1140
39	72	N&SWPB2	568	482	1079	1054		978	830
40	77	N&SBI43	1442	1190	1114	1475		1611	1620
41	79	N&SBI348	1333	1027	2239	2268		1747	1720
42	80	QBSA	134	81	57			87	83
43	81	UHUC1	500	813	422		548	650	780
44	83	UHUC11	516	958	433		569	760	800
45	101	PRS	654	885	630		1028	957	1240
46	102	PRL	969	1424	1307		1409	1579	1690

Table.9.2 Measured and estimated pile capacity (KN) for Type II Cases by methods

No.	Case #	Name	Schmertmann	de Ruiter	French	Meyerhof	Tumay	Proposed	TEST
1	13	JPNOT2	2903	3010	3989	3314		3971	3190
2	14	JPNOT3	2903	3010	3989	3314		3971	3250
3	19	LSUB12	3816	4991	3995		4431	4242	3960
4	24	LSUN216	1068	2325	1117		2345	2383	1890
5	25	LSUH1	1111	2666	1382		2412	2483	1935
6	26	LSUR24	1795	1976	1668		2069	2205	2025
7	28	UFL22	1632	1198	1978	1441		1623	1350
8	29	UFL52	1849	2232	3200	2883		2983	2070
9	30	UFL53	908	765	1643	1016		1149	1260
10	34	MUMB	1214	2906	831		1318	1512	1686
11	38	OKLAST	3006	3053	3561	4769		4868	3650
12	39	ALABA	3182	2539	2655	2925		2543	2130
13	40	SPB	2009	1845	1476	799		2721	3000
14	41	L&D13A	3136	2697	2151	3247		3560	2900
15	42	L&D16	3102	2660	2053	3163		3445	3600
16	44	L&D34	1959	1688	1373	2009		2089	1300
17	45	L&D37	2254	1963	1740	2569		2616	1800
18	46	L&D12	834	588	1230	1037		1406	1170
19	48	L&D21	824	1007	2087	1506		1802	1260
20	56	YOG1	687	356	355			388	430
21	57	YOG2	1206	781	627			795	700
22	62	A&N1	3043	2360	2430	3323		3779	3850
23	65	LTN930	1157	1073	990	491		1651	1385
24	66	LTN938	1519	1286	1933	886		1786	1370
25	69	PTSER	4933	4059	4284	5277		6018	5500
26	70	PT361	4773	4213	3697			4885	6000
27	73	N&SJC1	2263	2024	2645	1742		2848	1845
28	74	N&SBI215	825	597	1263	1066		1042	810
29	75	N&SBI316	1022	915	1441	1236		1517	1485
30	76	N&SBI42	531	400	644	765		917	660
31	85	PNTRA5	203	200	129			228	190
32	86	PNTRA6	208	215	140			420	460
33	87	CWDNC	350	458	239			438	400
34	88	CWDND	350	458	239			438	404
35	89	CWDNE	350	458	239			438	380
36	90	CWDNF	350	458	239			438	390
37	91	CWDNG	238	305	159			292	311
38	92	CWDNH	238	305	159			292	350
39	93	CWDNI	238	305	159			292	290
40	94	CWDNJ	238	305	159			292	280
41	95	CWDNK	238	305	159			292	350
42	96	ONSYA1	152	56	89			100	105
43	97	ONSYB1	553	207	331			373	444
44	98	LSTDA7	155	64	96			83	78
45	99	LSTDA8	160	78	106			55	86
46	100	LSTDB2	567	236	356			309	374

Table.9.3 Measured and estimated pile capacity (KN) for Type III Cases by methods

No.	Case #	Name	Schmertmann	de Ruiter	French	Meyerhof	Tumay	Proposed	TEST
1	103	A&M5	1195	2019	1022		2054	1447	1330
2	104	A&M6	445	703	405		895	521	800
3	105	A&M7	853	1412	760		1278	1092	1470
4	106	A&M8	1197	2015	989		1927	1593	1070
5	107	A&M11	835	1834	910		1192	1303	1050
6	108	A&M14	251	186	294	298		468	590
7	109	A&M16	1062	527	460	613		931	1070
8	110	A&M19	1197	2245	1414		1814	1500	1240
9	111	A&M20	1163	2466	1545		1810	1655	1330
10	112	A&M21	423	1116	545		770	497	470
11	113	A&M22	843	1194	1116	1925		1305	1250
12	114	A&M24	1773	1357	1613	1955		1562	1174
13	115	A&M26	614	452	840	1421		1033	600
14	116	A&M30	221	1294	1984	2073		2223	1420
15	117	A&M31	977	1762	827		1650	1063	1070
16	118	A&M32	1165	2310	814		1577	1586	1160
17	119	A&M33	1070	2057	727		1451	1449	1170
18	120	A&M34	1233	1266	693		1455	1133	880
19	121	A&M35	1140	1760	921		1710	1320	1170
20	122	A&M36	638	1007	566		1183	813	720
21	123	A&M38	1804	1183	1693	987		1326	870
22	124	A&M39	839	709	898	965		1435	1370
23	125	A&M40	1600	1095	1907	2071		1391	1070
24	126	A&M41	503	470	561	648		487	520
25	127	A&M46	1668	1803	1248	1877		1686	1140
26	128	A&M47	1473	1024	1886	1859		1609	1020
27	129	A&M48	860	540	975	980		904	620
28	130	A&M49	1191	738	1288	1196		1029	1170
29	131	A&M66	1988	1867	2486	2721		1880	1560
30	132	A&M69	866	1055	930	1724		1741	1780
31	133	A&M79	1077	1612	627		1257	1038	1320
32	134	A&M81	1800	894	1190	1149		1968	2100
33	135	A&M86	884	1692	780		1316	1160	1390
34	136	A&M87	656	973	685		973	749	640
35	137	A&M90	1550	2173	1482		2210	1873	1500
36	138	A&M93	564	1046	551		1006	1165	1240
37	139	A&M95	597	1232	586		1005	1347	1260
38	140	A&M97	704	1261	925		1041	1376	1201
39	141	A&M1	1094	886	1474	1727		1562	1140
40	142	A&M4	848	1577	740		1387	1140	1100

Table 9.4 Measured and estimated pile capacity (KN) for 24 cases including 14 compression and 10 tension tests

No.	Case #	Name	Schmertmann	de Ruiter	French	Meyerhof	Tumay	Proposed	TEST
Toe Resistance									
1	2	UBC3	238	238	347		238	291	315
2	3	UBC5	137	137	83	219		186	180
3	5	NWUP	94	45	50		94	57	62
4	7	FHWASF	267	267	209	460		355	355
5	8	BGHD1	215	215	158	351		334	360
6	9	BGHD2	430	430	350	616		524	480
7	10	POLA1	3849	3849	2876	3837		4521	4050
8	11	POLA2*	4600	4600	3038	3917		3542	3650
9	15	TWNTP4	1570	1570	1229	1830		2112	1600
10	17	TWNTP6	1177	1177	1215	1977		1652	1650
11	63	A&N2	1220	1220	940	1916		2305	1900
12	80	QBSA	14	7	8			9	9
13	81	UHUC1	214	118	109		214	232	240
14	83	UHUC11	175	125	104		175	227	245
Shaft Resistance									
	2	UBC3	193	324	286		759	339	315
	3	UBC5	688	734	970	782		950	920
	5	NWUP	839	1162	852		741	877	958
	7	FHWASF	59	70	212	75		148	135
	8	BGHD1	334	161	507	242		710	640
	9	BGHD2	609	300	876	450		1015	1120
	10	POLA1	1411	721	1466	1081		1449	1405
	15	TWNTP4	2042	2110	1923	1975		2678	2730
	17	TWNTP6	2233	2517	2187	2207		2691	2810
	63	A&N2	1667	1009	1862	1373		1958	2356
	80	QBSA	120	74	49			78	74
	81	UHUC1	286	495	313		334	418	540
	83	UHUC11	341	833	330		394	532	555
Tension Test									
15	16	TWNTP5	1517	1807	1896	2192		2516	2500
16	47	L&D314	538	380	788	714		958	1170
17	49	L&D35	388	270	558	517		686	630
18	50	L&D316	525	360	742	689		922	870
19	51	L&D32	328	227	468	433		568	560
20	52	L&D38	433	309	637	591		784	945
21	53	L&D315	525	360	742	689		921	817
22	78	N&SBI44	513	361	778	720		878	765
23	82	UHUT1	200	521	313		334	418	485
24	84	UHUT11	239	624	330		394	532	520

* shaft resistance was not measured

Table 9.5 Relative error (%) in pile capacity estimation by different methods

DESCRIPTION / METHOD	ERROR		24 cases used for calibration: 14 Compression Tests: Toe	24 cases used for calibration: 14 Compression Tests: Shaft	24 cases used for calibration: 14 Compression Tests: Total	24 cases used for calibration: 10 Tension Tests	24 cases used for calibration: 24 cases Total	Type I 46 cases	Type II 46 cases	Type III 40 cases	Type I and Type II 67*** cases	Type I, Type II, and Type III 142 cases
Schmertmann	Strict	*m* *	-7	-25	-17	-45	-29	-22	0	-7	-14	-12
		SD**	31	31	29	9	27	27	35	37	34	34
	Absolute	*m*	26	-35	30	45	36	29	28	28	31	30
		SD	16	18	15	9	15	19	21	25	21	21
European	Strict	*m*	-23	-22	-15	-42	-26	-17	-8	20	-16	-6
		SD	20	37	27	31	32	22	27	48	25	38
	Absolute	*m*	26	34	25	47	34	23	23	41	24	30
		SD	15	26	18	21	22	16	16	31	17	24
French	Strict	*m*	-33	-14	-24	-21	-23	-22	-11	-6	-24	-14
		SD	20	26	14	13	13	21	35	42	24	33
	Absolute	*m*	34	25	24	21	23	27	31	36	30	31
		SD	18	16	14	12	13	15	18	22	16	19
Meyerhof	Strict	*m*	13	-37	-13	-21	-17	-19	2	31	-21	-1
		SD	13	18	17	12	15	30	34	51	30	40
	Absolute	*m*	14	37	17	21	19	29	25	49	29	32
		SD	11	18	13	12	12	21	20	32	22	25
Tumay	Strict	*m*	-3	13	-5	-28	-12	-3	8	31	-5	13
		SD	37	86	42	5	35	41	19	32	41	38
	Absolute	*m*	29	58	34	28	32	28	17	38	29	32
		SD	17	56	17	5	14	29	10	22	29	24
Proposed	Strict	*m*	3	-2	-1	0	-1	2	11	15	0	8
		SD	12	11	7	12	9	13	21	25	14	21
	Absolute	*m*	8	8	6	10	7	11	19	24	11	17
		SD	9	6	4	7	6	8	14	18	8	14

* *m* = Mean

** SD = Standard Deviation

*** 46 cases of Type I and 21 cases of Type II which failed

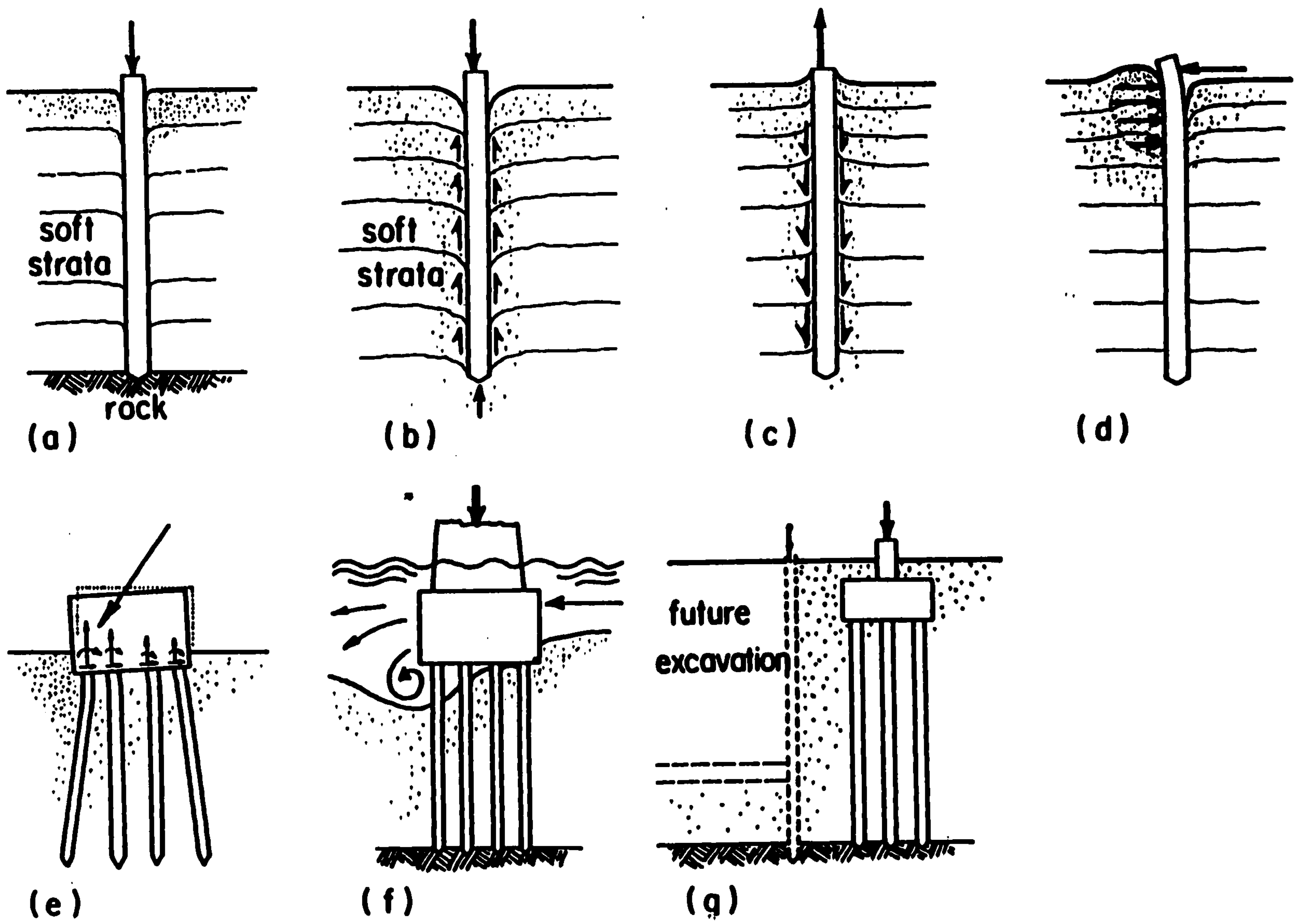

Fig. 2.1 Situation in which piles may be driven (after Vesic, 1977)

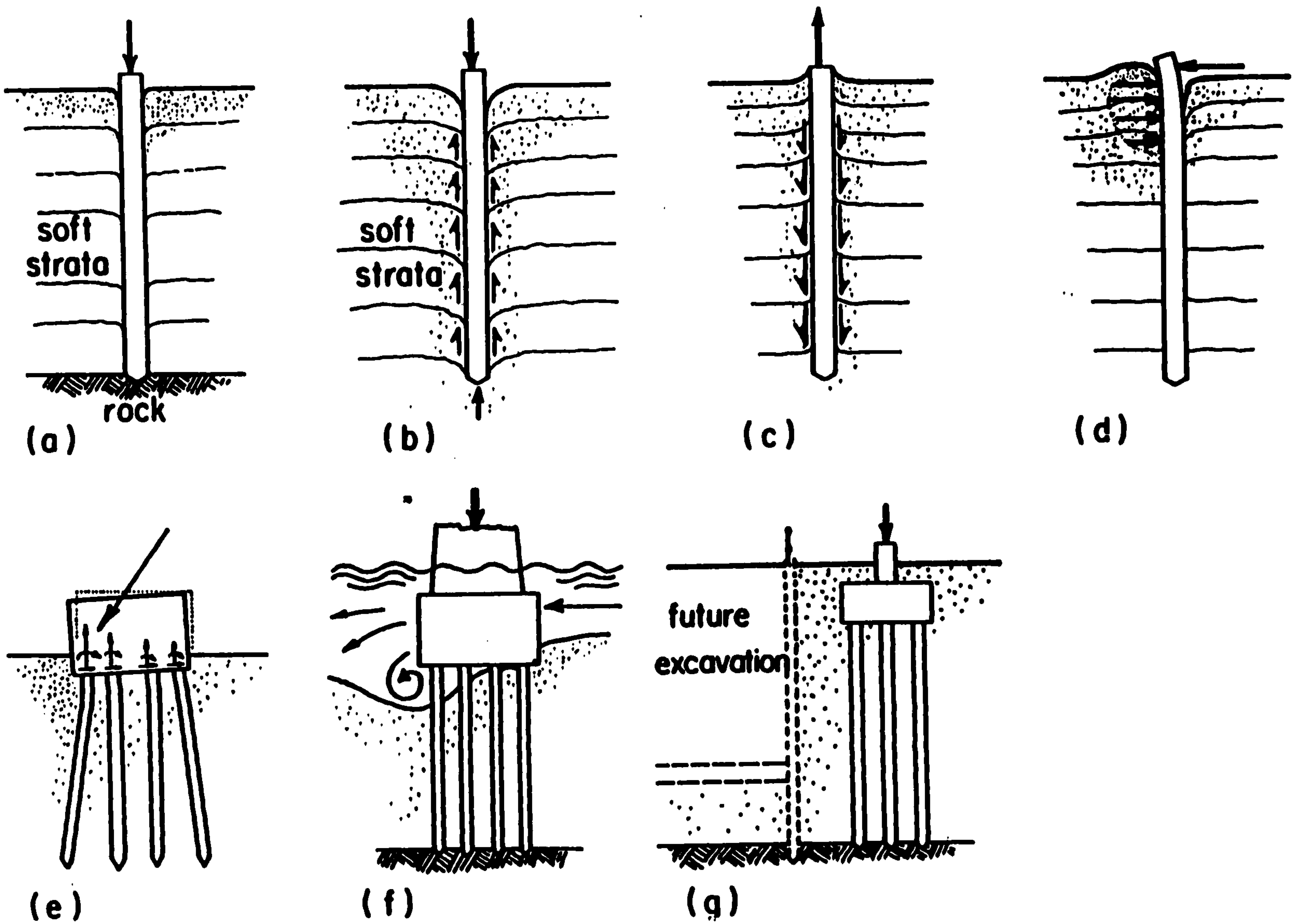

Fig. 2.1 Situation in which piles may be driven (after Vesic, 1977)

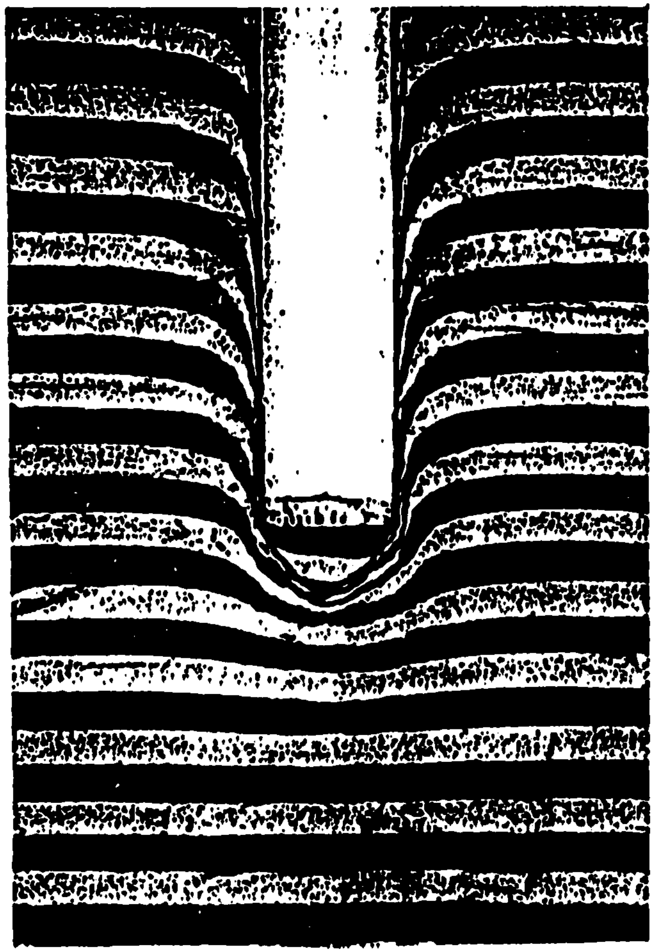
(a)

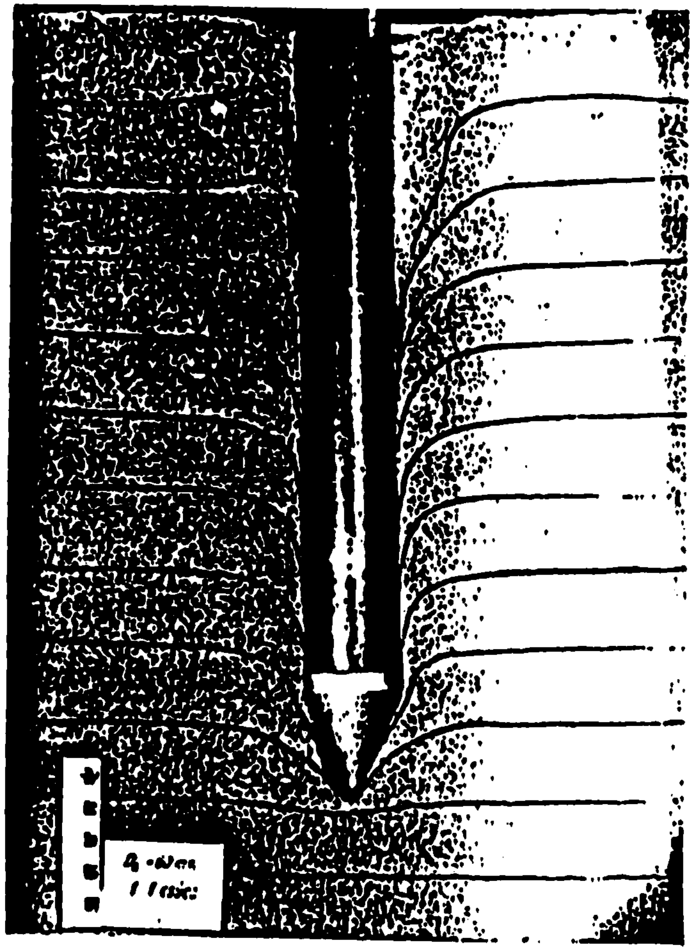
(b)

Fig. 2.2 Failure pattern under pile toe in (a) soft clay (after Rourk, 1961), (b) dense sand (after Ladanyi, 1961)

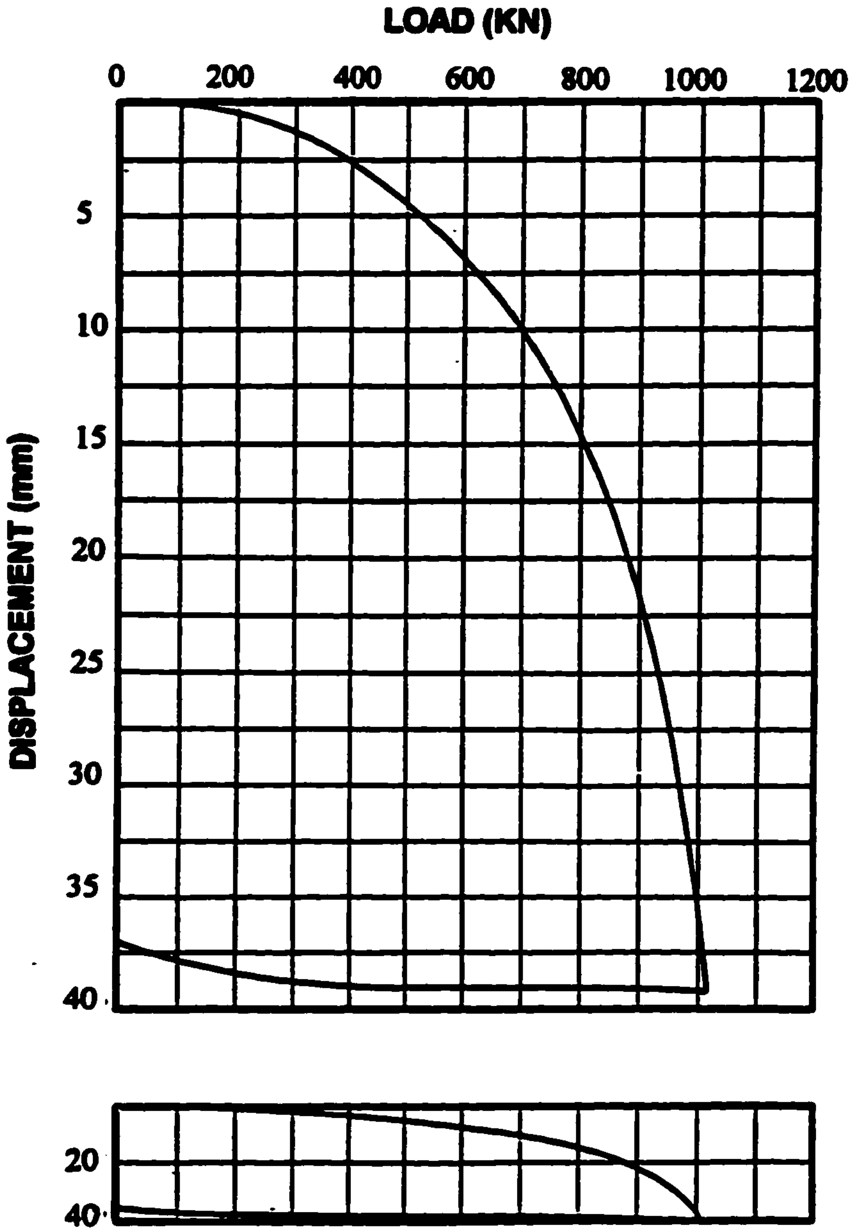

Fig. 2.3 Load-displacement diagram of a test pile drawn in two different scales (data from Van der Veen, 1953)

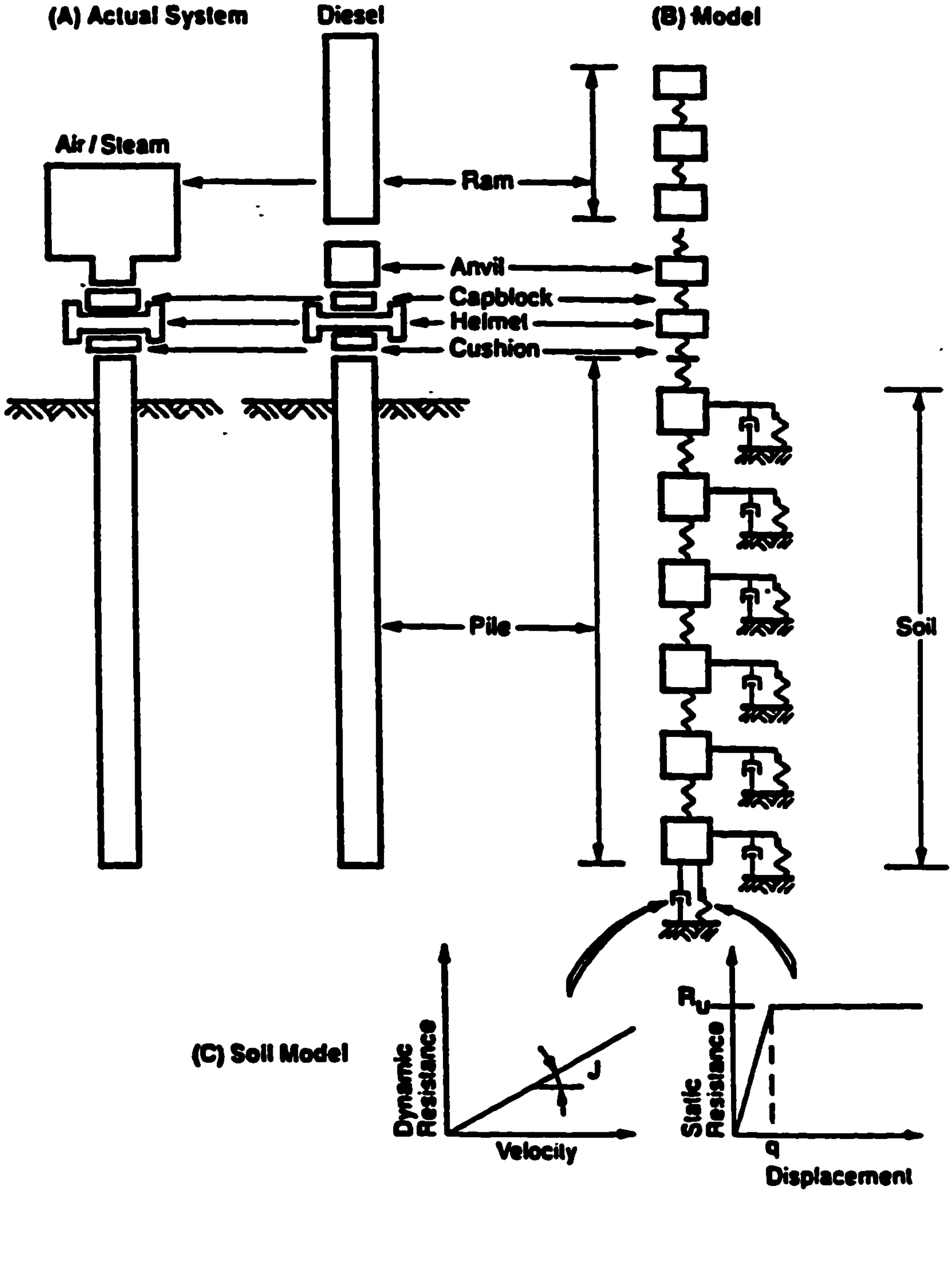

Fig. 2.4 Discrete-elements of the pile-soil system (after Smith, 1960)

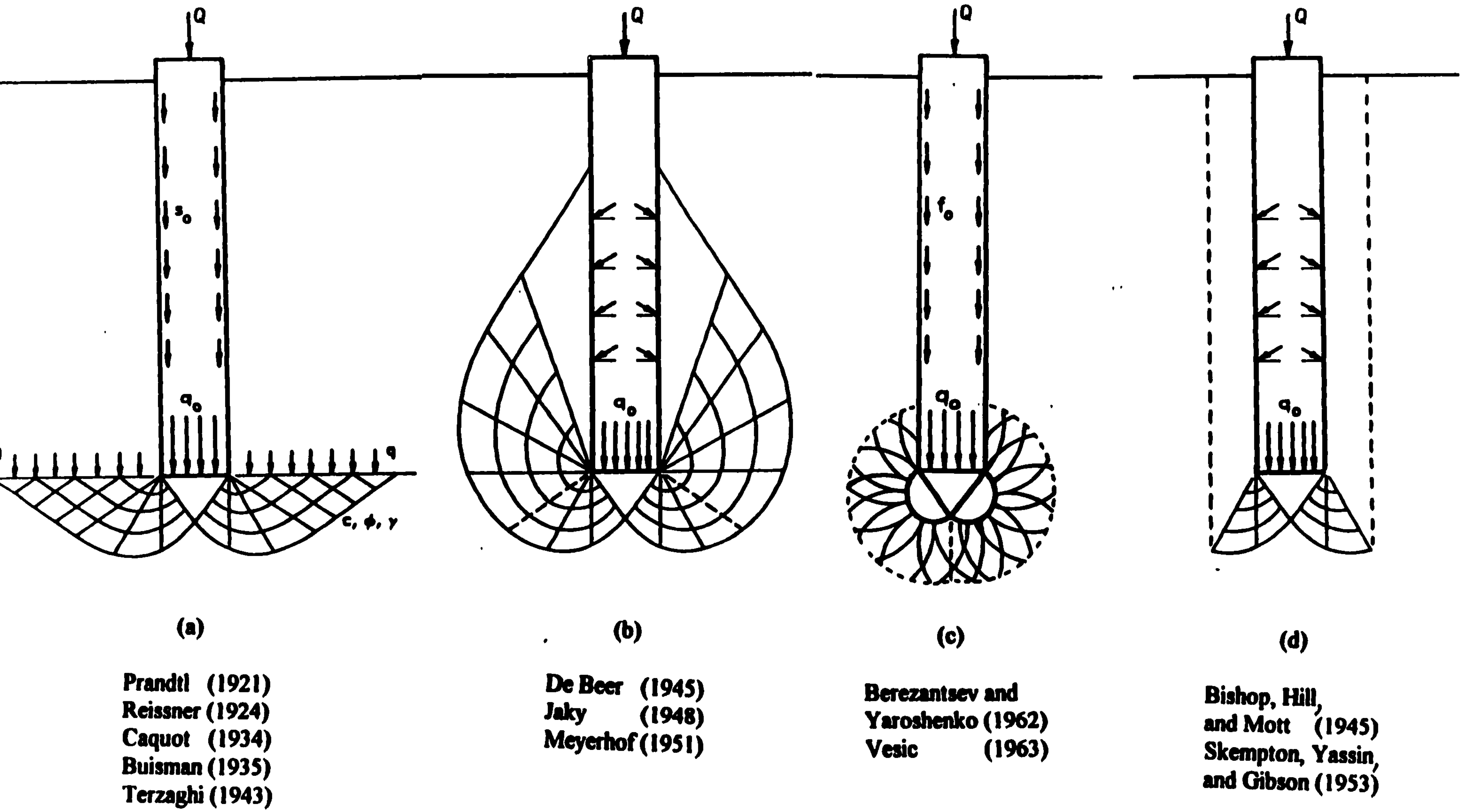

Fig. 2.5 Assumed failure mechanism under pile foundations (after Vesic, 1967)

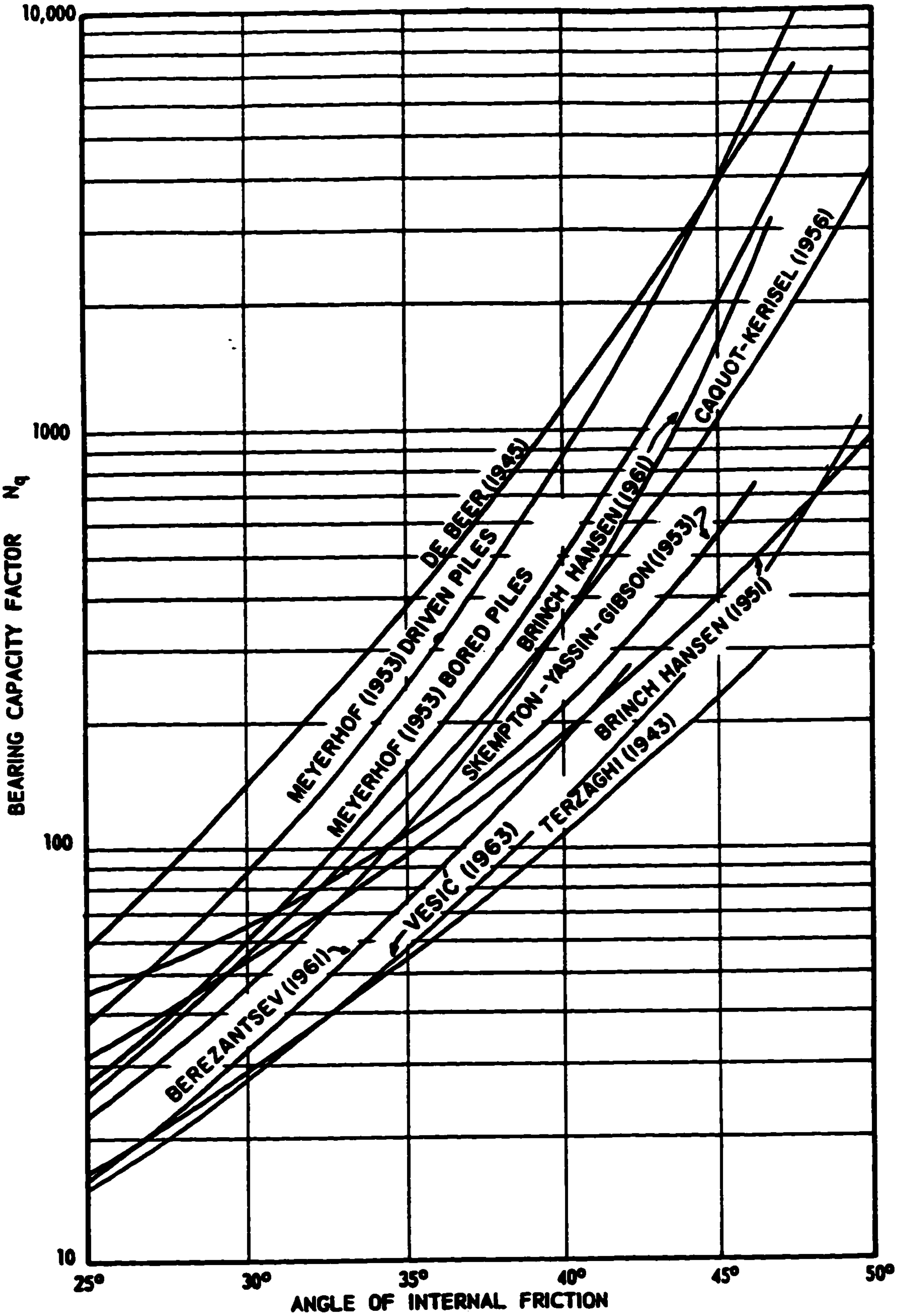

Fig. 2.6 Bearing capacity factor for deep circular foundations (after Vesic, 1964)

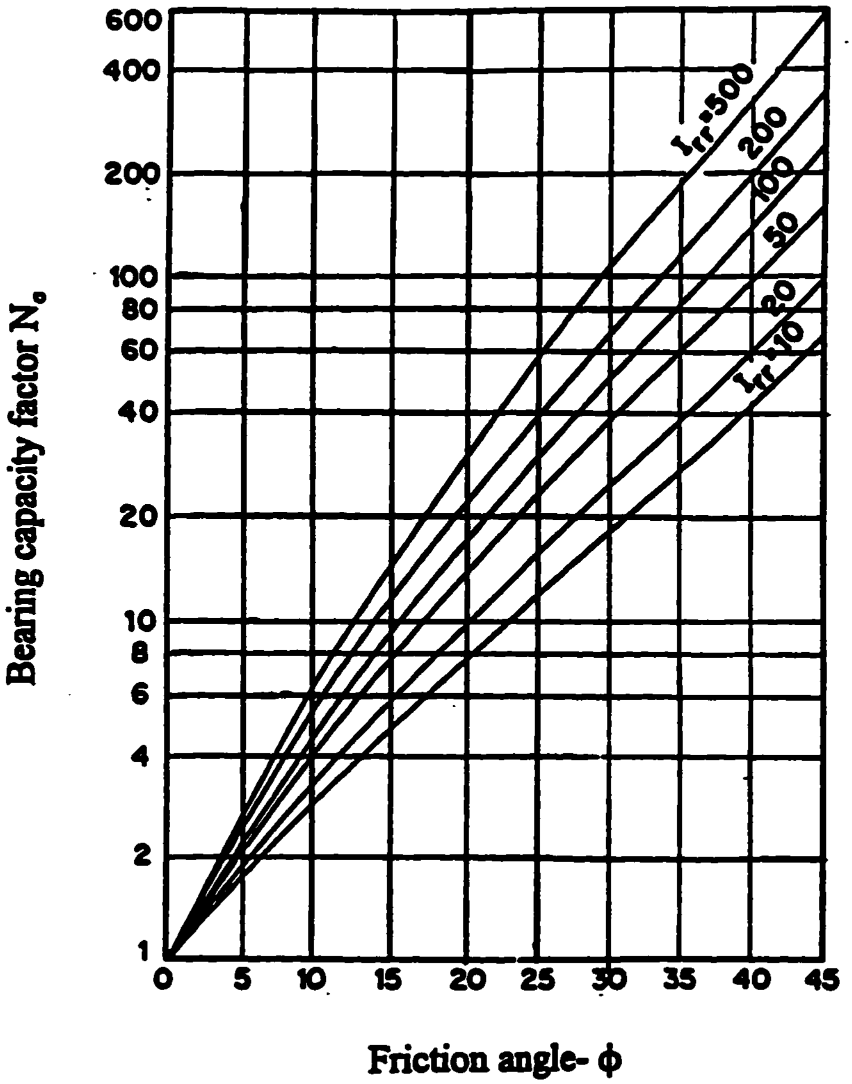

Fig. 2.7 Variation of bearing capacity factor with I_{rr} and ϕ angle (after Vesic, 1977)

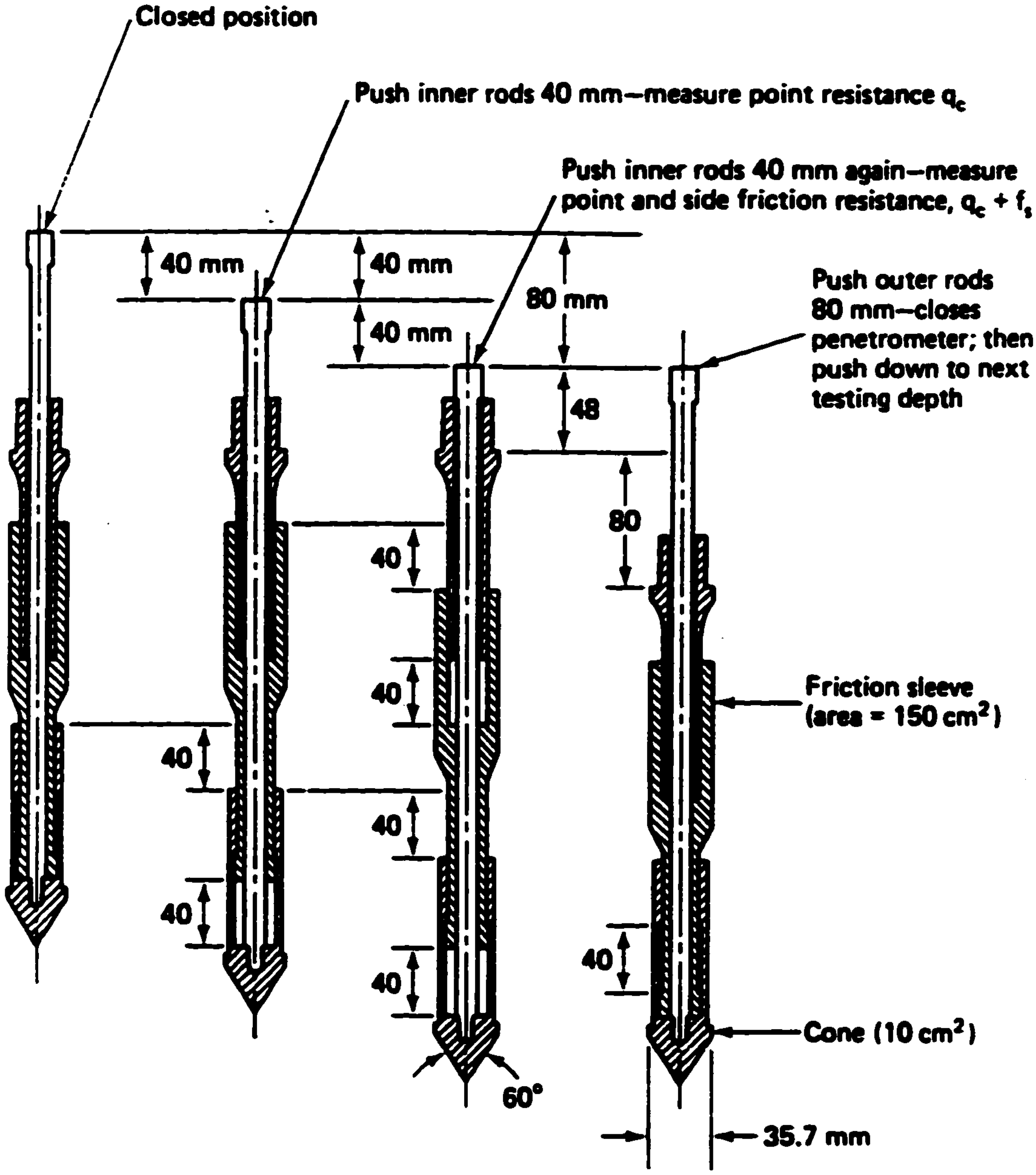

Fig. 3.1 Mechanical Friction-Cone Penetrometer (after Begemann, 1953)

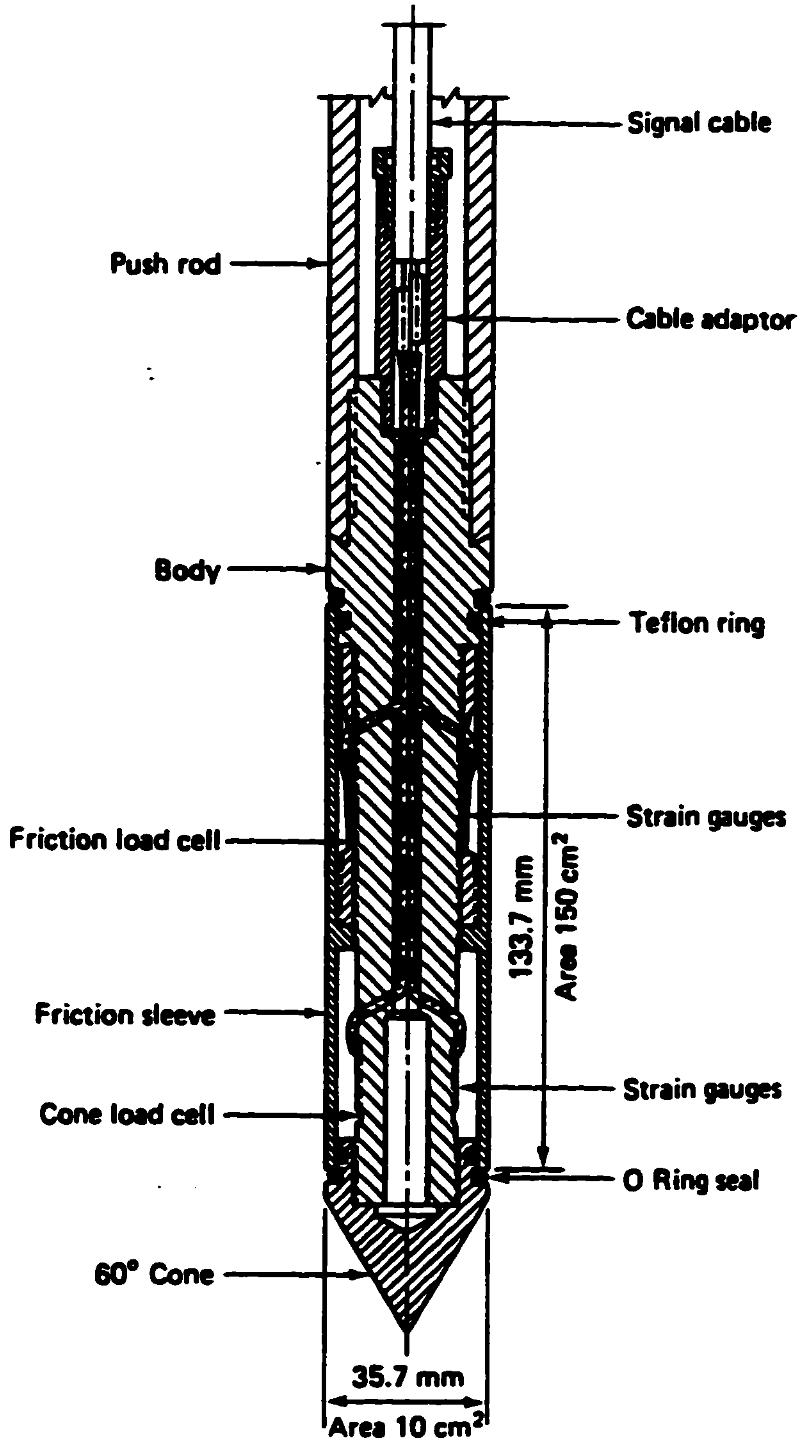

Fig. 3.2 Electrical Friction-Cone Penetrometer (after Holden, 1971)

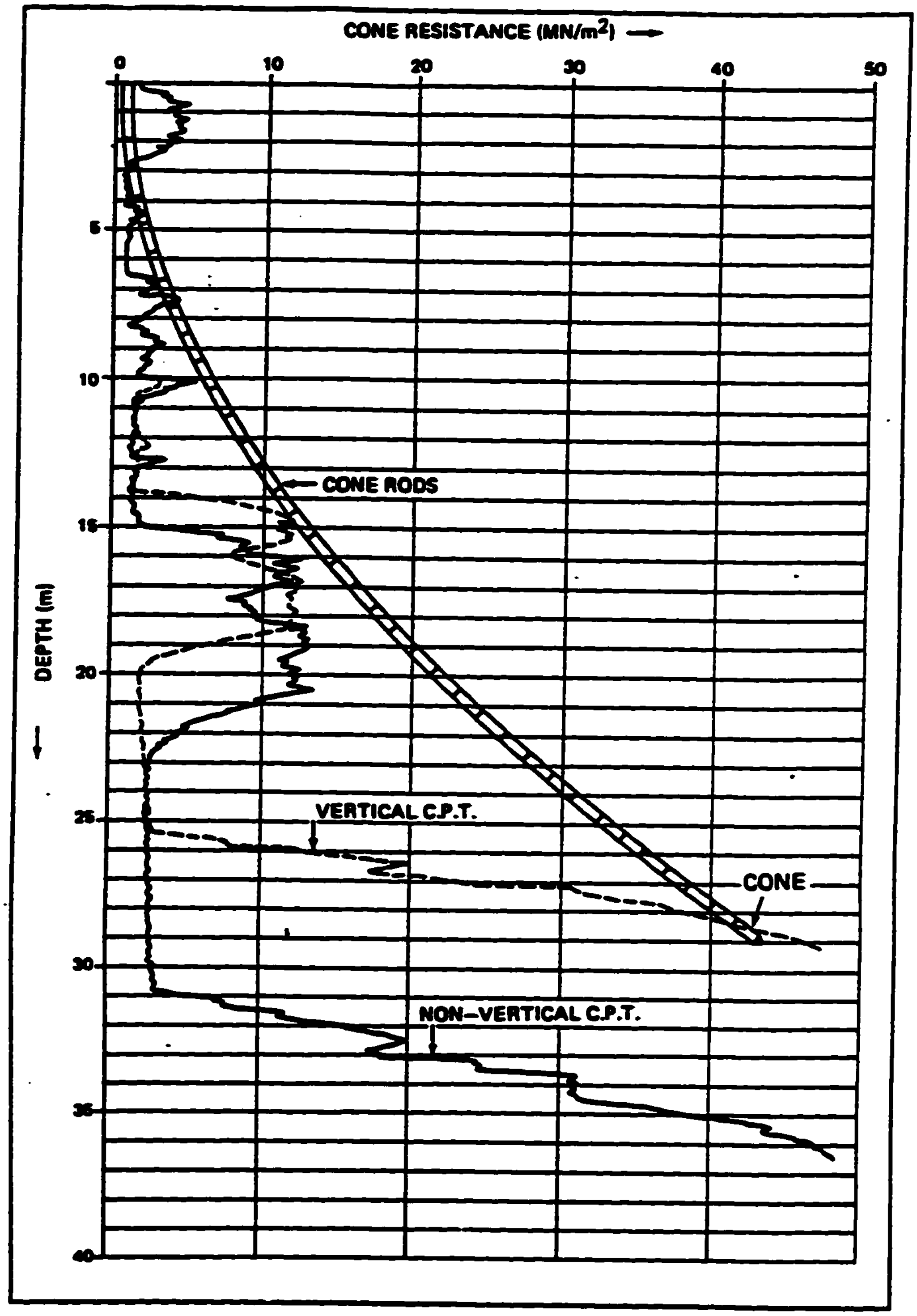

Fig. 3.3 Comparison of curved and vertical CPT (from de Ruiter, 1981)

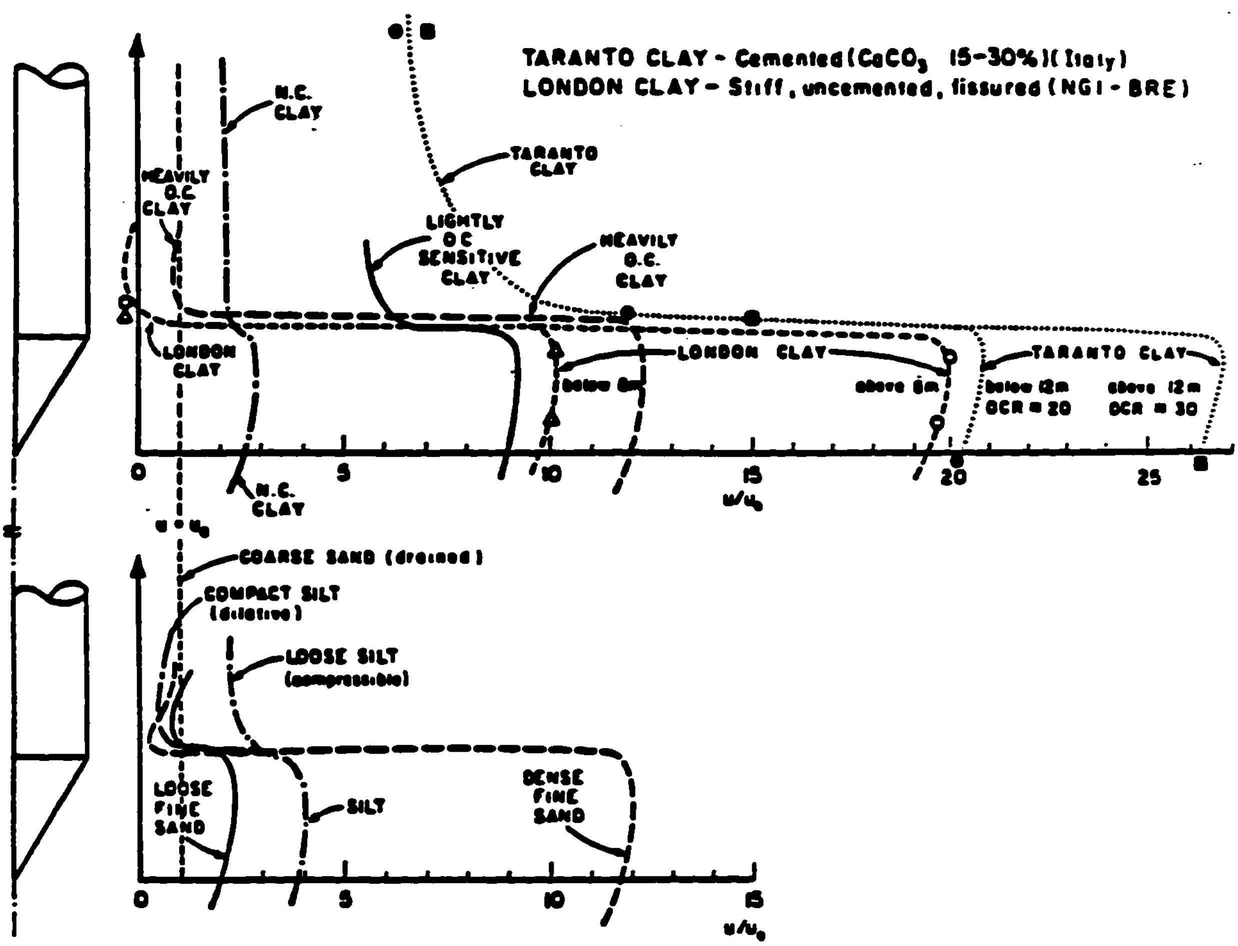

Fig. 3.4 Conceptual pore pressure distribution in saturated soil during CPT based on field measurements (after Robertson, 1986)

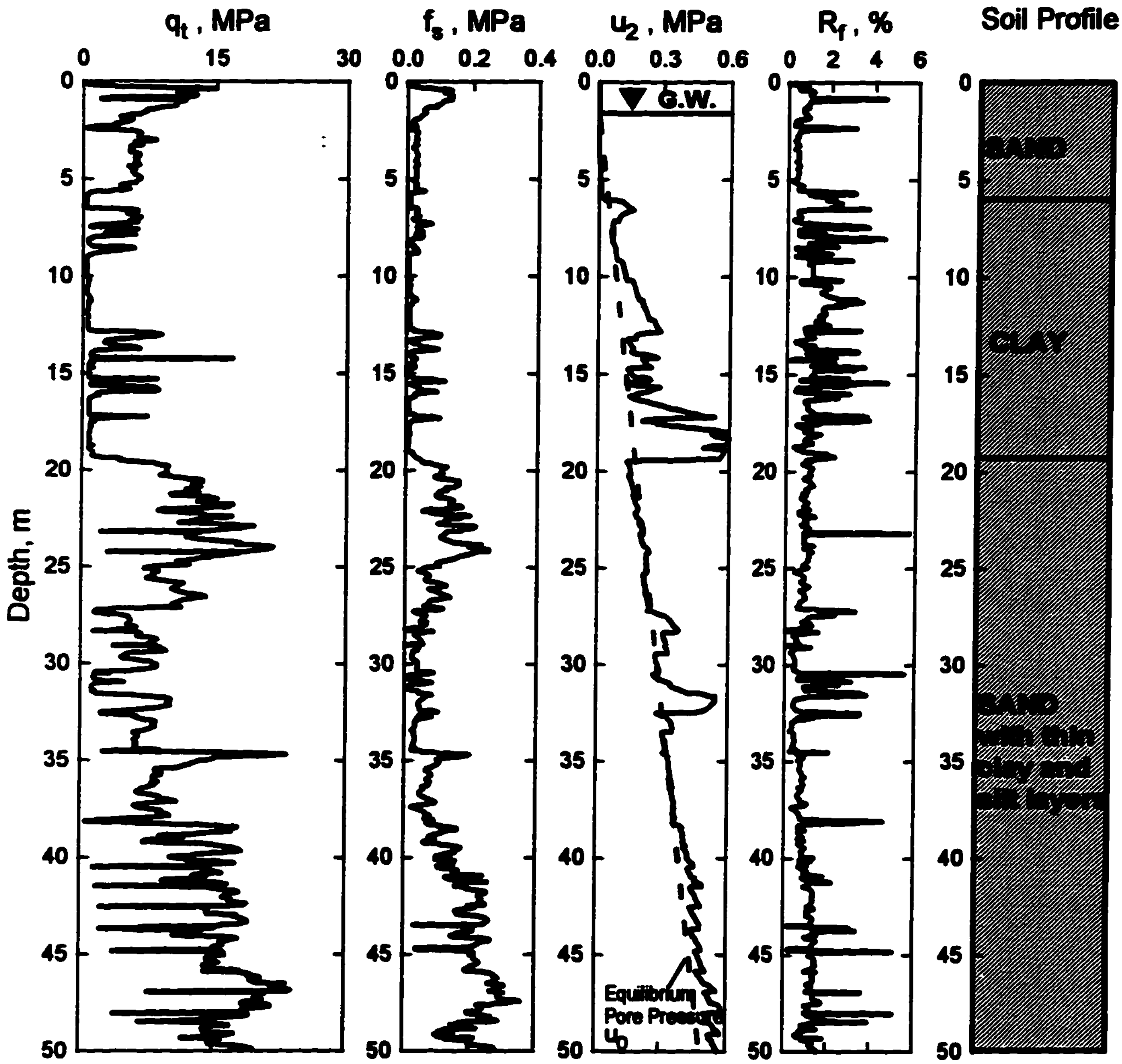

Fig. 3.5 Typical piezocone profile and interpreted soil profile using CPTu data (data from Yen et al., 1989)

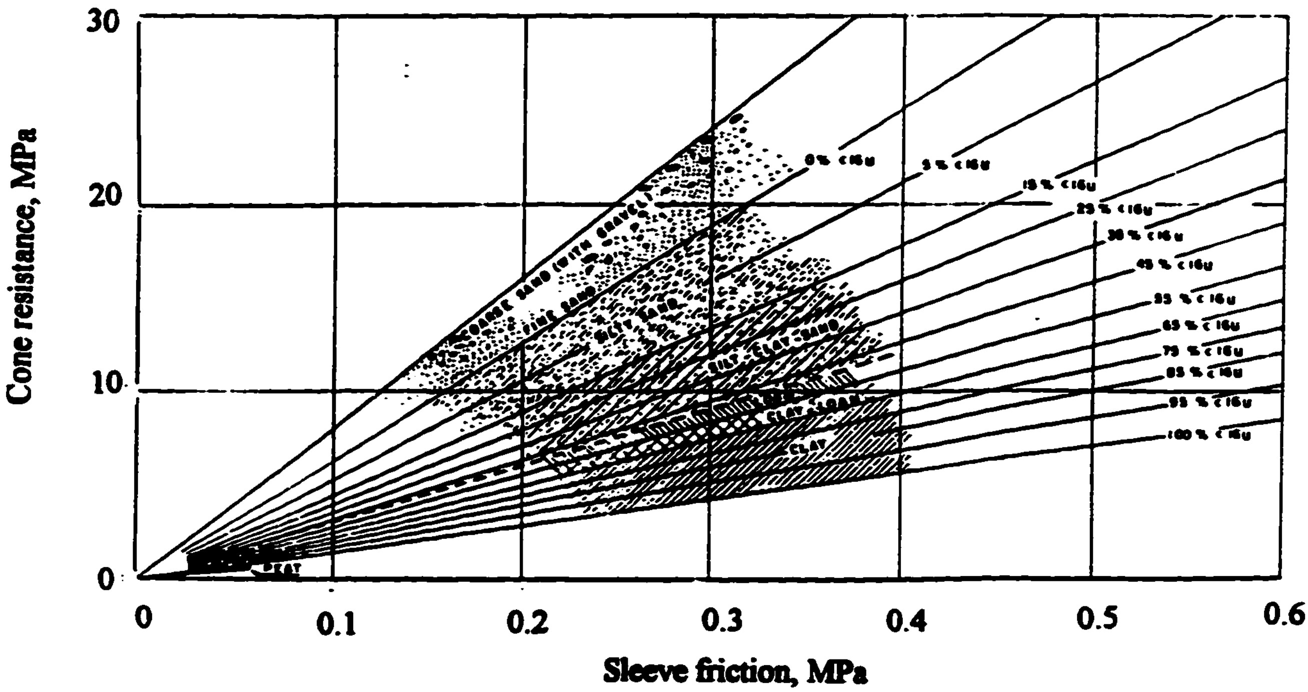

Fig. 3.6 Relationship between cone resistance, sleeve friction, and soil type (after Begemann, 1965)

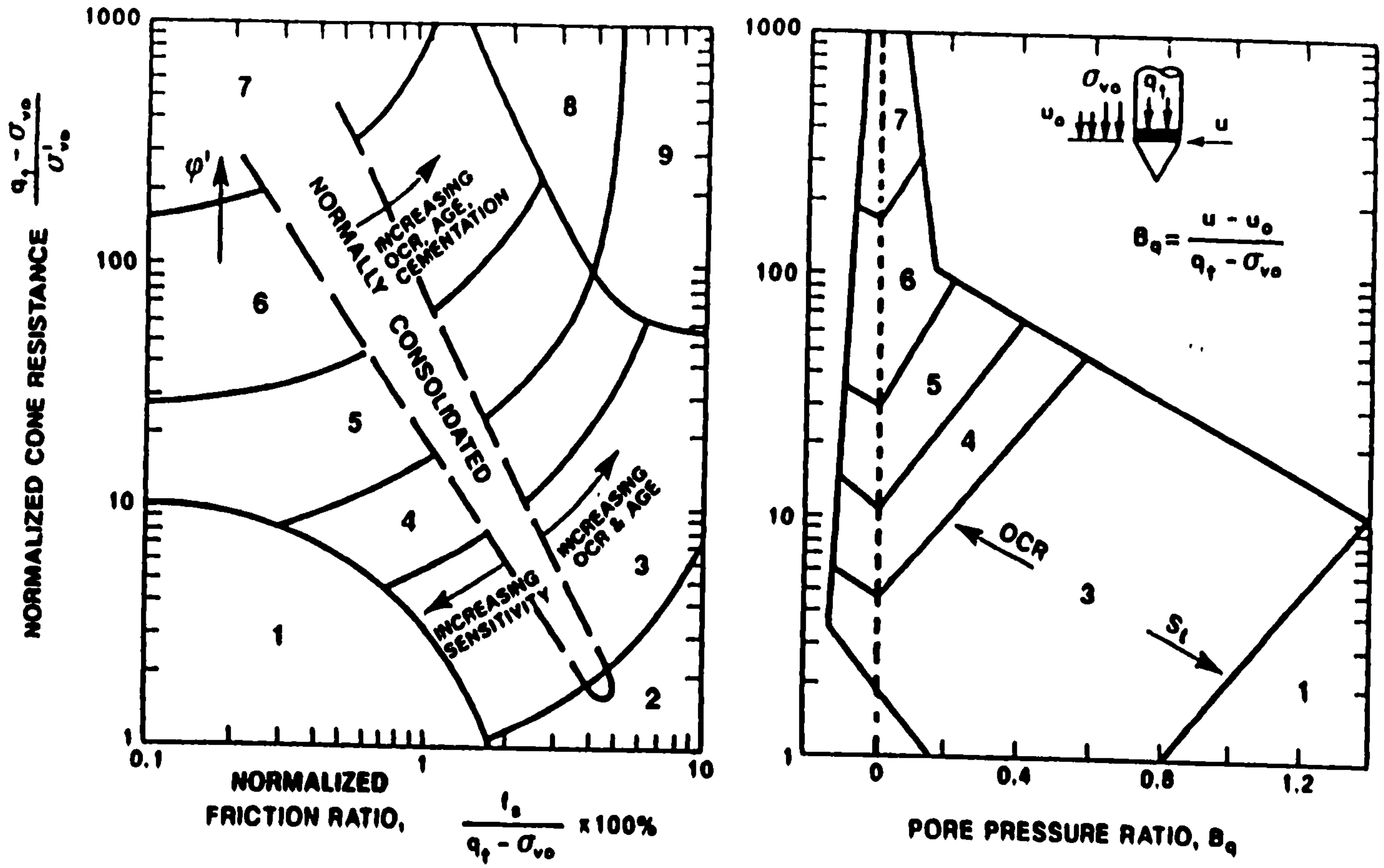

1. SENSITIVE, FINE GRAINED
2. ORGANIC SOILS – PEATS
3. CLAYS – CLAY TO SILTY CLAY
4. SILT MIXTURES – CLAYEY SILT TO SILTY CLAY
5. SAND MIXTURES – SILTY SAND TO SANDY SILT
6. SANDS – CLEAN SAND TO SILTY SAND
7. GRAVELLY SAND TO SAND
8. VERY STIFF SAND TO CLAYEY* SAND
9. VERY STIFF, FINE GRAINED*

(*) HEAVILY OVERCONSOLIDATED OR CEMENTED

Fig.3.7 Soil classification chart based on normalized CPTu data (after Robertson, 1990)

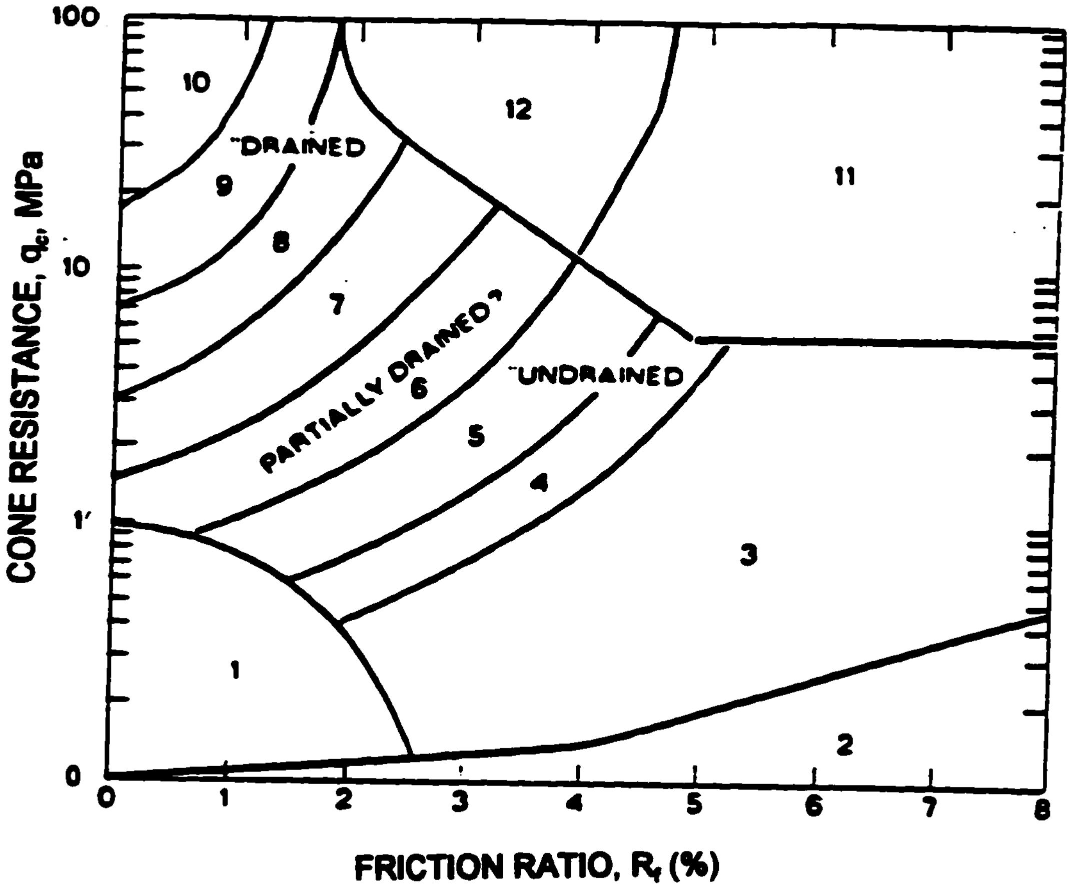

Zone	q_c/N	Soil Behaviour Type
1)	2	sensitive fine grained
2)	1	organic material
3)	1	clay
4)	1.5	silty clay to clay
5)	2	clayey silt to silty clay
6)	2.5	sandy silt to clayey silt
7)	3	silty sand to sandy silt
8)	4	sand to silty sand
9)	5	sand
10)	6	gravelly sand to sand
11)	1	very stiff fine grained (*)
12)	2	sand to clayey sand (*)

(*) overconsolidated or cemented

Fig. 3.8 Simplified soil classification chart based on CPT data (after Robertson et al., 1986; from CPTINT program, Campanella, 1993)

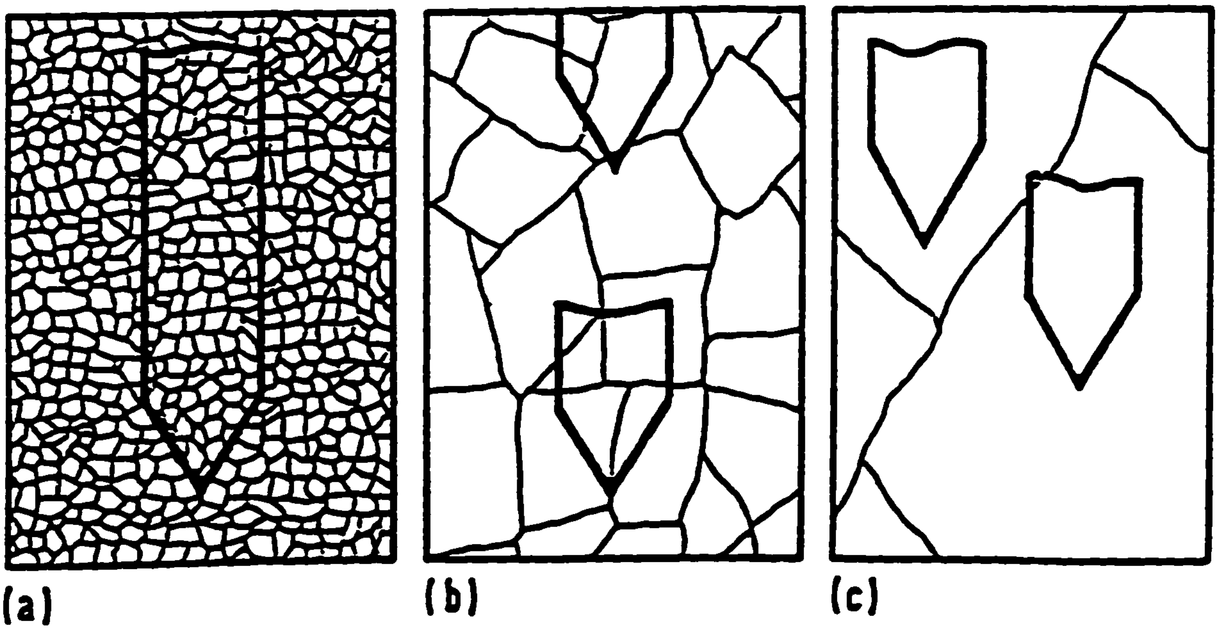

Fig. 3.9 Fissure patterns in OC clays related to scale of cone penetrometer tip (from Marsland and Quaterman, 1982)

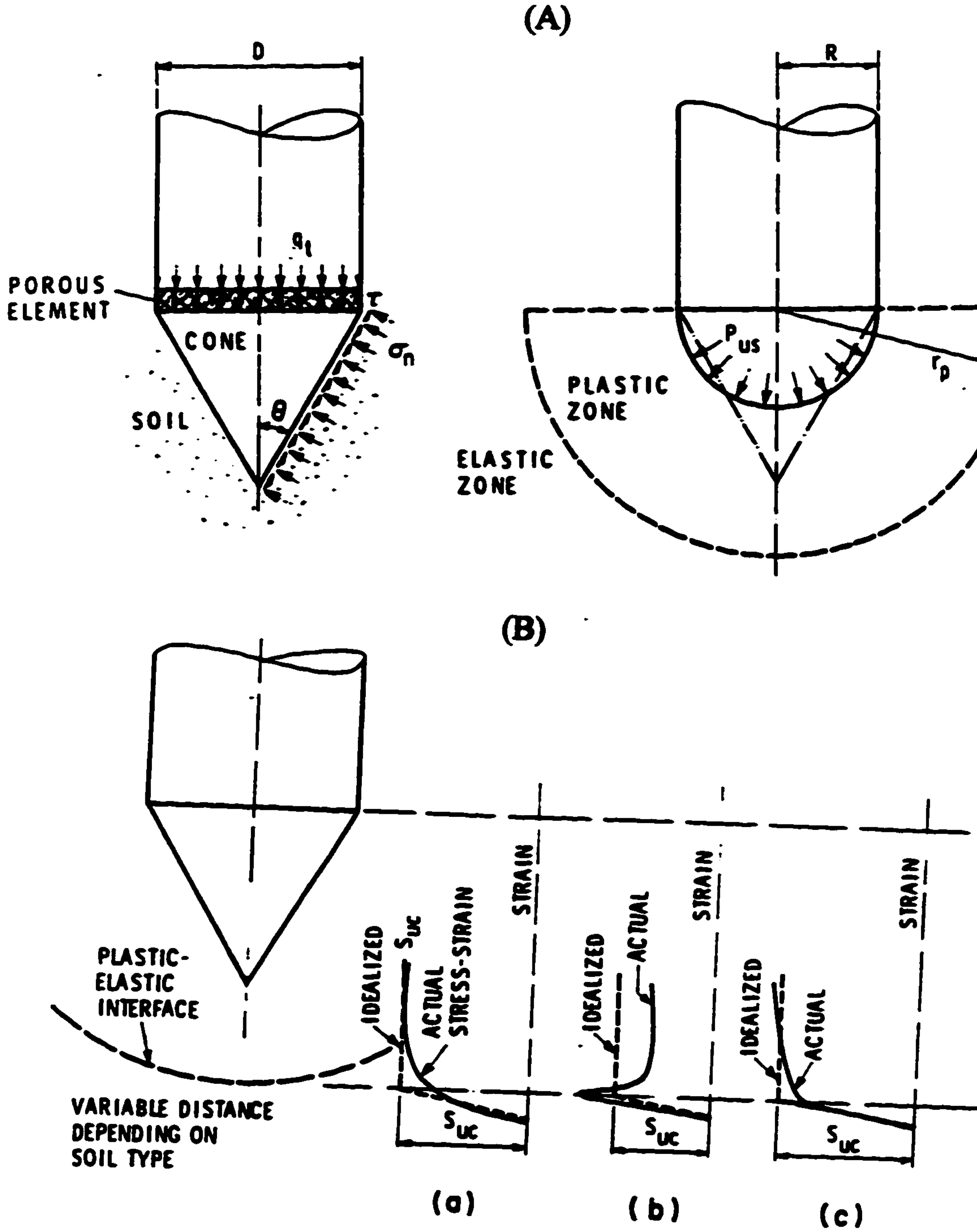

Fig. 3.10 **Proposed model for calculating undrained shear strength from cone resistance (A) proposed stress field acting on cone and expansion of spherical cavity (B) S_u mobilized by the cone in different soil types (a) normally consolidated (b) work softening (c) work hardening (Konrad and Law, 1987)**

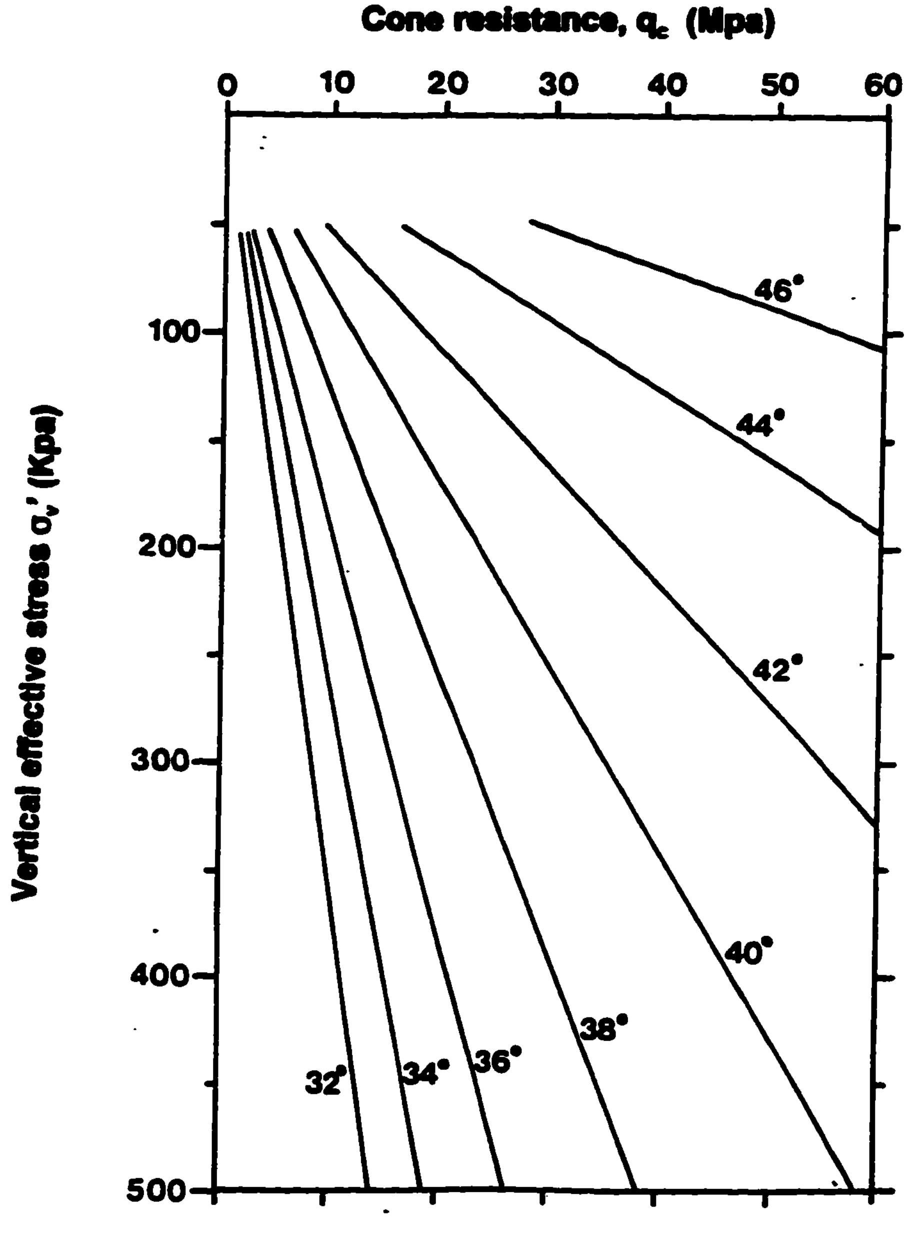

Fig. 3.11 Relationship between ϕ angle and cone resistance, q_c, for uncemented NC quartz sand (after Durgunoglu and Mitchell ,1975)

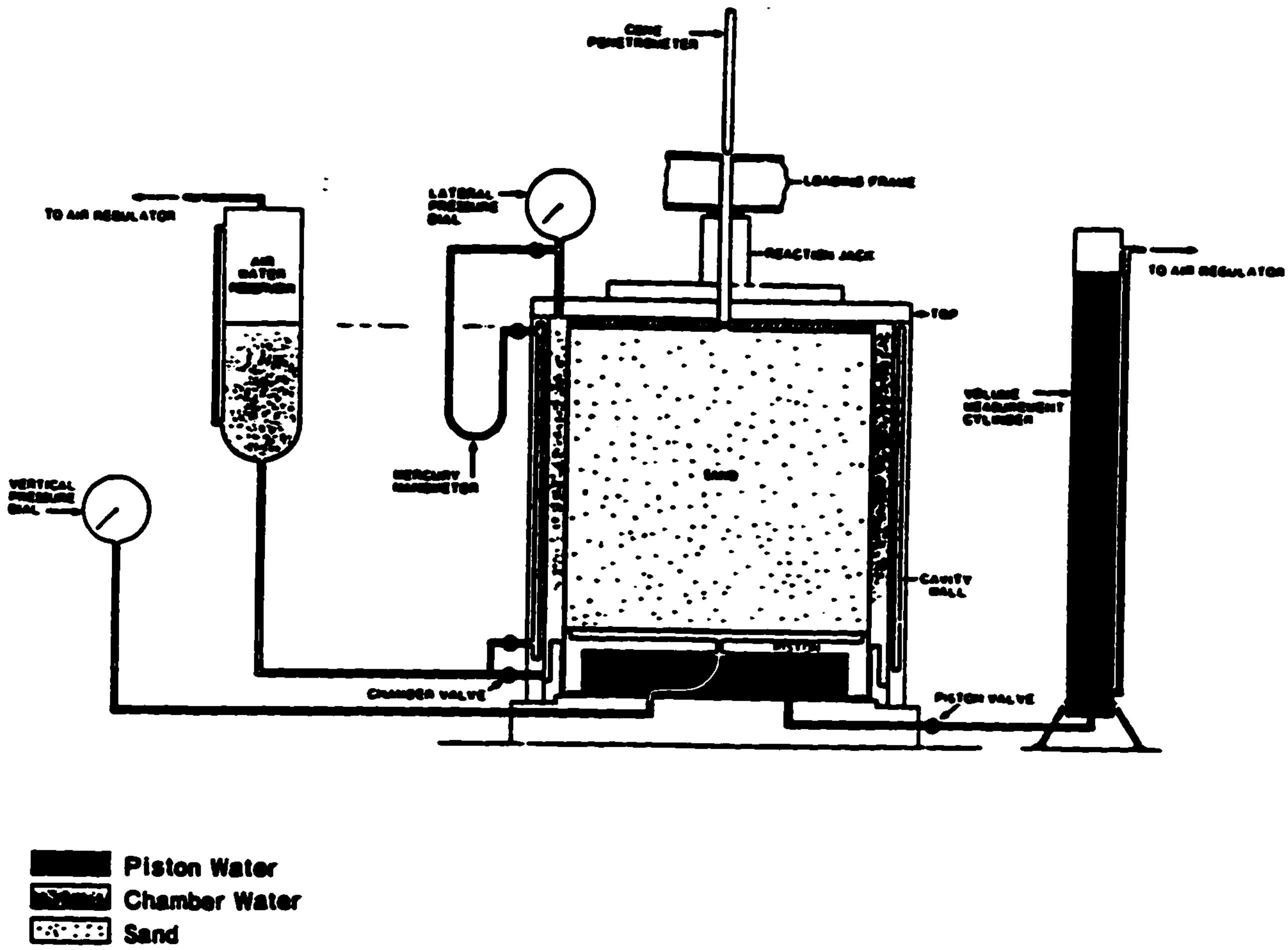

Fig. 4.1 The flexible-wall calibration chamber developed at The University of Florida (after Reese, 1975)

BC1	σ_v = const	σ_h = const
BC2	$\Delta\epsilon_v = \Delta\epsilon_h = 0$	
BC3	σ_v = const	$\Delta\epsilon_h = 0$
BC4	$\Delta\epsilon_v = 0$	σ_h = const

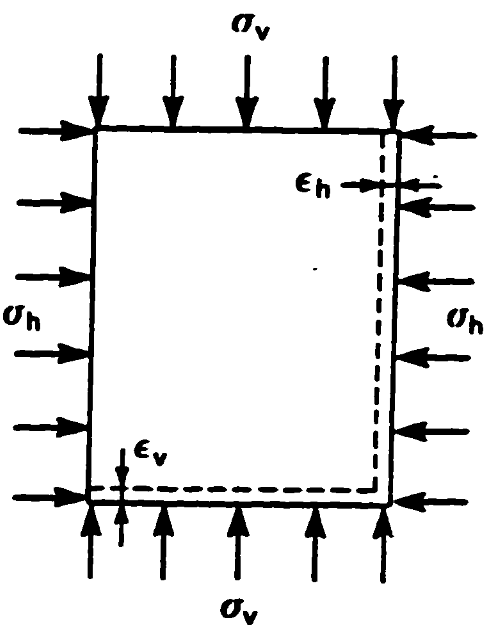

Fig. 4.2 Different boundary conditions for CPT in calibration chamber (after Veismanis, 1974)

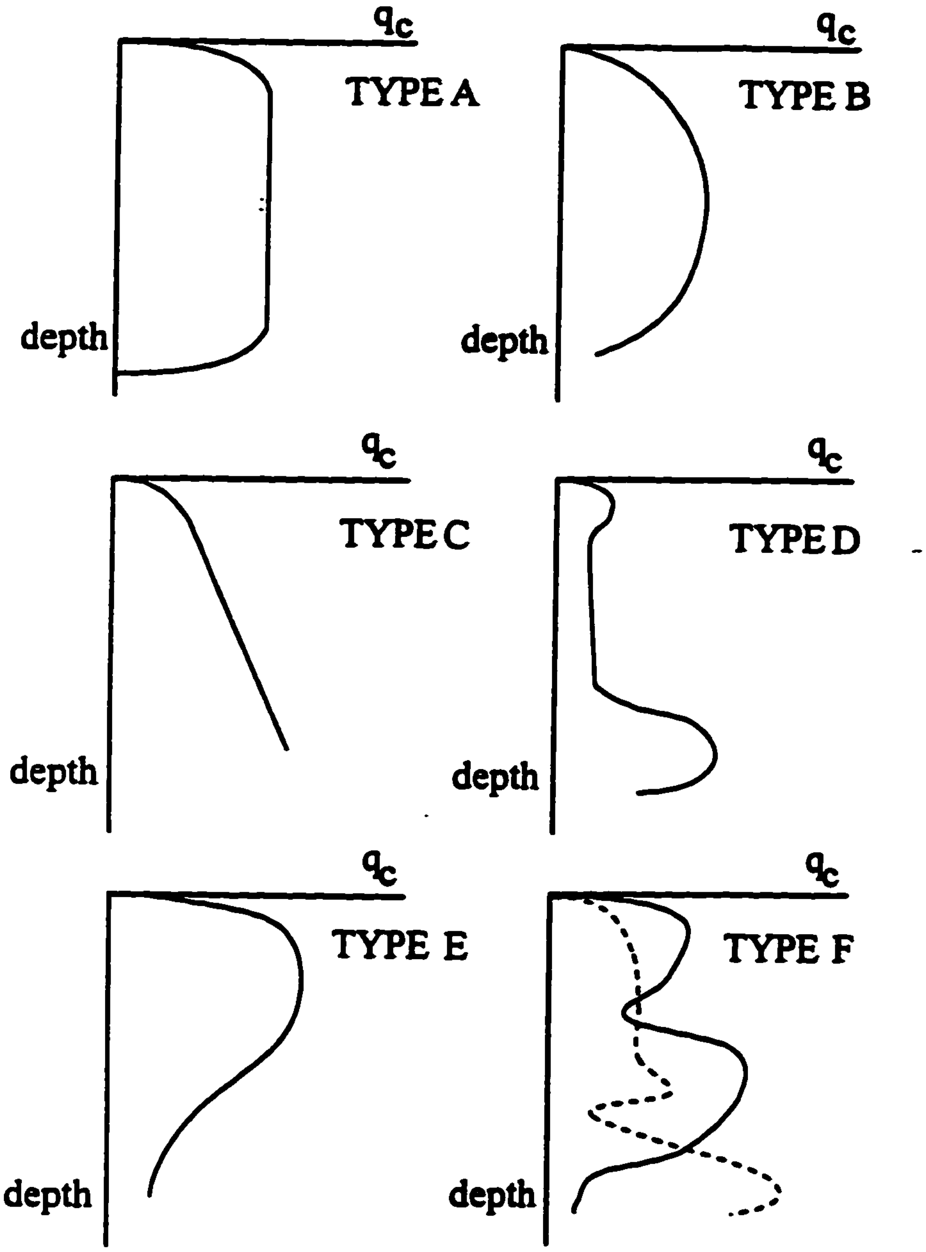

Fig. 4.3 Different types of cone resistance profile of CPT in calibration chamber test (after Salgado, 1993)

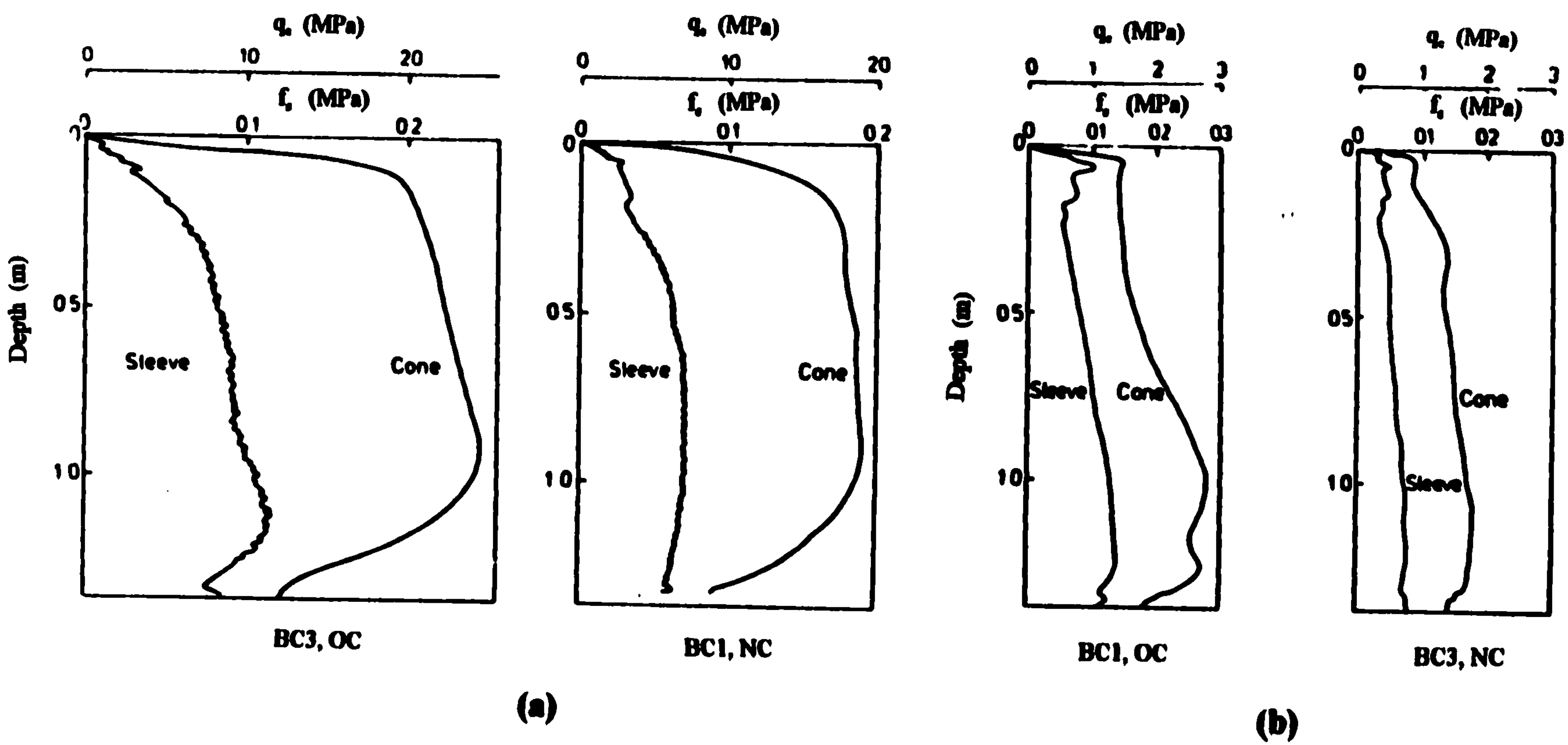

Fig. 4.4 Typical CPT traces in NGI chamber (a) Dense samples (b) Loose samples (from Parkin and Lunne, 1982)

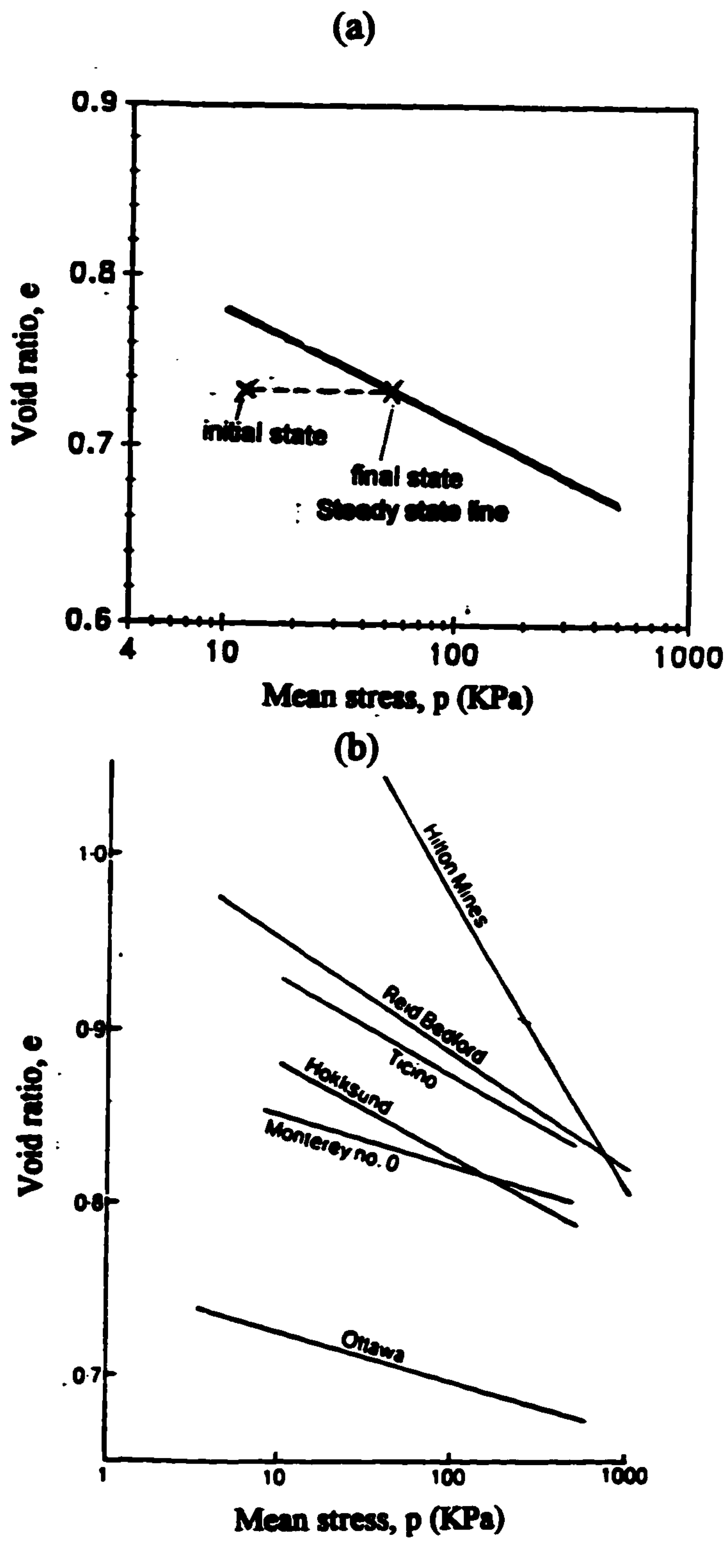

Fig. 4.5 (a) Typical state diagram (b) Steady state lines for different noncohesive soils tested in calibration chamber (modified after Been et al., 1985)

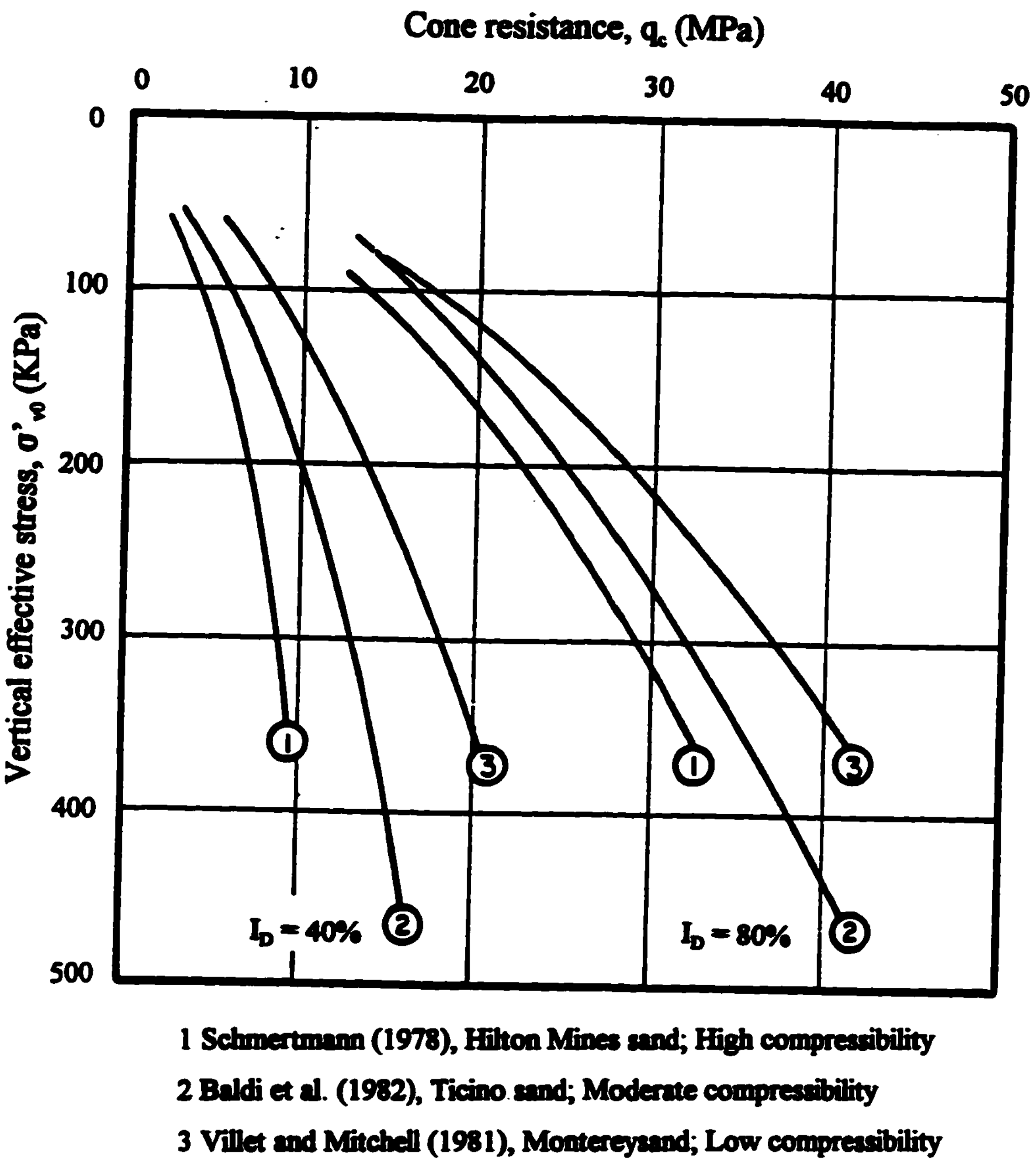

Fig. 4.6 Comparison of different relationships between density index, cone resistance, and vertical effective stress (modified after Robertson and Campanella, 1983)

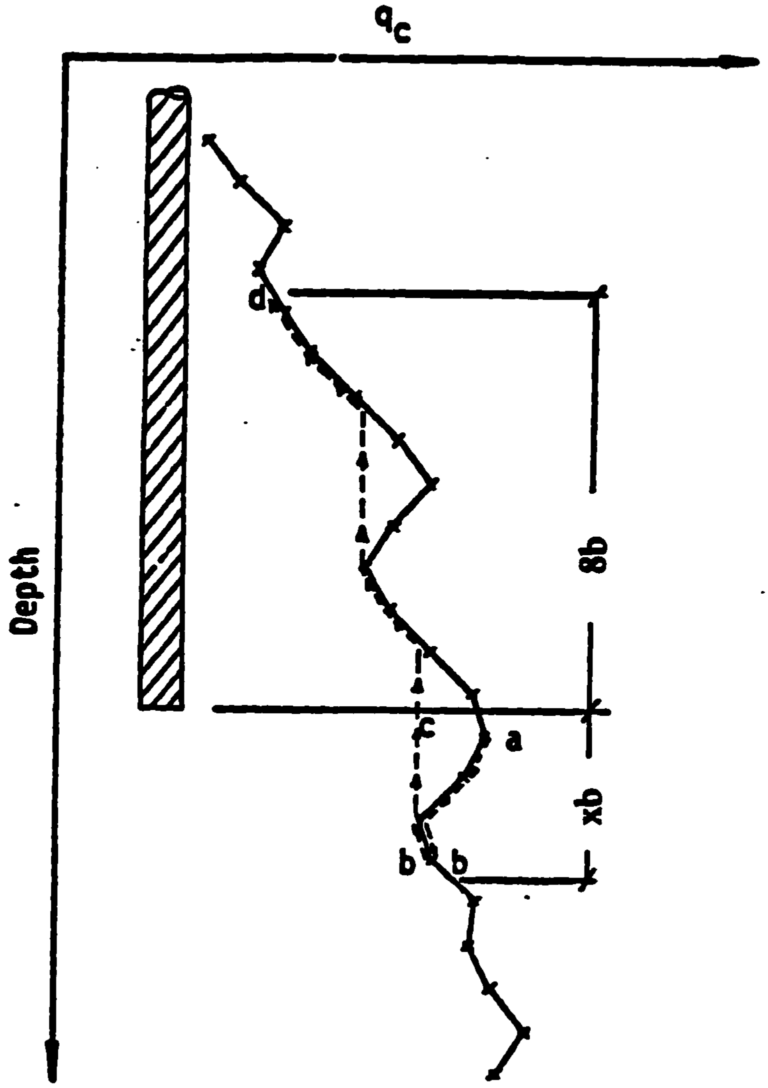

r_t = $(q_{c1}+q_{c2})/2$

q_{c1} = Average q_c over a distance of xb below the pile toe (path a-b-c). Sum q values in both the downward (path a-b) and upward (path b-c) directions. Use actual q_c values along path a-b and the minimum path rule along path b-c. Compute q_{c1} for x-values from 0.7 to 3.75 and use the minimum q_{c1} value obtained.

q_{c2} = Average q_c over a distance of 8b above the pile toe (path c-d). Use the minimum path rule as for path b-c in the q_{c1} computations.

Fig. 5.1 Begemann procedure for determining pile toe capacity from cone resistance (modified after Nottingham, 1975)

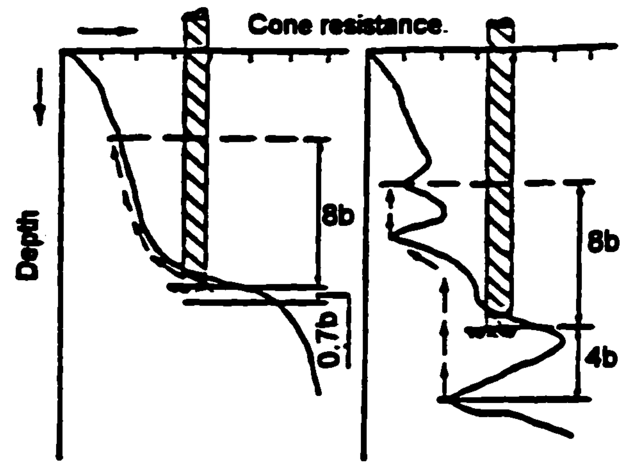

$$q_p = \frac{(q_I + q_{II})/2 + q_{III}}{2}$$

b = pile diameter

q_p = ultimate unit toe resistance of the pile

q_I = average cone resistance below the pile toe over a depth which may vary between 0.7b and 4b

q_{II} = minimum cone resistance recorded below the pile toe over the same depth of 0.7b to 4b

q_{III} = average of the envelope of minimum cone resistance recorded above the pile toe over a height which may vary between 6b and 8b. In determining this envelope, values above the minimum value selected under II are to be disregarded (II: zone for calculating q_{II})

Fig. 5.2a Application of CPT data to pile design (after Schmertmann, 1978)

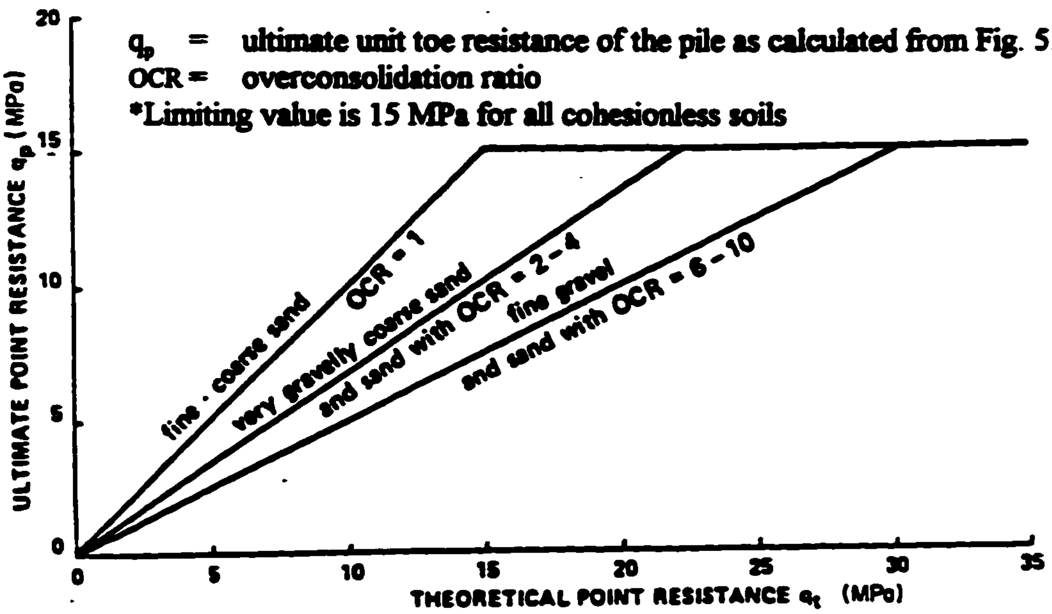

Fig. 5.2b Application of CPT data to pile design (after de Ruiter and Beringen, 1979)

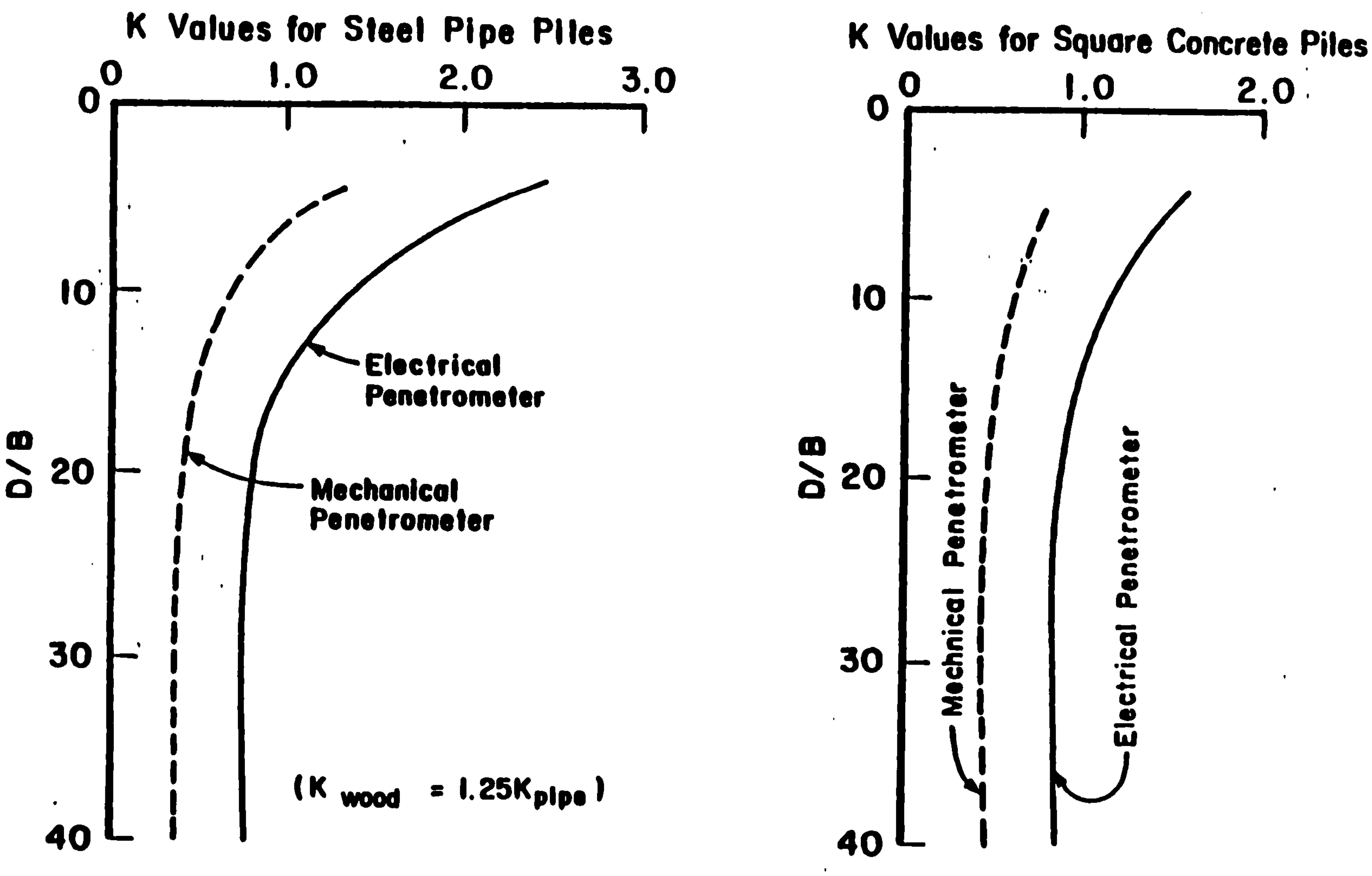

Fig. 5.3 Design curves for pile shaft resistance in sand (from Schmertmann, 1978)

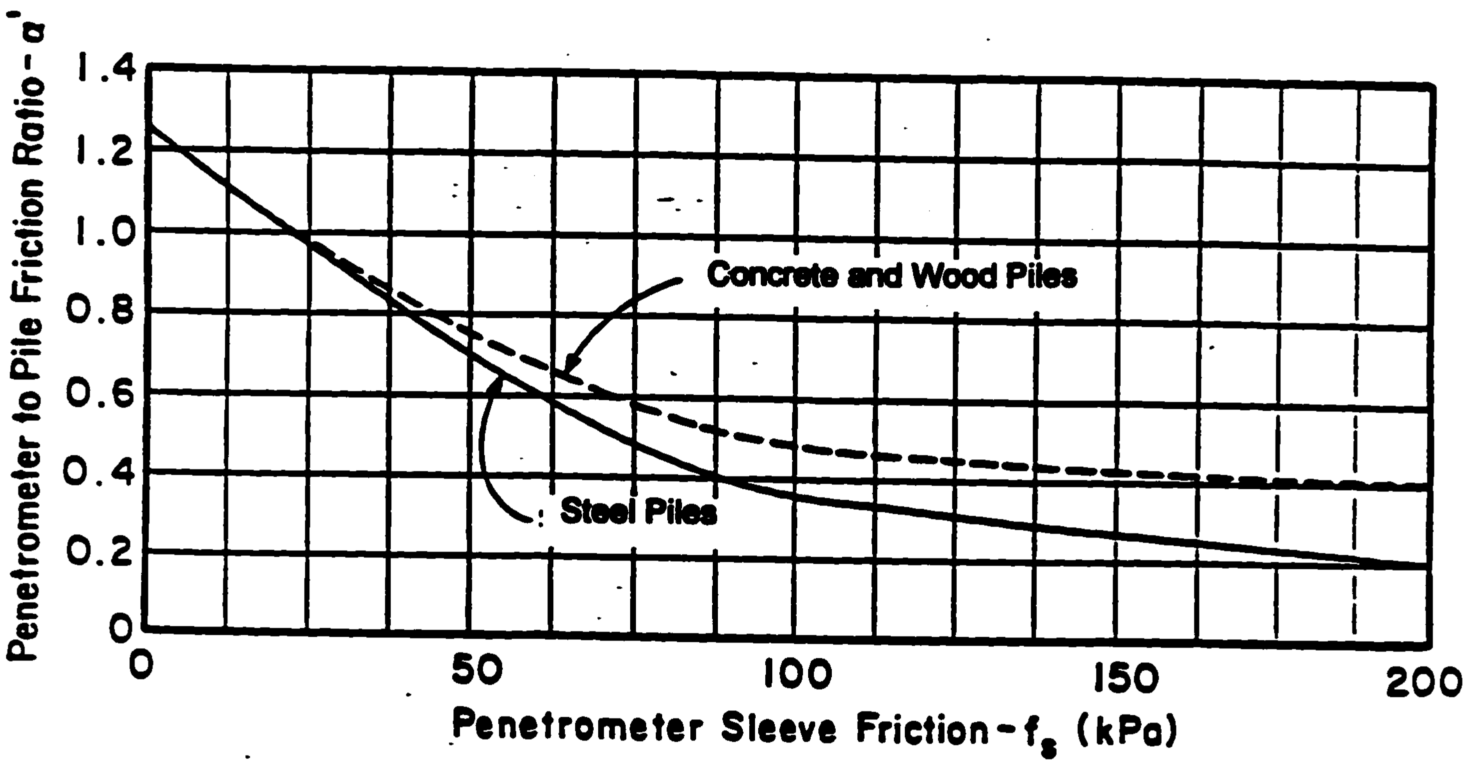

Fig. 5.4 Design curve for pile shaft resistance in clay (from Schmertmann, 1978)

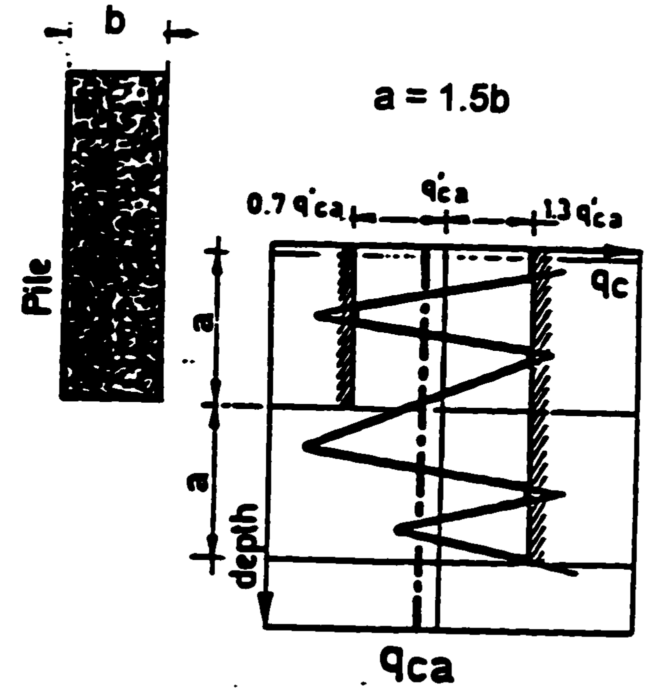

Fig. 5.5 LCPC CPT method to determine equivalent cone resistance at pile toe (after Bustamante and Gianeselli, 1982)

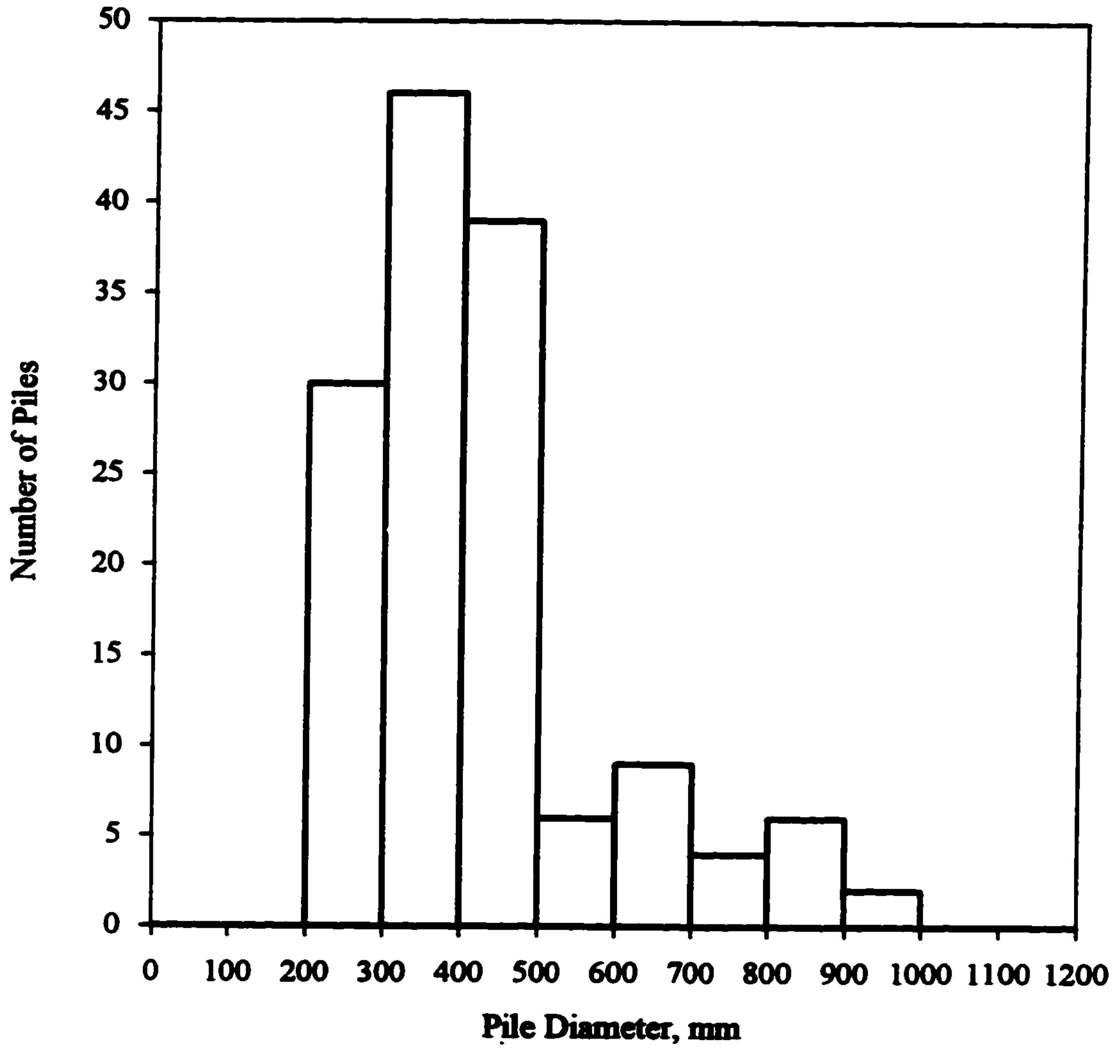

Fig. 6.1 Frequency distribution of pile diameter in the compiled database

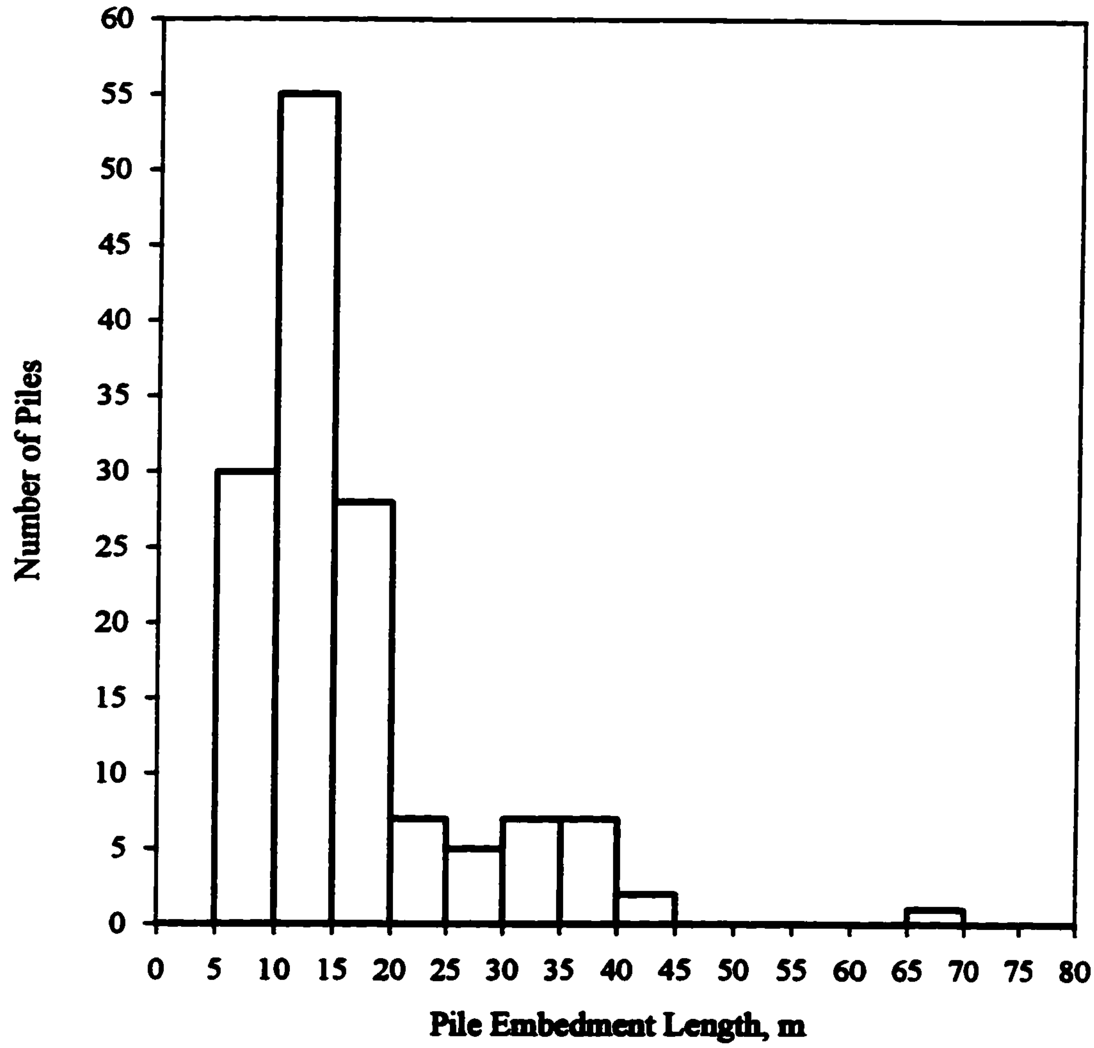

Fig. 6.2 Frequency distribution of pile embedment length in the compiled database

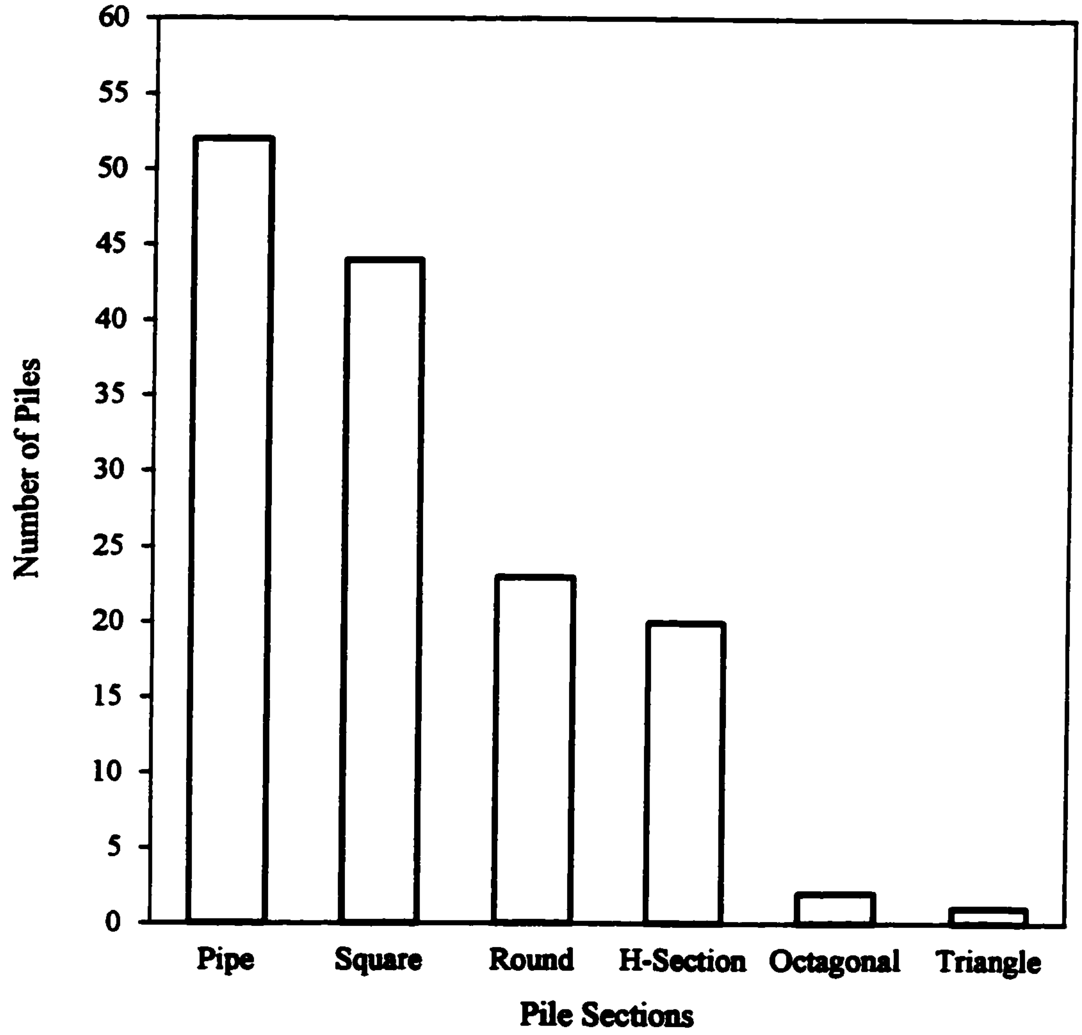

Fig. 6.3 Frequency distribution of pile sections in the compiled database

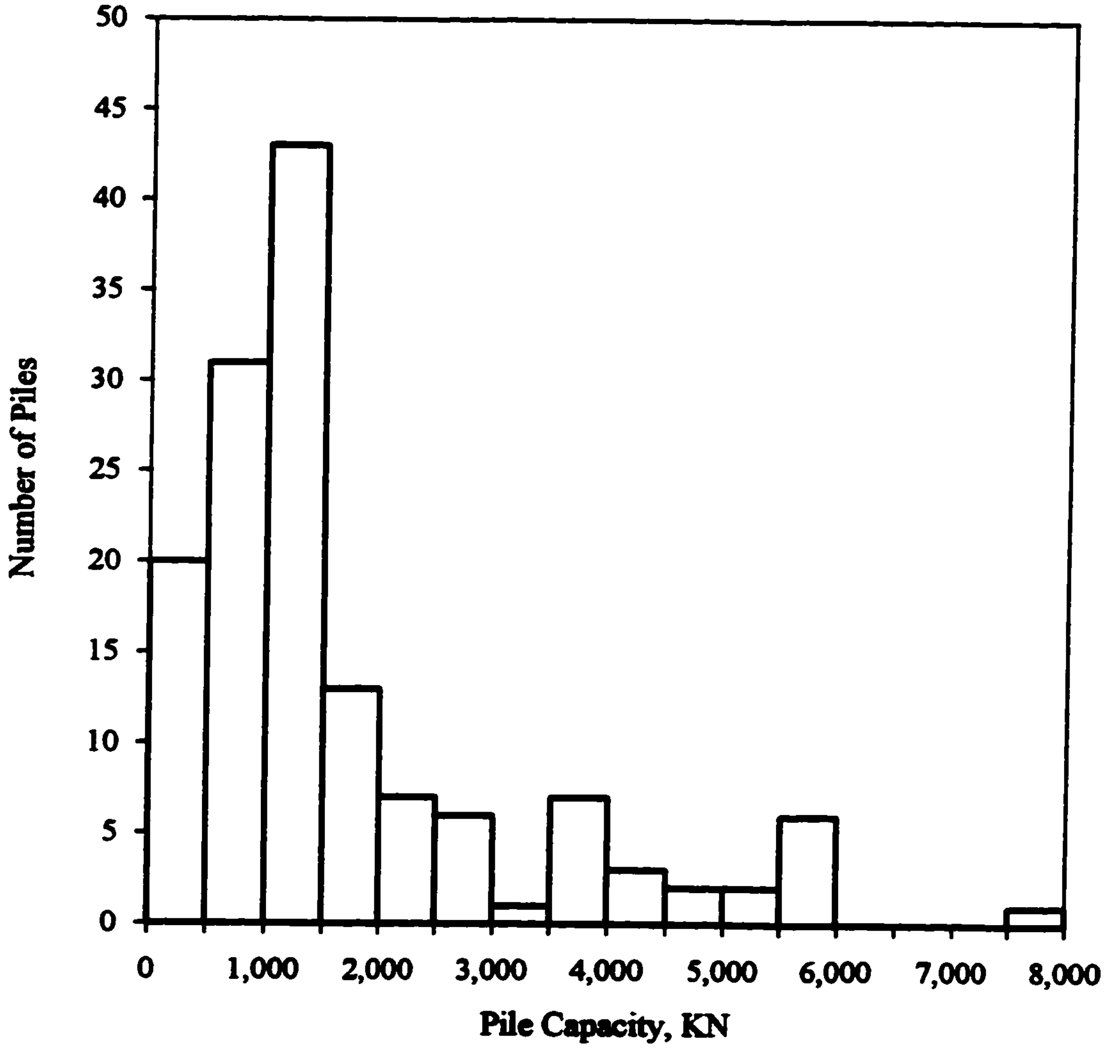

Fig. 6.4 Frequency distribution of pile capacity in the compiled database

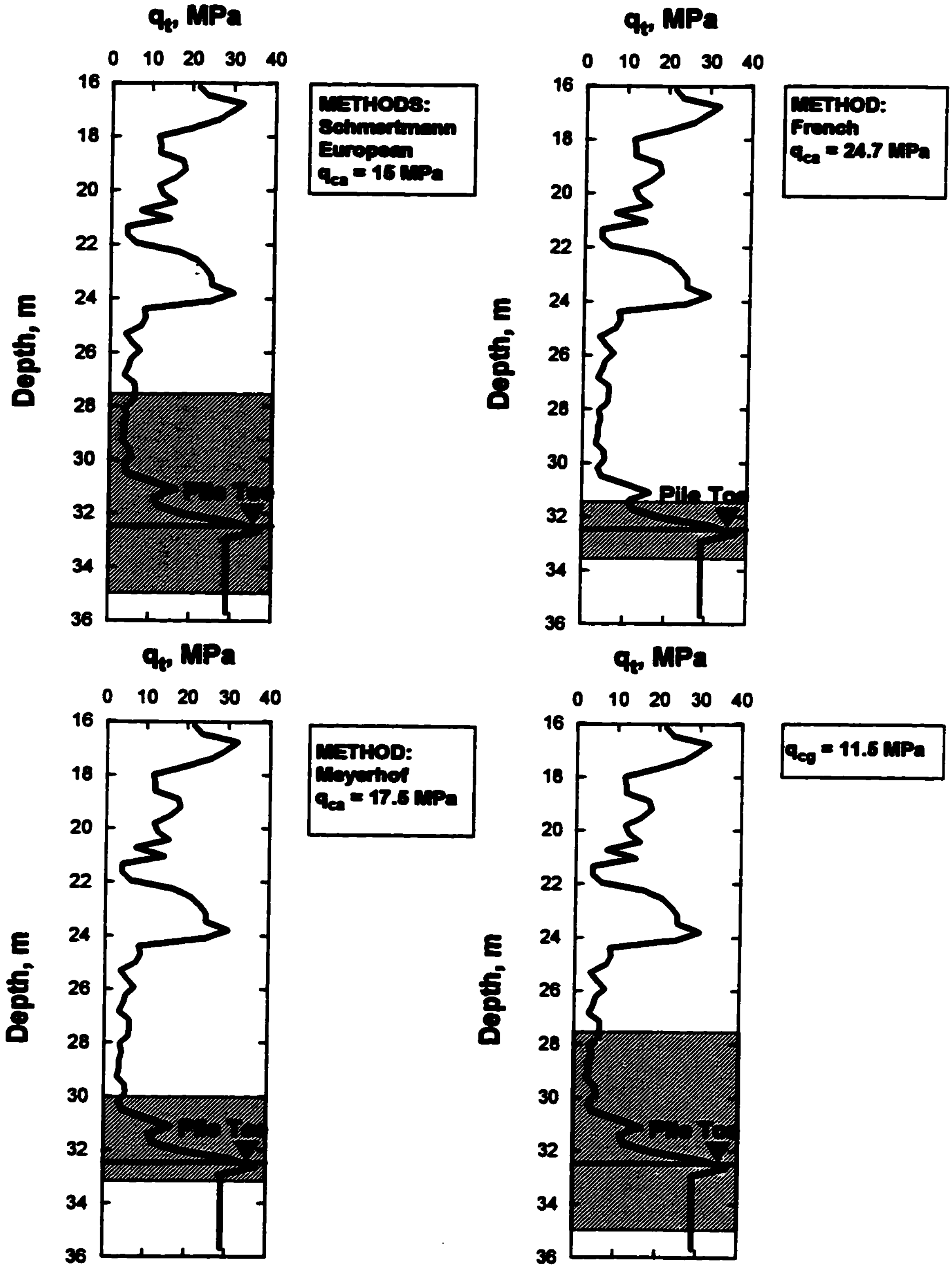

Fig. 7.1 Comparison of q_c -average for different CPT methods for Case #11, POLA2

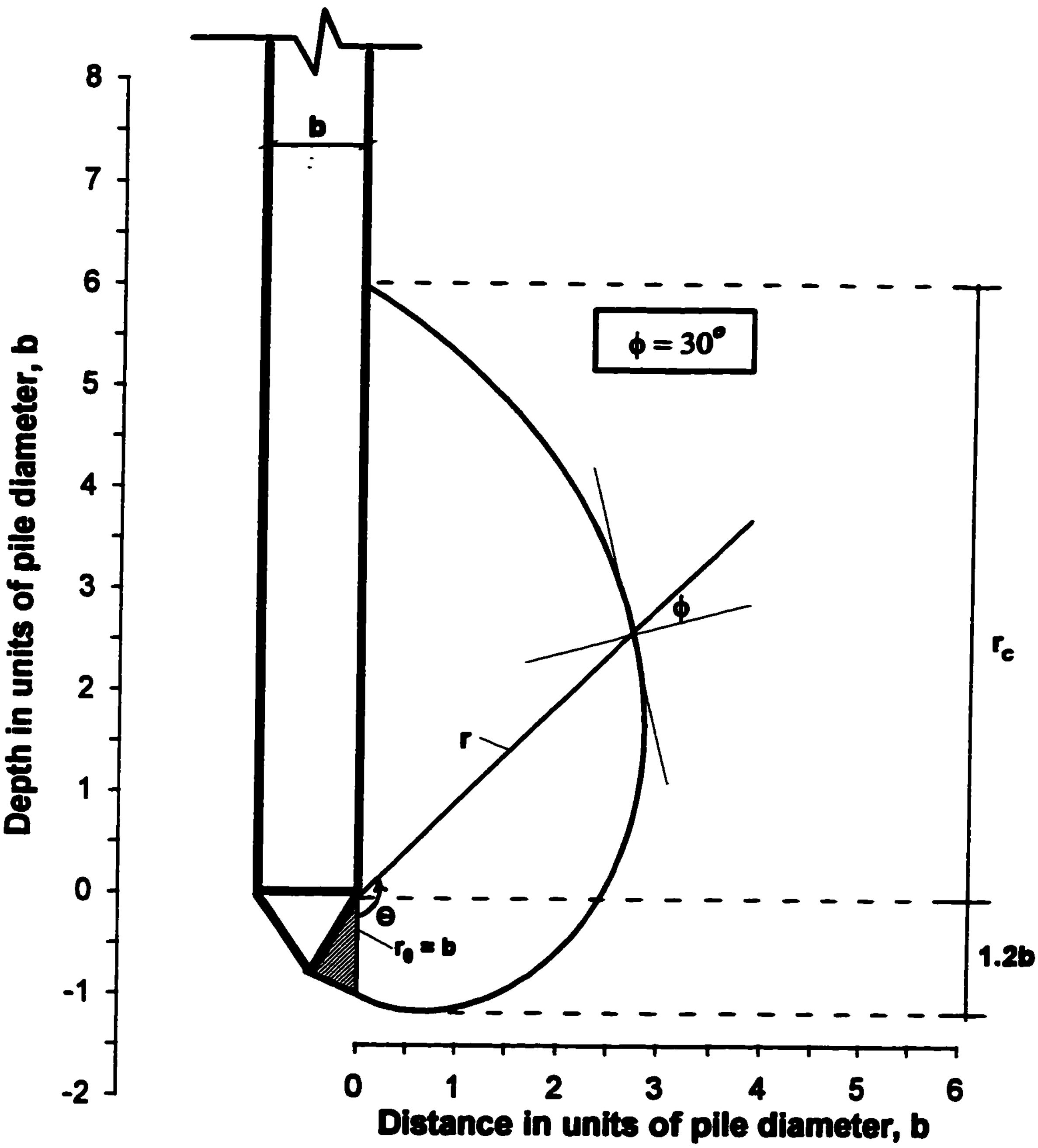

Fig. 7.2 Rupture surface around cone point and pile toe

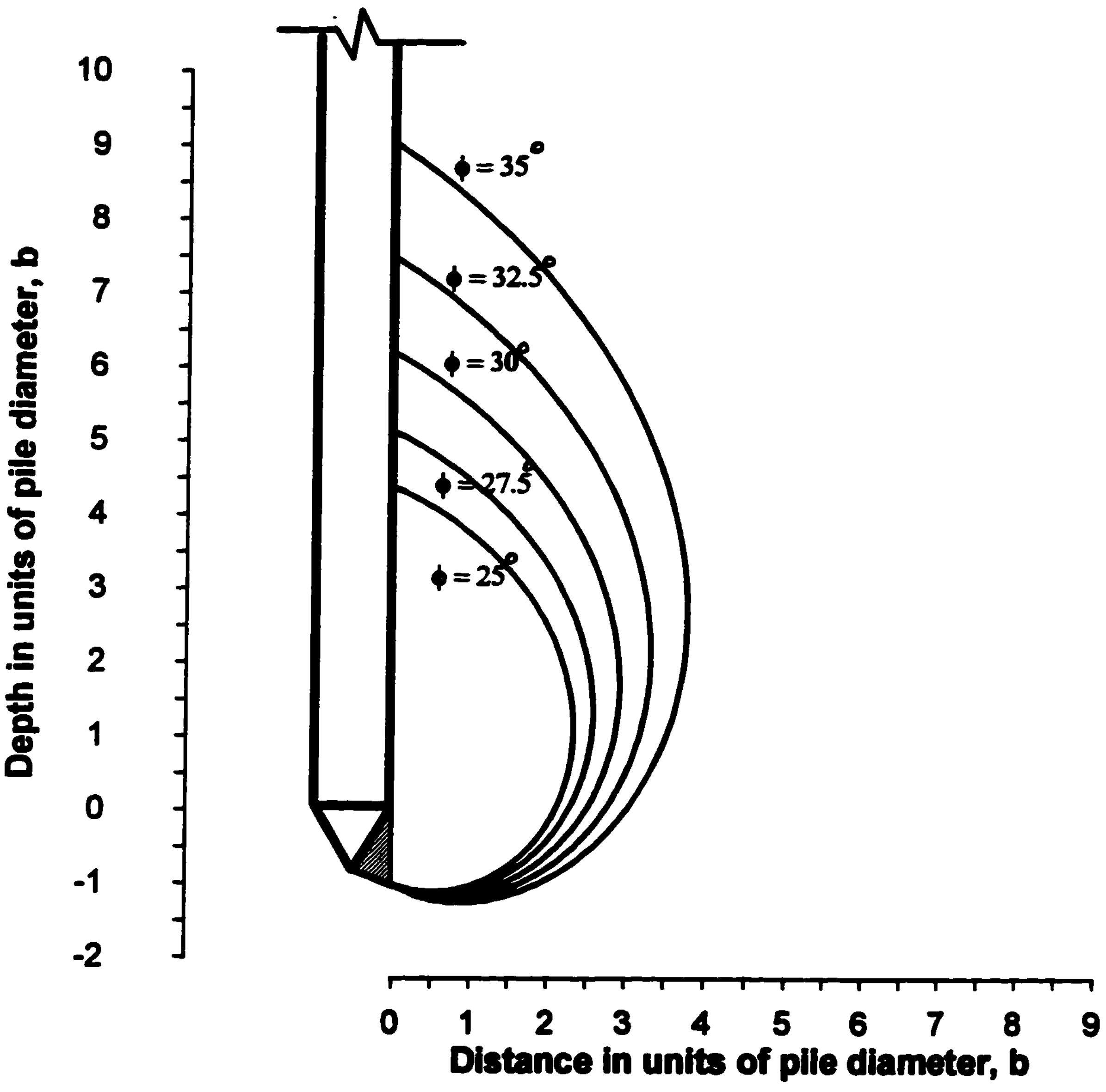

Fig. 7.3 Rupture surfaces around pile toe for different soils

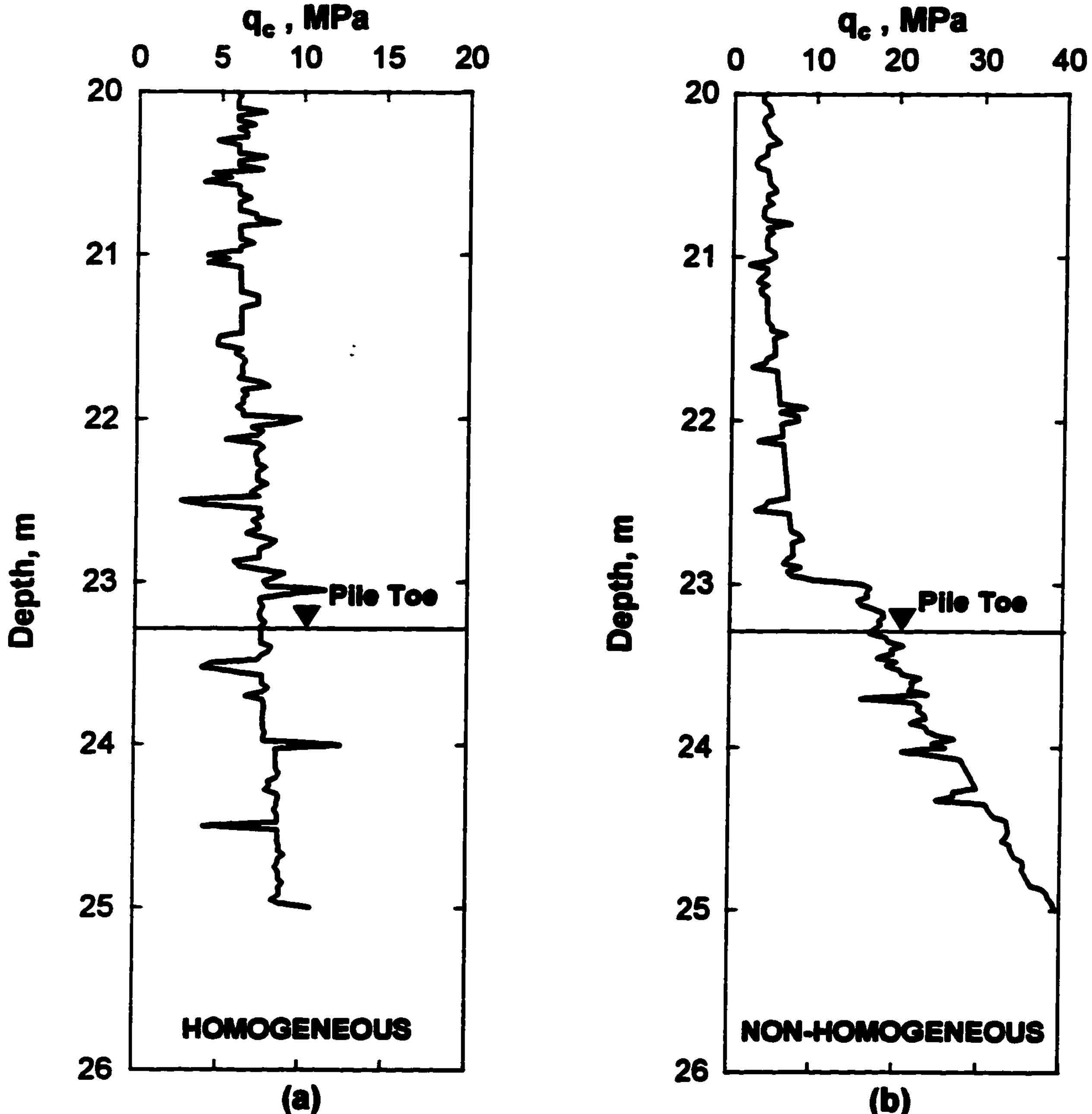

GEOMETRIC AVERAGE OF CONE RESISTANCE FOR DIFFERENT ZONES (b= 350 mm), MPa

ZONE	HOMOGENEOUS	NON-HOMOGENEOUS
2b-2b	7.66	16.13
2b-4b	7.43	11.79
2b-6b	7.09	9.06
2b-8b	6.93	8.06
4b-2b	7.89	19.92
4b-4b	7.65	14.89
4b-6b	7.38	11.97
4b-8b	7.15	10.11

Fig. 7.4 Comparison of pile unit toe resistance for different zones
(a) Homogeneous (b) Non-Homogeneous

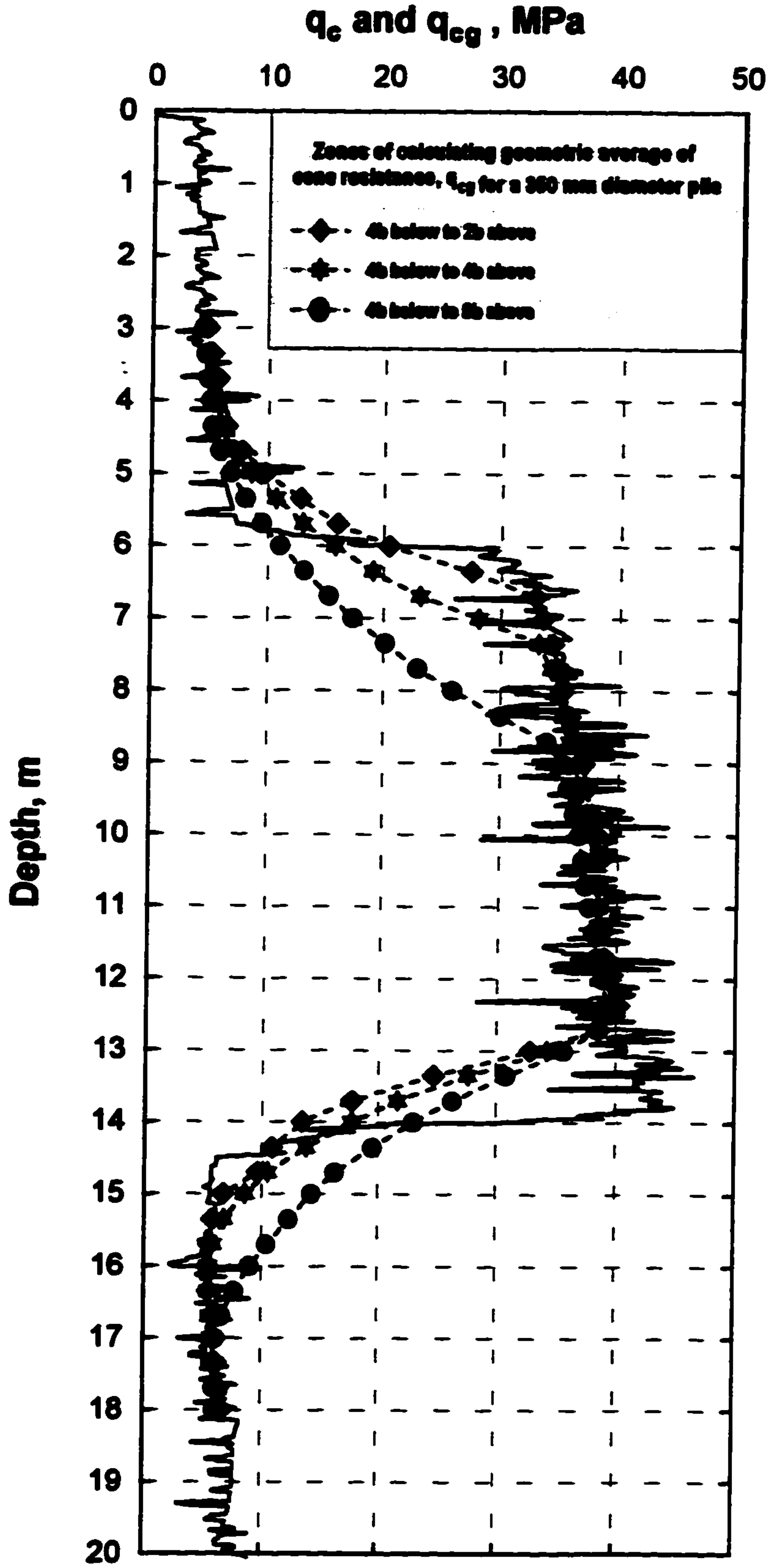

Fig. 7.5 Comparison of cone resistance and calculated geometric average as pile unit toe resistance in non-homogeneous soil for different zones

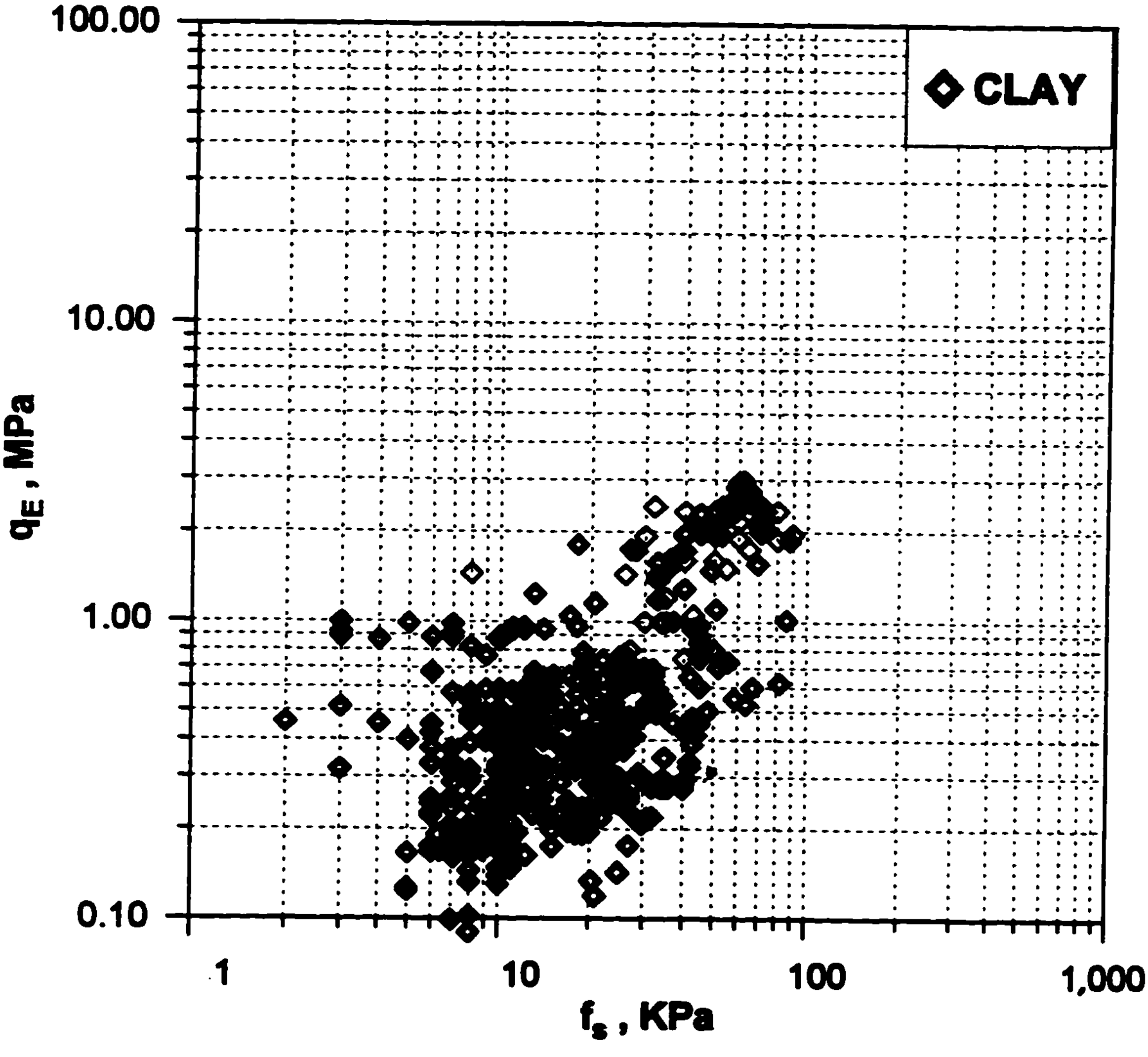

Fig. 7.6 Soil classification chart based on database- clay soils

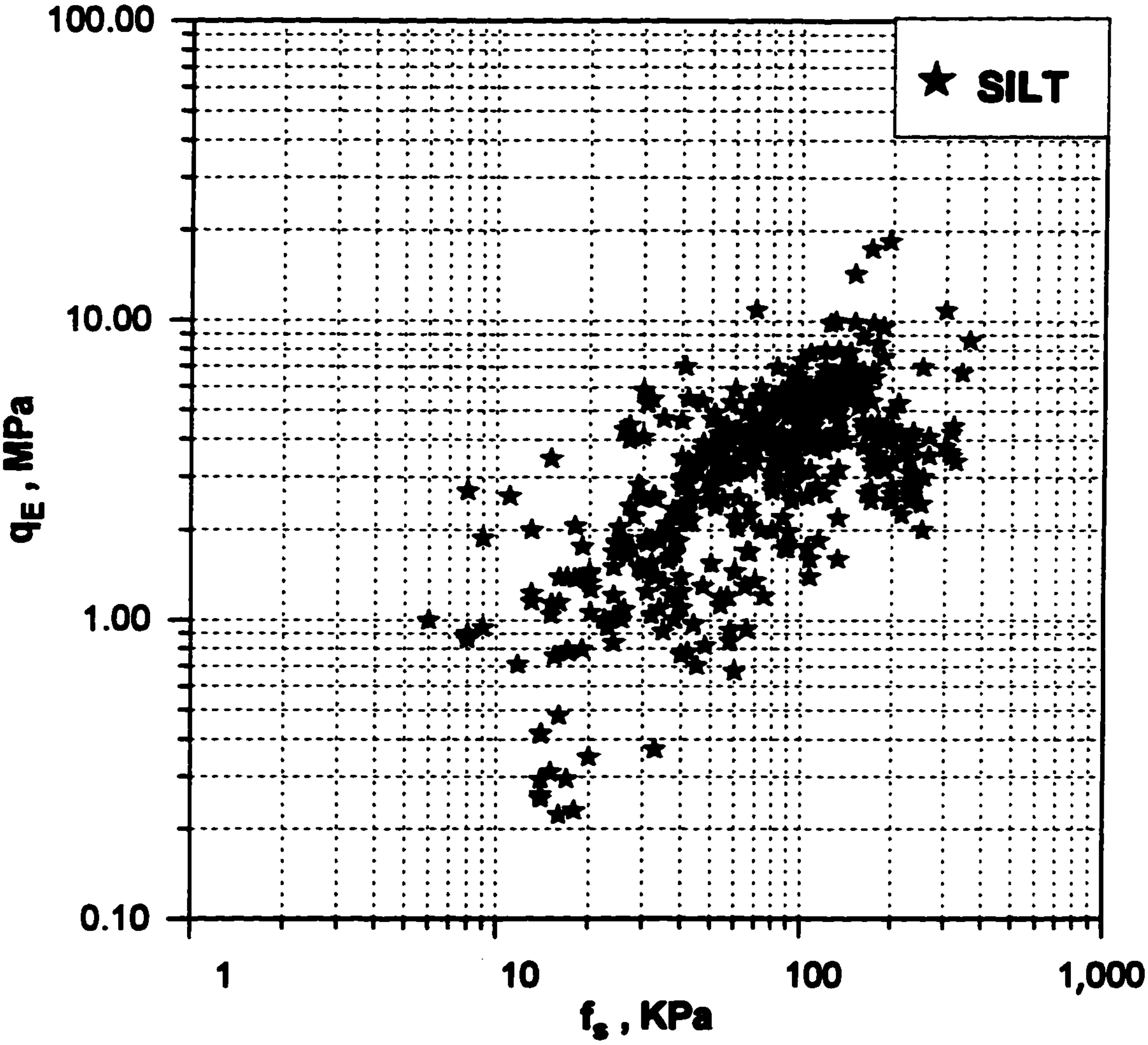

Fig. 7.7 Soil classification chart based on database- silt soils

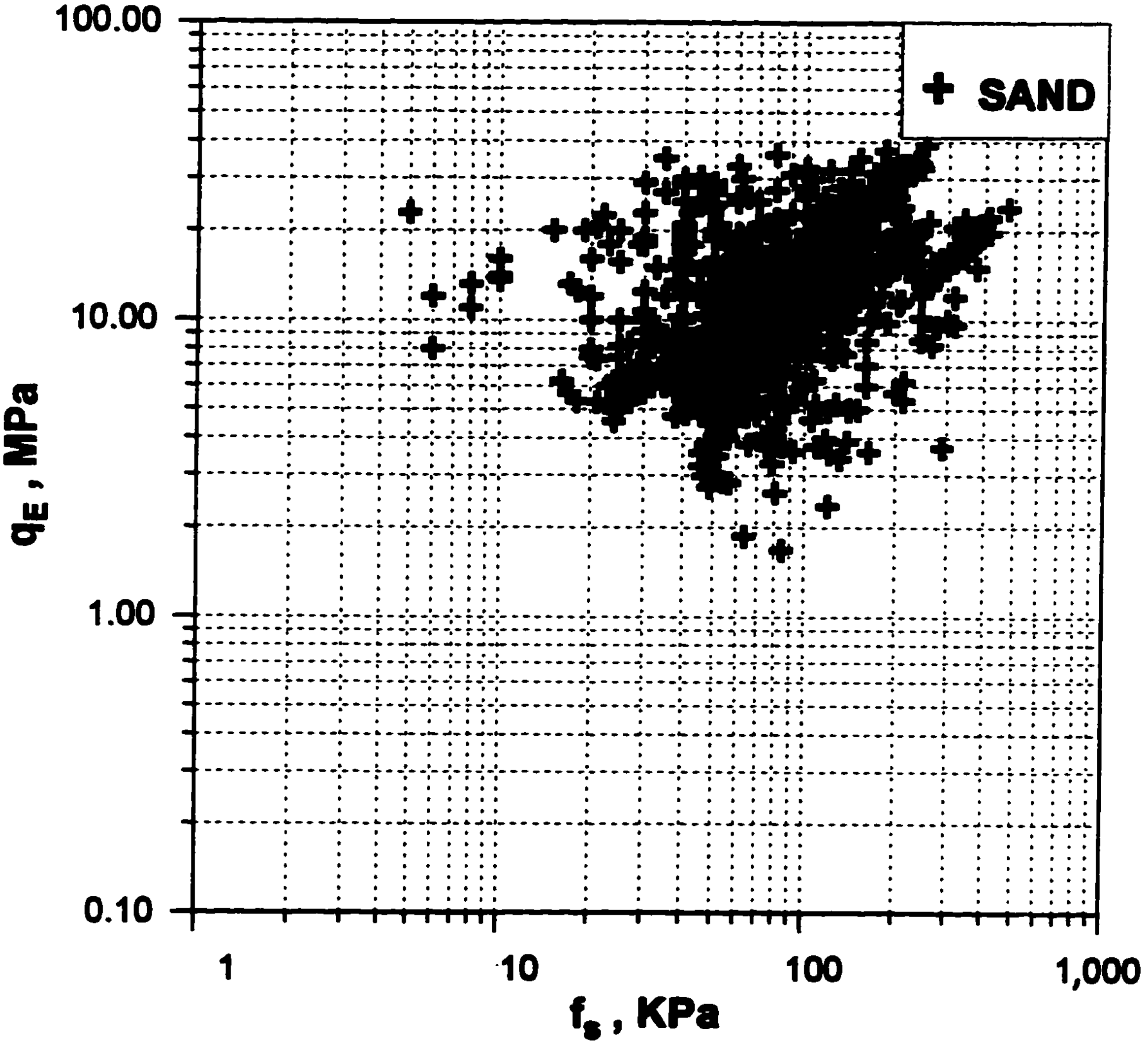

Fig. 7.8 Soil classification chart based on database- sand soils

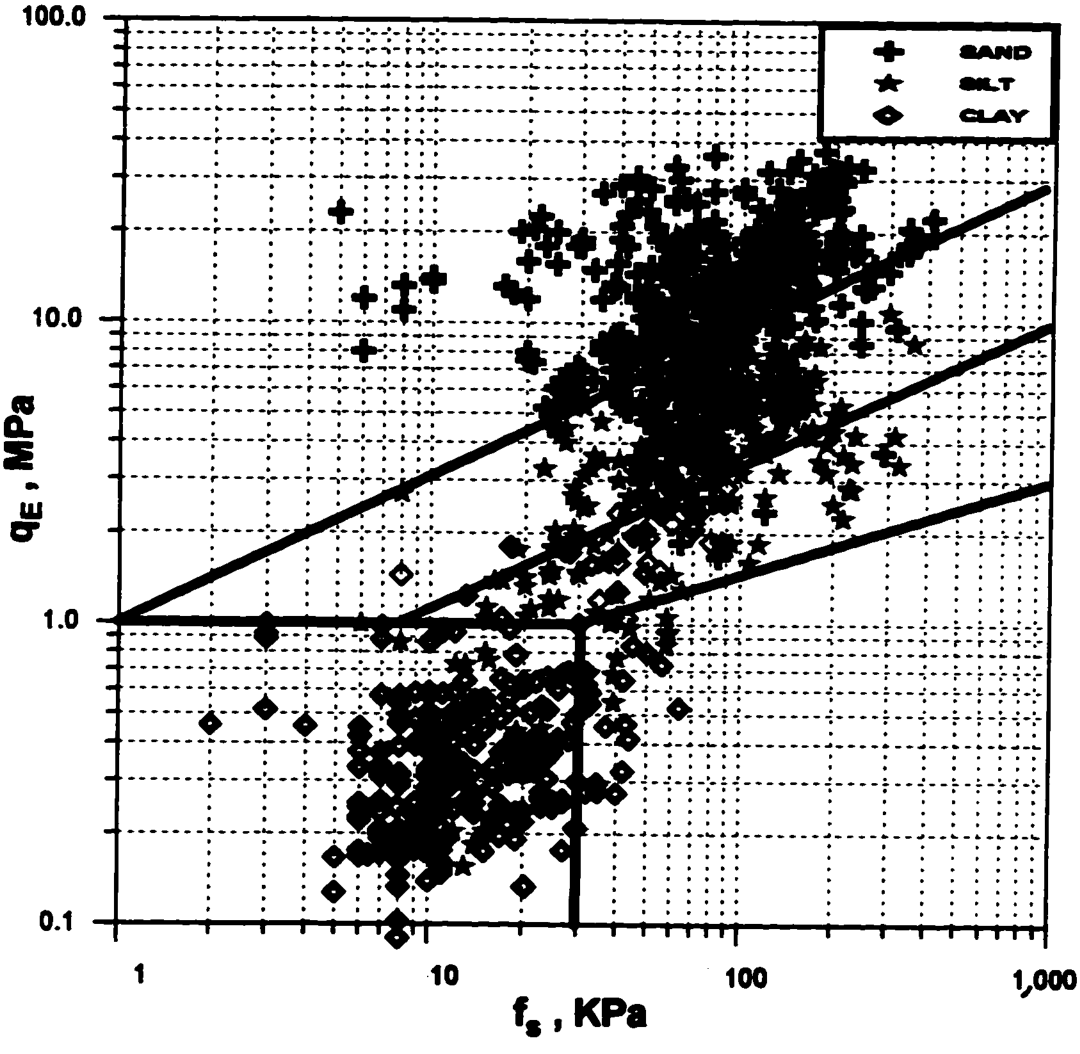

Fig. 7.9 Combination of different soils in new soil classification chart

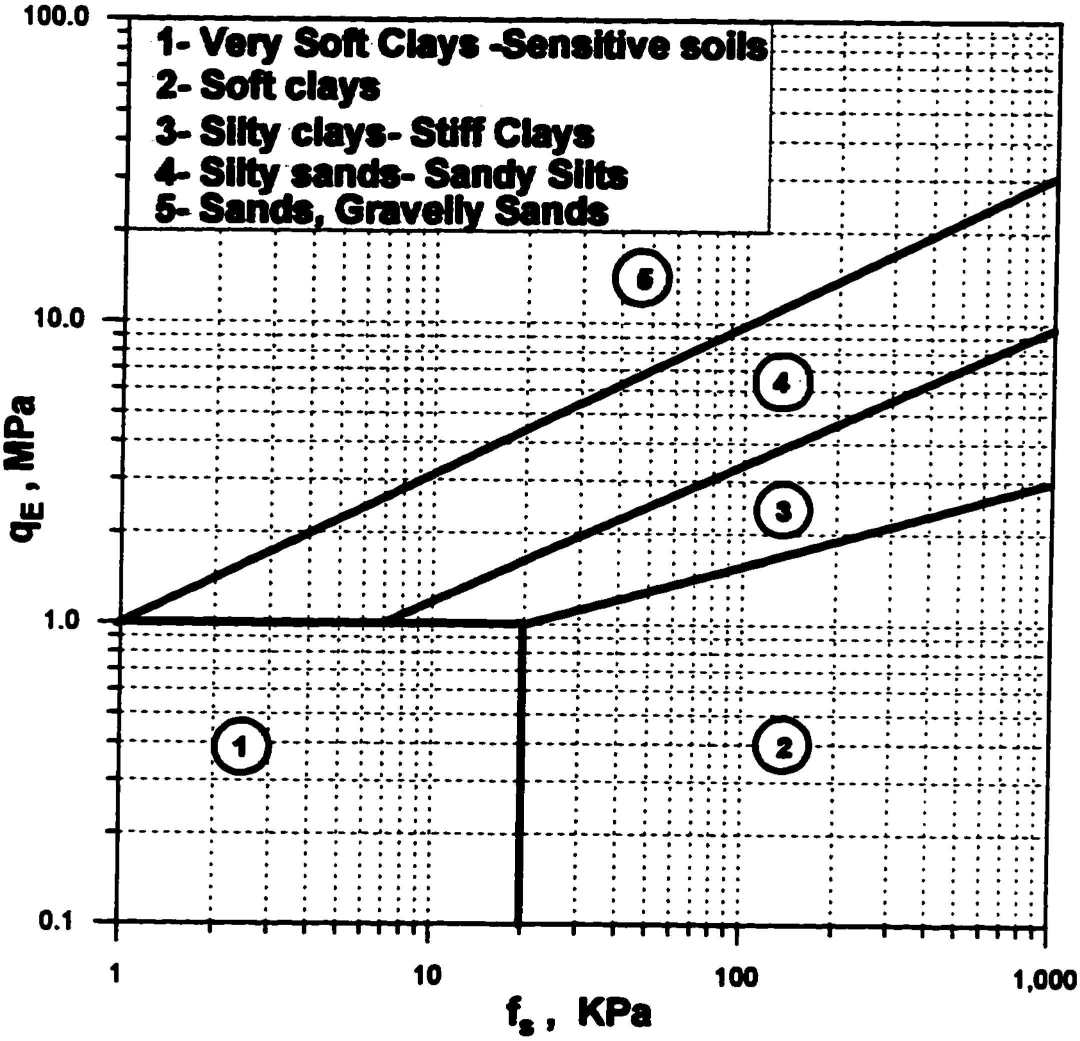

Fig. 7.10 Proposed soil classification chart based on delineation of soils in the database

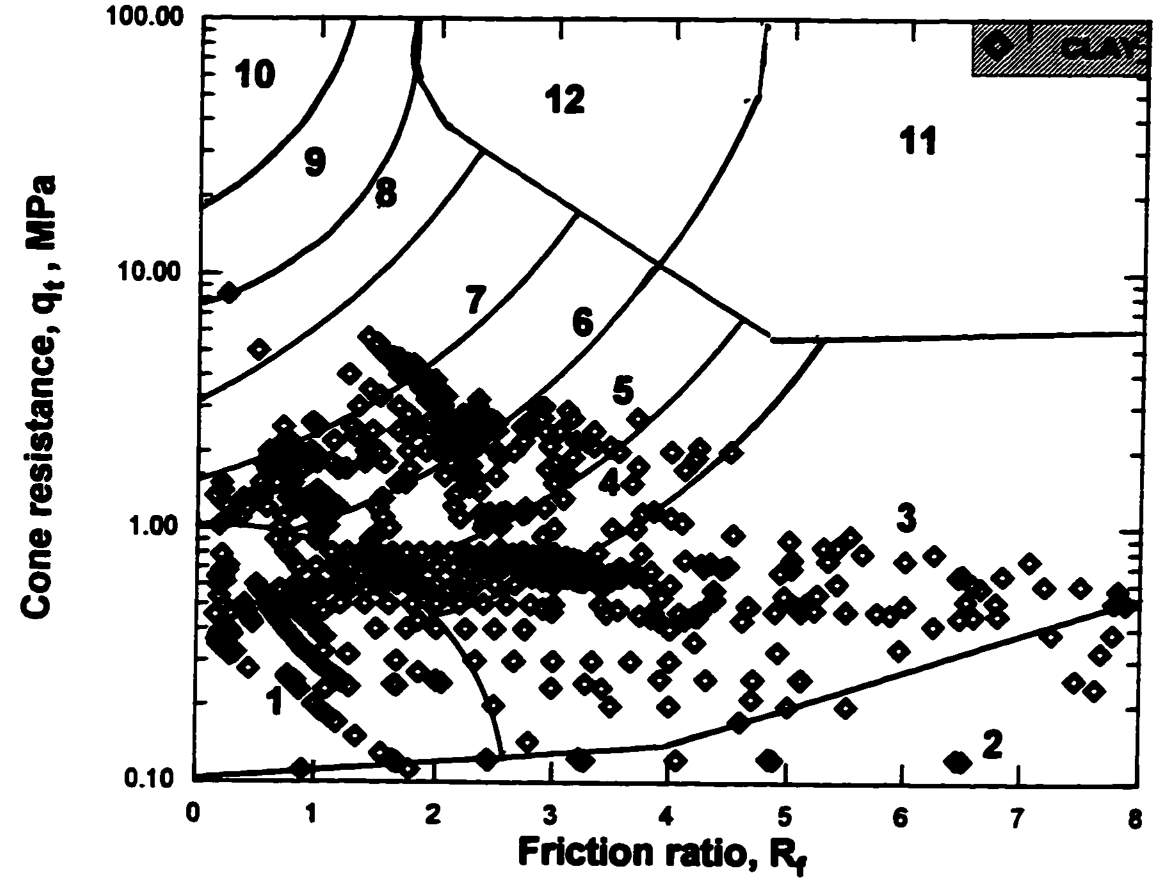

ZONE	SOIL BEHAVIOUR TYPE
1	Sensitive fine grained
2	Organic material
3	Clay
4	Silty clay to clay
5	Clayey silt to silty clay
6	Sandy silt to clayey silt
7	Silty sand to sandy silt
8	Sand to silty sand
9	Sand
10	Gravelly sand to sand
11	Very stiff fine grained *
12	Sand to clayey sand *

* overconsolidated or cemented

Fig. 7.11 Distribution of database soils (clay) in soil classification chart proposed by Robertson et al. (1986)

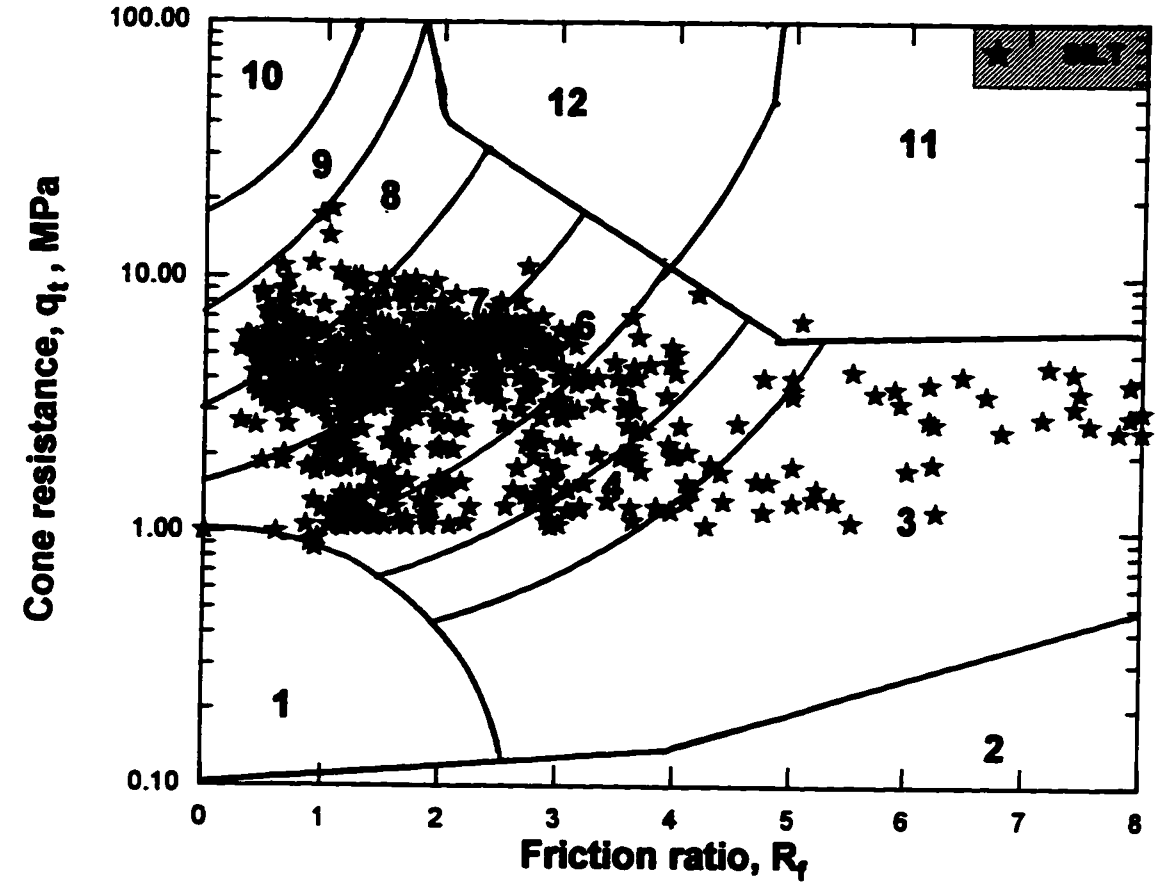

ZONE	SOIL BEHAVIOUR TYPE
1	Sensitive fine grained
2	Organic material
3	Clay
4	Silty clay to clay
5	Clayey silt to silty clay
6	Sandy silt to clayey silt
7	Silty sand to sandy silt
8	Sand to silty sand
9	Sand
10	Gravelly sand to sand
11	Very stiff fine grained *
12	Sand to clayey sand *

* overconsolidated or cemented

Fig. 7.12 Distribution of database soils (silt) in soil classification chart proposed by Robertson et al. (1986)

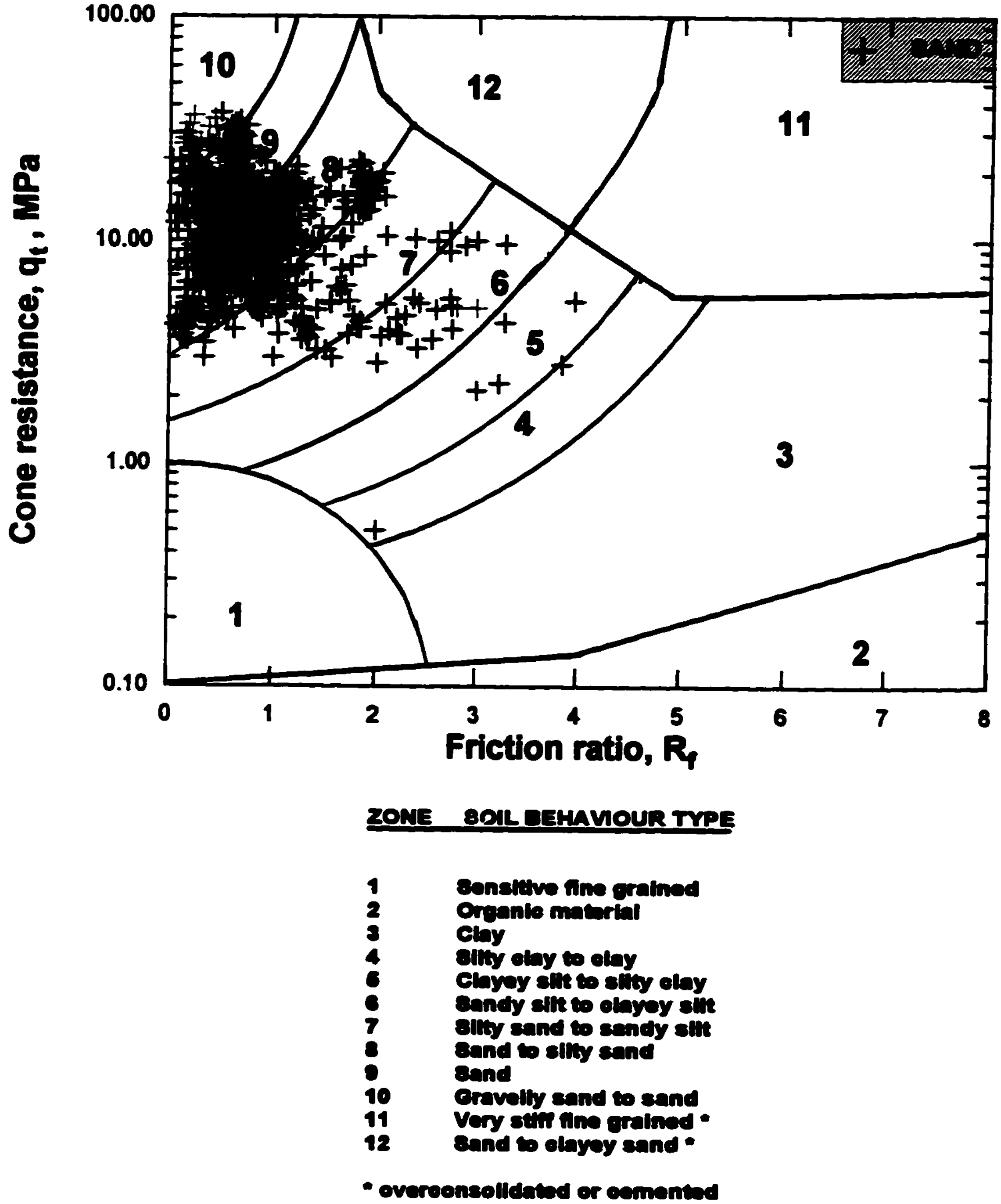

Fig. 7.13 Distribution of database soils (sand) in soil classification chart proposed by Robertson et al. (1986)

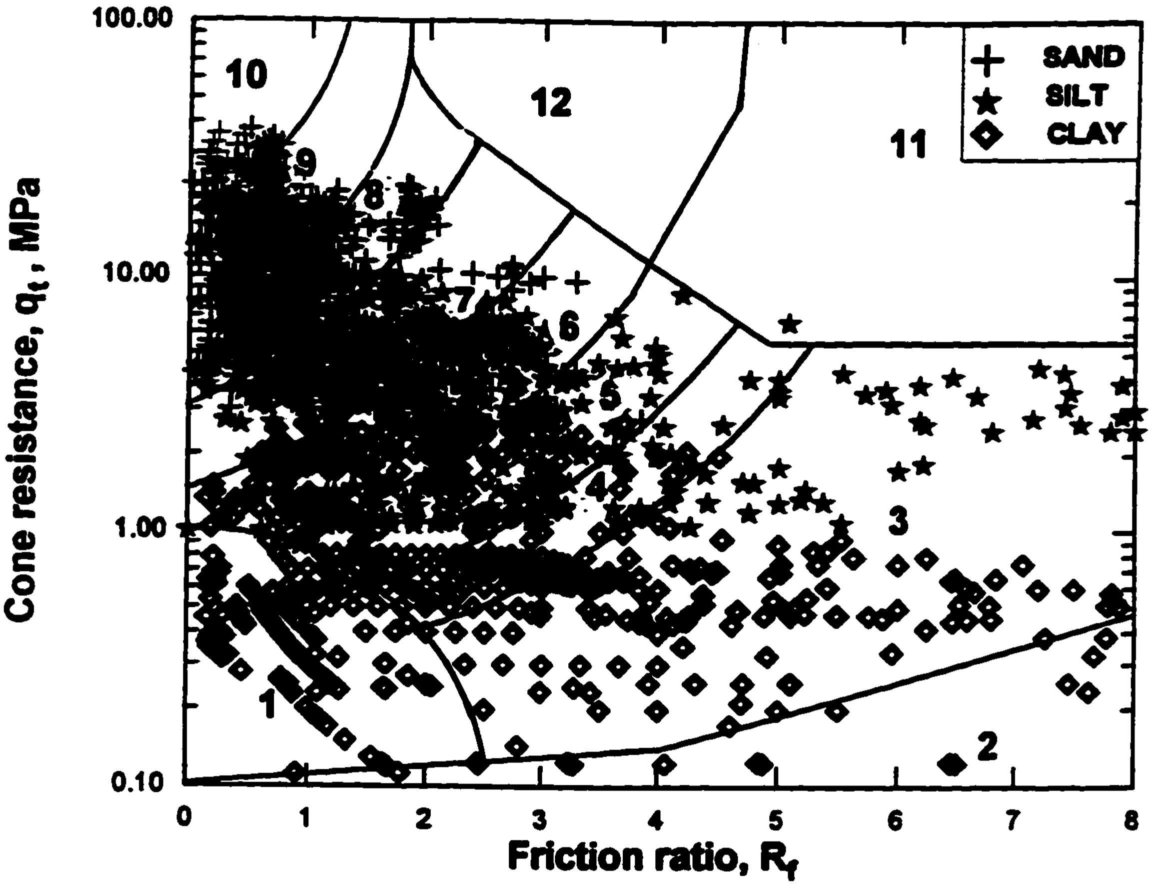

ZONE	SOIL BEHAVIOUR TYPE
1	Sensitive fine grained
2	Organic material
3	Clay
4	Silty clay to clay
5	Clayey silt to silty clay
6	Sandy silt to clayey silt
7	Silty sand to sandy silt
8	Sand to silty sand
9	Sand
10	Gravelly sand to sand
11	Very stiff fine grained *
12	Sand to clayey sand *

* overconsolidated or cemented

Fig. 7.14 Distribution of database soils in soil classification chart proposed by Robertson et al. (1986)

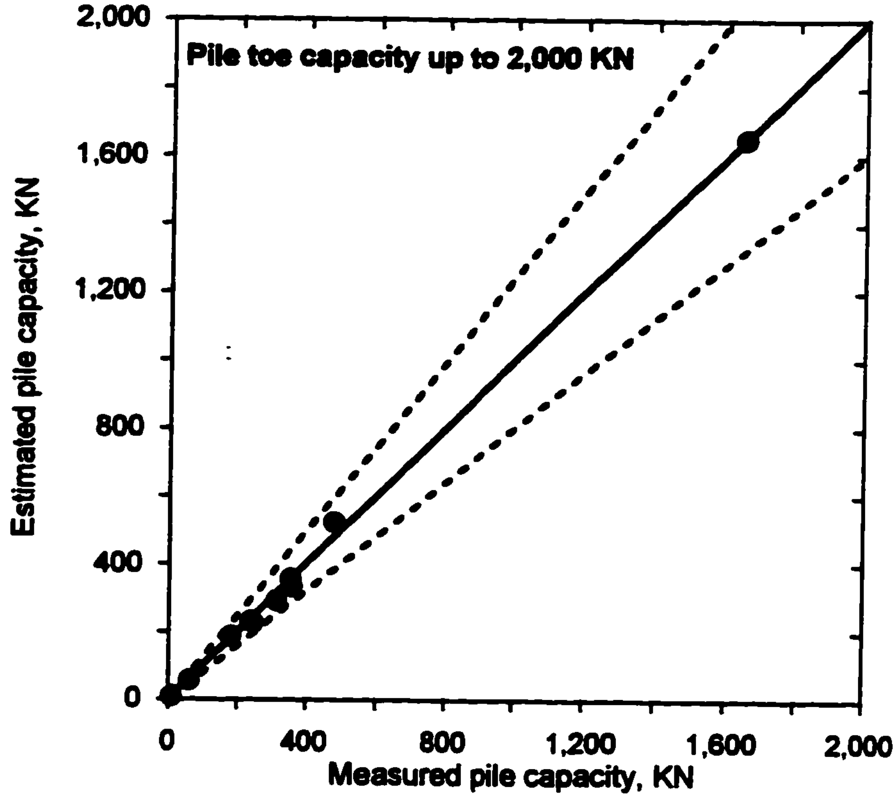

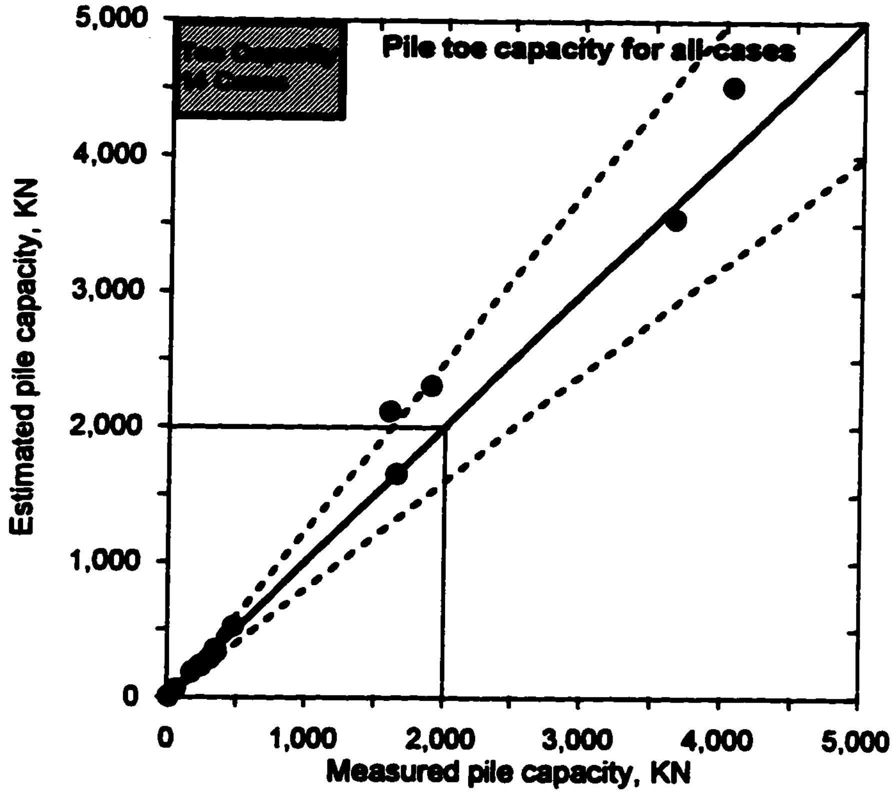

Fig. 8.1 Comparison of measured and estimated pile toe capacity by the proposed method

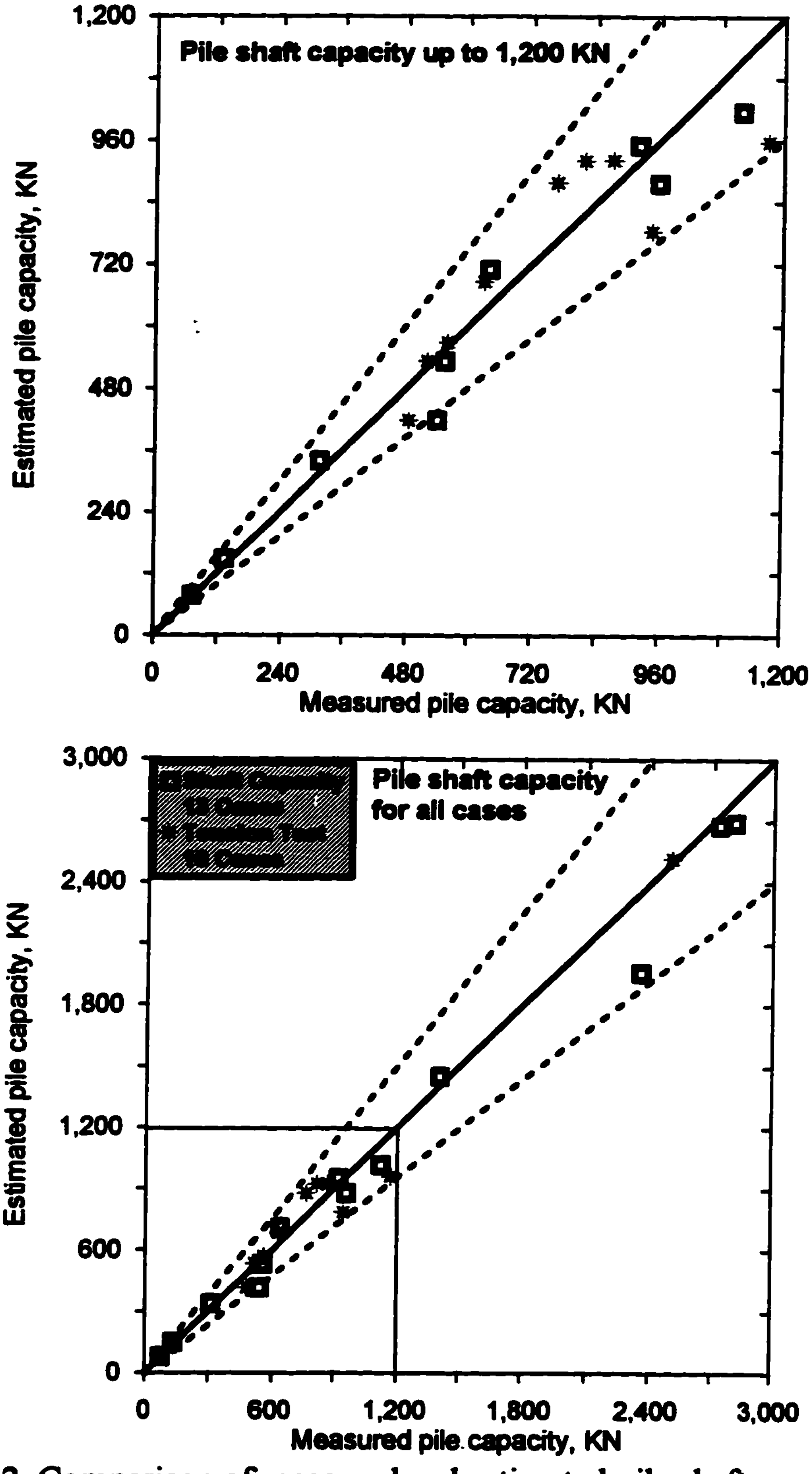

Fig. 8.2 Comparison of measured and estimated pile shaft capacity by the proposed method

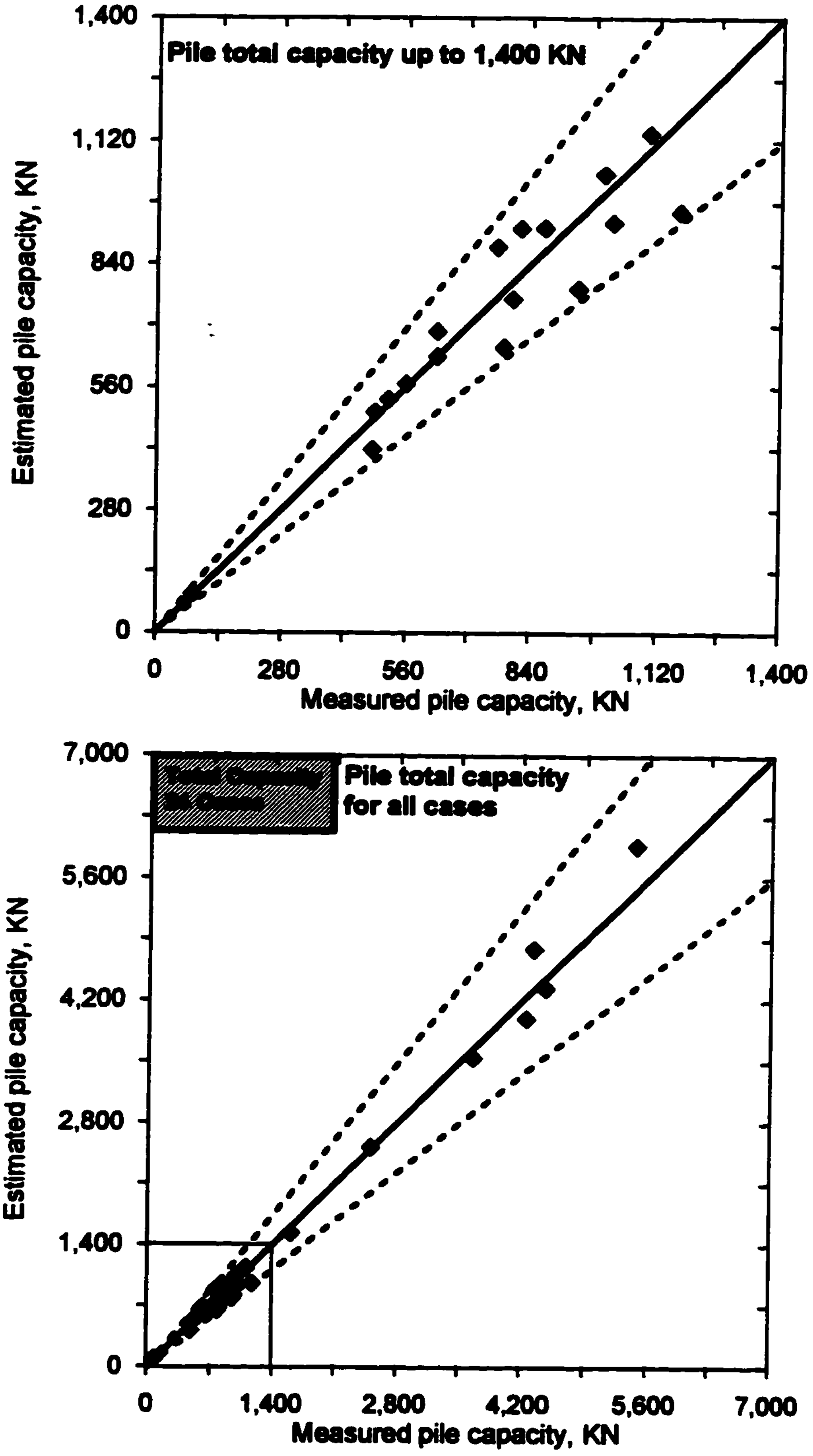

Fig. 8.3 Comparison of measured and estimated pile capacity by the proposed method

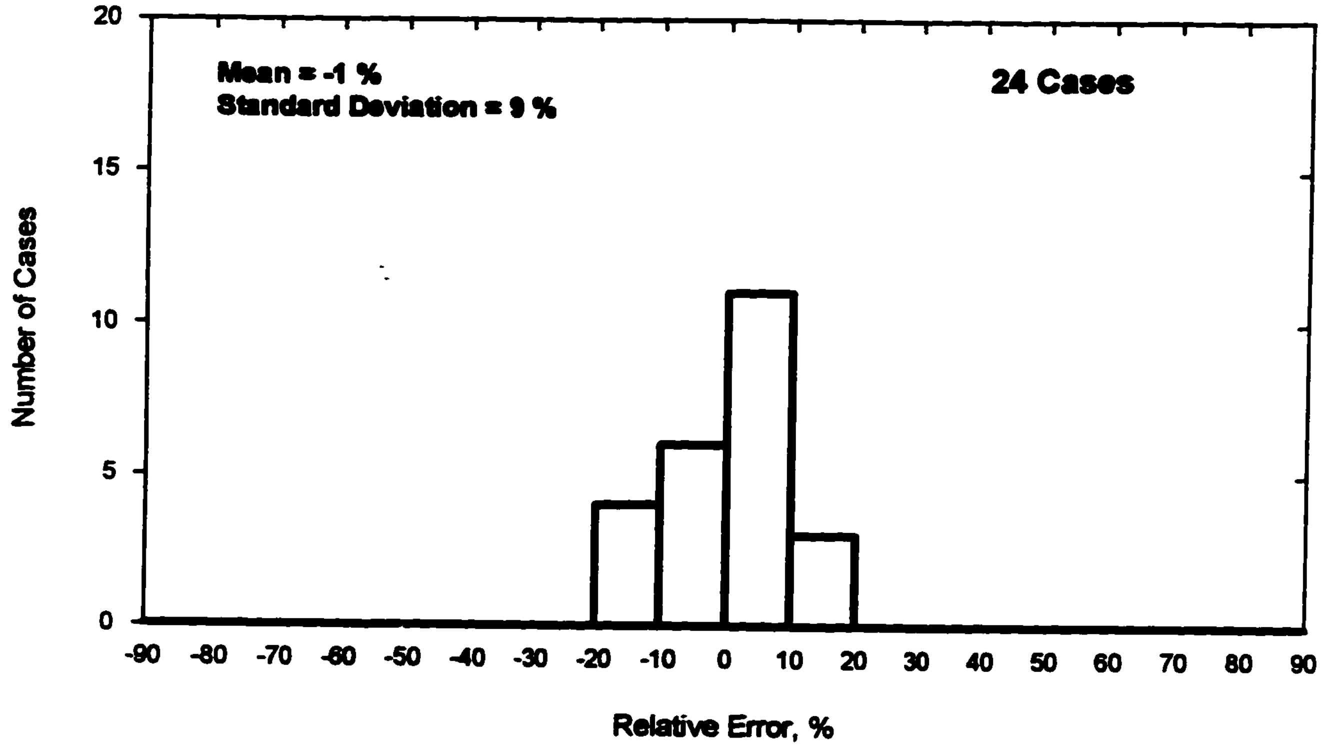

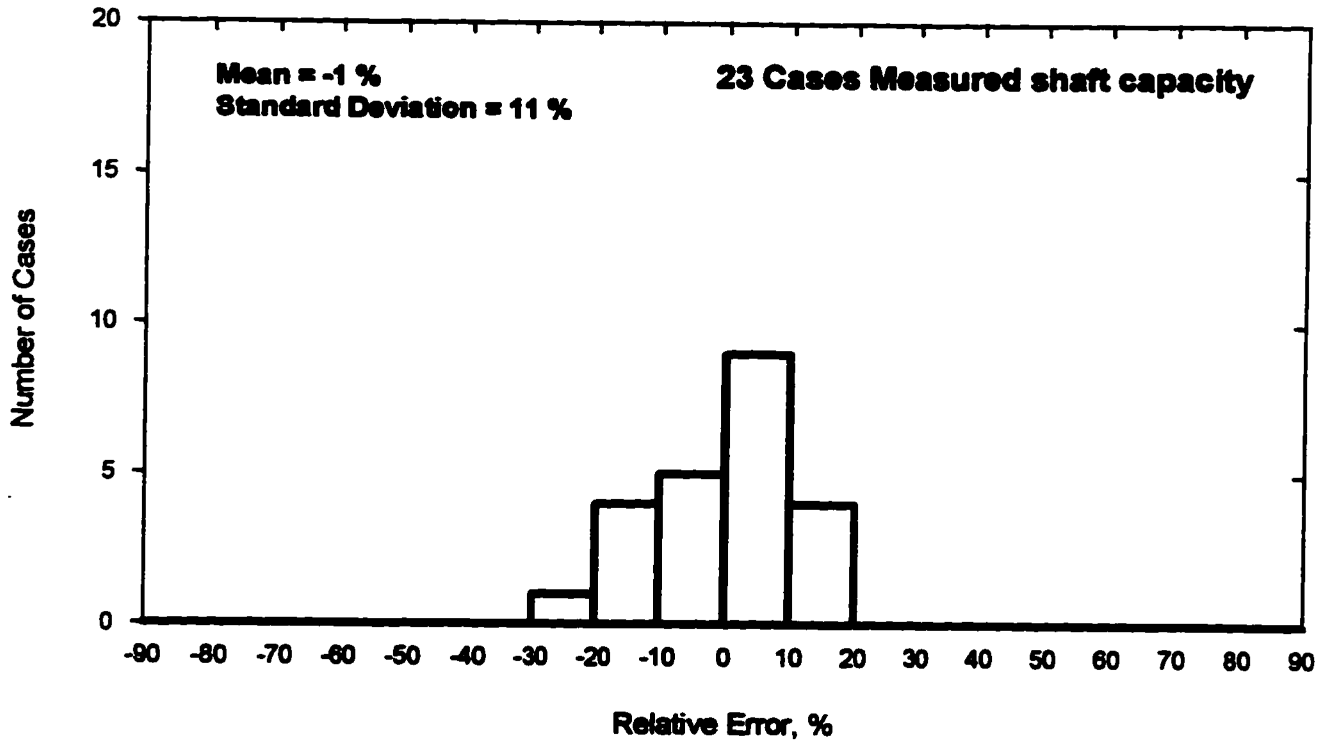

Fig. 8.4 Relative error (%) in pile capacity as determined by the proposed method

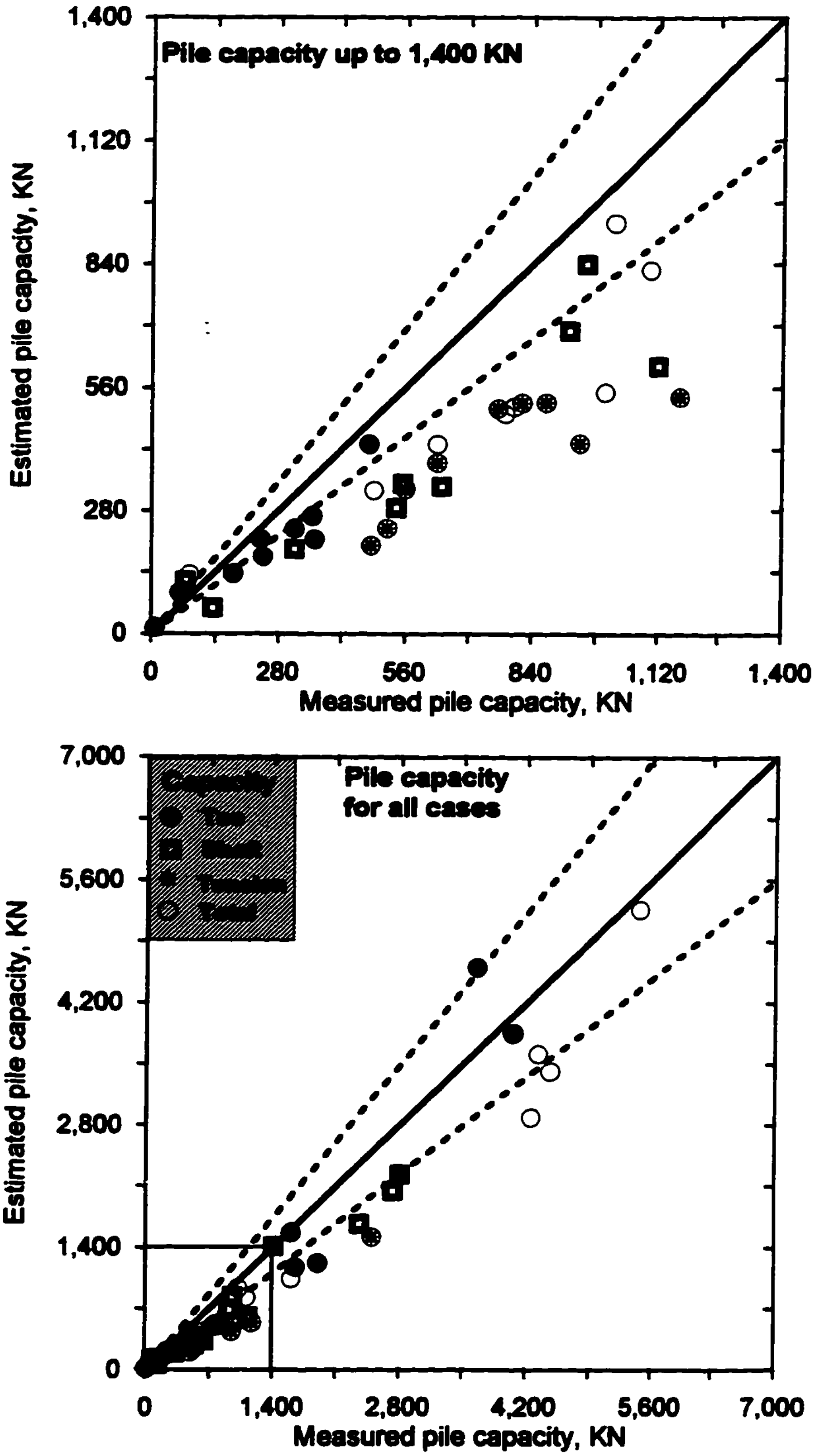

Fig. 9.1 Measured and estimated pile capacity for 24 cases by the Schmertmann method

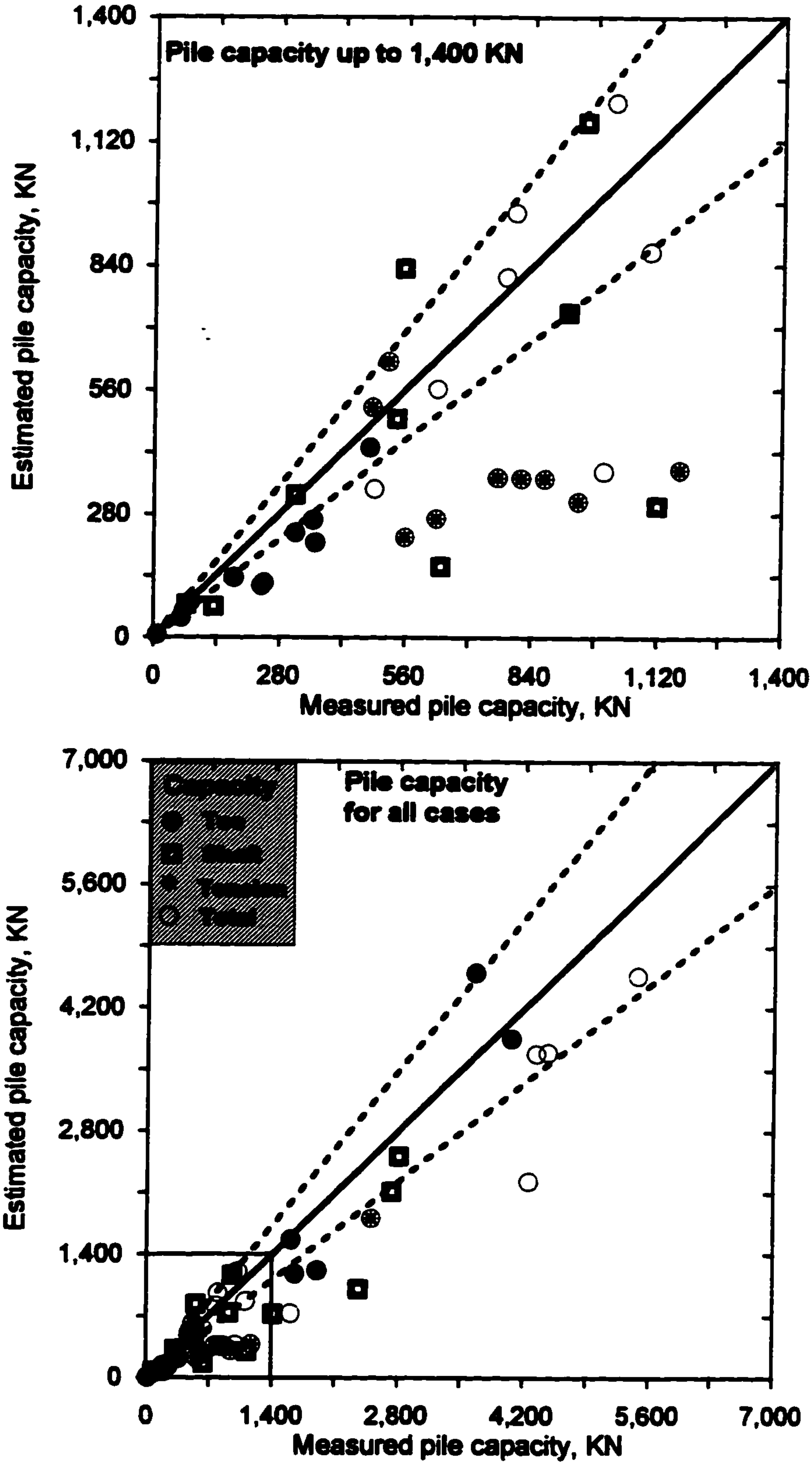

Fig. 9.2 Measured and estimated pile capacity for 24 cases by the European method

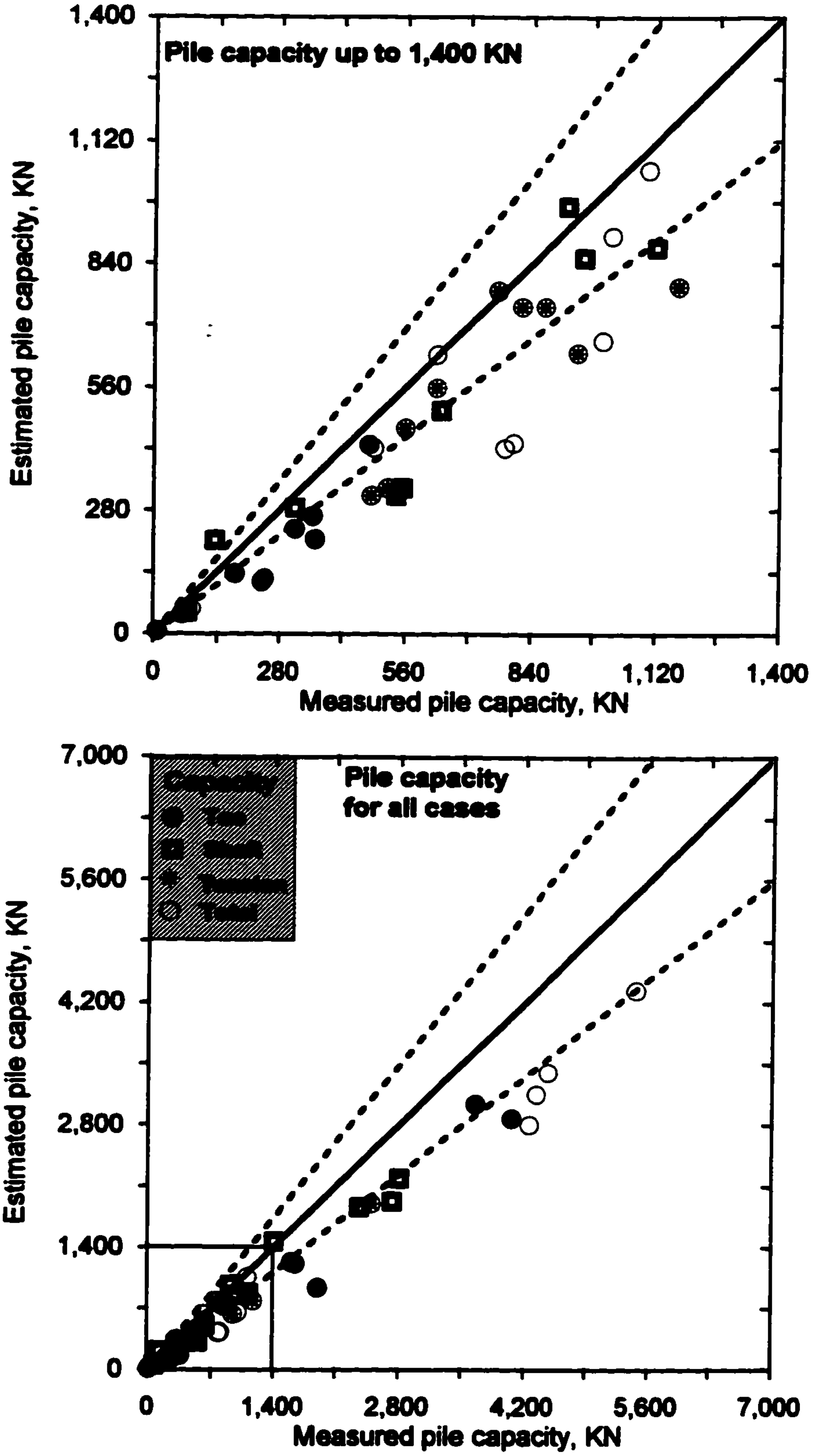

Fig. 9.3 Measured and estimated pile capacity for 24 cases by the French method

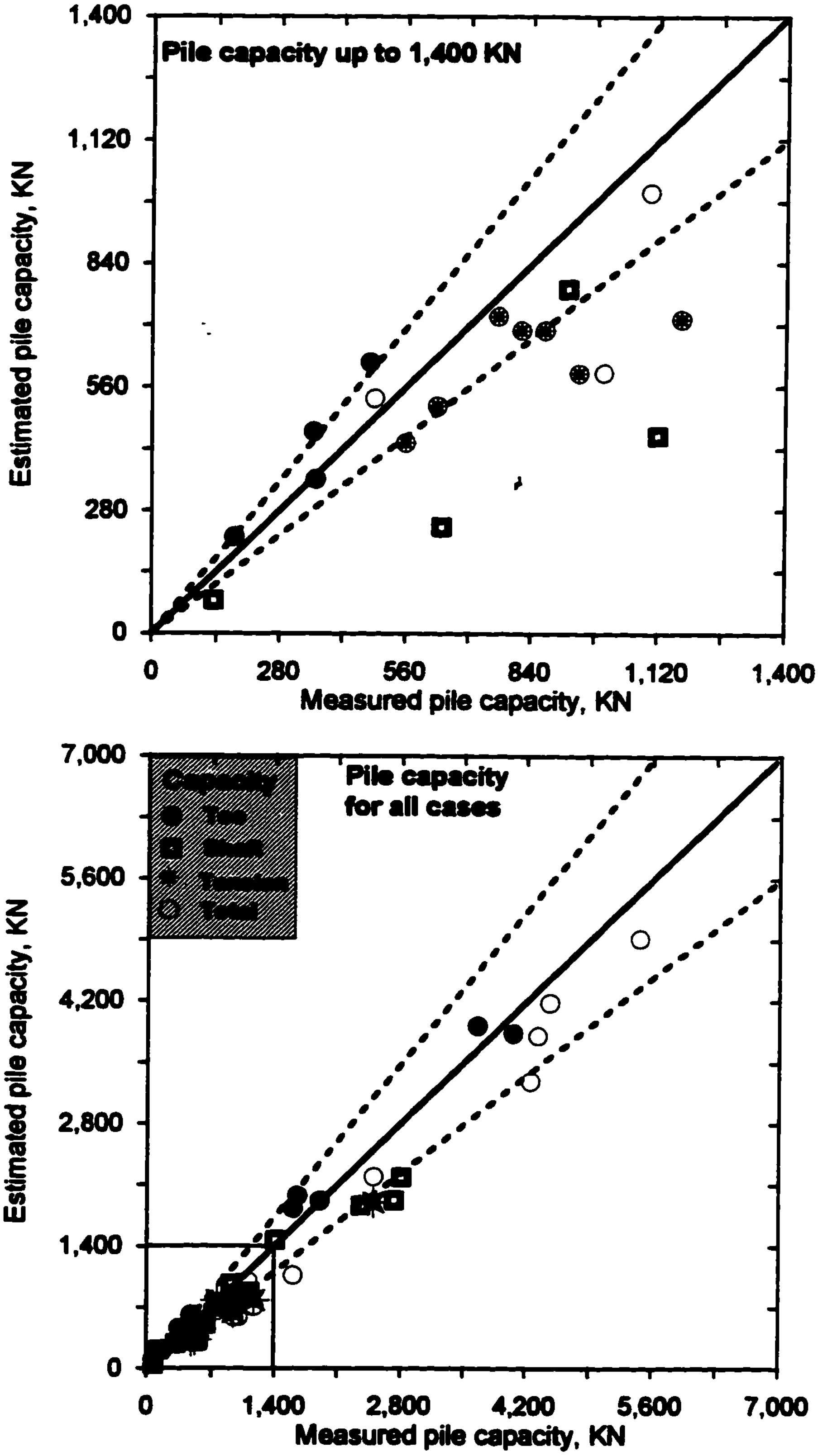

Fig. 9.4 Measured and estimated pile capacity for 17 cases by the Meyerhof method

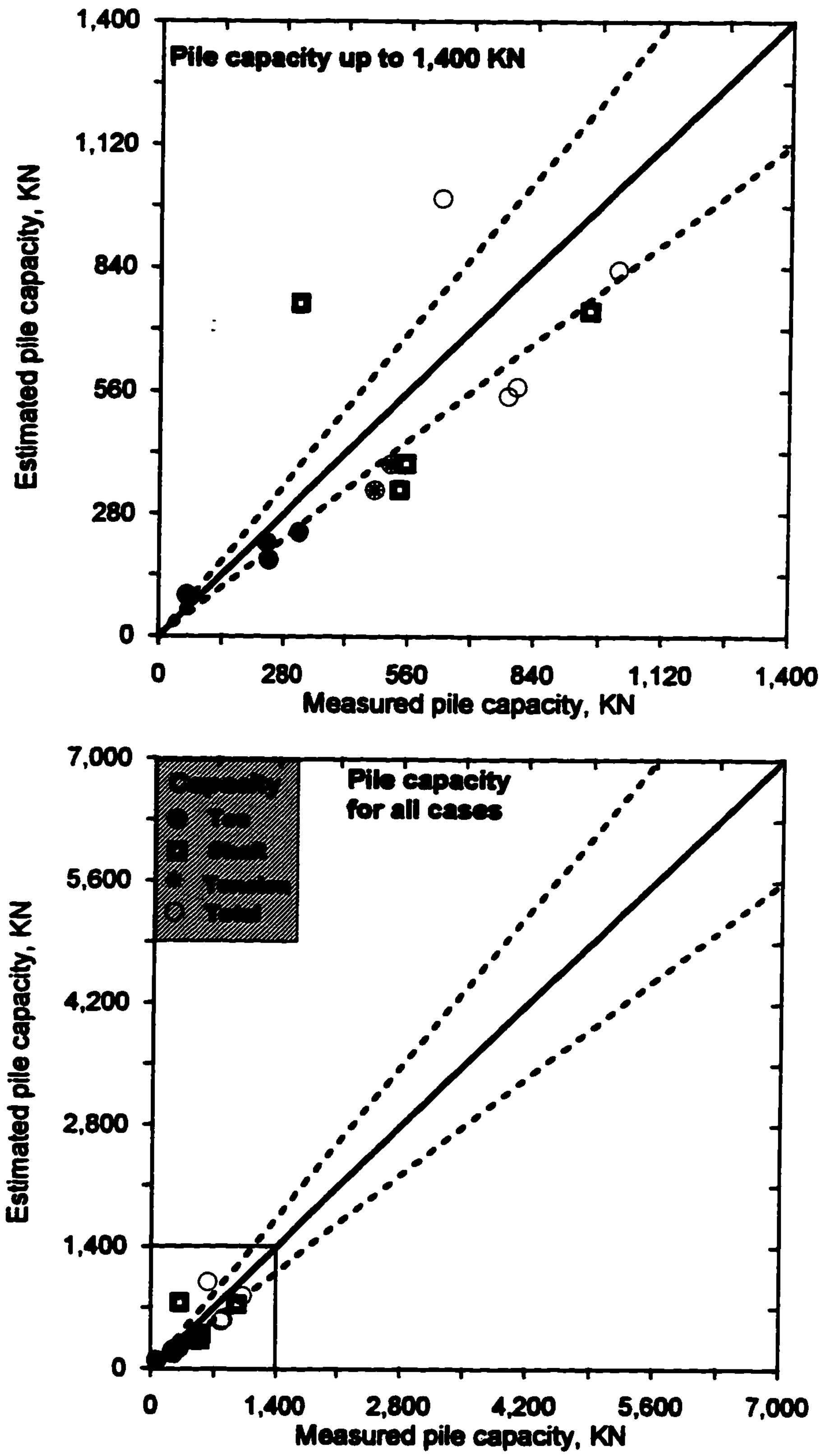

Fig. 9.5 Measured and estimated pile capacity for 6 cases by the Tumay method

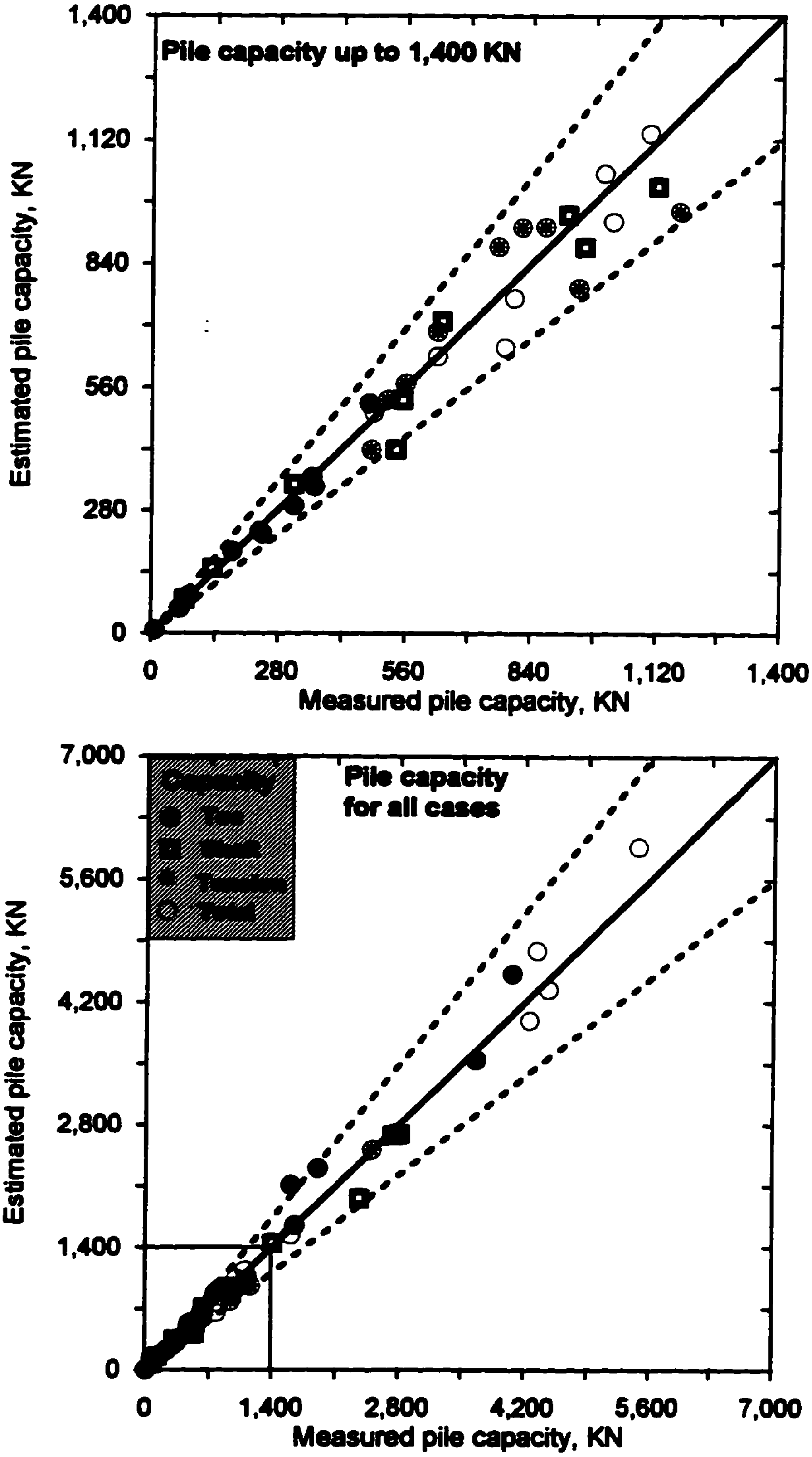

Fig. 9.6 Measured and estimated pile capacity for 24 cases by the proposed method

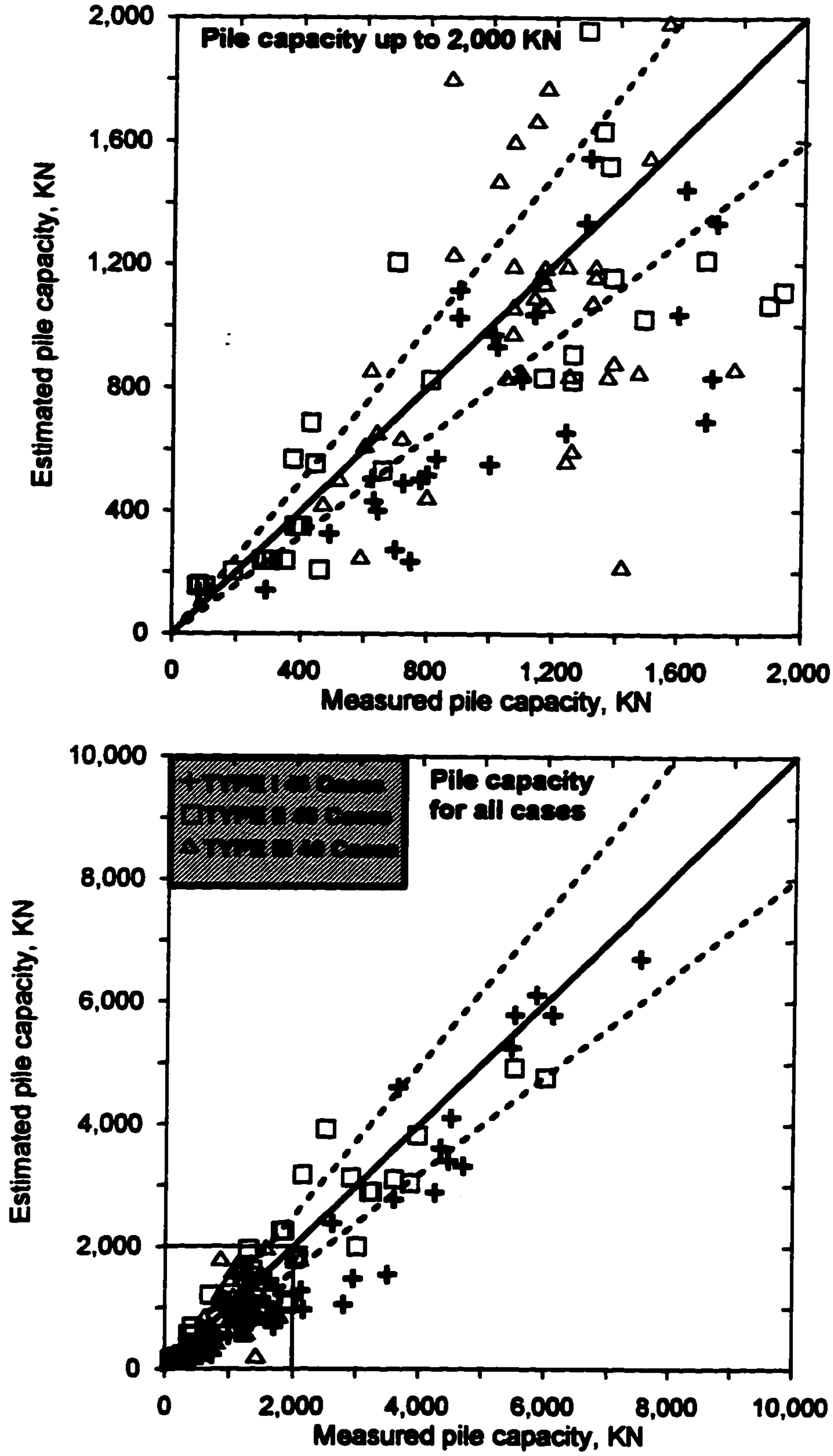

Fig. 9.7 Comparison of measured and estimated pile capacity by the Schmertmann method

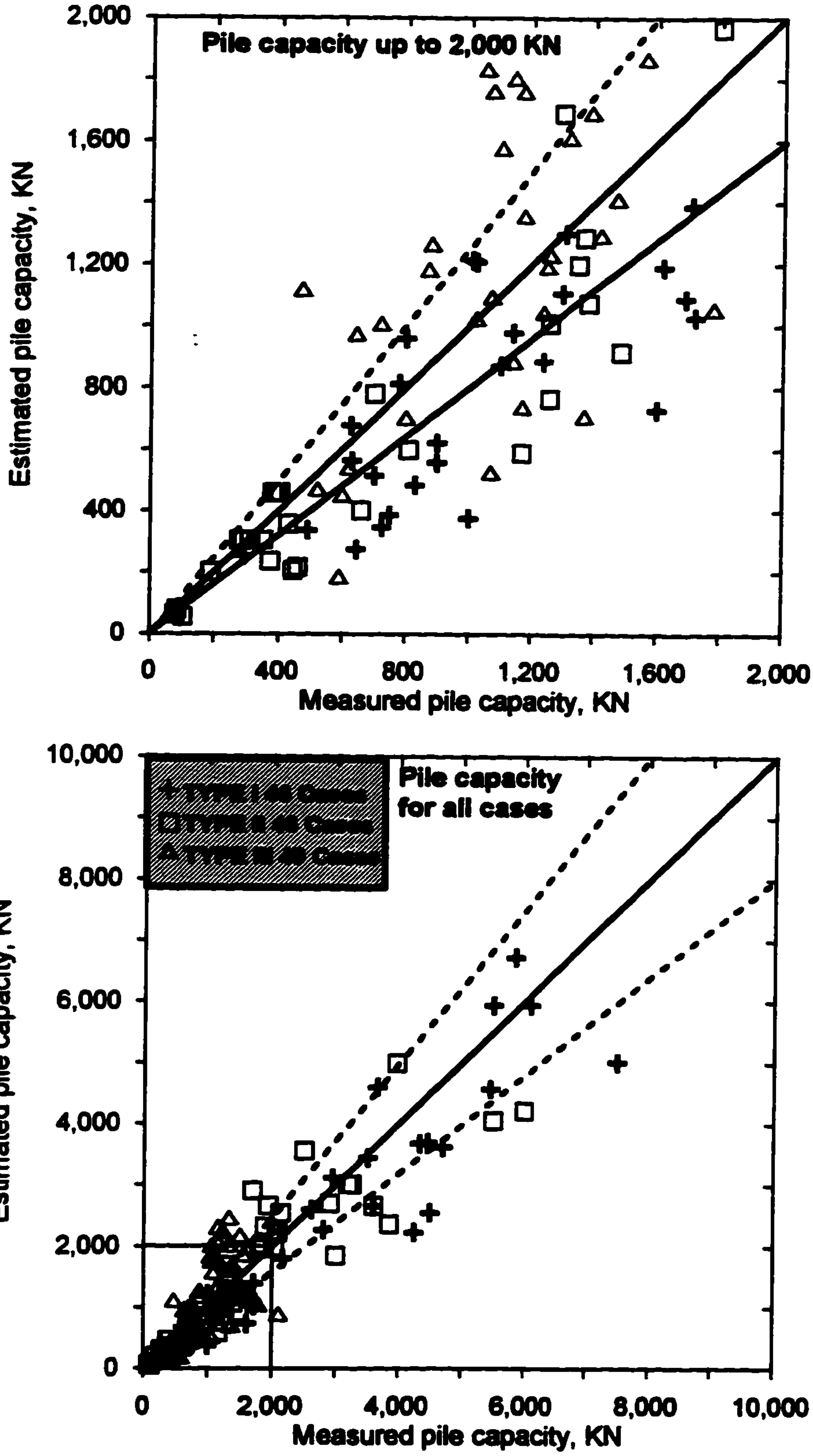

Fig. 9.8 Comparison of measured and estimated pile capacity by the European method

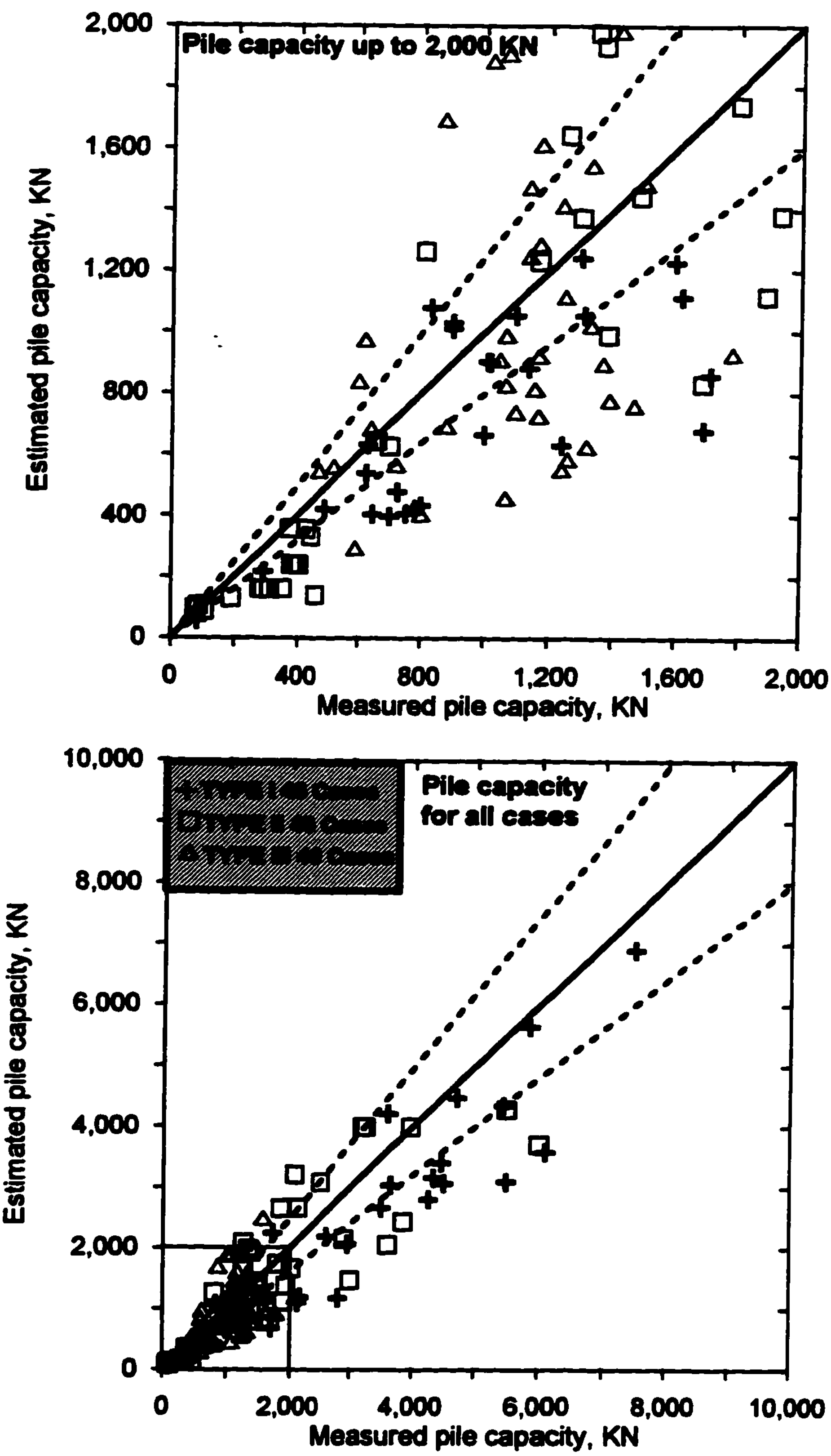

Fig. 9.9 Comparison of measured and estimated pile capacity by the French method

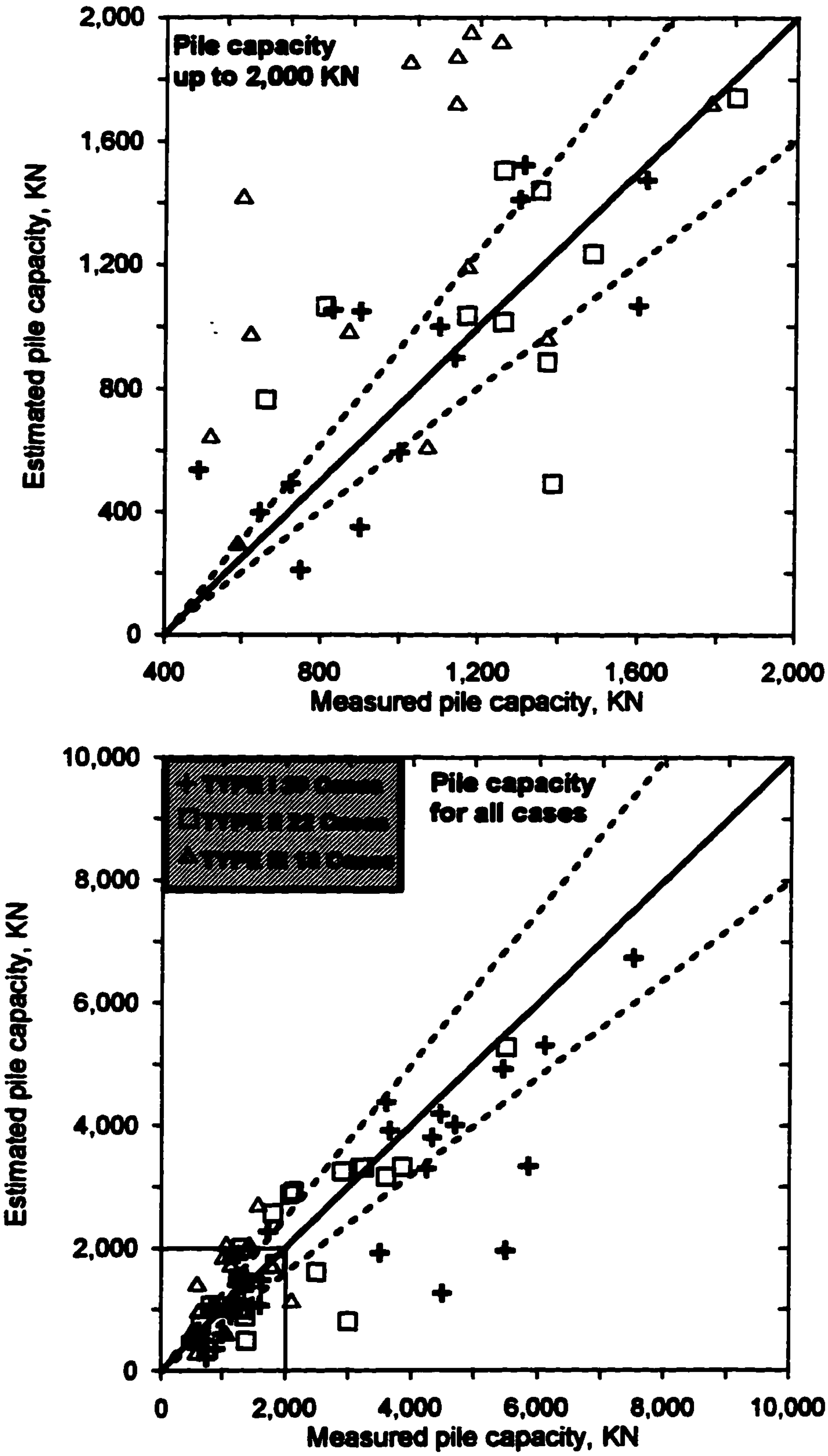

Fig. 9.10 Comparison of measured and estimated pile capacity by the Meyerhof method

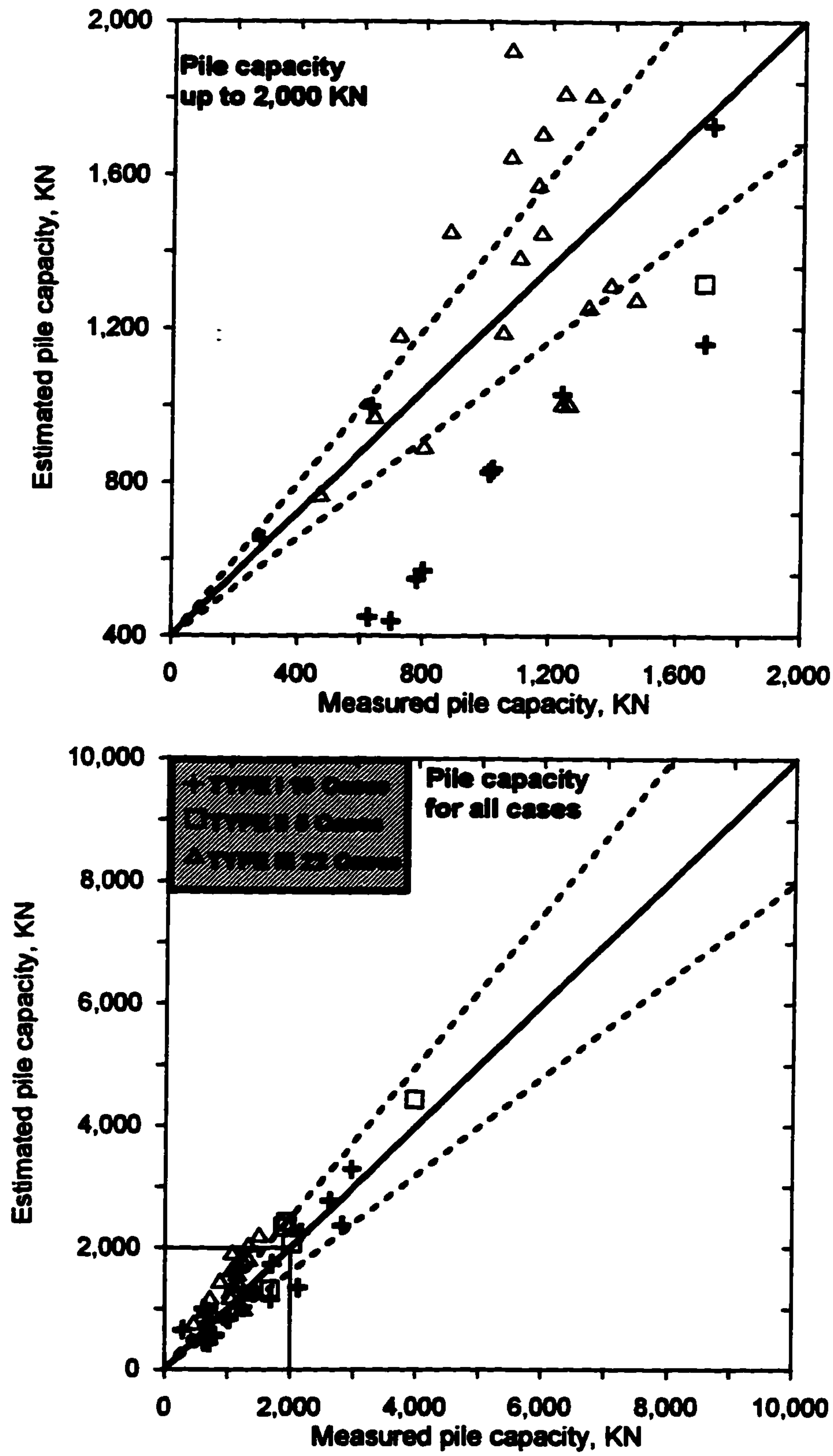

Fig. 9.11 Comparison of measured and estimated pile capacity by the Tumay method

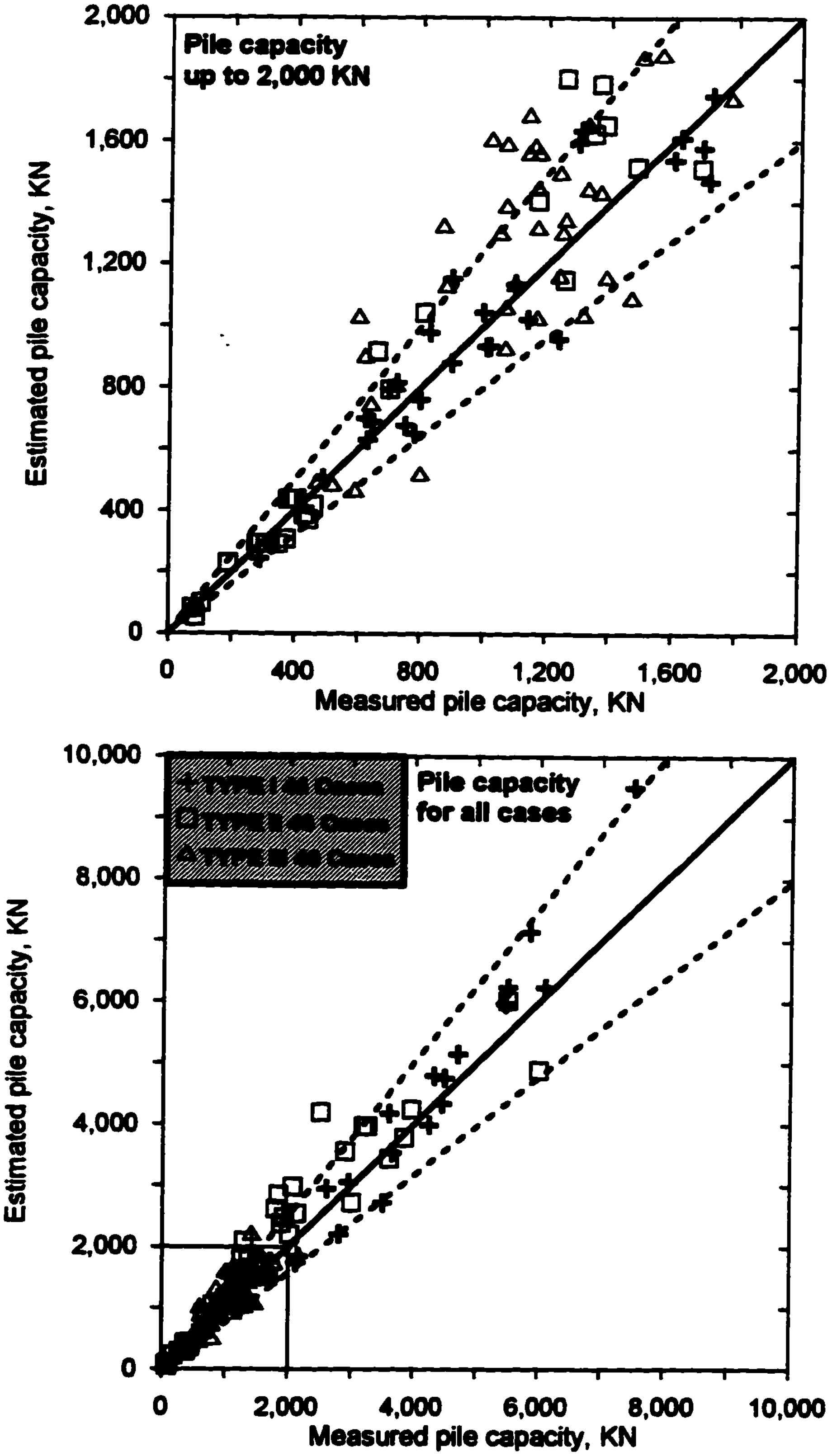

Fig. 9.12 Comparison of measured and estimated pile capacity by the proposed method

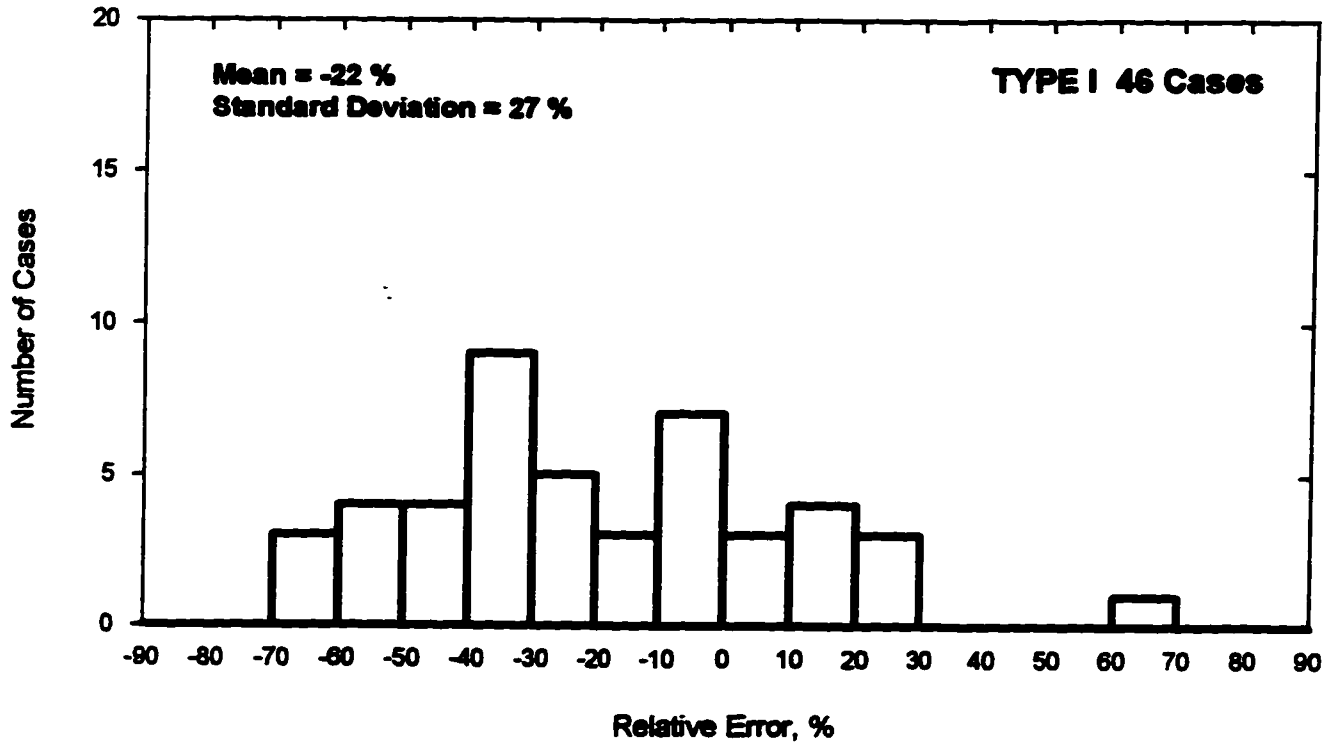

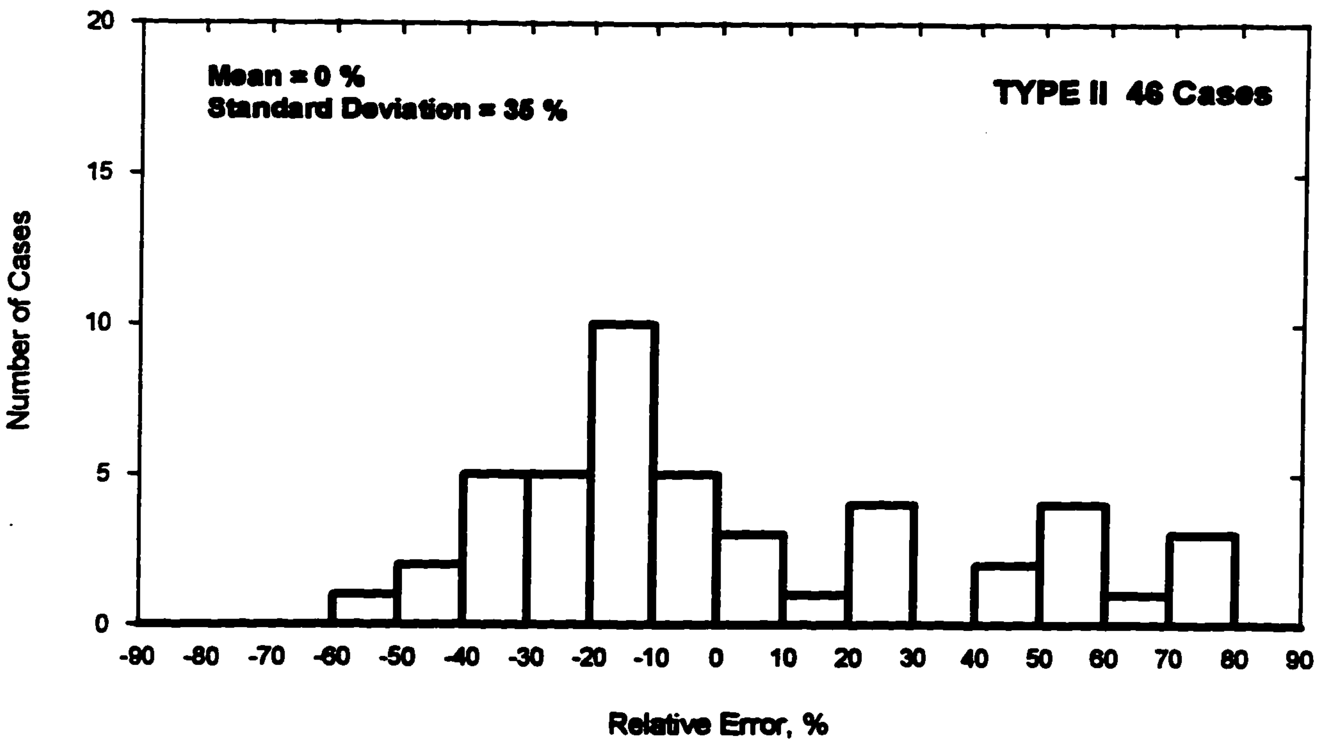

Fig. 9.13 Relative error (%) in pile capacity as determined by the Schmertmann method

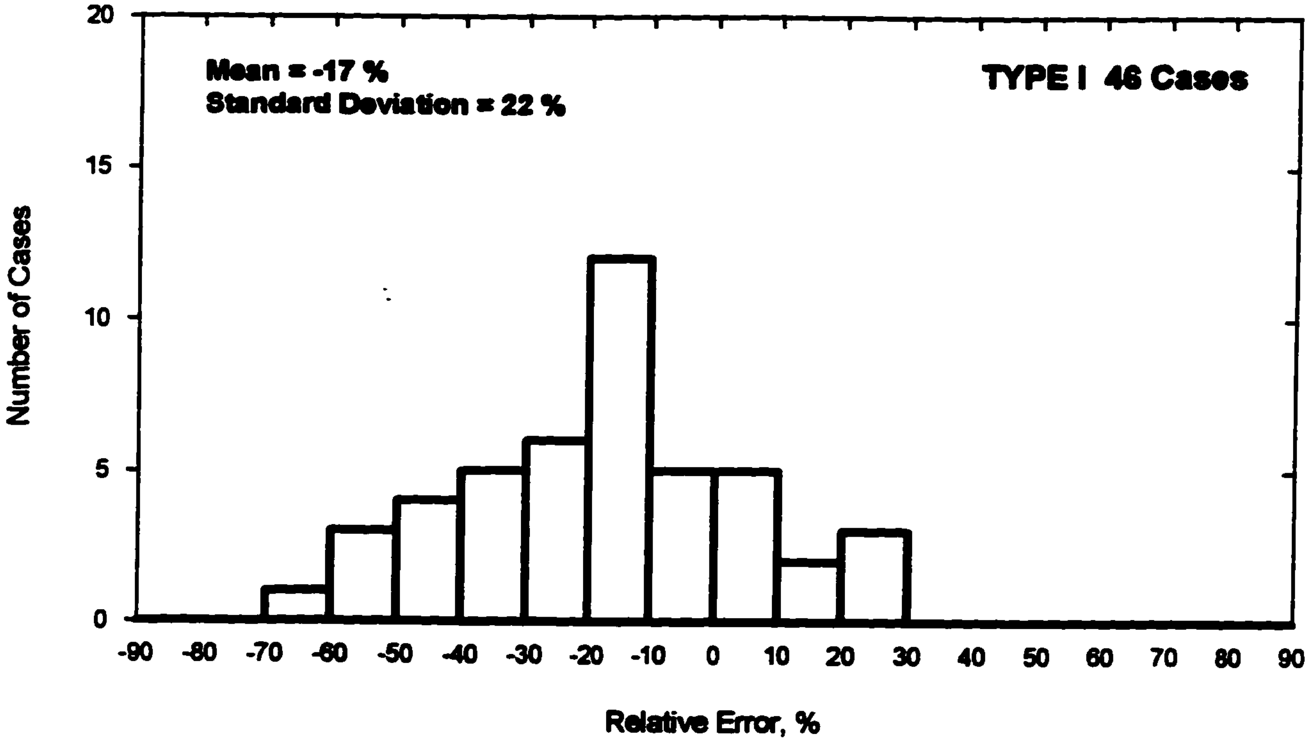

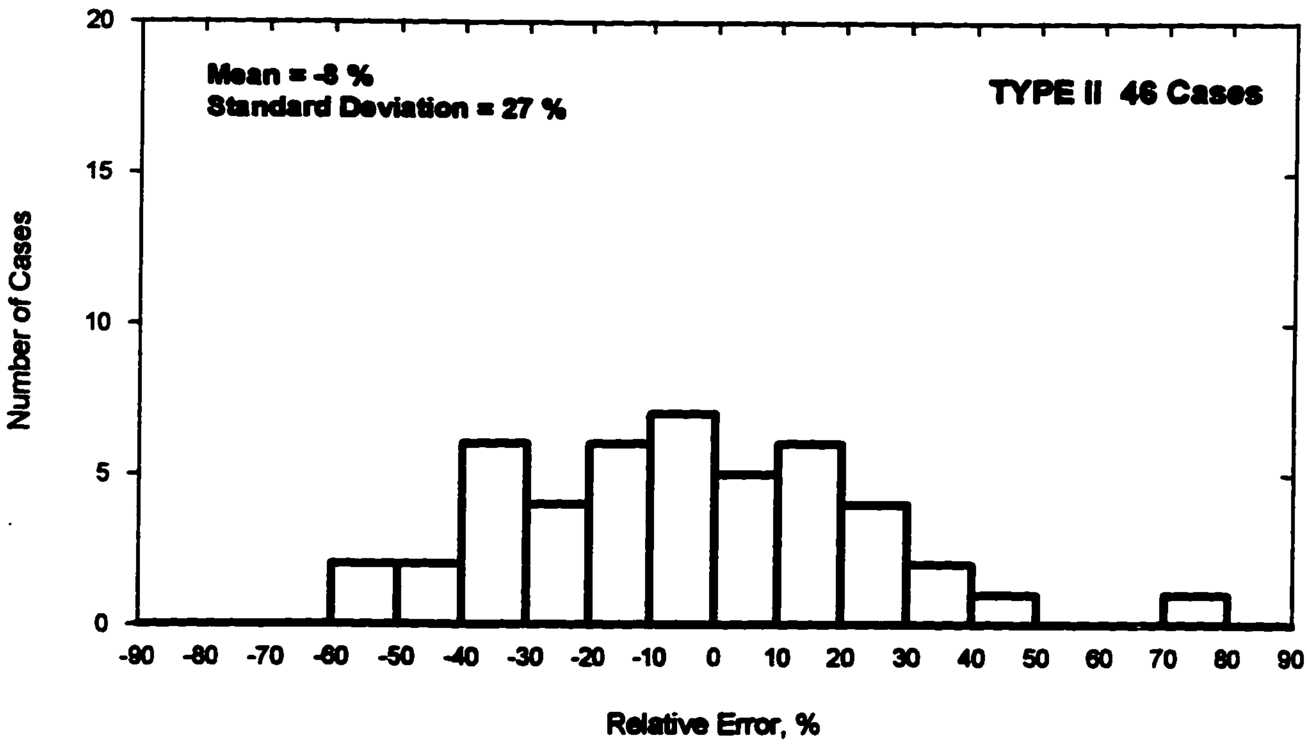

Fig. 9.14 Relative error (%) in pile capacity as determined by the European method

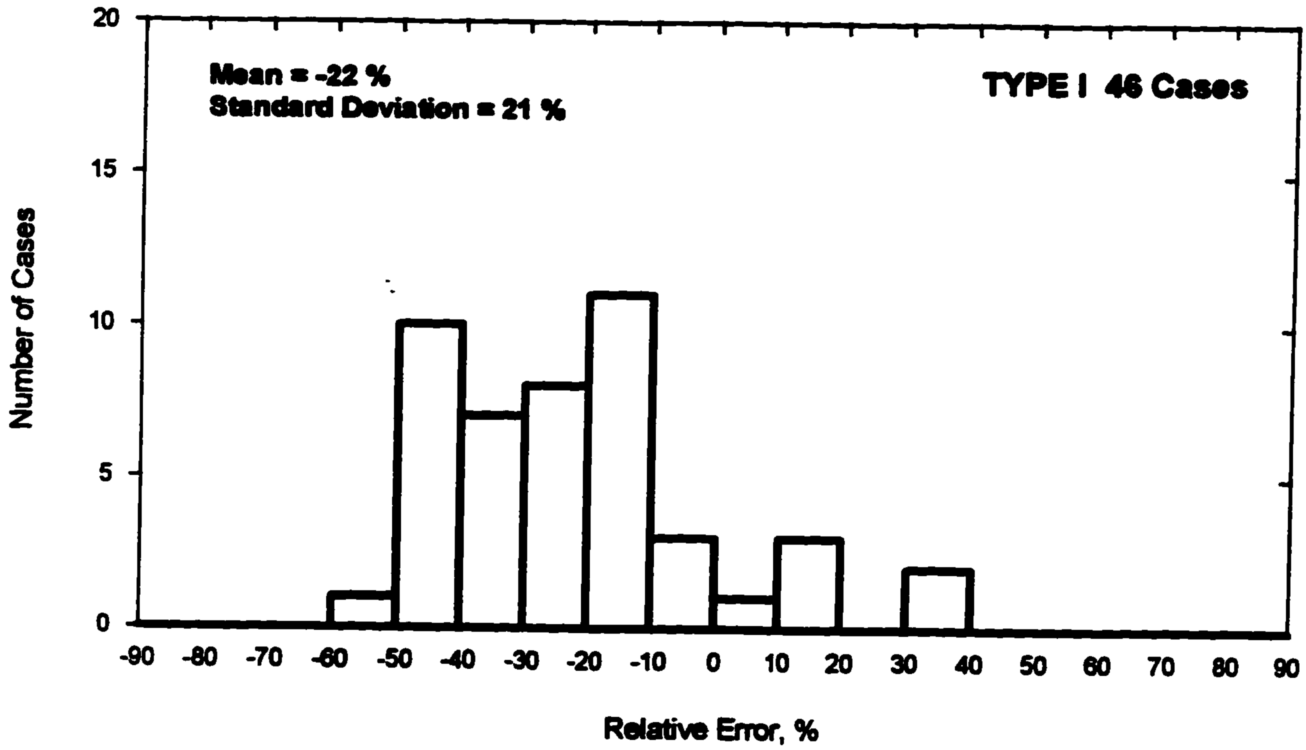

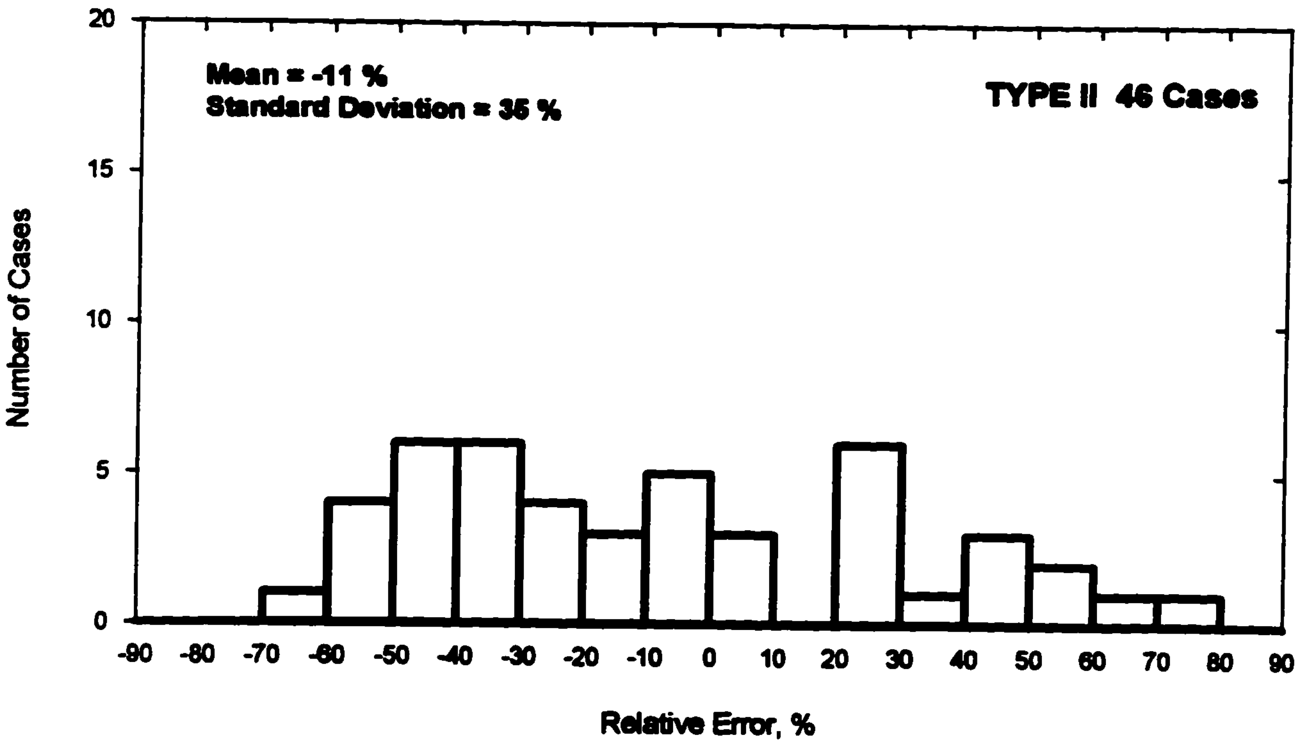

Fig. 9.15 Relative error (%) in pile capacity as determined by the French method

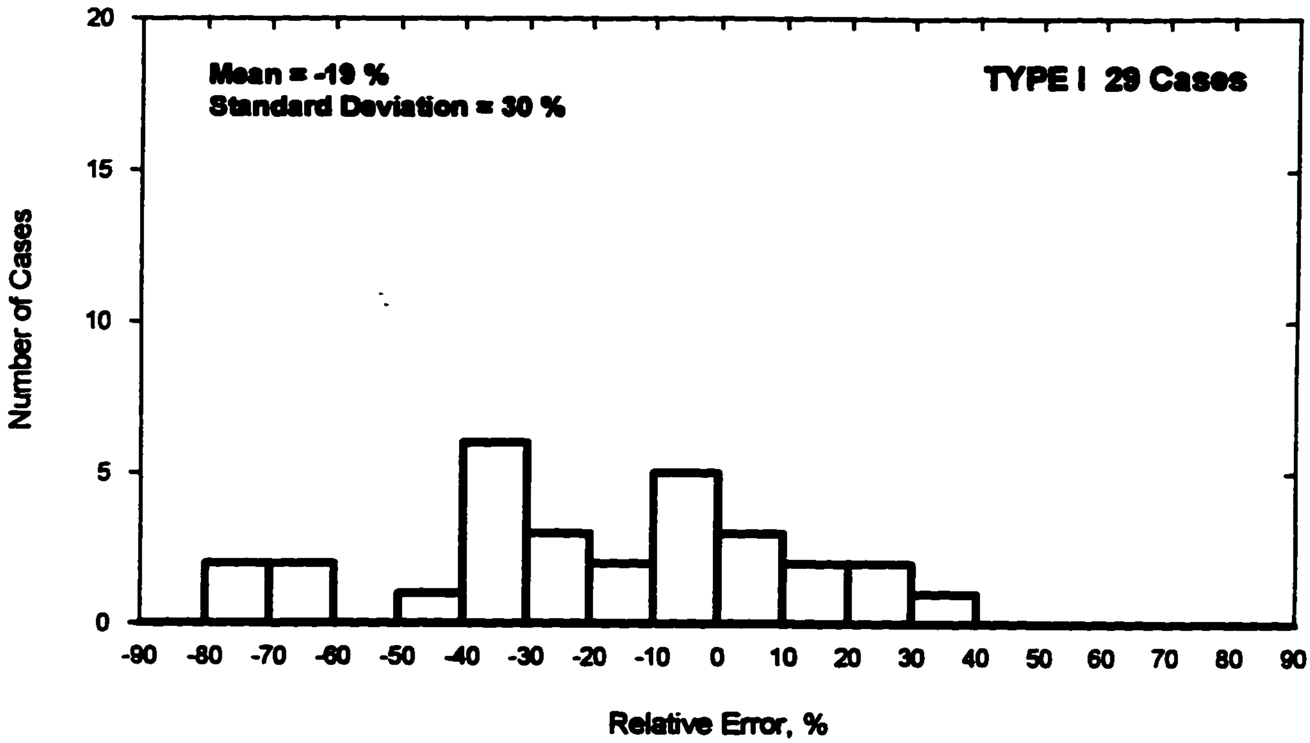

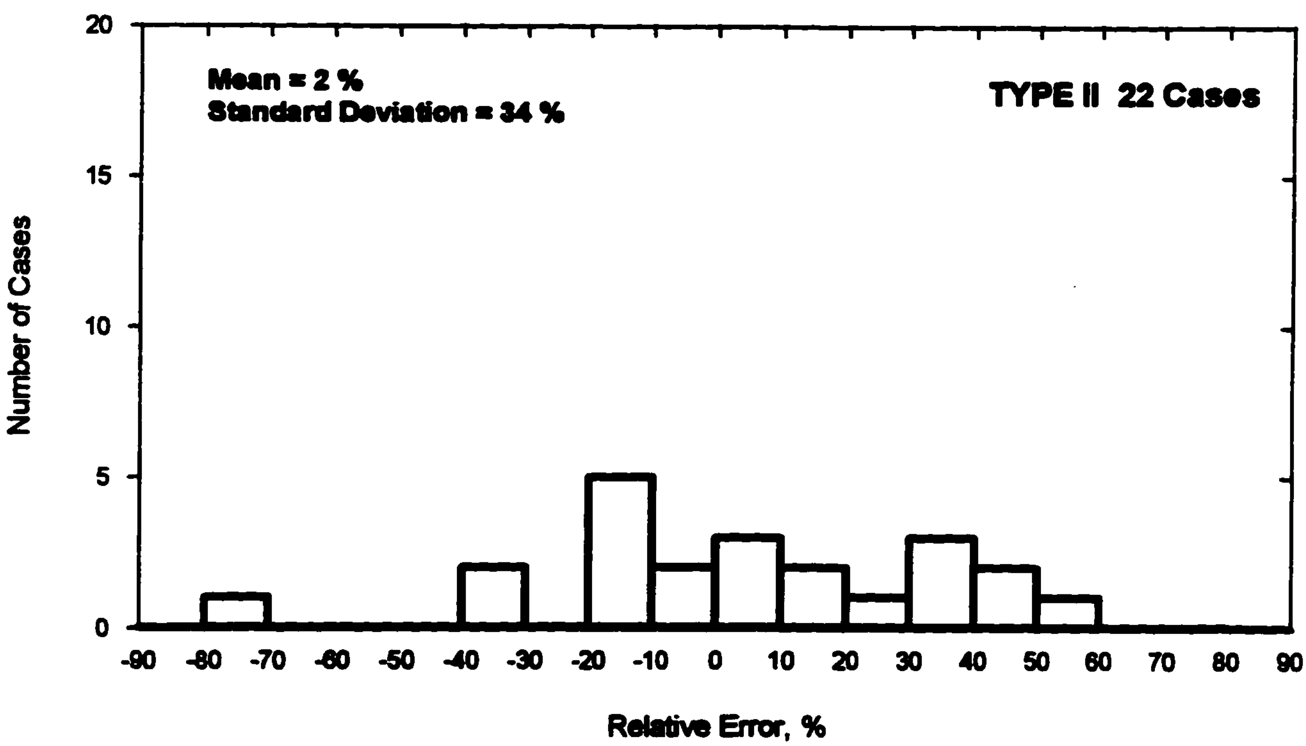

Fig. 9.16 Relative error (%) in pile capacity as determined by the Meyerhof method

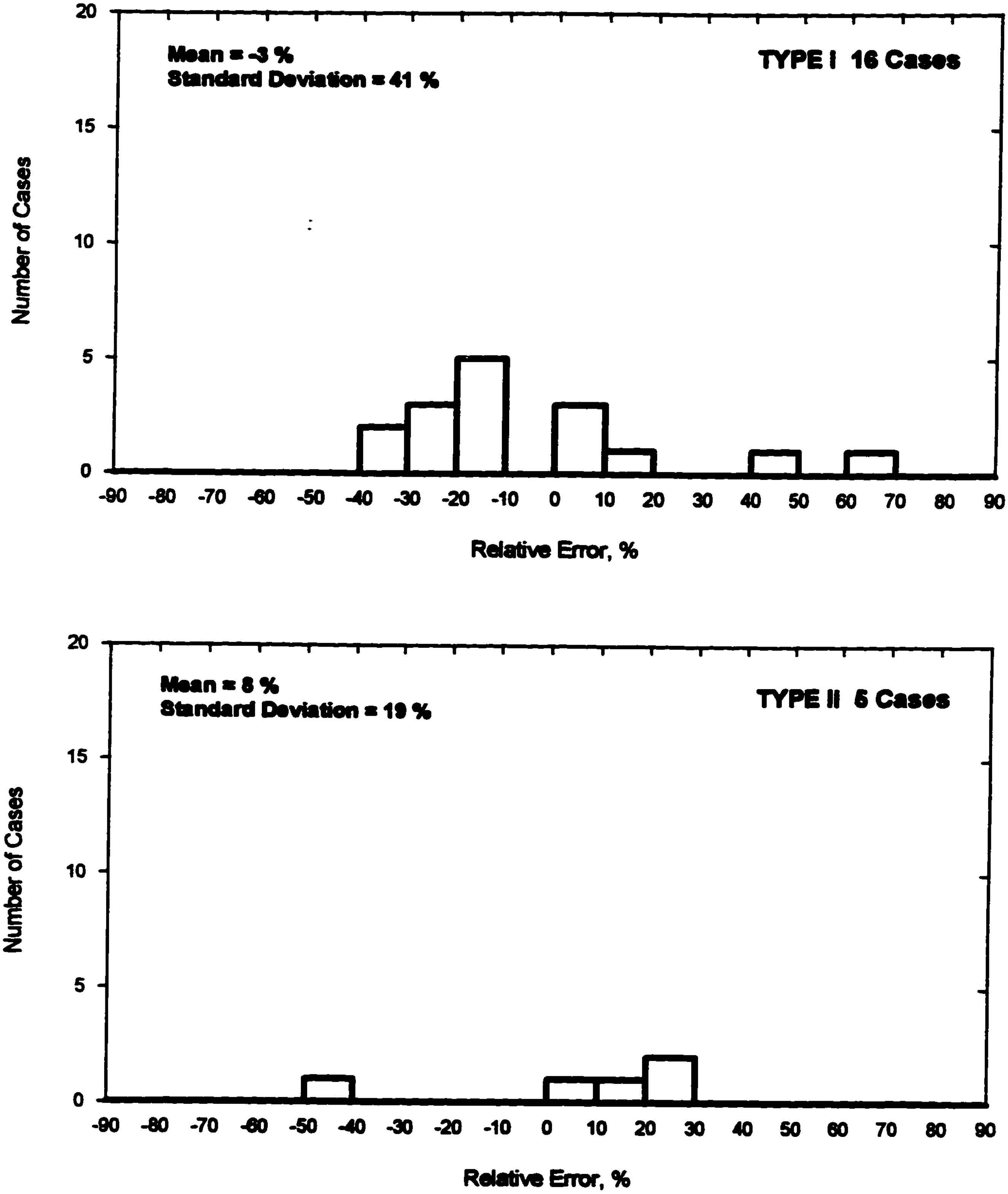

Fig. 9.17 Relative error (%) in pile capacity as determined by the Tumay method

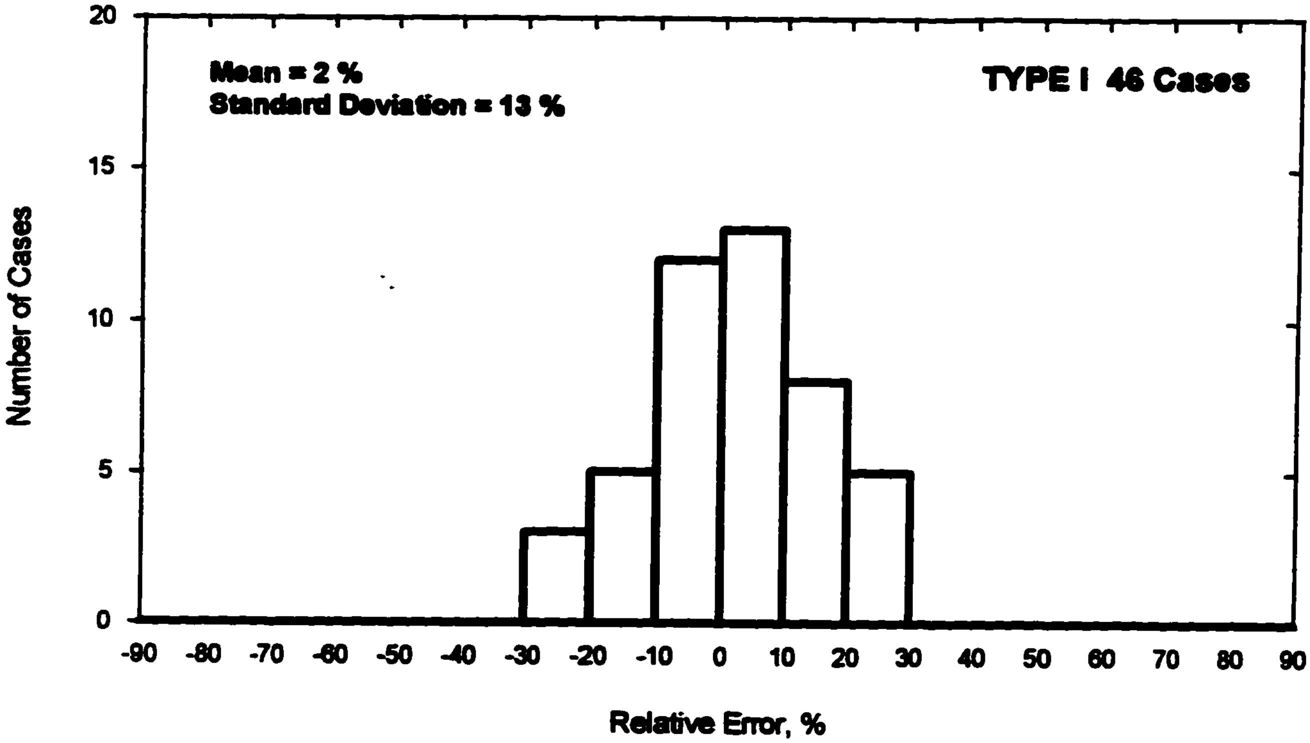

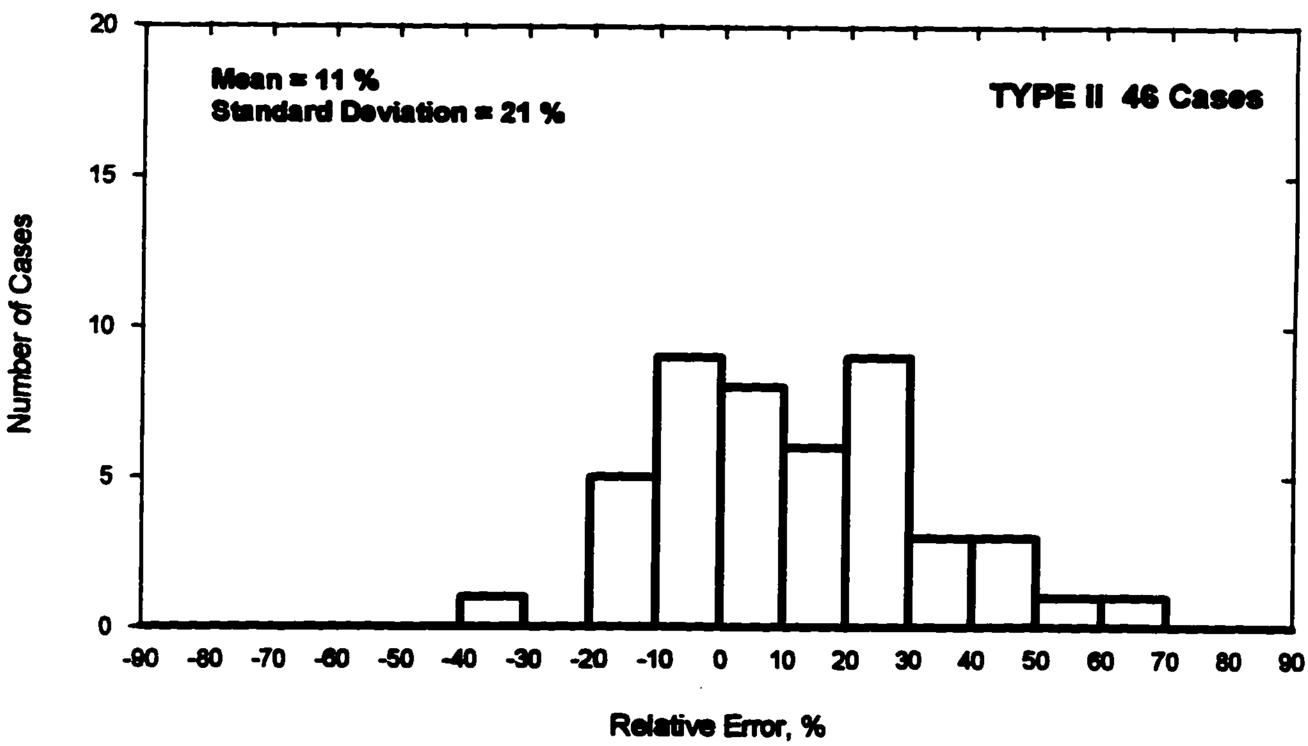

Fig. 9.18 Relative error (%) in pile capacity as determined by the proposed method

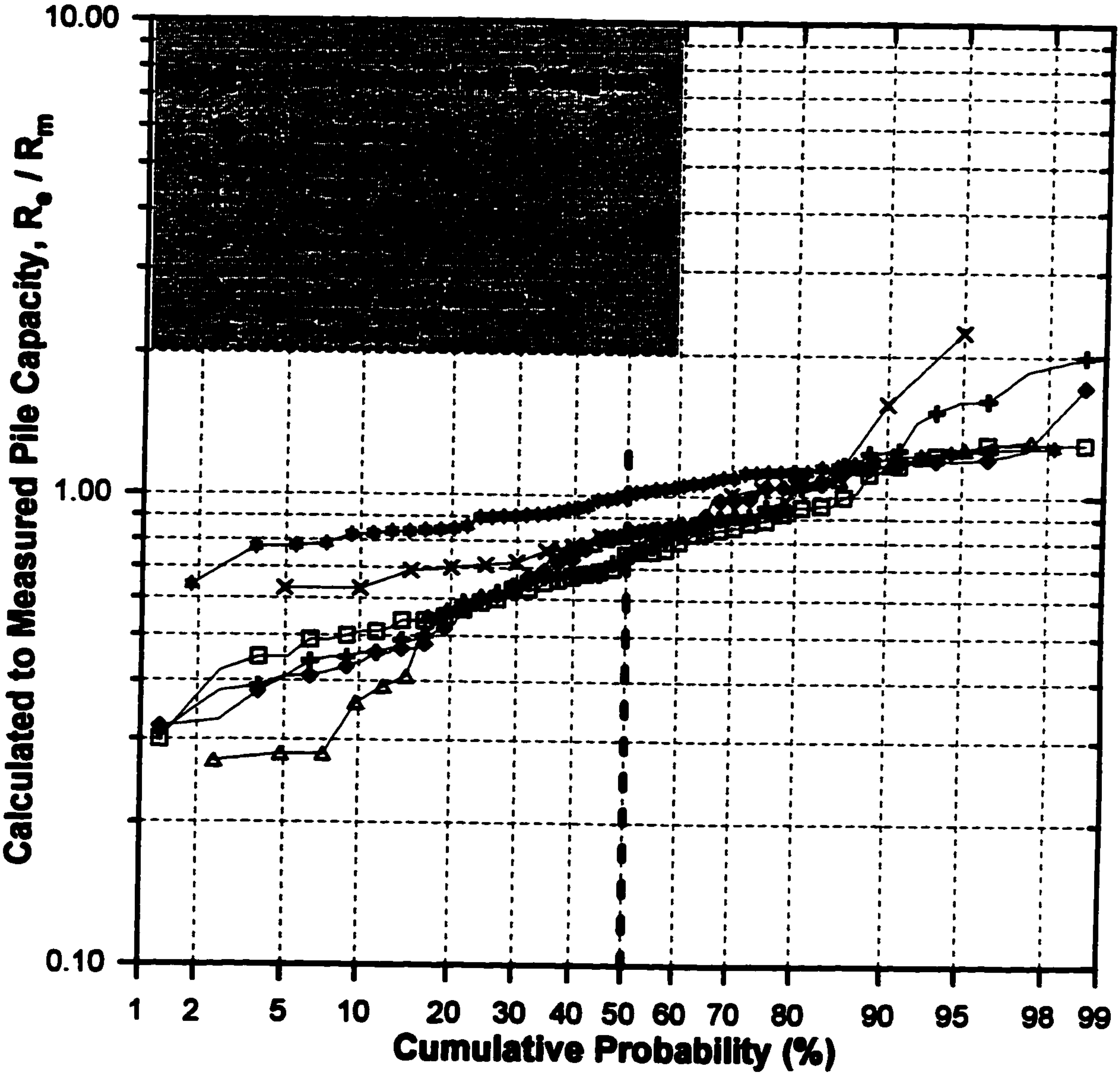

Fig. 9.19 Comparison of the methods estimation using probability approach

APPENDIX

Case Records

Sheet "a" CPT Profile

Sheet "b" Pile Characteristics

Case 1 UBC2
Sheet a CPT data

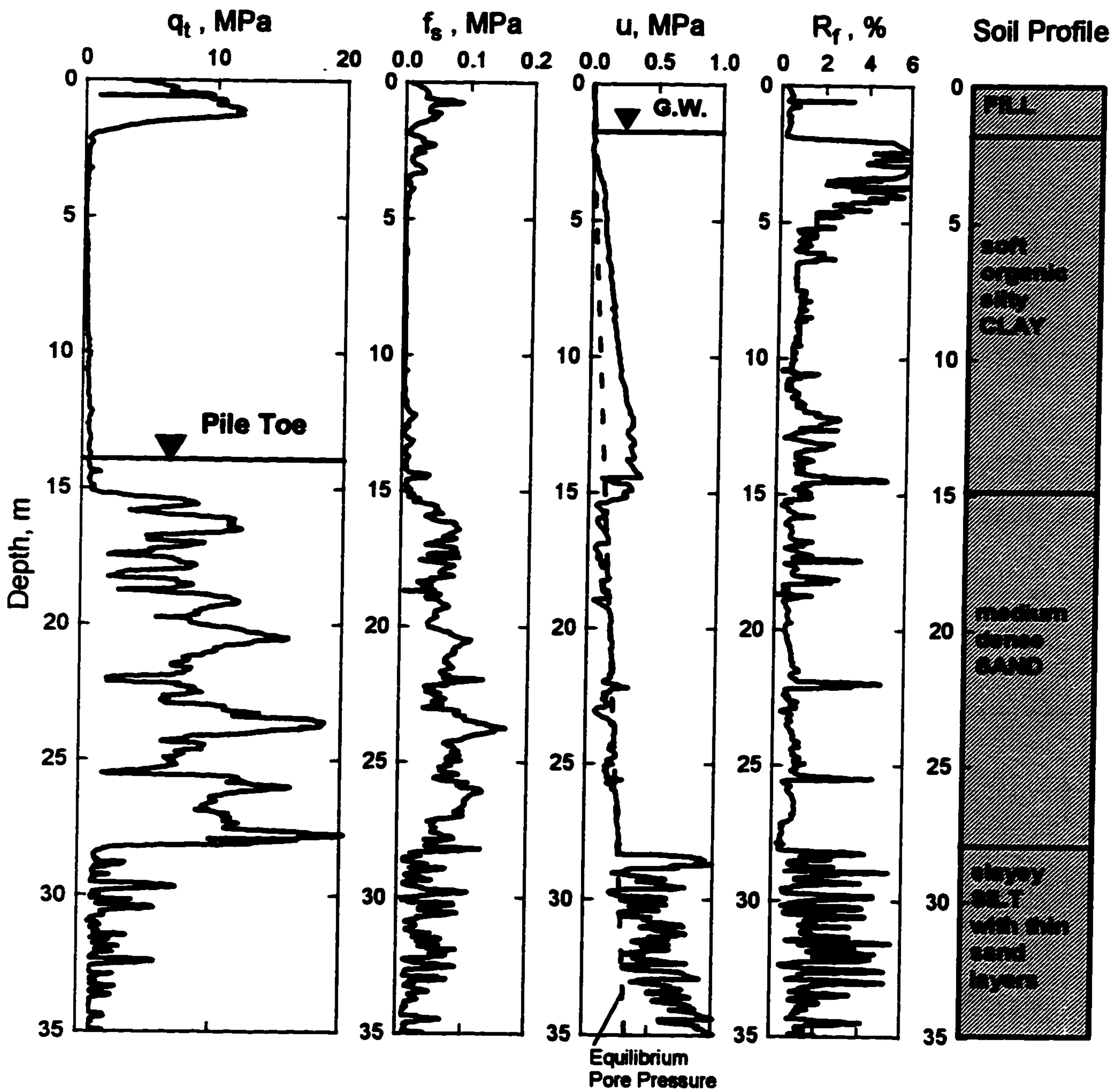

Case 1 UBC2
Sheet b Pile data

	DETAIL	DESCRIPTION
1	Site	Vancouver, Canada
2	Reference	Campanella et al., 1989
3	Shape, Material, and Installation	Pipe, Steel, Driven
4	Diameter, b, and Wall Thickness, t, mm	324 9.5
5	Embedment Length D, m	13.7
6	Cross Sectional Area A_t, m^2	0.082
7	Unit Circumferential Area, A_s, m^2/m	1.018
8	Toe, Closed or Open	Closed
9	Type of Test and Loading	Static Compression, QML
10	Toe Capacity, R_t, KN	
11	Shaft Capacity, R_s, KN	
12	*Capacity, R_u, KN	290

SCHEMATIC PROFILE

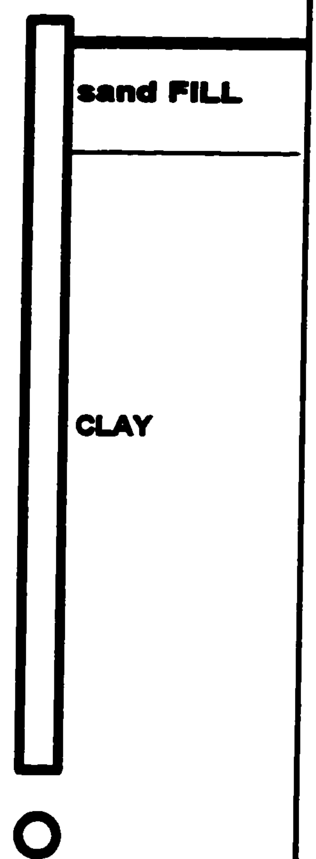

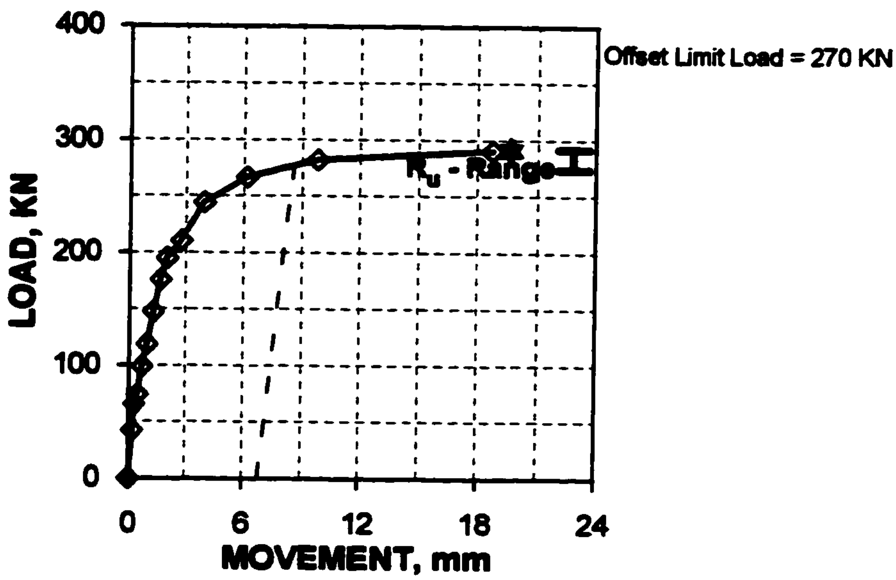

Case 2 UBC3
Sheet a CPT data

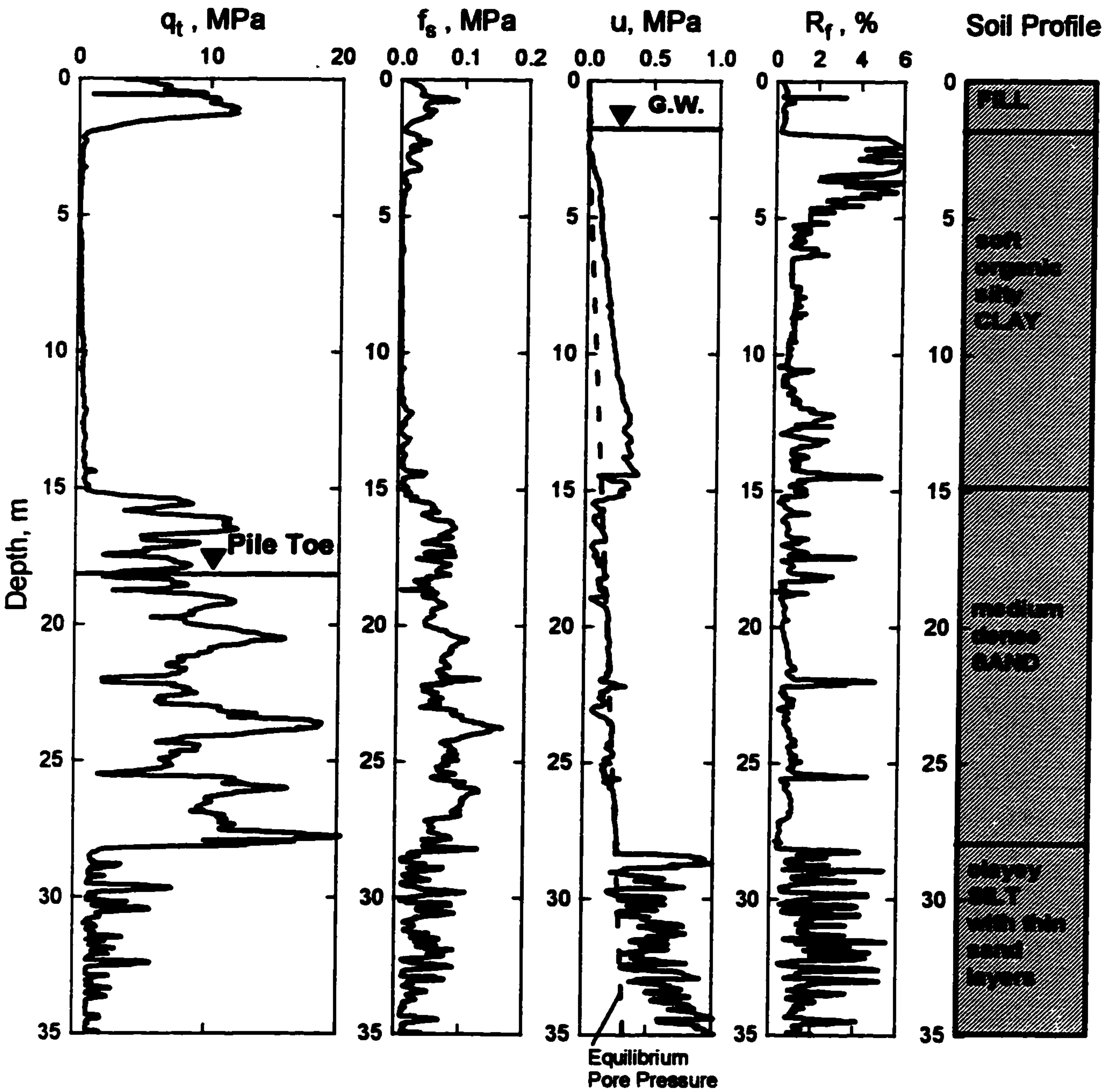

Case 2 UBC3
Sheet b Pile data

DETAIL		DESCRIPTION
1	Site	Vancouver, Canada
2	Reference	Campanella et al., 1989
3	Shape, Material, and Installation	Pipe, Steel, Driven
4	Diameter, b, and Wall Thickness, t, mm	324 9.5
5	Embedment Length D, m	16.8
6	Cross Sectional Area A_t, m^2	0.082
7	Unit Circumferential Area, A_s, m^2 /m	1.018
8	Toe, Closed or Open	Closed
9	Type of Test and Loading	Static Compression, QML
10	Toe Capacity, R_t, KN	315
11	Shaft Capacity, R_s, KN	315
12	*Capacity, R_u, KN	630

SCHEMATIC PROFILE

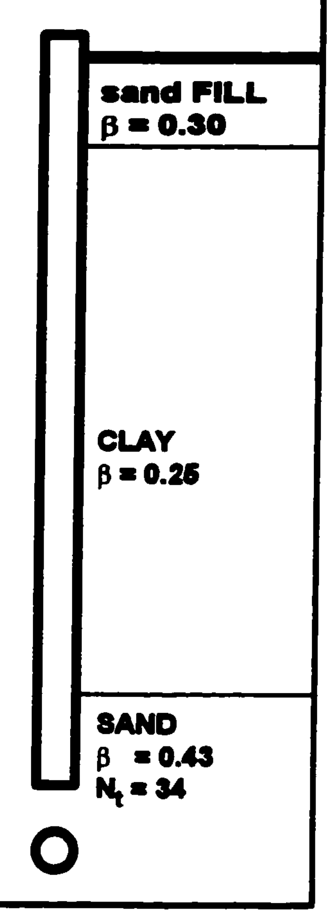

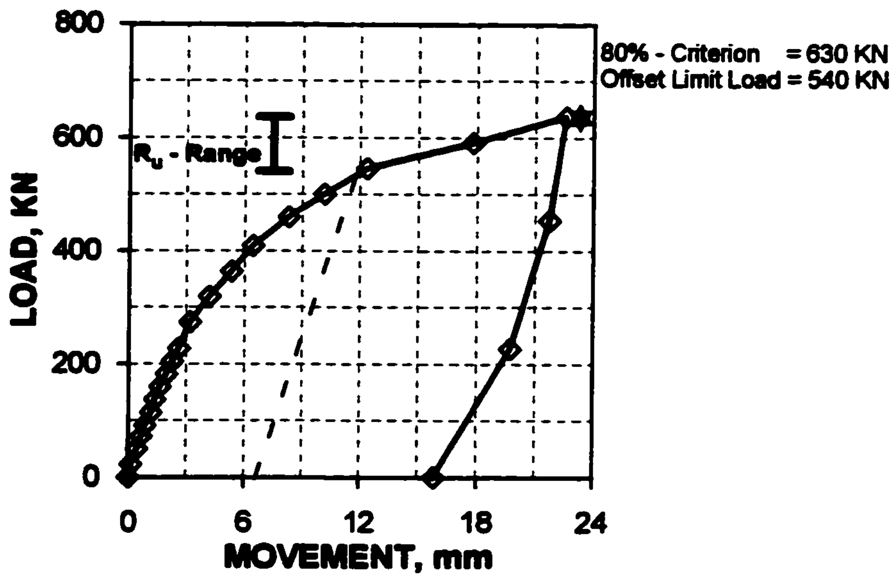

Case 3 UBC5
Sheet a CPT data

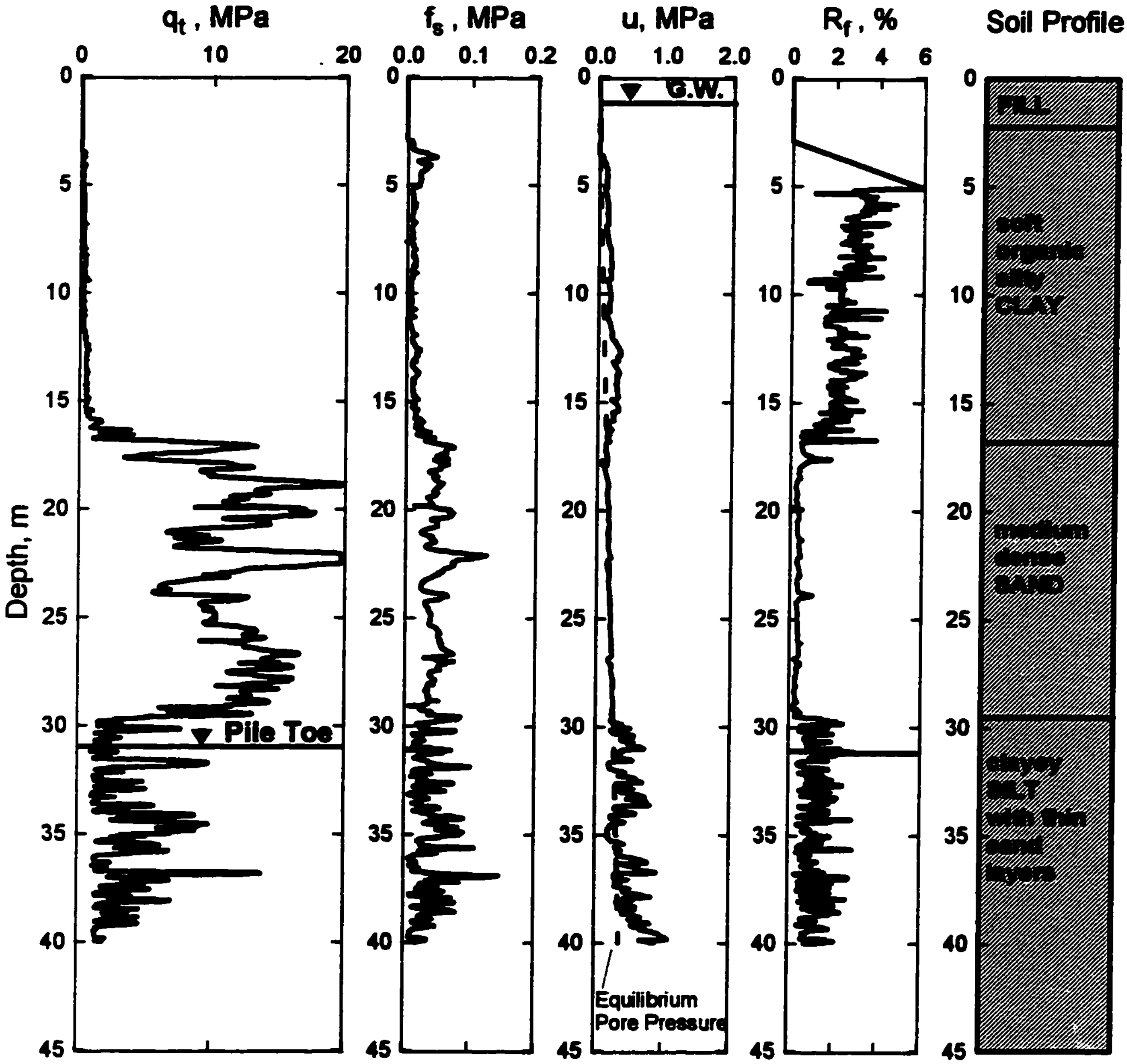

Case 3 UBC5
Sheet b Pile data

	DETAIL	DESCRIPTION
1	Site	Vancouver, Canada
2	Reference	Campanella et al., 1989
3	Shape, Material, and Installation	Pipe, Steel, Driven
4	Diameter, b, and Wall Thickness, t, mm	324 11.5
5	Embedment Length D, m	31.1
6	Cross Sectional Area A_t, m^2	0.082
7	Unit Circumferential Area, A_s, m^2/m	1.018
8	Toe, Closed or Open	Closed
9	Type of Test and Loading	Static Compression, QML
10	Toe Capacity, R_t, KN	180
11	Shaft Capacity, R_s, KN	920
12	*Capacity, R_u, KN	1,100

SCHEMATIC PROFILE

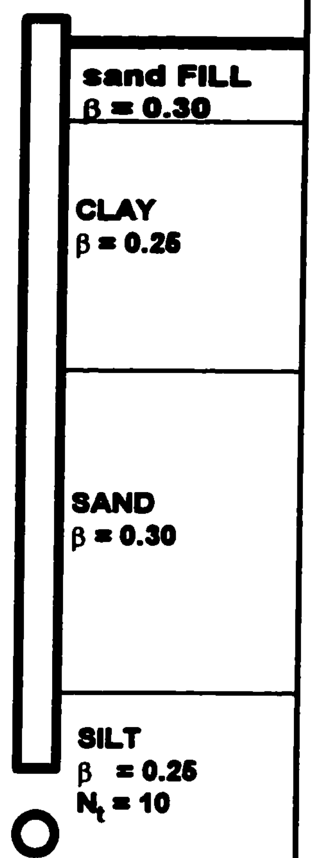

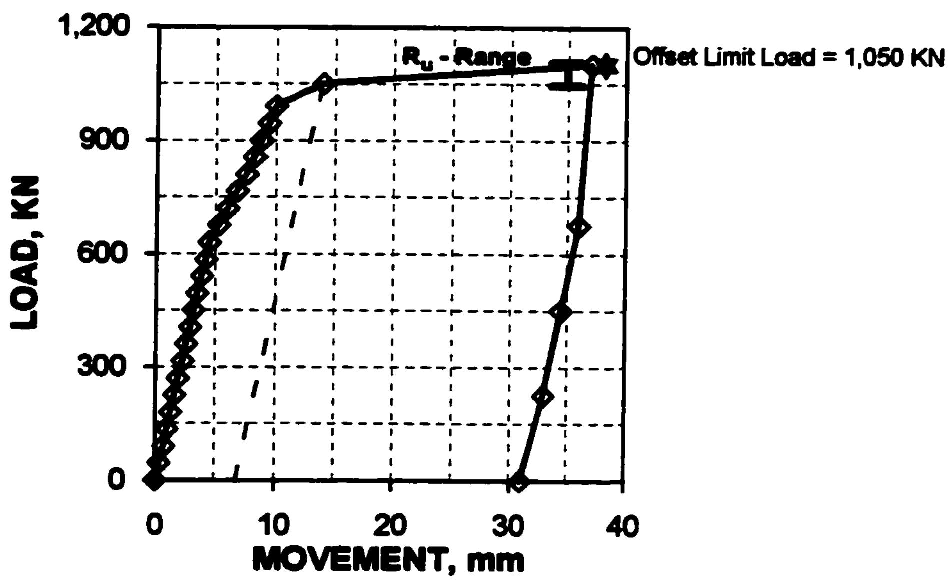

Case 4 UBCA
Sheet a CPT data

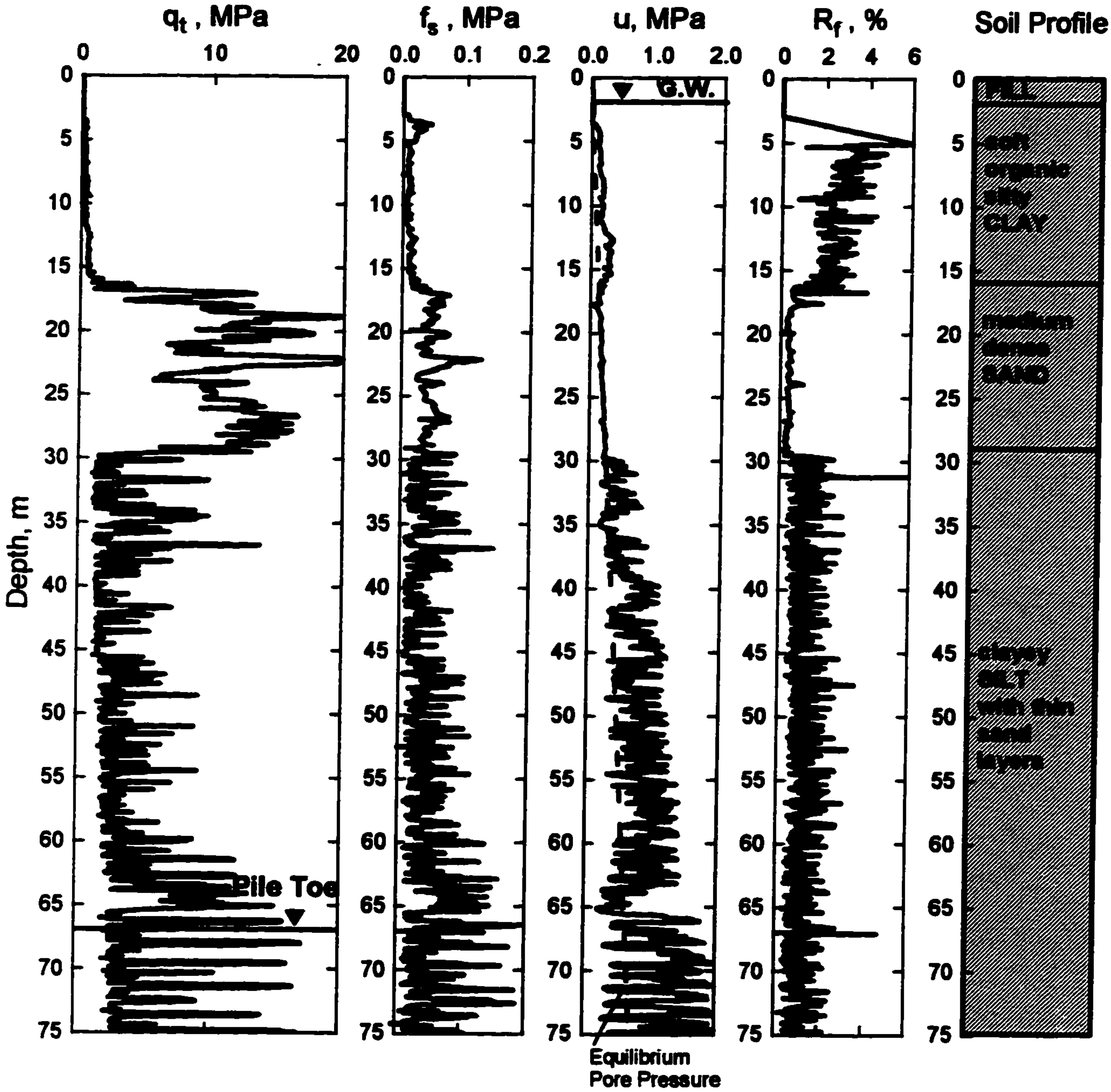

Case 4 UBCA
Sheet b Pile data

	DETAIL	DESCRIPTION
1	Site	Vancouver, Canada
2	Reference	Campanella et al., 1989
3	Shape, Material, and Installation	Pipe, Steel, Driven
4	Diameter, b, and Wall Thickness, t, mm	915 19
5	Embedment Length D, m	67
6	Cross Sectional Area A_t, m^2	0.658
7	Unit Circumferential Area, A_s, m^2/m	2.87
8	Toe, Closed or Open	Open
9	Type of Test and Loading	Static Compression, SML
10	Toe Capacity, R_t, KN	
11	Shaft Capacity, R_s, KN	
12	*Capacity, R_u, KN	7,500

SCHEMATIC PROFILE

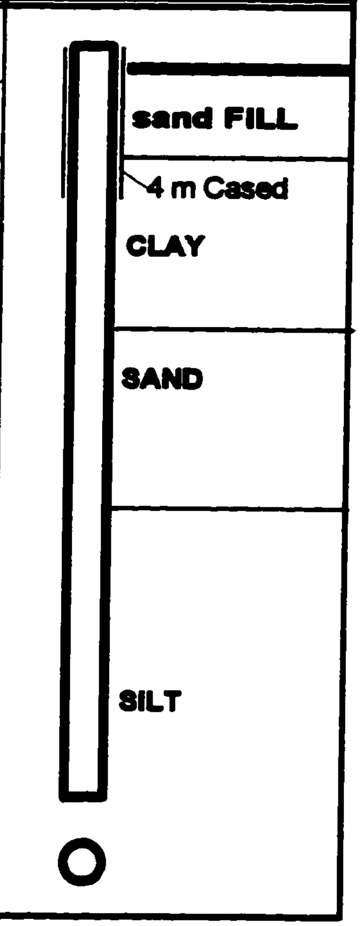

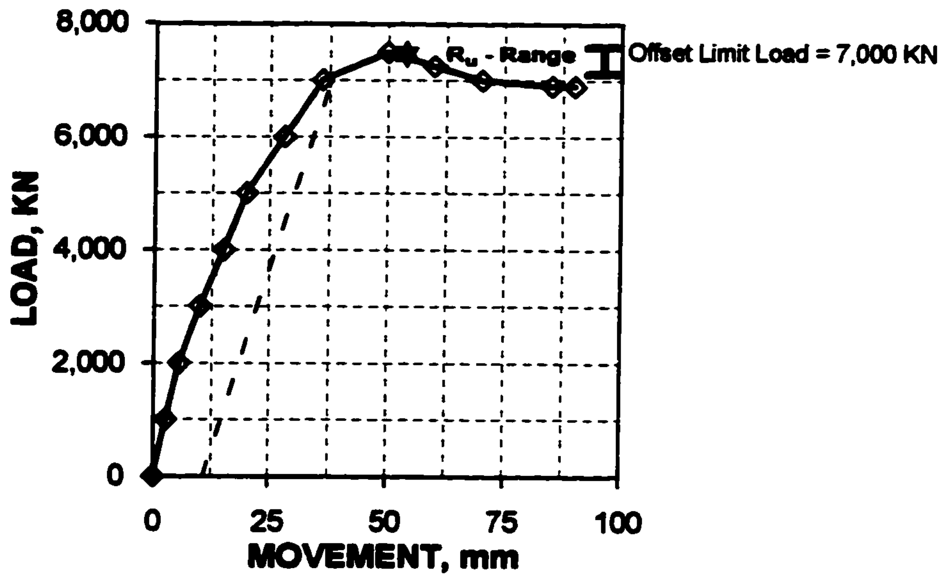

Case 5 NWUP
Sheet a CPT data

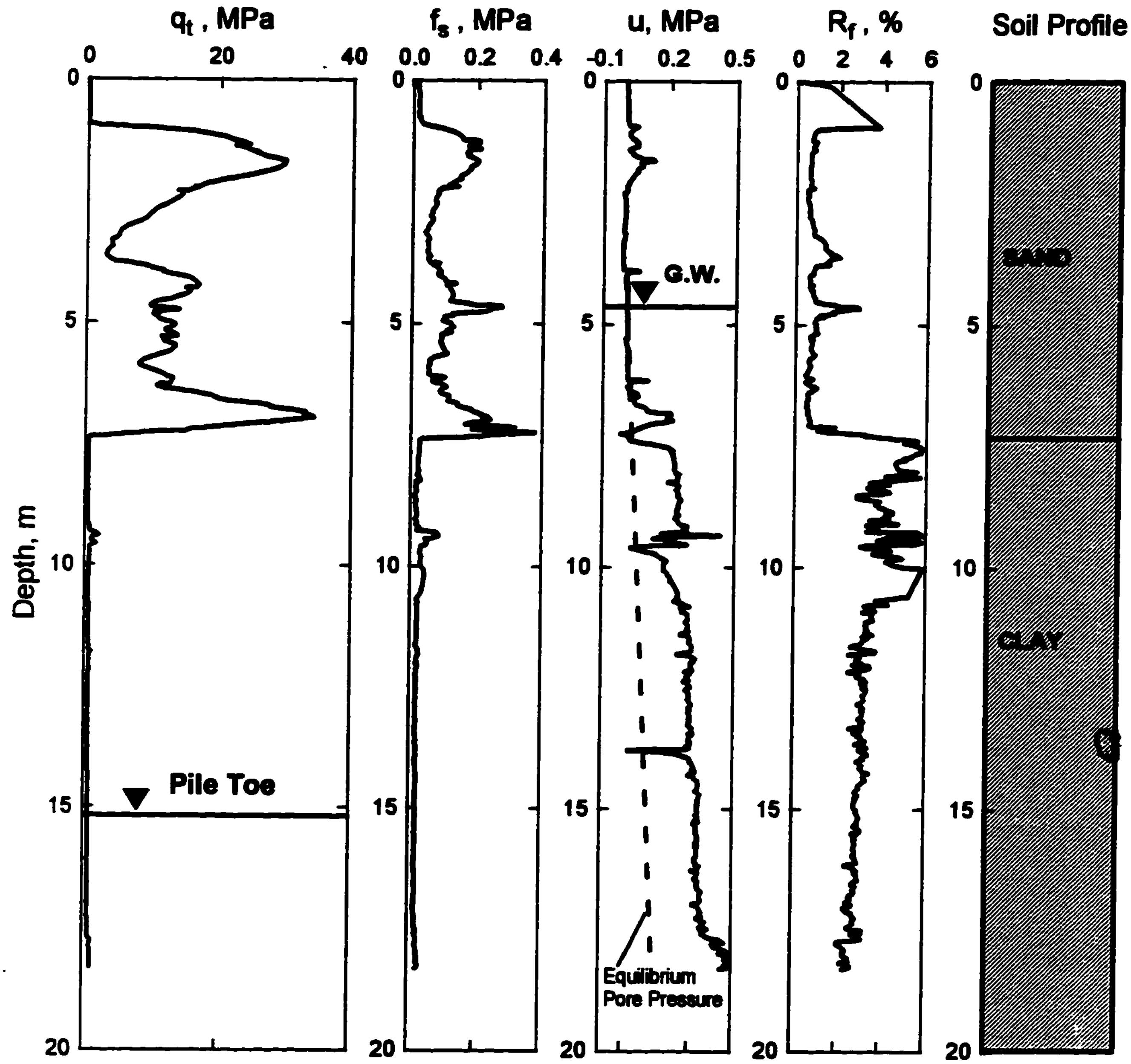

Case 5 NWUP
Sheet b Pile data

	DETAIL	DESCRIPTION	SCHEMATIC PROFILE
1	Site	Evanston, IL, USA	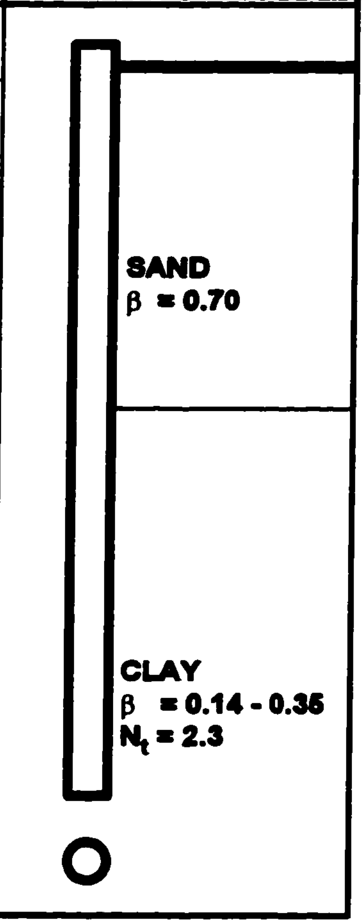
2	Reference	Finno, 1989	
3	Shape, Material, and Installation	Pipe, Steel, Driven	
4	Diameter, b, and Wall Thickness, t, mm	450 9.5	
5	Embedment Length D, m	15.2	
6	Cross Sectional Area A_t, m^2	0.159	
7	Unit Circumferential Area, A_s, m^2/m	1.41	
8	Toe, Closed or Open	Closed	
9	Type of Test and Loading	Static Compression, SML	
10	Toe Capacity, R_t, KN	62	
11	Shaft Capacity, R_s, KN	958	
12	*Capacity, R_u, KN	1,020	

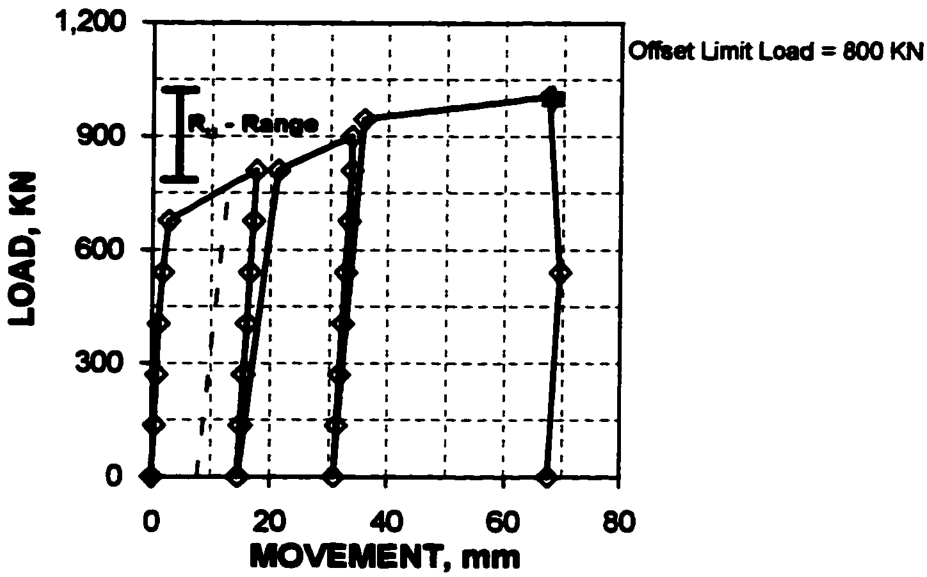

Case 6 NWUH
Sheet a CPT data

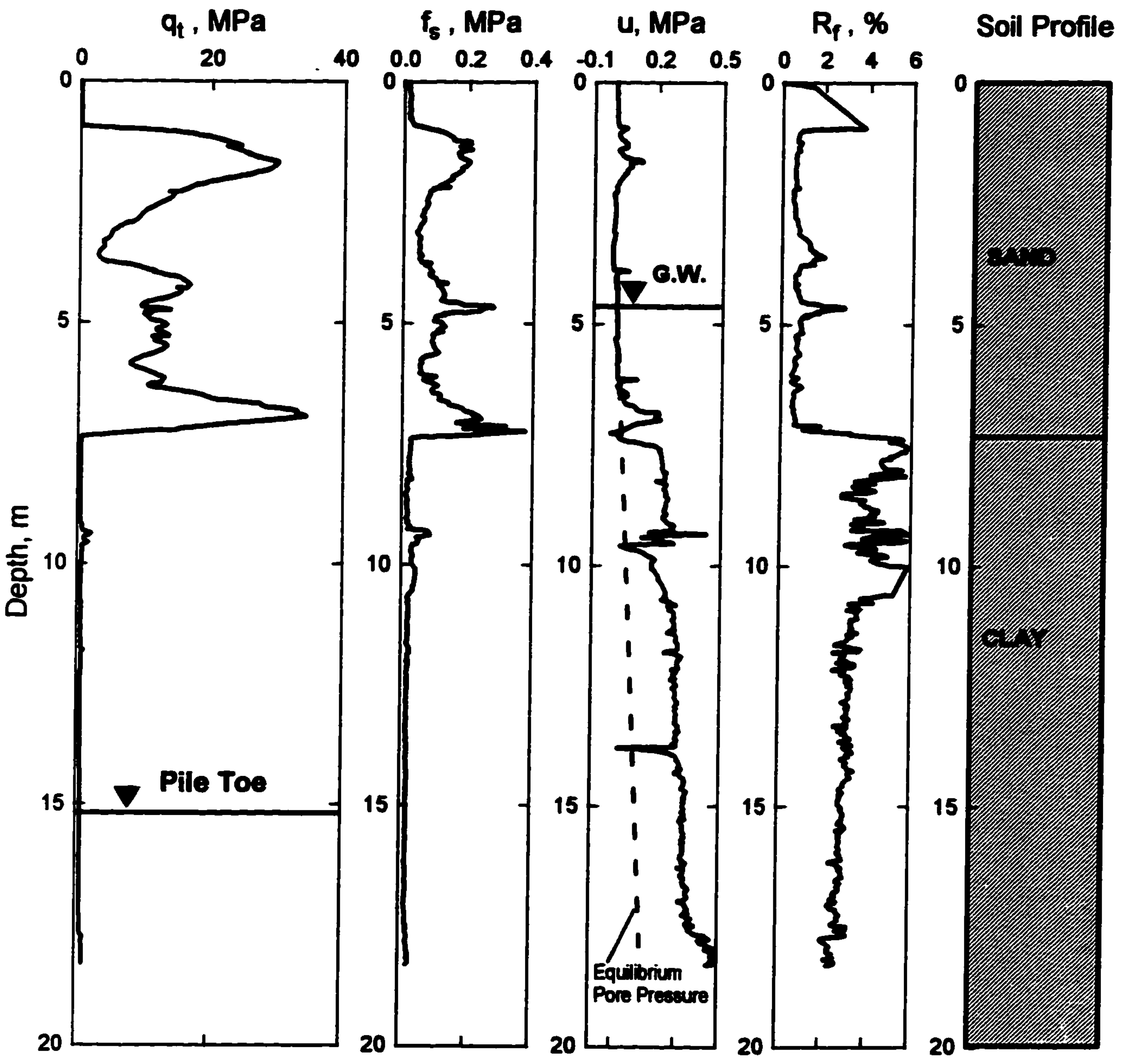

Case 6 NWUH
Sheet b Pile data

	DETAL	DESCRIPTION
1	Site	Evanston, IL, USA
2	Reference	Finno, 1989
3	Shape, Material, and Installation	H-Pile, Steel, Driven
4	Diameter, b, and Wall Thickness, t, mm	371*346
5	Embedment Length D, m	15.2
6	Cross Sectional Area A_t, m^2	0.128
7	Unit Circumferential Area, A_s, m^2/m	1.43
8	Toe, Closed or Open	Closed
9	Type of Test and Loading	Static Compression, SML
10	Toe Capacity, R_t, KN	50
11	Shaft Capacity, R_s, KN	960
12	*Capacity, R_u, KN	1,010

SCHEMATIC PROFILE

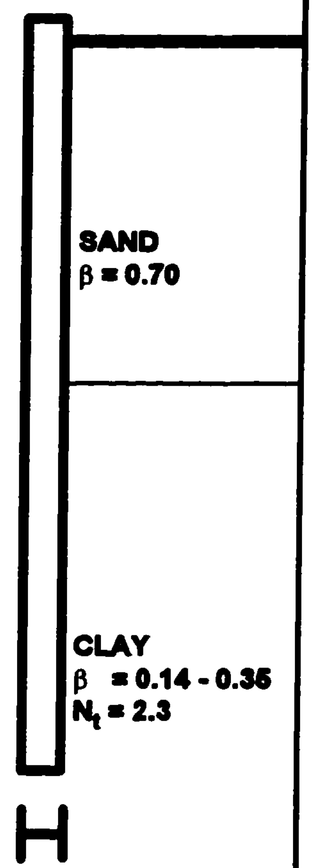

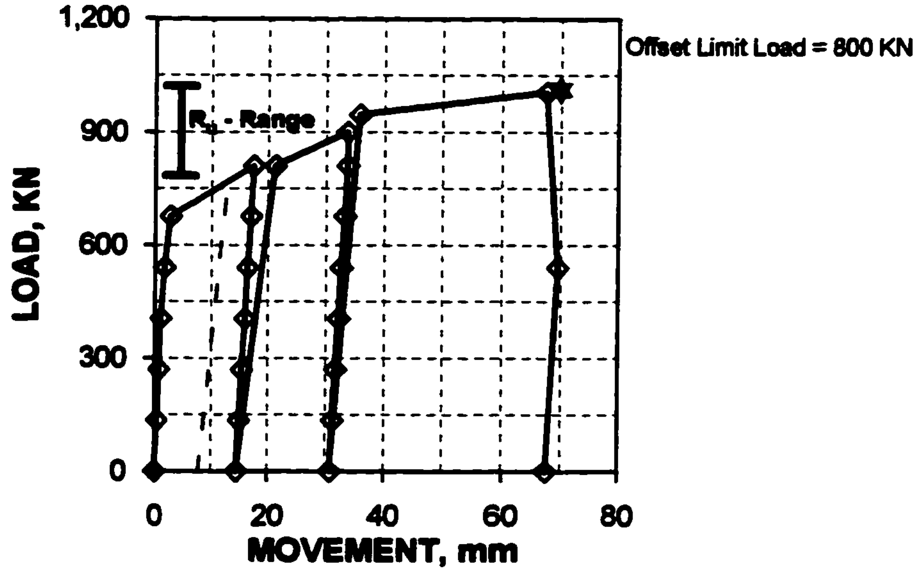

Case 7 FHWASF
Sheet a CPT data

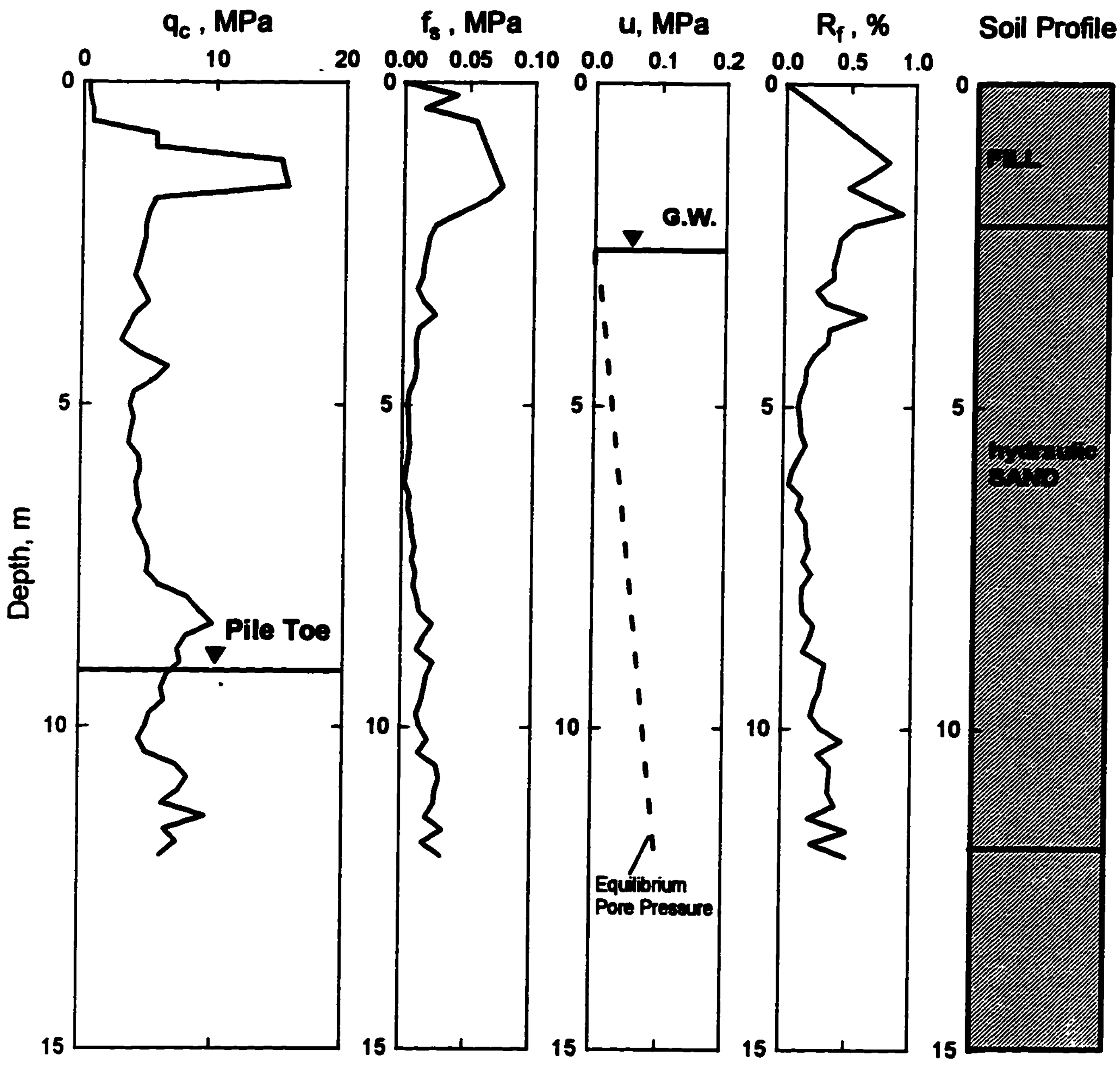

Case 7 FHWASF
Sheet b Pile data

	DETAIL	DESCRIPTION	SCHEMATIC PROFILE
1	Site	SF, California, USA	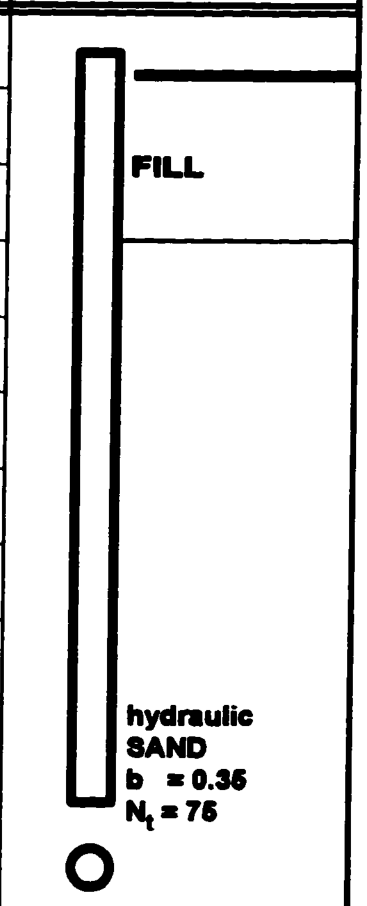
2	Reference	O'Neill, 1988	
3	Shape, Material, and Installation	Pipe, Steel, Driven	
4	Diameter, b, and Wall Thickness, t, mm	273 9.1	
5	Embedment Length D, m	9.2	
6	Cross Sectional Area A_t, m^2	0.059	
7	Unit Circumferential Area, A_s, m^2/m	0.858	
8	Toe, Closed or Open	Closed	
9	Type of Test and Loading	Static Compression, SML	
10	Toe Capacity, R_t, KN	355	
11	Shaft Capacity, R_s, KN	135	
12	*Capacity, R_u, KN	490	

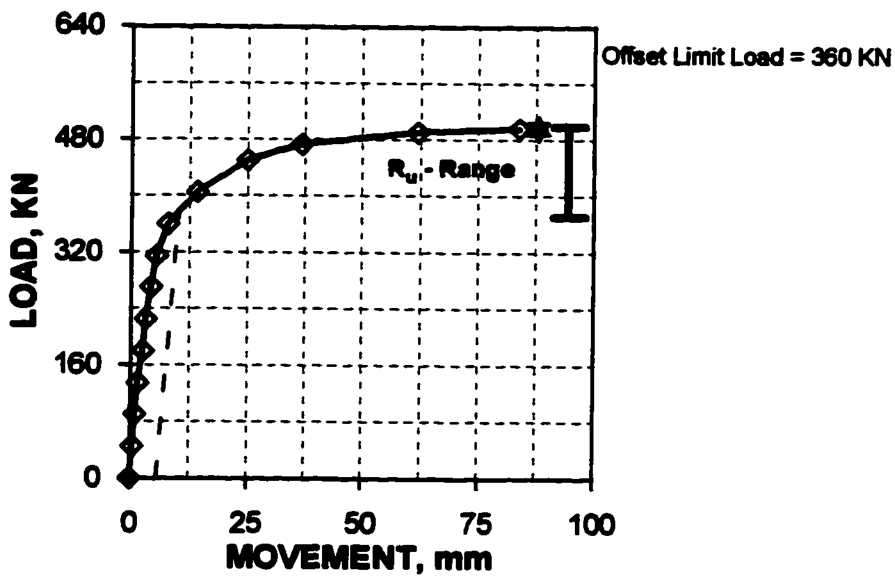

Case 8 BGHD1
Sheet a CPT data

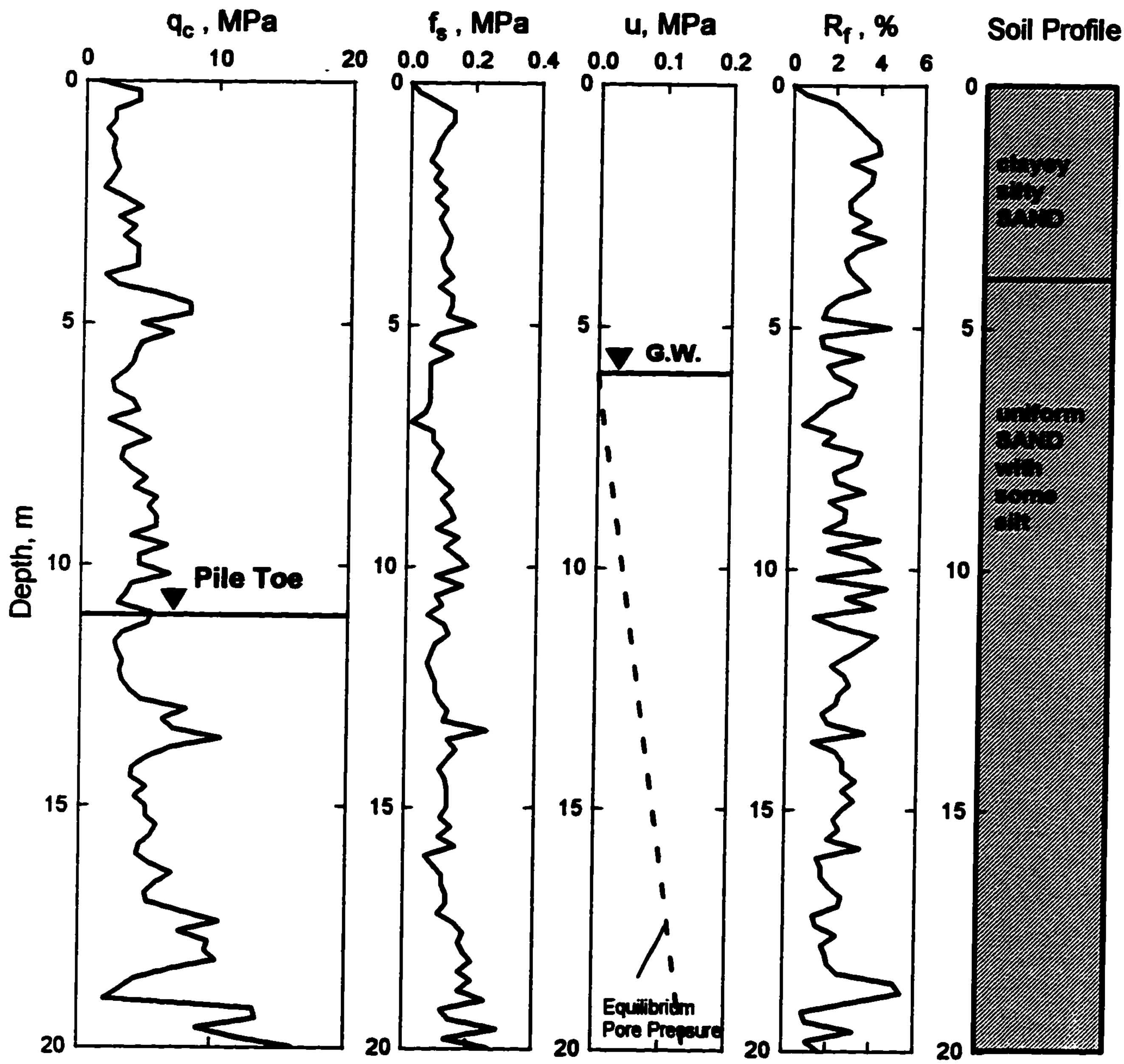

Case 8 BGHD1
Sheet b Pile data

	DETAIL	DESCRIPTION
1	Site	Baghdad, Iraq
2	Reference	Altaee et al., 1992
3	Shape, Material, and Installation	Square, Concrete, Driven
4	Diameter, b, and Wall Thickness, t, mm	285
5	Embedment Length D, m	11
6	Cross Sectional Area A_t, m^2	0.081
7	Unit Circumferential Area, A_s, m^2/m	1.14
8	Toe, Closed or Open	Closed
9	Type of Test and Loading	Static Compression, SML
10	Toe Capacity, R_t, KN	360
11	Shaft Capacity, R_s, KN	640
12	*Capacity, R_u, KN	1,000

SCHEMATIC PROFILE

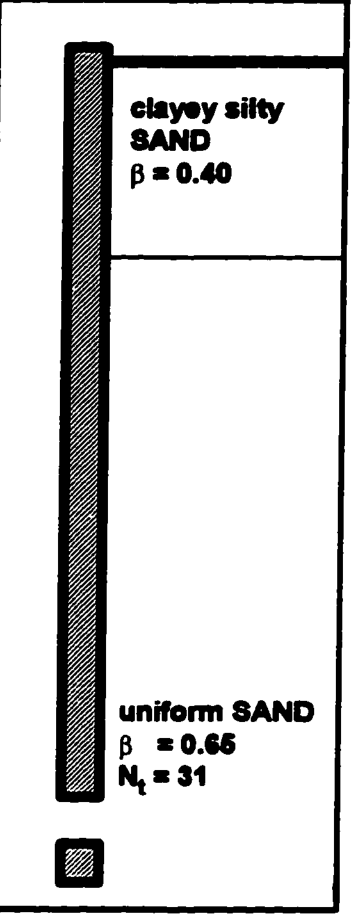

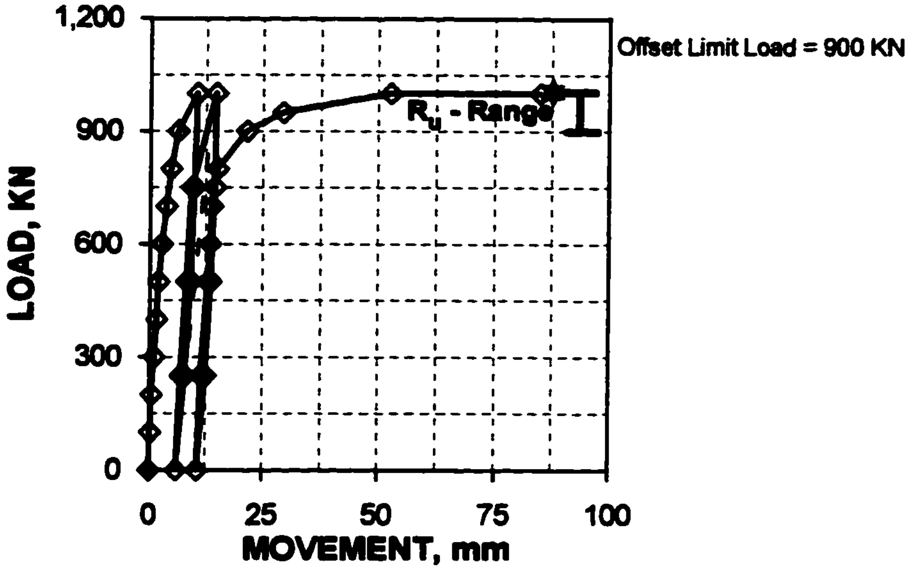

Case 9 BGHD2
Sheet a CPT data

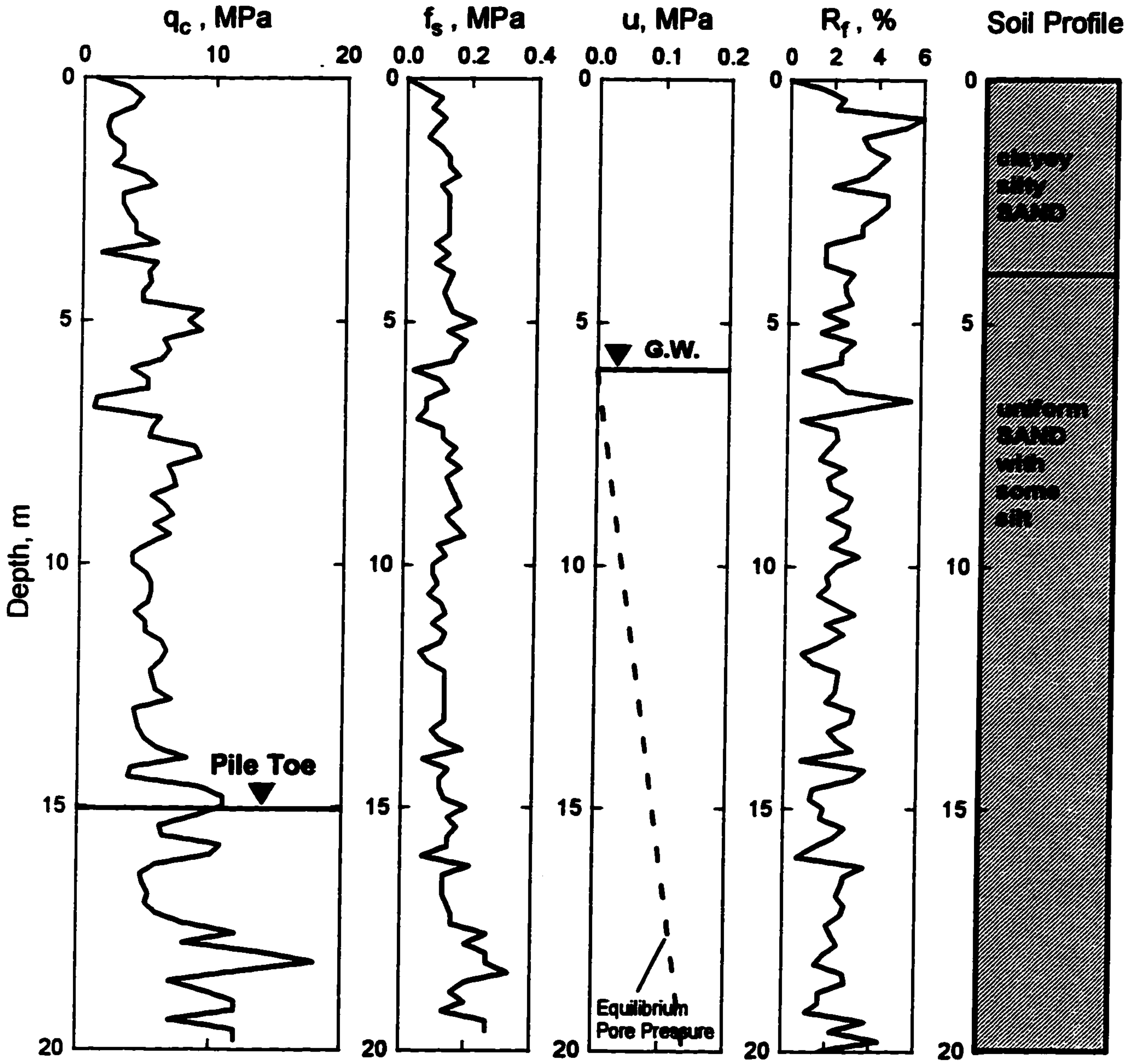

Case 9 BGHD2
Sheet b Pile data

	DETAIL	DESCRIPTION
1	Site	Baghdad, Iraq
2	Reference	Altaee et al., 1992
3	Shape, Material, and Installation	Square, Concrete, Driven
4	Diameter, b, and Wall Thickness, t, mm	285
5	Embedment Length D, m	15
6	Cross Sectional Area A_t, m^2	0.081
7	Unit Circumferential Area, A_s, m^2/m	1.14
8	Toe, Closed or Open	Closed
9	Type of Test and Loading	Static Compression, SML
10	Toe Capacity, R_t, KN	480
11	Shaft Capacity, R_s, KN	1,120
12	*Capacity, R_u, KN	1,600

SCHEMATIC PROFILE

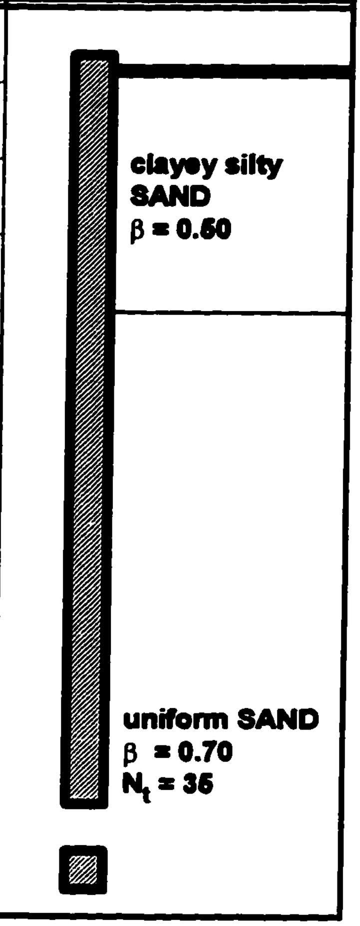

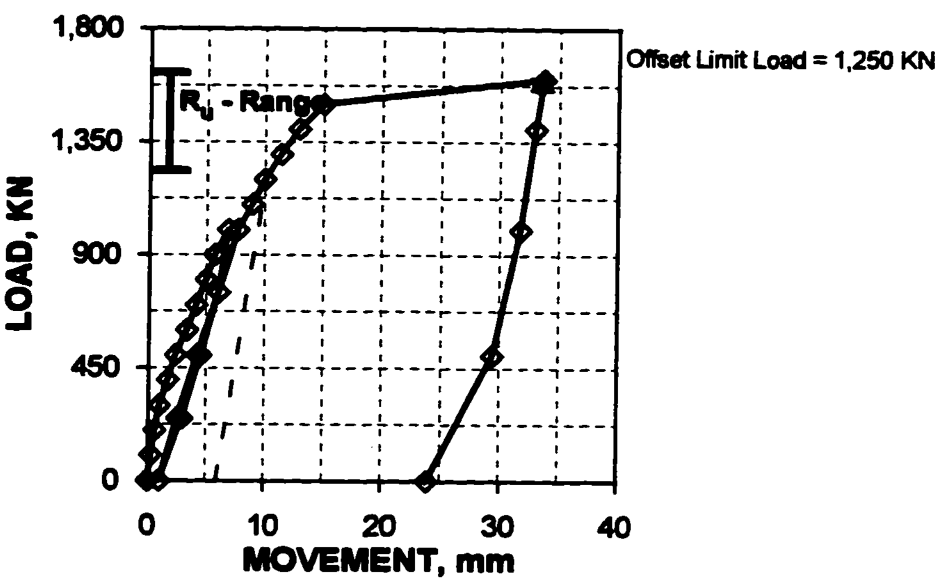

Case 10 POLA1
Sheet a CPT data

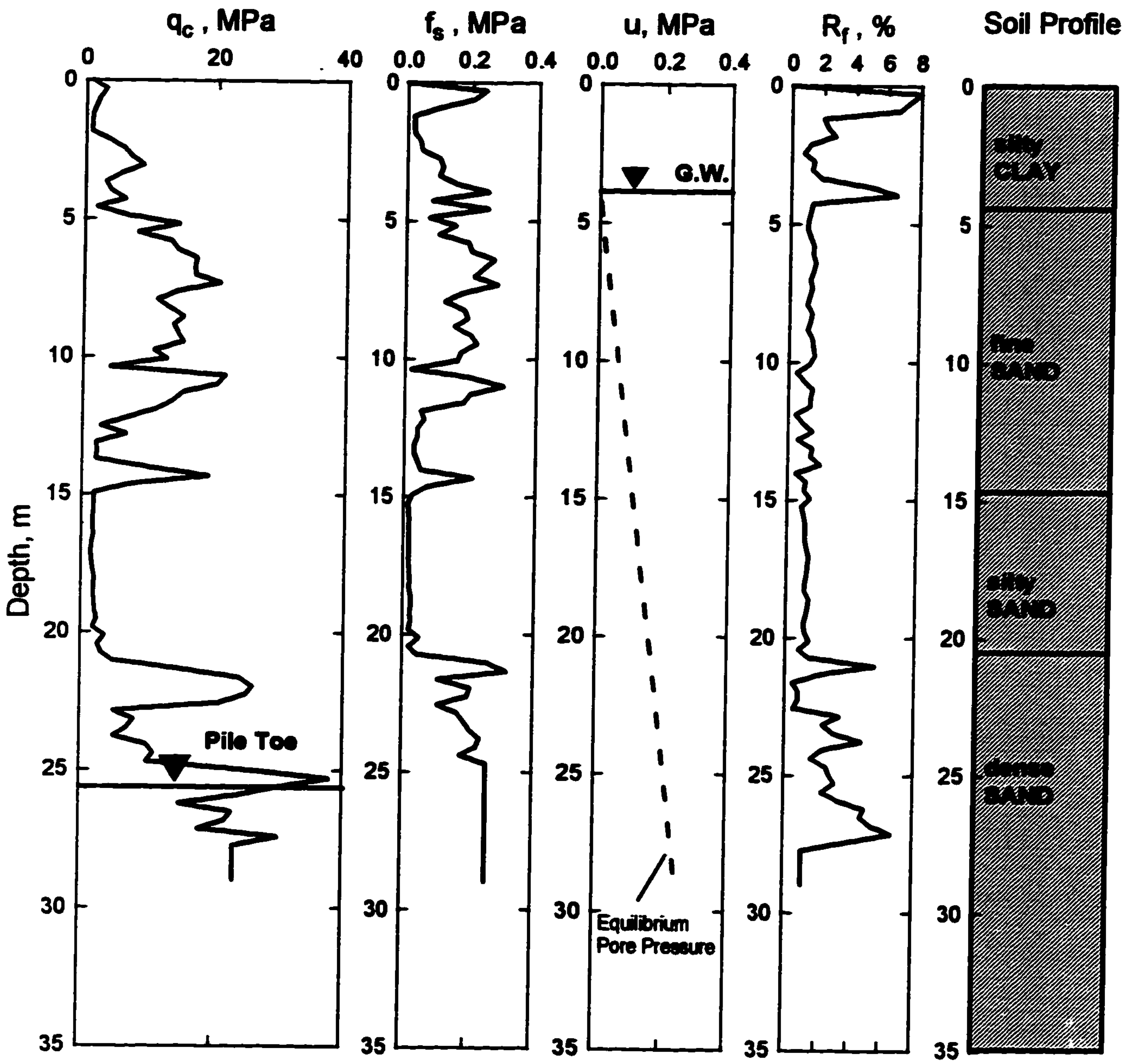

Case 10 POLA1
Sheet b Pile data

	DETAIL	DESCRIPTION
1	Site	Port of Los Angeles, USA
2	Reference	CH2M Hill, 1982
3	Shape, Material, and Installation	Octagonal, Concrete, Driven
4	Diameter, b, and Wall Thickness, t, mm	600
5	Embedment Length D, m	25.8
6	Cross Sectional Area A_t, m^2	0.308
7	Unit Circumferential Area, A_s, m^2/m	2.02
8	Toe, Closed or Open	Closed
9	Type of Test and Loading	Static Compression, QML
10	Toe Capacity, R_t, KN	4,050
11	Shaft Capacity, R_s, KN	1,735 (330 KN for sleeved part)
12	*Capacity, R_u, KN	5,785

SCHEMATIC PROFILE

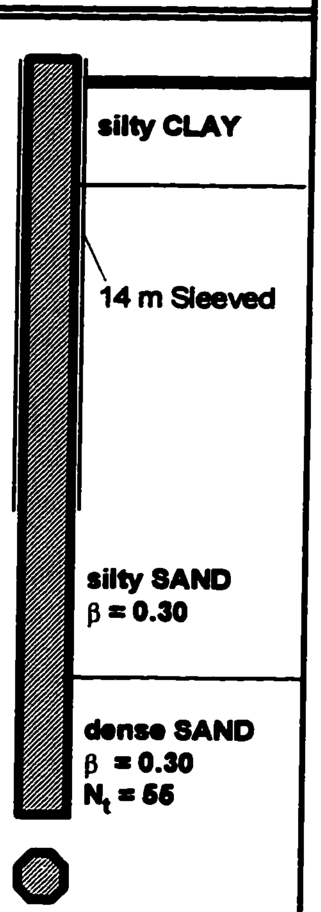

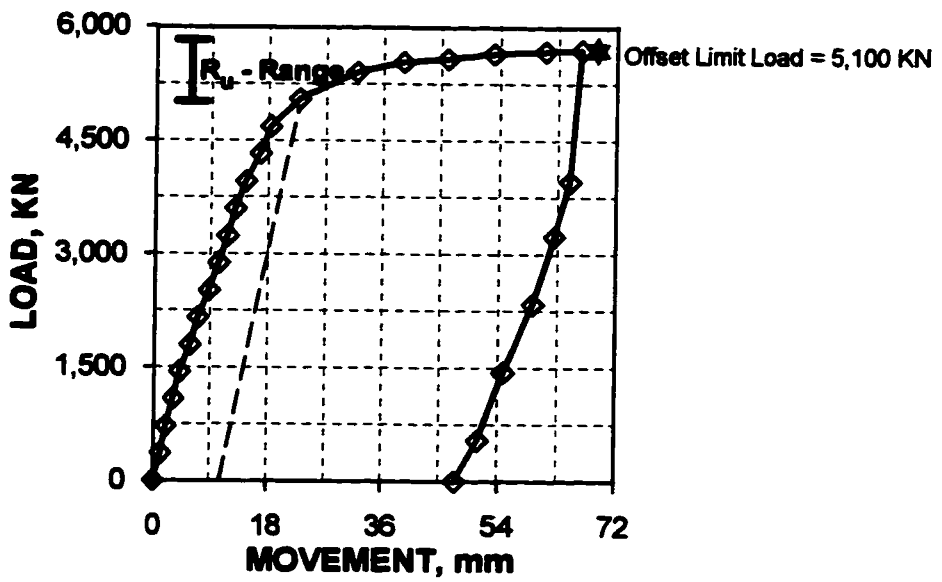

Case 11 POLA2
Sheet a CPT data

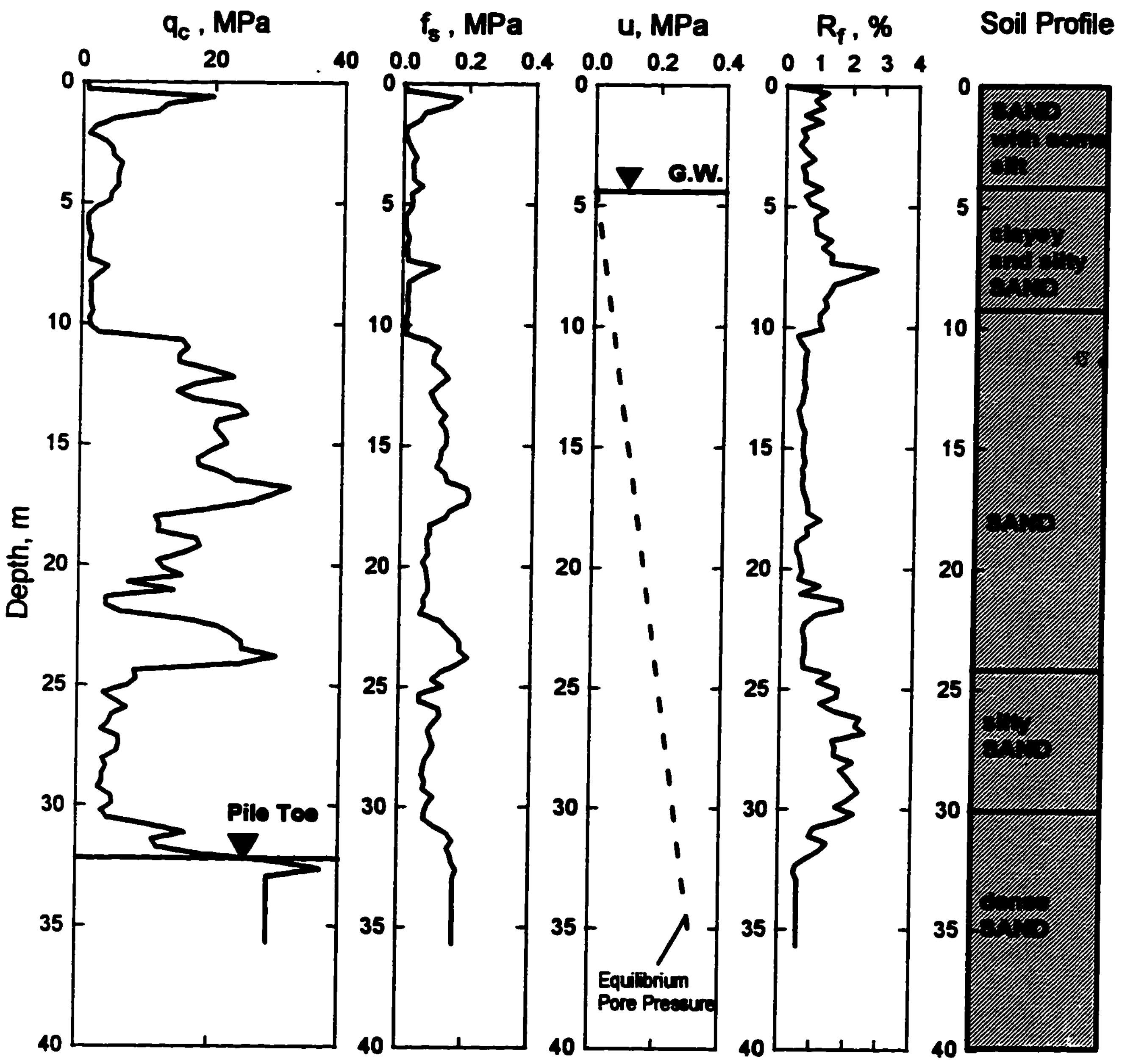

Case 11 POLA2
Sheet b Pile data

	DETAIL	DESCRIPTION	SCHEMATIC PROFILE
1	Site	Port of Los Angeles, USA	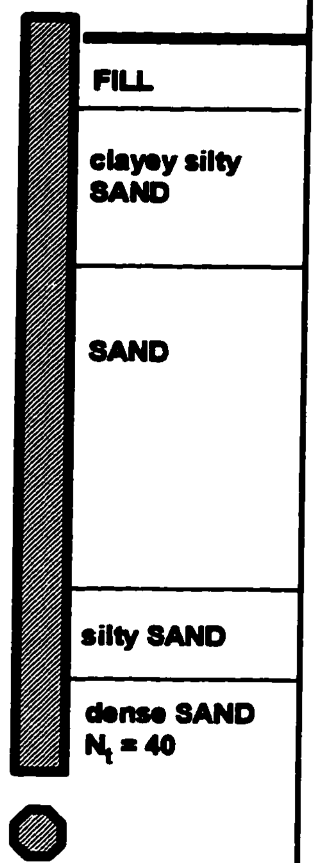
2	Reference	Fellenius, 1995	
3	Shape, Material, and Installation	Octagonal, Concrete, Driven	
4	Diameter, b, and Wall Thickness, t, mm	600	
5	Embedment Length D, m	32.6	
6	Cross Sectional Area A_t, m^2	0.308	
7	Unit Circumferential Area, A_s, m^2/m	2.02	
8	Toe, Closed or Open	Closed	
9	Type of Test and Loading	Static Compression, SML	
10	Toe Capacity, R_t, KN	3560 (from CAPWAP analysis)	
11	Shaft Capacity, R_s, KN	(jetted during driving)	
12	Capacity, R_u, KN		

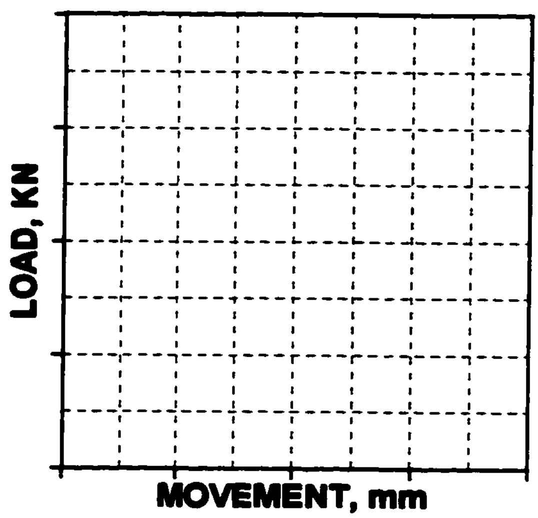

Case 12 JPNOT1
Sheet a CPT data

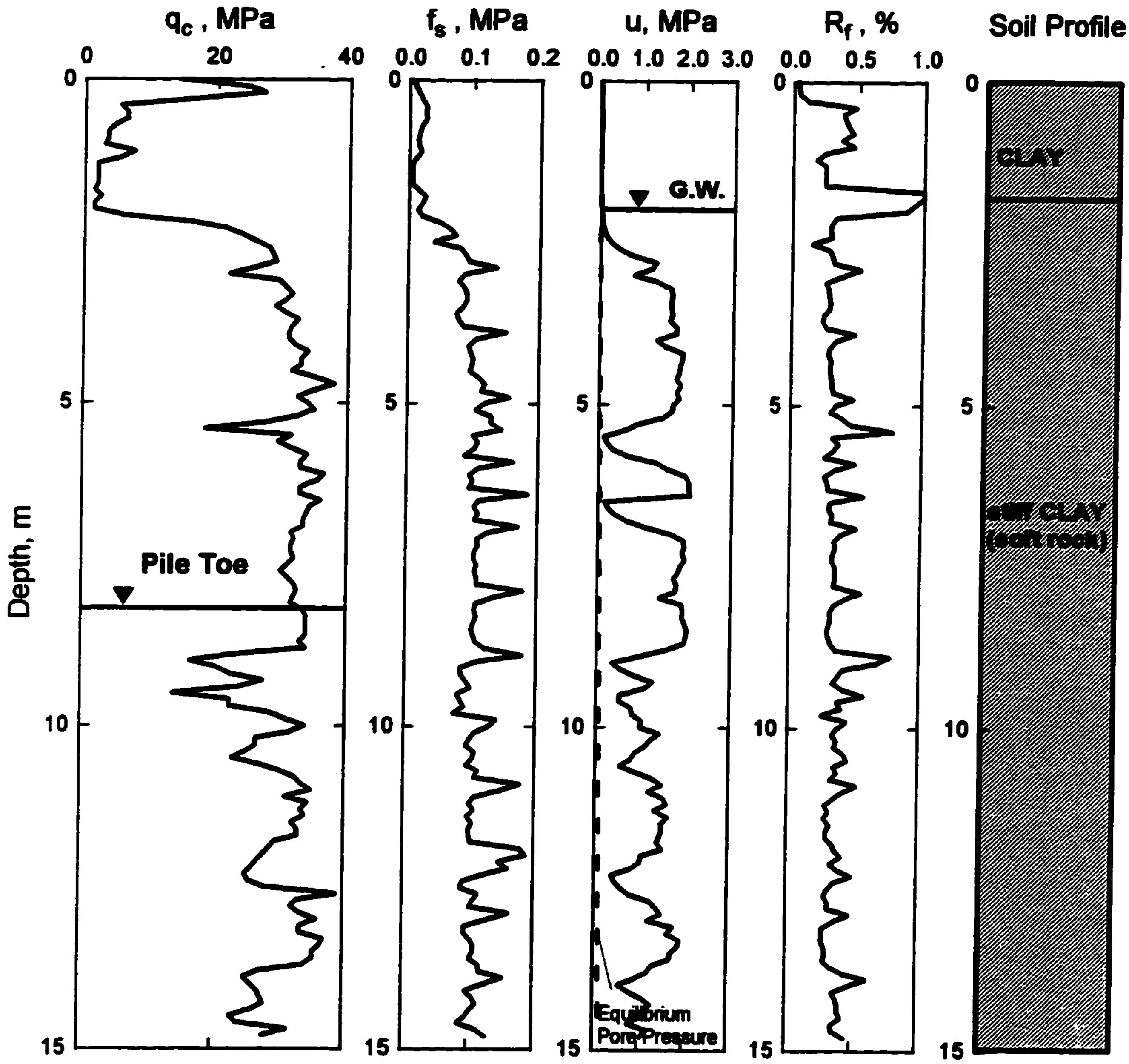

Case 12 JPNOT1
Sheet b Pile data

	DETAIL	DESCRIPTION	SCHEMATIC PROFILE
1	Site	Noto Island, Japan	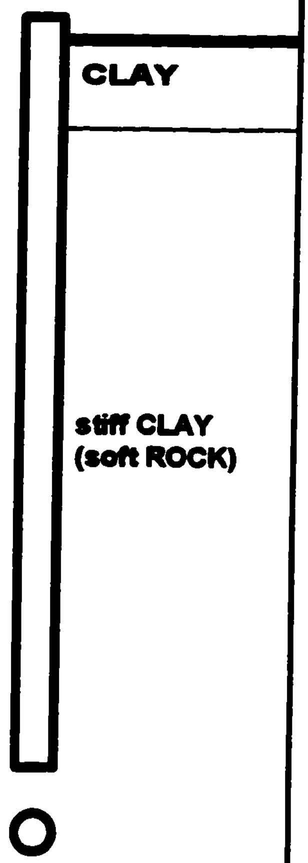
2	Reference	Matrumoto et al., 1995	
3	Shape, Material, and Installation	Pipe, Steel, Driven	
4	Diameter, b, and Wall Thickness, t, mm	800 12.1	
5	Embedment Length D, m	8.2 (L = 11 m)	
6	Cross Sectional Area A_t, m^2	0.041	
7	Unit Circumferential Area, A_s, m^2/m	2.51 + 2.44 (inside + outside)	
8	Toe, Closed or Open	Open	
9	Type of Test and Loading	Static Compression, SML	
10	Toe Capacity, R_t, KN	1,200	
11	Shaft Capacity, R_s, KN	3,500 (7 m soil plug inside the pile)	
12	*Capacity, R_u, KN	4,700	

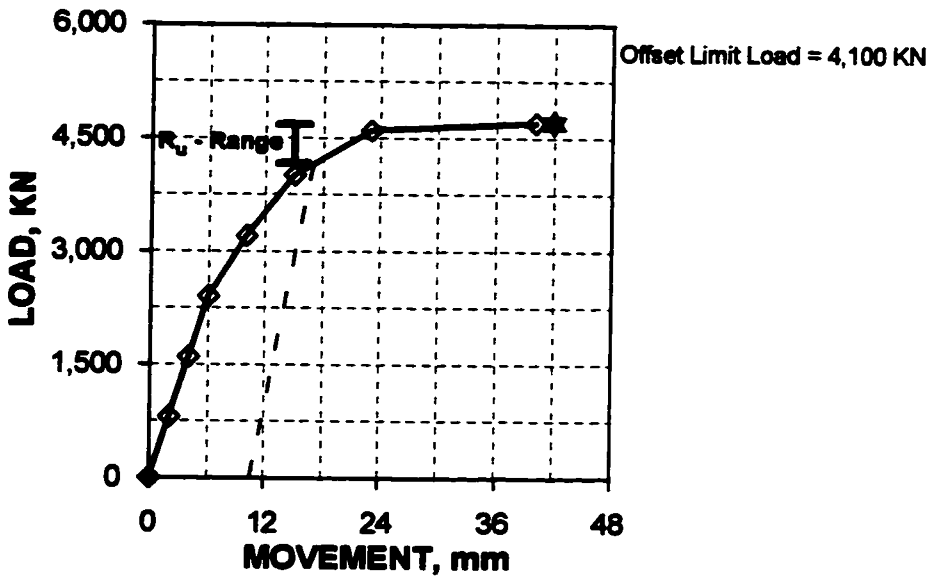

Case 13 JPNOT2
Sheet a CPT data

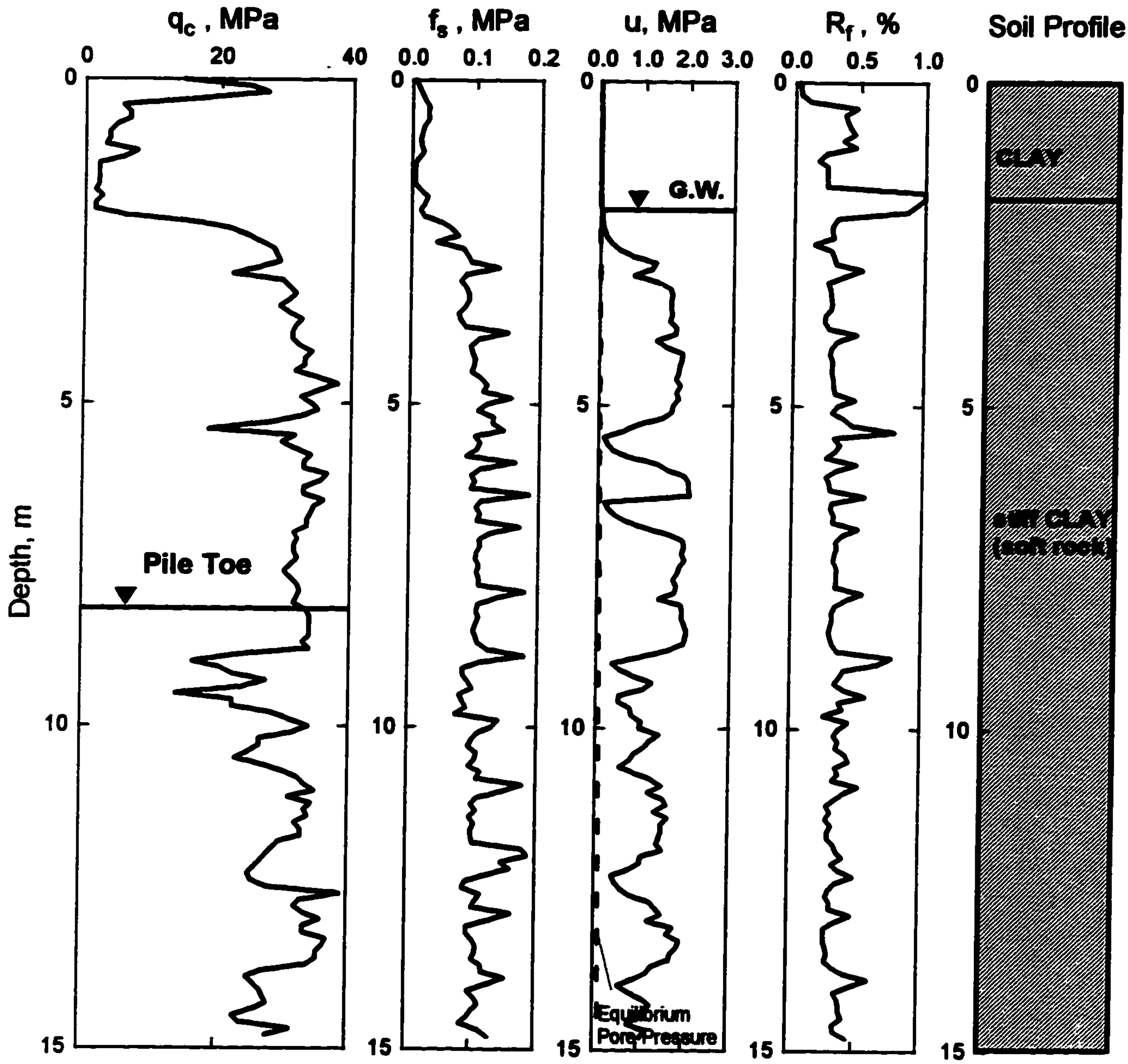

Case 13 JPNOT2
Sheet b Pile data

	DETAIL	DESCRIPTION
1	Site	Noto Island, Japan
2	Reference	Matrumoto et al., 1995
3	Shape, Material, and Installation	Pipe, Steel, Driven
4	Diameter, b, and Wall Thickness, t, mm	800 12.1
5	Embedment Length D, m	8.2 (L = 11 m)
6	Cross Sectional Area A_t, m^2	0.041
7	Unit Circumferential Area, A_s, m^2/m	2.51
8	Toe, Closed or Open	Open
9	Type of Test and Loading	Static Compression, SML
10	Toe Capacity, R_t, KN	500
11	Shaft Capacity, R_s, KN	3,190
12	*Capacity, R_u, KN	3,690

SCHEMATIC PROFILE

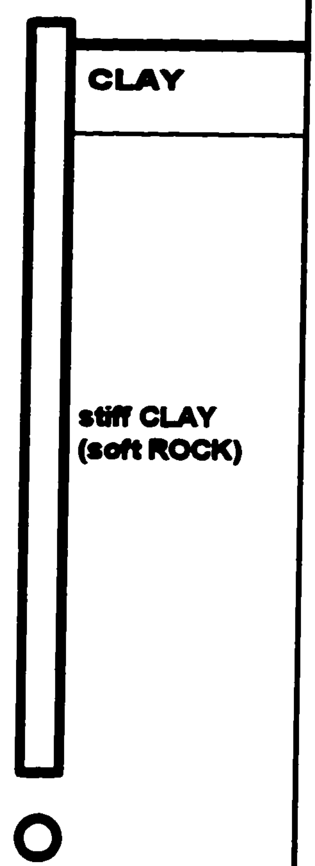

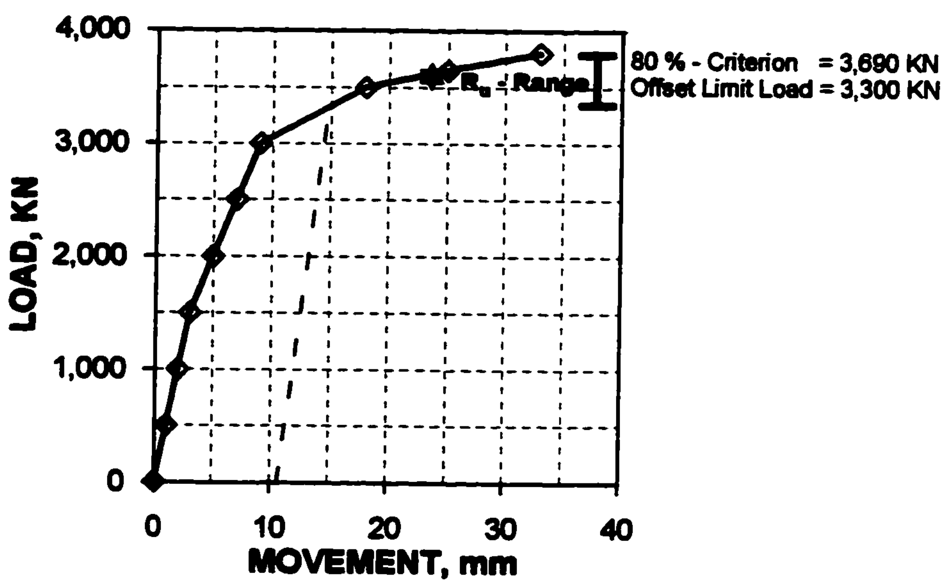

Case 14 JPNOT3
Sheet a CPT data

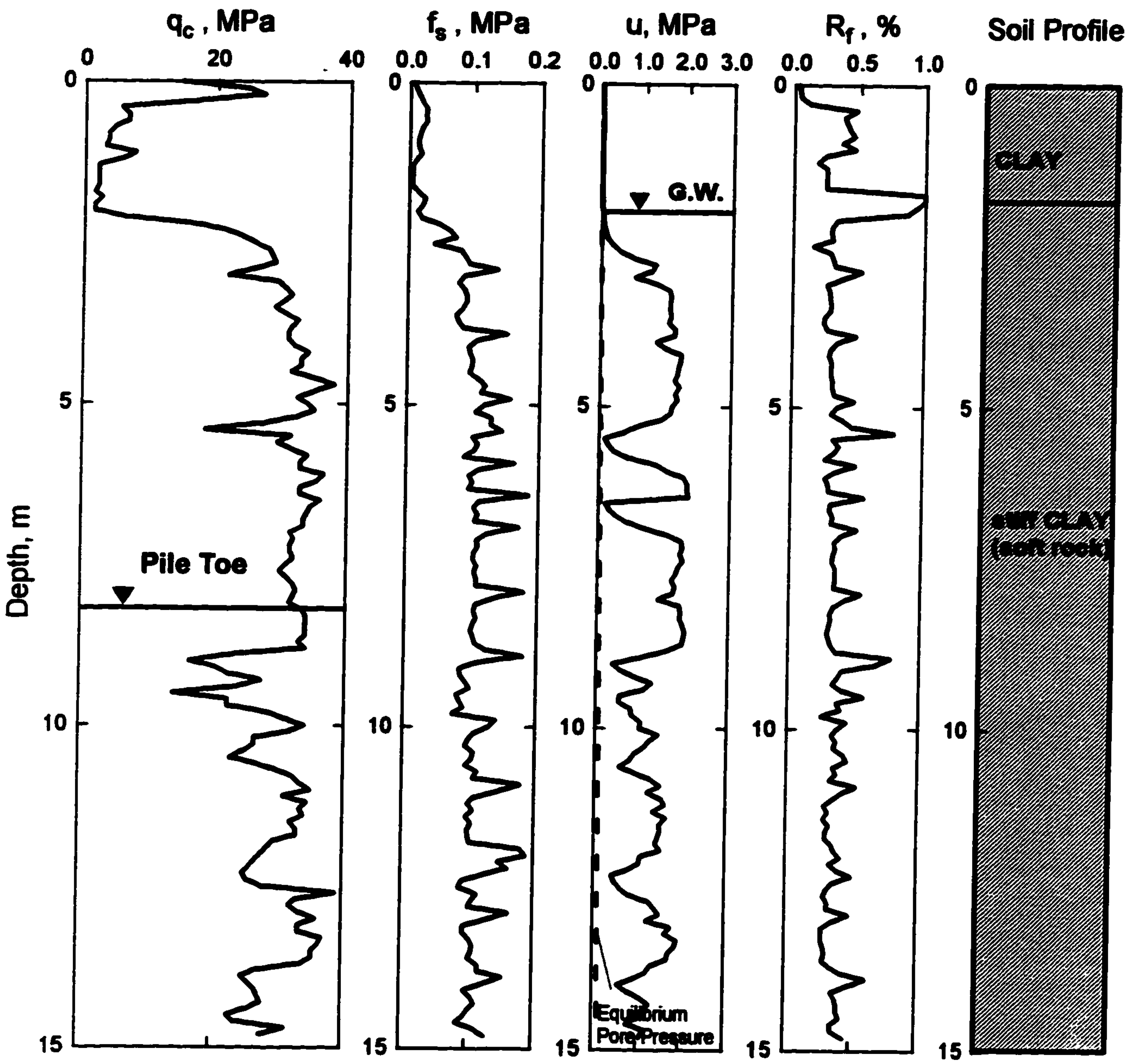

Case 14 JPNOT3
Sheet b Pile data

	DETAIL	DESCRIPTION
1	Site	Noto Island, Japan
2	Reference	Matrumoto et al., 1995
3	Shape, Material, and Installation	Pipe, Steel, Driven
4	Diameter, b, and Wall Thickness, t, mm	800 12.1
5	Embedment Length D, m	8.2 (L = 11 m)
6	Cross Sectional Area A_t, m^2	0.041
7	Unit Circumferential Area, A_s, m^2/m	2.51
8	Toe, Closed or Open	Open
9	Type of Test and Loading	Static Tension, SML
10	Toe Capacity, R_t, KN	
11	Shaft Capacity, R_s, KN	3,250
12	*Capacity, R_u, KN	

SCHEMATIC PROFILE

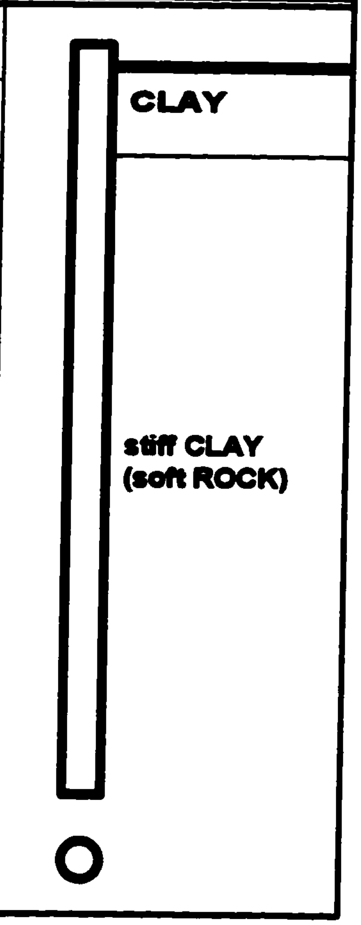

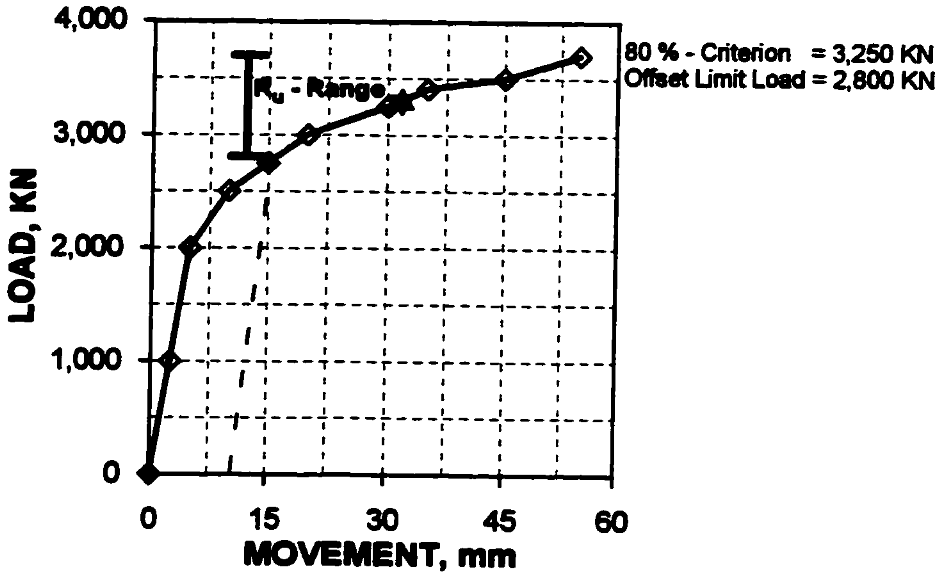

Case 15 TWNTP4
Sheet a CPT data

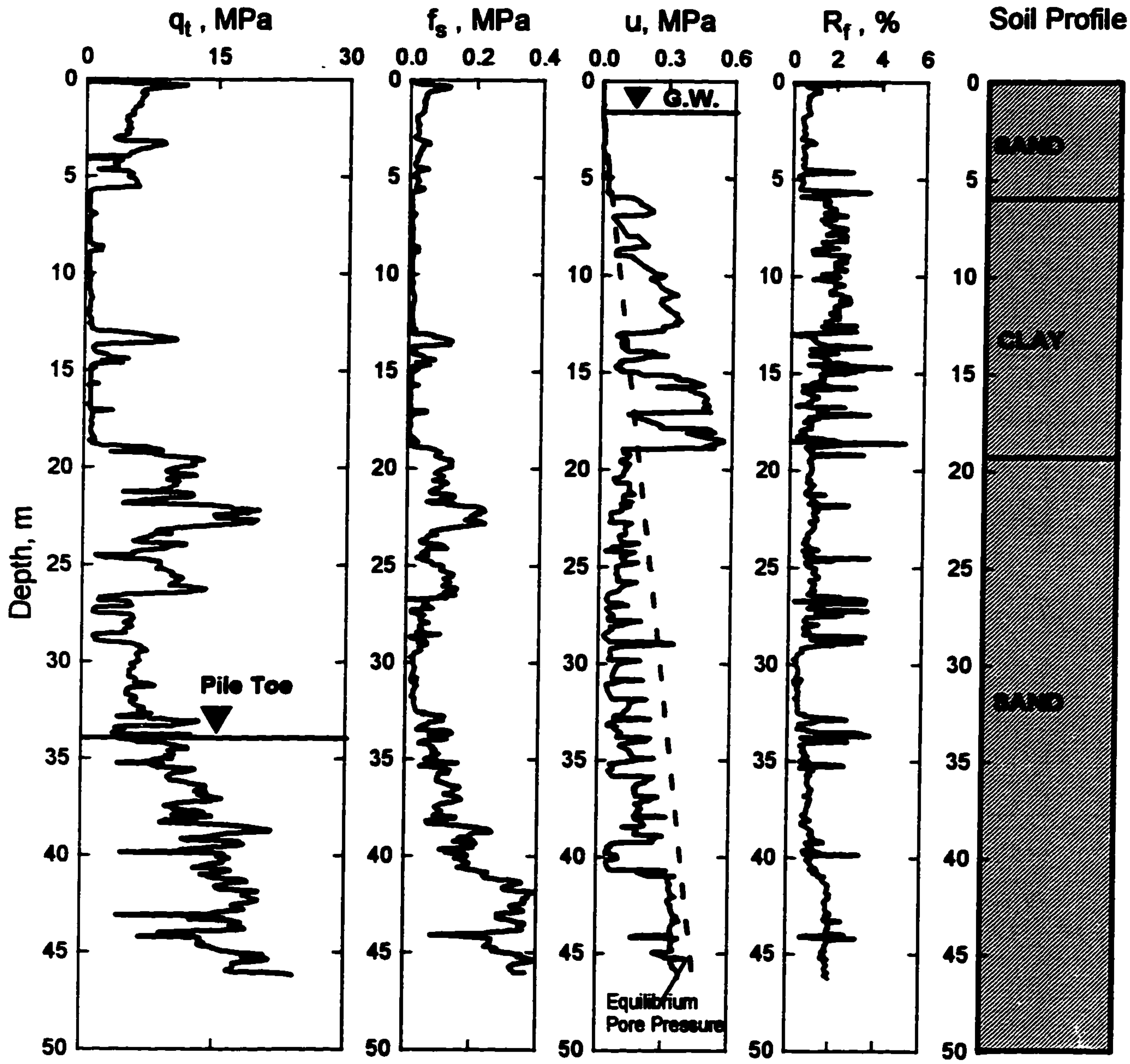

Case 15 TWNTP4
Sheet b Pile data

	DETAIL	DESCRIPTION
1	Site	Taiwan
2	Reference	Yen et al., 1989
3	Shape, Material, and Installation	Pipe, Steel, Driven
4	Diameter, b, and Wall Thickness, t, mm	609 12
5	Embedment Length D, m	34.25
6	Cross Sectional Area A_t, m^2	0.291
7	Unit Circumferential Area, A_s, m^2/m	1.91
8	Toe, Closed or Open	Closed
9	Type of Test and Loading	Static Compression, SML
10	Toe Capacity, R_t, KN	1,600
11	Shaft Capacity, R_s, KN	2,730
12	*Capacity, R_u, KN	4,330

SCHEMATIC PROFILE

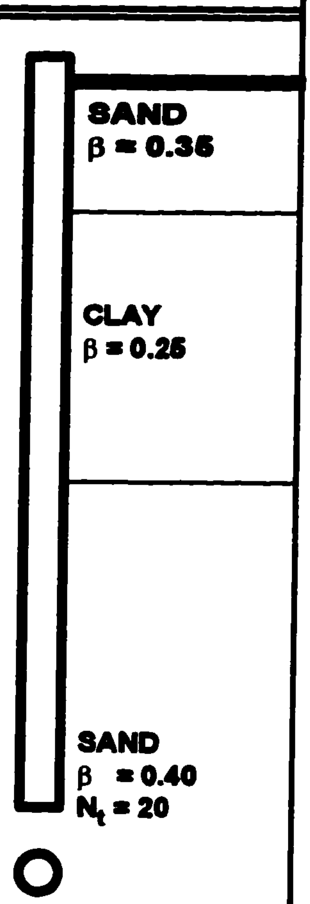

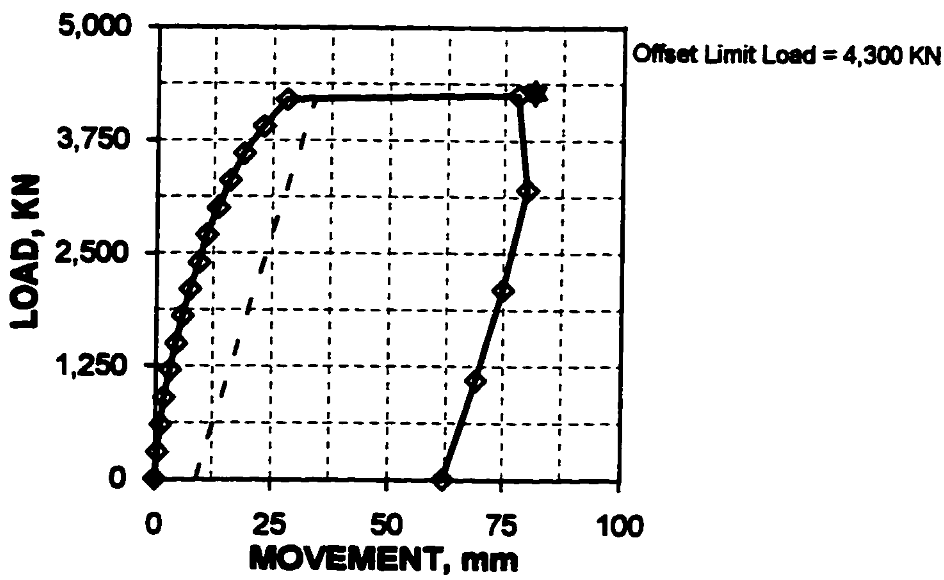

Case 16 TWNTP5
Sheet a CPT data

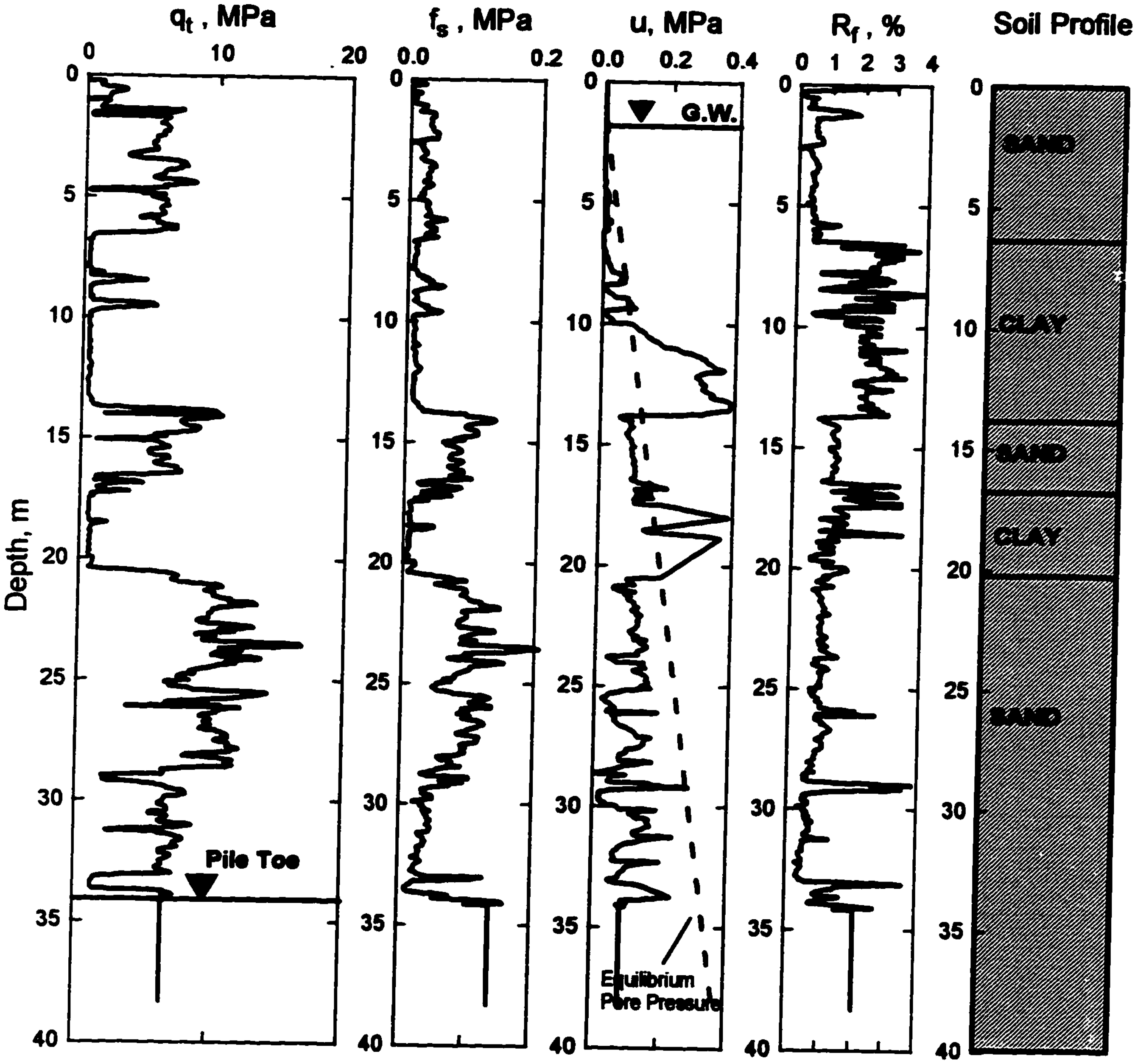

Case 16 TWNTP5
Sheet b Pile data

	DETAIL	DESCRIPTION	SCHEMATIC PROFILE
1	Site	Taiwan	
2	Reference	Yen et al., 1989	
3	Shape, Material, and Installation	Pipe, Steel, Driven	
4	Diameter, b, and Wall Thickness, t, mm	609 12	
5	Embedment Length D, m	34.25	
6	Cross Sectional Area A_t, m^2	0.291	
7	Unit Circumferential Area, A_s, m^2/m	1.91	
8	Toe, Closed or Open	Closed	
9	Type of Test and Loading	Static Tension, SML	
10	Toe Capacity, R_t, KN		
11	*Shaft Capacity, R_s, KN	2,500	
12	Capacity, R_u, KN		

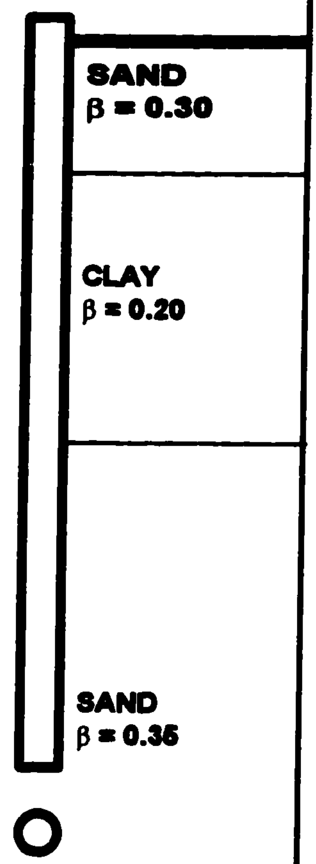

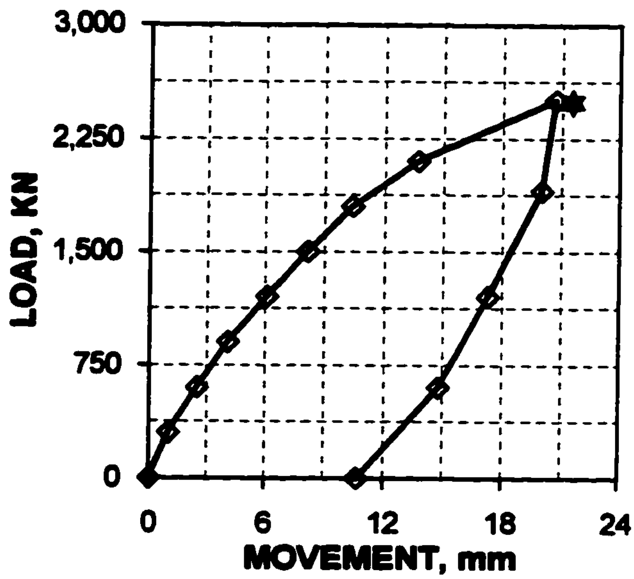

Case 17 TWNTP6
Sheet a CPT data

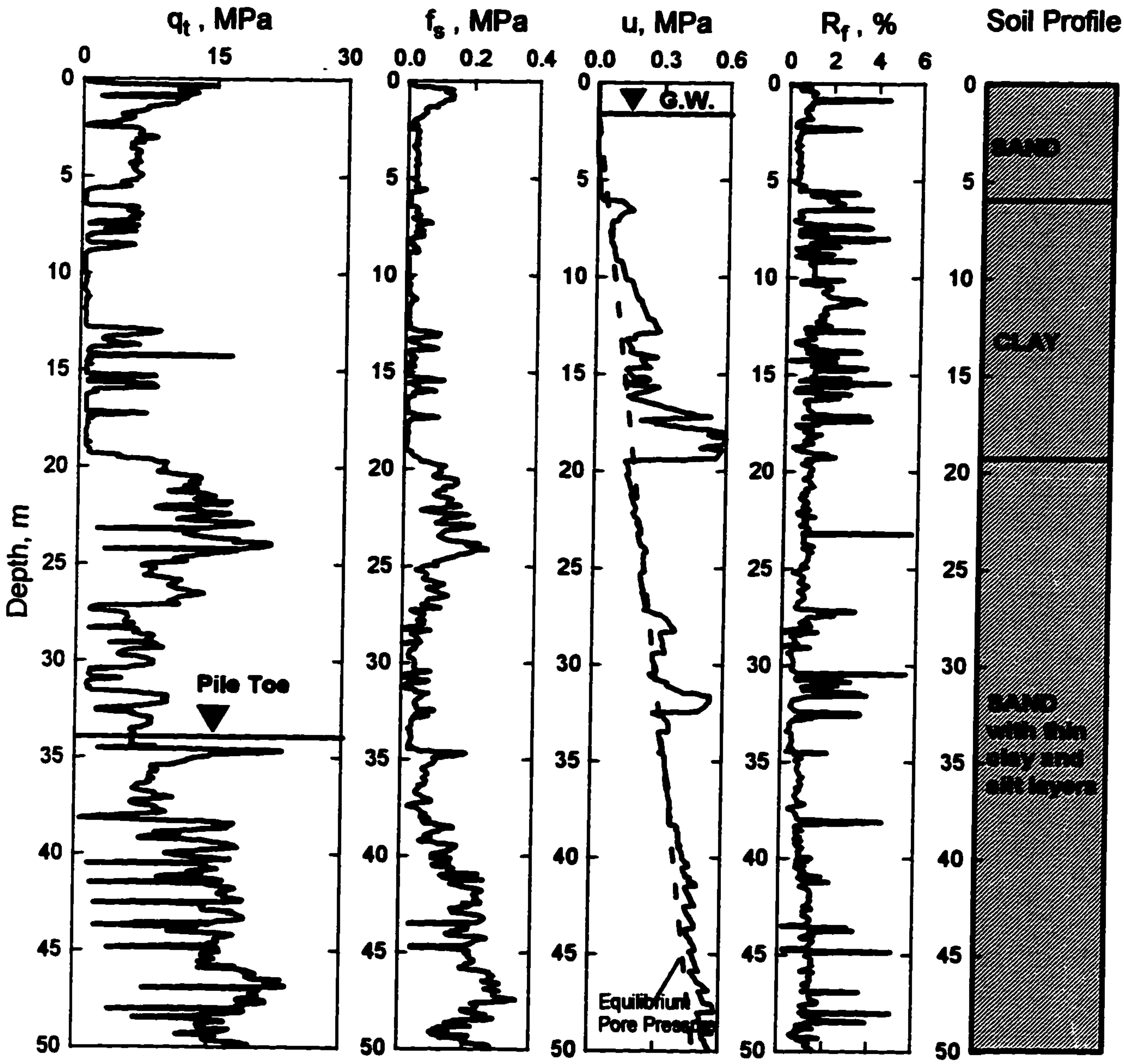

Case 17 TWNTP6
Sheet b Pile data

	DETAIL	DESCRIPTION
1	Site	Taiwan
2	Reference	Yen et al., 1989
3	Shape, Material, and Installation	Pipe, Steel, Driven
4	Diameter, b, and Wall Thickness, t, mm	609 12
5	Embedment Length D, m	34.25
6	Cross Sectional Area A_t, m^2	0.291
7	Unit Circumferential Area, A_s, m^2/m	1.91
8	Toe, Closed or Open	Closed
9	Type of Test and Loading	Static Compression, SML
10	Toe Capacity, R_t, KN	1,650
11	Shaft Capacity, R_s, KN	2,810
12	*Capacity, R_u, KN	4,460

SCHEMATIC PROFILE

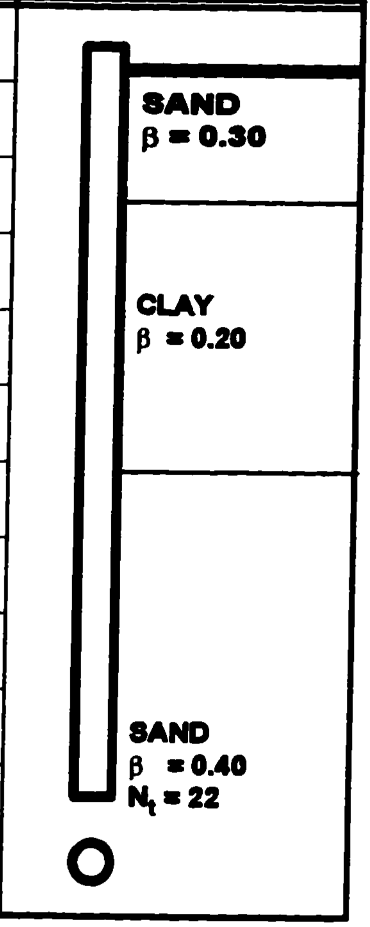

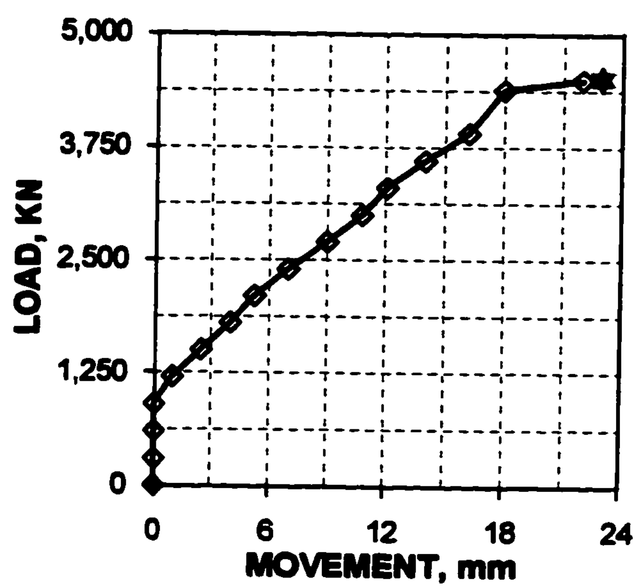

Case 18 LSUA1
Sheet a CPT data

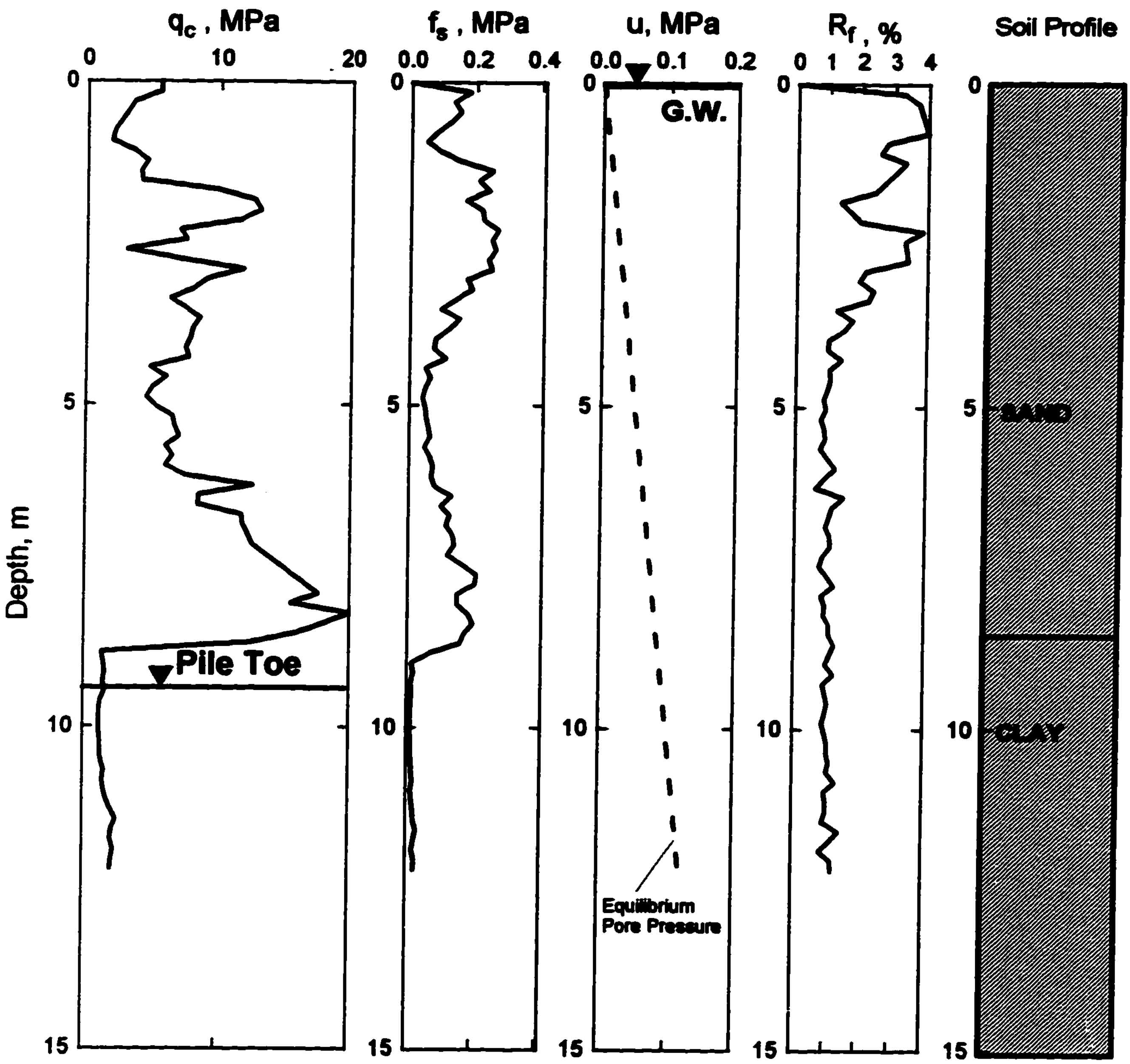

Case 18 LSUA1
Sheet b Pile data

	DETAIL	DESCRIPTION
1	Site	Louisiana, USA
2	Reference	Tumay and Fakhroo, 1981
3	Shape, Material, and Installation	Square, Concrete, Driven
4	Diameter, b, and Wall Thickness, t, mm	350
5	Embedment Length D, m	9.5
6	Cross Sectional Area A_t, m²	0.096
7	Unit Circumferential Area, A_s, m²/m	1.1
8	Toe, Closed or Open	Closed
9	Type of Test and Loading	Static Compression, SML
10	Toe Capacity, R_t, KN	
11	Shaft Capacity, R_s, KN	
12	*Capacity, R_u, KN	900

SCHEMATIC PROFILE

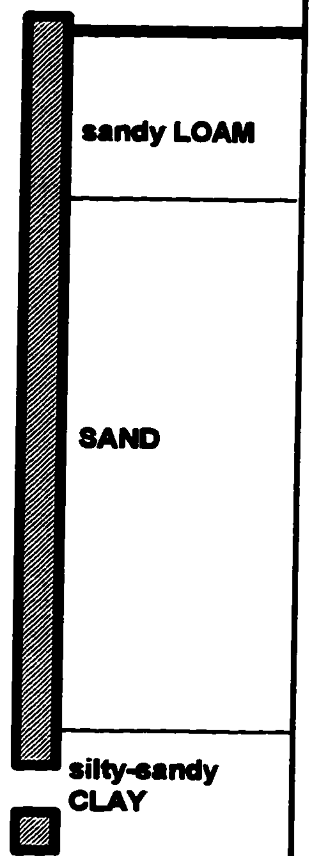

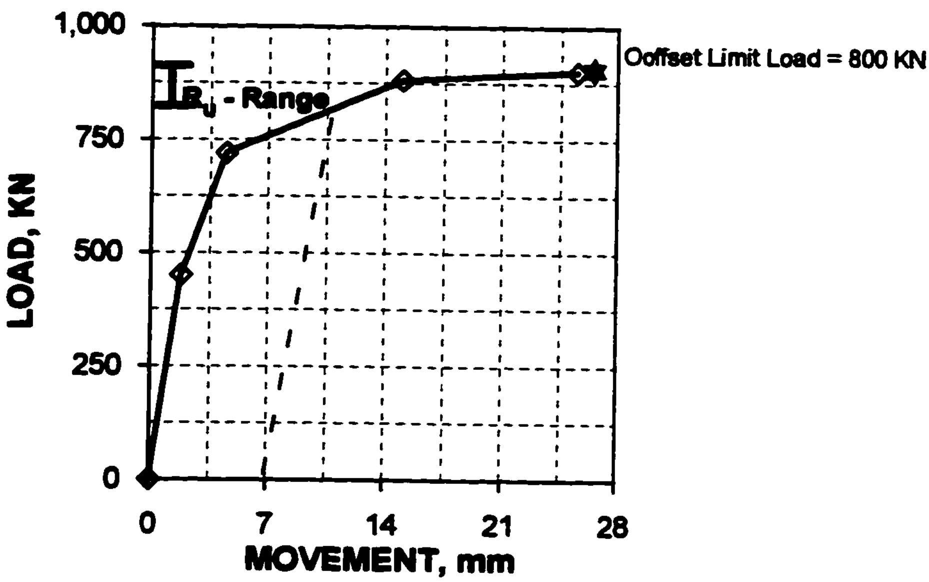

Case 19 LSUB12
Sheet a CPT data

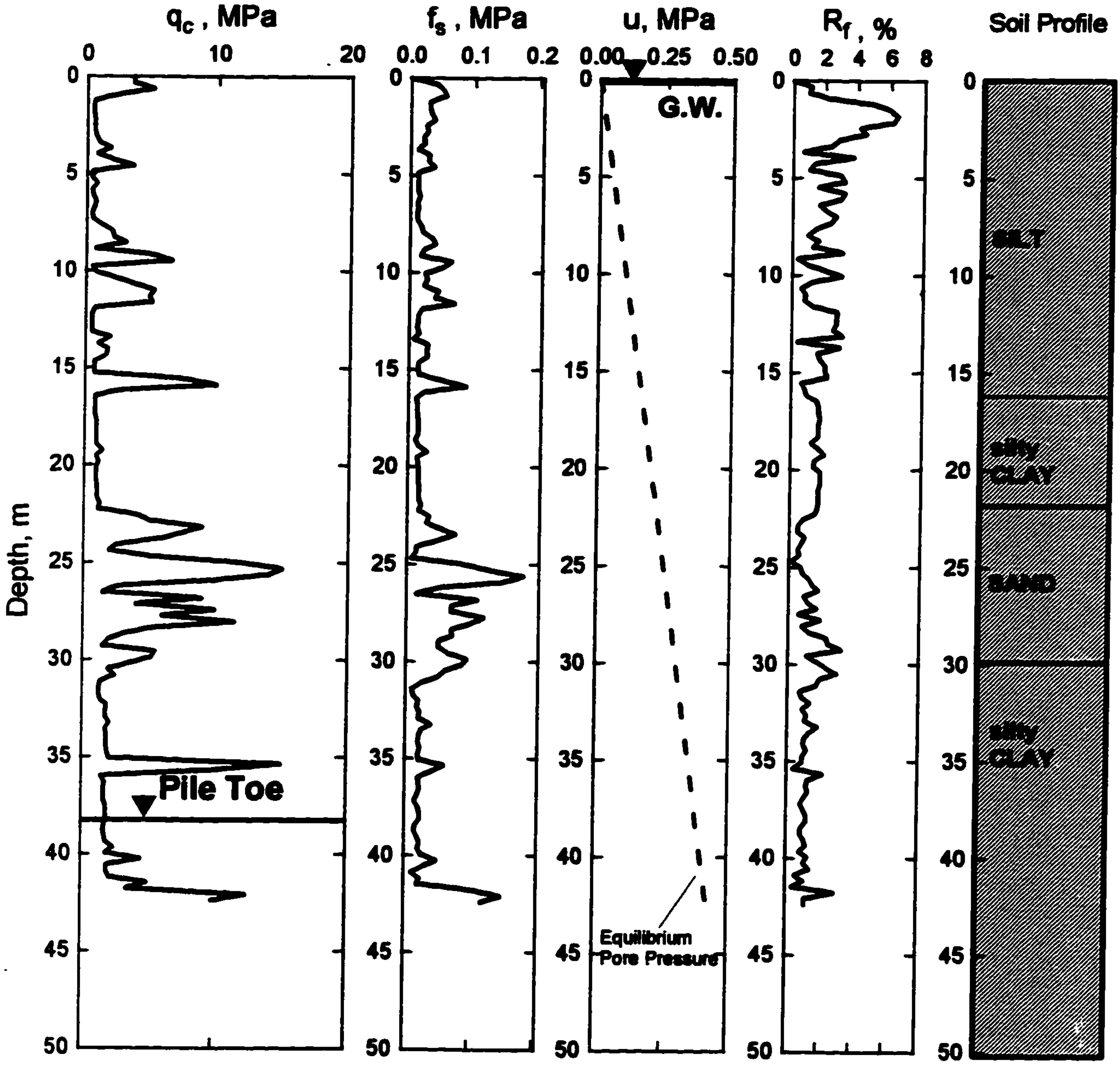

Case 19 LSUB12
Sheet b Pile data

	DETAIL	DESCRIPTION	SCHEMATIC PROFILE
1	Site	Louisiana, USA	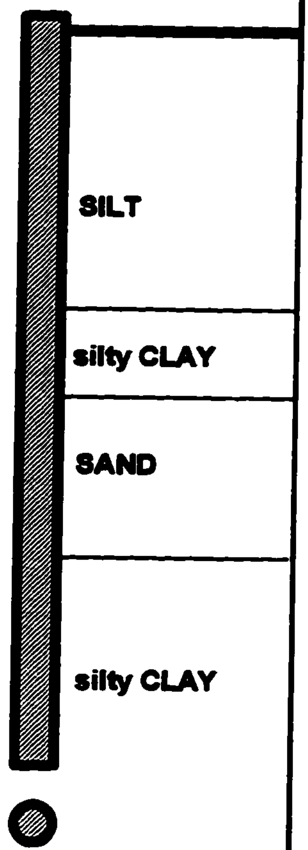
2	Reference	Tumay and Fakhroo, 1981	
3	Shape, Material, and Installation	Round, Concrete, Driven	
4	Diameter, b, and Wall Thickness, t, mm	900	
5	Embedment Length D, m	37.8	
6	Cross Sectional Area A_t, m²	0.636	
7	Unit Circumferential Area, A_s, m²/m	2.83	
8	Toe, Closed or Open	Closed	
9	Type of Test and Loading	Static Compression, QML	
10	Toe Capacity, R_t, KN		
11	Shaft Capacity, R_s, KN		
12	*Capacity, R_u, KN	3,960	

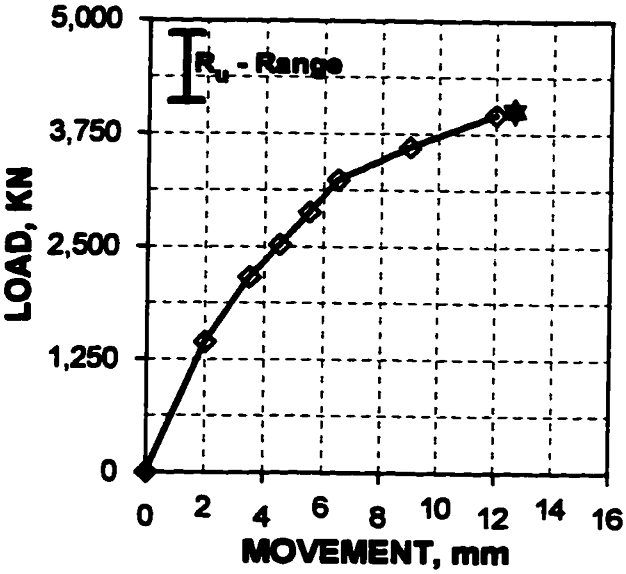

Case 20 LSUN11
Sheet a CPT data

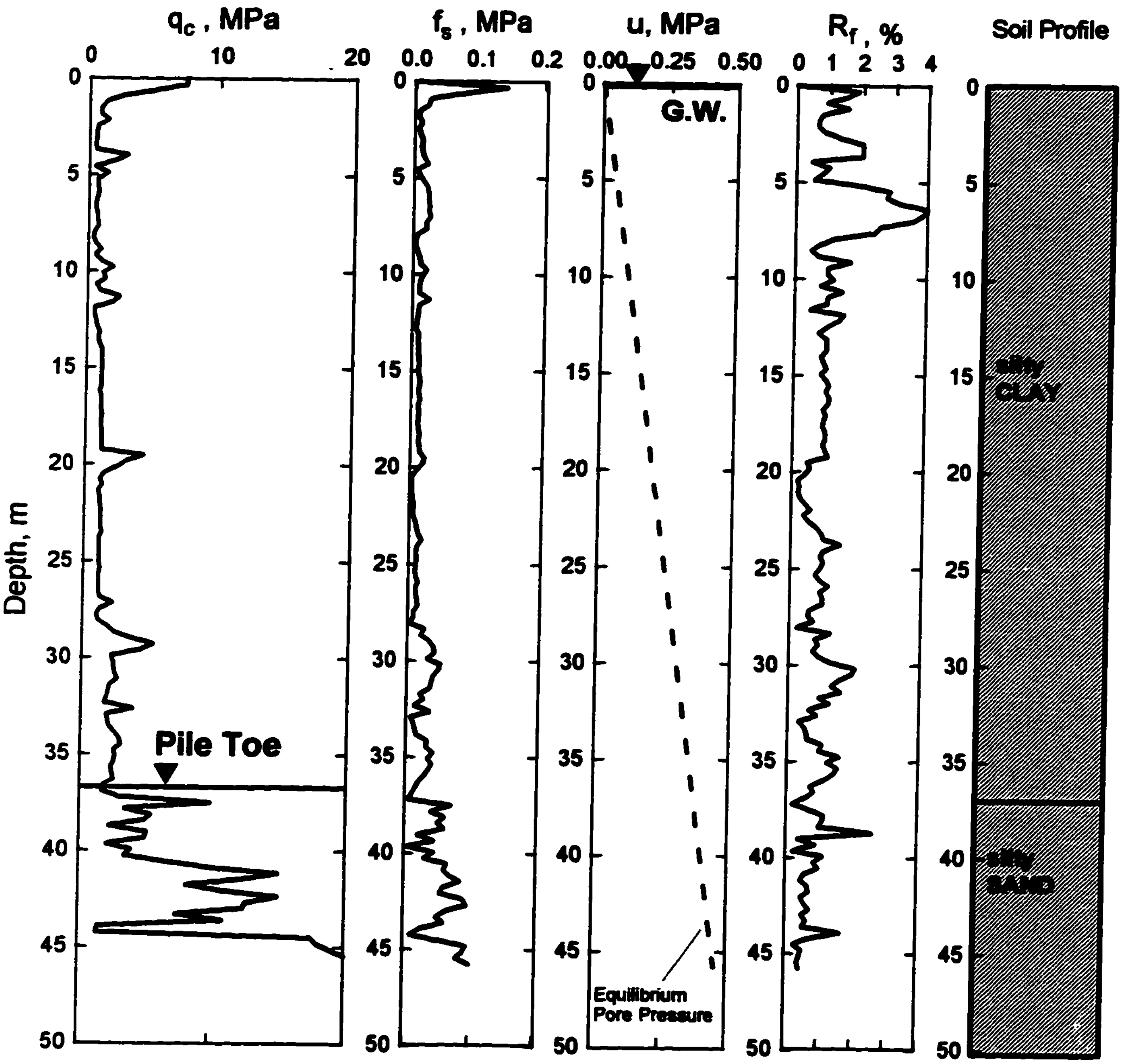

Case 20 LSUN11
Sheet b Pile data

	DETAIL	DESCRIPTION
1	Site	Louisiana, USA
2	Reference	Tumay and Fakhroo, 1981
3	Shape, Material, and Installation	Square, Concrete, Driven
4	Diameter, b, and Wall Thickness, t, mm	450
5	Embedment Length D, m	36.5
6	Cross Sectional Area A_t, m^2	0.203
7	Unit Circumferential Area, A_s, m^2/m	1.8
8	Toe, Closed or Open	Closed
9	Type of Test and Loading	Static Compression, SML
10	Toe Capacity, R_t, KN	
11	Shaft Capacity, R_s, KN	
12	*Capacity, R_u, KN	2,950

SCHEMATIC PROFILE

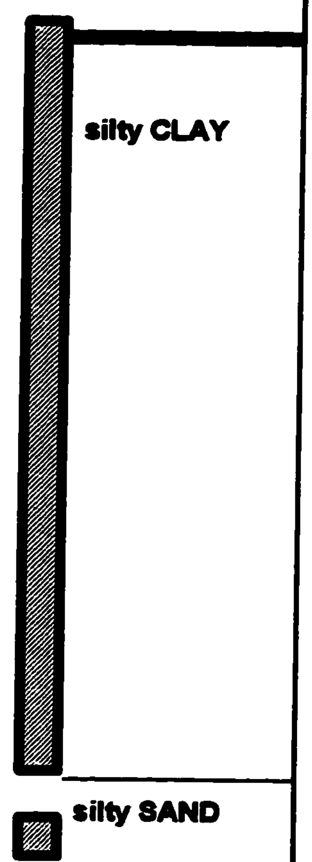

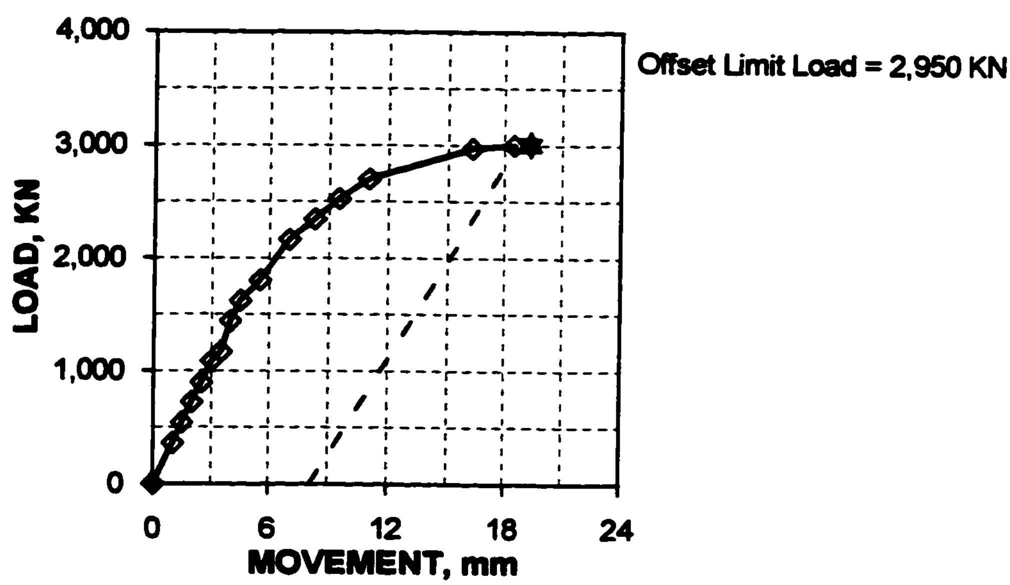

Case 21 LSUN15
Sheet a CPT data

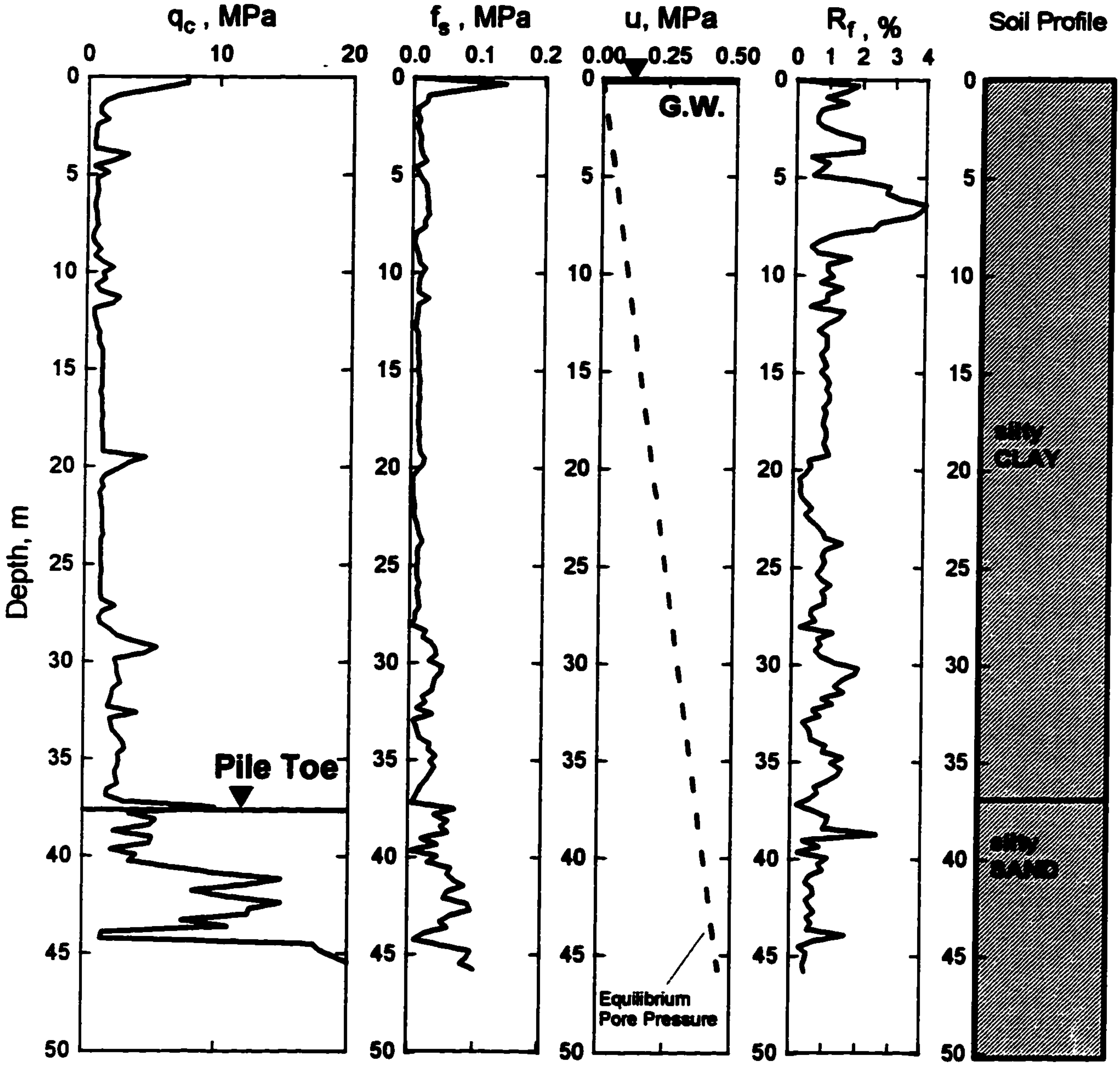

Case 21 LSUN15
Sheet b Pile data

	DETAIL	DESCRIPTION	SCHEMATIC PROFILE
1	Site	Louisiana, USA	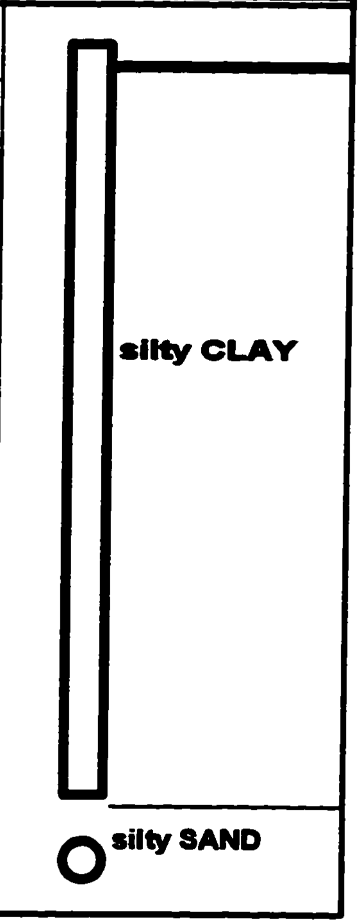
2	Reference	Tumay and Fakhroo, 1981	
3	Shape, Material, and Installation	Pipe, Steel, Driven	
4	Diameter, b, and Wall Thickness, t, mm	400	
5	Embedment Length D, m	37.5	
6	Cross Sectional Area A_t, m^2	0.126	
7	Unit Circumferential Area, A_s, m^2/m	1.257	
8	Toe, Closed or Open	Closed	
9	Type of Test and Loading	Static Compression, QML	
10	Toe Capacity, R_t, KN		
11	Shaft Capacity, R_s, KN		
12	*Capacity, R_u, KN	2,800	

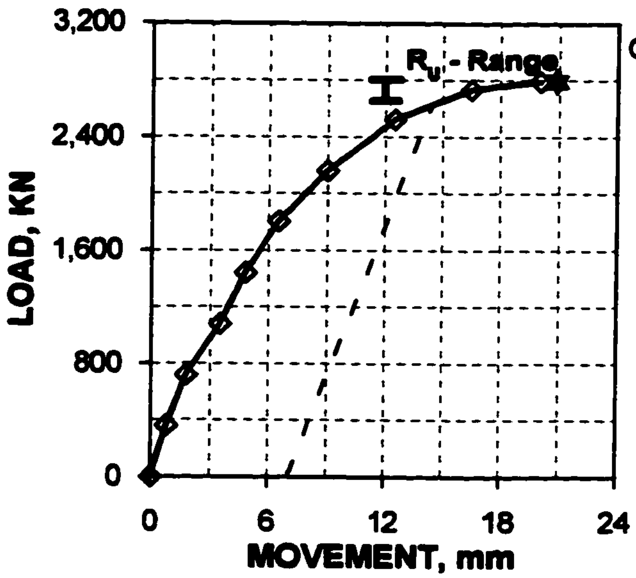

Offset Limit Load = 2,600 KN

Case 22 LSUN28
Sheet a CPT data

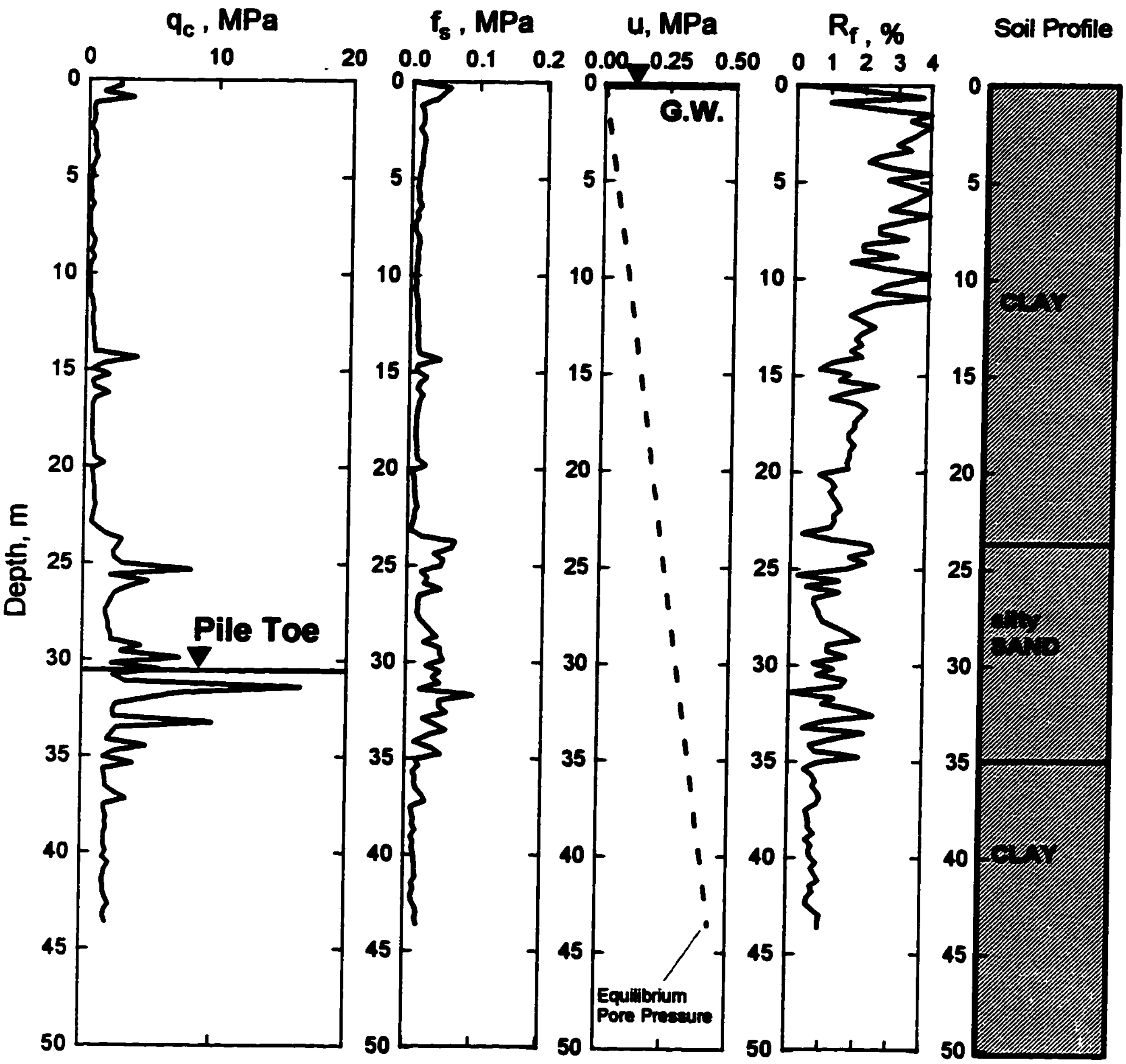

Case 22 LSUN28
Sheet b Pile data

DETAIL		DESCRIPTION	SCHEMATIC PROFILE
1	Site	Louisiana, USA	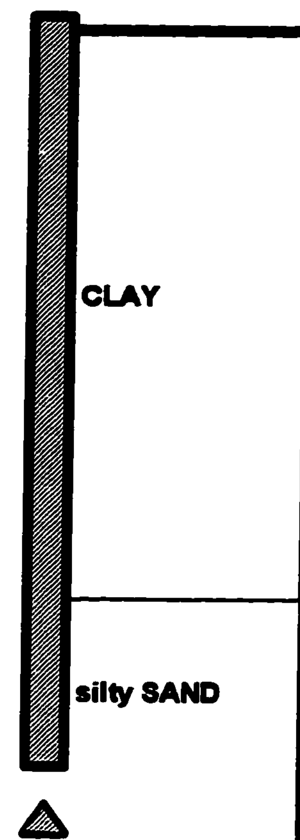
2	Reference	Tumay and Fakhroo, 1981	
3	Shape, Material, and Installation	Triangle, Concrete, Driven	
4	Diameter, b, and Wall Thickness, t, mm	500	
5	Embedment Length D, m	30.5	
6	Cross Sectional Area A_t , m^2	0.1075	
7	Unit Circumferential Area, A_s , m^2 /m	1.5	
8	Toe, Closed or Open	Closed	
9	Type of Test and Loading	Static Compression, SML	
10	Toe Capacity, R_t , KN		
11	Shaft Capacity, R_s , KN		
12	*Capacity, R_u , KN	2,160	

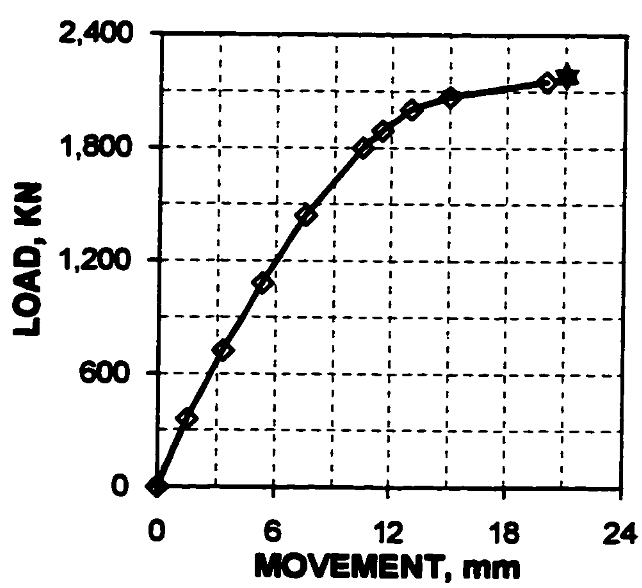

Case 23 LSUN215
Sheet a CPT data

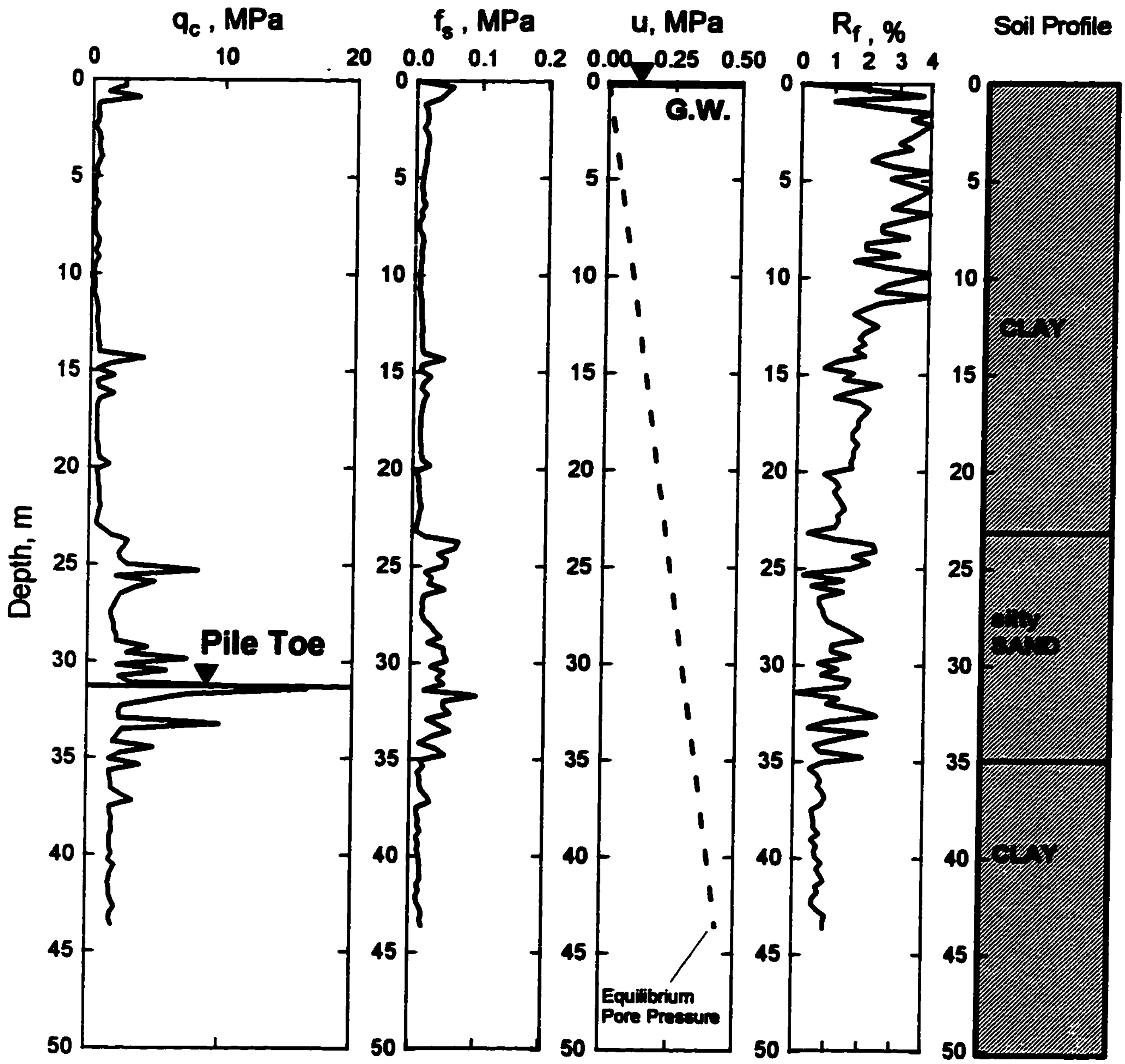

Case 23 LSUN215
Sheet b Pile data

	DETAIL	DESCRIPTION
1	Site	Louisiana, USA
2	Reference	Tumay and Fakhroo, 1981
3	Shape, Material, and Installation	Pipe, Steel, Driven
4	Diameter, b, and Wall Thickness, t, mm	350
5	Embedment Length D, m	31.1
6	Cross Sectional Area A_t, m^2	0.096
7	Unit Circumferential Area, A_s, m^2/m	1.01
8	Toe, Closed or Open	Closed
9	Type of Test and Loading	Static Compression, QML
10	Toe Capacity, R_t, KN	
11	Shaft Capacity, R_s, KN	
12	*Capacity, R_u, KN	1,710

SCHEMATIC PROFILE

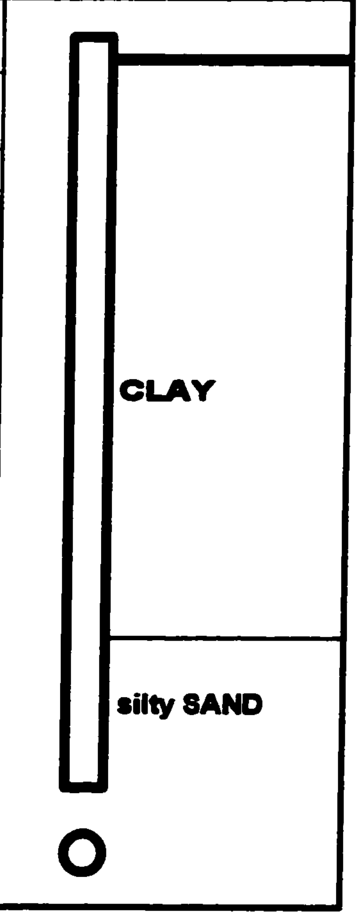

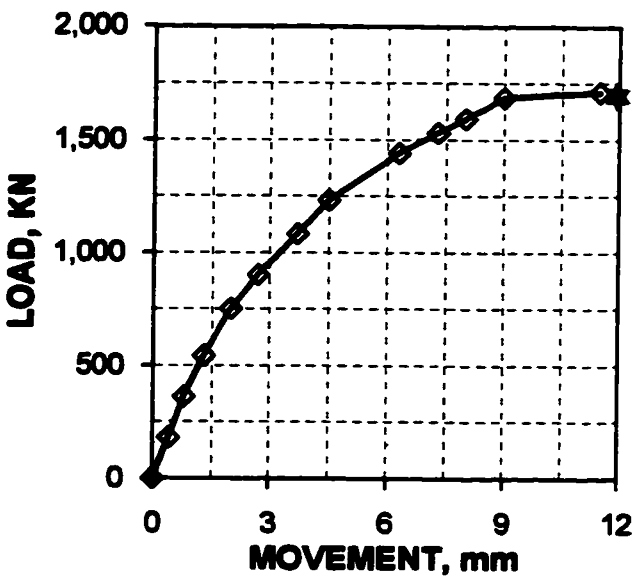

Case 24 LSUN216
Sheet a CPT data

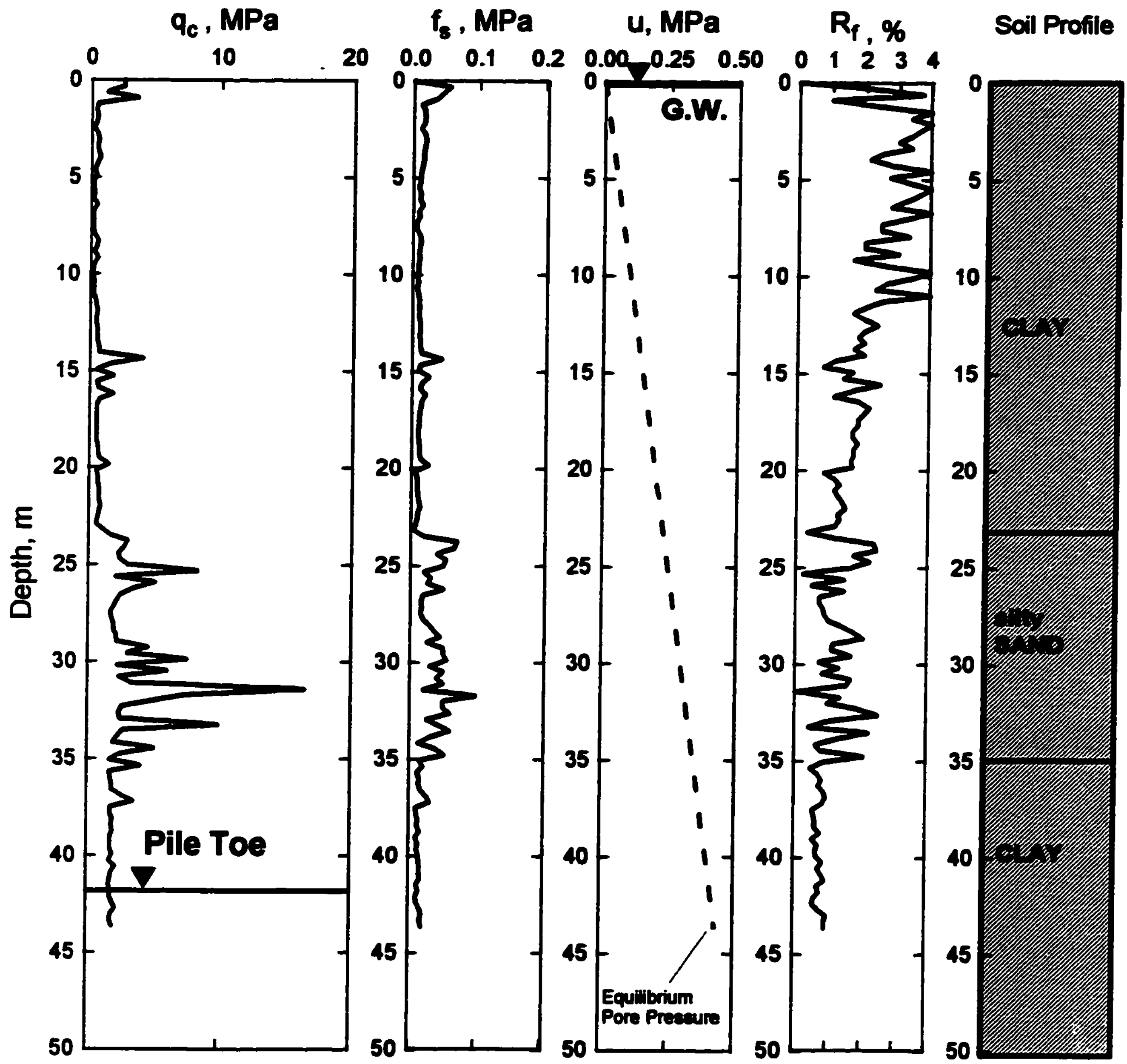

Case 24 LSUN216
Sheet b Pile data

	DETAIL	DESCRIPTION
1	Site	Louisiana, USA
2	Reference	Tumay and Fakhroo, 1981
3	Shape, Material, and Installation	Pipe, Steel, Driven
4	Diameter, b, and Wall Thickness, t, mm	400
5	Embedment Length D, m	41.8
6	Cross Sectional Area A_t, m^2	0.126
7	Unit Circumferential Area, A_s, m^2/m	1.26
8	Toe, Closed or Open	Closed
9	Type of Test and Loading	Static Compression, QML
10	Toe Capacity, R_t, KN	
11	Shaft Capacity, R_s, KN	
12	*Capacity, R_u, KN	1,890

SCHEMATIC PROFILE

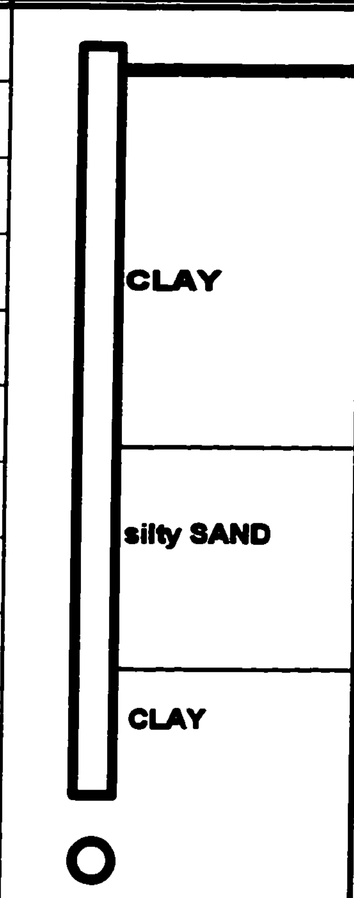

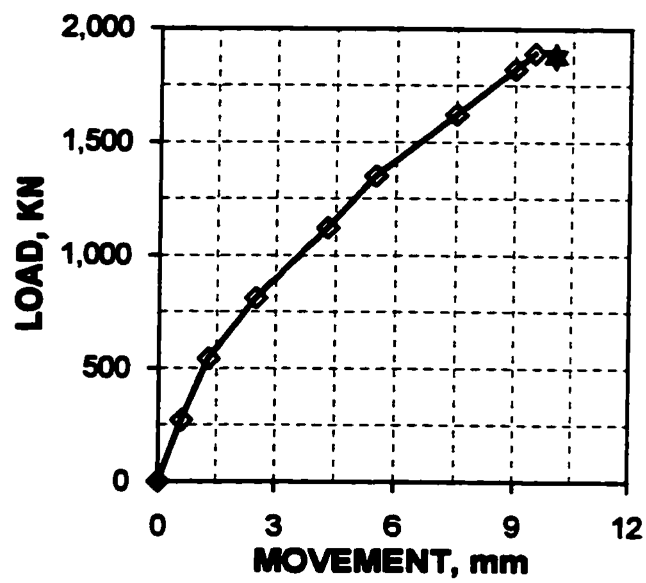

Case 25 LSUH1
Sheet a CPT data

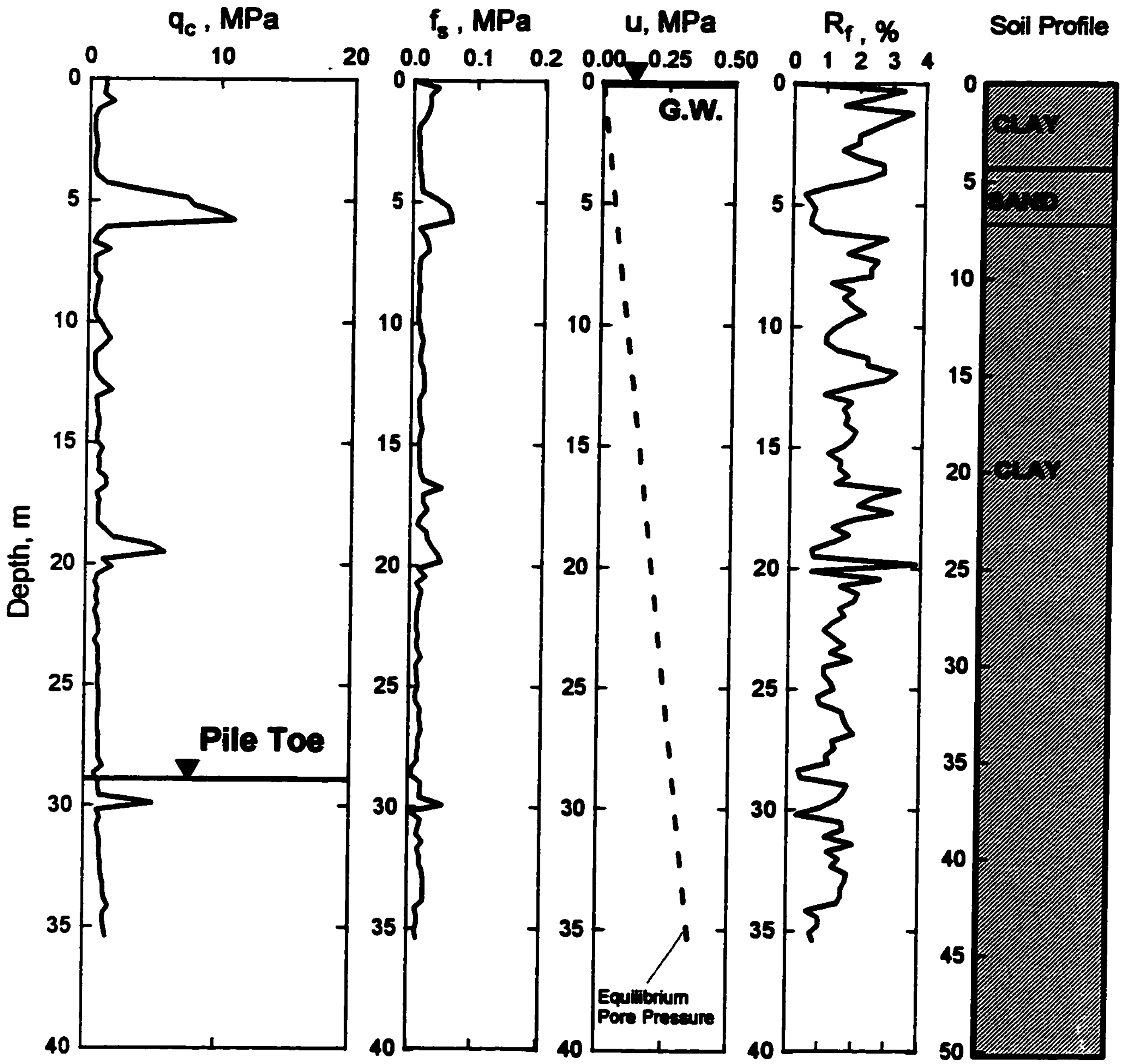

Case 25 LSUH1
Sheet b Pile data

	DETAIL	DESCRIPTION
1	Site	Louisiana, USA
2	Reference	Tumay and Fakhroo, 1981
3	Shape, Material, and Installation	Square, Concrete, Driven
4	Diameter, b, and Wall Thickness, t, mm	450
5	Embedment Length D, m	29
6	Cross Sectional Area A_t, m^2	0.203
7	Unit Circumferential Area, A_s, m^2/m	1.8
8	Toe, Closed or Open	Closed
9	Type of Test and Loading	Static Compression, SML
10	Toe Capacity, R_t, KN	
11	Shaft Capacity, R_s, KN	
12	*Capacity, R_u, KN	1,935

SCHEMATIC PROFILE

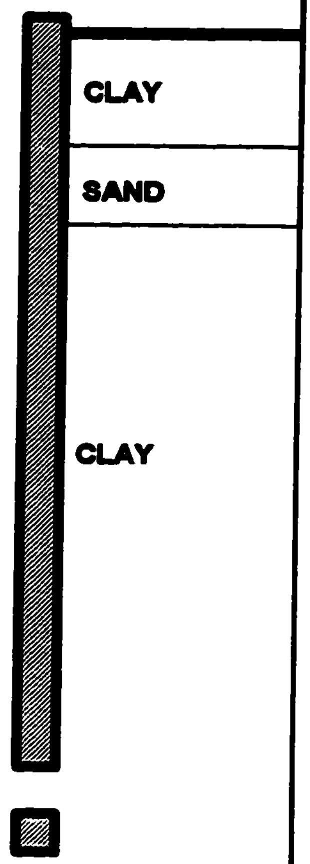

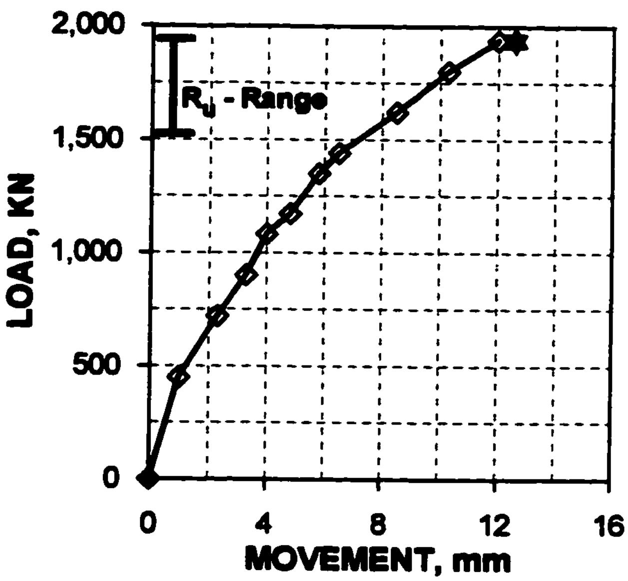

Case 26 LSUR24
Sheet a CPT data

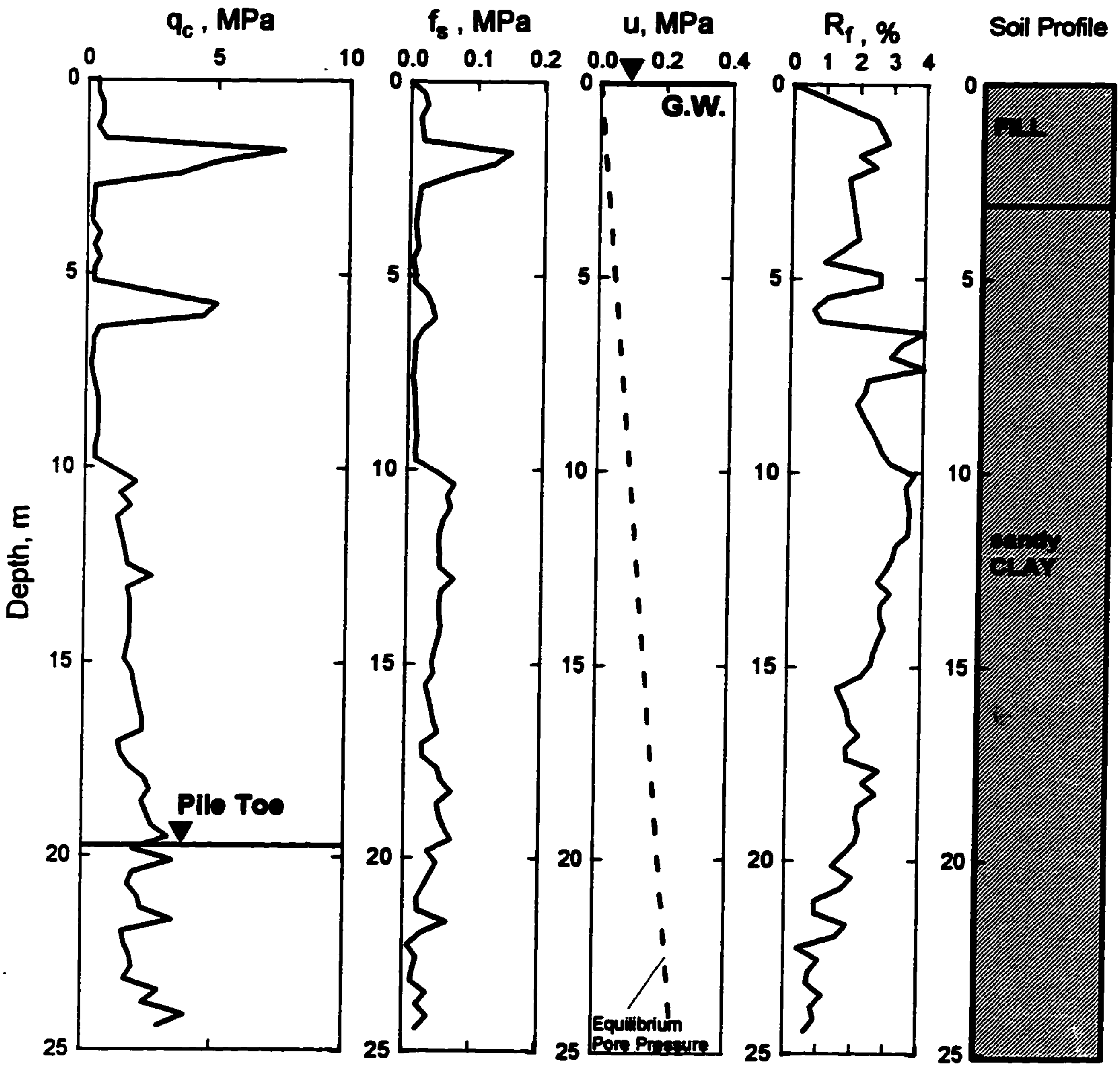

Case 26 LSUR24
Sheet b Pile data

	DETAIL	DESCRIPTION
1	Site	Louisiana, USA
2	Reference	Tumay and Fakhroo, 1981
3	Shape, Material, and Installation	Square, Concrete, Driven
4	Diameter, b, and Wall Thickness, t, mm	600
5	Embedment Length D, m	19.8
6	Cross Sectional Area A_t, m^2	0.360
7	Unit Circumferential Area, A_s, m^2/m	2.4
8	Toe, Closed or Open	Closed
9	Type of Test and Loading	Static Compression, SML
10	Toe Capacity, R_t, KN	
11	Shaft Capacity, R_s, KN	
12	*Capacity, R_u, KN	2,025

SCHEMATIC PROFILE

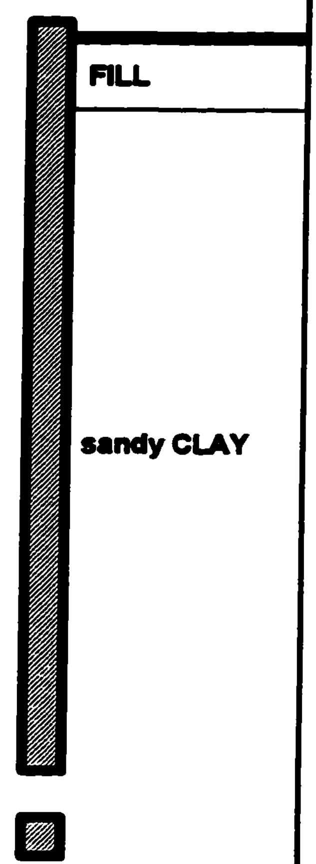

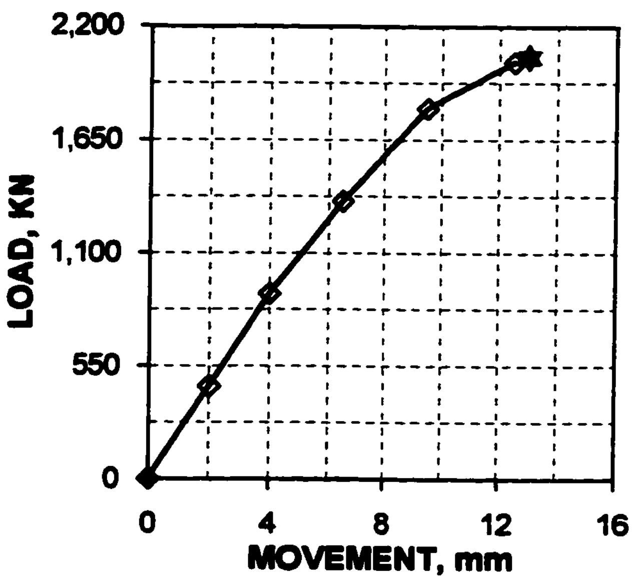

Case 27 LSUR30
Sheet a CPT data

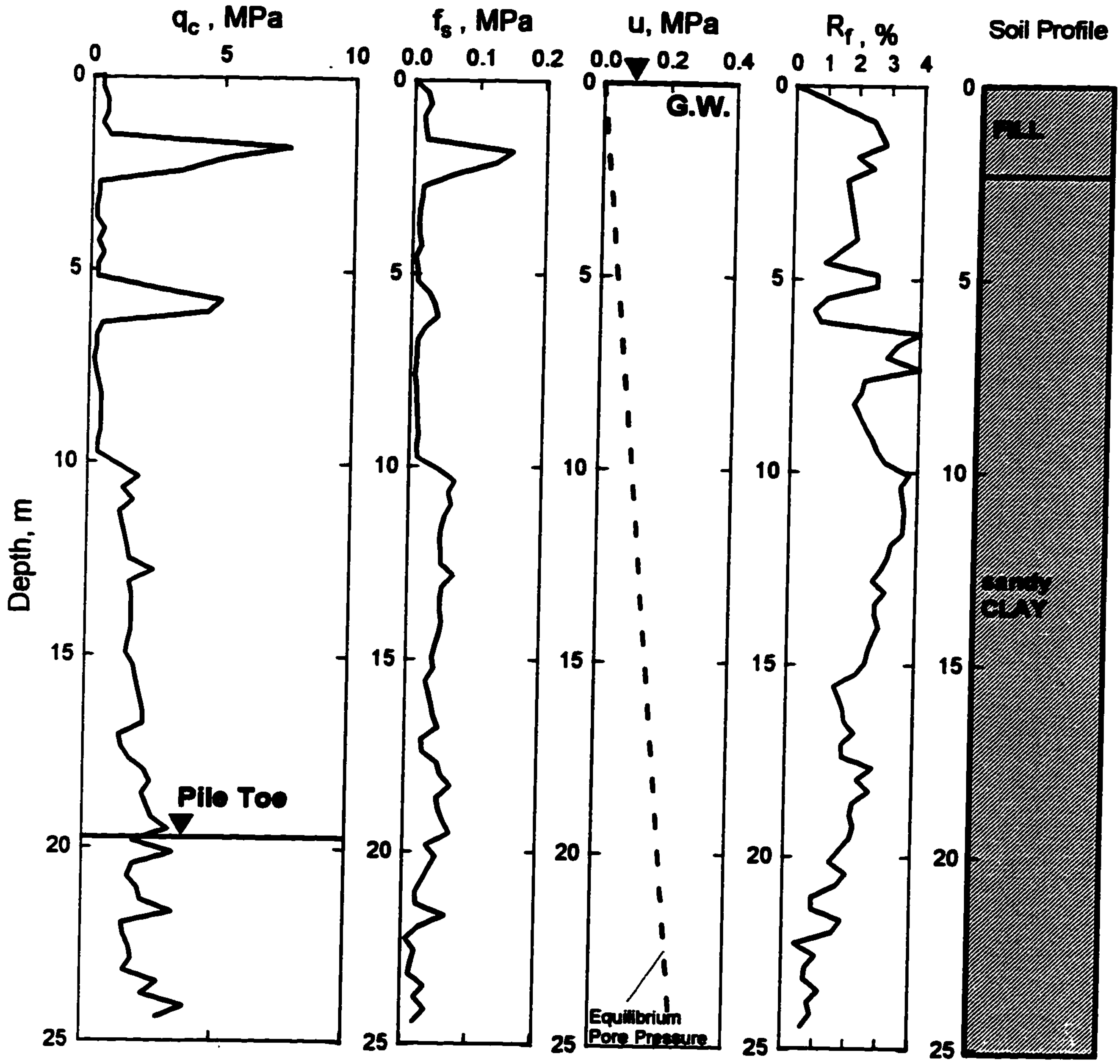

Case 27 LSUR30
Sheet b Pile data

DETAIL		DESCRIPTION
1	Site	Louisiana, USA
2	Reference	Tumay and Fakhroo, 1981
3	Shape, Material, and Installation	Square, Concrete, Driven
4	Diameter, b, and Wall Thickness, t, mm	750
5	Embedment Length D, m	19.8
6	Cross Sectional Area A_t, m^2	0.563
7	Unit Circumferential Area, A_s, m^2/m	3.0
8	Toe, Closed or Open	Closed
9	Type of Test and Loading	Static Compression, SML
10	Toe Capacity, R_t, KN	
11	Shaft Capacity, R_s, KN	
12	*Capacity, R_u, KN	2,610

SCHEMATIC PROFILE

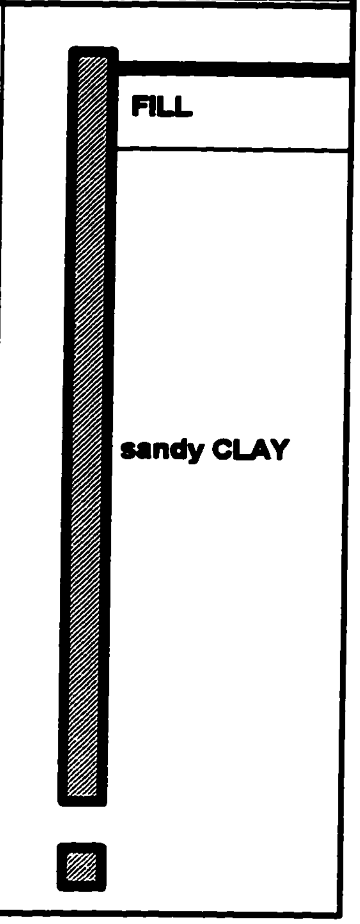

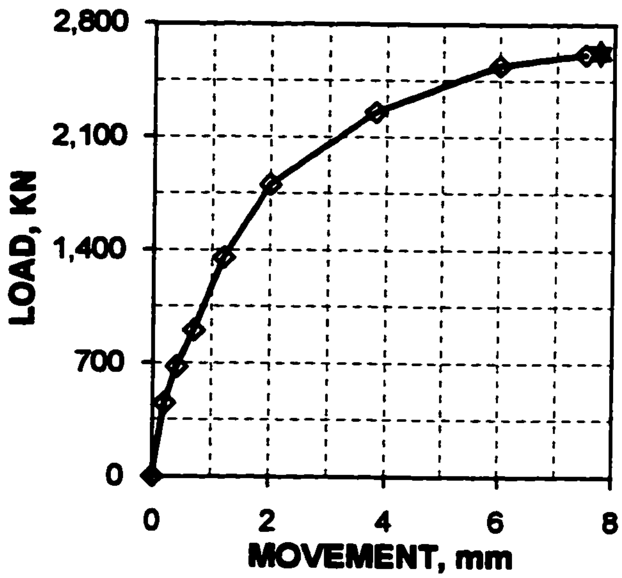

Case 28 UFL22
Sheet a CPT data

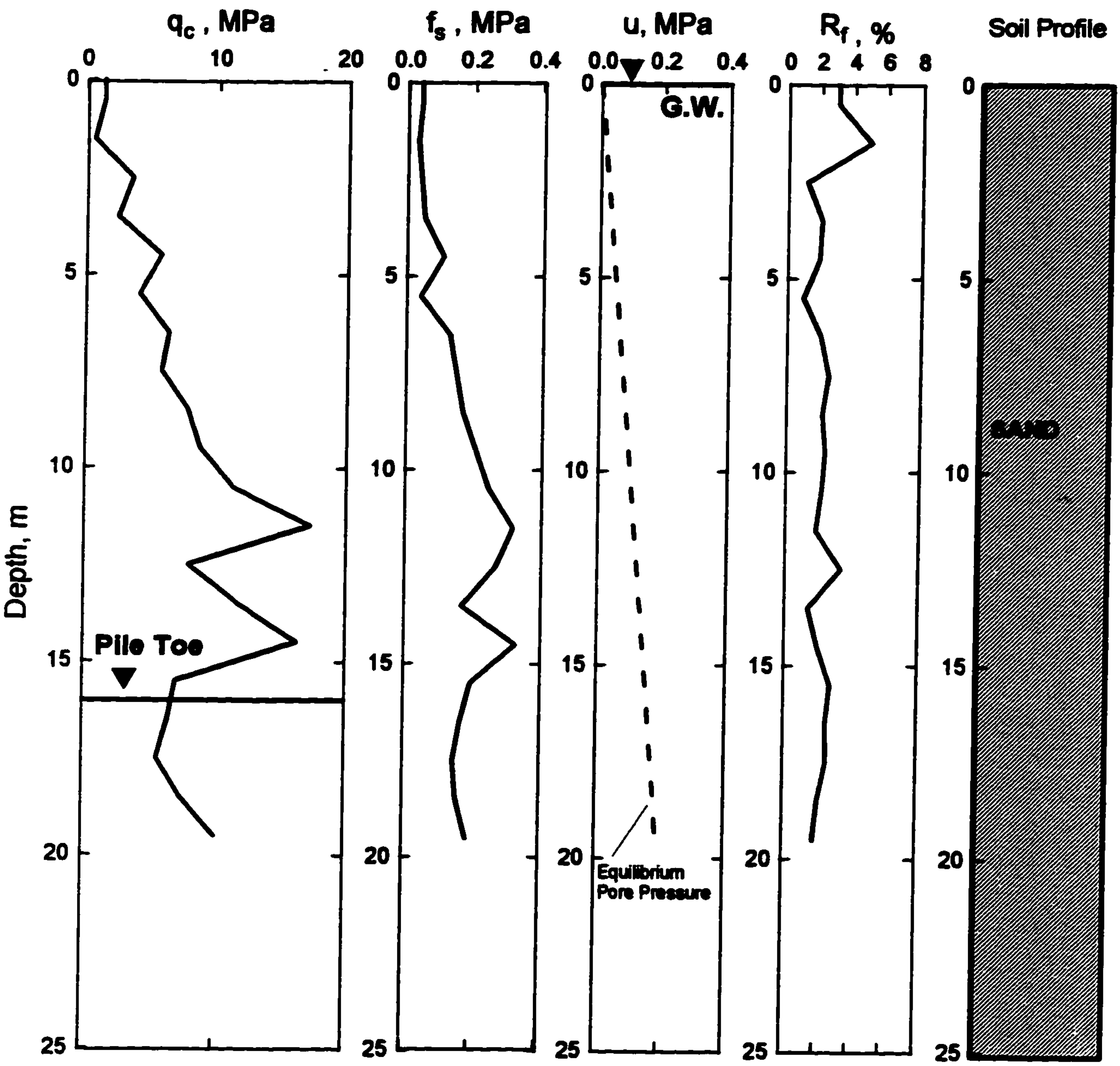

Case 28 UFL22
Sheet b Pile data

	DETAIL	DESCRIPTION
1	Site	Florida, USA
2	Reference	Avasarala et al., 1994
3	Shape, Material, and Installation	Square, Concrete, Driven
4	Diameter, b, and Wall Thickness, t, mm	350
5	Embedment Length D, m	16
6	Cross Sectional Area A_t, m^2	0.096
7	Unit Circumferential Area, A_s, m^2/m	1.1
8	Toe, Closed or Open	Closed
9	Type of Test and Loading	Static Compression, SML
10	Toe Capacity, R_t, KN	
11	Shaft Capacity, R_s, KN	
12	*Capacity, R_u, KN	1,350

SCHEMATIC PROFILE

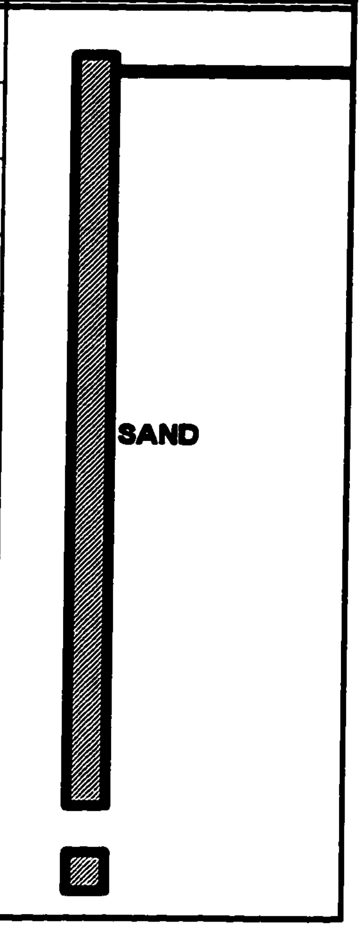

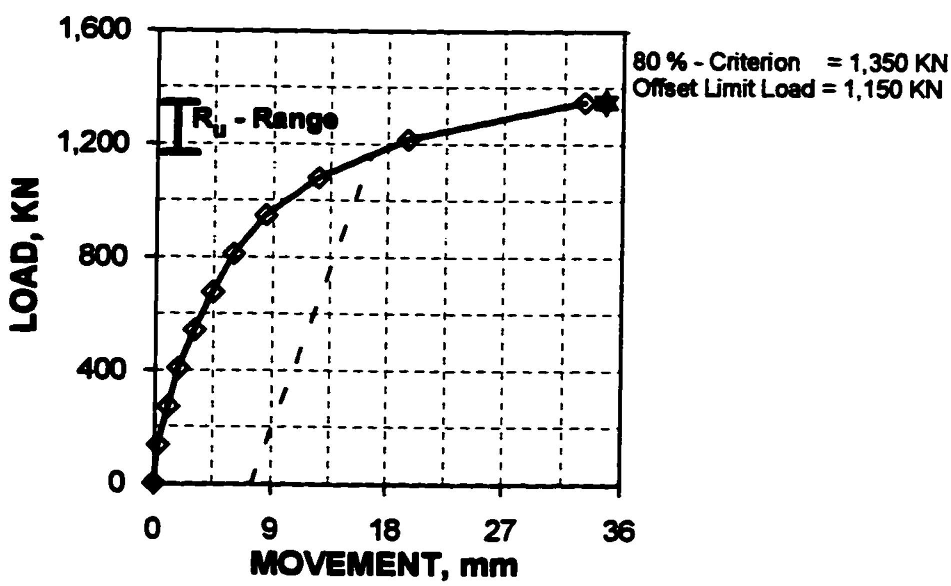

Case 29 UFL52
Sheet a CPT data

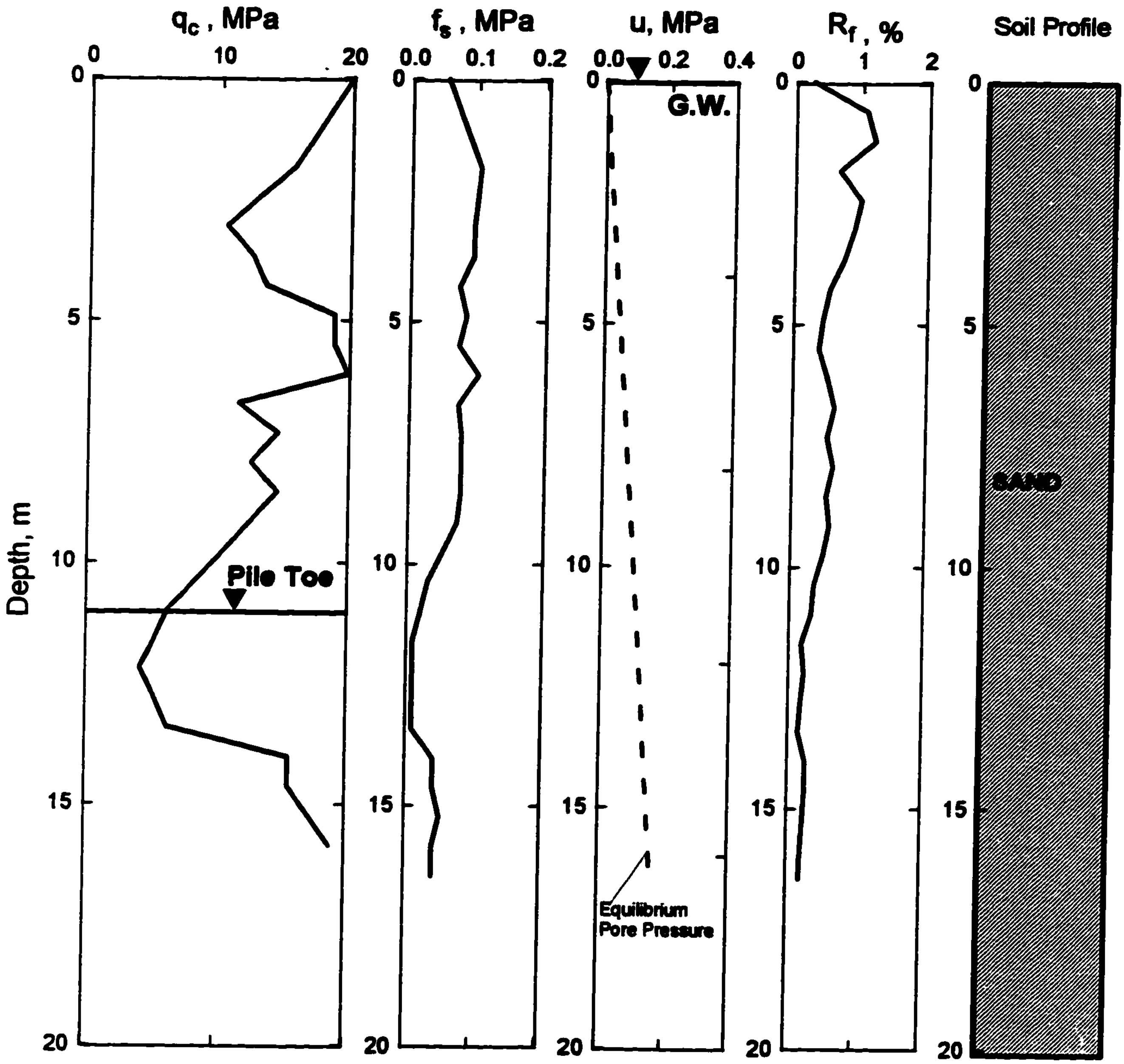

Case 29 UFL52
Sheet b Pile data

	DETAIL	DESCRIPTION	SCHEMATIC PROFILE
1	Site	Florida, USA	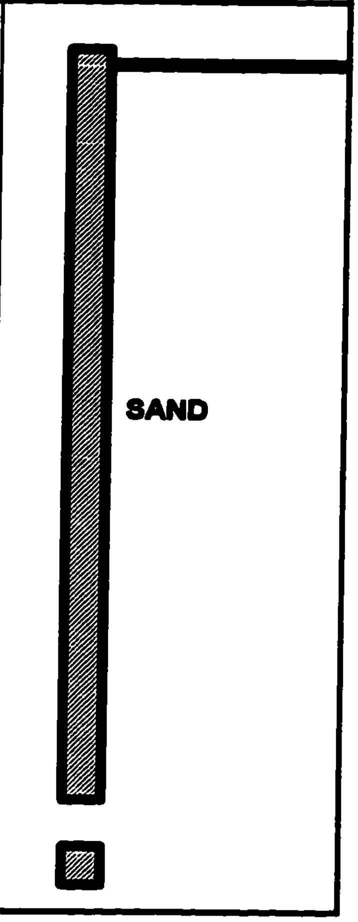
2	Reference	Avasarala et al., 1994	
3	Shape, Material, and Installation	Square, Concrete, Driven	
4	Diameter, b, and Wall Thickness, t, mm	500	
5	Embedment Length D, m	11	
6	Cross Sectional Area A_t, m^2	0.25	
7	Unit Circumferential Area, A_s, m^2 /m	2.0	
8	Toe, Closed or Open	Closed	
9	Type of Test and Loading	Static Compression, SML	
10	Toe Capacity, R_t, KN		
11	Shaft Capacity, R_s, KN		
12	*Capacity, R_u, KN	2,070	

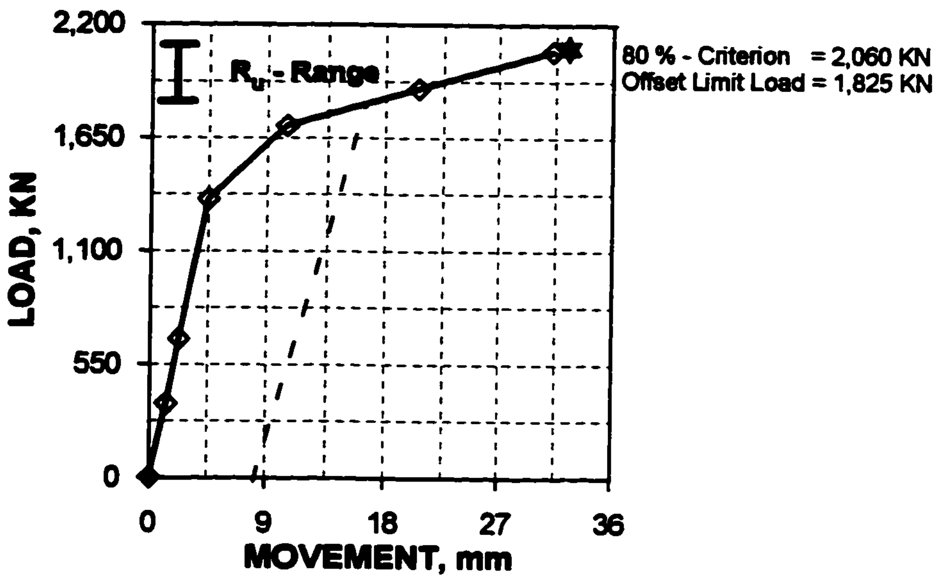

Case 30 UFL53
Sheet a CPT data

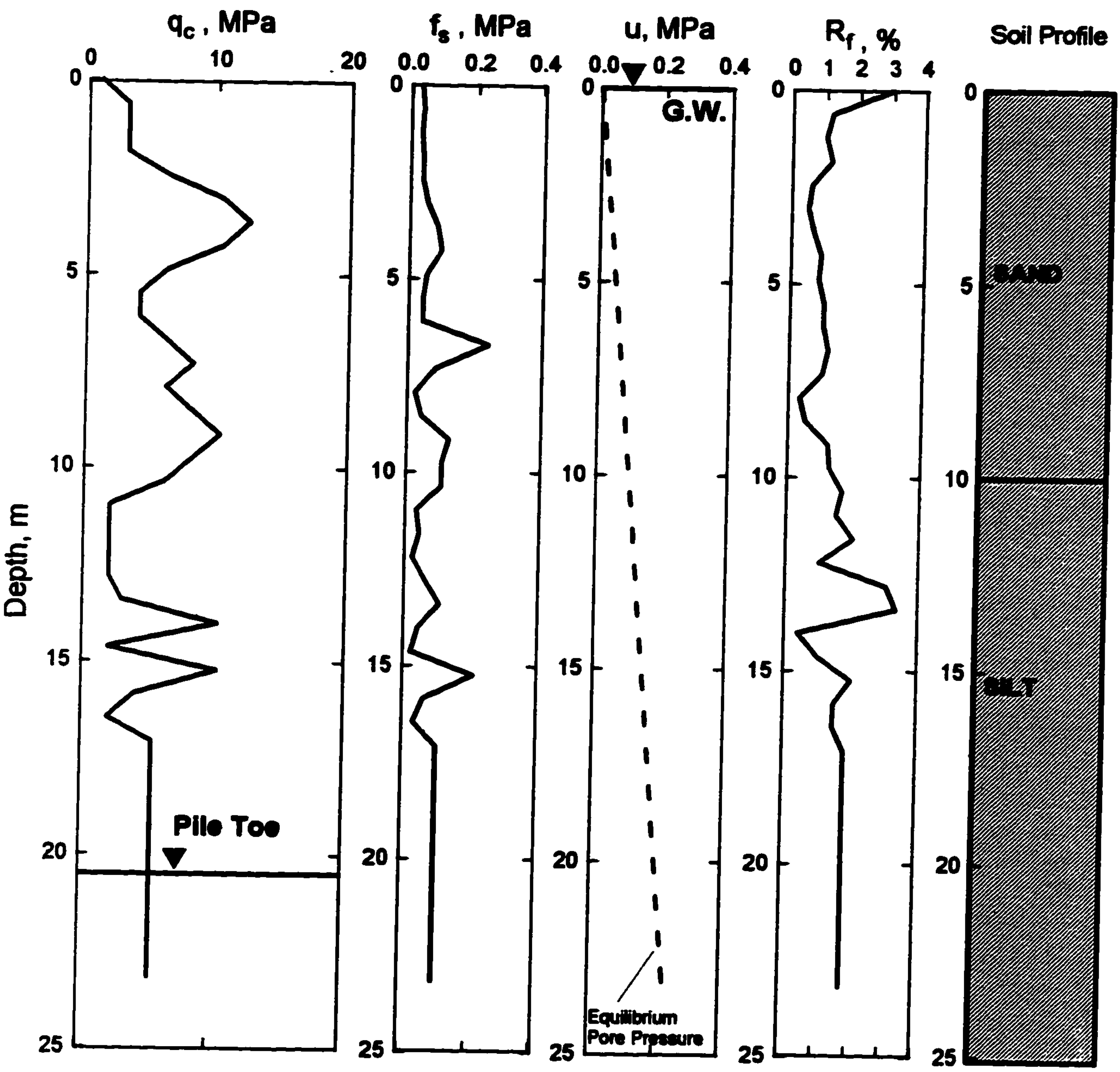

Case 30 UFL53
Sheet b Pile data

	DETAIL	DESCRIPTION	SCHEMATIC PROFILE
1	Site	Florida, USA	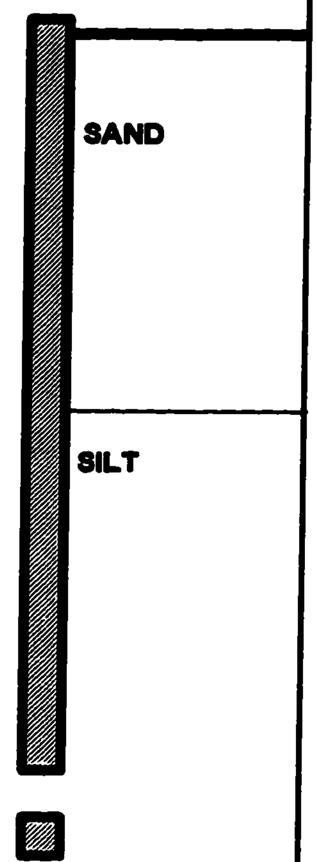
2	Reference	Avasarala et al., 1994	
3	Shape, Material, and Installation	Square, Concrete, Driven	
4	Diameter, b, and Wall Thickness, t, mm	350	
5	Embedment Length D, m	20.4	
6	Cross Sectional Area A_t, m^2	0.096	
7	Unit Circumferential Area, A_s, m^2/m	1.1	
8	Toe, Closed or Open	Closed	
9	Type of Test and Loading	Static Compression, SML	
10	Toe Capacity, R_t, KN		
11	Shaft Capacity, R_s, KN		
12	*Capacity, R_u, KN	1,260	

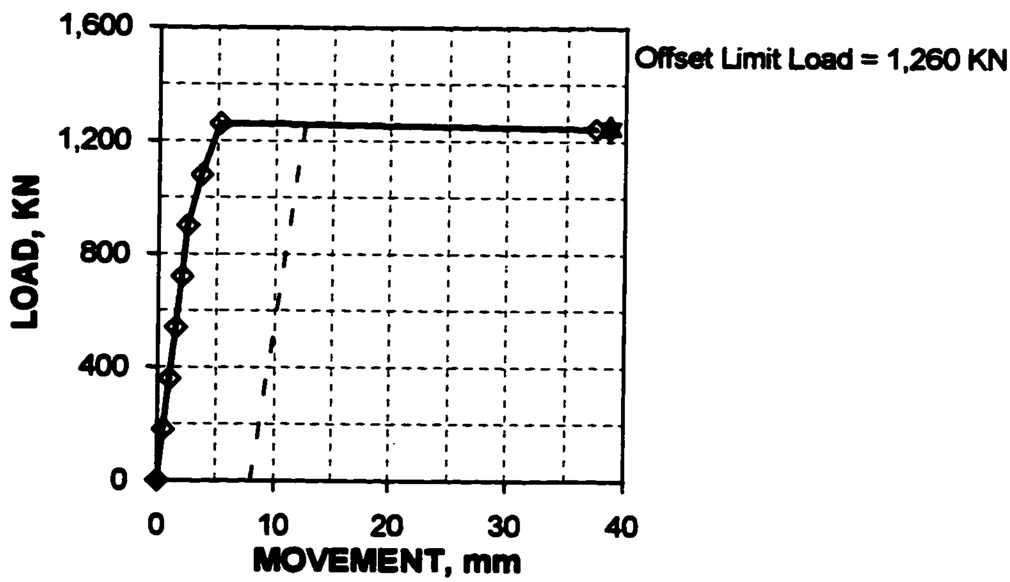

Case 31 LTN741
Sheet a CPT data

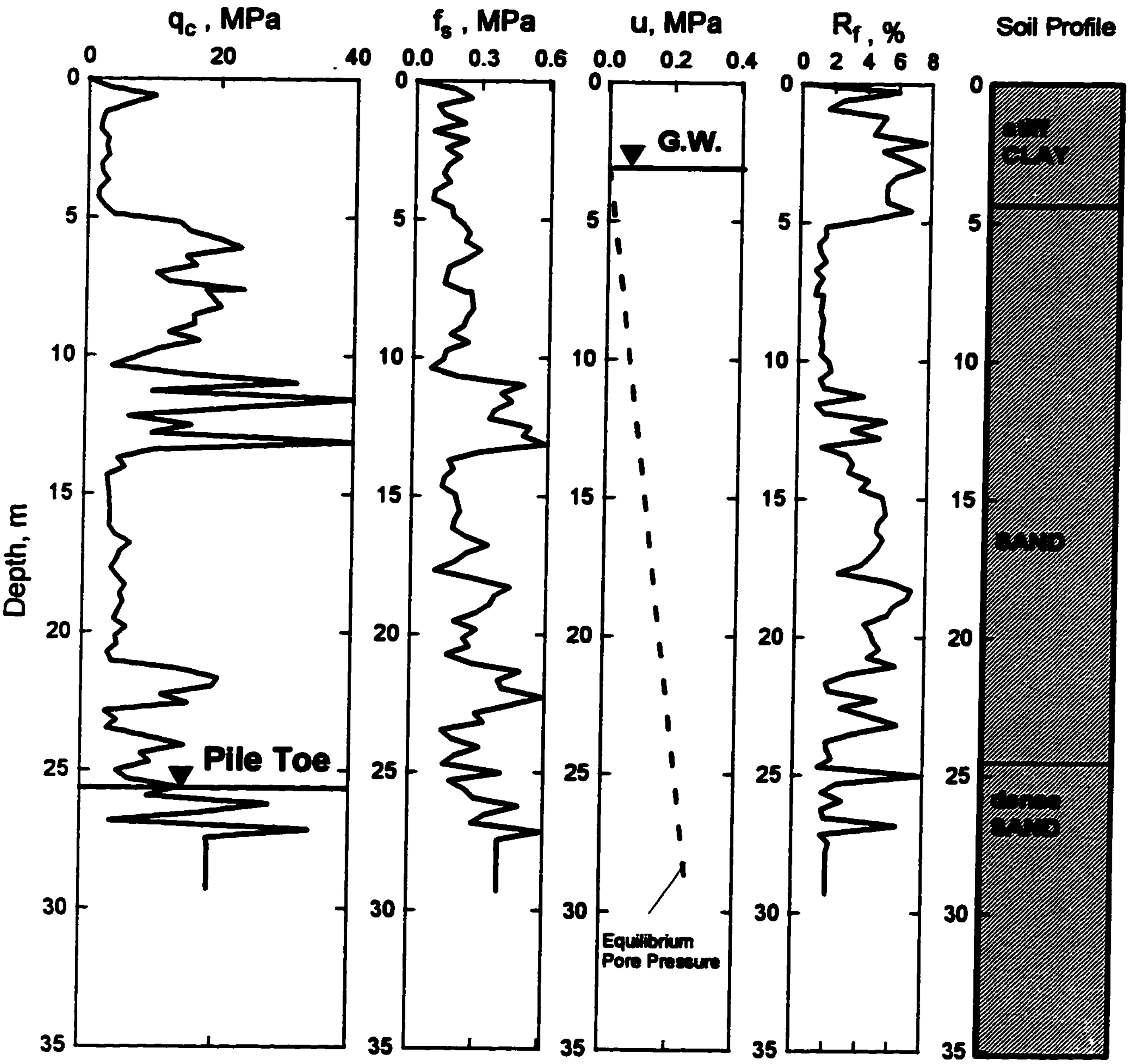

Case 31 LTN 741
Sheet b Pile data

	DETAIL	DESCRIPTION
1	Site	Texas, USA
2	Reference	Reese et al., 1988
3	Shape, Material, and Installation	Round, Concrete, Bored
4	Diameter, b, and Wall Thickness, t, mm	810
5	Embedment Length D, m	24.1
6	Cross Sectional Area A_t, m^2	0.503
7	Unit Circumferential Area, A_s, m^2/m	2.51
8	Toe, Closed or Open	Closed
9	Type of Test and Loading	Static Compression,SML
10	Toe Capacity, R_t, KN	
11	Shaft Capacity, R_s, KN	
12	*Capacity, R_u, KN	7,830

SCHEMATIC PROFILE

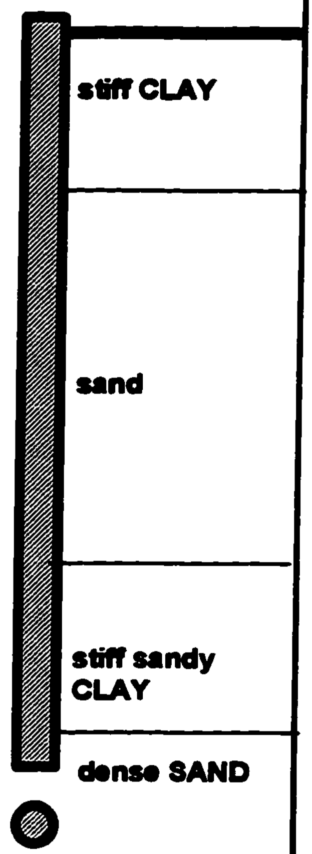

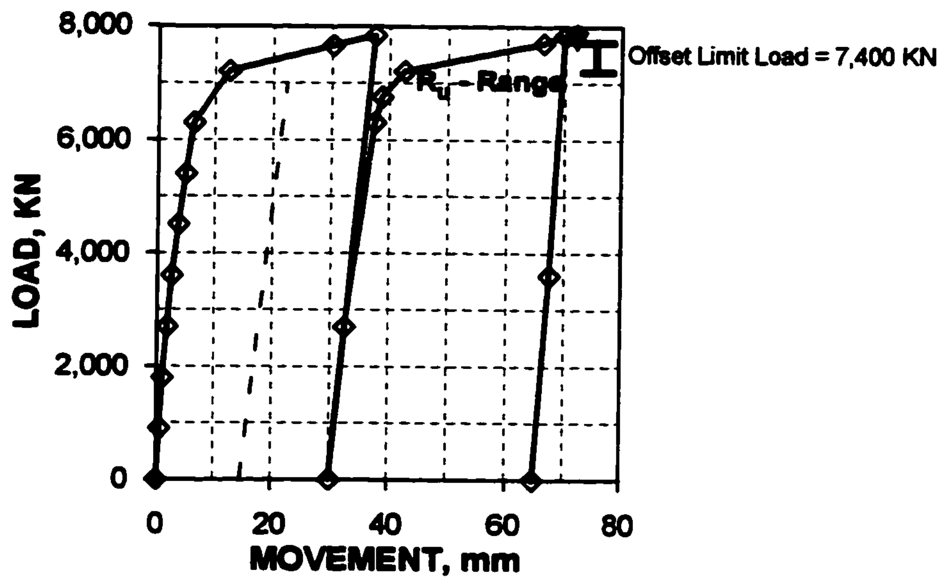

Case 32 LTN484
Sheet a CPT data

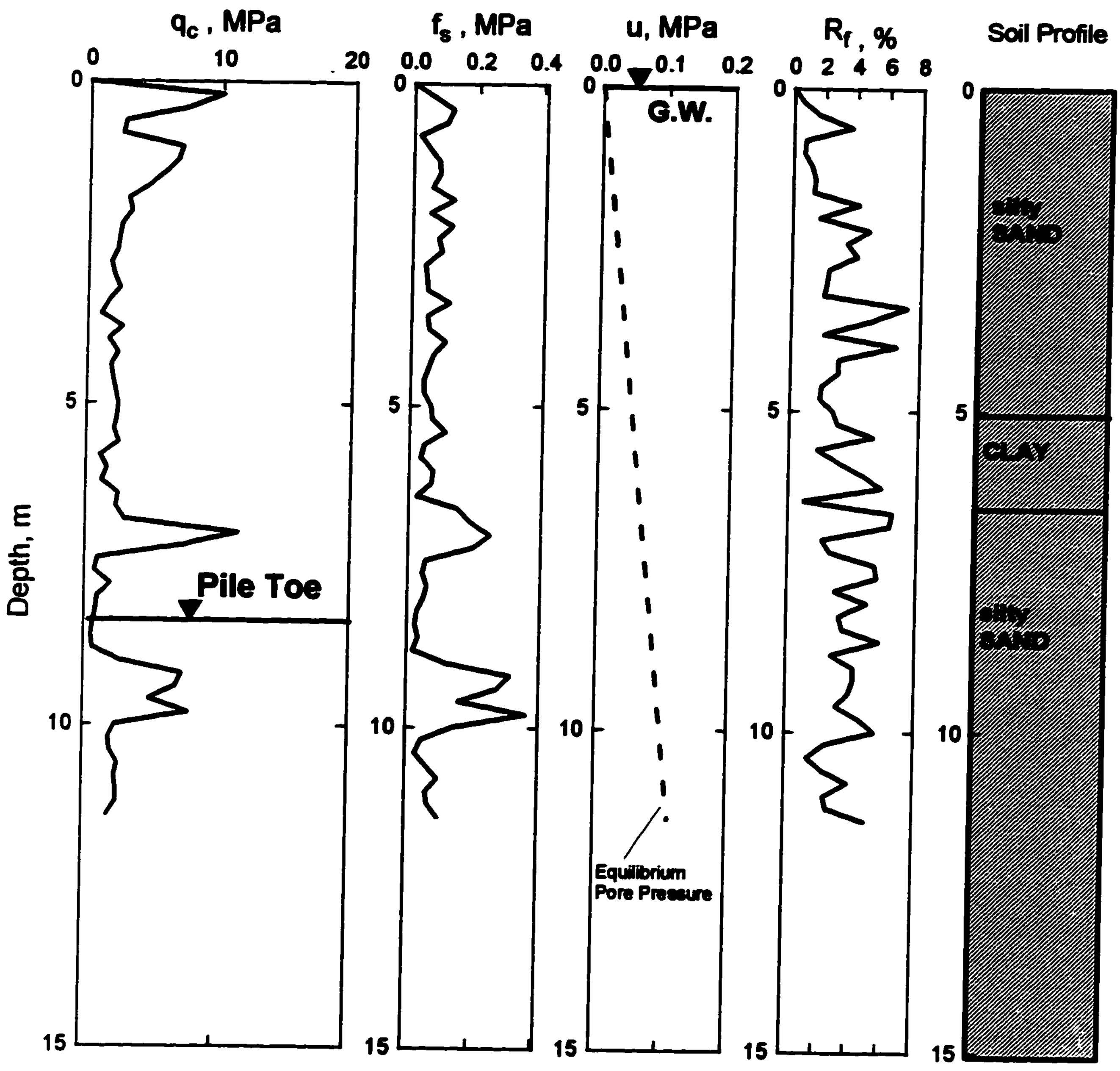

Case 32 LTN 484
Sheet b Pile data

	DETAIL	DESCRIPTION	SCHEMATIC PROFILE
1	Site	Holland, Netherlands	
2	Reference	Kruizinga, 1985	
3	Shape, Material, and Installation	Round, Concrete, Bored	
4	Diameter, b, and Wall Thickness, t, mm	450	
5	Embedment Length D, m	7.6	
6	Cross Sectional Area A_t, m²	0.159	
7	Unit Circumferential Area, A_s, m² /m	1.41	
8	Toe, Closed or Open	Closed	
9	Type of Test and Loading	Static Tension, SML	
10	Toe Capacity, R_t, KN		
11	Shaft Capacity, R_s, KN		
12	*Capacity, R_u, KN	750	

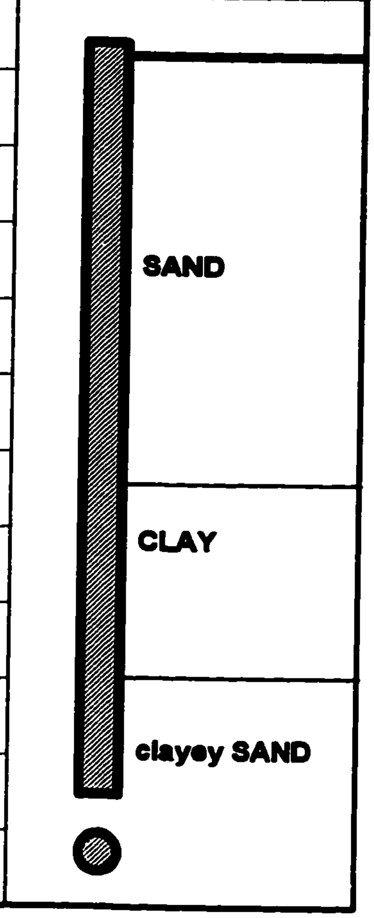

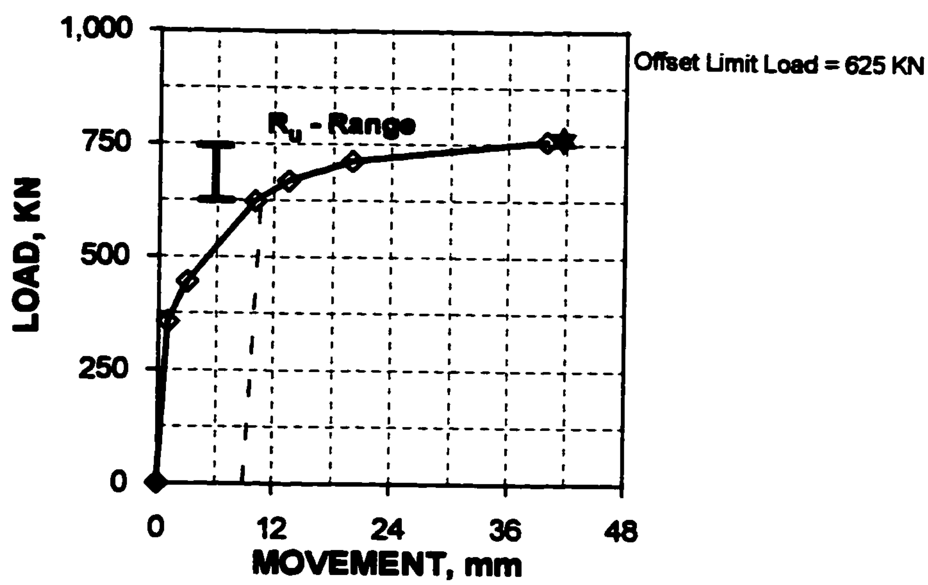

Case 33 LTN742
Sheet a CPT data

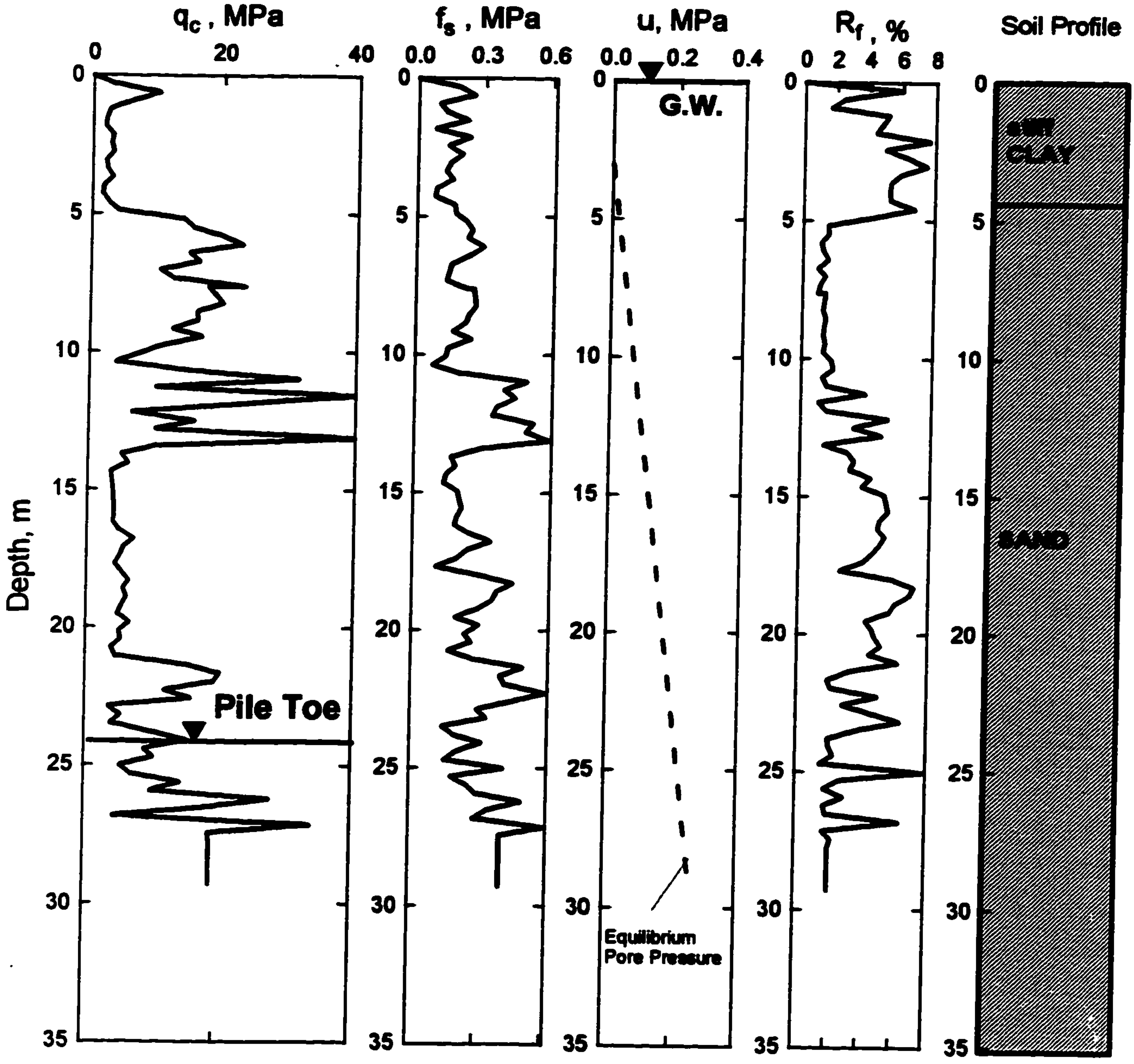

Case 33 LTN 742
Sheet b Pile data

	DETAIL	DESCRIPTION	SCHEMATIC PROFILE
1	Site	Texas, USA	
2	Reference	Reese et al., 1988	
3	Shape, Material, and Installation	Round, Concrete, Bored	
4	Diameter, b, and Wall Thickness, t, mm	810	
5	Embedment Length D, m	24.1	
6	Cross Sectional Area A_t , m^2	0.503	
7	Unit Circumferential Area, A_s , m^2 /m	2.51	
8	Toe, Closed or Open	Closed	
9	Type of Test and Loading	Static Compression,SML	
10	Toe Capacity, R_t , KN		
11	Shaft Capacity, R_s , KN		
12	*Capacity, R_u , KN	5,850	

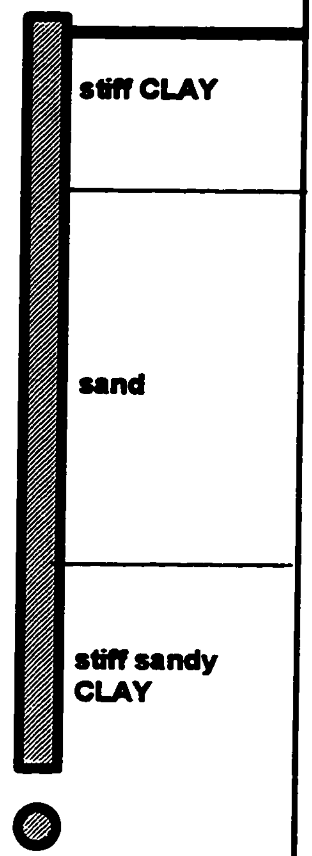

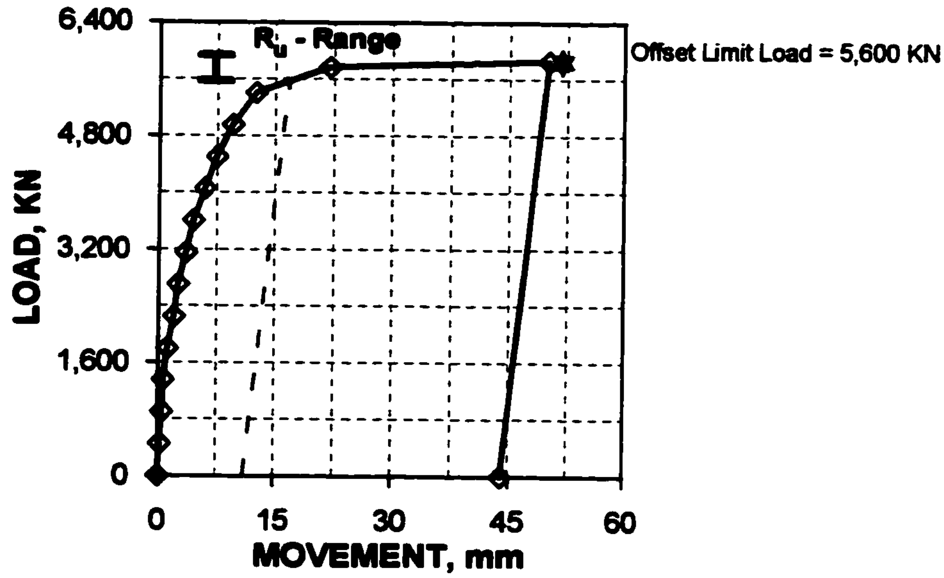

Case 34 MUMB
Sheet a CPT data

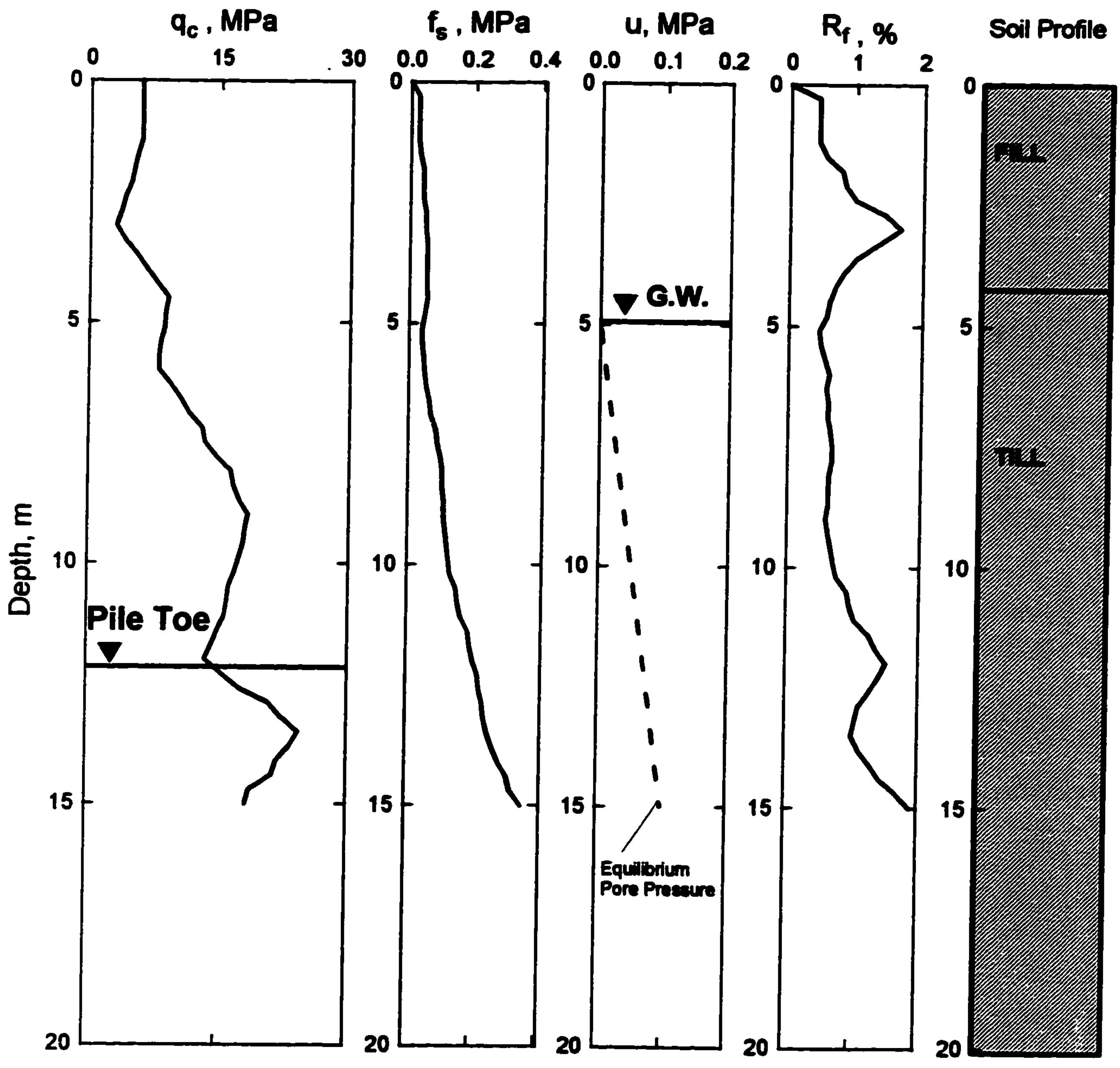

Case 34 MUMB
Sheet b Pile data

	DETAIL	DESCRIPTION
1	Site	Milwaukee, USA
2	Reference	Hunt, 1993
3	Shape, Material, and Installation	Pipe, Steel, Driven
4	Diameter, b, and Wall Thickness, t, mm	273 5.6
5	Embedment Length D, m	12.2
6	Cross Sectional Area A_t, m^2	0.059
7	Unit Circumferential Area, A_s, m^2/m	0.858
8	Toe, Closed or Open	Closed
9	Type of Test and Loading	Static Compression, SML
10	Toe Capacity, R_t, KN	534
11	Shaft Capacity, R_s, KN	1152
12	*Capacity, R_u, KN	1686 (from CAPWAP analysis)

SCHEMATIC PROFILE

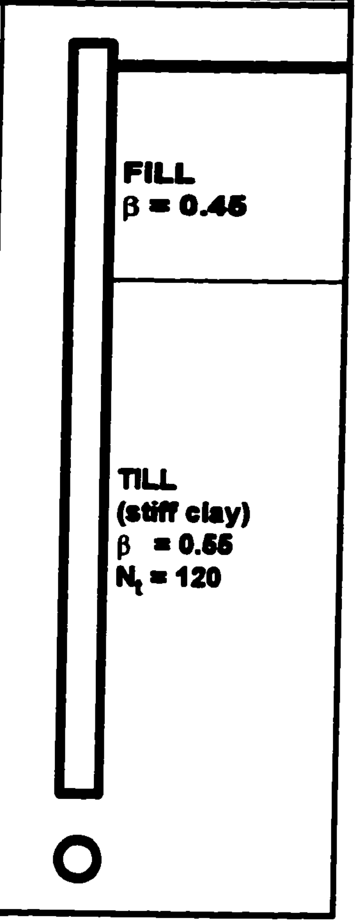

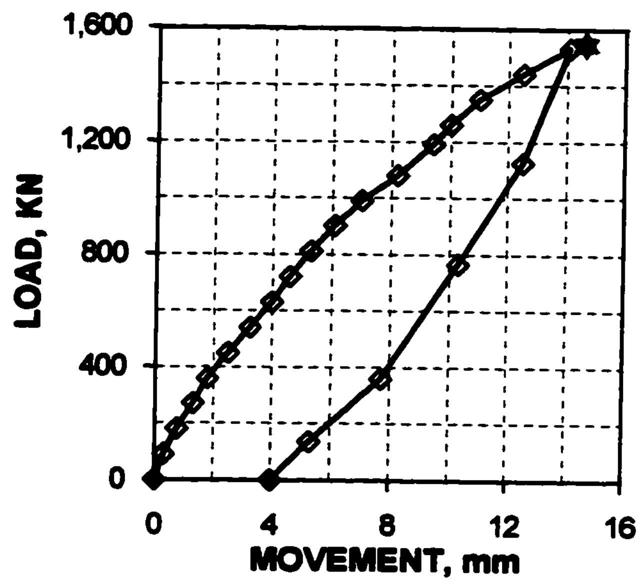

Case 35 NETH2
Sheet a CPT data

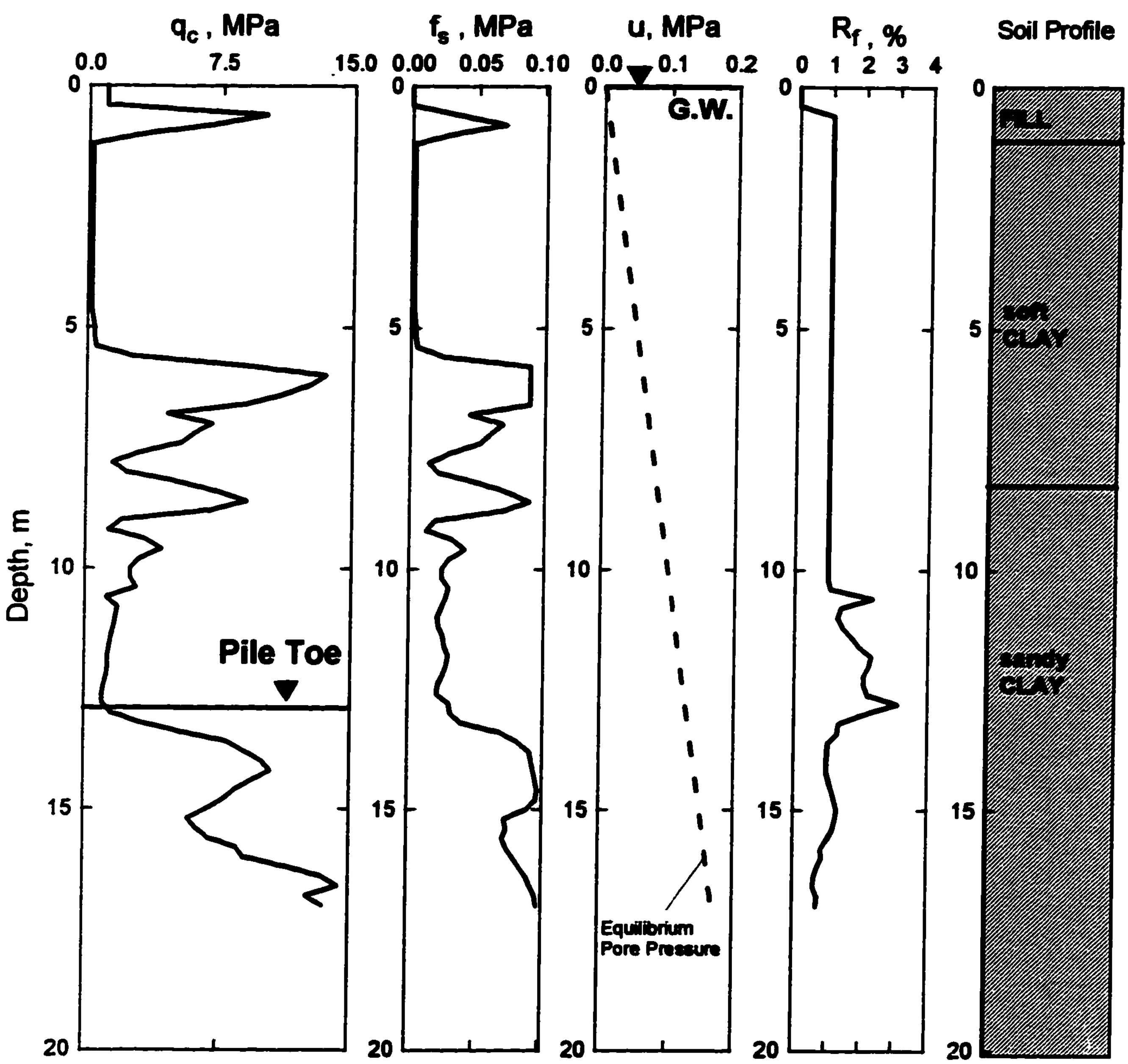

Case 35 NETH2
Sheet b Pile data

	DETAIL	DESCRIPTION
1	Site	Almere, Netherlands
2	Reference	Viergever, 1982
3	Shape, Material, and Installation	Square, Concrete, Driven
4	Diameter, b, and Wall Thickness, t, mm	250
5	Embedment Length D, m	9.25
6	Cross Sectional Area A_t, m^2	0.063
7	Unit Circumferential Area, A_s, m^2 /m	1.0
8	Toe, Closed or Open	Closed
9	Type of Test and Loading	Static Compression, SML
10	Toe Capacity, R_t, KN	
11	Shaft Capacity, R_s, KN	
12	*Capacity, R_u, KN	700

SCHEMATIC PROFILE

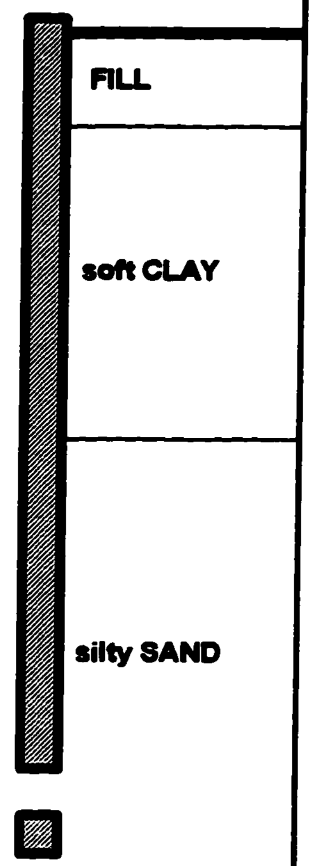

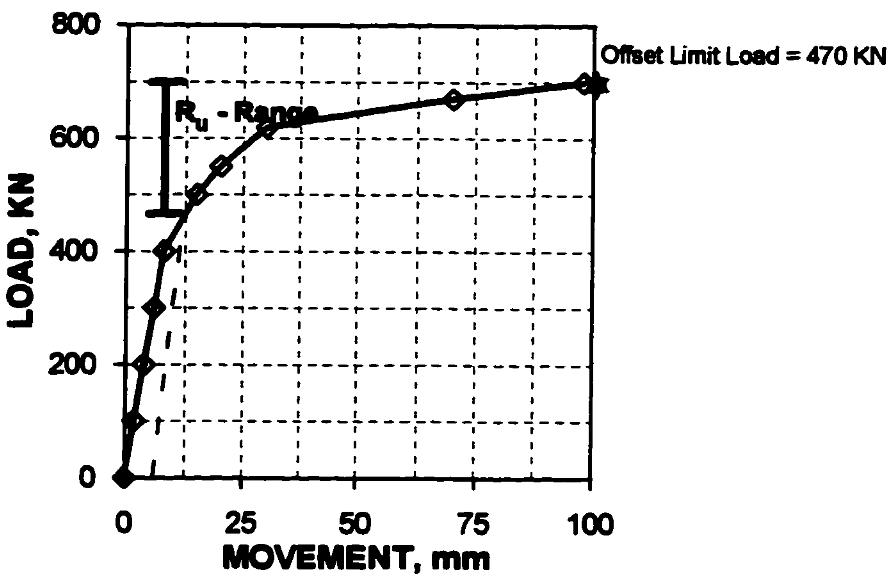

Case 36 MILANO
Sheet a CPT data

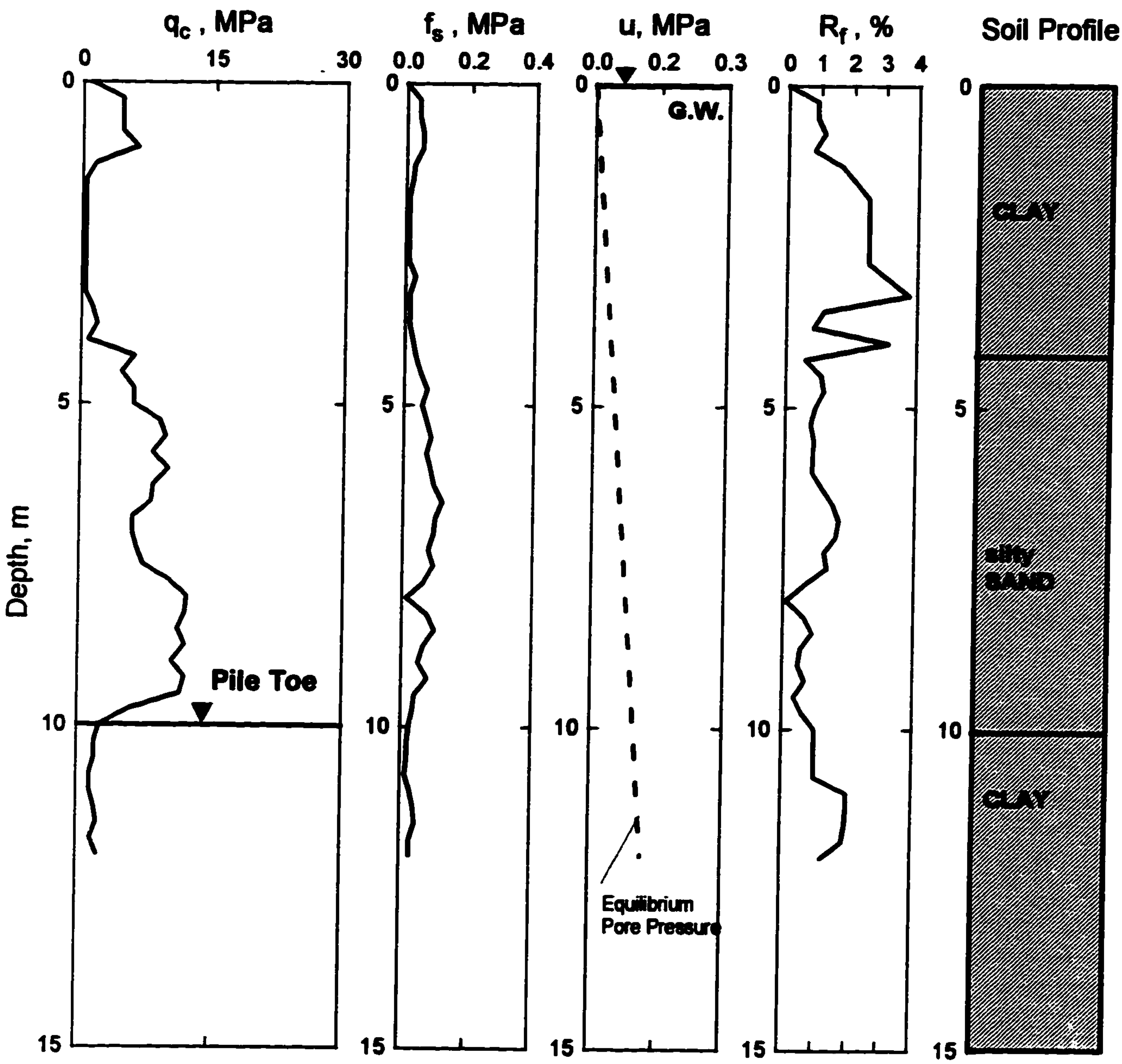

Case 36 MILANO
Sheet b Pile data

	DETAIL	DESCRIPTION
1	Site	Milan, Italy
2	Reference	Gambini, 1985
3	Shape, Material, and Installation	Pipe, Steel, Driven
4	Diameter, b, and Wall Thickness, t, mm	330 10
5	Embedment Length D, m	10
6	Cross Sectional Area A_t, m^2	0.086
7	Unit Circumferential Area, A_s, m^2/m	1.037
8	Toe, Closed or Open	Closed
9	Type of Test and Loading	Static Compression, SML
10	Toe Capacity, R_t, KN	
11	Shaft Capacity, R_s, KN	
12	*Capacity, R_u, KN	625

SCHEMATIC PROFILE

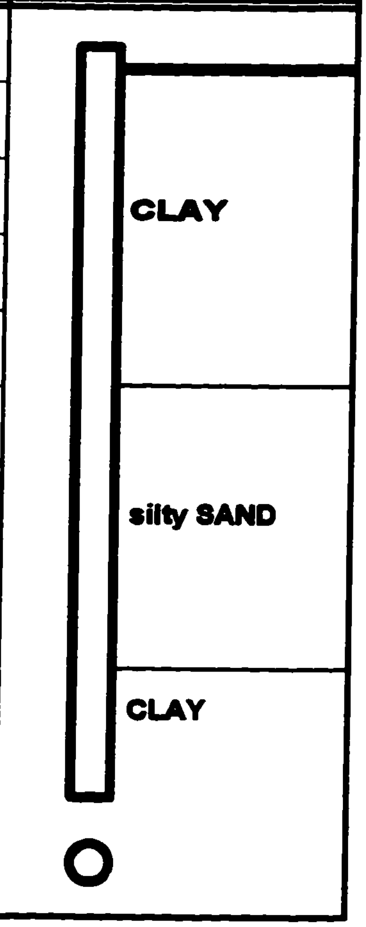

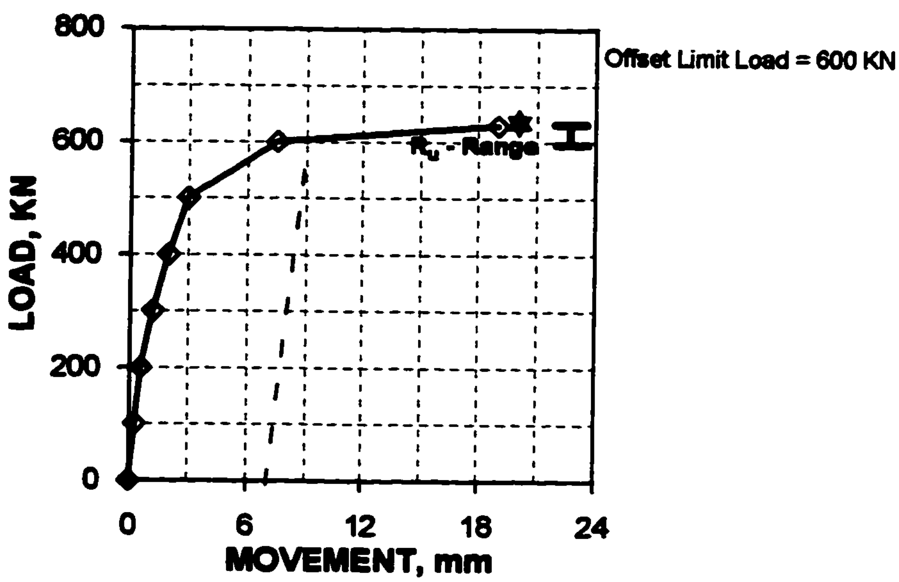

Case 37 OKLACO
Sheet a CPT data

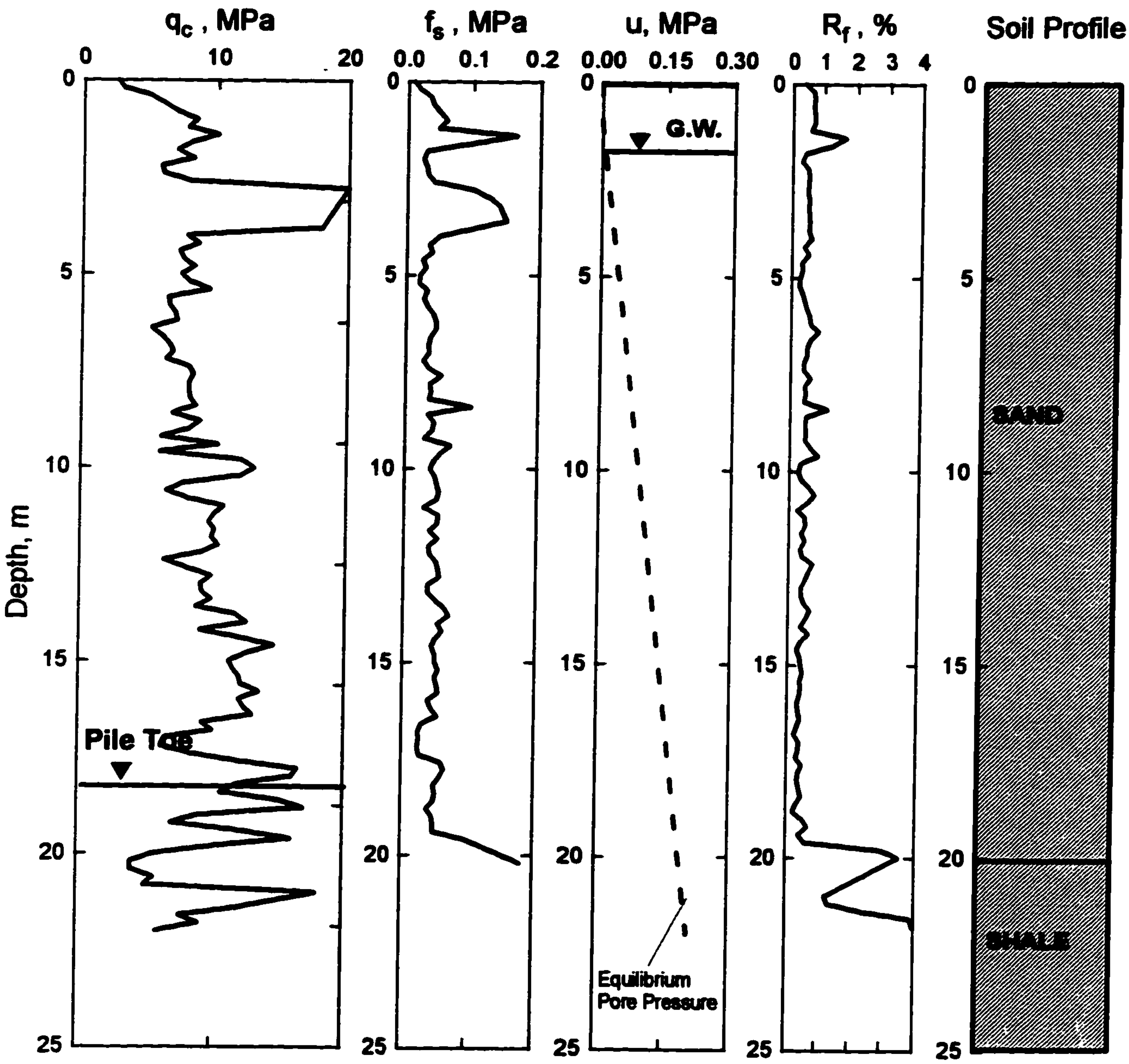

Case 37 OKLACO
Sheet b Pile data

	DETAIL	DESCRIPTION
1	Site	Oklahama, USA
2	Reference	Neveles, 1994
3	Shape, Material, and Installation	Round, Concrete, Driven
4	Diameter, b, and Wall Thickness, t, mm	610
5	Embedment Length D, m	18.2
6	Cross Sectional Area A_t, m^2	0.292
7	Unit Circumferential Area, A_s, m^2/m	1.92
8	Toe, Closed or Open	Closed
9	Type of Test and Loading	Static Compression, QML
10	Toe Capacity, R_t, KN	
11	Shaft Capacity, R_s, KN	
12	*Capacity, R_u, KN	3,600

SCHEMATIC PROFILE

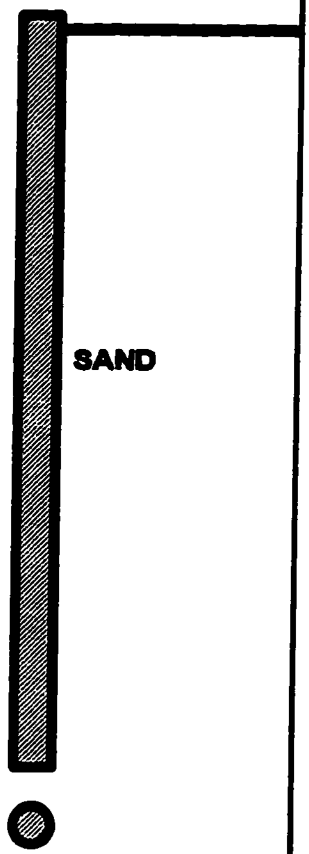

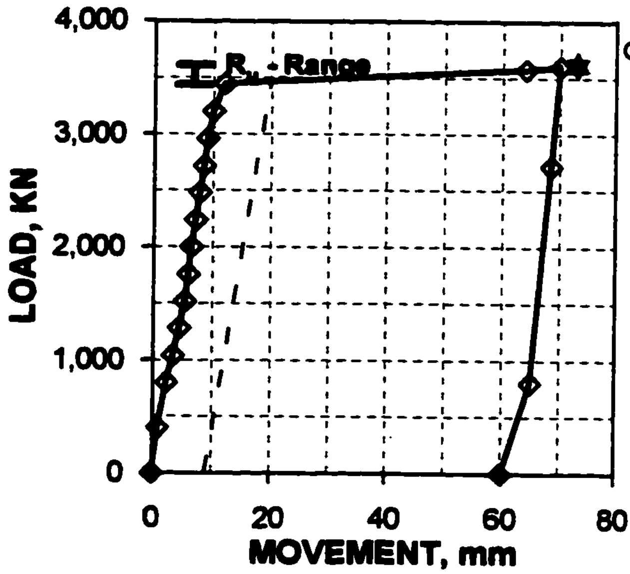

Offset Limit Load = 3,450 KN

Case 38 OKLAST
Sheet a CPT data

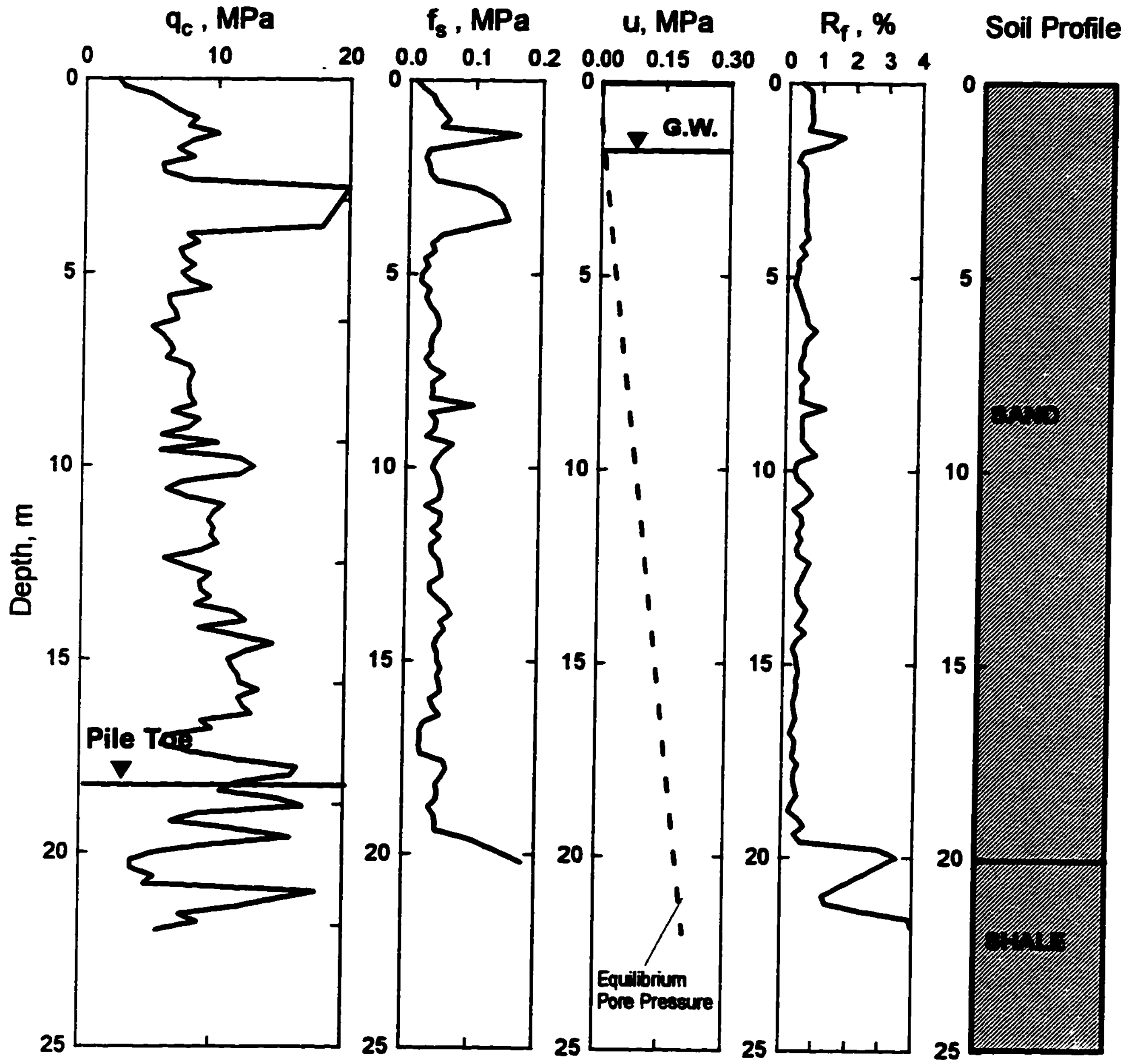

Case 38 OKLAST
Sheet b Pile data

	DETAIL	DESCRIPTION
1	Site	Oklahama, USA
2	Reference	Neveles, 1994
3	Shape, Material, and Installation	Pipe, Steel, Driven
4	Diameter, b, and Wall Thickness, t, mm	660 12
5	Embedment Length D, m	18.2
6	Cross Sectional Area A_t, m^2	0.342
7	Unit Circumferential Area, A_s, m^2/m	2.07
8	Toe, Closed or Open	Closed
9	Type of Test and Loading	Static Compression, SML
10	Toe Capacity, R_t, KN	
11	Shaft Capacity, R_s, KN	
12	*Capacity, R_u, KN	3,650

SCHEMATIC PROFILE

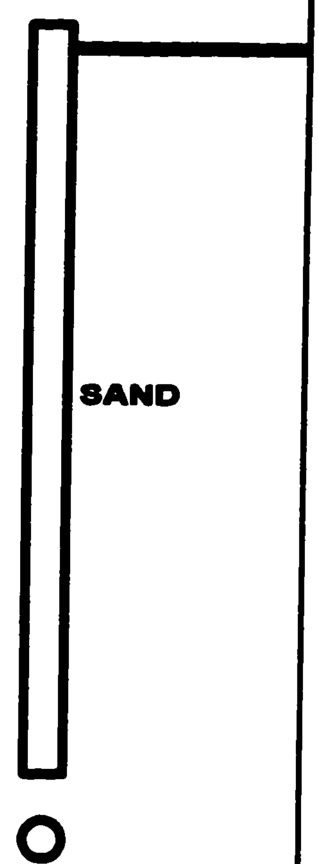

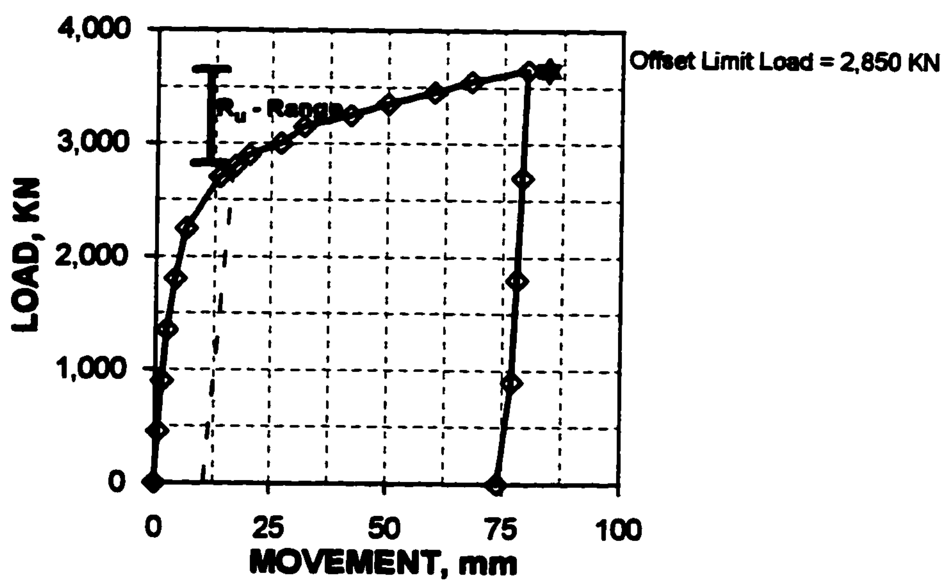

Case 39 ALABA
Sheet a CPT data

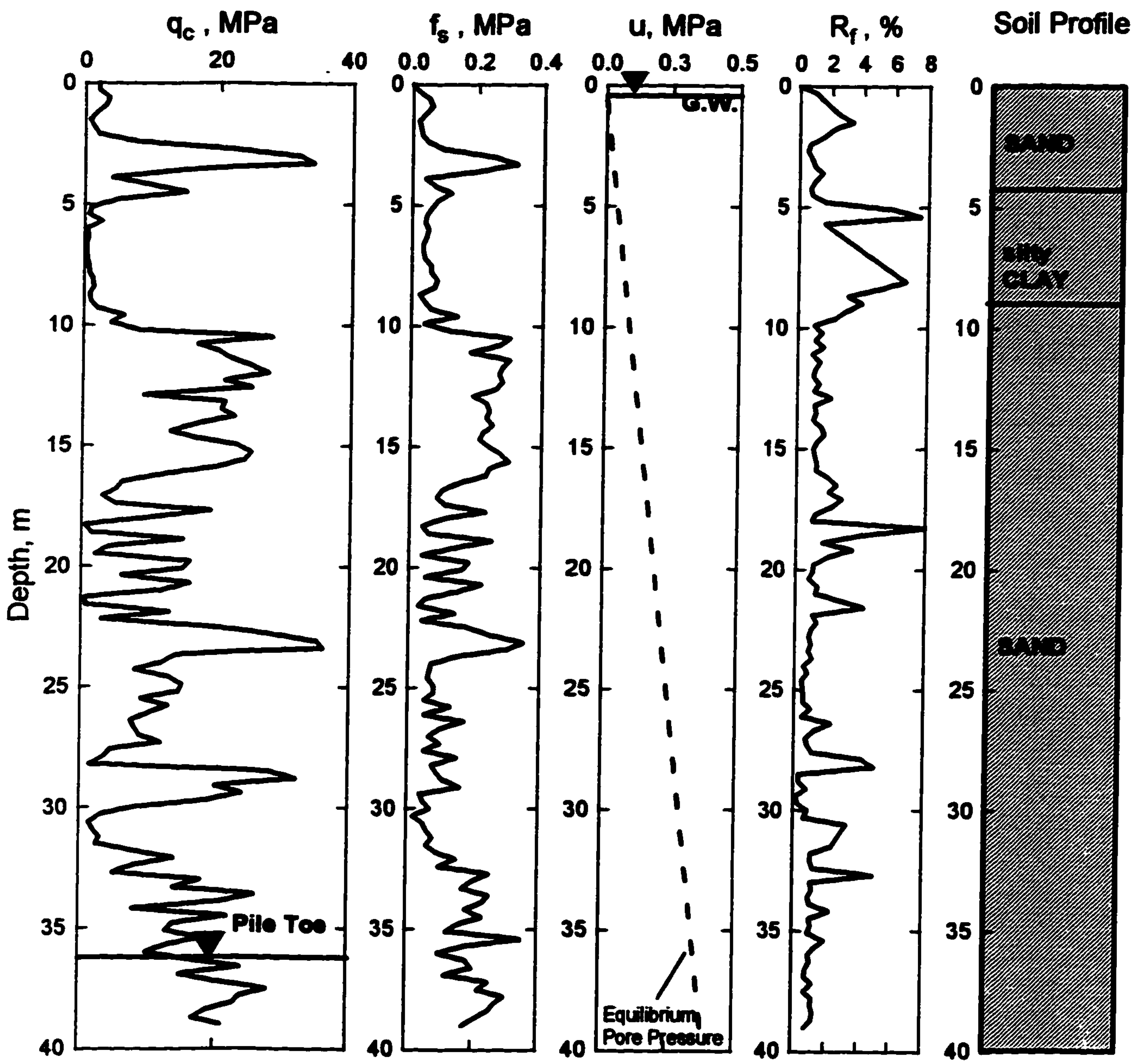

Case 39 ALABA
Sheet b Pile data

	DETAIL	DESCRIPTION
1	Site	Alabama, USA
2	Reference	Laier, 1994
3	Shape, Material, and Installation	H-Pile, Steel, Driven
4	Diameter, b, and Wall Thickness, t, mm	308*310
5	Embedment Length D, m	36.3
6	Cross Sectional Area A_t, m²	0.014
7	Unit Circumferential Area, A_s, m²/m	1.23
8	Toe, Closed or Open	
9	Type of Test and Loading	Static Compression, SML
10	Toe Capacity, R_t, KN	
11	Shaft Capacity, R_s, KN	
12	*Capacity, R_u, KN	2,130

SCHEMATIC PROFILE

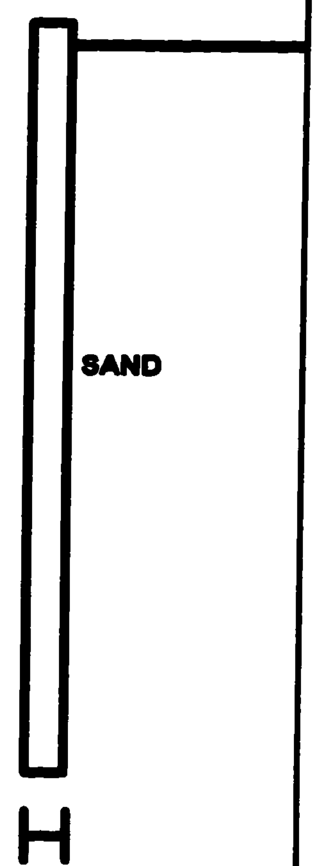

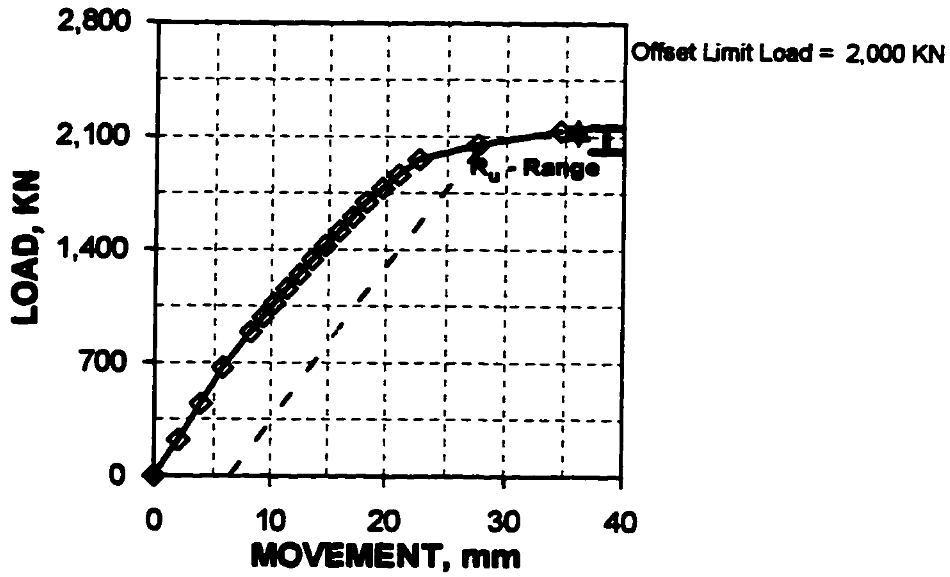

Case 40 SPB
Sheet a CPT data

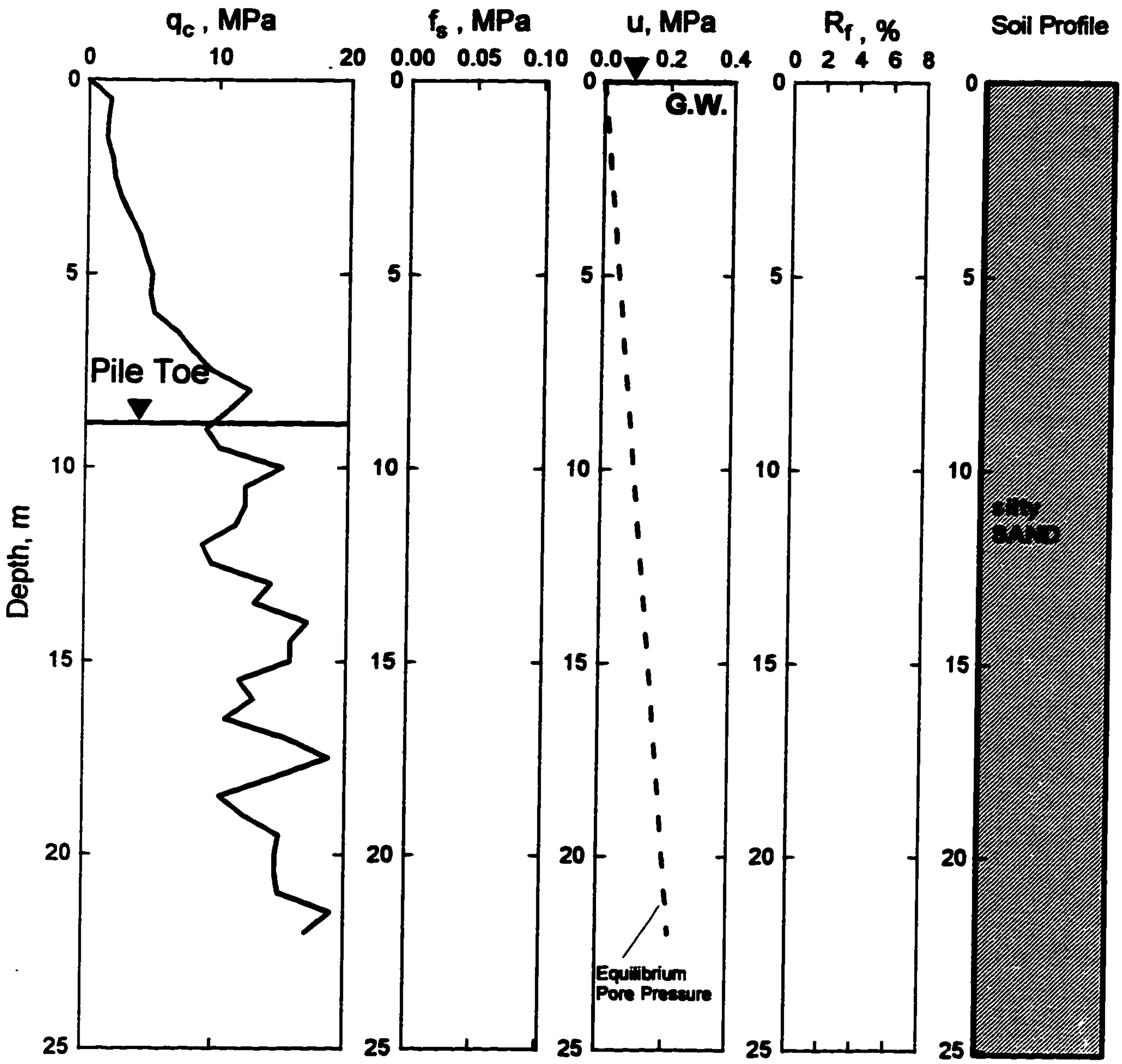

Case 40 SPB
Sheet b Pile data

	DETAIL	DESCRIPTION
1	Site	Sao Poulo, Brazil
2	Reference	Decourt et al., 1994
3	Shape, Material, and Installation	Round, Concrete, Bored
4	Diameter, b, and Wall Thickness, t, mm	500
5	Embedment Length D, m	8.7
6	Cross Sectional Area A_t, m^2	0.196
7	Unit Circumferential Area, A_s, m^2/m	1.57
8	Toe, Closed or Open	Closed
9	Type of Test and Loading	Static Compression,SML
10	Toe Capacity, R_t, KN	2,000
11	Shaft Capacity, R_s, KN	1,000
12	*Capacity, R_u, KN	3,000

SCHEMATIC PROFILE

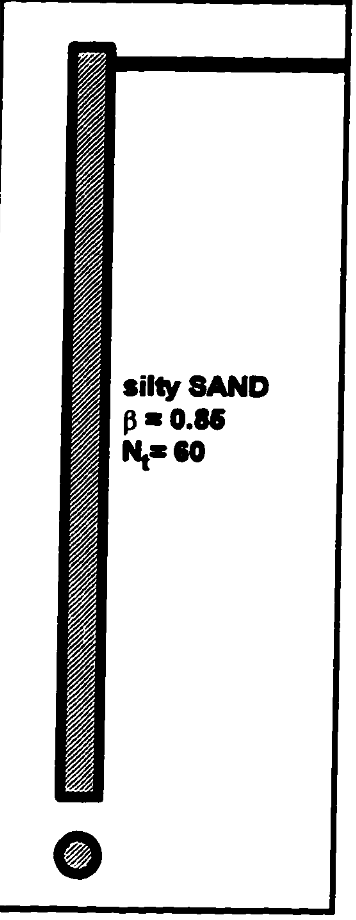

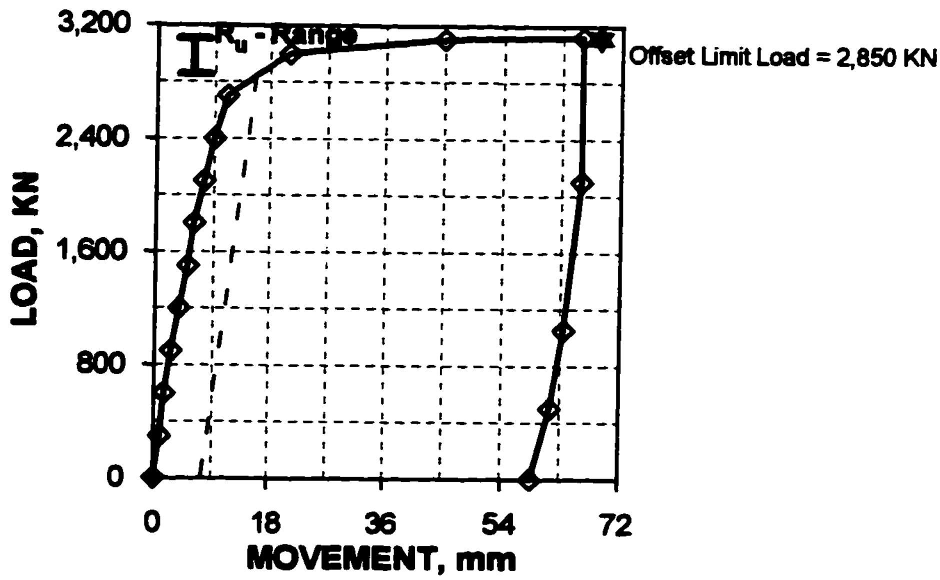

Case 41 L&D13A
Sheet a CPT data

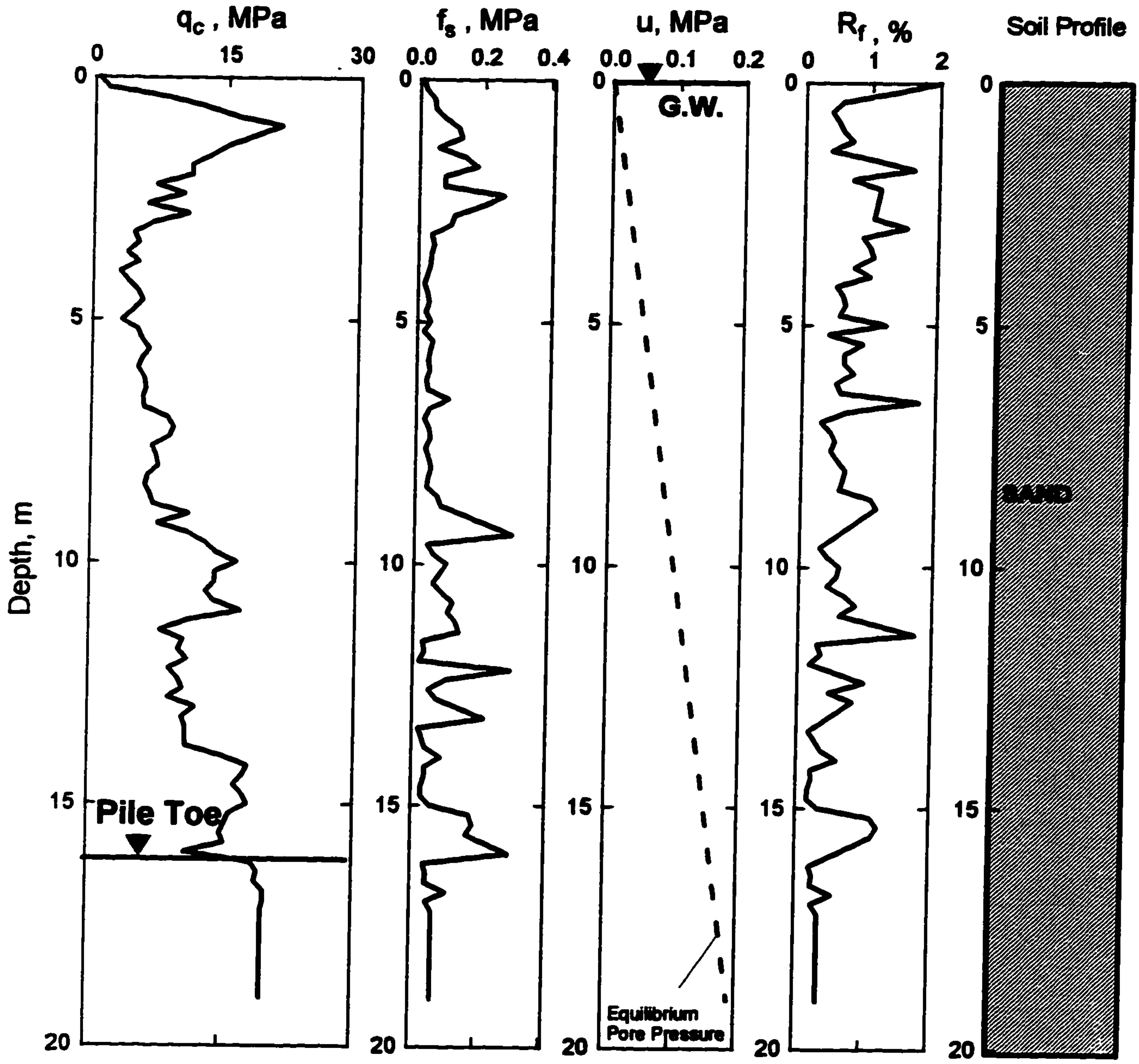

Case 41 L&D13A
Sheet b Pile data

	DETAIL	DESCRIPTION	SCHEMATIC PROFILE
1	Site	Lock and Dam 26, SL, USA	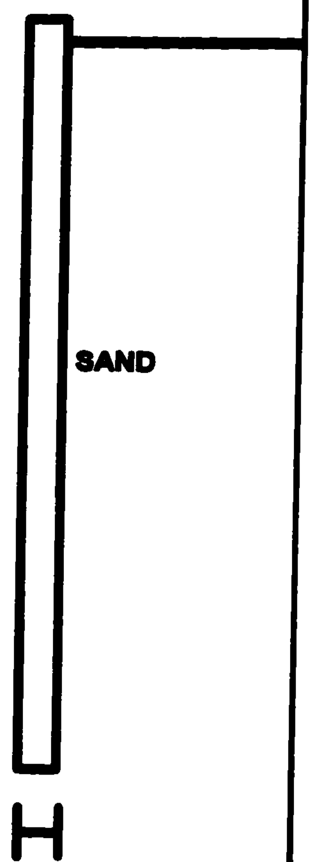
2	Reference	Tucker and Briaud, 1988	
3	Shape, Material, and Installation	H-Pile, Steel, Driven	
4	Diameter, b, and Wall Thickness, t, mm	346*371	
5	Embedment Length D, m	16.5	
6	Cross Sectional Area A_t, m^2	0.014	
7	Unit Circumferential Area, A_s, m^2/m	1.43	
8	Toe, Closed or Open		
9	Type of Test and Loading	Static Compression, SML	
10	Toe Capacity, R_t, KN		
11	Shaft Capacity, R_s, KN		
12	*Capacity, R_u, KN	2,900	

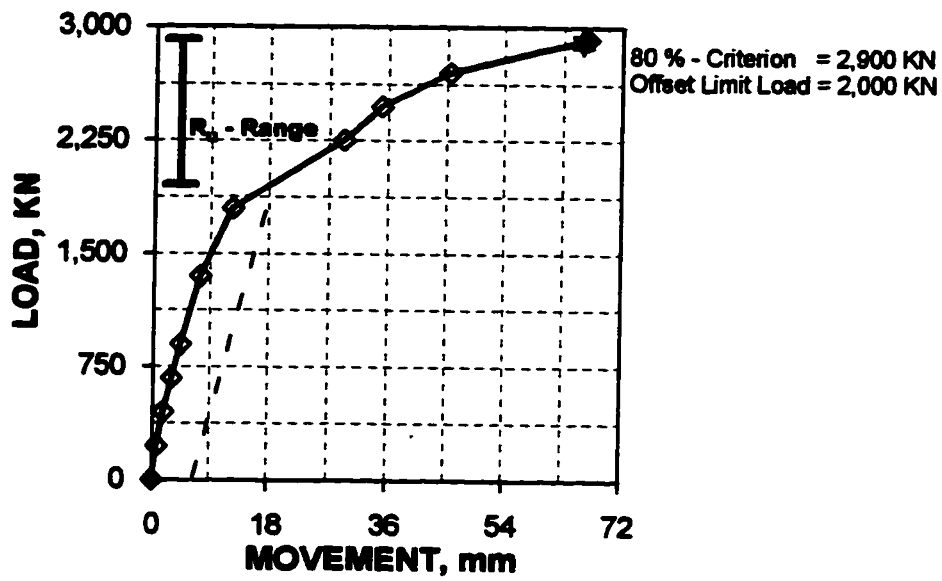

Case 42 L&D16
Sheet a CPT data

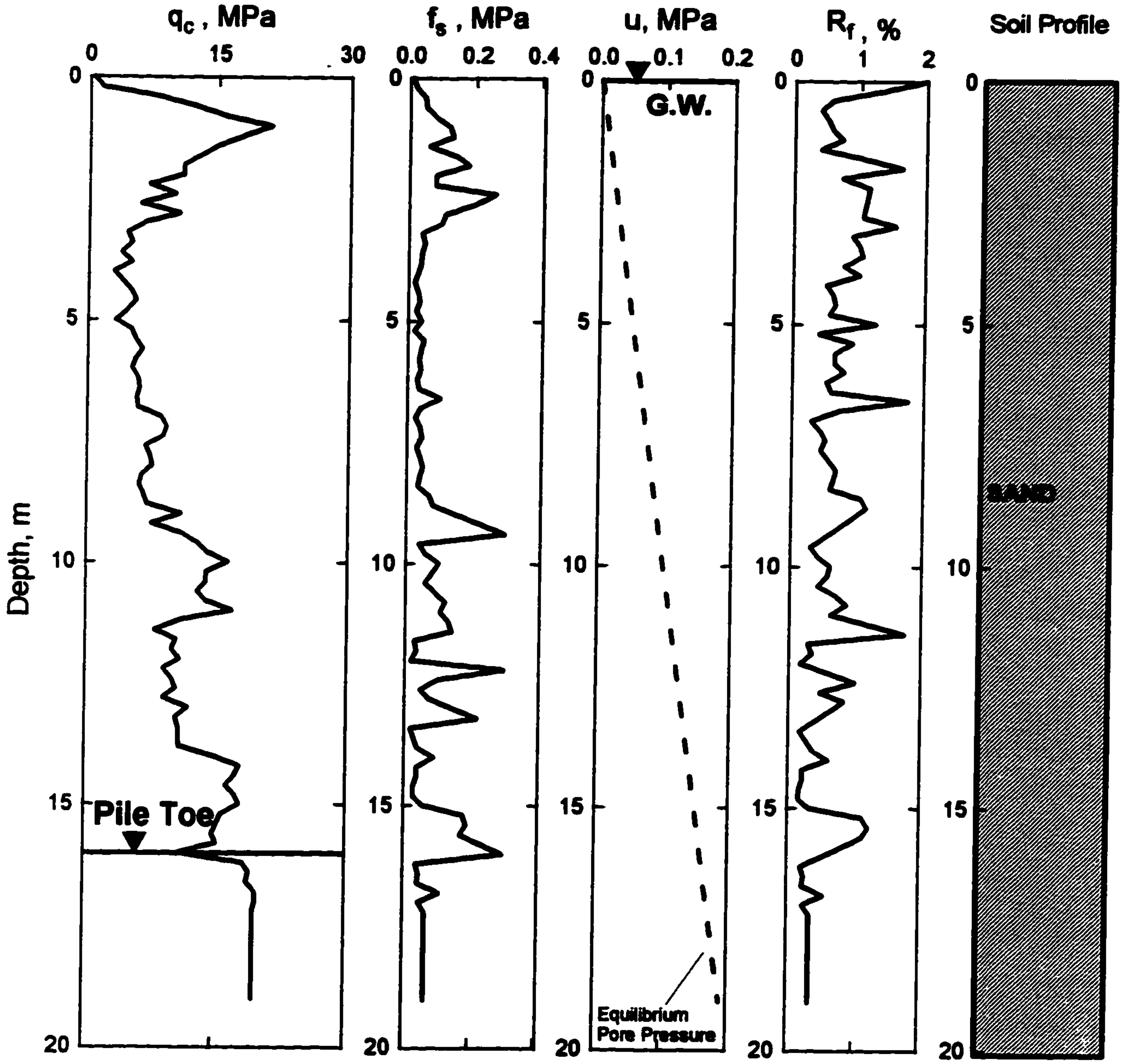

Case 42 L&D16
Sheet b Pile data

	DETAIL	DESCRIPTION	SCHEMATIC PROFILE
1	Site	Lock and Dam 26, SL, USA	
2	Reference	Tucker and Briaud, 1988	
3	Shape, Material, and Installation	H-Pile, Steel, Driven	
4	Diameter, b, and Wall Thickness, t, mm	346*371	
5	Embedment Length D, m	16.2	
6	Cross Sectional Area A_t, m^2	0.014	
7	Unit Circumferential Area, A_s, m^2/m	1.43	
8	Toe, Closed or Open		
9	Type of Test and Loading	Static Compression, QML	
10	Toe Capacity, R_t, KN		
11	Shaft Capacity, R_s, KN		
12	*Capacity, R_u, KN	3,600	

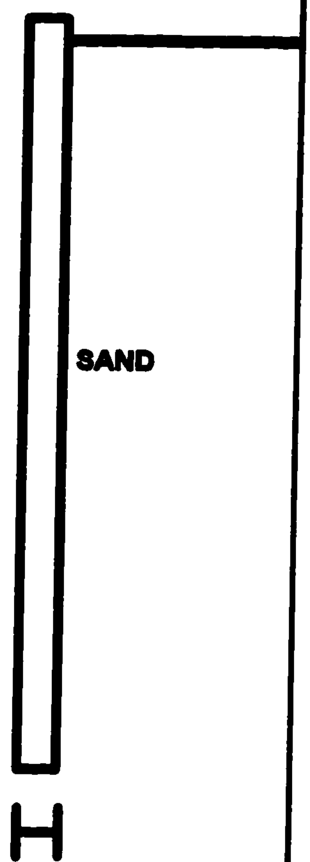

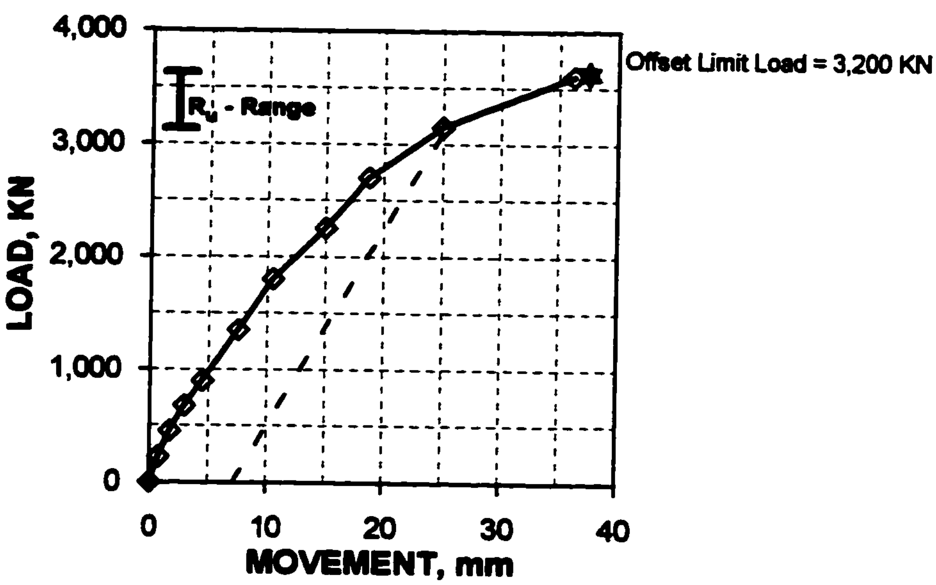

Case 43 L&D31
Sheet a CPT data

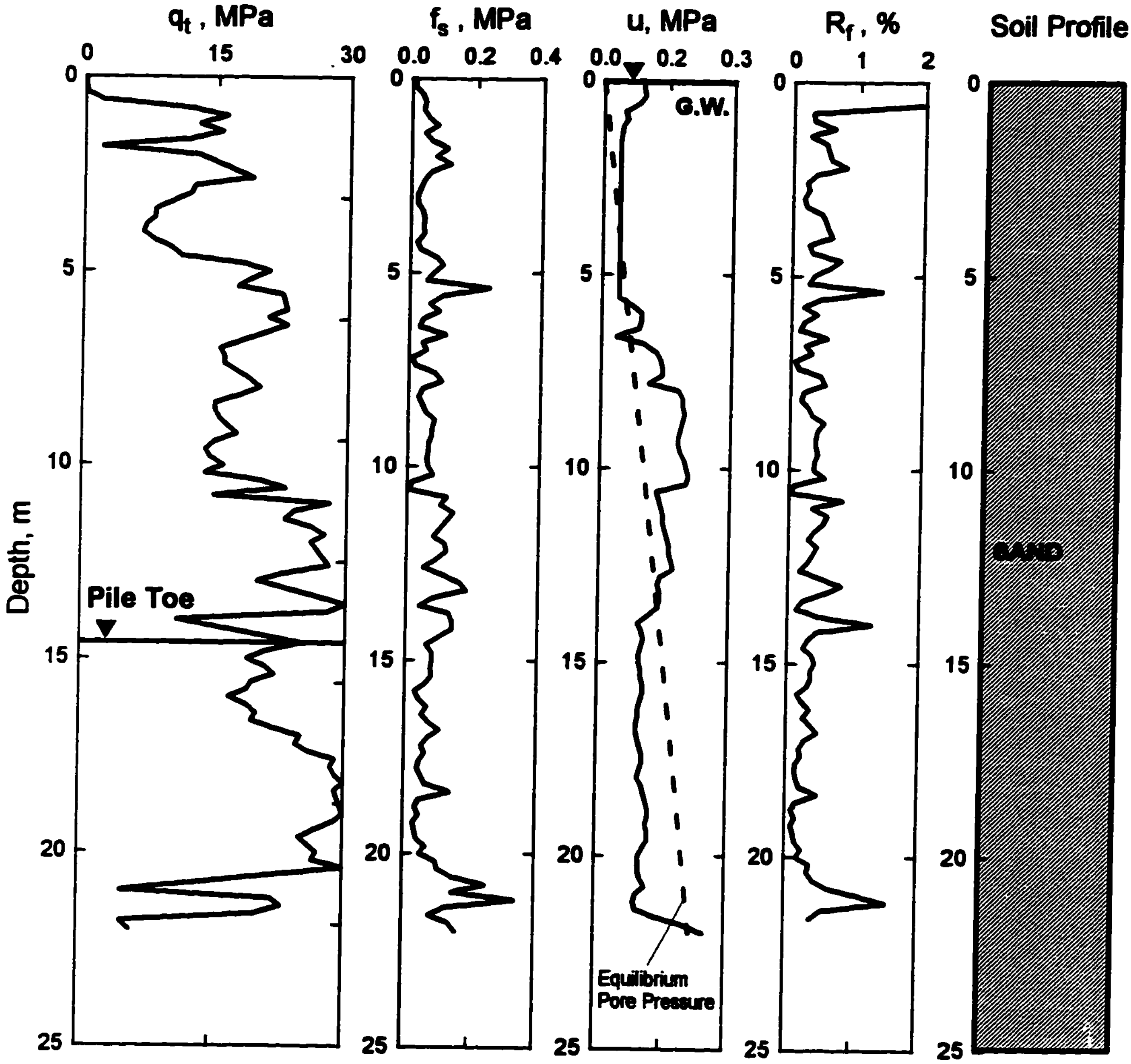

Case 43 L&D31
Sheet b   Pile data

	DETAIL	DESCRIPTION	SCHEMATIC PROFILE
1	Site	Lock and Dam 26, USA	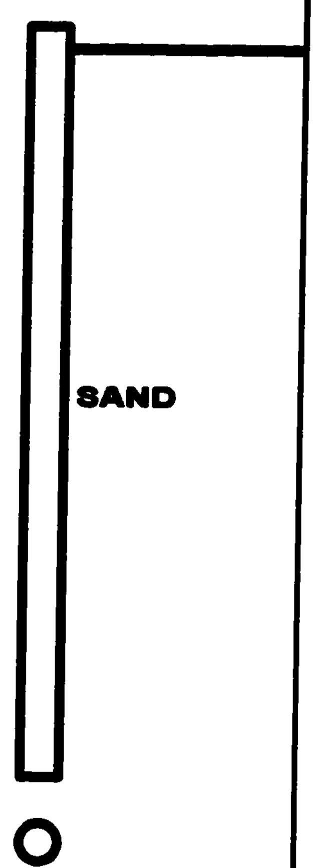
2	Reference	Tucker and Briaud, 1988	
3	Shape, Material, and Installation	Pipe, Steel, Driven	
4	Diameter, b, and Wall Thickness, t, mm	300 9.5	
5	Embedment Length D, m	16.2	
6	Cross Sectional Area A_t, m^2	0.071	SAND
7	Unit Circumferential Area, A_s, m^2/m	0.94	
8	Toe, Closed or Open	Closed	
9	Type of Test and Loading	Static Compression, SML	
10	Toe Capacity, R_t, KN		
11	Shaft Capacity, R_s, KN		
12	*Capacity, R_u, KN	1,310	

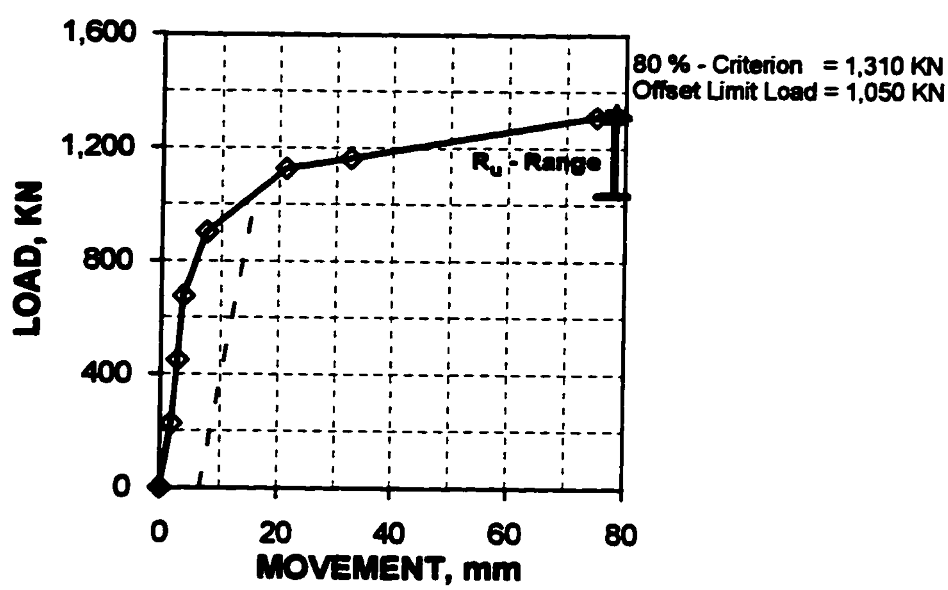

Case 44 L&D34
Sheet a CPT data

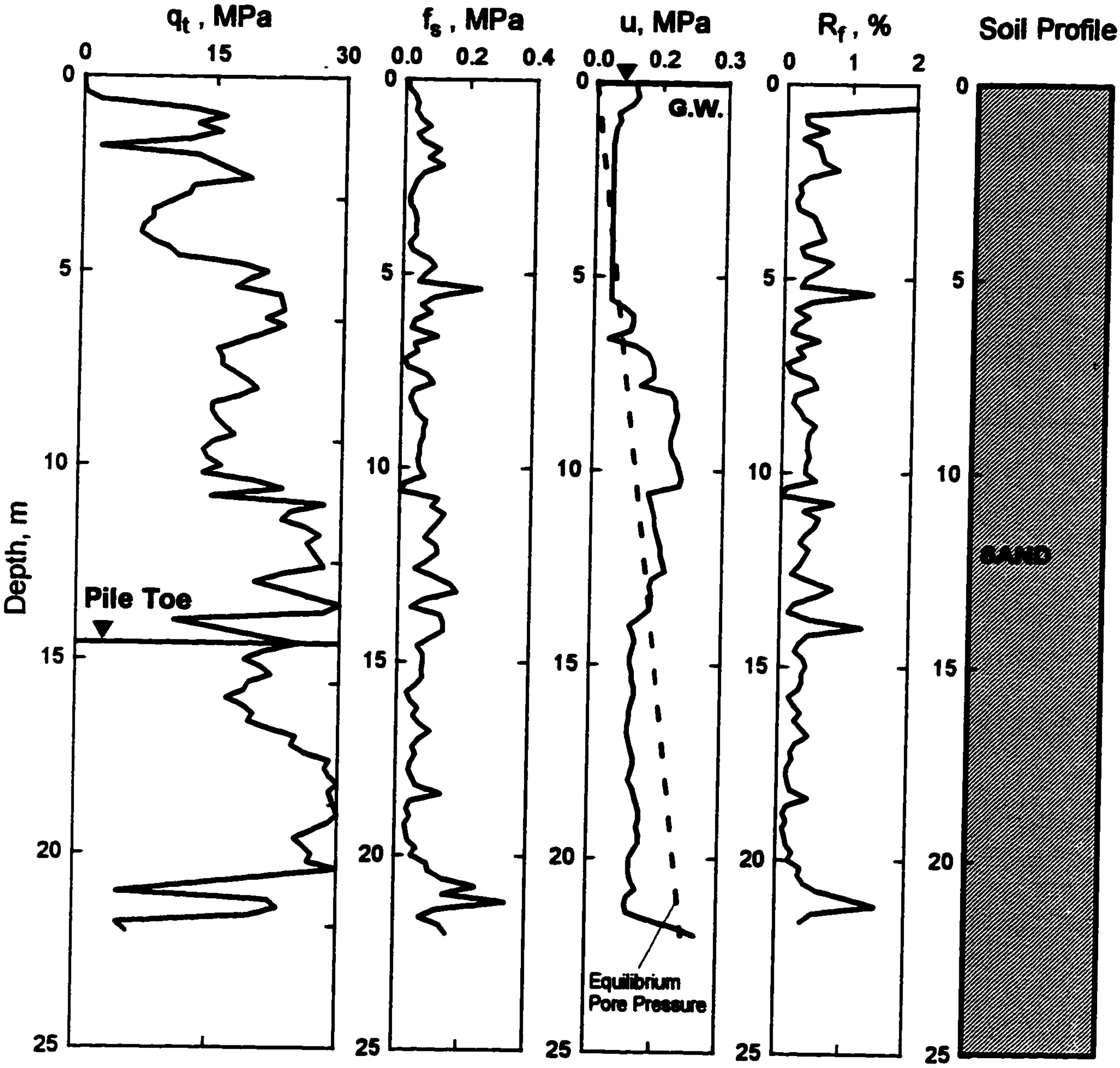

Case 44 L&D34
Sheet b Pile data

	DETAIL	DESCRIPTION
1	Site	Lock and Dam 26, USA
2	Reference	Tucker and Briaud, 1988
3	Shape, Material, and Installation	Pipe, Steel. Driven
4	Diameter, b, and Wall Thickness, t, mm	350 9.5
5	Embedment Length D, m	14.4
6	Cross Sectional Area A_t, m^2	0.096
7	Unit Circumferential Area, A_s, m^2/m	1.1
8	Toe, Closed or Open	Closed
9	Type of Test and Loading	Static Compression, SML
10	Toe Capacity, R_t, KN	
11	Shaft Capacity, R_s, KN	
12	*Capacity, R_u, KN	1,300

SCHEMATIC PROFILE

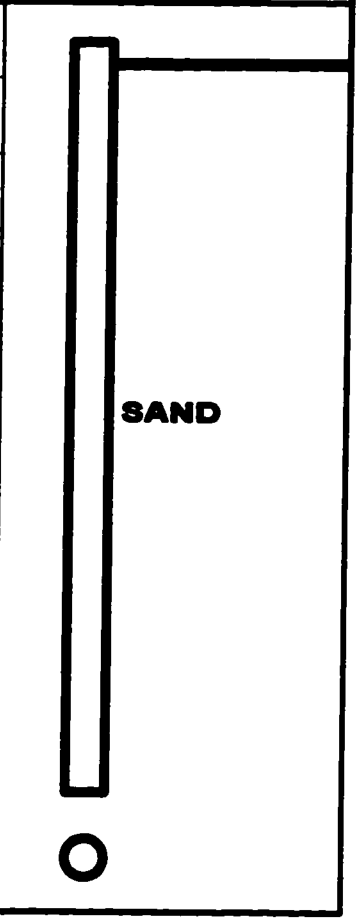

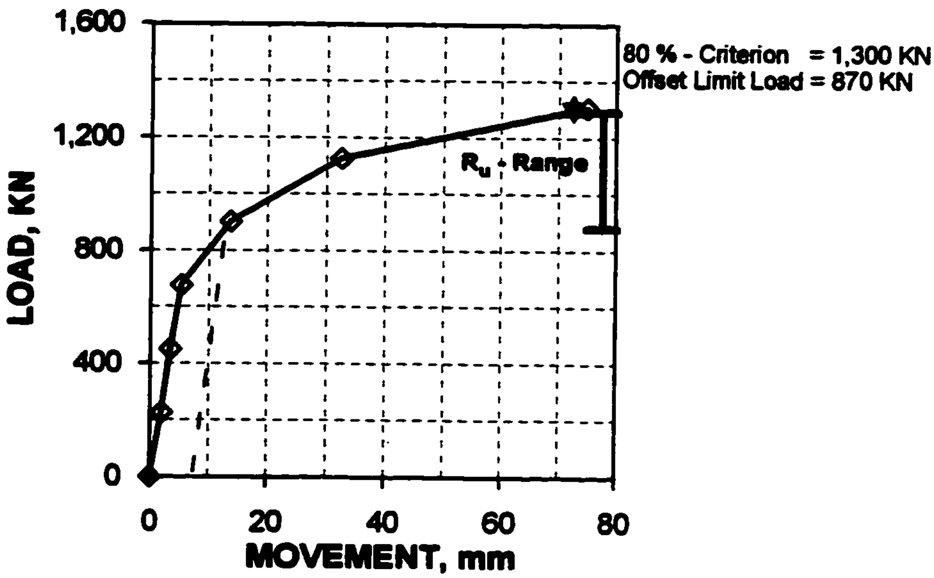

Case 45 L&D37
Sheet a CPT data

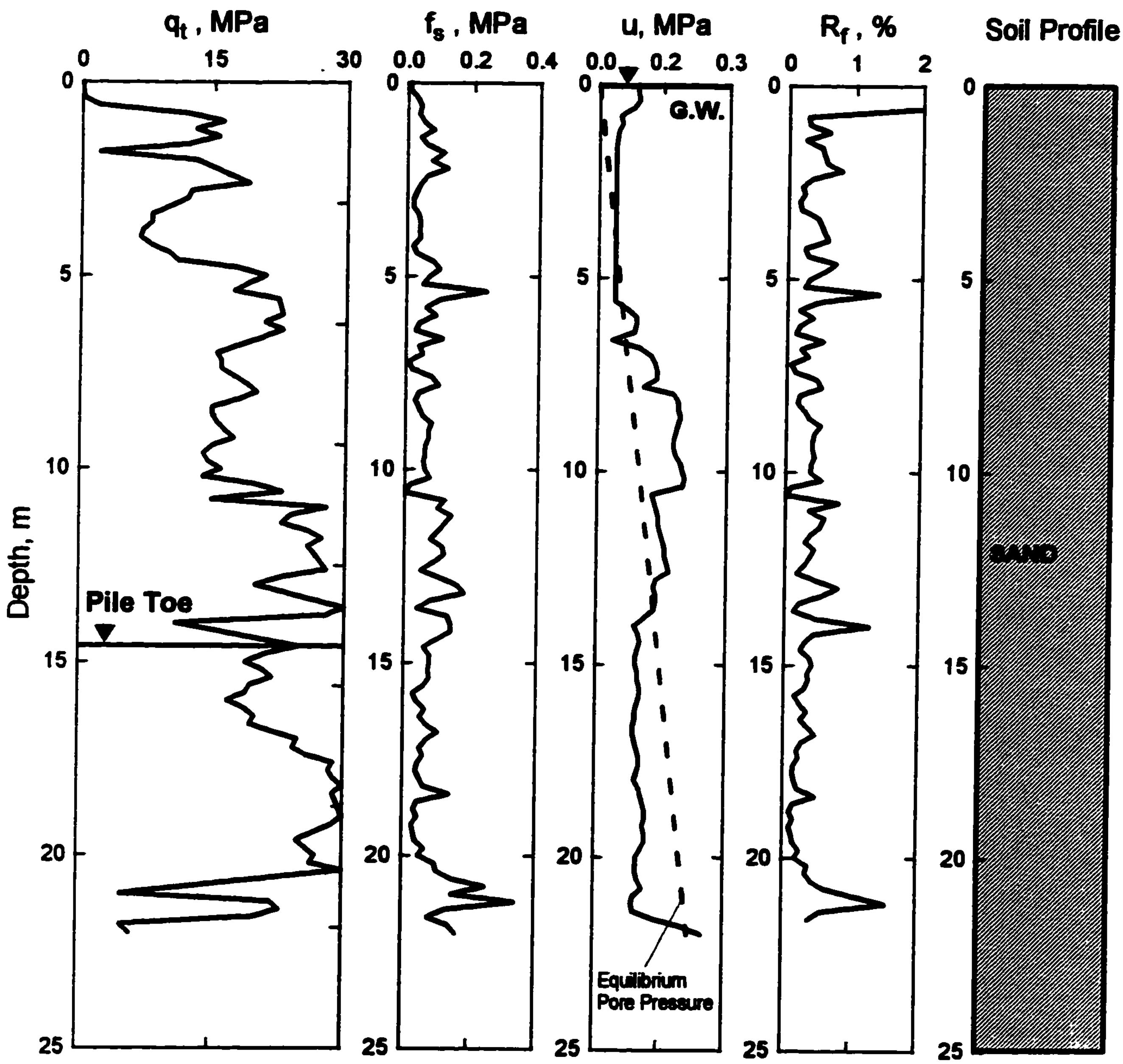

Case 45 L&D37
Sheet b Pile data

	DETAIL	DESCRIPTION
1	Site	Lock and Dam 26, USA
2	Reference	Tucker and Briaud, 1988
3	Shape, Material, and Installation	Pipe, Steel, Driven
4	Diameter, b, and Wall Thickness, t, mm	400 9.5
5	Embedment Length D, m	14.6
6	Cross Sectional Area A_t, m^2	0.126
7	Unit Circumferential Area, A_s, m^2/m	1.26
8	Toe, Closed or Open	Closed
9	Type of Test and Loading	Static Compression, SML
10	Toe Capacity, R_t, KN	
11	Shaft Capacity, R_s, KN	
12	*Capacity, R_u, KN	1,800

SCHEMATIC PROFILE

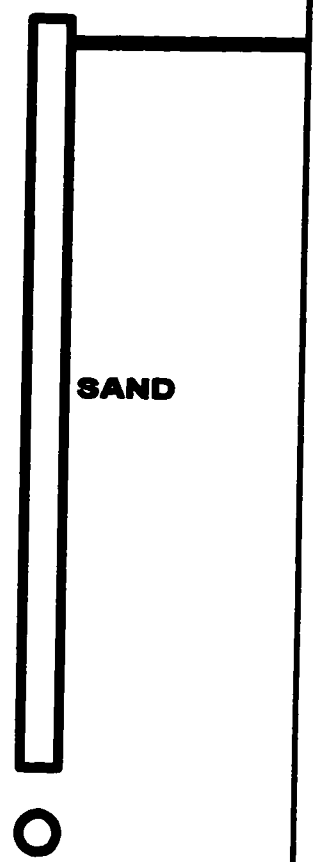

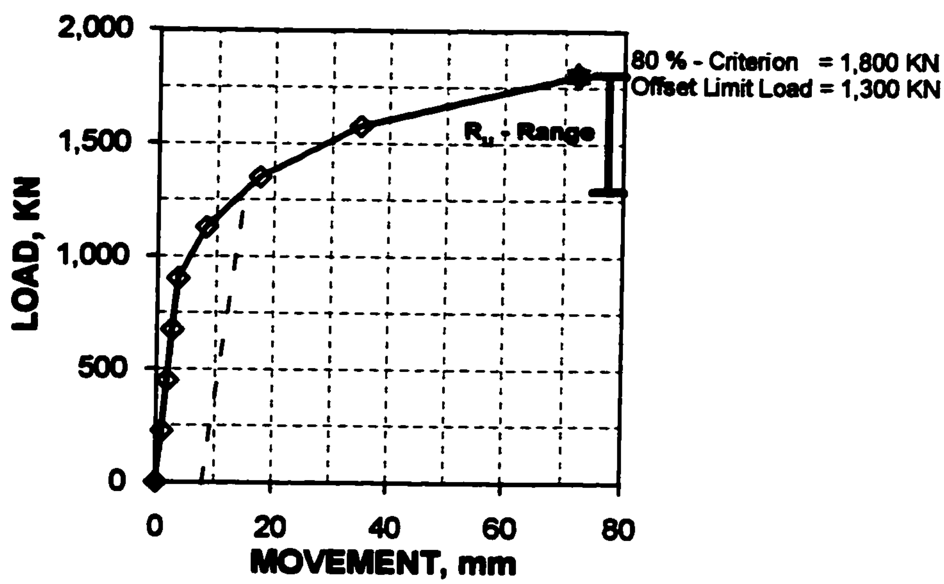

Case 46 L&D12
Sheet a CPT data

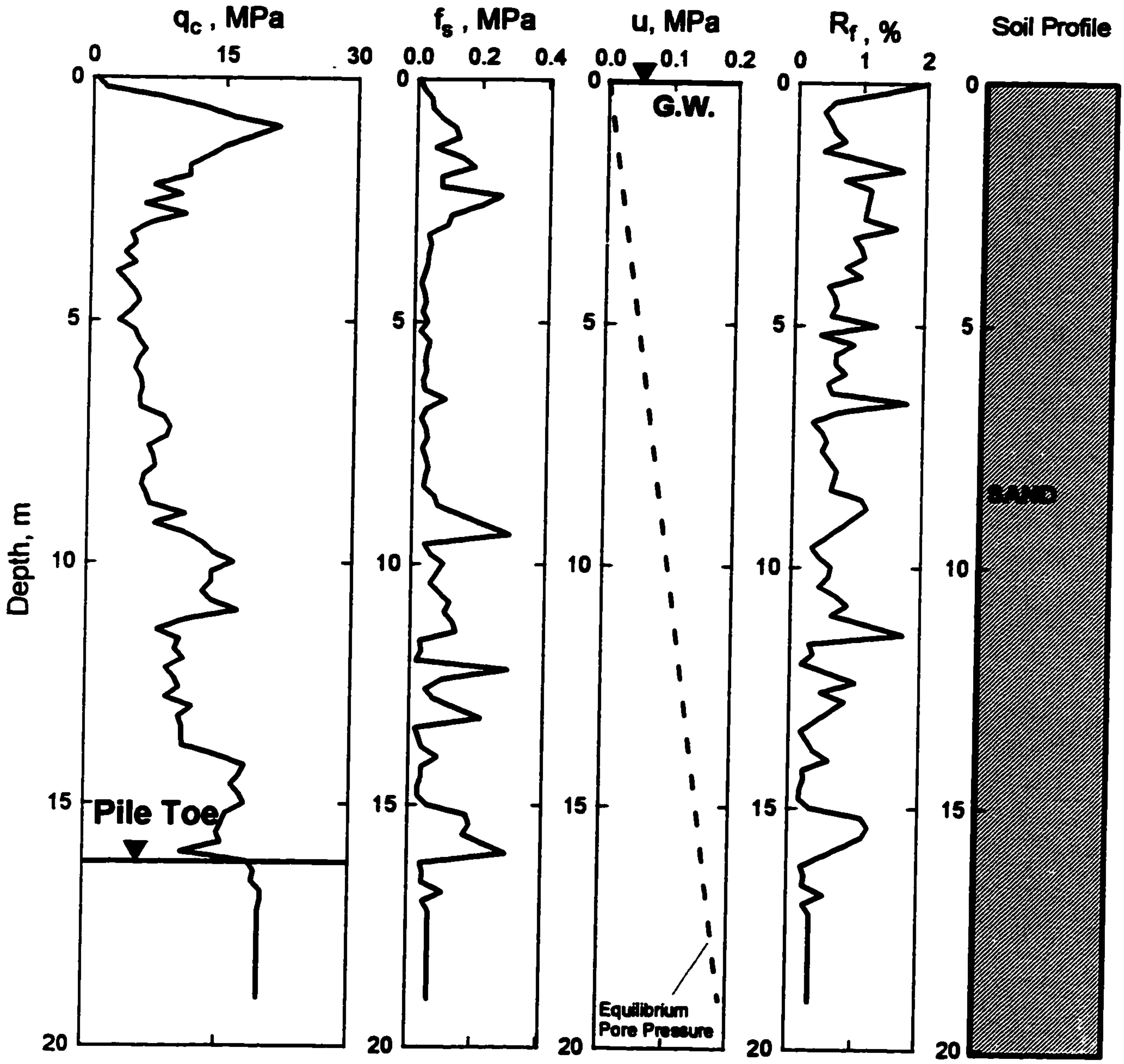

Case 46 L&D12
Sheet b Pile data

	DETAIL	DESCRIPTION
1	Site	Lock and Dam 26, SL, USA
2	Reference	Tucker and Briaud, 1988
3	Shape, Material, and Installation	H-Pile, Steel, Driven
4	Diameter, b, and Wall Thickness, t, mm	346*371
5	Embedment Length D, m	16.2
6	Cross Sectional Area A_t, m^2	0.014
7	Unit Circumferential Area, A_s, m^2/m	1.43
8	Toe, Closed or Open	Open
9	Type of Test and Loading	Static Tension, SML
10	Toe Capacity, R_t, KN	
11	Shaft Capacity, R_s, KN	
12	*Capacity, R_u, KN	1,170

SCHEMATIC PROFILE

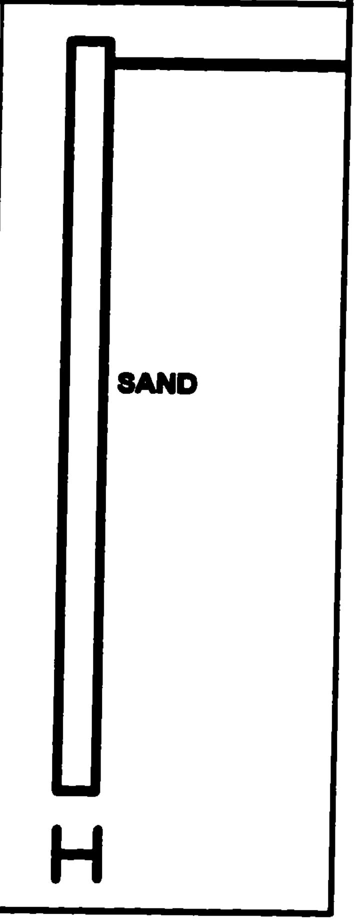

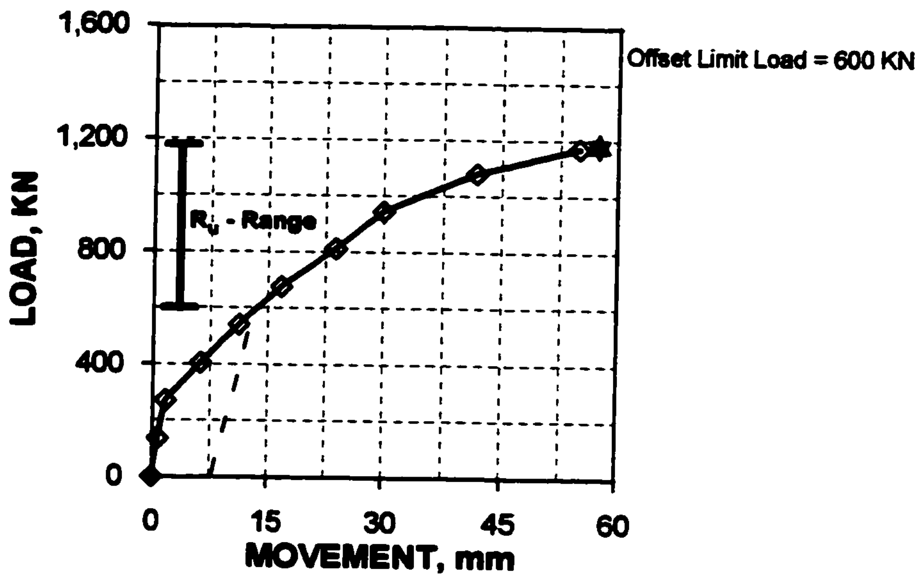

Case 47 L&D314
Sheet a CPT data

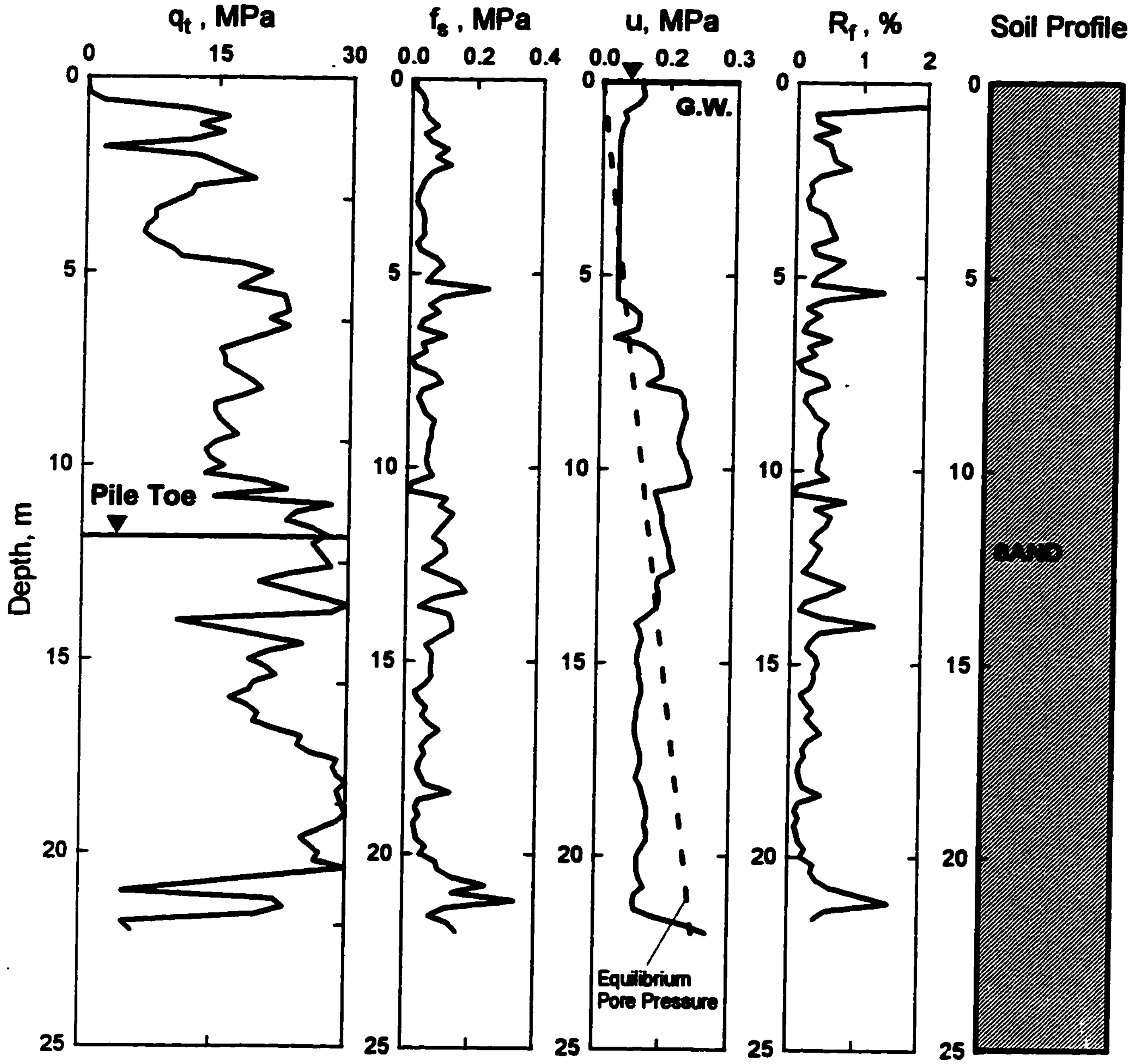

Case 47 L&D314
Sheet b Pile data

	DETAIL	DESCRIPTION
1	Site	Lock and Dam 26, SL, USA
2	Reference	Tucker and Briaud, 1988
3	Shape, Material, and Installation	H-Pile, Steel, Driven
4	Diameter, b, and Wall Thickness, t, mm	346*371
5	Embedment Length D, m	12
6	Cross Sectional Area A_t, m^2	0.014
7	Unit Circumferential Area, A_s, m^2/m	1.43
8	Toe, Closed or Open	Open
9	Type of Test and Loading	Static Tension, SML
10	Toe Capacity, R_t, KN	
11	Shaft Capacity, R_s, KN	
12	*Capacity, R_u, KN	1,170

SCHEMATIC PROFILE

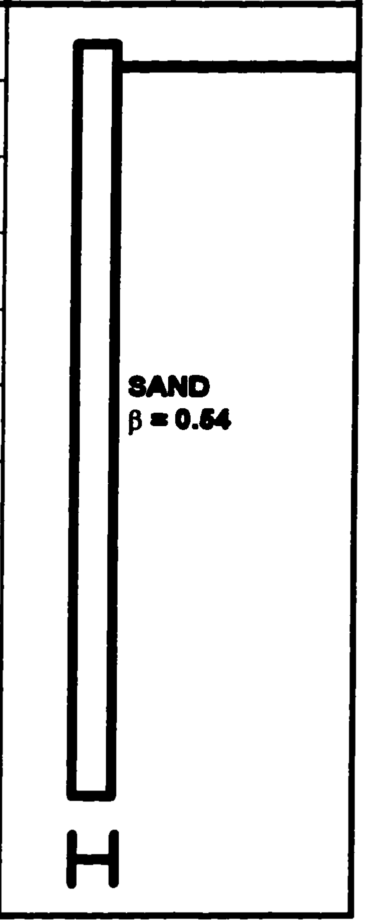

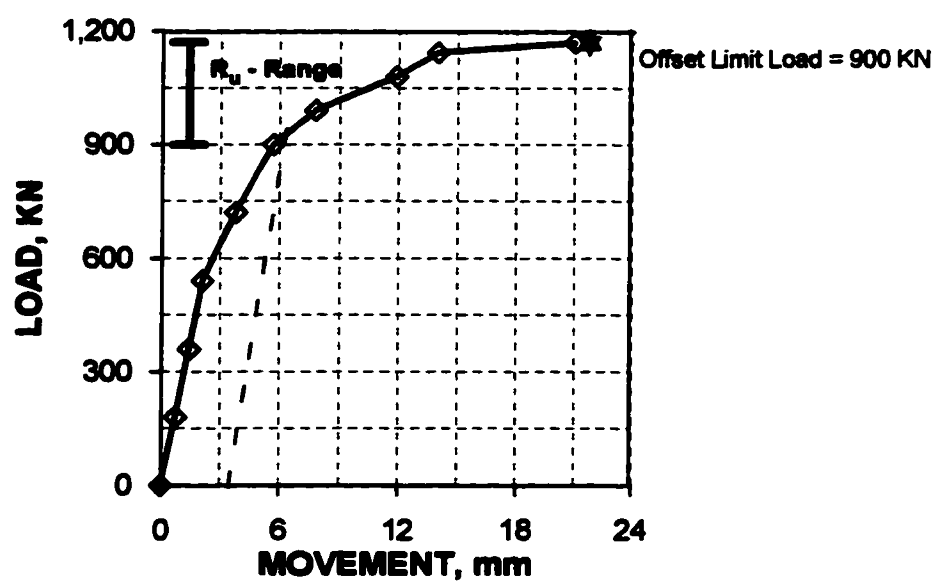

Case 48 L&D21
Sheet a CPT data

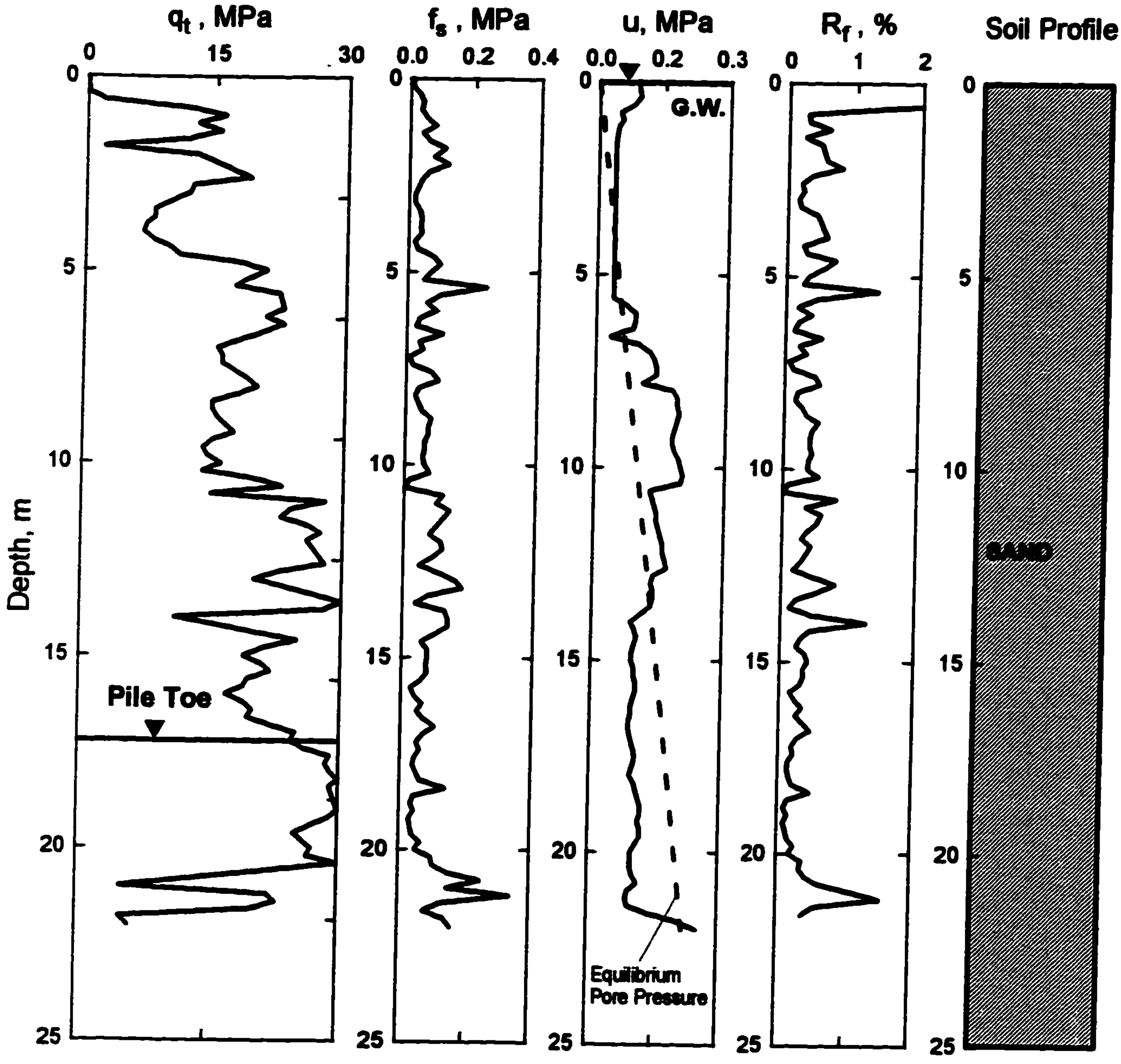

Case 48 L&D21
Sheet b Pile data

	DETAIL	DESCRIPTION
1	Site	Lock and Dam 26, SL, USA
2	Reference	Tucker and Briaud, 1988
3	Shape, Material, and Installation	H-Pile, Steel, Driven
4	Diameter, b, and Wall Thickness, t, mm	346*371
5	Embedment Length D, m	16.8
6	Cross Sectional Area A_t, m^2	0.014
7	Unit Circumferential Area, A_s, m^2/m	1.43
8	Toe, Closed or Open	Open
9	Type of Test and Loading	Static Tension, QML
10	Toe Capacity, R_t, KN	
11	Shaft Capacity, R_s, KN	
12	*Capacity, R_u, KN	1,260

SCHEMATIC PROFILE

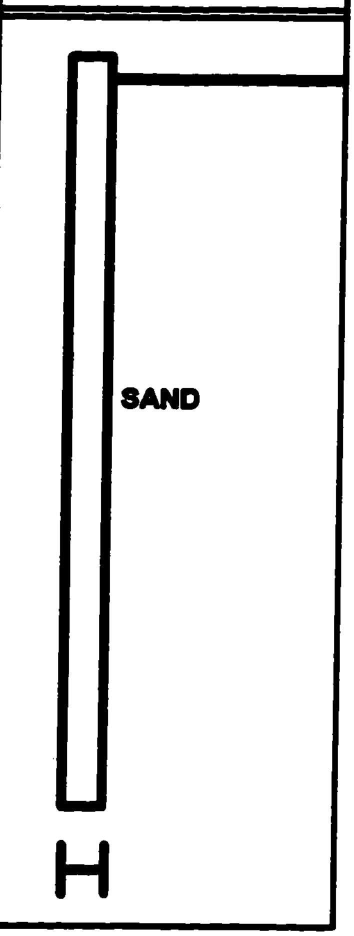

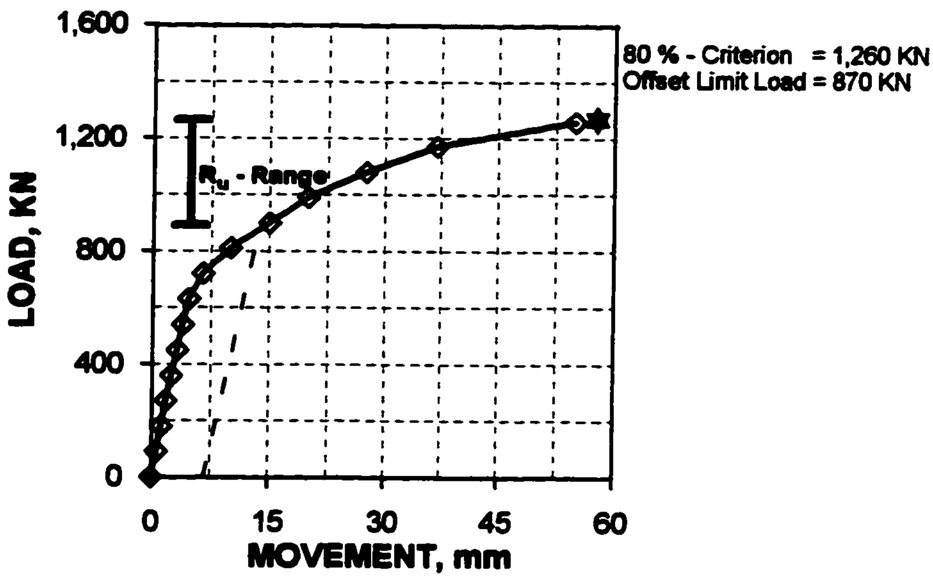

Case 49 L&D35
Sheet a CPT data

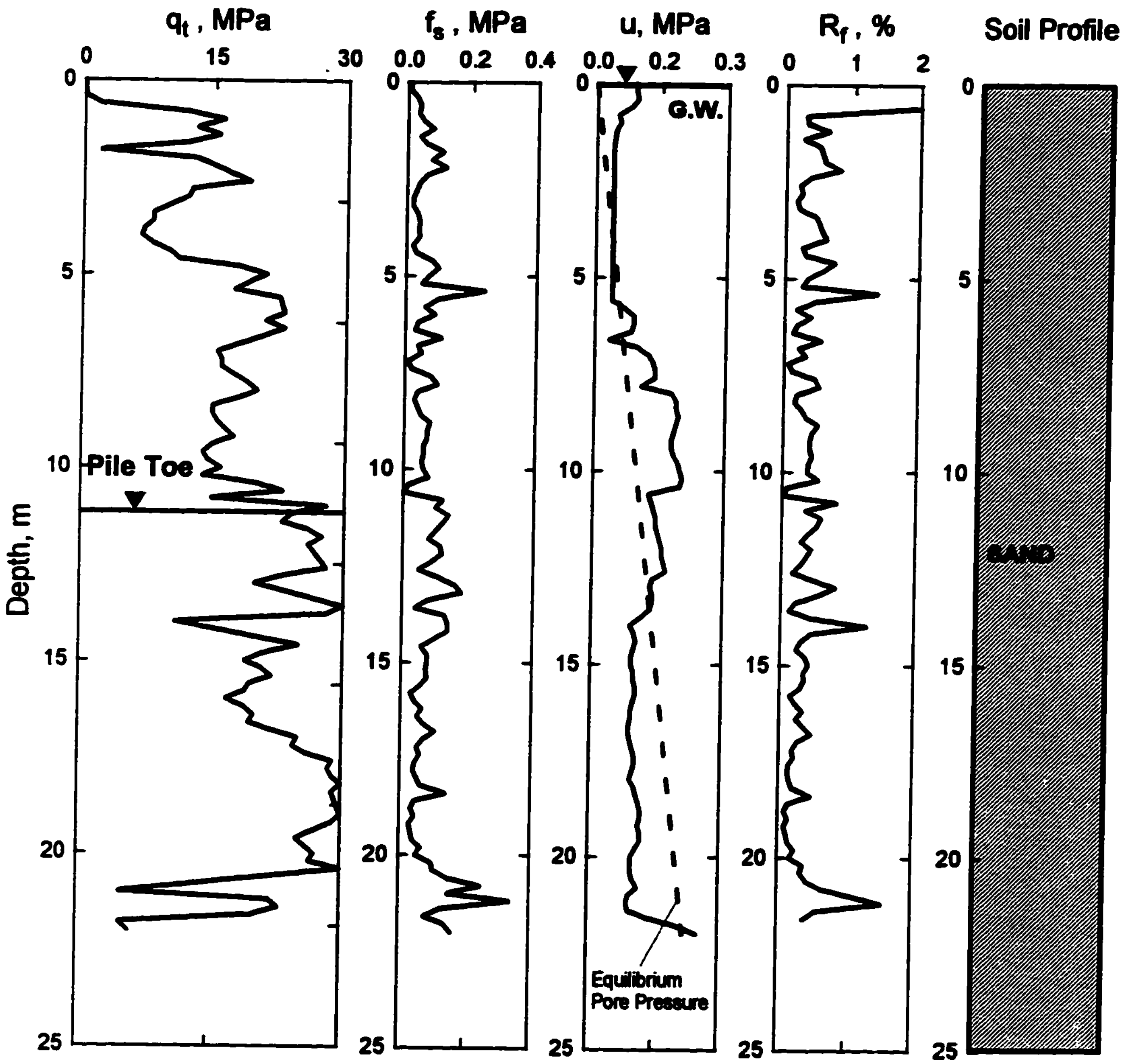

Case 49 L&D35
Sheet b Pile data

	DETAIL	DESCRIPTION	SCHEMATIC PROFILE
1	Site	Lock and Dam 26, USA	
2	Reference	Tucker and Briaud, 1988	
3	Shape, Material, and Installation	Pipe, Steel, Driven	
4	Diameter, b, and Wall Thickness, t, mm	350 9.5	
5	Embedment Length D, m	11.1	
6	Cross Sectional Area A_t, m^2	0.096	
7	Unit Circumferential Area, A_s, m^2/m	1.1	
8	Toe, Closed or Open	Closed	
9	Type of Test and Loading	Static Tension, SML	
10	Toe Capacity, R_t, KN		
11	Shaft Capacity, R_s, KN		
12	*Capacity, R_u, KN	630	

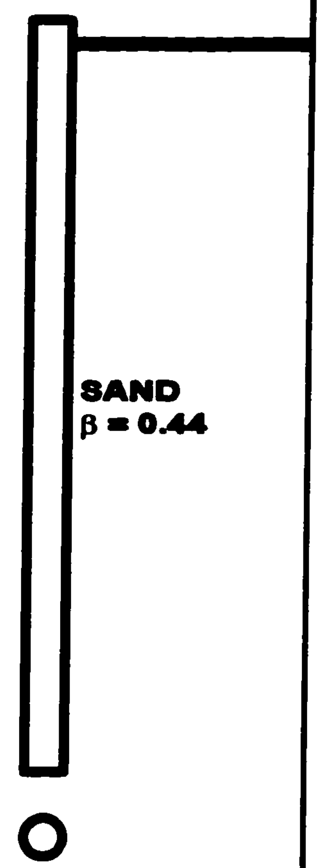

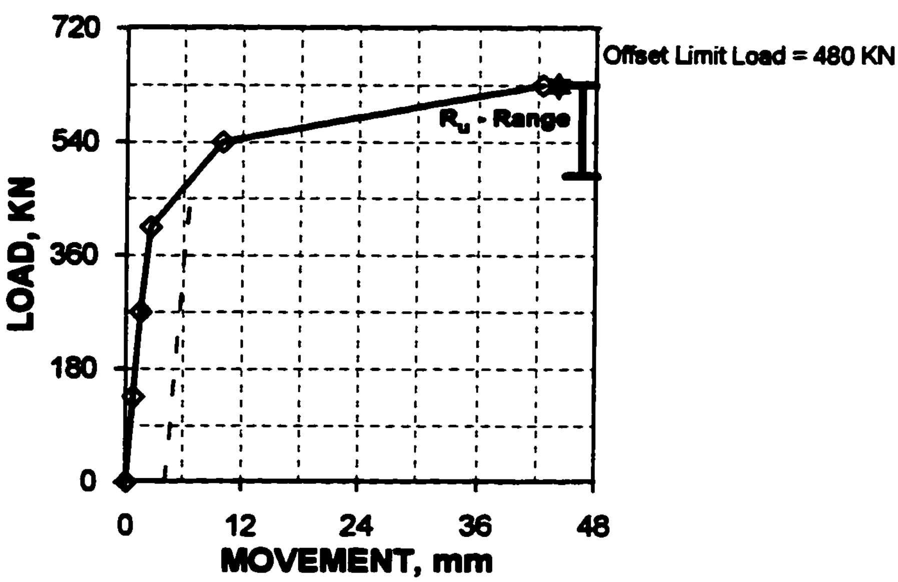

Case 50 L&D316
Sheet a CPT data

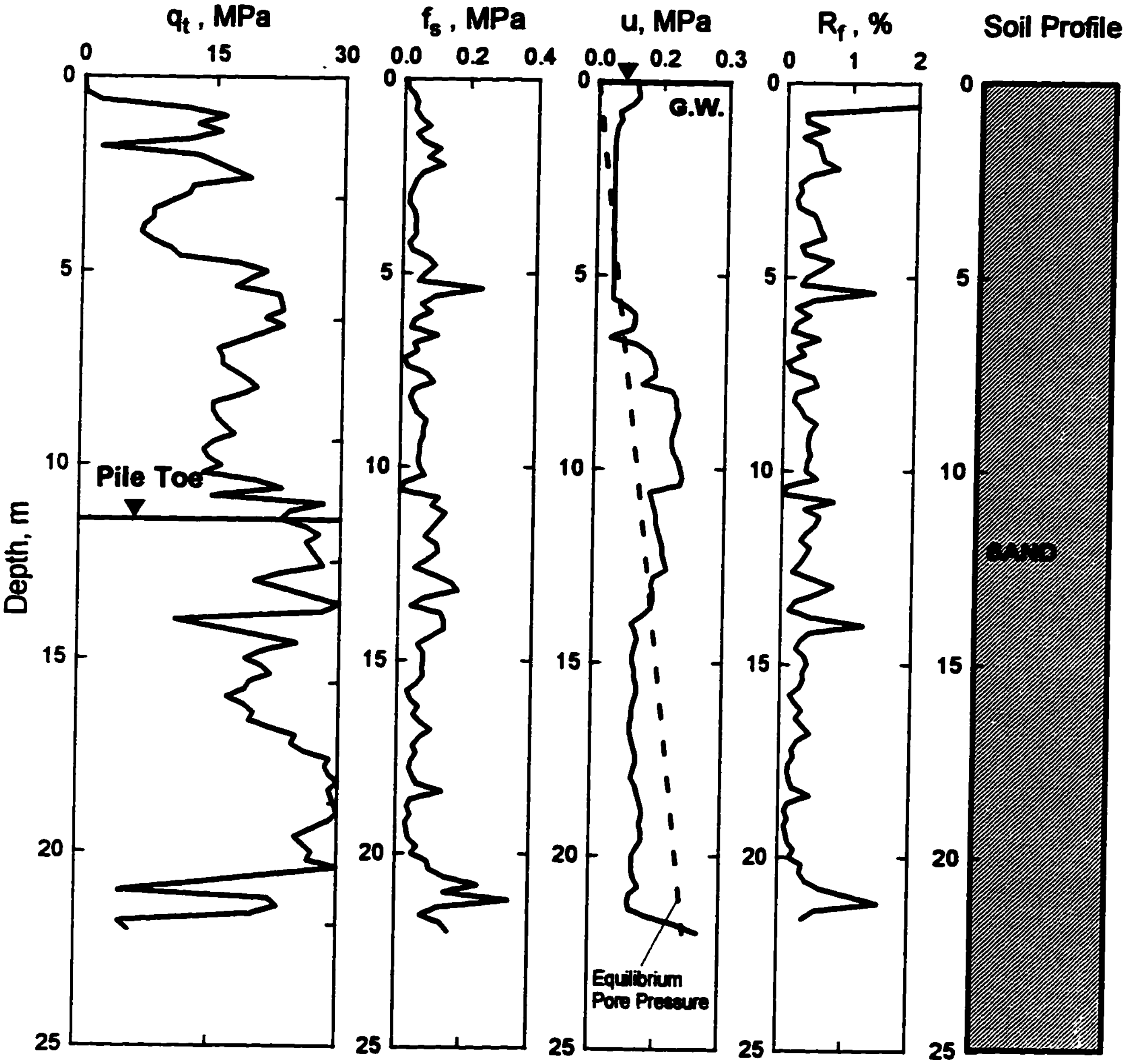

Case 50 L&D316
Sheet b Pile data

DETAIL		DESCRIPTION
1	Site	Lock and Dam 26, SL, USA
2	Reference	Tucker and Briaud, 1988
3	Shape, Material, and Installation	H-Pile, Steel, Driven
4	Diameter, b, and Wall Thickness, t, mm	346*371
5	Embedment Length D, m	11.3
6	Cross Sectional Area A_t, m^2	0.014
7	Unit Circumferential Area, A_s, m^2/m	1.43
8	Toe, Closed or Open	Open
9	Type of Test and Loading	Static Tension, SML
10	Toe Capacity, R_t, KN	
11	Shaft Capacity, R_s, KN	
12	*Capacity, R_u, KN	870

SCHEMATIC PROFILE

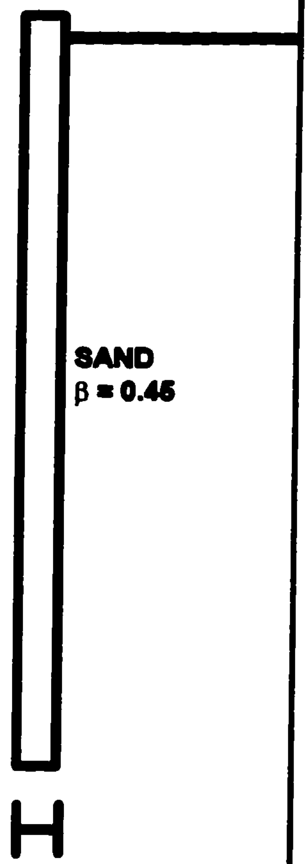

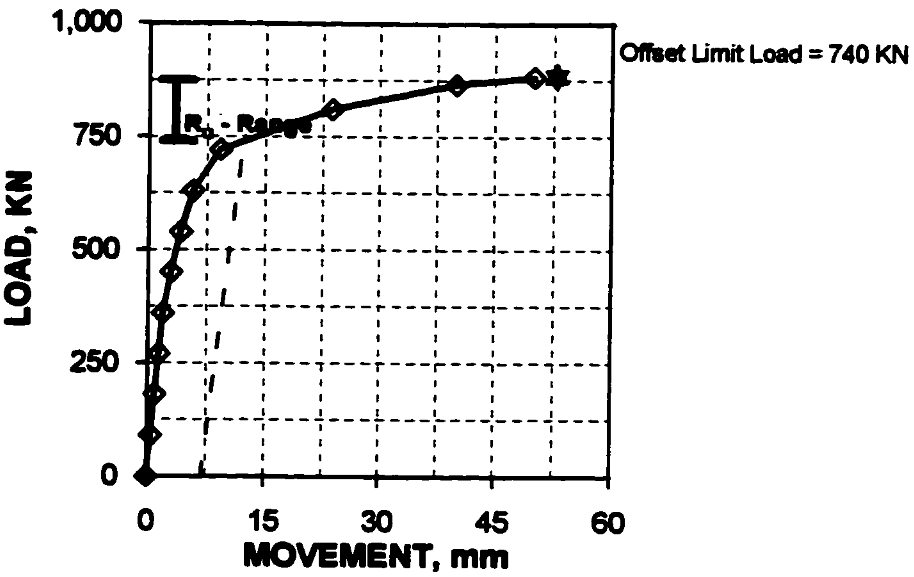

Case 51 L&D32
Sheet a CPT data

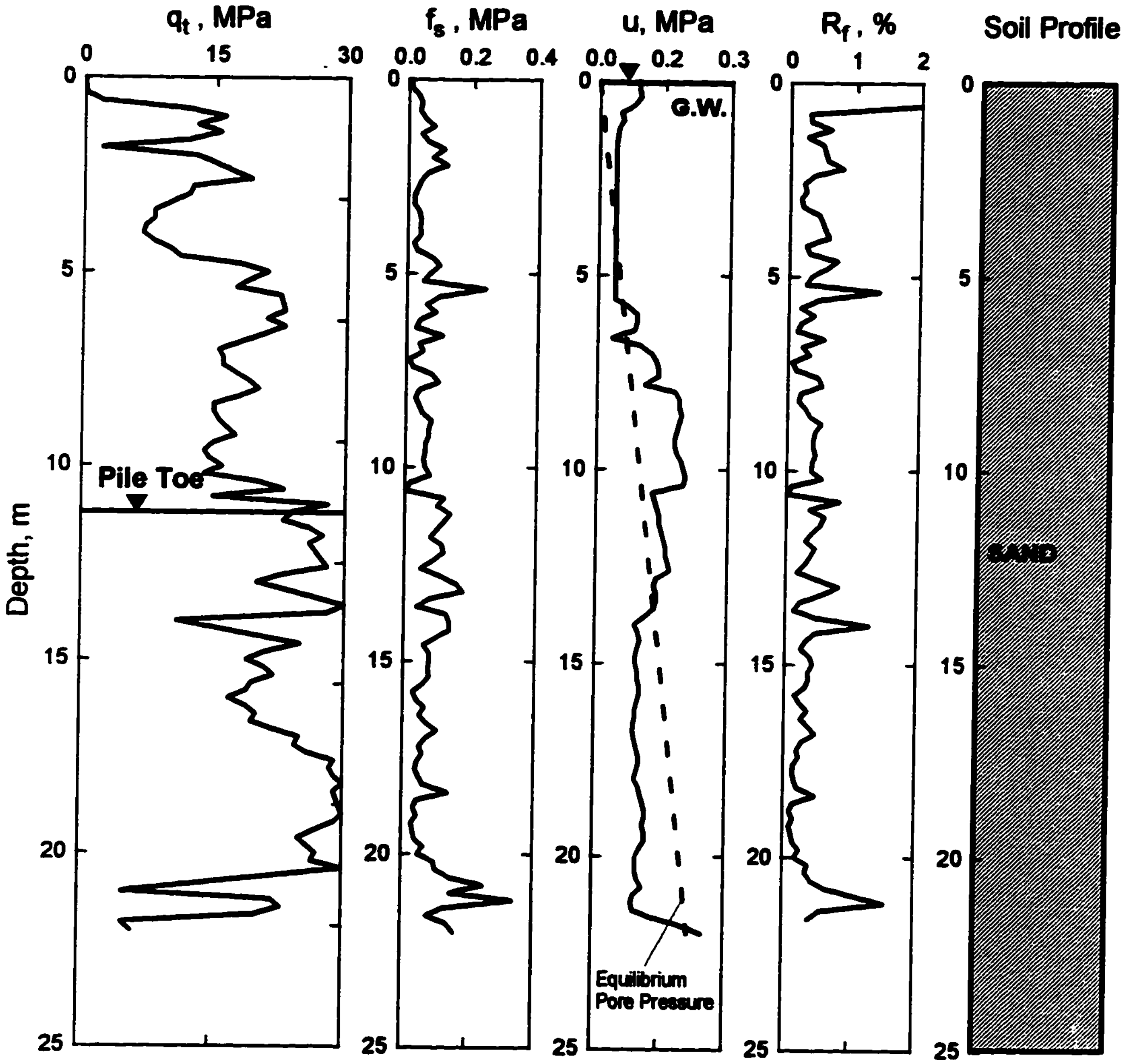

Case 51 L&D32
Sheet b Pile data

DETAIL		DESCRIPTION	SCHEMATIC PROFILE
1	Site	Lock and Dam 26, USA	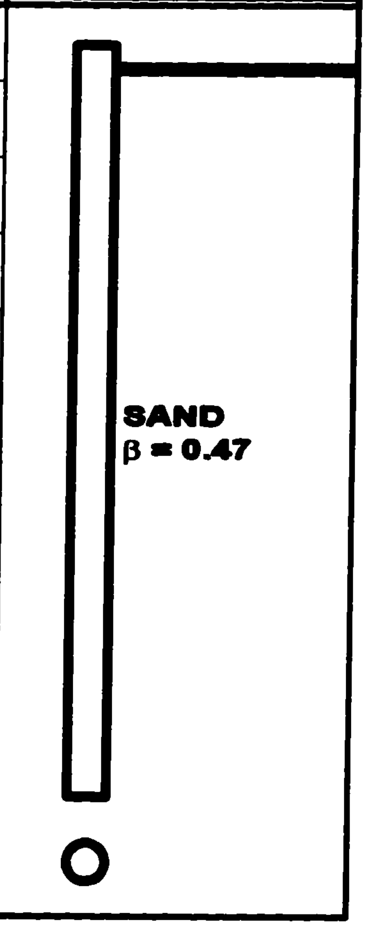
2	Reference	Tucker and Briaud, 1988	
3	Shape, Material, and Installation	Pipe, Steel, Driven	
4	Diameter, b, and Wall Thickness, t, mm	300 9.5	
5	Embedment Length D, m	11	
6	Cross Sectional Area A_t, m^2	0.071	
7	Unit Circumferential Area, A_s, m^2/m	0.94	
8	Toe, Closed or Open	Closed	
9	Type of Test and Loading	Static Tension, SML	
10	Toe Capacity, R_t, KN		
11	Shaft Capacity, R_s, KN		
12	*Capacity, R_u, KN	560	

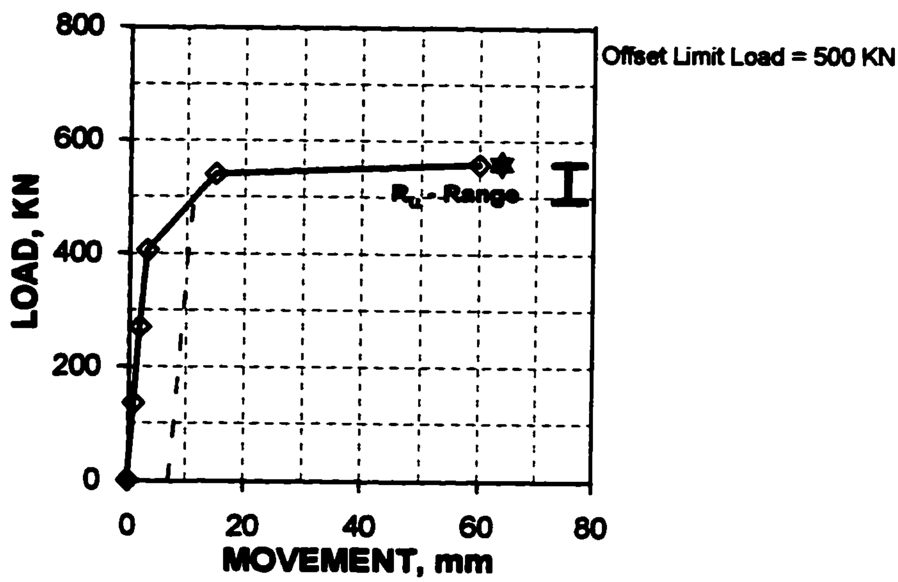

Case 52 L&D38
Sheet a CPT data

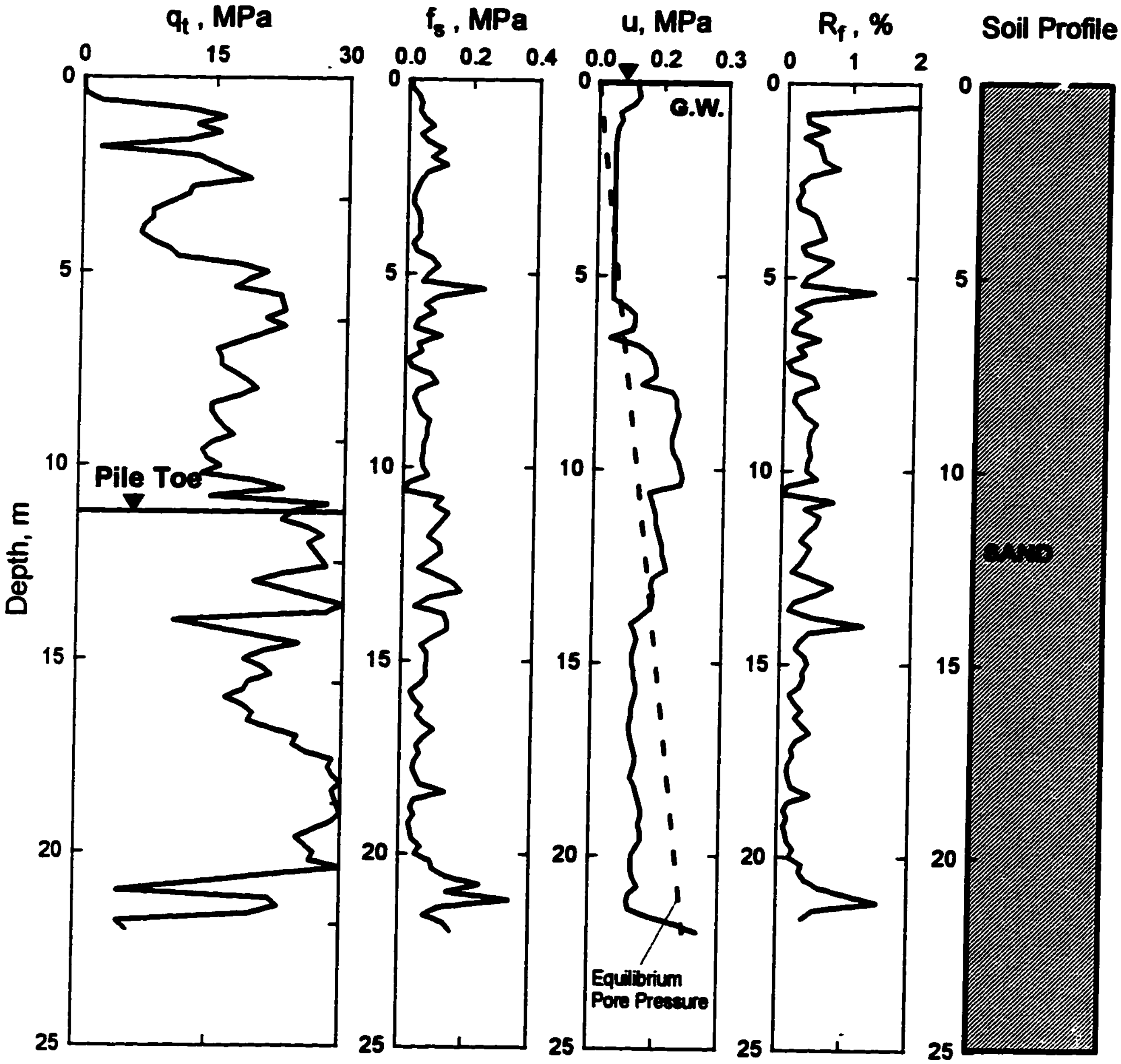

Case 52 L&D38
Sheet b Pile data

	DETAIL	DESCRIPTION	SCHEMATIC PROFILE
1	Site	Lock and Dam 26, USA	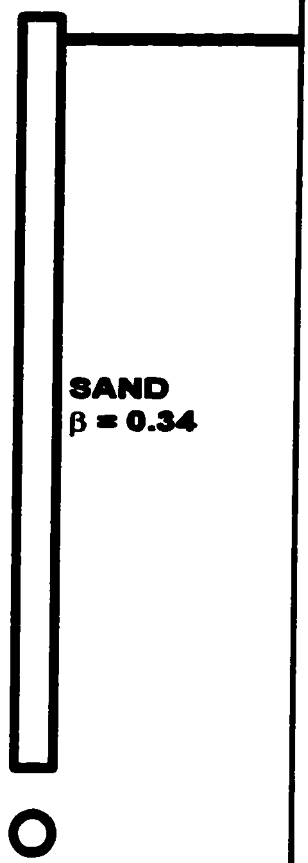
2	Reference	Tucker and Briaud, 1988	
3	Shape, Material, and Installation	Pipe, Steel, Driven	
4	Diameter, b, and Wall Thickness, t, mm	400 9.5	
5	Embedment Length D, m	14.6	
6	Cross Sectional Area A_t, m^2	0.126	
7	Unit Circumferential Area, A_s, m^2/m	1.26	
8	Toe, Closed or Open	Closed	
9	Type of Test and Loading	Static Tension, SML	
10	Toe Capacity, R_t, KN		
11	Shaft Capacity, R_s, KN		
12	*Capacity, R_u, KN	945	

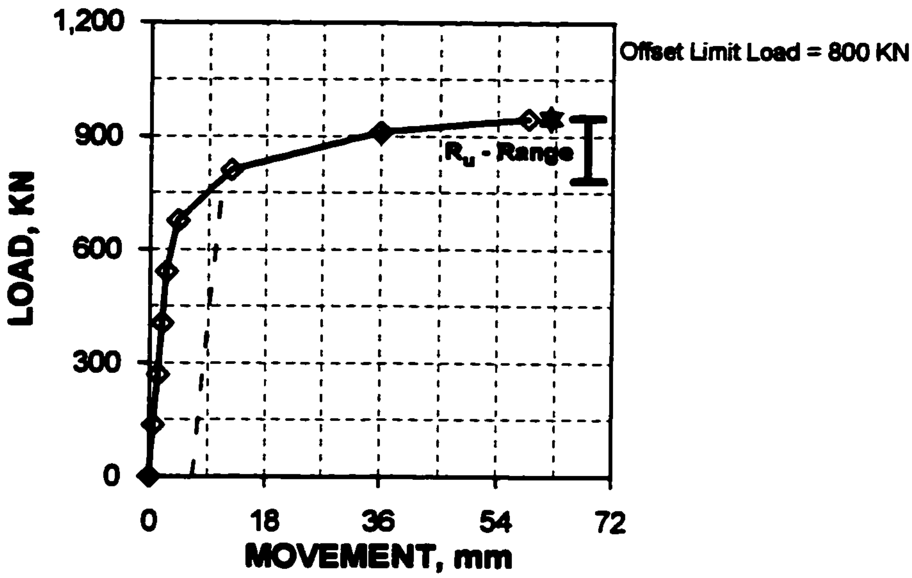

Case 53 L&D315
Sheet a CPT data

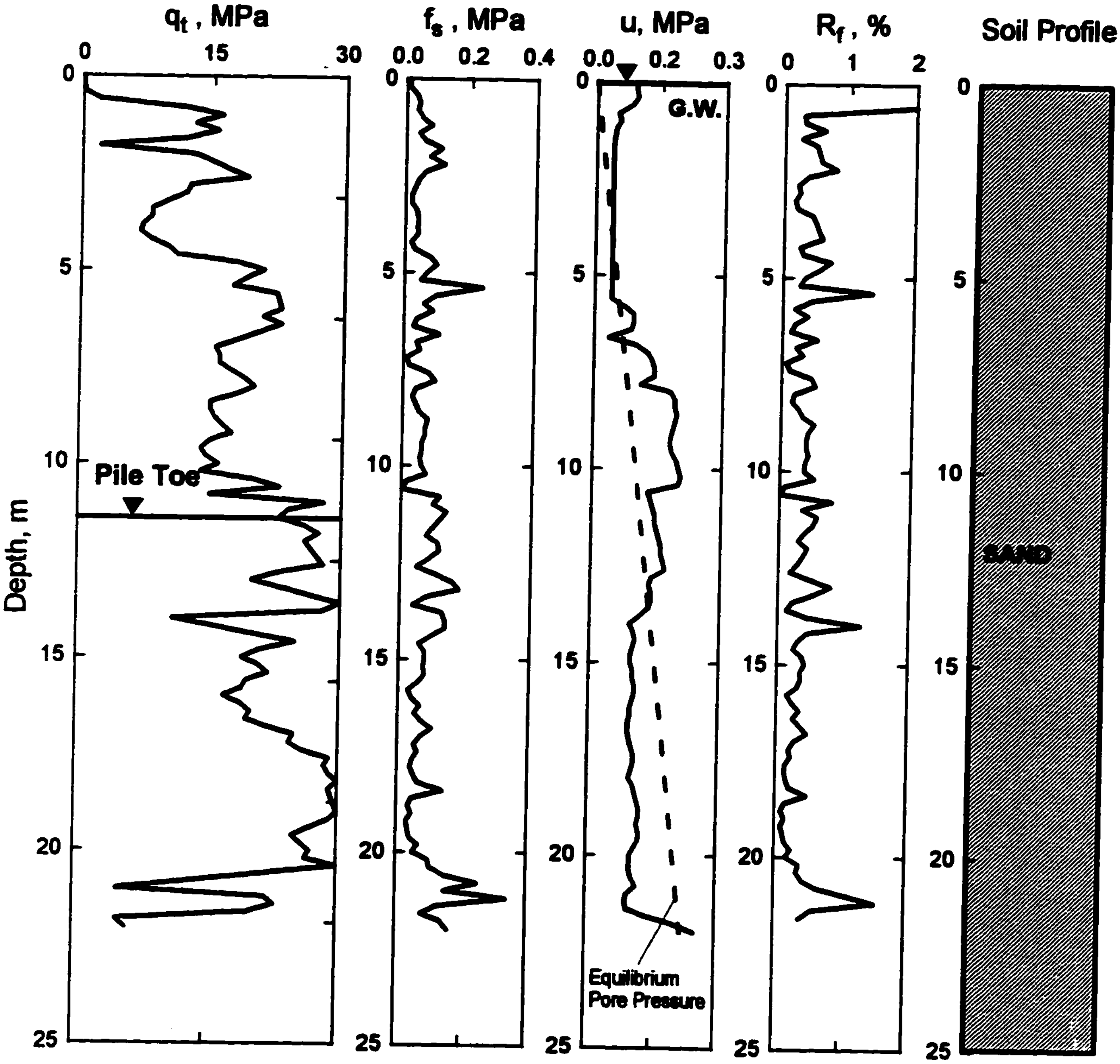

Case 53 L&D315
Sheet b Pile data

	DETAIL	DESCRIPTION
1	Site	Lock and Dam 26, SL, USA
2	Reference	Tucker and Briaud, 1988
3	Shape, Material, and Installation	H-Pile, Steel, Driven
4	Diameter, b, and Wall Thickness, t, mm	346*371
5	Embedment Length D, m	11.3
6	Cross Sectional Area A_t, m^2	0.014
7	Unit Circumferential Area, A_s, m^2/m	1.43
8	Toe, Closed or Open	Open
9	Type of Test and Loading	Static Tension, SML
10	Toe Capacity, R_t, KN	
11	Shaft Capacity, R_s, KN	
12	*Capacity, R_u, KN	817

SCHEMATIC PROFILE

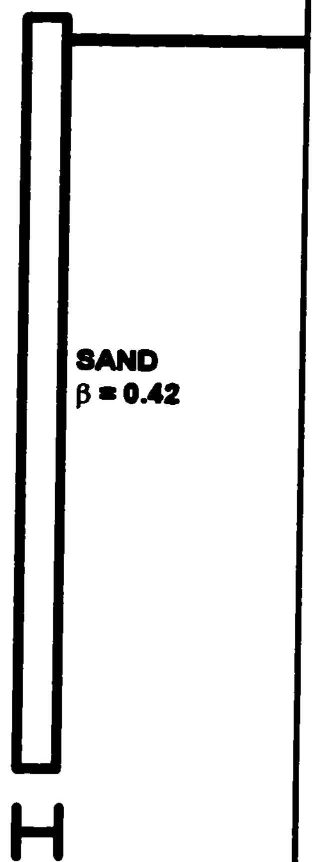

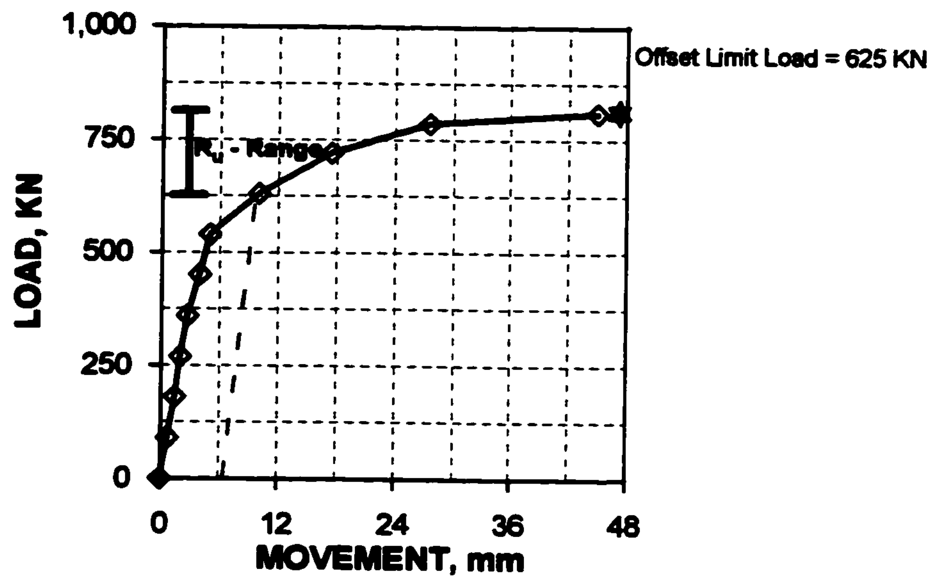

Case 54 SEATW
Sheet a CPT data

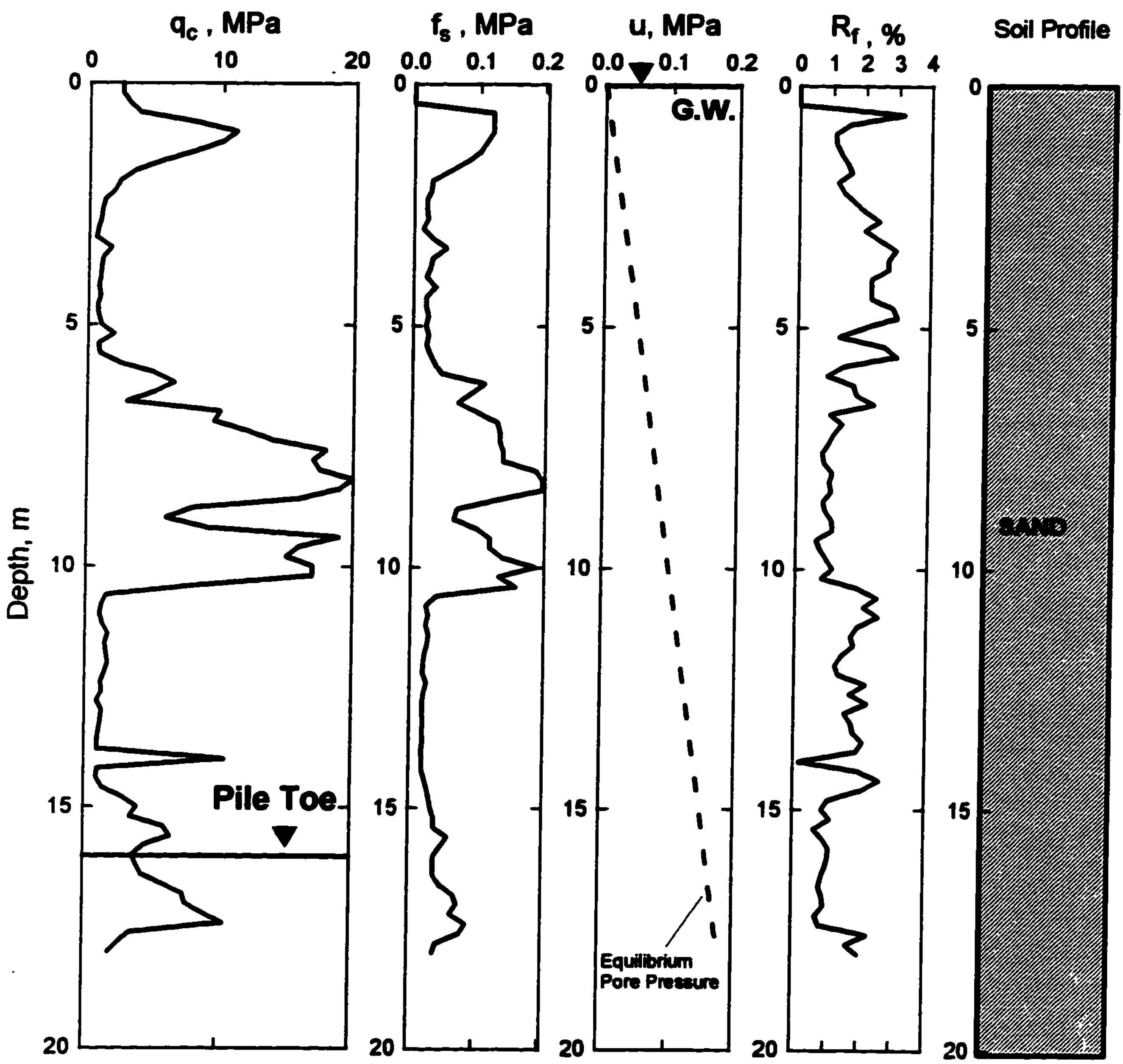

Case 54 SEATW
Sheet b Pile data

DETAIL		DESCRIPTION	SCHEMATIC PROFILE
1	Site	Seatle, USA	
2	Reference	Horvitz et al., 1986	
3	Shape, Material, and Installation	Round, Concrete, Bored	
4	Diameter, b, and Wall Thickness, t, mm	350	
5	Embedment Length D, m	15.8	
6	Cross Sectional Area A_t, m^2	0.096	
7	Unit Circumferential Area, A_s, m^2 /m	1.1	
8	Toe, Closed or Open	Closed	
9	Type of Test and Loading	Static Compression,SML	
10	Toe Capacity, R_t, KN		
11	Shaft Capacity, R_s, KN		
12	*Capacity, R_u, KN	900	

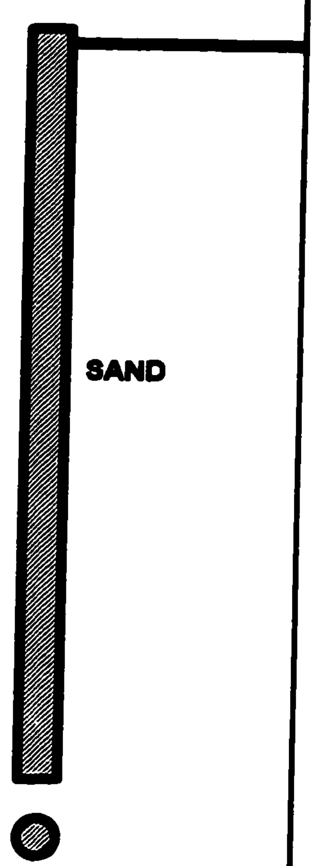

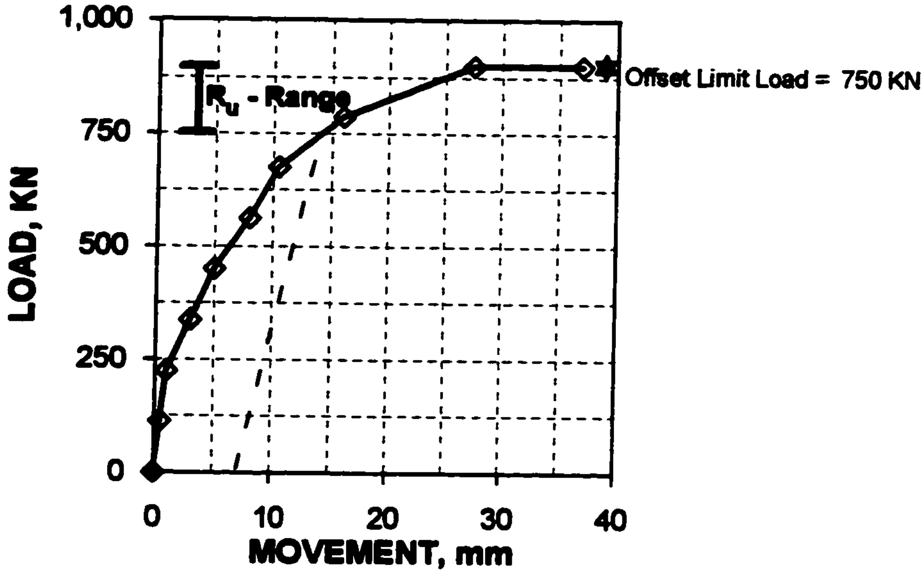

Case 55 GIT1
Sheet a CPT data

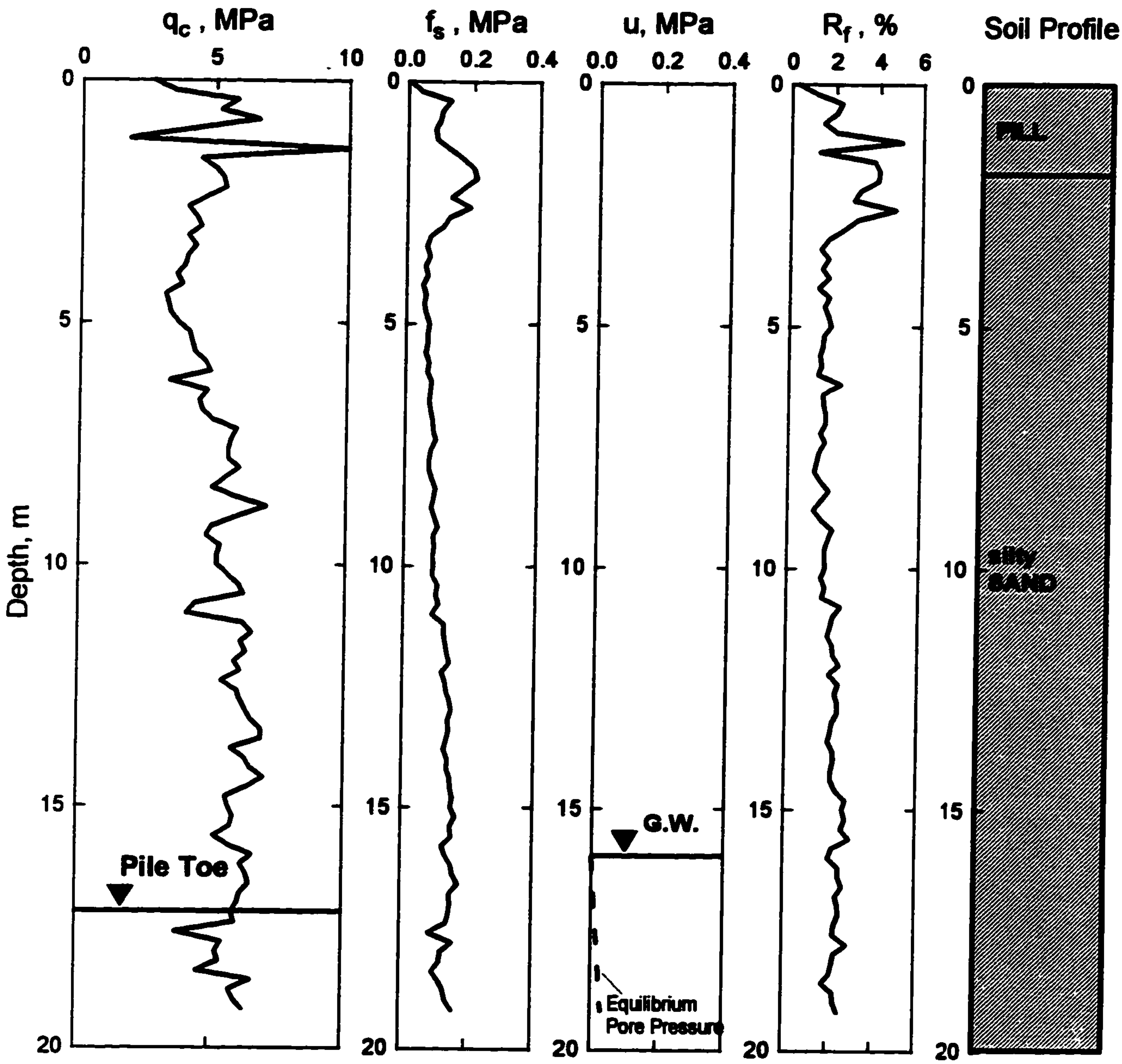

Case 55 GIT1
Sheet b Pile data

	DETAIL	DESCRIPTION
1	Site	Georgia, USA
2	Reference	Mayne, 1993
3	Shape, Material, and Installation	Round, Concrete, Bored
4	Diameter, b, and Wall Thickness, t, mm	750
5	Embedment Length D, m	16.8
6	Cross Sectional Area A_t, m^2	0.442
7	Unit Circumferential Area, A_s, m^2/m	2.36
8	Toe, Closed or Open	Closed
9	Type of Test and Loading	Static Compression,SML
10	Toe Capacity, R_t, KN	
11	Shaft Capacity, R_s, KN	
12	*Capacity, R_u, KN	4,500

SCHEMATIC PROFILE

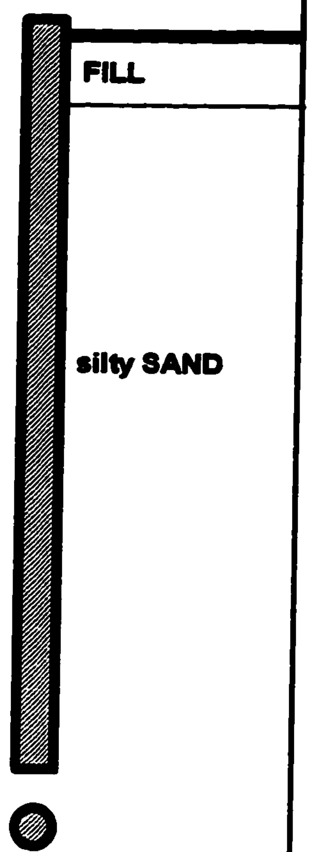

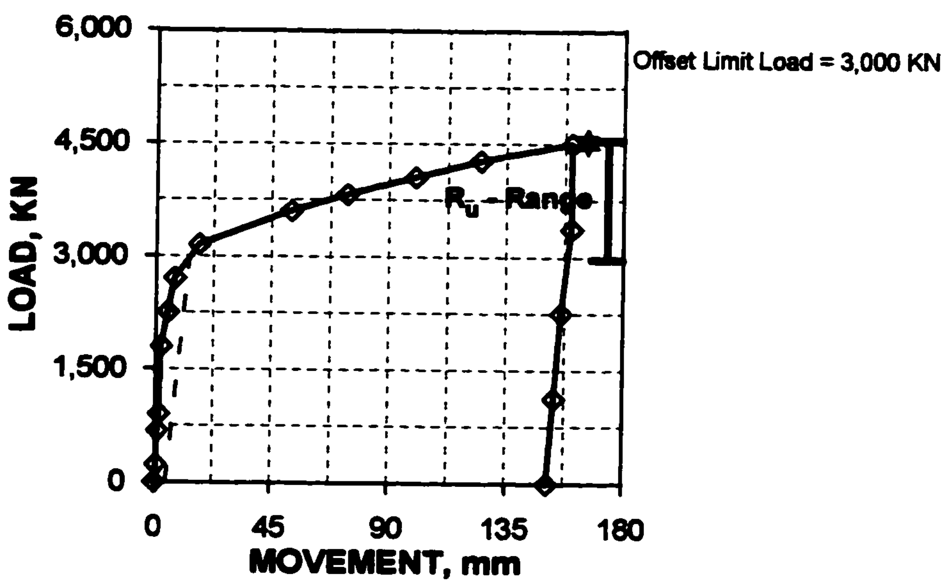

Case 56 YOG1
Sheet a CPT data

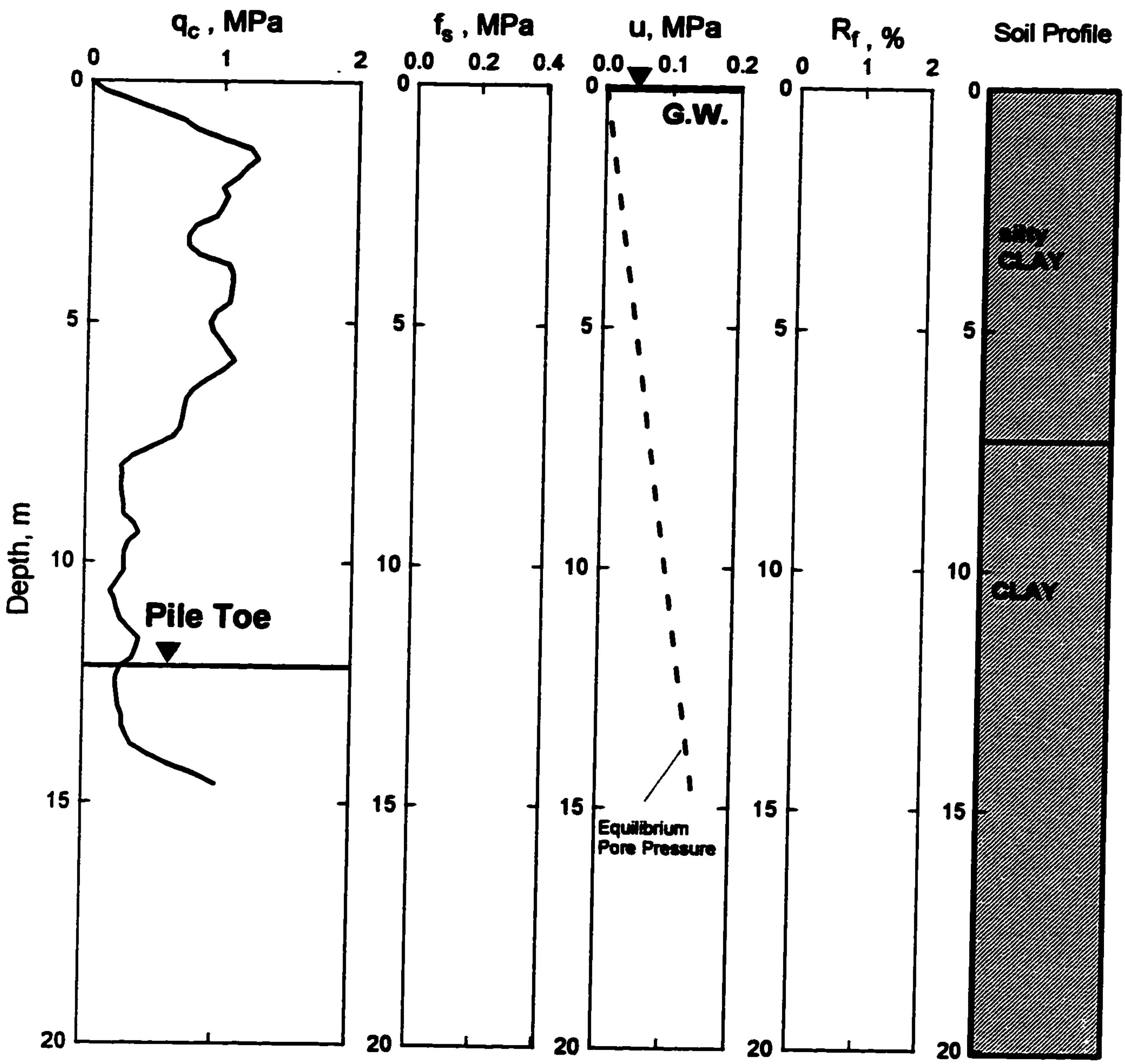

Case 56 YOG1
Sheet b Pile data

	DETAIL	DESCRIPTION
1	Site	Yogoslavia, 1982
2	Reference	Milovic et al., 1982
3	Shape, Material, and Installation	Round, Concrete, Driven
4	Diameter, b, and Wall Thickness, t, mm	520
5	Embedment Length D, m	12
6	Cross Sectional Area A_t, m^2	0.21
7	Unit Circumferential Area, A_s, m^2/m	1.63
8	Toe, Closed or Open	Closed
9	Type of Test and Loading	Static Compression,SML
10	Toe Capacity, R_t, KN	
11	Shaft Capacity, R_s, KN	
12	*Capacity, R_u, KN	430

SCHEMATIC PROFILE

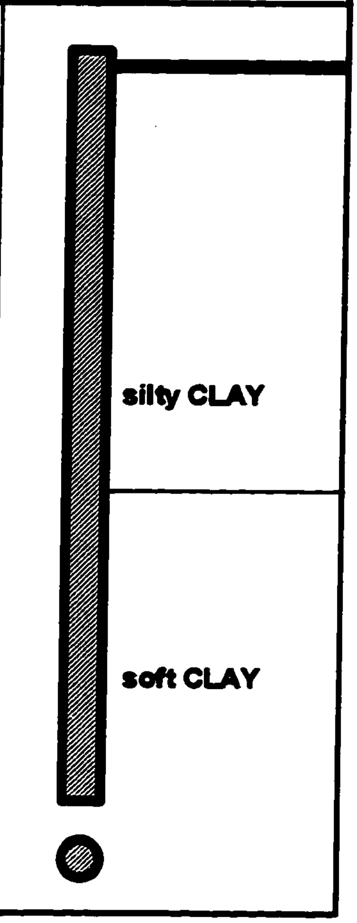

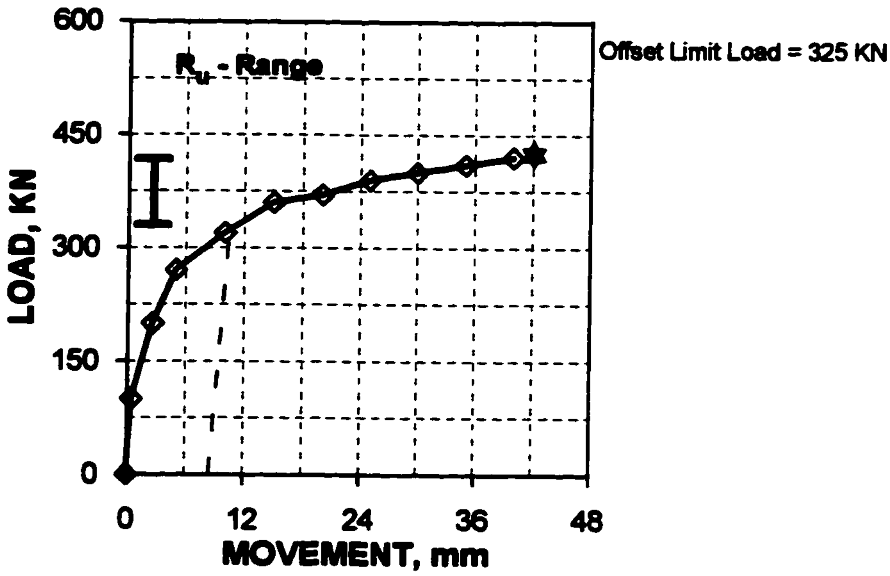

Case 57 YOG2
Sheet a CPT data

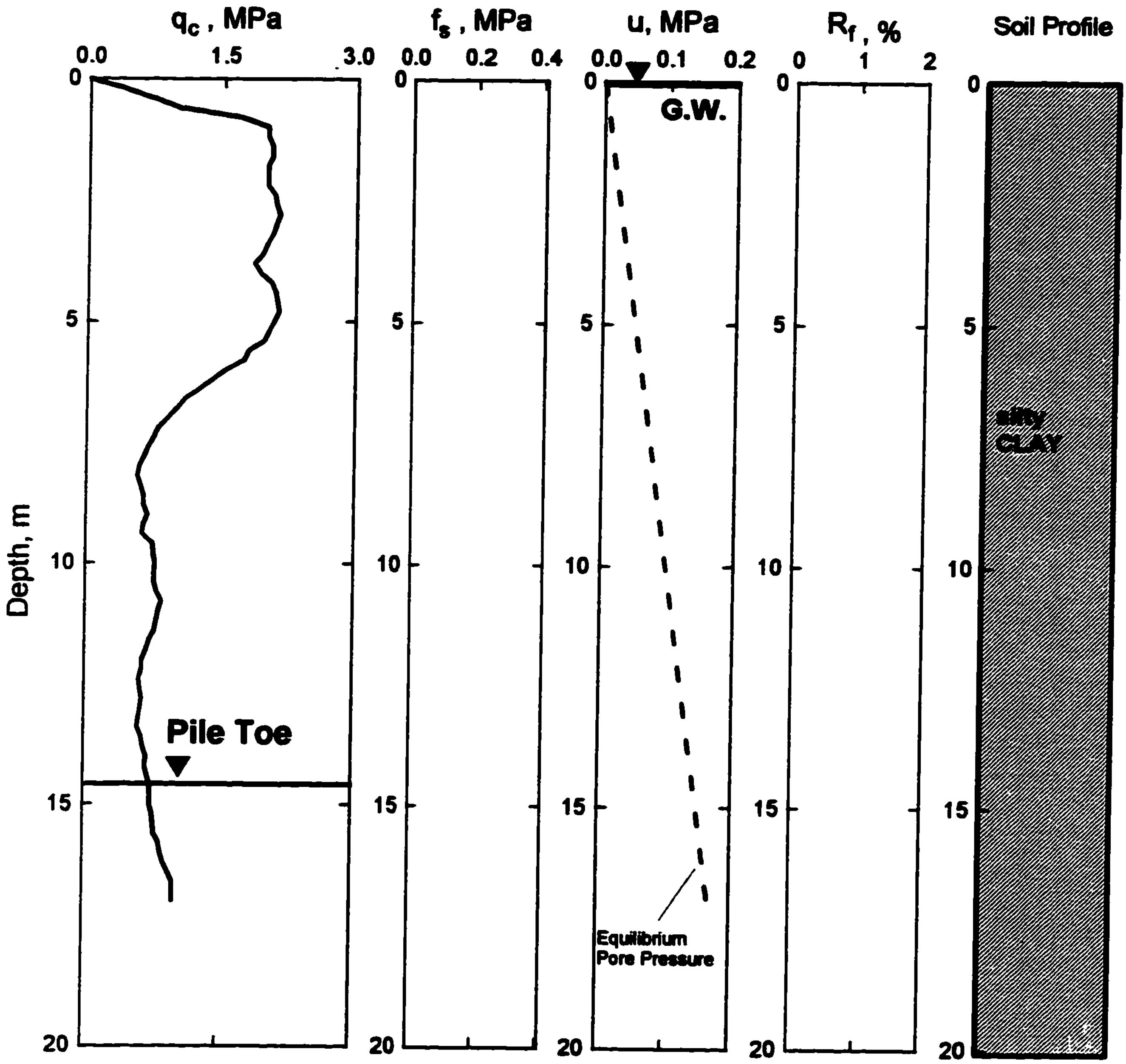

Case 57 YOG2
Sheet b Pile data

	DETAIL	DESCRIPTION
1	Site	Yogoslavia, 1982
2	Reference	Milovic et al., 1982
3	Shape, Material, and Installation	Round, Concrete, Driven
4	Diameter, b, and Wall Thickness, t, mm	520
5	Embedment Length D, m	14.5
6	Cross Sectional Area A_t, m^2	0.21
7	Unit Circumferential Area, A_s, m^2/m	1.63
8	Toe, Closed or Open	Closed
9	Type of Test and Loading	Static Compression,SML
10	Toe Capacity, R_t, KN	
11	Shaft Capacity, R_s, KN	
12	*Capacity, R_u, KN	700

SCHEMATIC PROFILE

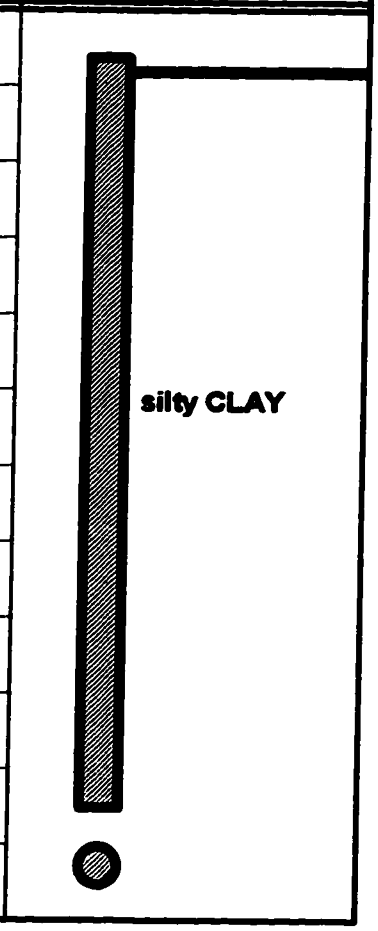

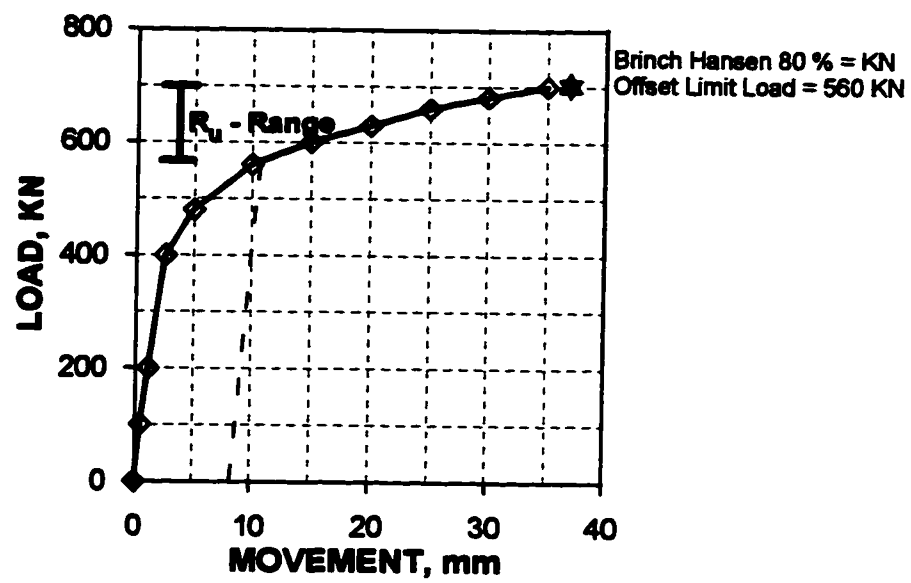

Case 58 KP1
Sheet a CPT data

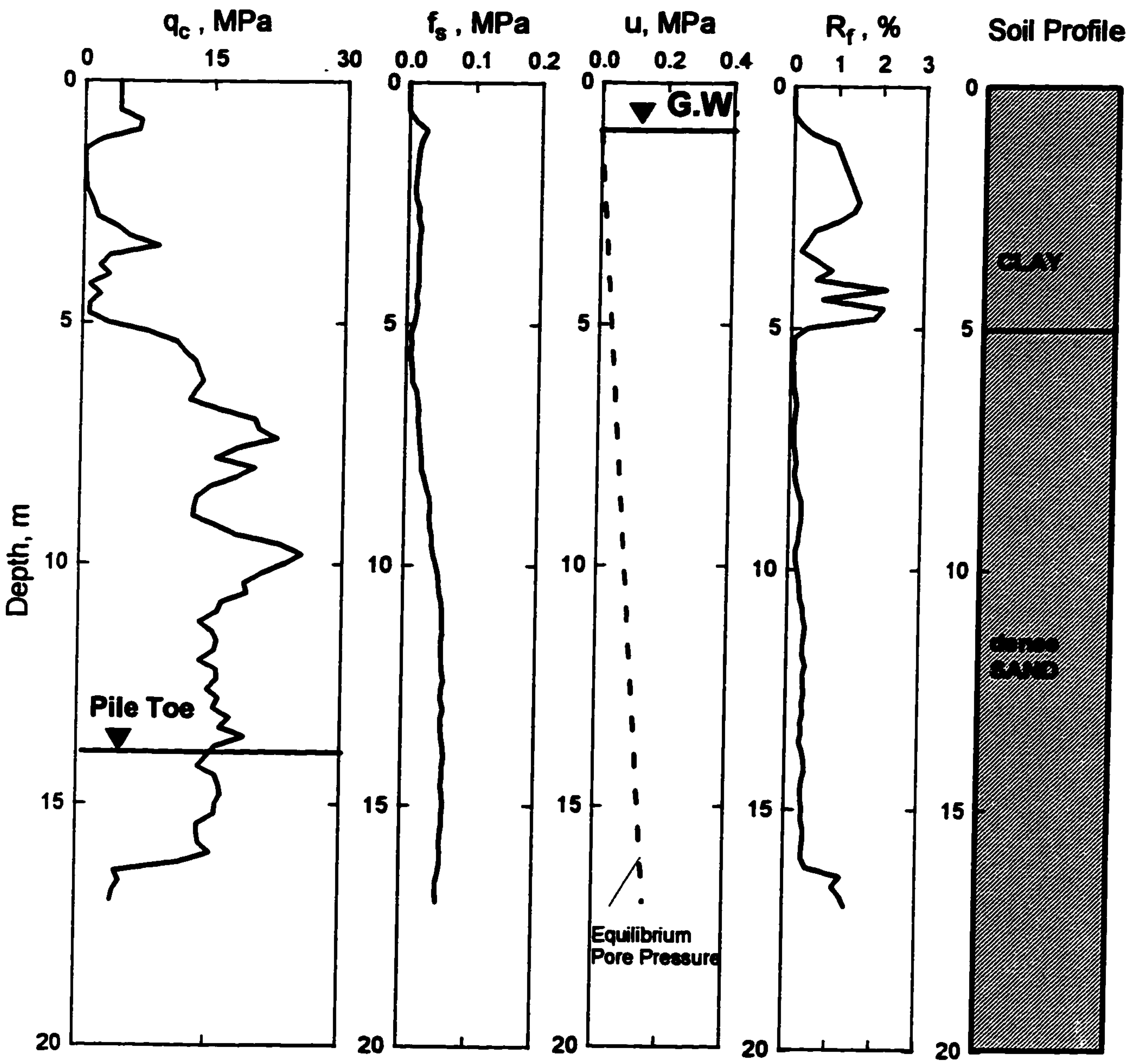

Case 58 KP1
Sheet b Pile data

	DETAIL	DESCRIPTION
1	Site	Kallo, Belgium
2	Reference	Weber, 1987
3	Shape, Material, and Installation	H-Pile, Steel, Driven
4	Diameter, b, and Wall Thickness, t, mm	368*400
5	Embedment Length D, m	14
6	Cross Sectional Area A_t, m²	0.046
7	Unit Circumferential Area, A_s, m² /m	1.54
8	Toe, Closed or Open	Open
9	Type of Test and Loading	Static Tension, SML
10	Toe Capacity, R_t, KN	1,000
11	Shaft Capacity, R_s, KN	2,500
12	*Capacity, R_u, KN	3,500

SCHEMATIC PROFILE

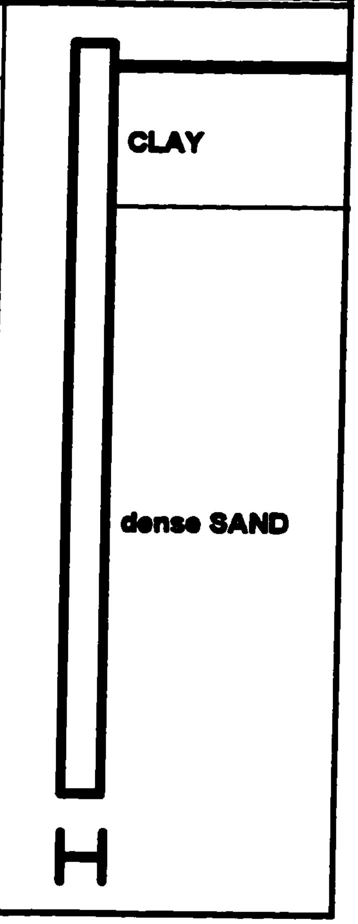

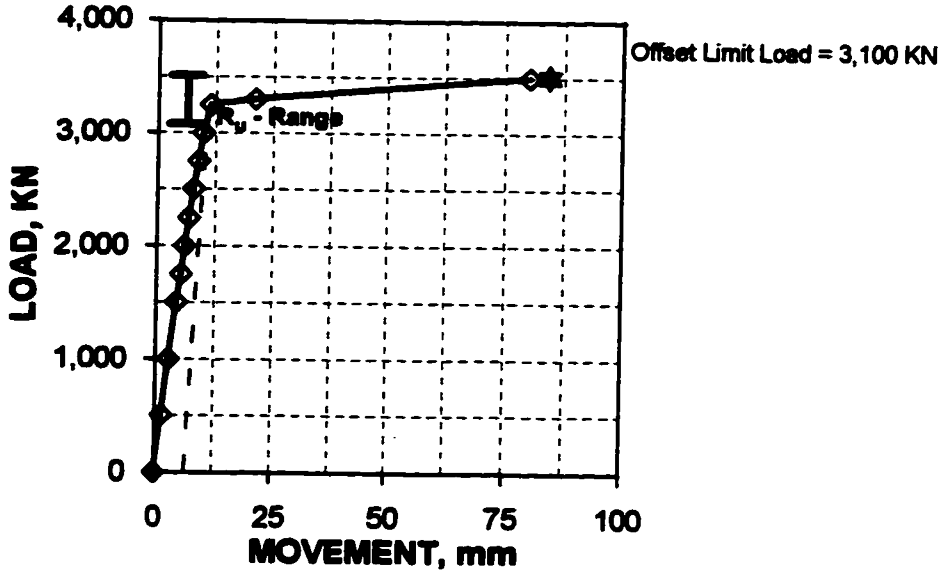

Case 59 MP1
Sheet a CPT data

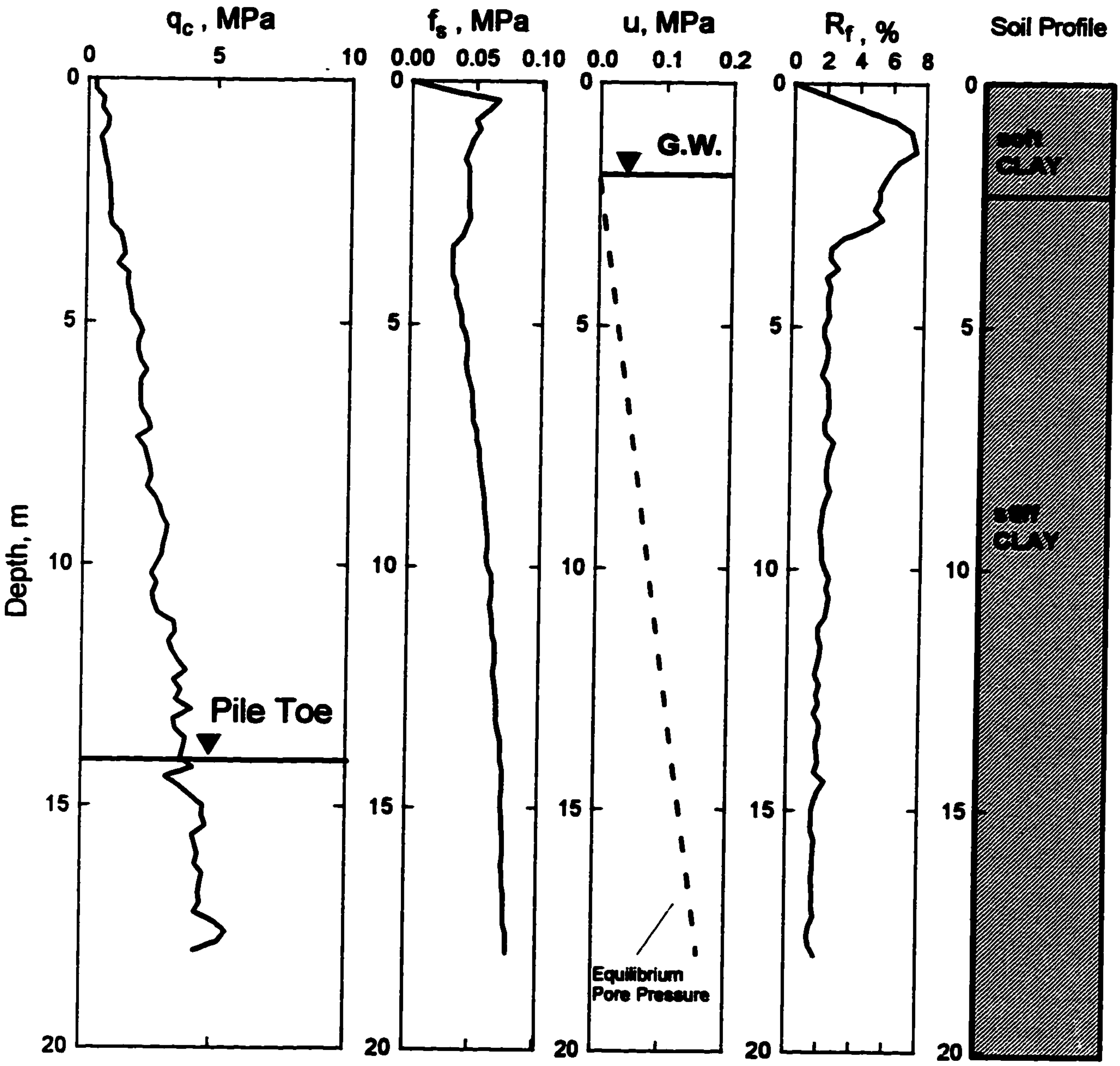

Case 59 MP1
Sheet b Pile data

DETAIL		DESCRIPTION	SCHEMATIC PROFILE
1	Site	Merville, France	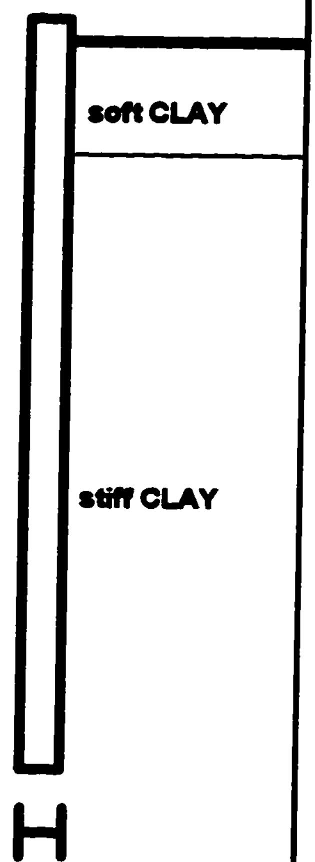
2	Reference	Weber, 1987	
3	Shape, Material, and Installation	H-Pile, Steel, Driven	
4	Diameter, b, and Wall Thickness, t, mm	368*400	
5	Embedment Length D, m	14	
6	Cross Sectional Area A_t, m^2	0.046	
7	Unit Circumferential Area, A_s, m^2/m	1.54	
8	Toe, Closed or Open	Open	
9	Type of Test and Loading	Static Tension, SML	
10	Toe Capacity, R_t, KN	200	
11	Shaft Capacity, R_s, KN	1,925	
12	*Capacity, R_u, KN	2,125	

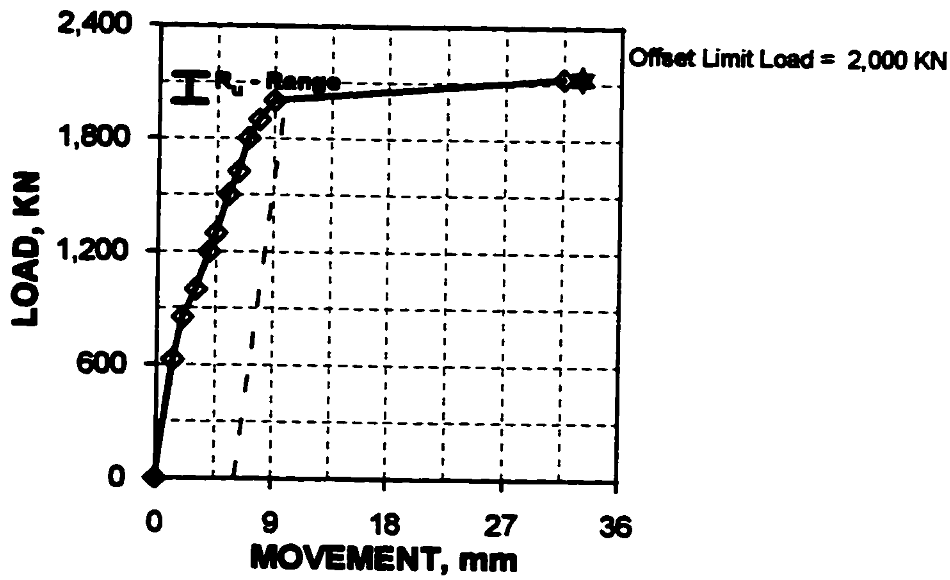

Case 60 KLO14A
Sheet a CPT data

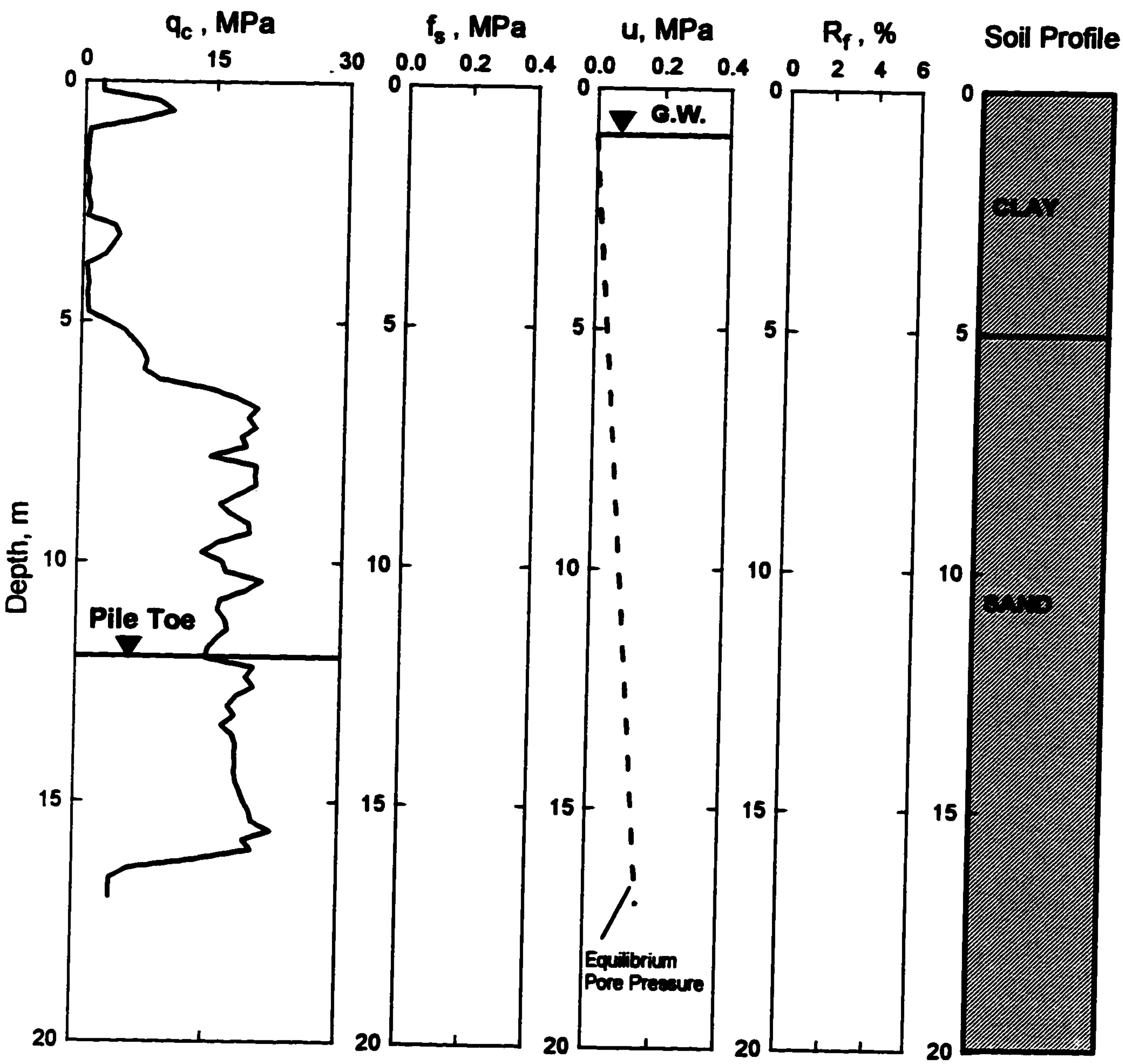

Case 60 KLO14A
Sheet b Pile data

	DETAIL	DESCRIPTION	SCHEMATIC PROFILE
1	Site	Kallo, Belgium	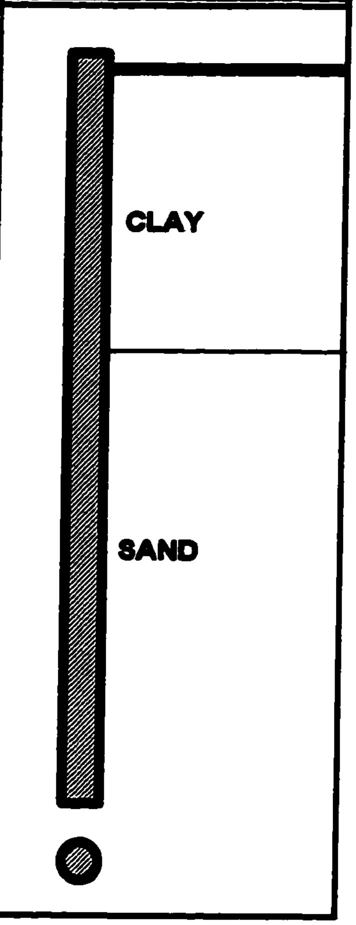
2	Reference	Van Impe and de Beer, 1988	
3	Shape, Material, and Installation	Round, Concrete, Bored	
4	Diameter, b, and Wall Thickness, t, mm	600	
5	Embedment Length D, m	12	
6	Cross Sectional Area A_t, m^2	0.283	
7	Unit Circumferential Area, A_s, m^2/m	1.88	
8	Toe, Closed or Open	Closed	
9	Type of Test and Loading	Static Compression,SML	
10	Toe Capacity, R_t, KN		
11	Shaft Capacity, R_s, KN		
12	*Capacity, R_u, KN	5,500	

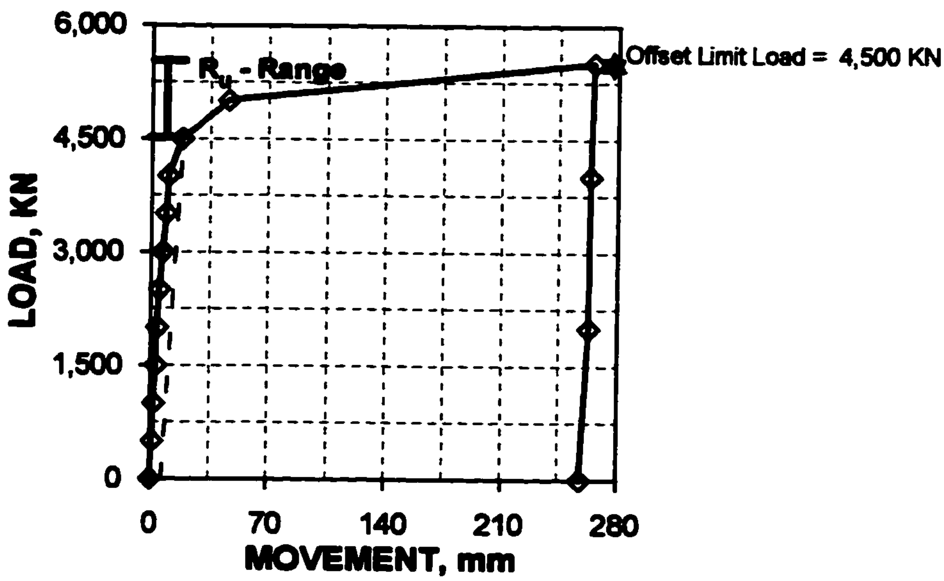

Case 61 KLO14B
Sheet a CPT data

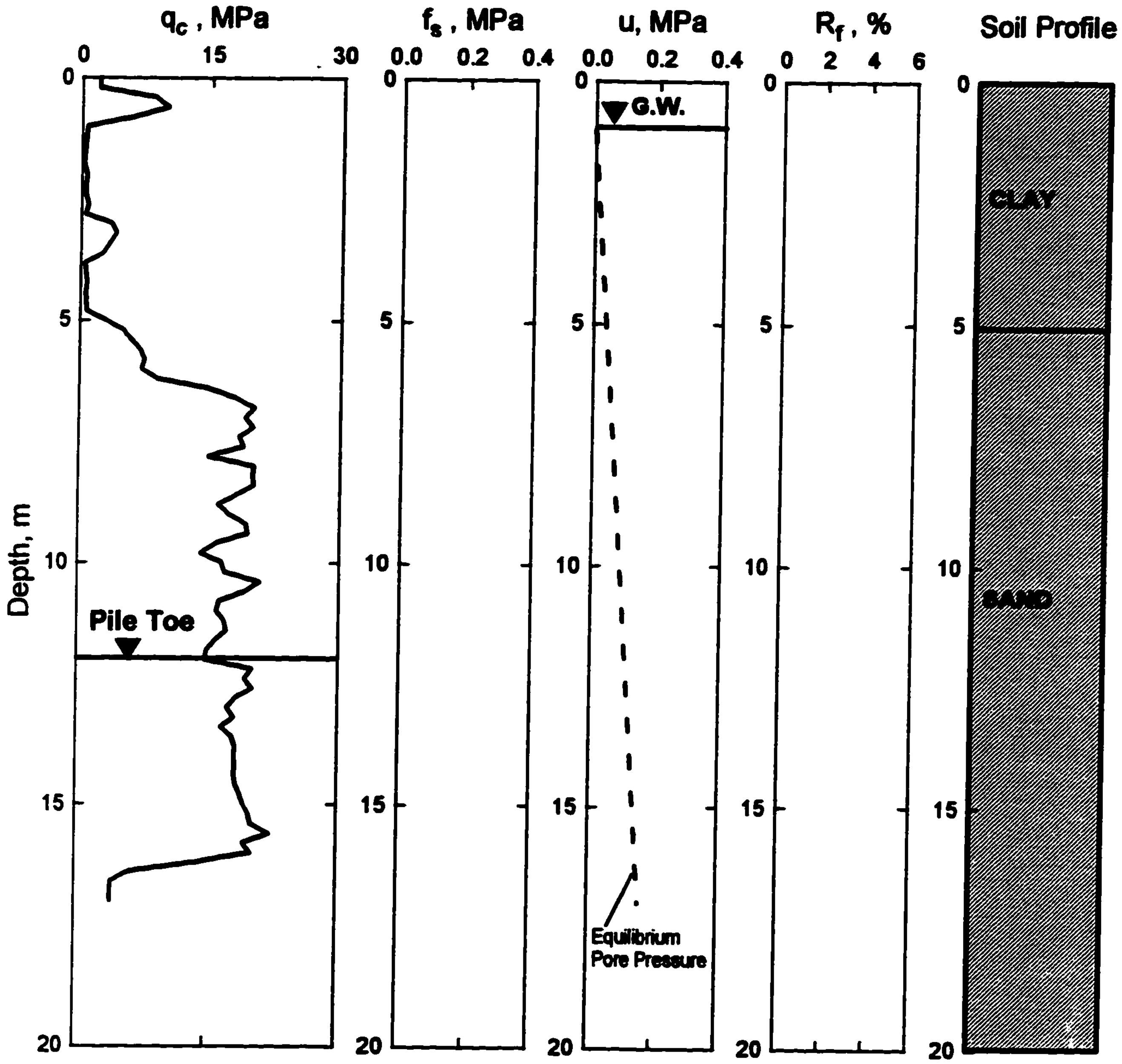

Case 61 KLO14B
Sheet b Pile data

	DETAIL	DESCRIPTION
1	Site	Kallo, Belgium
2	Reference	Van Impe and de Beer, 1988
3	Shape, Material, and Installation	Round, Concrete, Driven
4	Diameter, b, and Wall Thickness, t, mm	600
5	Embedment Length D, m	12
6	Cross Sectional Area A_t, m^2	0.283
7	Unit Circumferential Area, A_s, m^2/m	1.88
8	Toe, Closed or Open	Closed
9	Type of Test and Loading	Static Compression,SML
10	Toe Capacity, R_t, KN	
11	Shaft Capacity, R_s, KN	
12	*Capacity, R_u, KN	6,100

SCHEMATIC PROFILE

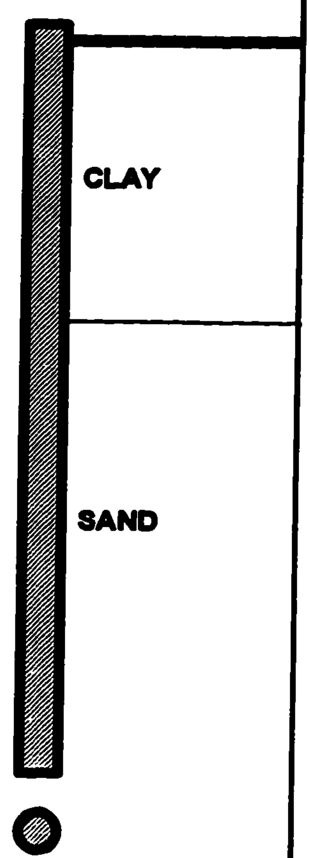

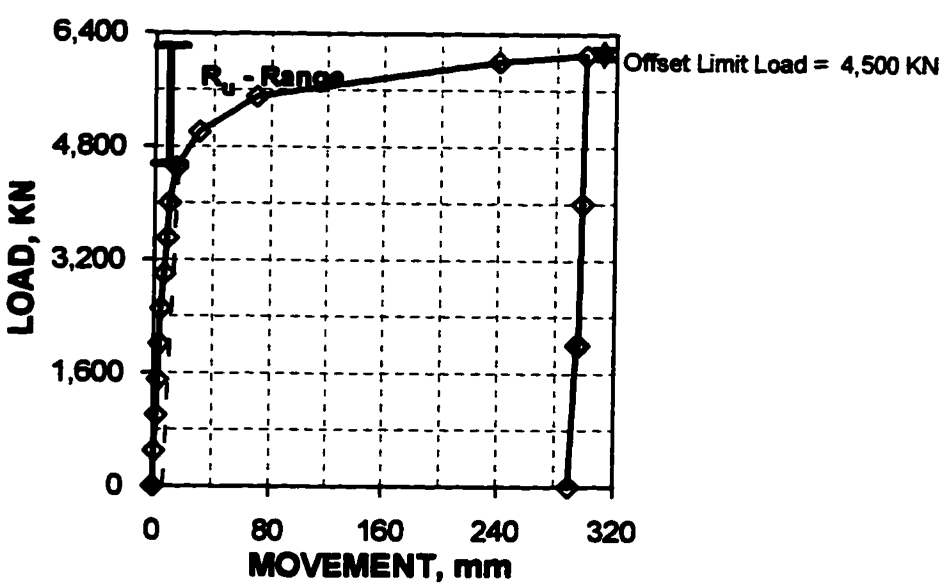

Case 62 A&N1
Sheet a CPT data

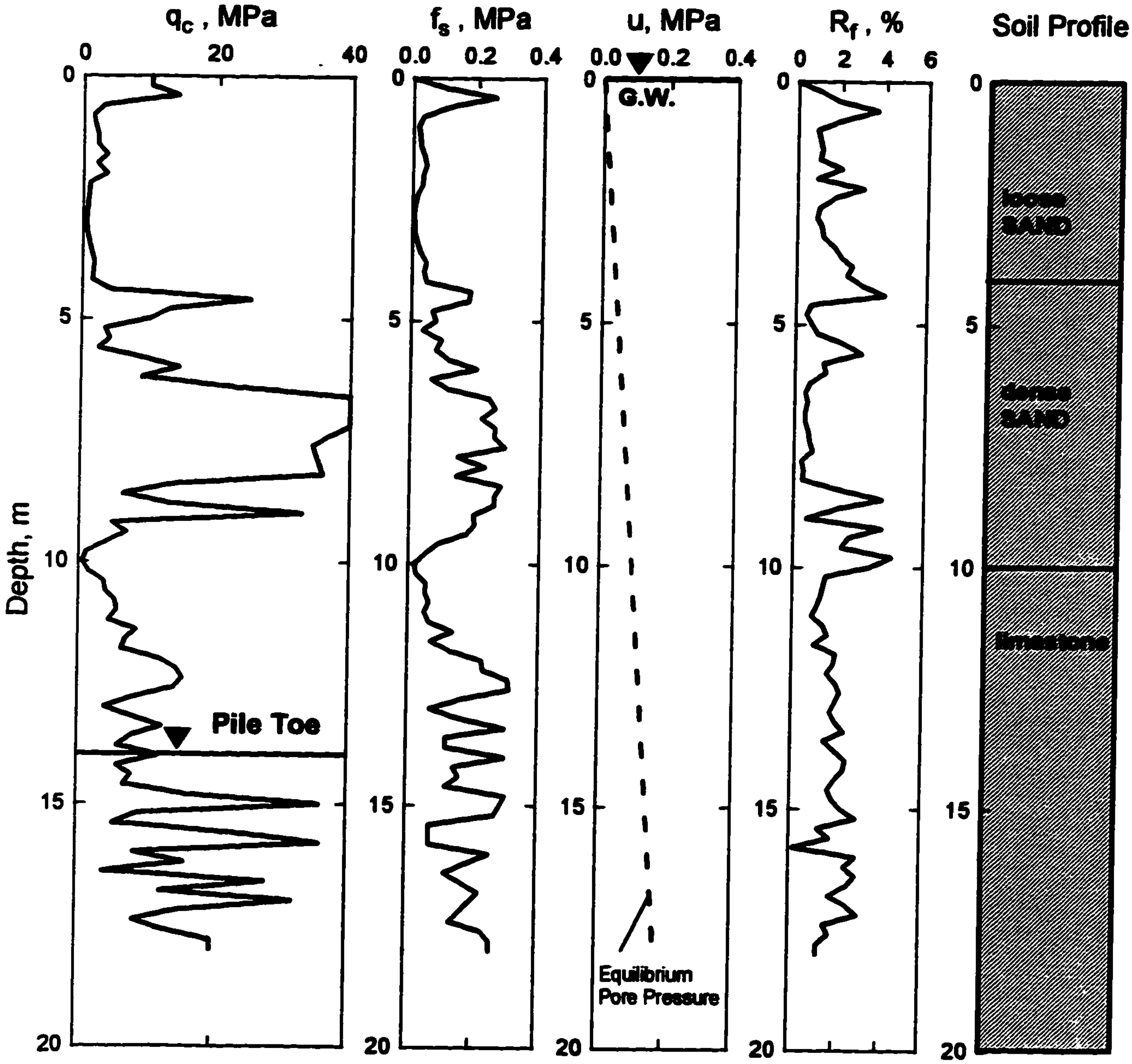

Case 62 A&N1
Sheet b Pile data

DETAIL		DESCRIPTION	SCHEMATIC PROFILE
1	Site	Victoria, Australia	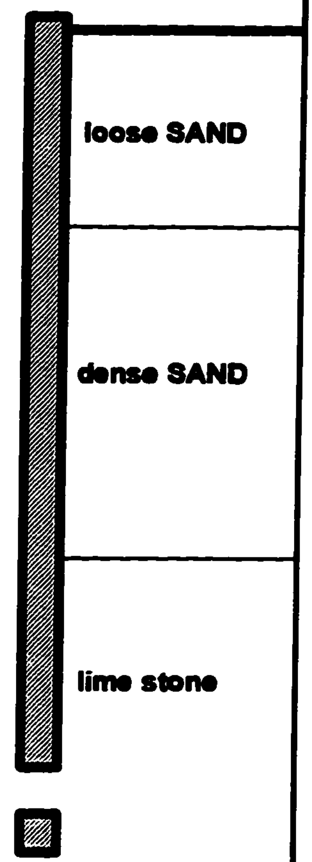
2	Reference	Haustorfer, et al., 1988	
3	Shape, Material, and Installation	Square, Concrete, Driven	
4	Diameter, b, and Wall Thickness, t, mm	450	
5	Embedment Length D, m	14	
6	Cross Sectional Area A_t, m^2	0.203	
7	Unit Circumferential Area, A_s, m^2/m	1.8	
8	Toe, Closed or Open	Closed	
9	Type of Test and Loading	Dynamic Testing	
10	Toe Capacity, R_t, KN	1,500 (from CAPWAP analysis)	
11	Shaft Capacity, R_s, KN	2,350 (from CAPWAP analysis)	
12	*Capacity, R_u, KN	3,850	

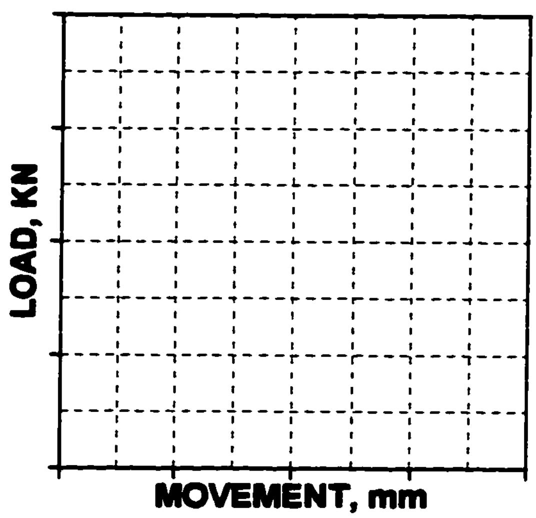

Case 63 A&N2
Sheet a CPT data

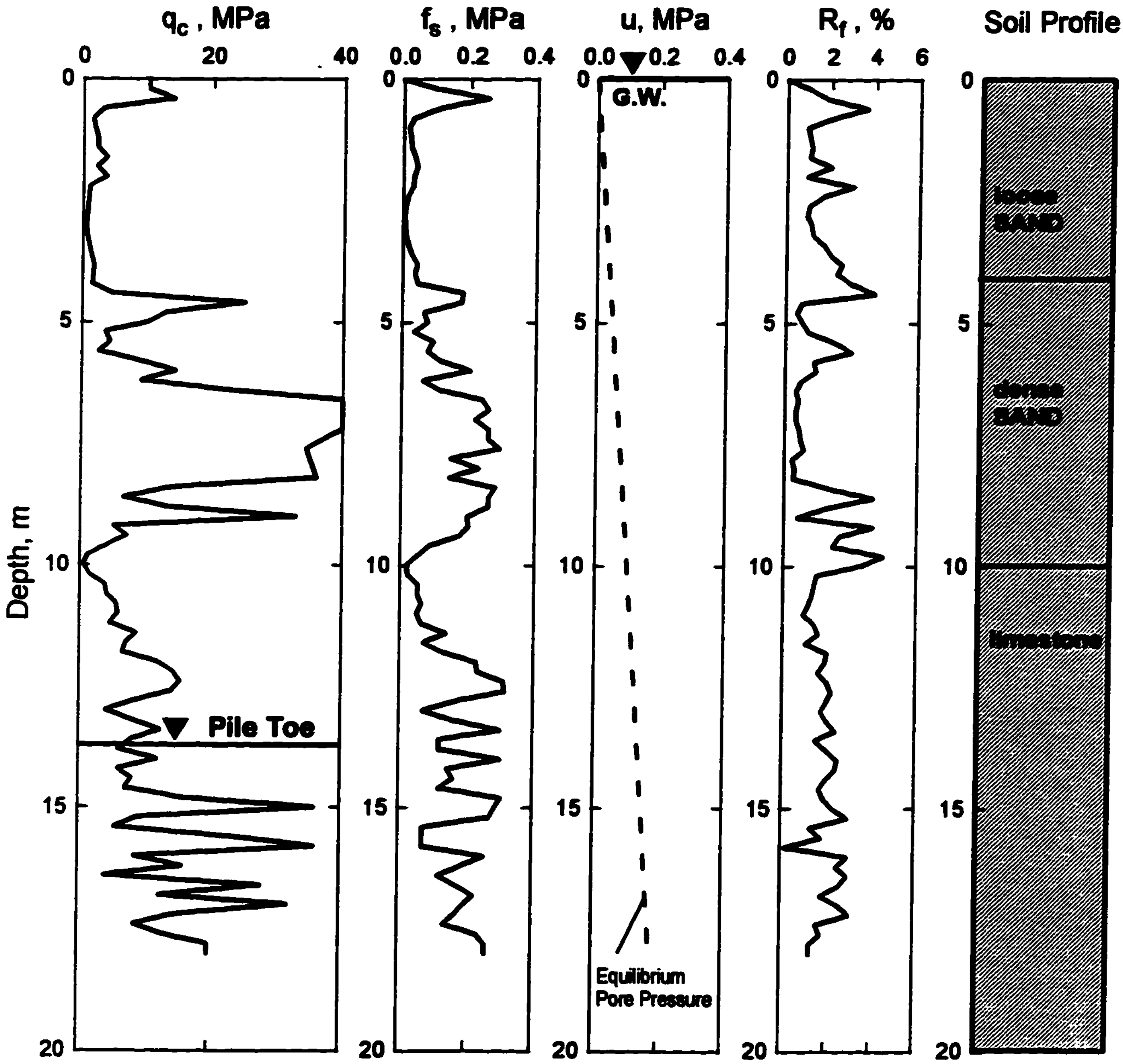

Case 63 A&N2
Sheet b Pile data

	DETAIL	DESCRIPTION	SCHEMATIC PROFILE
1	Site	Victoria, Australia	
2	Reference	Haustorfer, et al., 1988	
3	Shape, Material, and Installation	Square, Concrete, Driven	
4	Diameter, b, and Wall Thickness, t, mm	450	
5	Embedment Length D, m	13.75	
6	Cross Sectional Area A_t, m^2	0.203	
7	Unit Circumferential Area, A_s, m^2/m	1.8	
8	Toe, Closed or Open	Closed	
9	Type of Test and Loading	Static Compression, SML	
10	Toe Capacity, R_t, KN	1,900	
11	Shaft Capacity, R_s, KN	2,350	
12	*Capacity, R_u, KN	4,250	

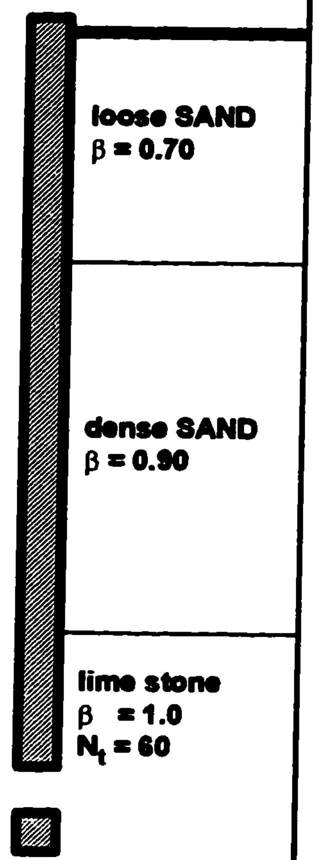

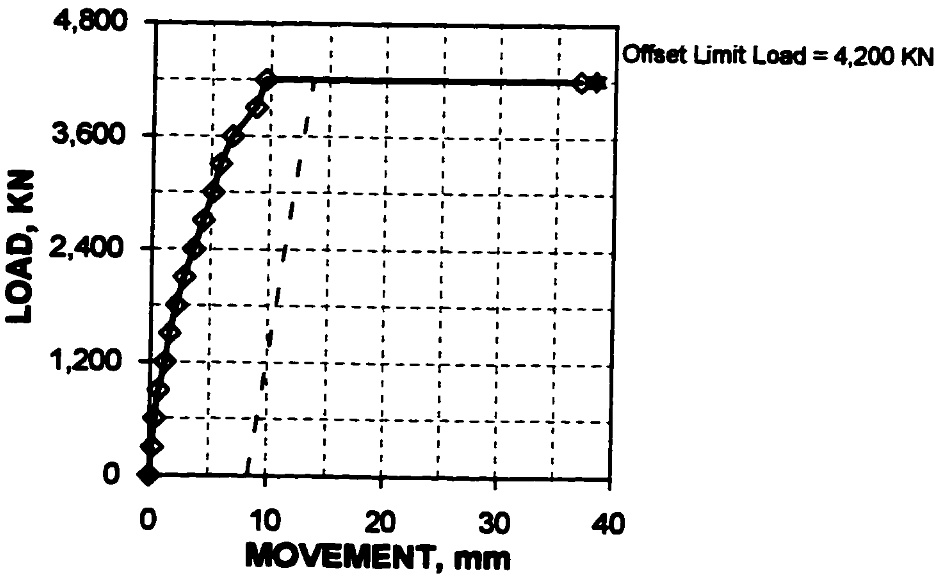

Case 64 A&N3
Sheet a CPT data

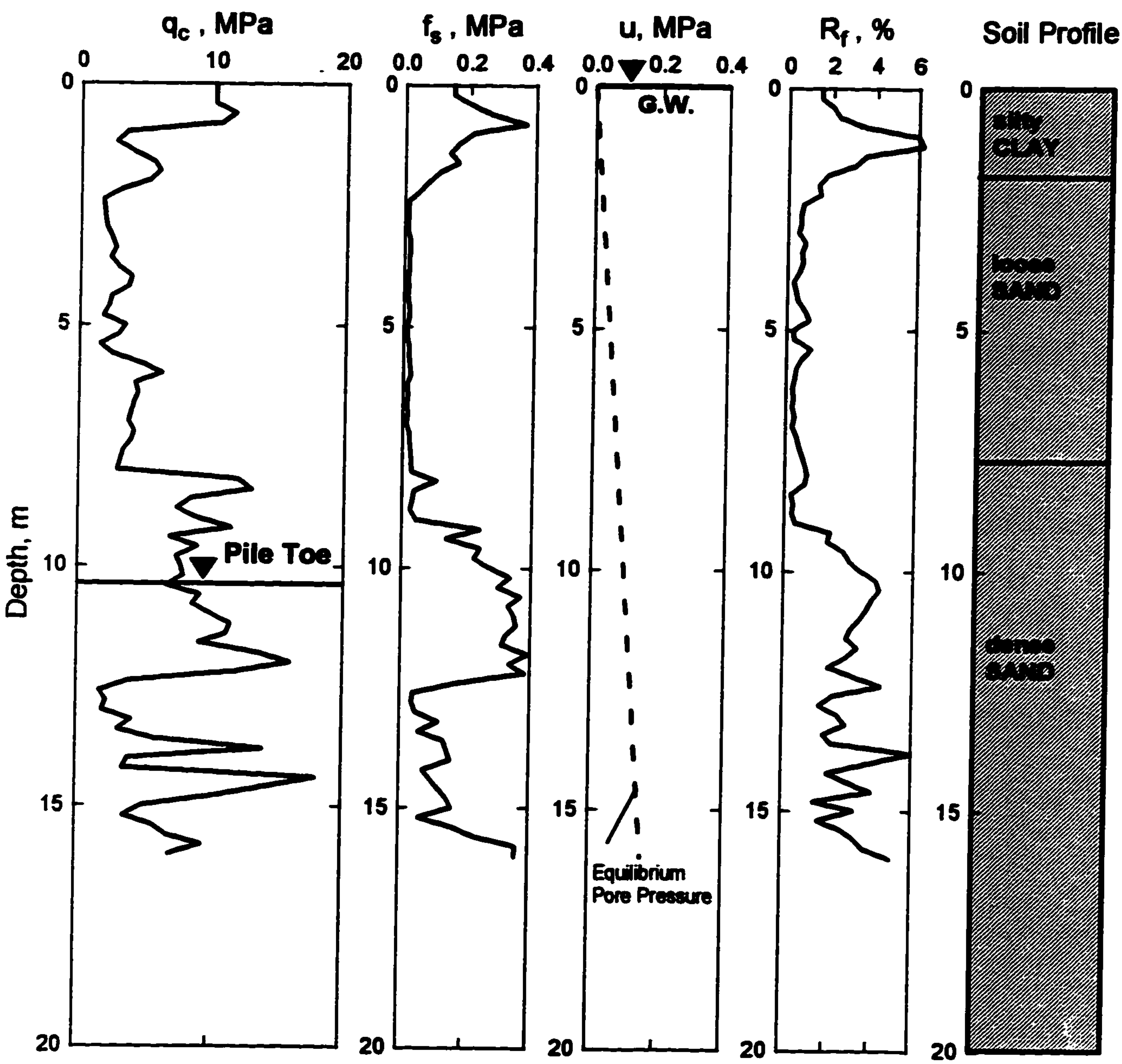

Case 64 A&N3
Sheet b Pile data

	DETAIL	DESCRIPTION
1	Site	Victoria, Australia
2	Reference	Haustorfer, et al., 1988
3	Shape, Material, and Installation	Square, Concrete, Driven
4	Diameter, b, and Wall Thickness, t, mm	355
5	Embedment Length D, m	10.2
6	Cross Sectional Area A_t, m²	0.126
7	Unit Circumferential Area, A_s, m² /m	1.42
8	Toe, Closed or Open	Closed
9	Type of Test and Loading	Static Compression, SML
10	Toe Capacity, R_t, KN	
11	Shaft Capacity, R_s, KN	
12	*Capacity, R_u, KN	1,300

SCHEMATIC PROFILE

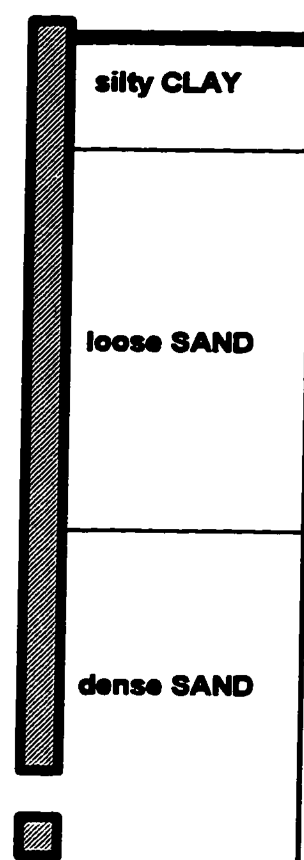

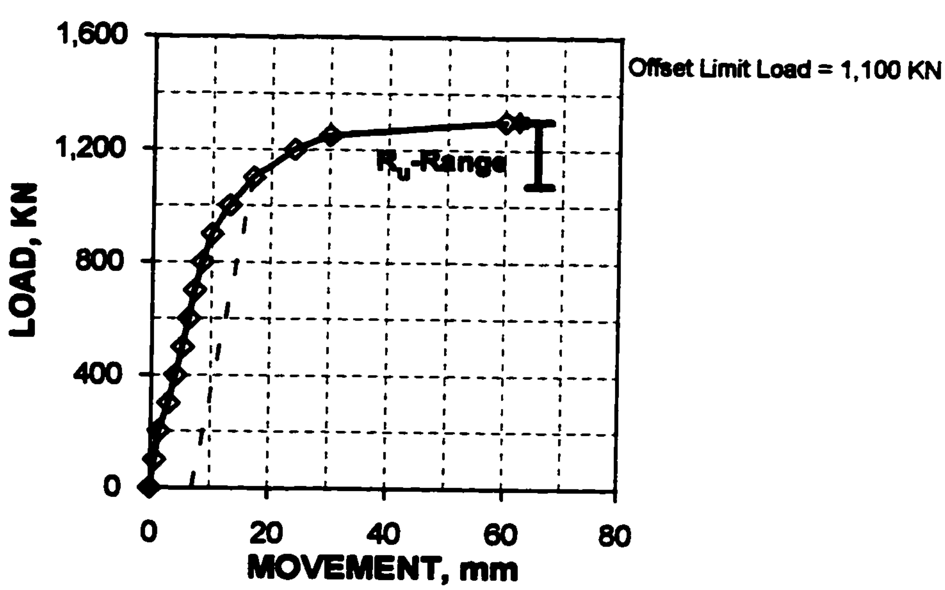

Case 65 LTN930
Sheet a CPT data

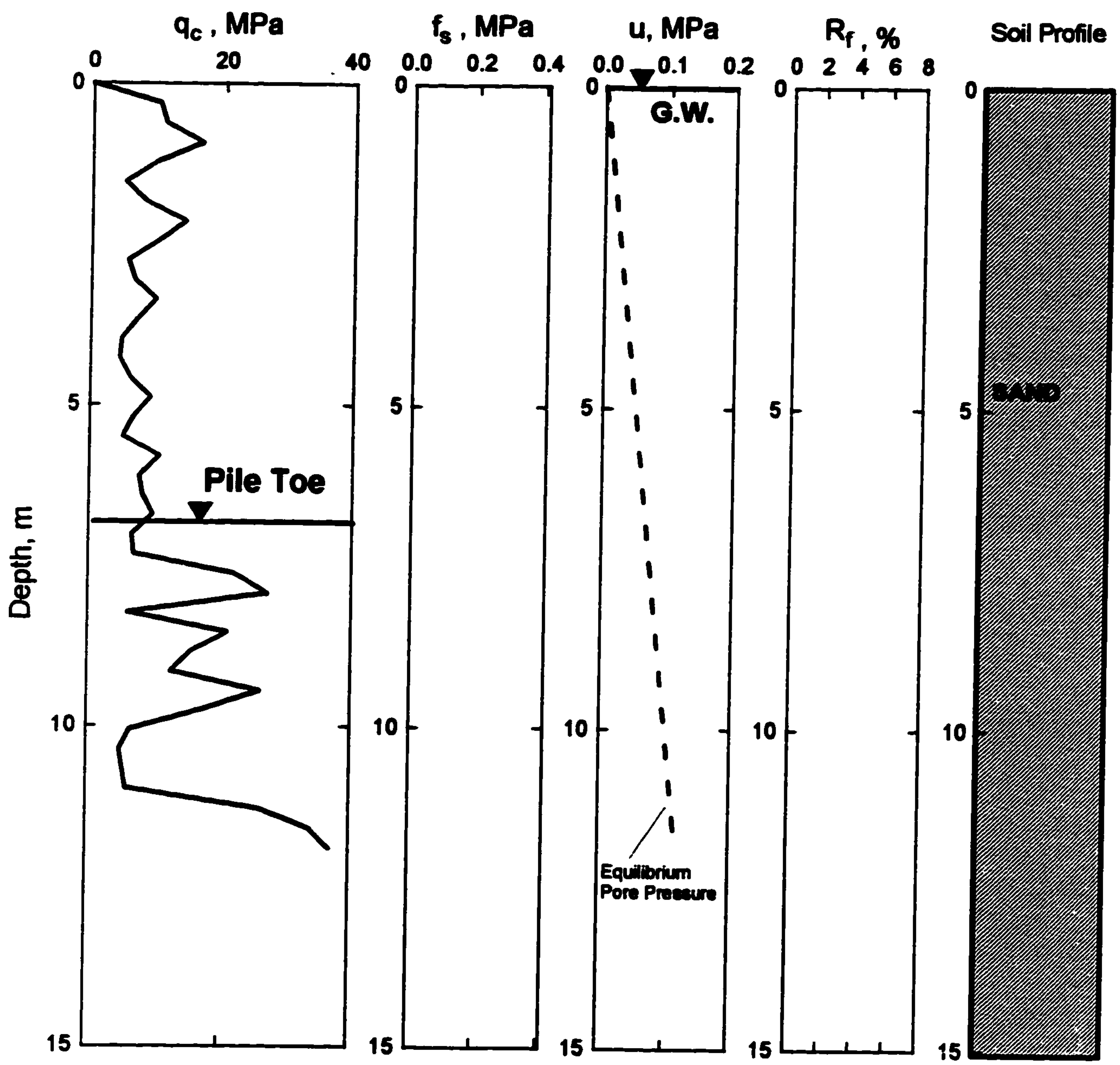

Case 65 LTN 930
Sheet b Pile data

DETAIL		DESCRIPTION
1	Site	California, USA
2	Reference	Richmann et al., 1989
3	Shape, Material, and Installation	Round, Concrete, Bored
4	Diameter, b, and Wall Thickness, t, mm	400
5	Embedment Length D, m	6.5
6	Cross Sectional Area A_t, m²	0.126
7	Unit Circumferential Area, A_s, m²/m	1.26
8	Toe, Closed or Open	Closed
9	Type of Test and Loading	Static Compression,SML
10	Toe Capacity, R_t, KN	
11	Shaft Capacity, R_s, KN	
12	*Capacity, R_u, KN	1,385

SCHEMATIC PROFILE

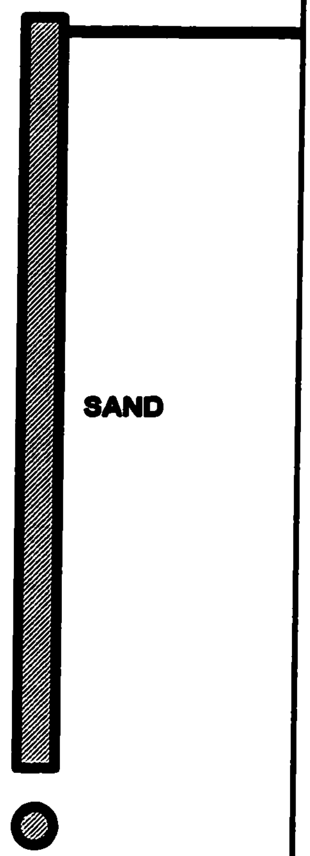

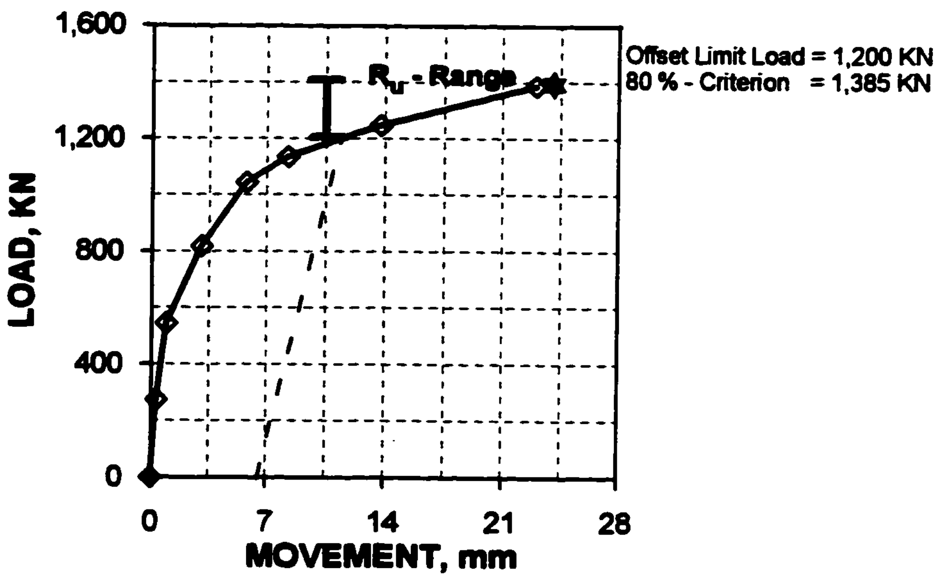

Case 66 LTN938
Sheet a CPT data

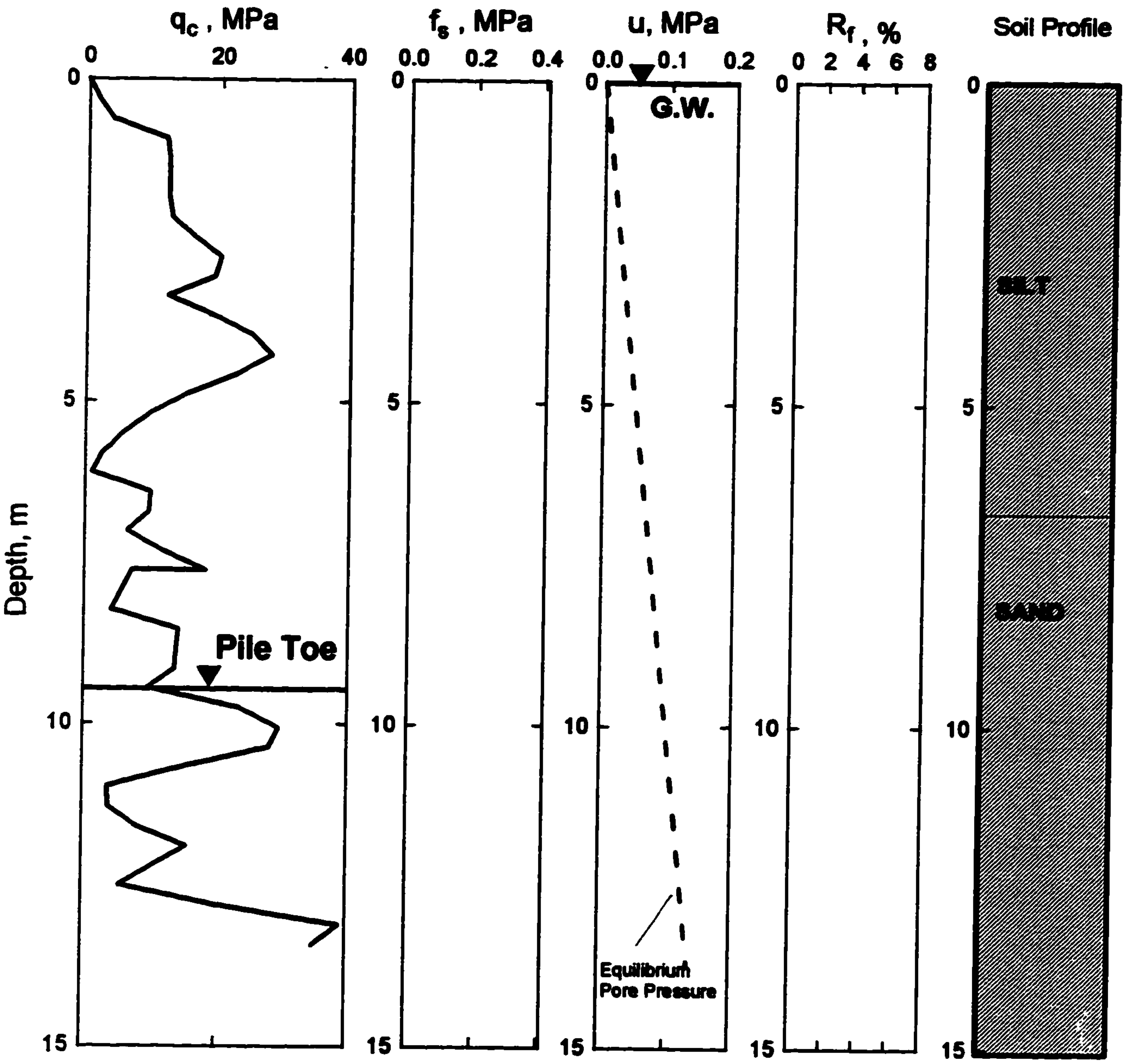

Case 66 LTN 938
Sheet b Pile data

	DETAIL	DESCRIPTION	SCHEMATIC PROFILE
1	Site	California, USA	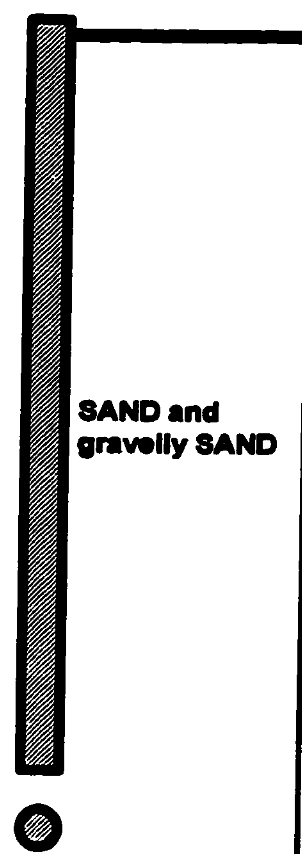
2	Reference	Richmann et al., 1989	
3	Shape, Material, and Installation	Round, Concrete, Bored	
4	Diameter, b, and Wall Thickness, t, mm	400	
5	Embedment Length D, m	9.3	
6	Cross Sectional Area A_t, m^2	0.126	
7	Unit Circumferential Area, A_s, m^2/m	1.26	
8	Toe, Closed or Open	Closed	
9	Type of Test and Loading	Static Compression,SML	
10	Toe Capacity, R_t, KN		
11	Shaft Capacity, R_s, KN		
12	*Capacity, R_u, KN	1,370	

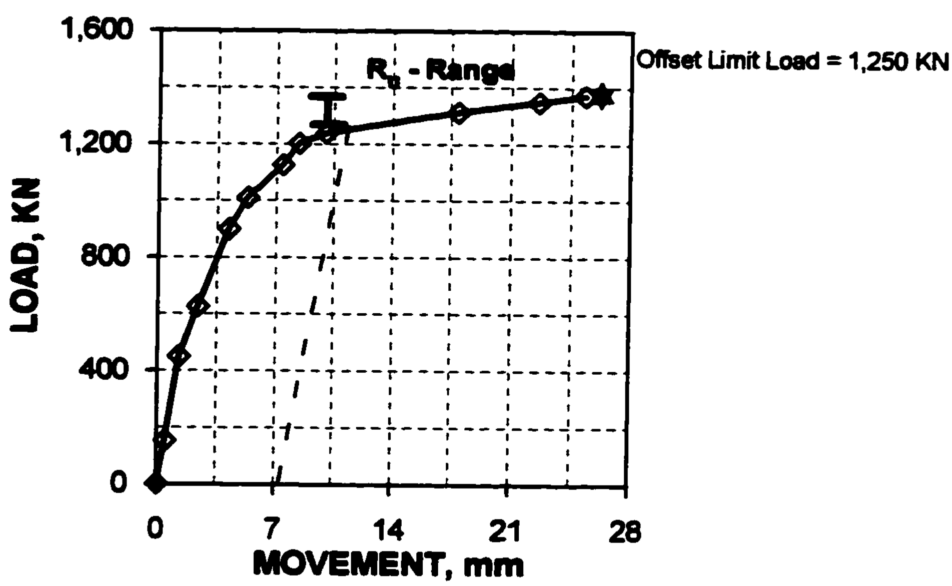

Case 67 USPB1
Sheet a CPT data

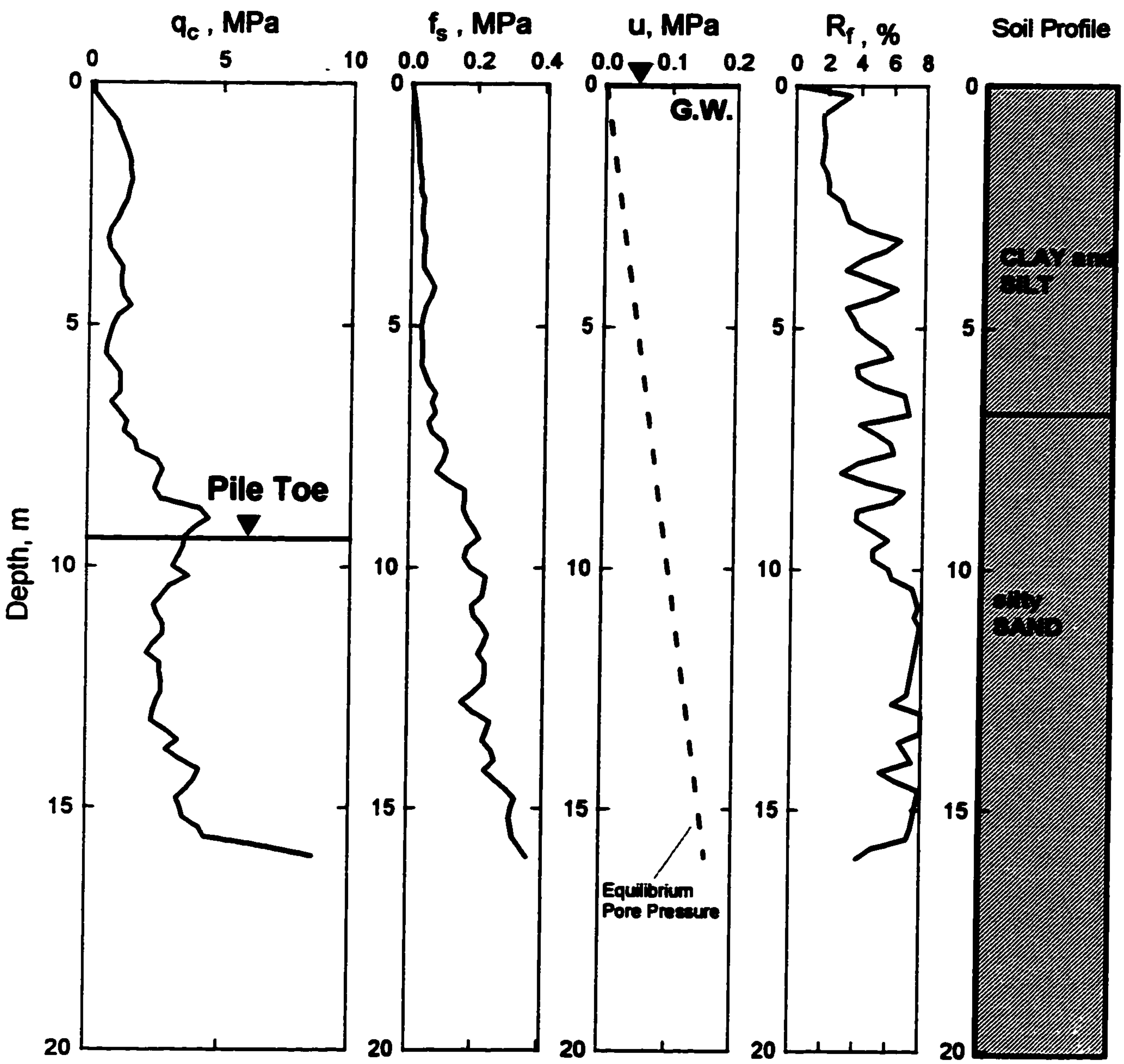

Case 67 USPB1
Sheet b Pile data

DETAIL		DESCRIPTION
1	Site	Sao Poulo, Brazil
2	Reference	Albiero et al., 1995
3	Shape, Material, and Installation	Round, Concrete, Bored
4	Diameter, b, and Wall Thickness, t, mm	350
5	Embedment Length D, m	9.4
6	Cross Sectional Area A_t, m^2	0.096
7	Unit Circumferential Area, A_s, m^2/m	1.1
8	Toe, Closed or Open	Closed
9	Type of Test and Loading	Static Compression,SML
10	Toe Capacity, R_t, KN	240
11	Shaft Capacity, R_s, KN	405
12	*Capacity, R_u, KN	645

SCHEMATIC PROFILE

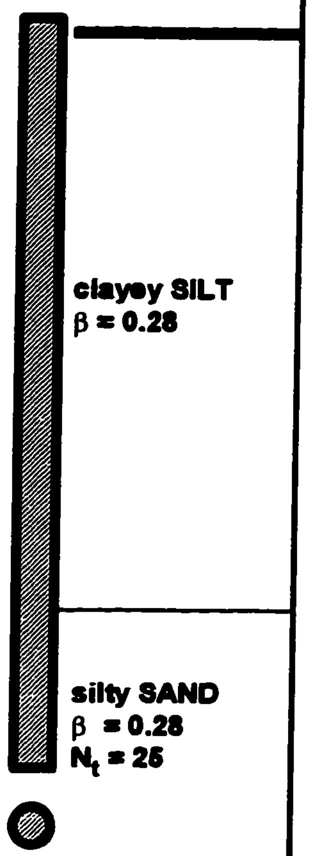

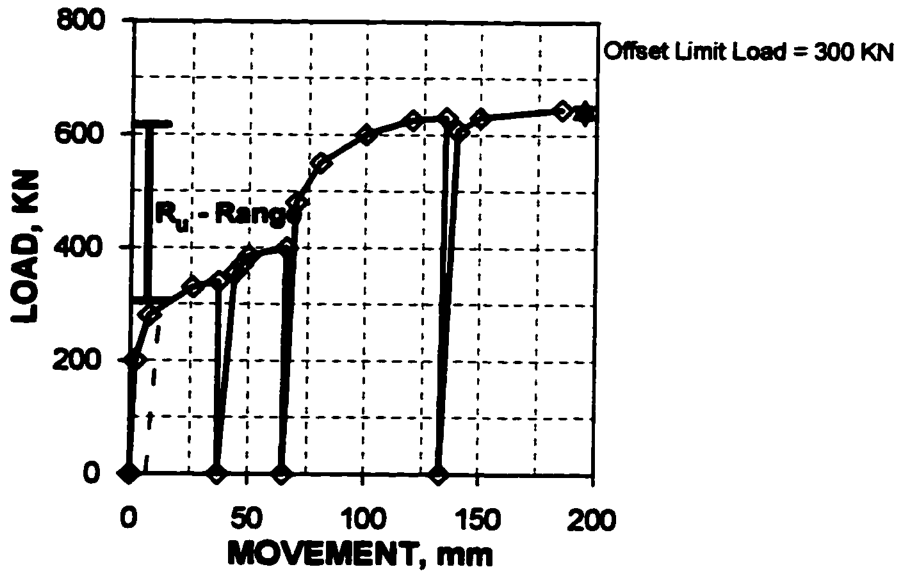

Case 68 USPB2
Sheet a CPT data

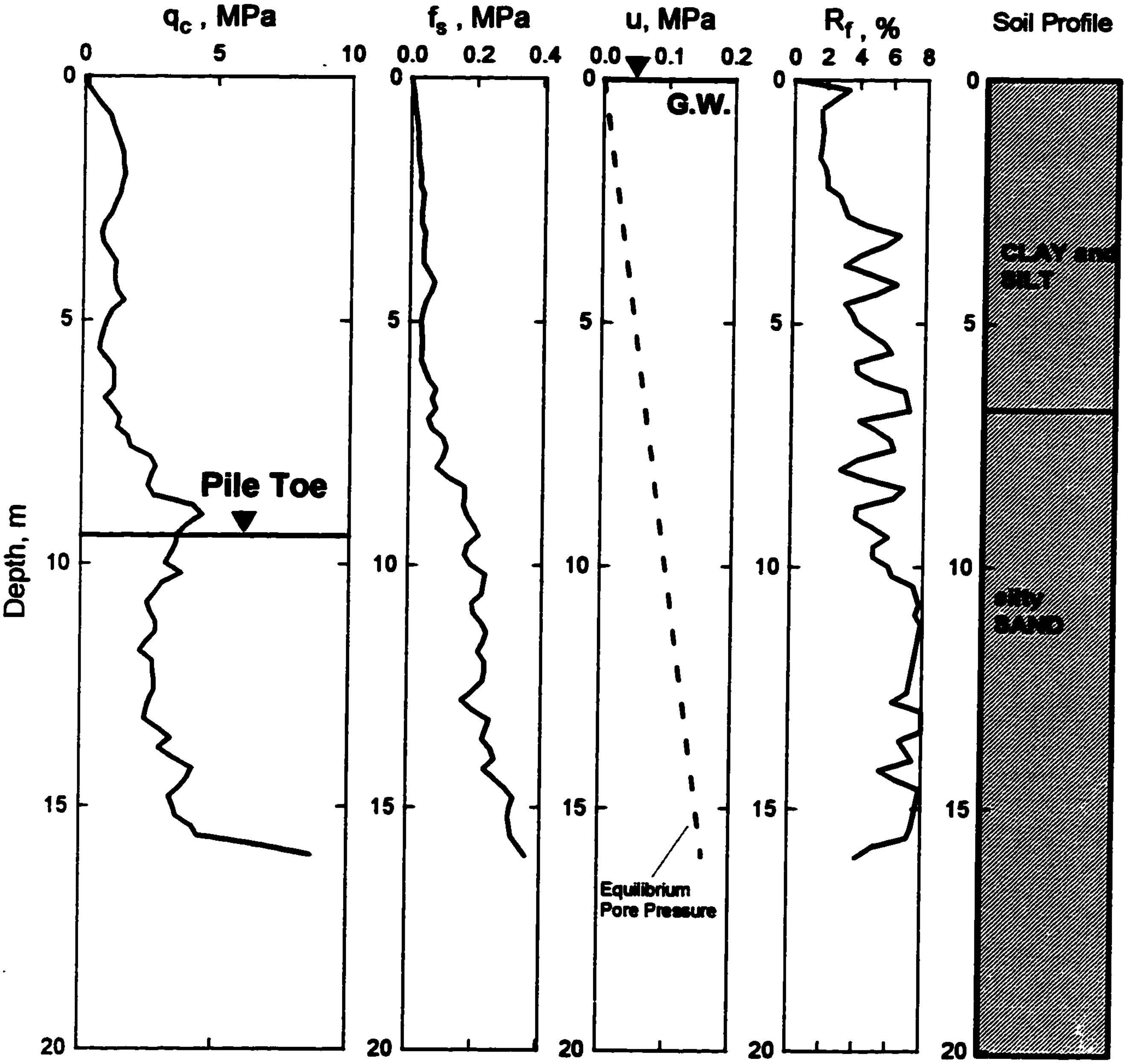

Case 68 USPB2
Sheet b Pile data

	DETAIL	DESCRIPTION	SCHEMATIC PROFILE
1	Site	Sao Poulo, Brazil	
2	Reference	Albiero et al., 1995	
3	Shape, Material, and Installation	Round, Concrete, Bored	
4	Diameter, b, and Wall Thickness, t, mm	400	
5	Embedment Length D, m	9.4	
6	Cross Sectional Area A_t, m^2	0.126	
7	Unit Circumferential Area, A_s, m^2/m	1.26	
8	Toe, Closed or Open	Closed	
9	Type of Test and Loading	Static Compression,SML	
10	Toe Capacity, R_t, KN	310	
11	Shaft Capacity, R_s, KN	415	
12	*Capacity, R_u, KN	725	

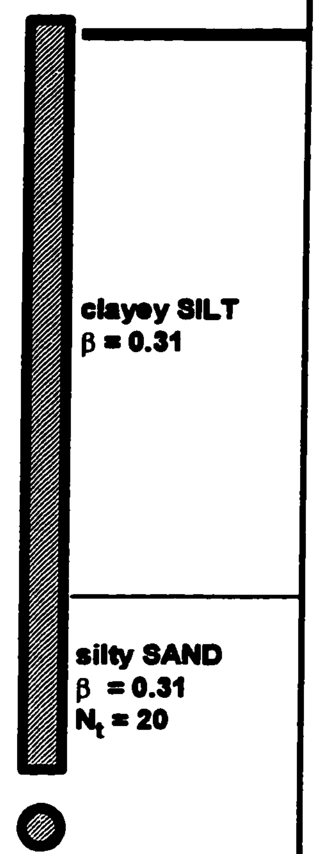

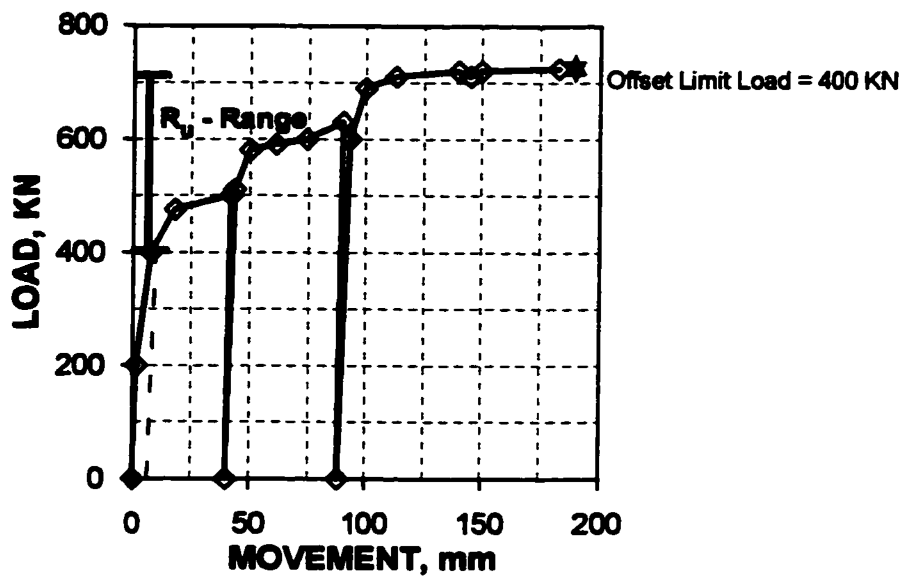

Case 69 PTSER
Sheet a CPT data

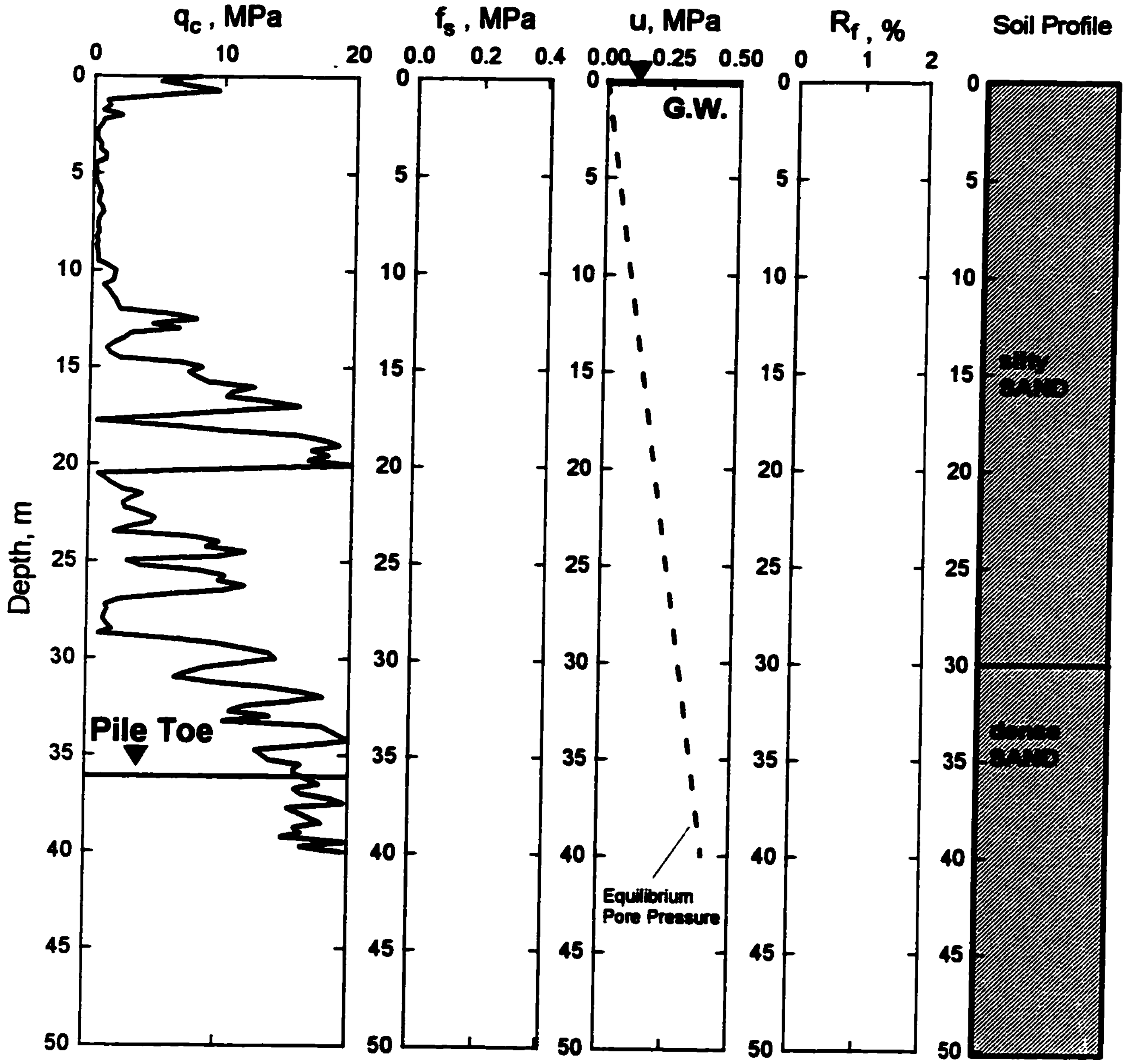

Case 69 PTSER
Sheet b Pile data

	DETAIL	DESCRIPTION
1	Site	Porto Tole Italy
2	Reference	Apendino, 1981
3	Shape, Material, and Installation	Round, Concrete, Driven
4	Diameter, b, and Wall Thickness, t, mm	508
5	Embedment Length D, m	35.85
6	Cross Sectional Area A_t, m^2	0.202
7	Unit Circumferential Area, A_s, m^2/m	1.6
8	Toe, Closed or Open	Closed
9	Type of Test and Loading	Static Compression,SML
10	Toe Capacity, R_t, KN	3,000
11	Shaft Capacity, R_s, KN	2,500
12	*Capacity, R_u, KN	5,500

SCHEMATIC PROFILE

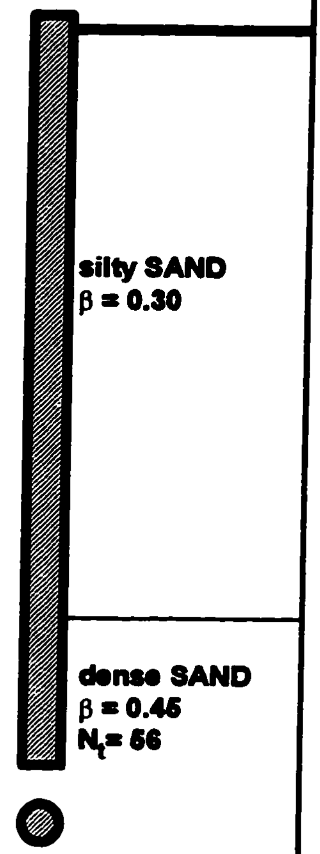

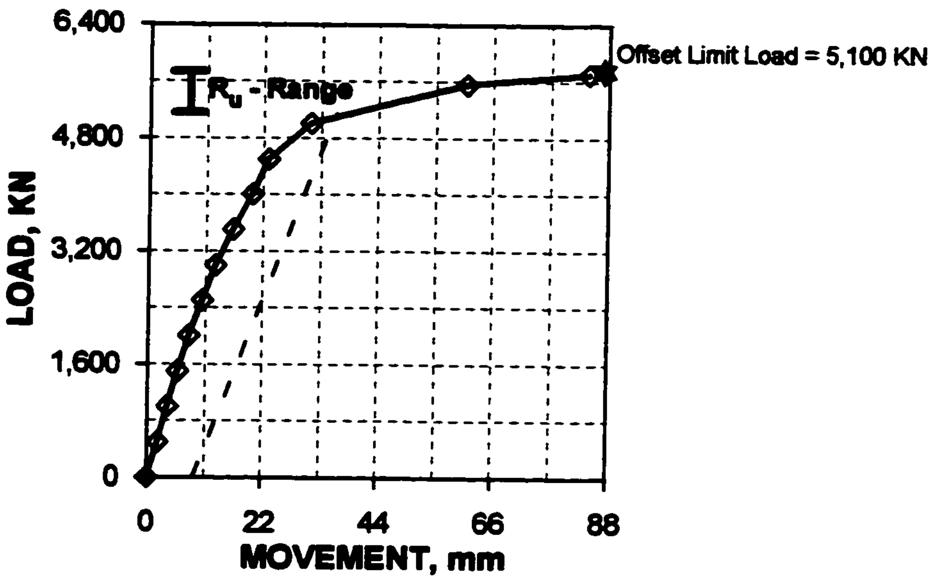

Case 70 PT361
Sheet a CPT data

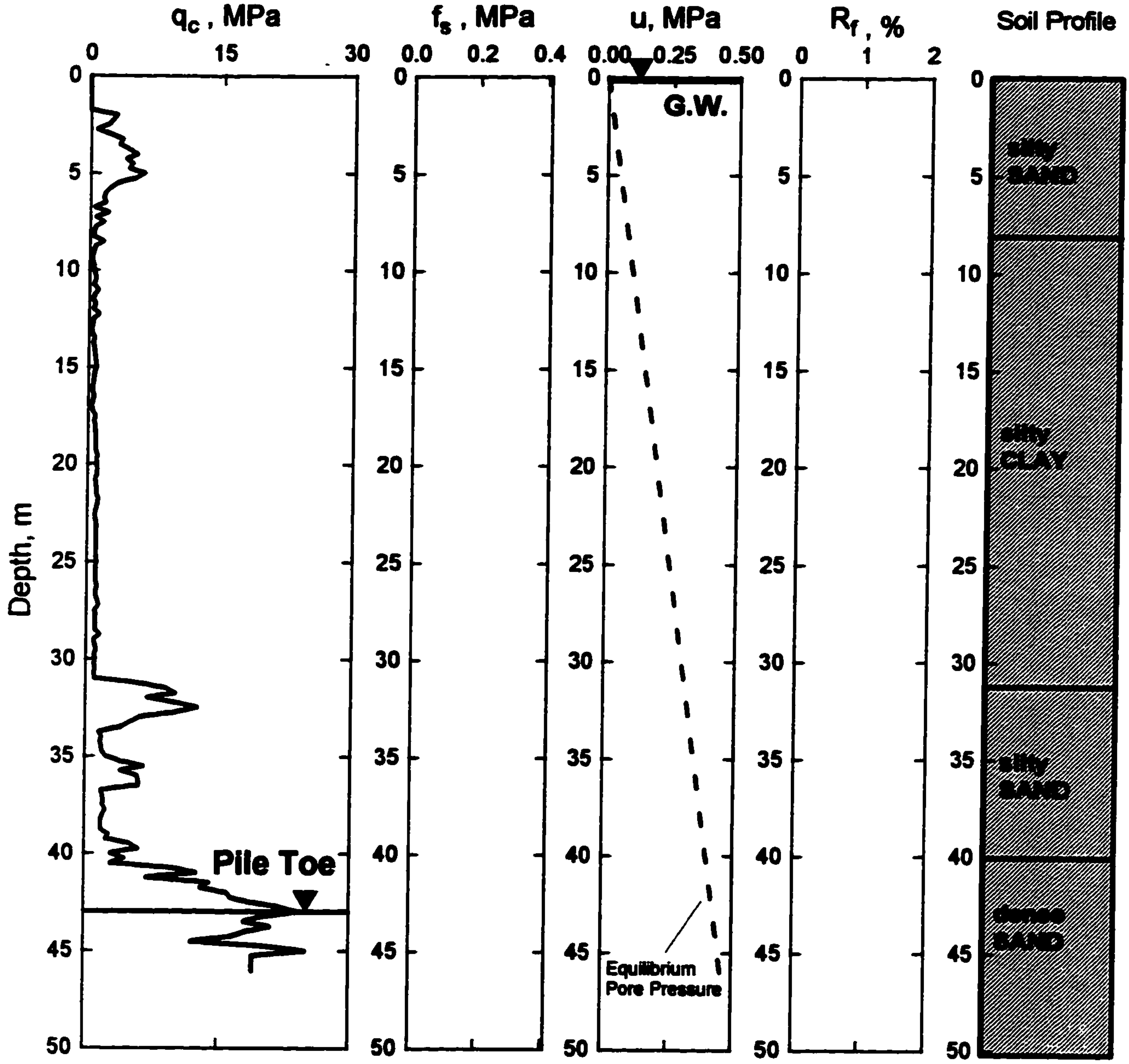

Case 70 PT361
Sheet b Pile data

	DETAIL	DESCRIPTION
1	Site	Porto Tole Italy
2	Reference	Apendino, 1981
3	Shape, Material, and Installation	Round, Concrete, Driven
4	Diameter, b, and Wall Thickness, t, mm	508
5	Embedment Length D, m	43
6	Cross Sectional Area A_t, m^2	0.202
7	Unit Circumferential Area, A_s, m^2/m	1.6
8	Toe, Closed or Open	Closed
9	Type of Test and Loading	Static Compression,SML
10	Toe Capacity, R_t, KN	2,600
11	Shaft Capacity, R_s, KN	3,400
12	*Capacity, R_u, KN	6,000

SCHEMATIC PROFILE

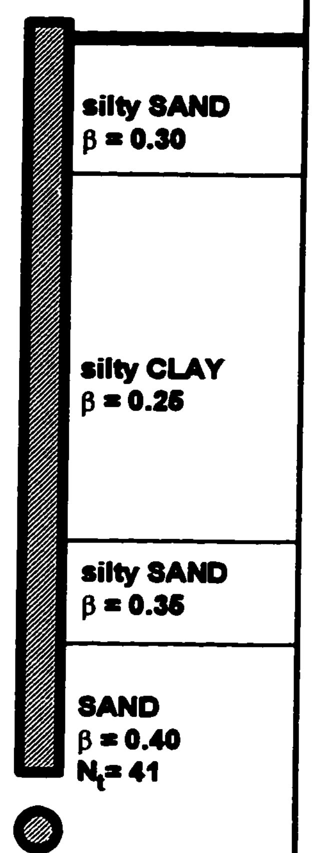

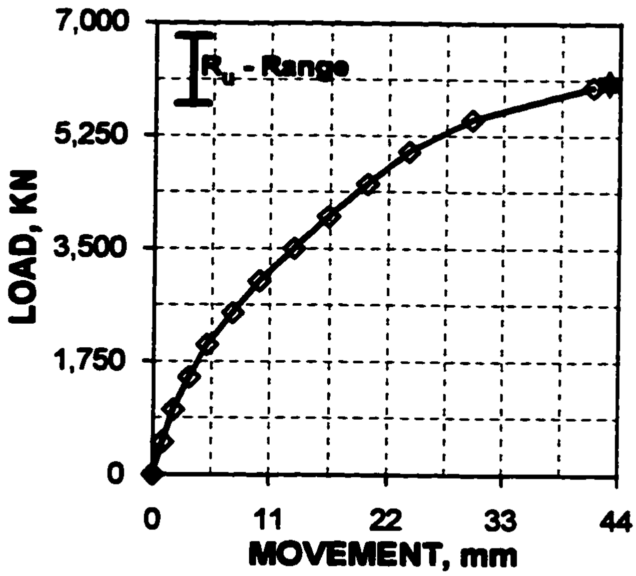

Case 71 N&SWB1
Sheet a CPT data

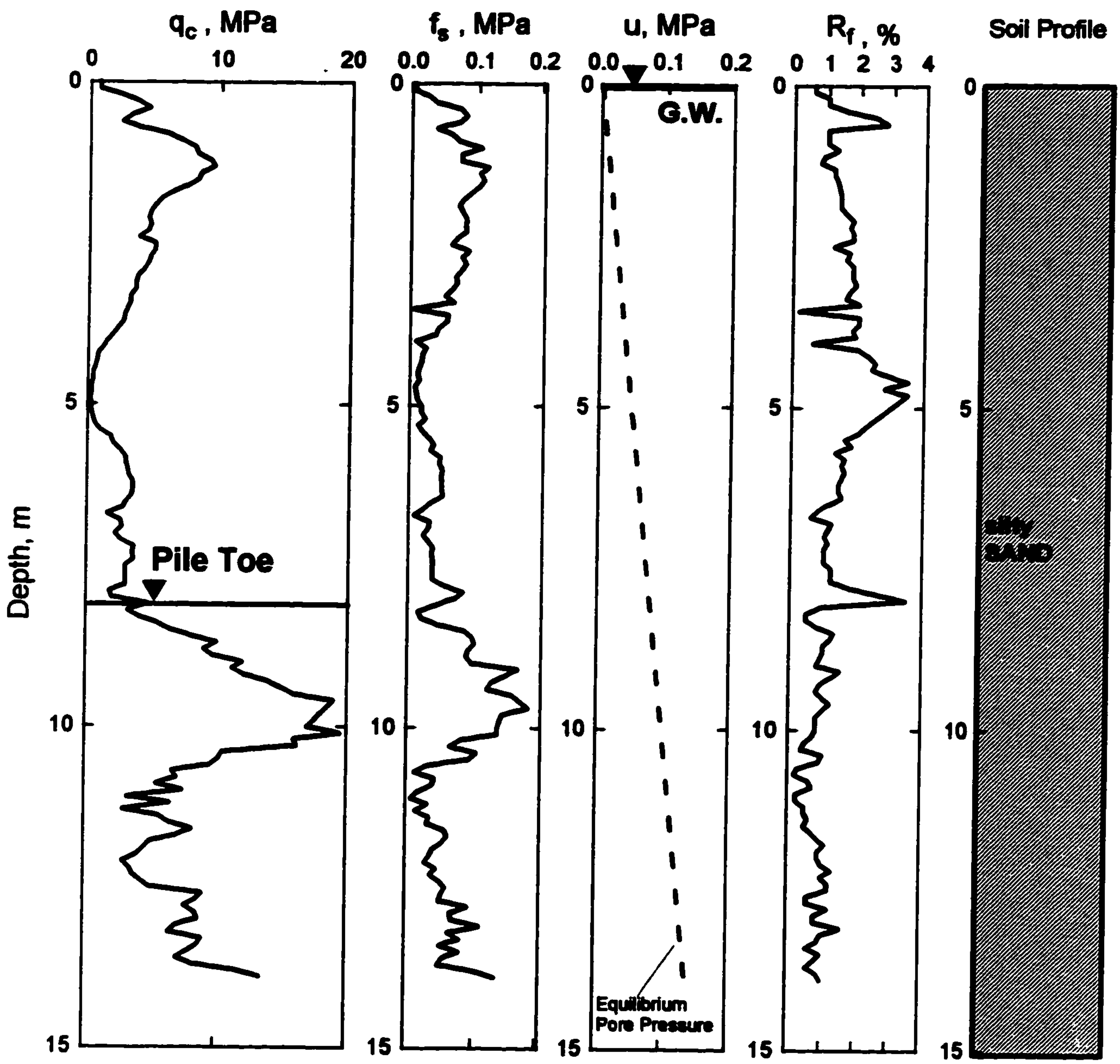

Case 71 N&SWP1
Sheet b Pile data

No.	CASE	DESCRIPTION	SCHEMATIC PROFILE
1	Site	West Palm Beach, USA	
2	Reference	Nottingham, 1975	
3	Shape, Material, and Installation	Square, Concrete, Driven	
4	Diameter, b, and Wall Thickness, t, mm	450	
5	Embedment Length D, m	8	
6	Cross Sectional Area A_t, m^2	0.203	
7	Unit Circumferential Area, A_s, m^2/m	1.8	
8	Toe, Closed or Open	Closed	
9	Type of Test and Loading	Static Compression, SML	
10	Toe Capacity, R_t, KN		
11	Shaft Capacity, R_s, KN		
12	*Capacity, R_u, KN	1,140	

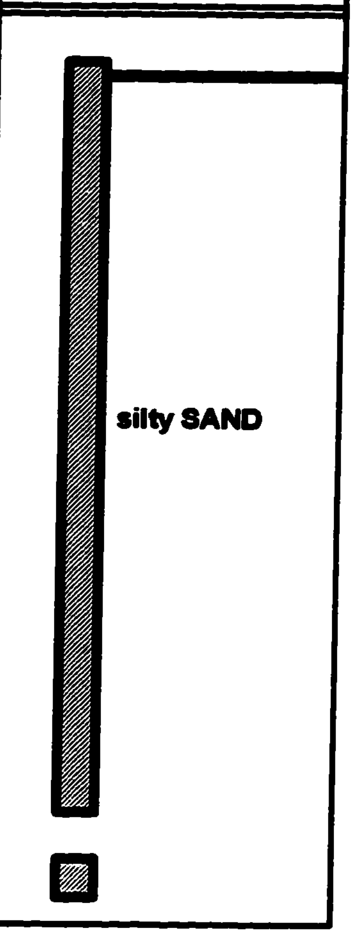

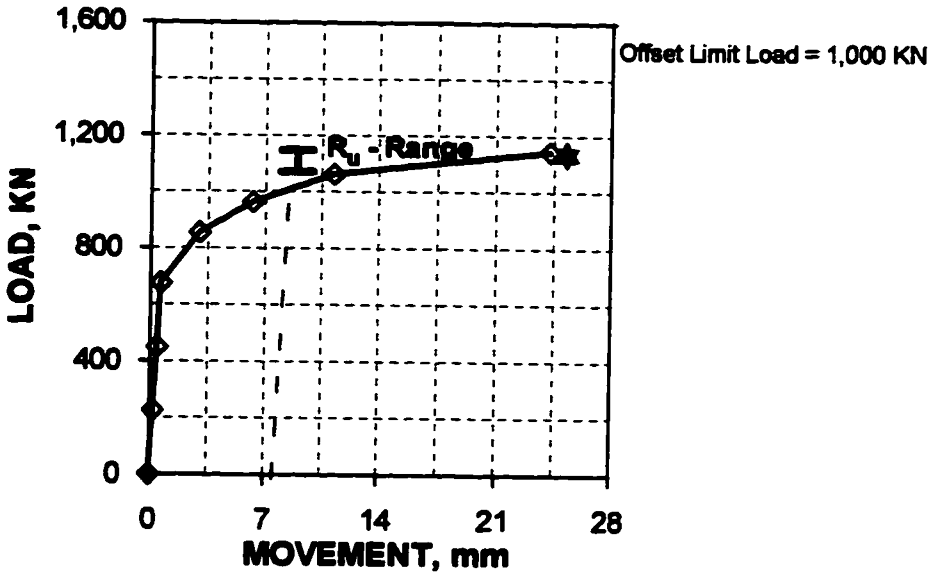

Case 72 N&SWB2
Sheet a CPT data

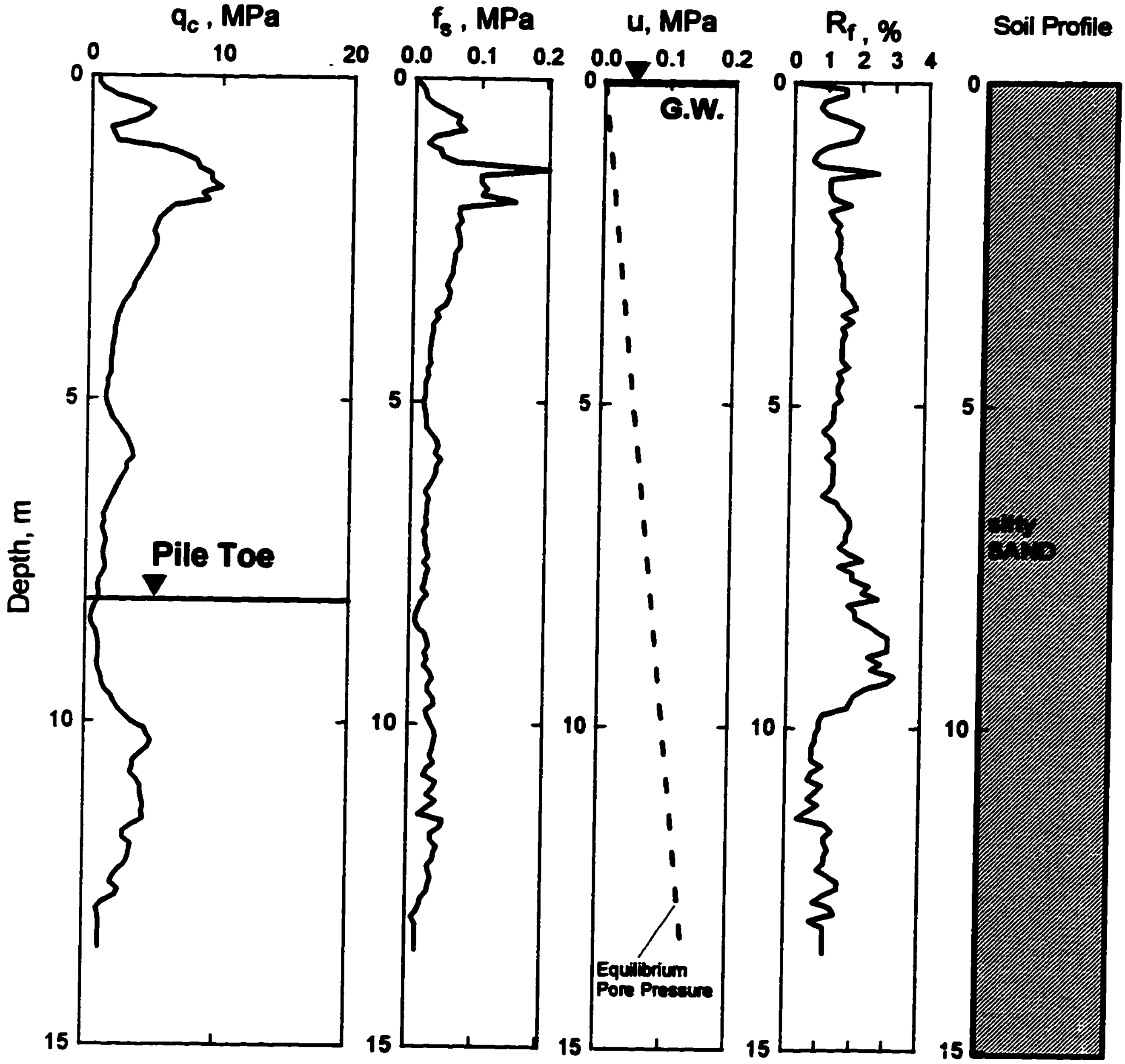

Case 72 N&SWP2
Sheet b Pile data

No.	CASE	DESCRIPTION	SCHEMATIC PROFILE
1	Site	West Palm Beach, USA	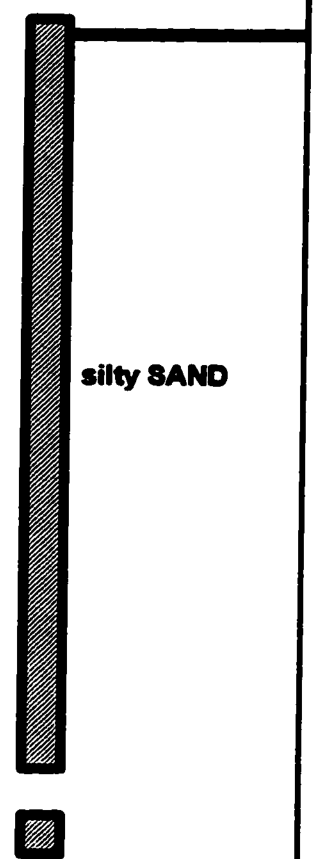
2	Reference	Nottingham, 1975	
3	Shape, Material, and Installation	Square, Concrete, Driven	
4	Diameter, b, and Wall Thickness, t, mm	450	
5	Embedment Length D, m	11.3	
6	Cross Sectional Area A_t, m^2	0.203	
7	Unit Circumferential Area, A_s, m^2 /m	1.8	
8	Toe, Closed or Open	Closed	
9	Type of Test and Loading	Static Compression, SML	
10	Toe Capacity, R_t, KN		
11	Shaft Capacity, R_s, KN		
12	*Capacity, R_u, KN	830	

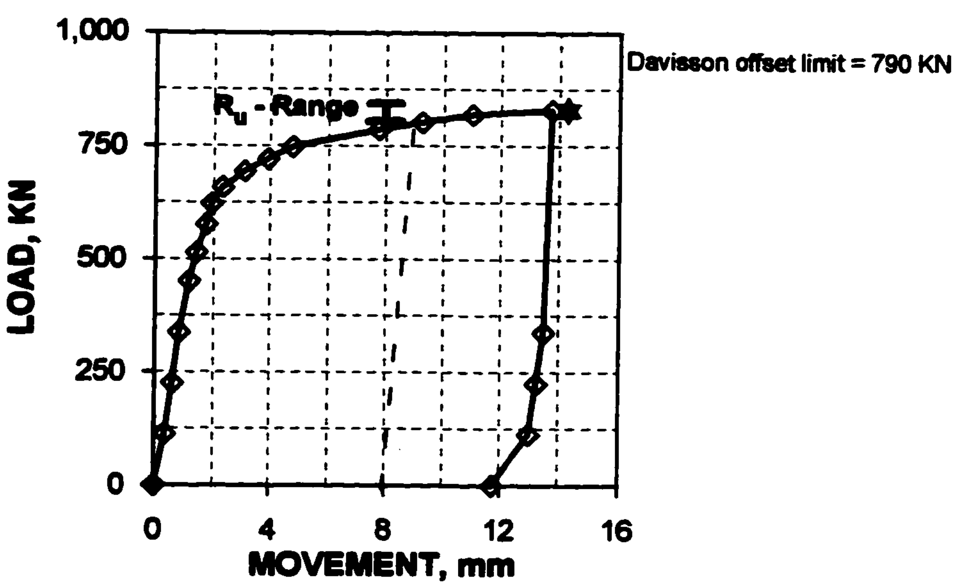

Case 73 N&SJC1
Sheet a CPT data

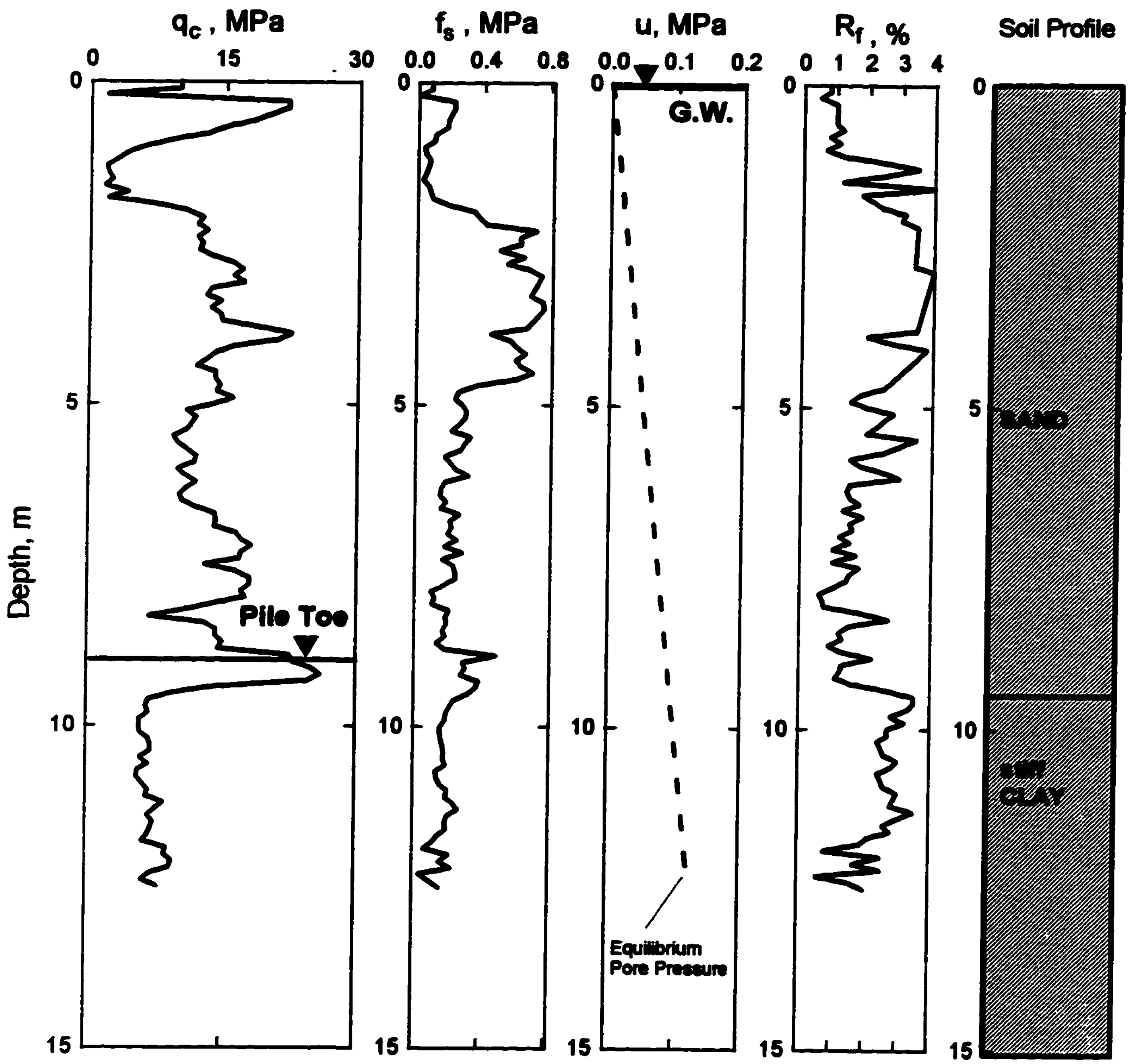

Case 73 N&SJC1
Sheet b Pile data

	DETAIL	DESCRIPTION
1	Site	Jefferson County, USA
2	Reference	Nottingham, 1975
3	Shape, Material, and Installation	Square, Concrete, Driven
4	Diameter, b, and Wall Thickness, t, mm	450
5	Embedment Length D, m	9.15
6	Cross Sectional Area A_t, m^2	0.203
7	Unit Circumferential Area, A_s, m^2 /m	1.8
8	Toe, Closed or Open	Closed
9	Type of Test and Loading	Static Compression, SML
10	Toe Capacity, R_t, KN	
11	Shaft Capacity, R_s, KN	
12	*Capacity, R_u, KN	1,845

SCHEMATIC PROFILE

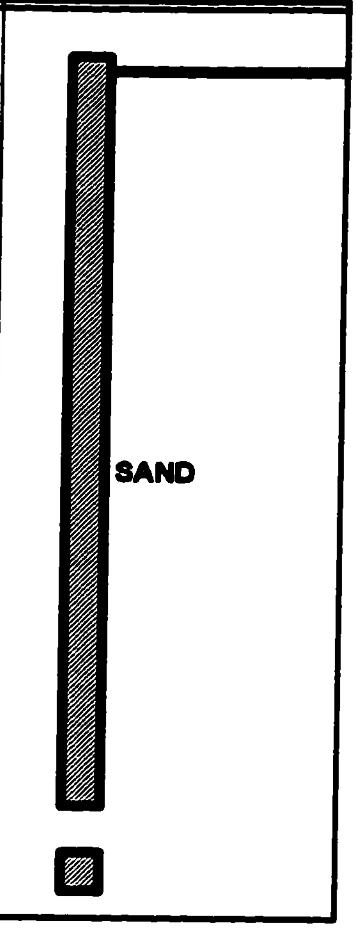

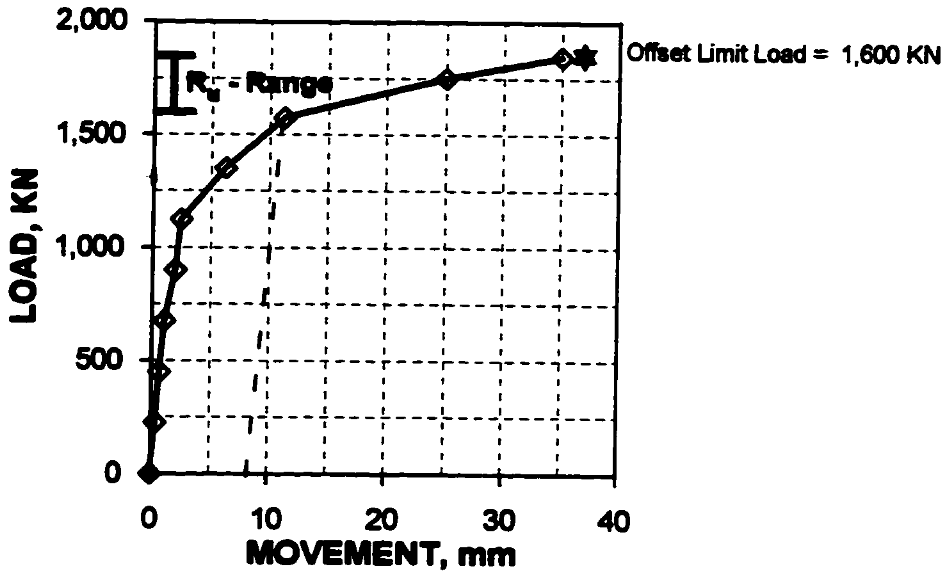

Case 74 N&SBI215
Sheet a CPT data

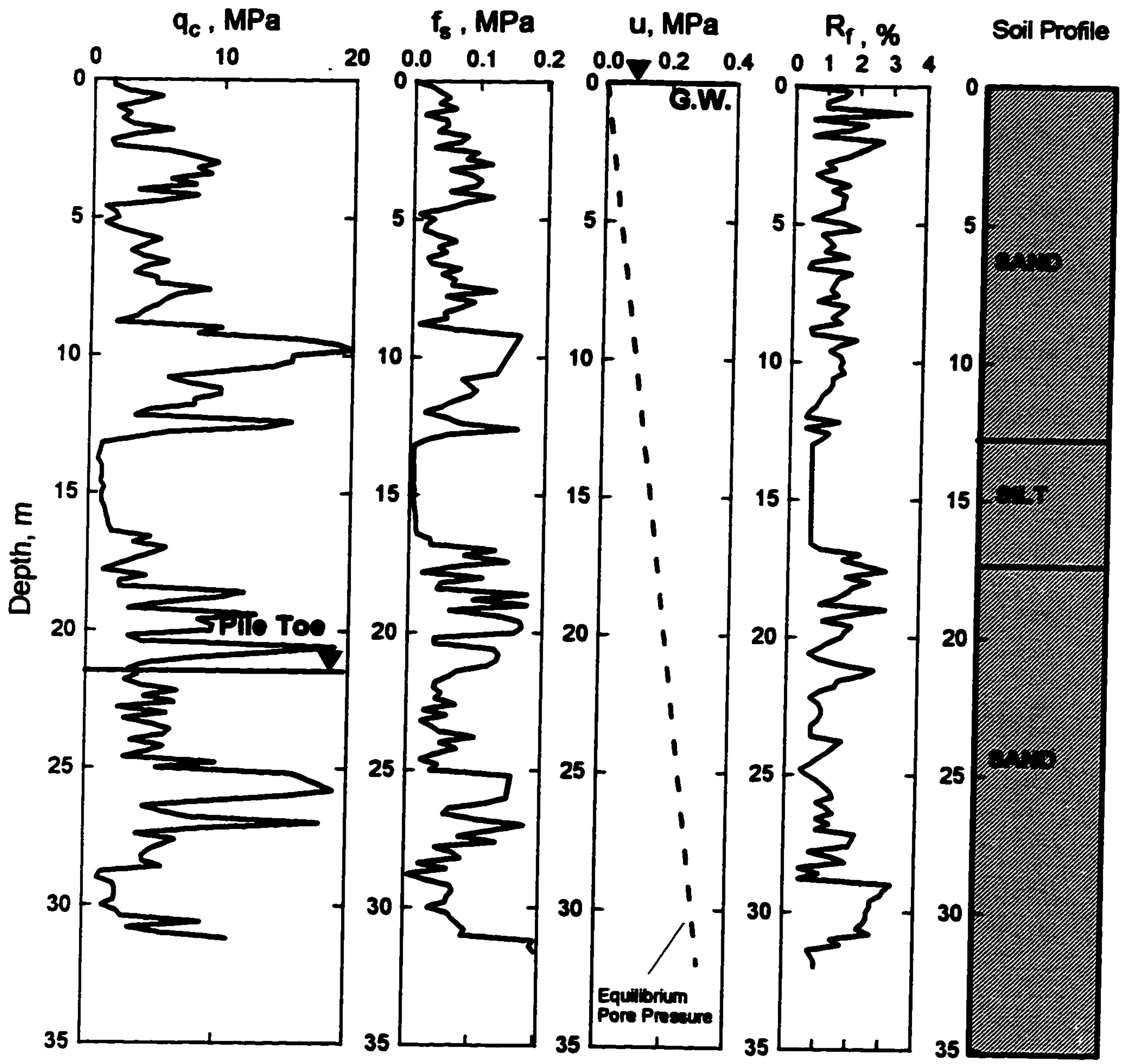

Case 74 N&S215
Sheet b Pile data

	DETAIL	DESCRIPTION	SCHEMATIC PROFILE
1	Site	Blount Island, USA	
2	Reference	Nottingham, 1975	
3	Shape, Material, and Installation	Square, Concrete, Driven	
4	Diameter, b, and Wall Thickness, t, mm	250	
5	Embedment Length D, m	21.3	
6	Cross Sectional Area A_t, m^2	0.049	
7	Unit Circumferential Area, A_s, m^2/m	0.785	
8	Toe, Closed or Open	Closed	
9	Type of Test and Loading	Static Compression, SML	
10	Toe Capacity, R_t, KN		
11	Shaft Capacity, R_s, KN		
12	*Capacity, R_u, KN	810	

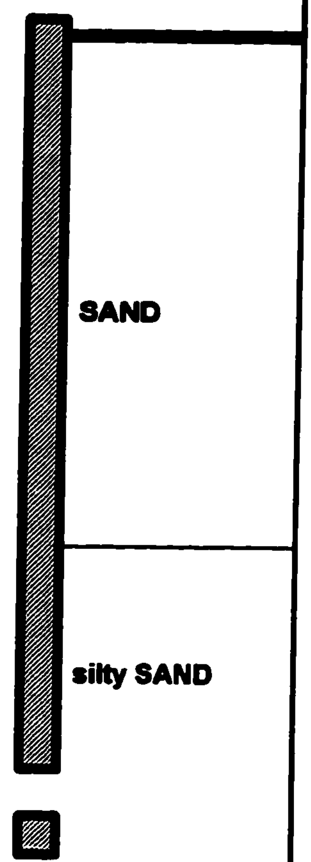

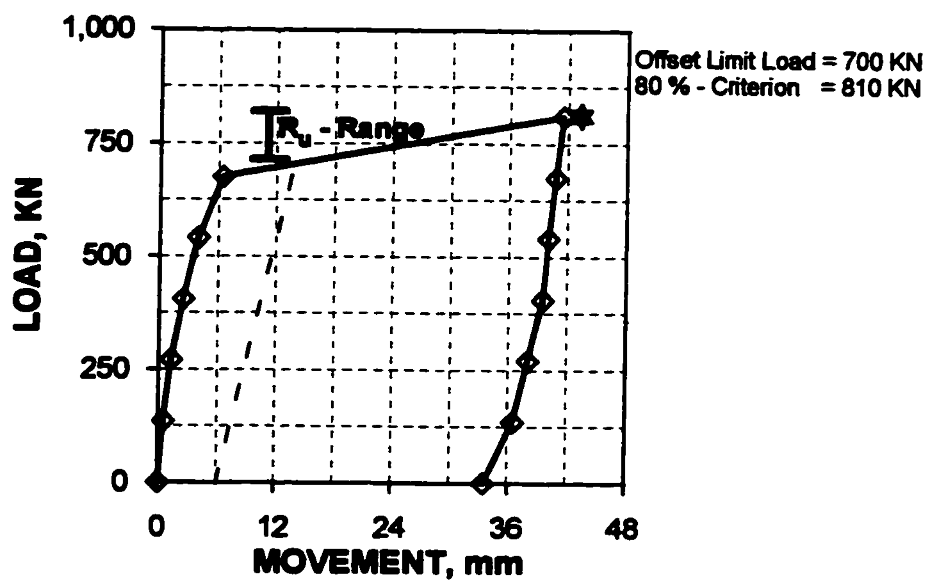

Case 75 N&SBI316
Sheet a CPT data

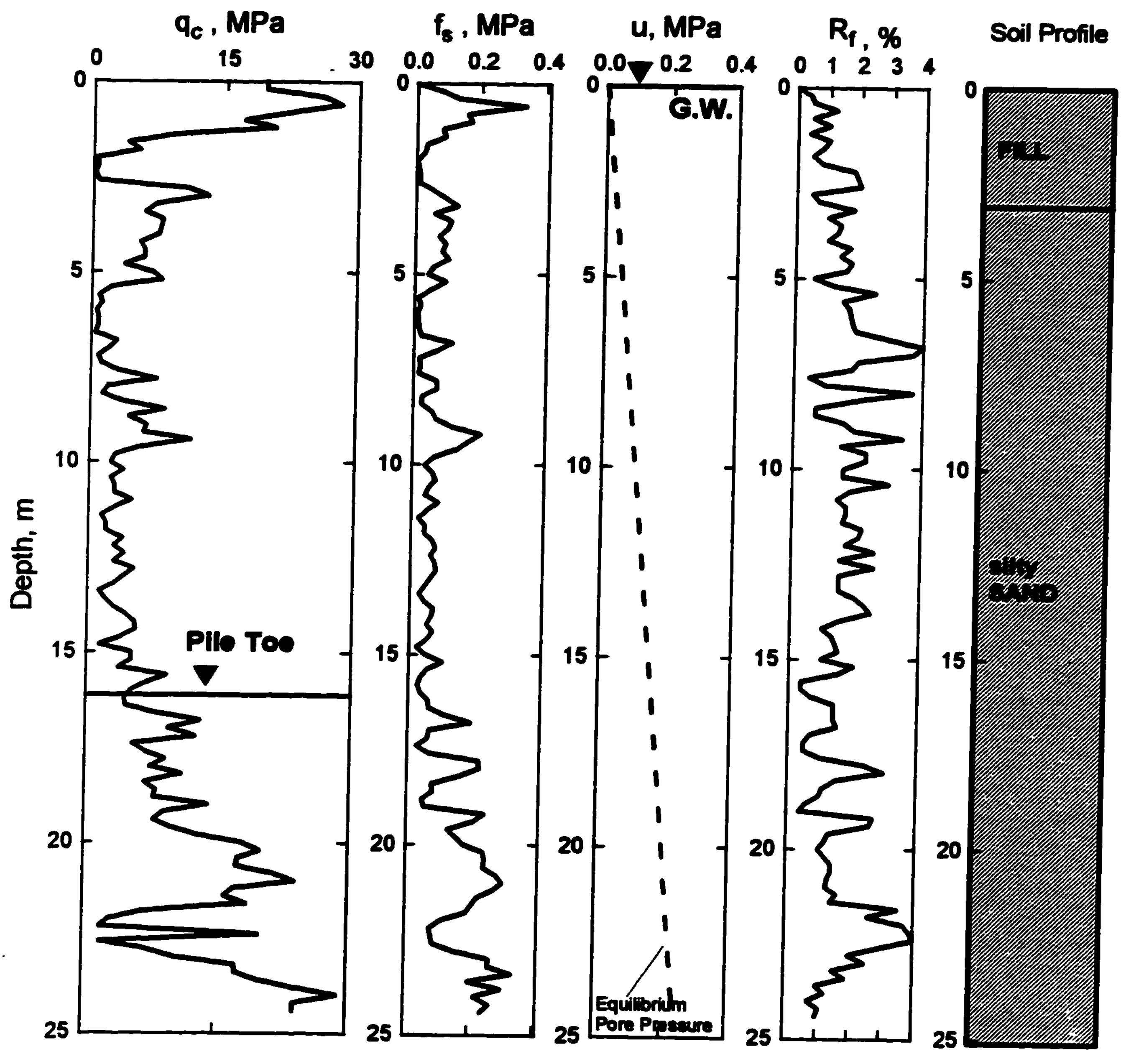

Case 75 N&S316
Sheet b Pile data

	DETAIL	DESCRIPTION
1	Site	Blount Island, USA
2	Reference	Nottingham, 1975
3	Shape, Material, and Installation	Square, Concrete, Driven
4	Diameter, b, and Wall Thickness, t, mm	350
5	Embedment Length D, m	15.85
6	Cross Sectional Area A_t, m^2	0.123
7	Unit Circumferential Area, A_s, m^2/m	1.4
8	Toe, Closed or Open	Closed
9	Type of Test and Loading	Static Compression, SML
10	Toe Capacity, R_t, KN	
11	Shaft Capacity, R_s, KN	
12	*Capacity, R_u, KN	1,485

SCHEMATIC PROFILE

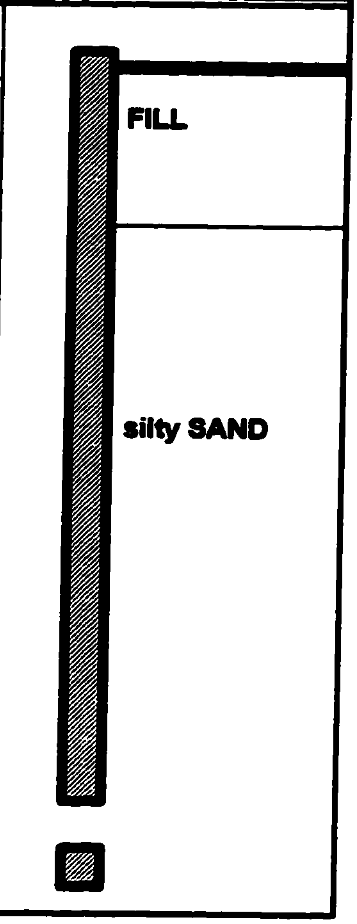

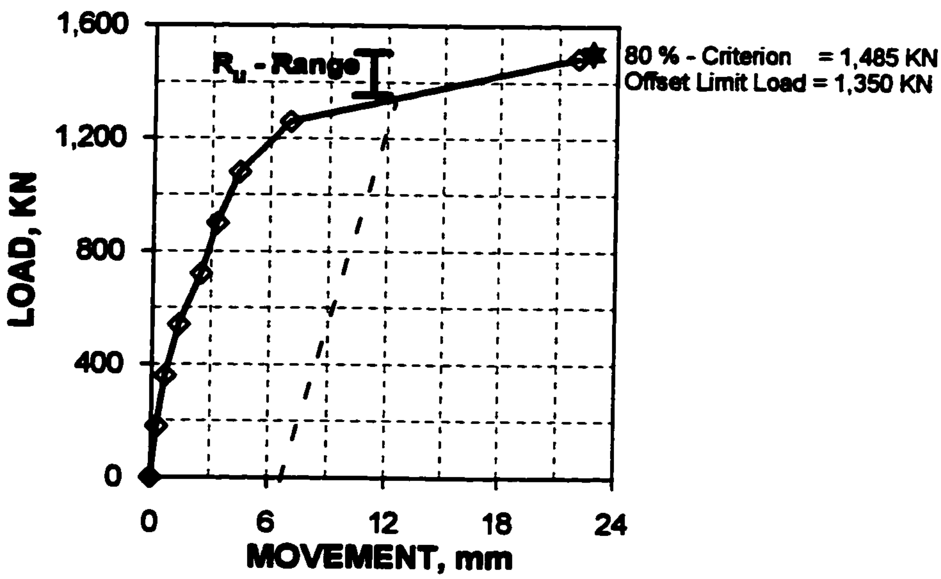

Case 76 N&SBI42
Sheet a CPT data

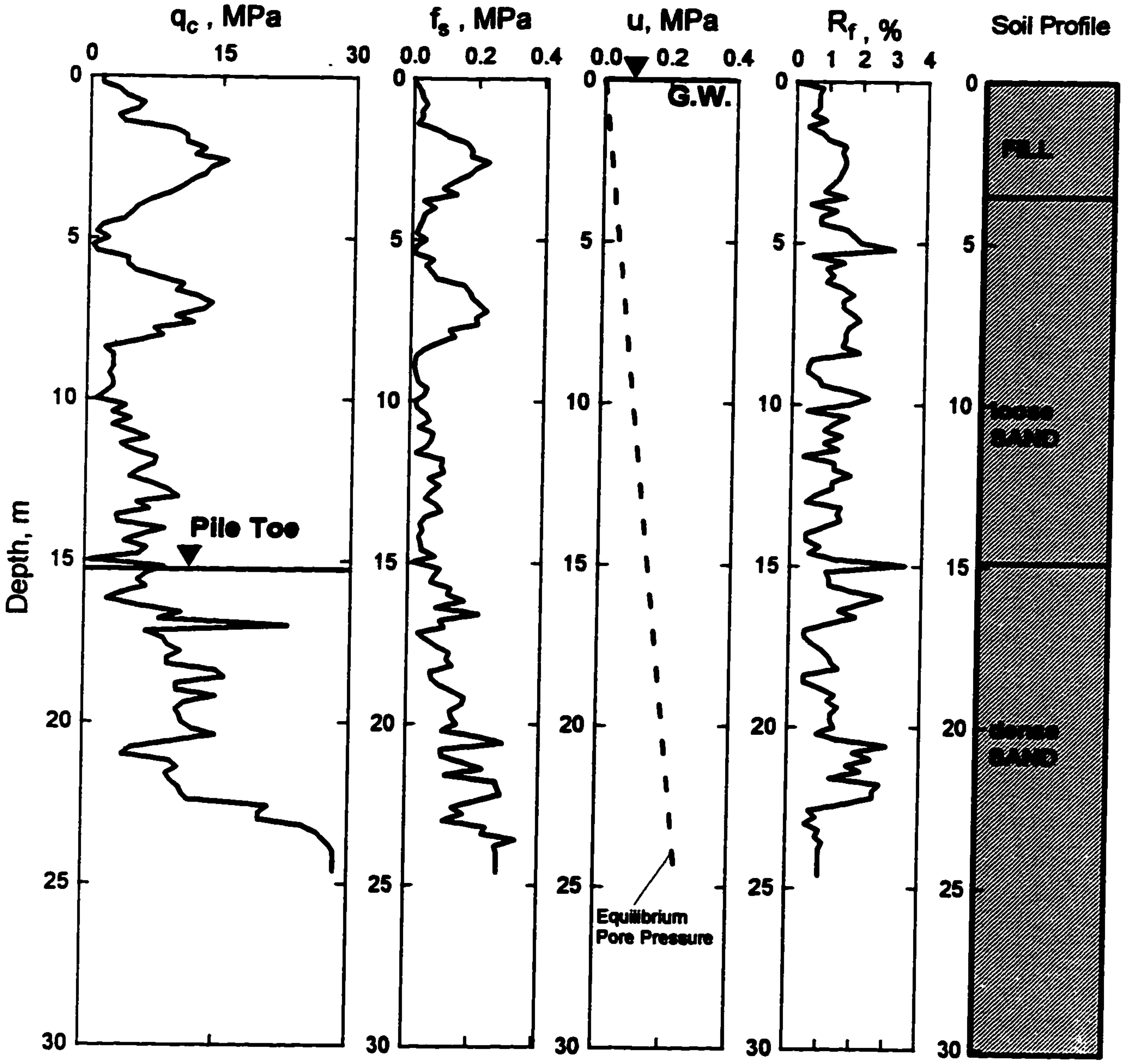

Case 76 N&SBI42
Sheet b Pile data

	DETAIL	DESCRIPTION
1	Site	Blount Island, USA
2	Reference	Nottingham, 1975
3	Shape, Material, and Installation	Pipe, Steel, Driven
4	Diameter, b, and Wall Thickness, t, mm	273 9
5	Embedment Length D, m	15.2
6	Cross Sectional Area A_t, m^2	0.059
7	Unit Circumferential Area, A_s, m^2/m	0.858
8	Toe, Closed or Open	Closed
9	Type of Test and Loading	Static Compression, SML
10	Toe Capacity, R_t, KN	
11	Shaft Capacity, R_s, KN	
12	*Capacity, R_u, KN	675

SCHEMATIC PROFILE

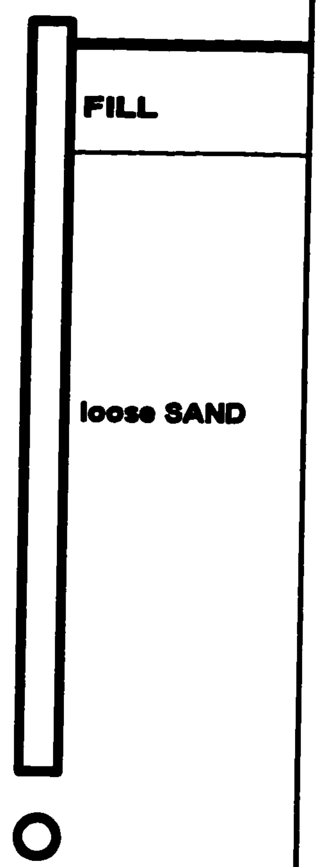

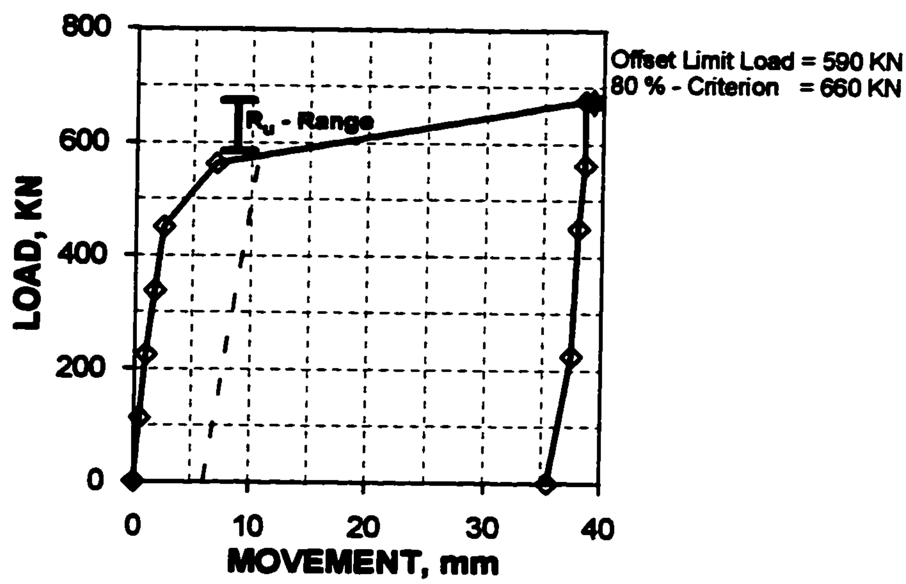

Case 77 N&SBI43
Sheet CPT data

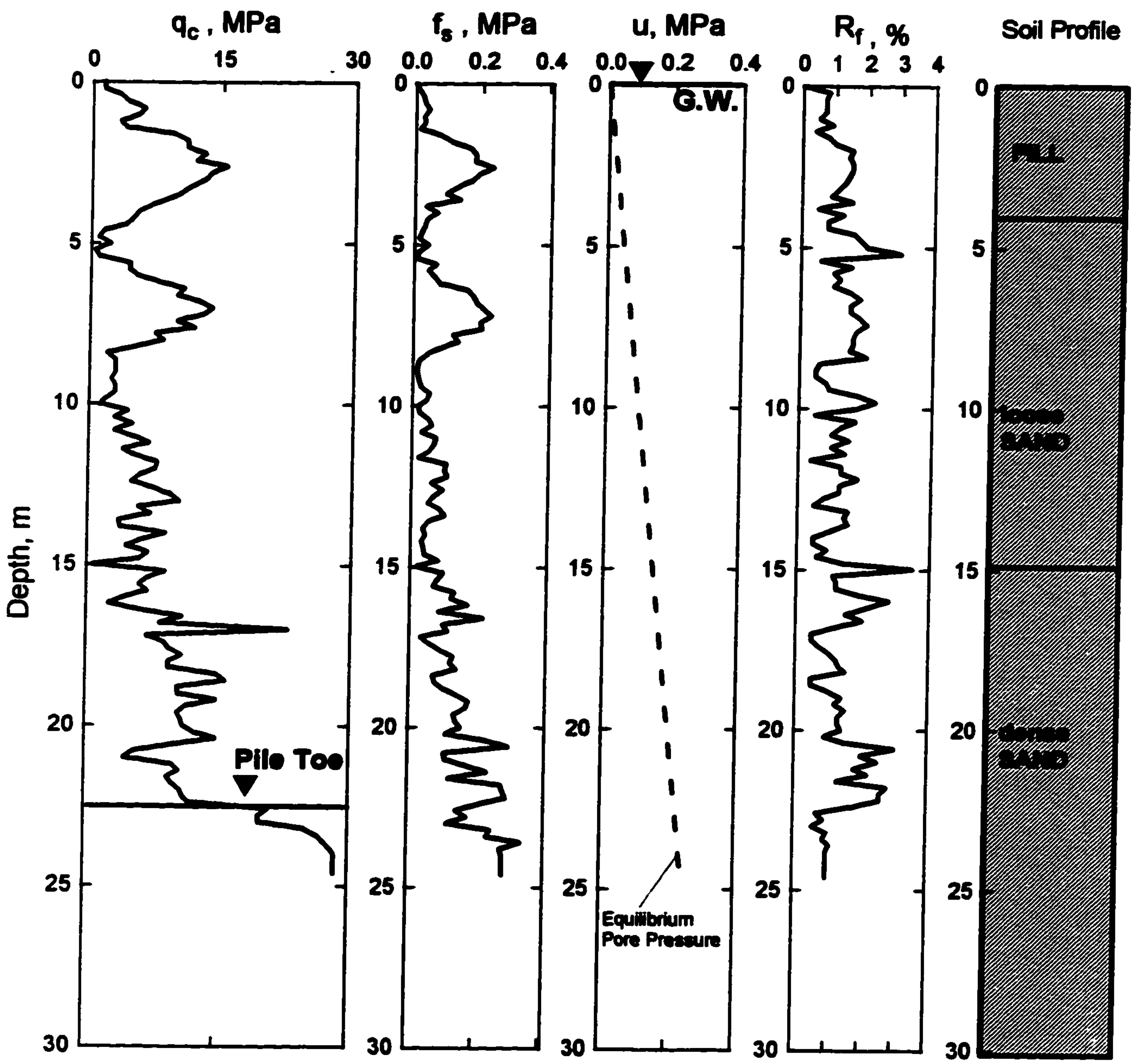

Case 77 N&SBI43
Sheet b Pile data

	DETAIL	DESCRIPTION
1	Site	Blount Island, USA
2	Reference	Nottingham, 1975
3	Shape, Material, and Installation	Pipe, Steel, Driven
4	Diameter, b, and Wall Thickness, t, mm	273 9
5	Embedment Length D, m	22.5
6	Cross Sectional Area A_t, m^2	0.059
7	Unit Circumferential Area, A_s, m^2/m	0.858
8	Toe, Closed or Open	Closed
9	Type of Test and Loading	Static Compression, SML
10	Toe Capacity, R_t, KN	
11	Shaft Capacity, R_s, KN	
12	*Capacity, R_u, KN	1,620

SCHEMATIC PROFILE

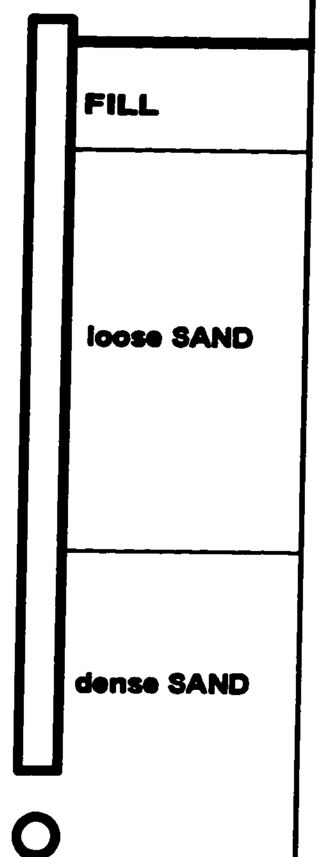

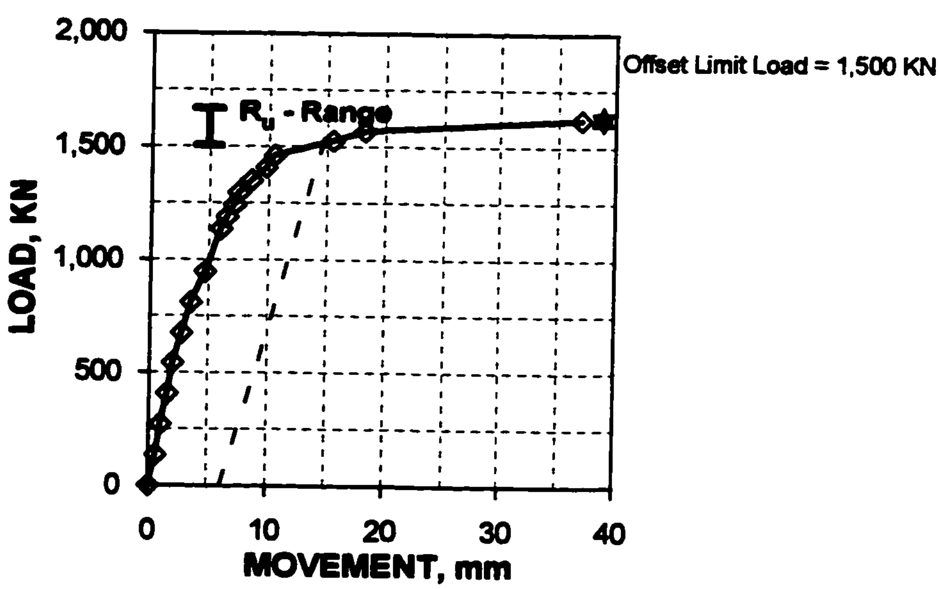

Case 78 N&SBI44
Sheet a CPT data

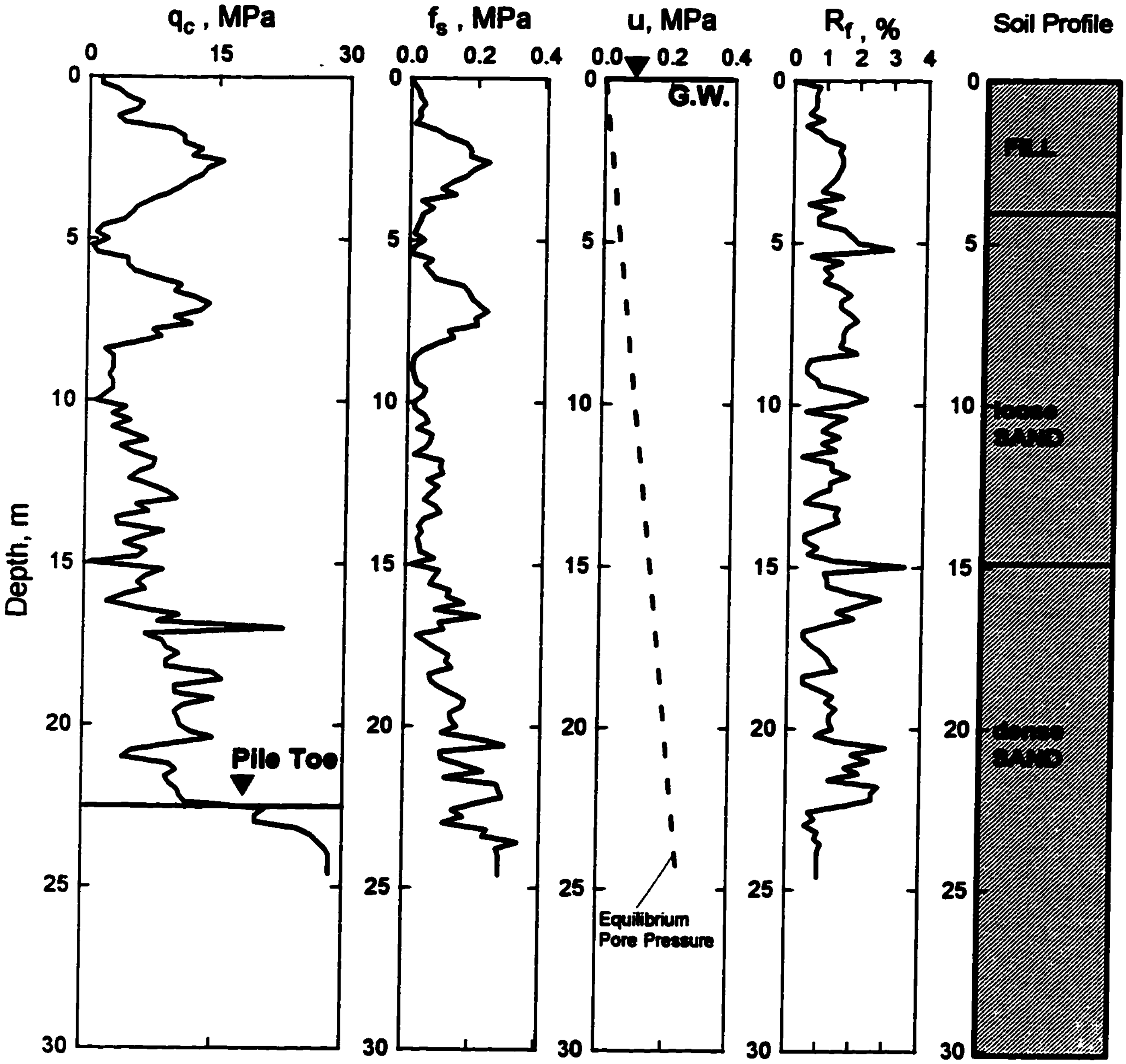

Case 78 N&SBI44
Sheet b Pile data

DETAIL		DESCRIPTION	SCHEMATIC PROFILE
1	Site	Blount Island, USA	
2	Reference	Nottingham, 1975	
3	Shape, Material, and Installation	Pipe, Steel, Driven	
4	Diameter, b, and Wall Thickness, t, mm	273 9	
5	Embedment Length D, m	22.5	
6	Cross Sectional Area A_t, m^2	0.059	
7	Unit Circumferential Area, A_s, m^2/m	0.858	
8	Toe, Closed or Open	Closed	
9	Type of Test and Loading	Static Tension, SML	
10	Toe Capacity, R_t, KN		
11	Shaft Capacity, R_s, KN		
12	*Capacity, R_u, KN	765	

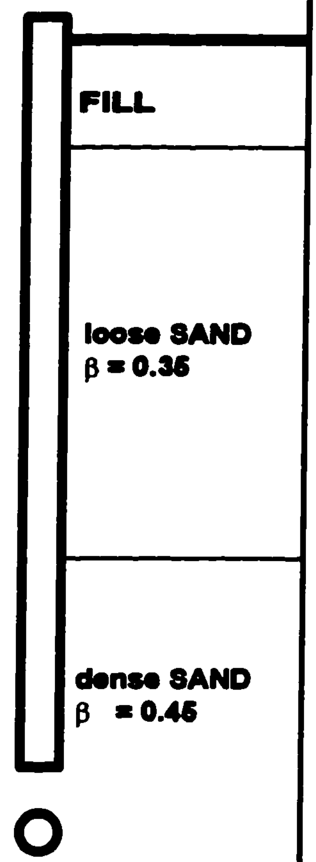

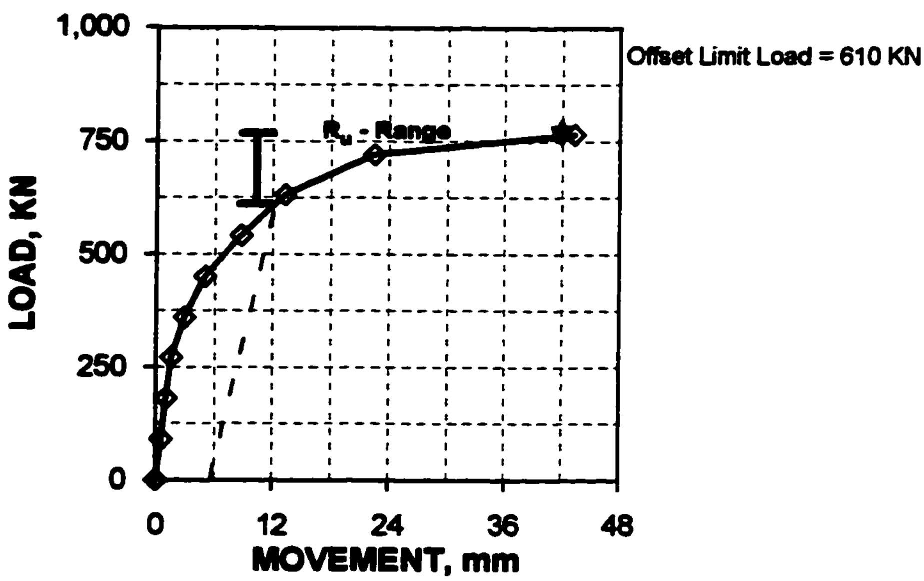

Case 79 N&SBI348
Sheet a CPT data

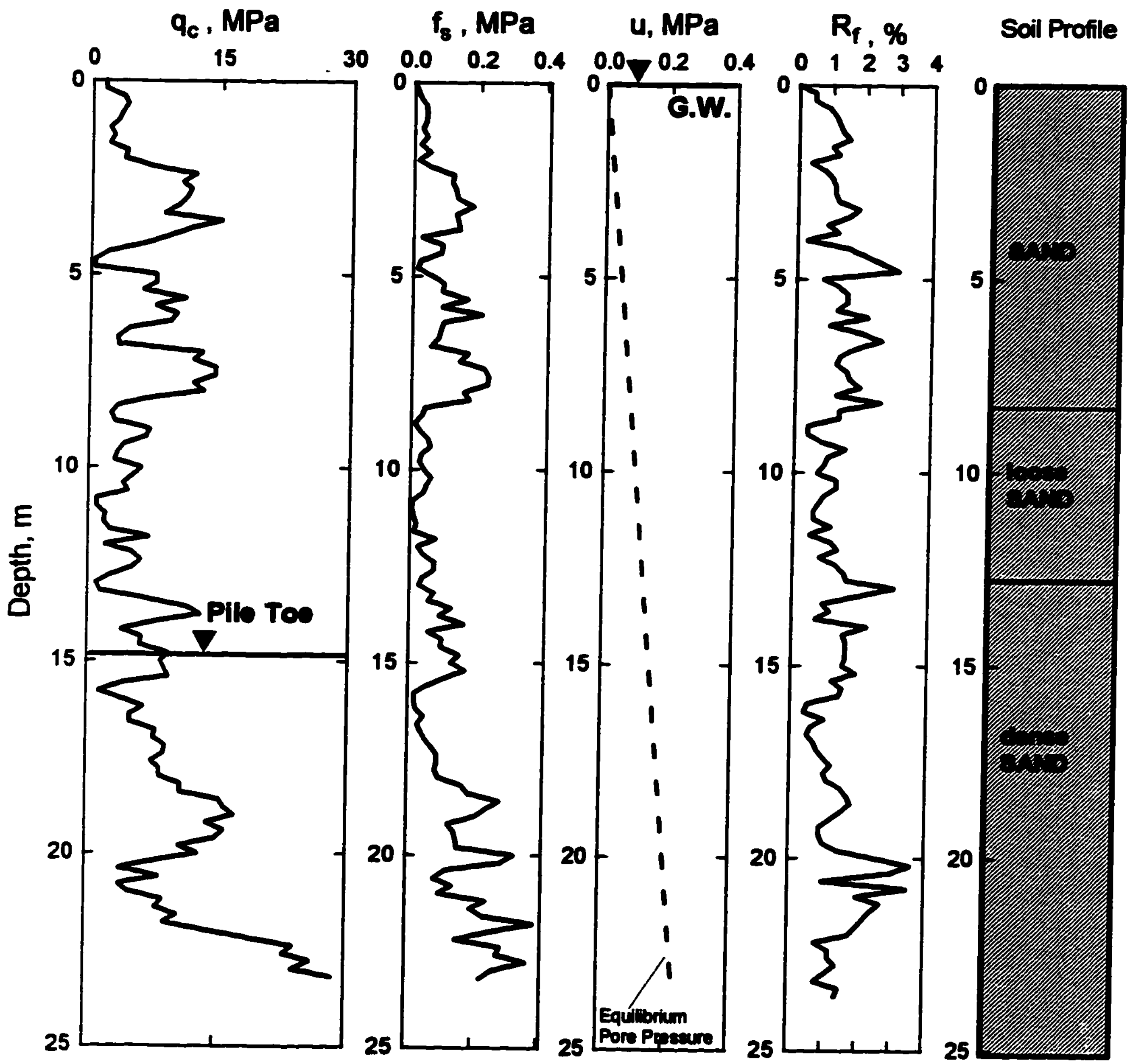

Case 79 N&S348
Sheet b Pile data

	DETAIL	DESCRIPTION
1	Site	Blount Island, USA
2	Reference	Nottingham, 1975
3	Shape, Material, and Installation	Square, Concrete, Driven
4	Diameter, b, and Wall Thickness, t, mm	450
5	Embedment Length D, m	14.9
6	Cross Sectional Area A_t, m^2	0.202
7	Unit Circumferential Area, A_s, m^2/m	1.8
8	Toe, Closed or Open	Closed
9	Type of Test and Loading	Static Compression, SML
10	Toe Capacity, R_t, KN	
11	Shaft Capacity, R_s, KN	
12	*Capacity, R_u, KN	1755

SCHEMATIC PROFILE

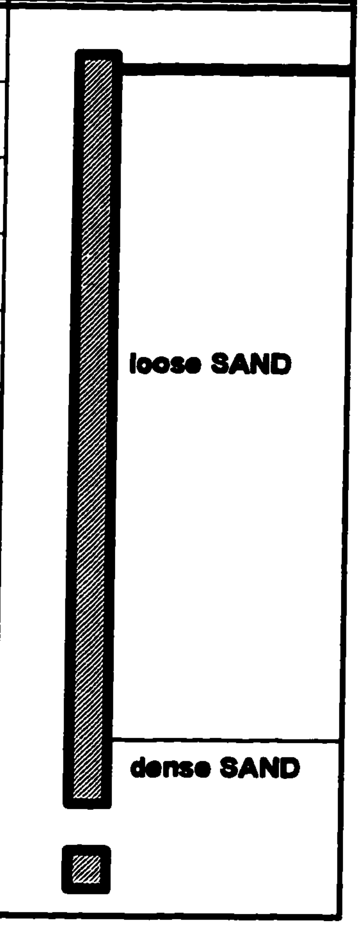

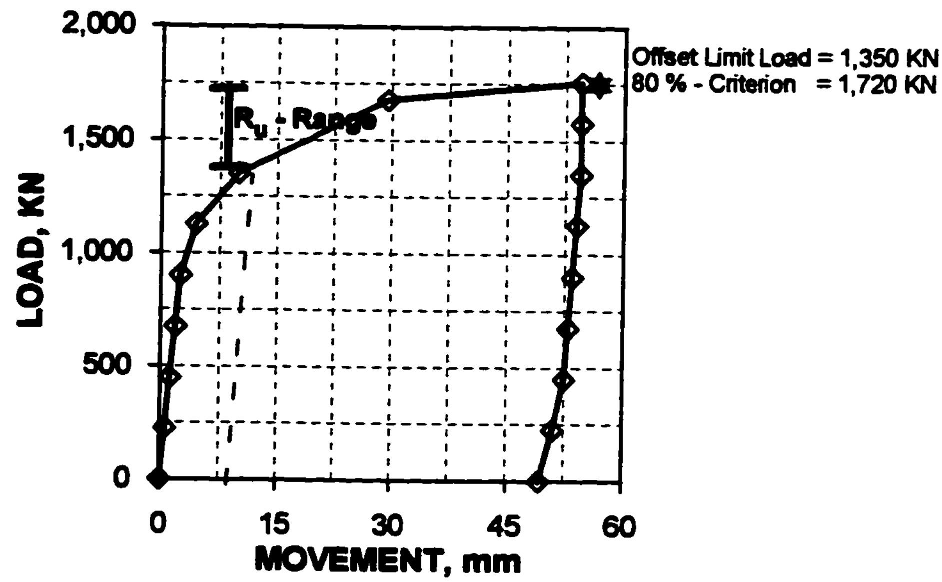

Case 80 QBSA
Sheet a CPT data

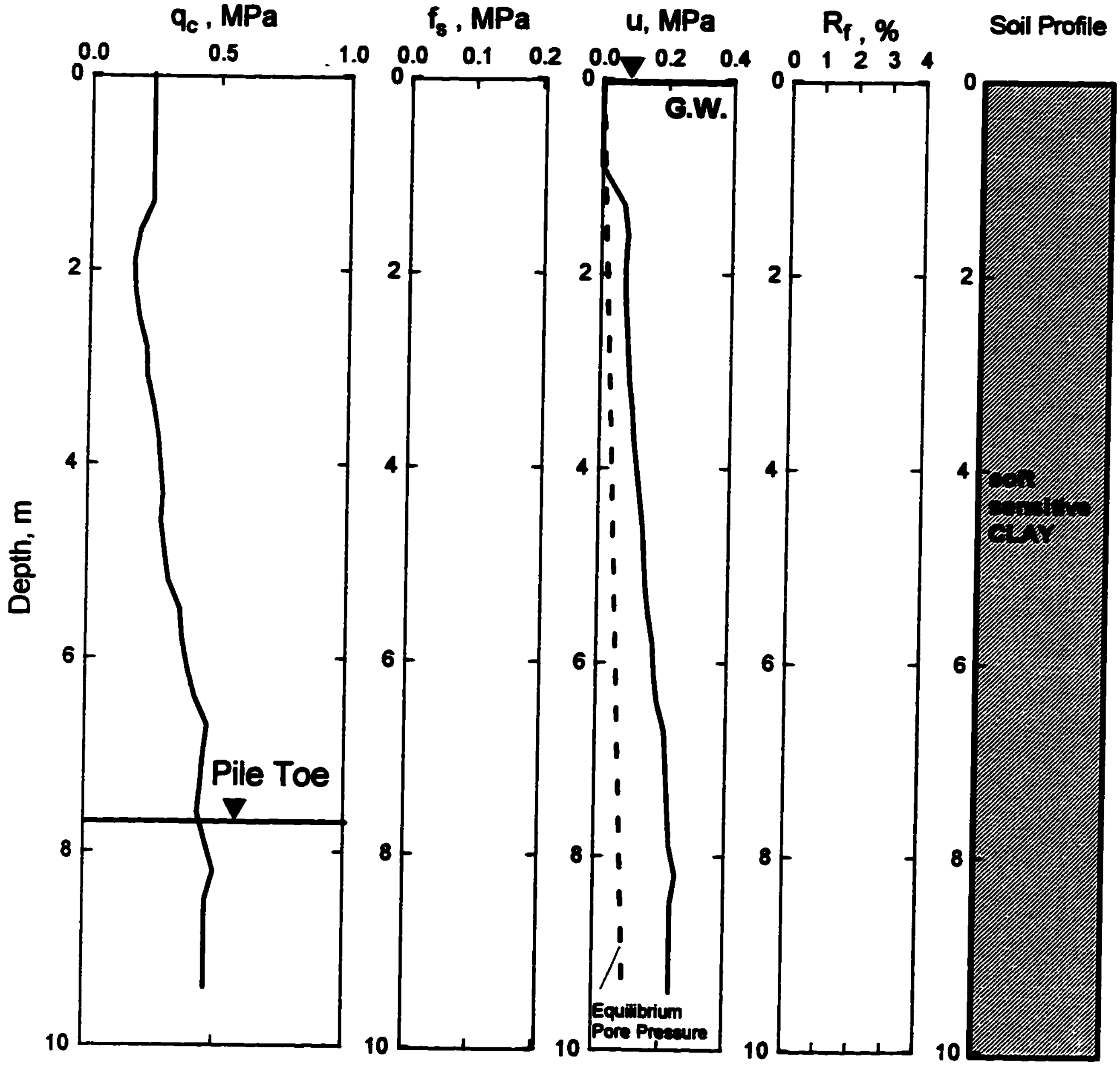

Case 80 QBSA
Sheet b Pile data

	DETAIL	DESCRIPTION	SCHEMATIC PROFILE
1	Site	Quebec, Canada	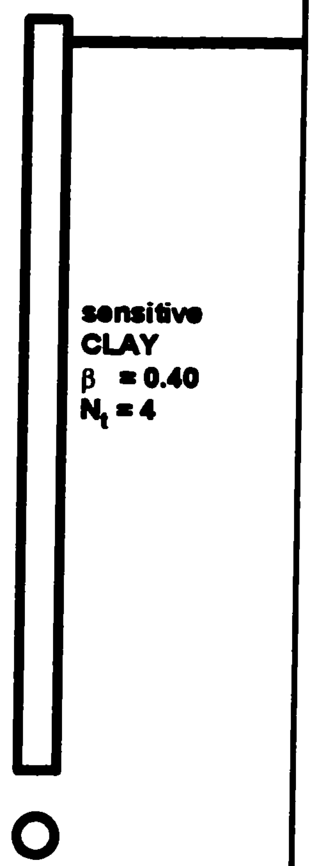
2	Reference	Roy et al., 1986	
3	Shape, Material, and Installation	Pipe, Steel, Driven	
4	Diameter, b, and Wall Thickness, t, mm	220	
5	Embedment Length D, m	7.5	sensitive CLAY β = 0.40 N_t = 4
6	Cross Sectional Area A_t, m^2	0.038	
7	Unit Circumferential Area, A_s, m^2 /m	0.69	
8	Toe, Closed or Open	Closed	
9	Type of Test and Loading	Static Compression, SML	
10	Toe Capacity, R_t, KN	9	
11	Shaft Capacity, R_s, KN	74	
12	*Capacity, R_u, KN	83	

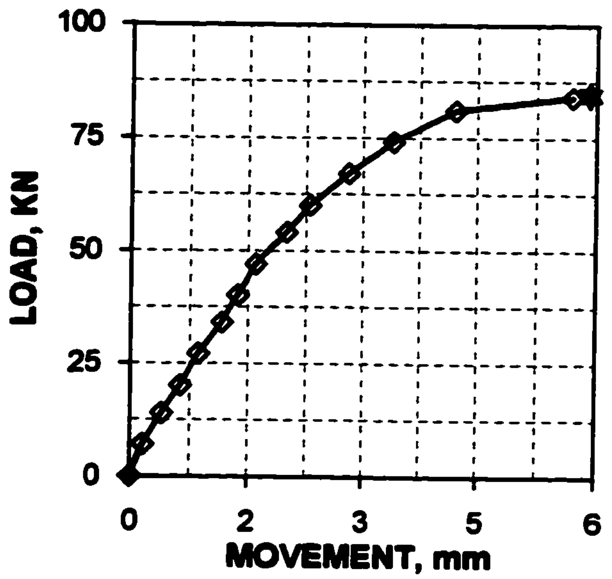

Case 81 UHUC1
Sheet a CPT data

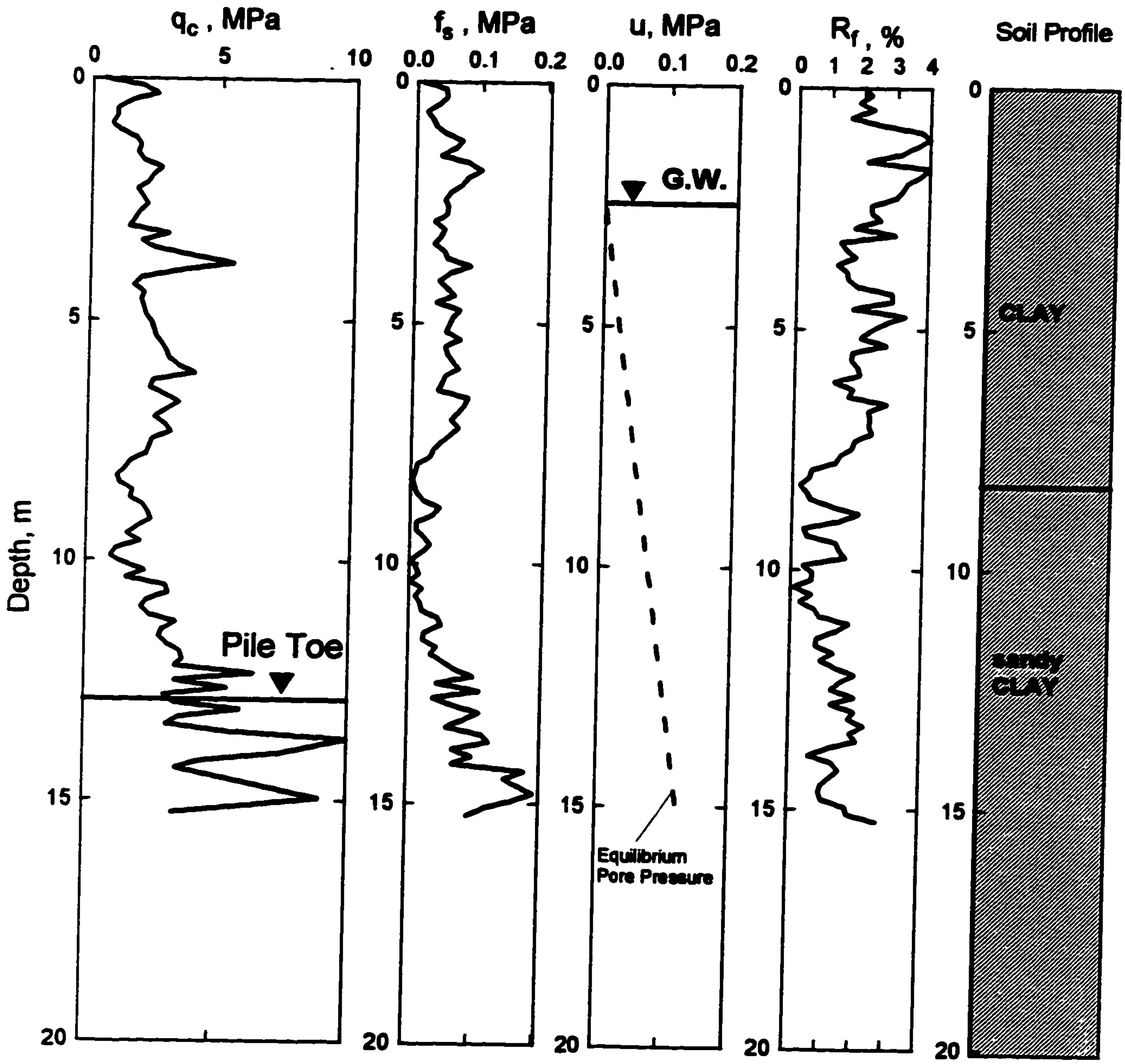

Case 81 UHUC1
Sheet b Pile data

	DETAIL	DESCRIPTION	SCHEMATIC PROFILE
1	Site	Houston, USA	CLAY β = 0.50; sandy CLAY β = 0.60, N_t = 27
2	Reference	FHWA, 1981; O'Neill, 1986	
3	Shape, Material, and Installation	Pipe, Steel, Driven	
4	Diameter, b, and Wall Thickness, t, mm	273 9	
5	Embedment Length D, m	13	
6	Cross Sectional Area A_t , m²	0.059	
7	Unit Circumferential Area, A_s , m² /m	0.858	
8	Toe, Closed or Open	Closed	
9	Type of Test and Loading	Static Compression, SML	
10	Toe Capacity, R_t , KN	240	
11	Shaft Capacity, R_s , KN	540	
12	*Capacity, R_u , KN	780	

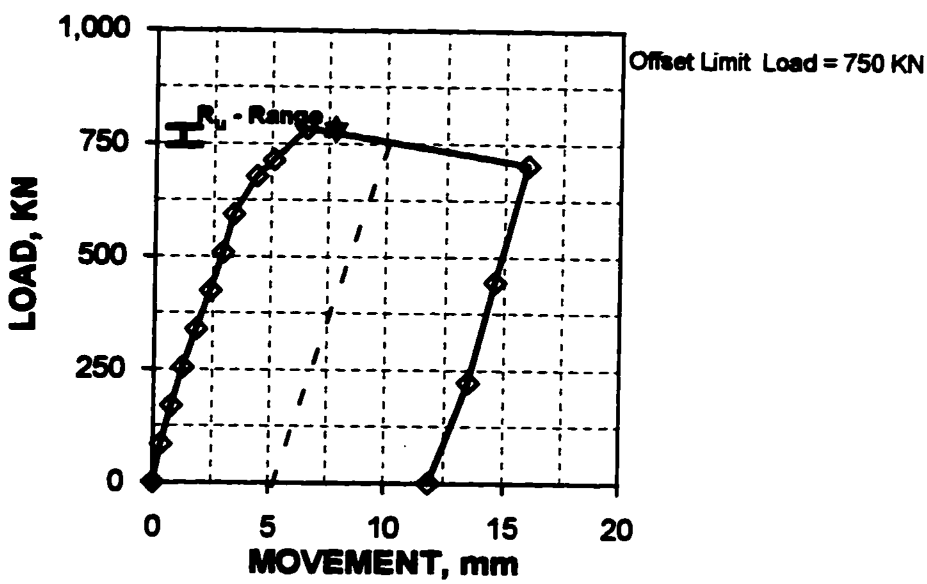

Case 82 UHUT1
Sheet a CPT data

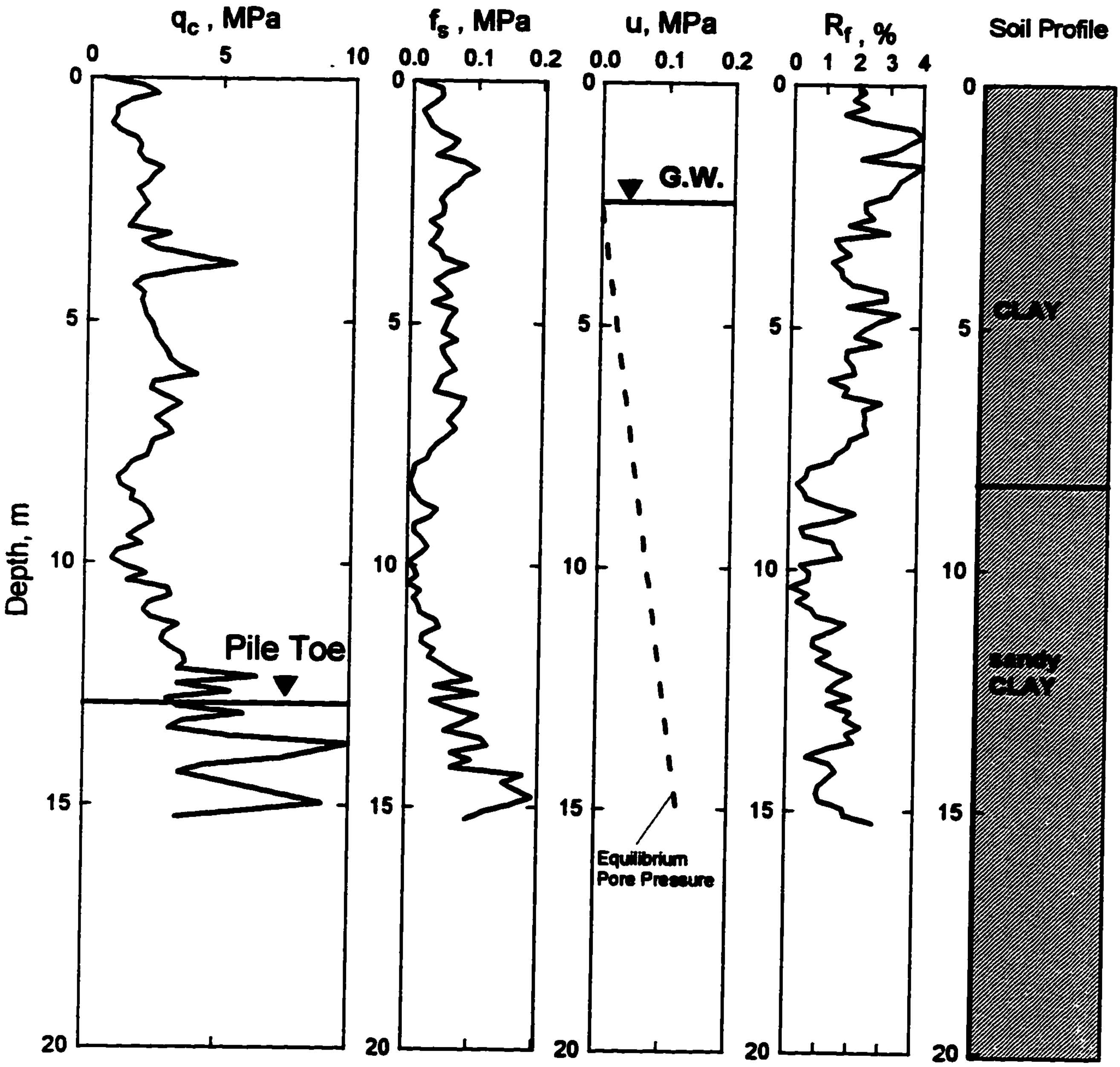

Case 82 UHUT1
Sheet b Pile data

No.	CASE	DESCRIPTION	SCHEMATIC PROFILE
1	Site	Houston, USA	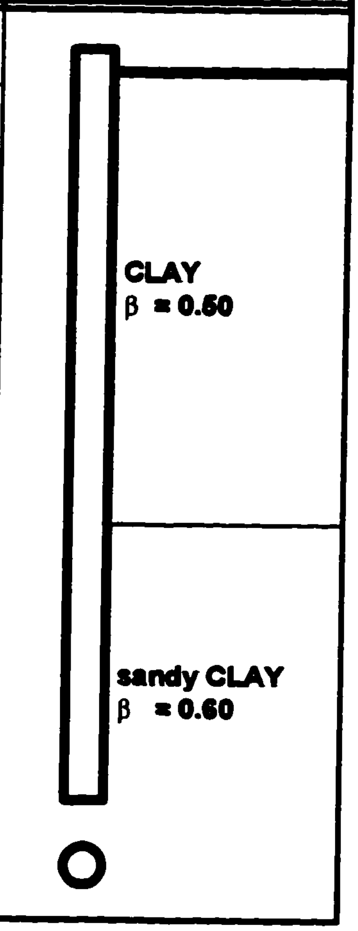
2	Reference	FHWA, 1981; O'Neill, 1986	
3	Shape, Material, and Installation	Pipe, Steel, Driven	
4	Diameter, b, and Wall Thickness, t, mm	273	
5	Embedment Length D, m	13	
6	Cross Sectional Area A_t, m^2	0.059	
7	Unit Circumferential Area, A_s, m^2/m	0.858	
8	Toe, Closed or Open	Closed	
9	Type of Test and Loading	Static Tension, SML	
10	Toe Capacity, R_t, KN		
11	Shaft Capacity, R_s, KN	485	
12	*Capacity, R_u, KN		

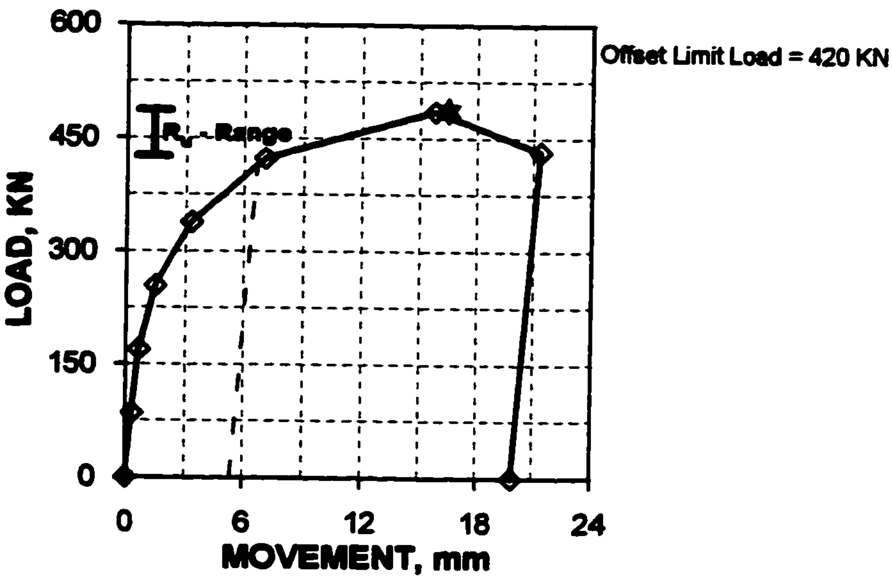

Case 83 UHUC11
Sheet a CPT data

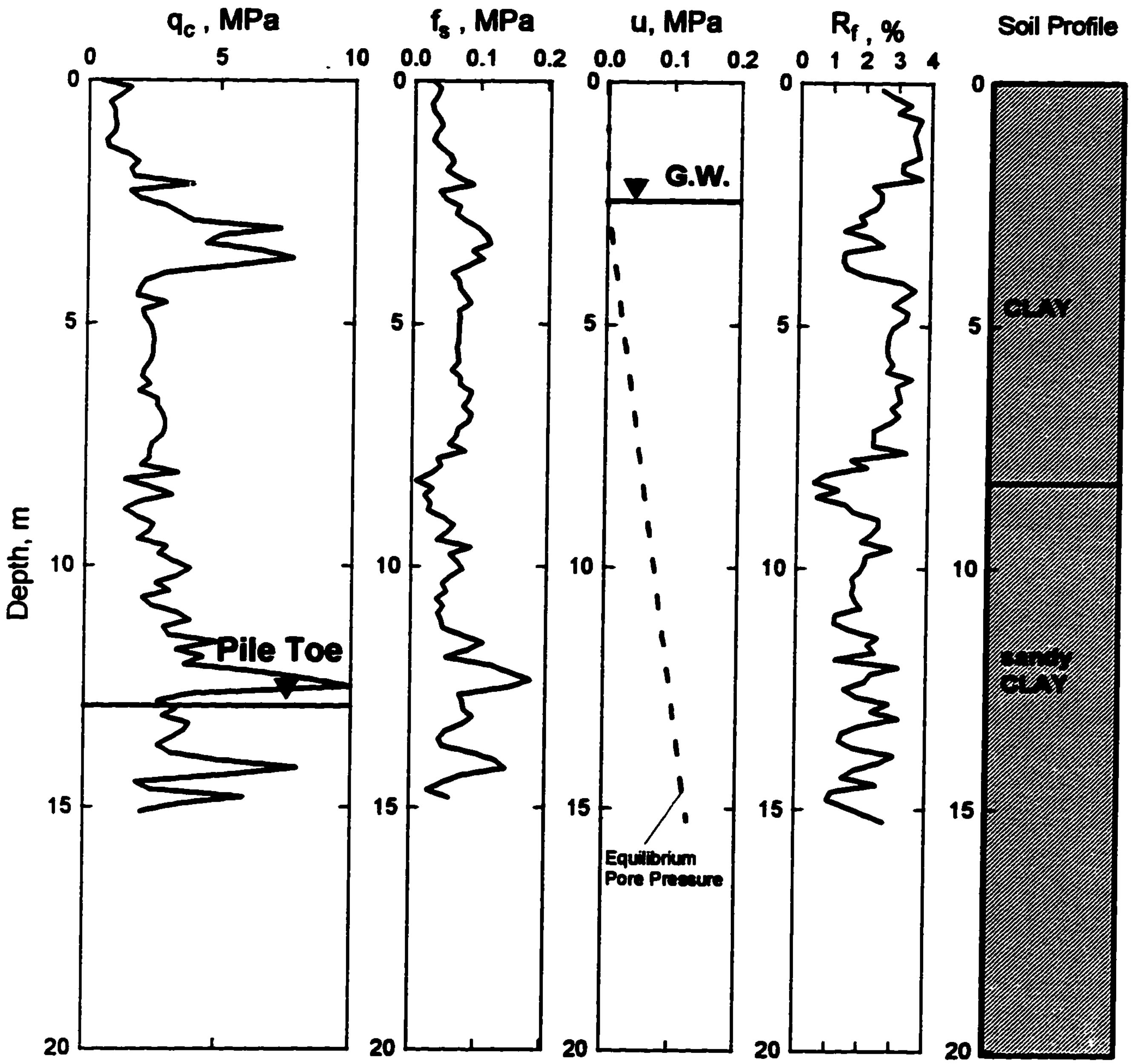

Case 83 UHUC11
Sheet b Pile data

	DETAIL	DESCRIPTION	SCHEMATIC PROFILE
1	Site	Houston, USA	
2	Reference	FHWA, 1981; O'Neill, 1986	
3	Shape, Material, and Installation	Pipe, Steel, Driven	
4	Diameter, b, and Wall Thickness, t, mm	273	
5	Embedment Length D, m	13	
6	Cross Sectional Area A_t, m²	0.059	
7	Unit Circumferential Area, A_s, m²/m	0.858	
8	Toe, Closed or Open	Closed	
9	Type of Test and Loading	Static Compression, SML	
10	Toe Capacity, R_t, KN	245	
11	Shaft Capacity, R_s, KN	538	
12	*Capacity, R_u, KN	800	

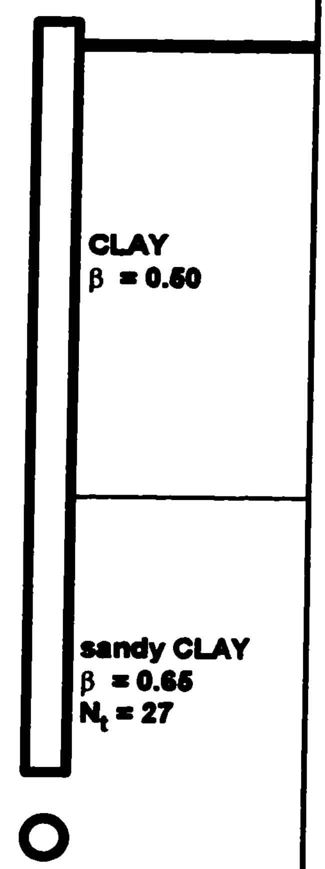

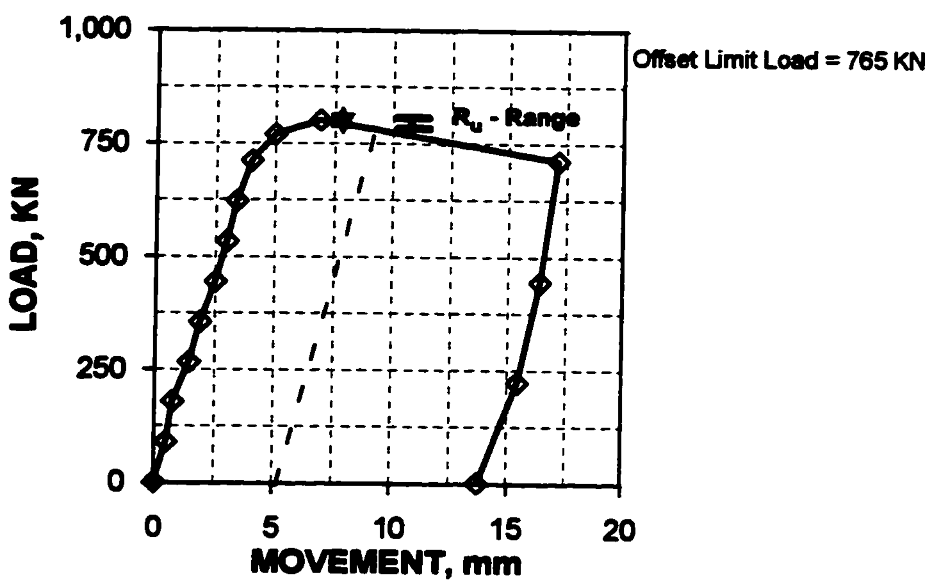

Case 84 UHUT11
Sheet a CPT data

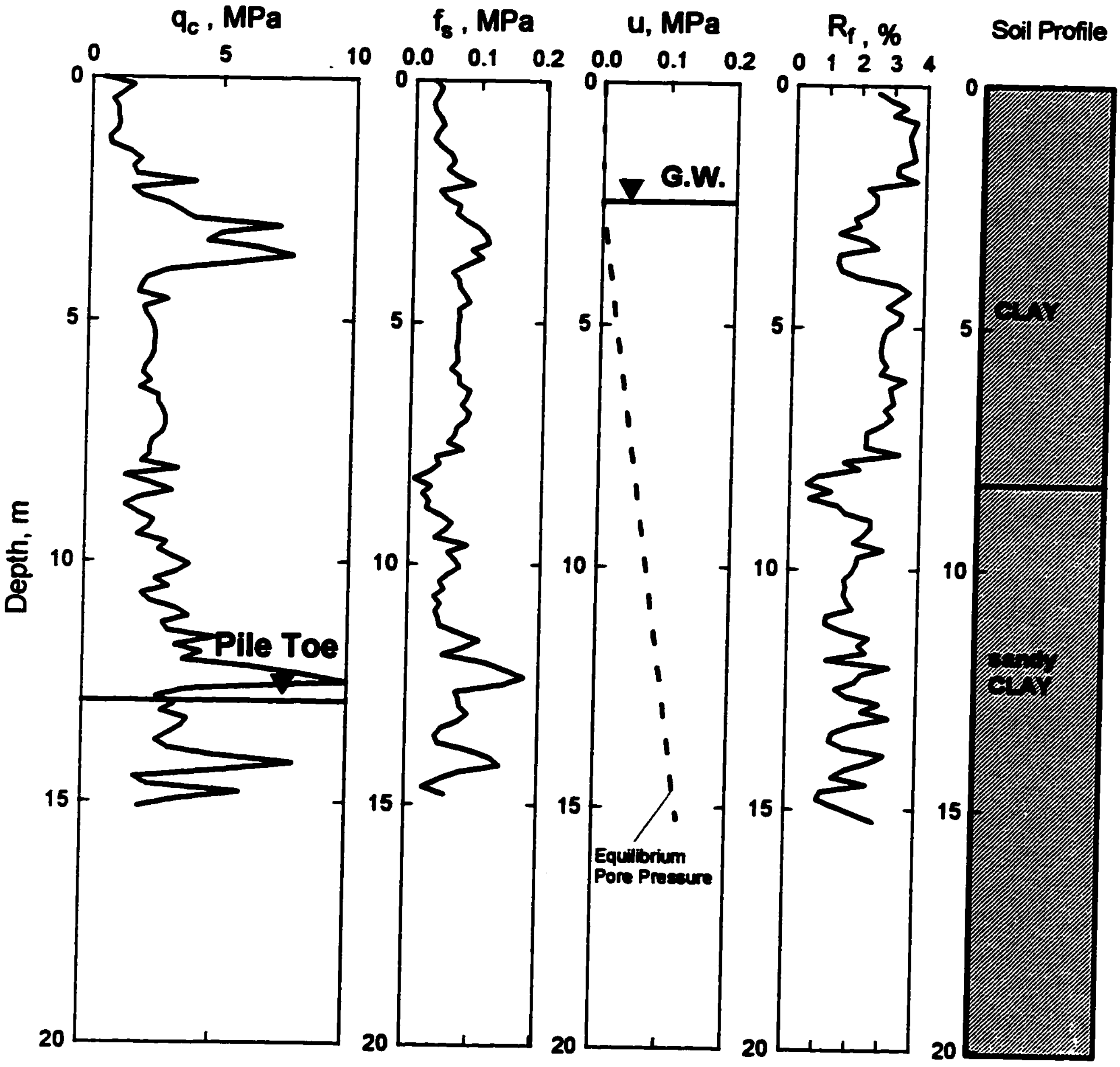

Case 84 UHUT11
Sheet b Pile data

	DETAIL	DESCRIPTION
1	Site	Houston, USA
2	Reference	FHWA, 1981; O'Neill, 1986
3	Shape, Material, and Installation	Pipe, Steel, Driven
4	Diameter, b, and Wall Thickness, t, mm	273
5	Embedment Length D, m	13
6	Cross Sectional Area A_t, m^2	0.059
7	Unit Circumferential Area, A_s, m^2/m	0.858
8	Toe, Closed or Open	Closed
9	Type of Test and Loading	Static Tension, SML
10	Toe Capacity, R_t, KN	
11	Shaft Capacity, R_s, KN	520
12	*Capacity, R_u, KN	

SCHEMATIC PROFILE

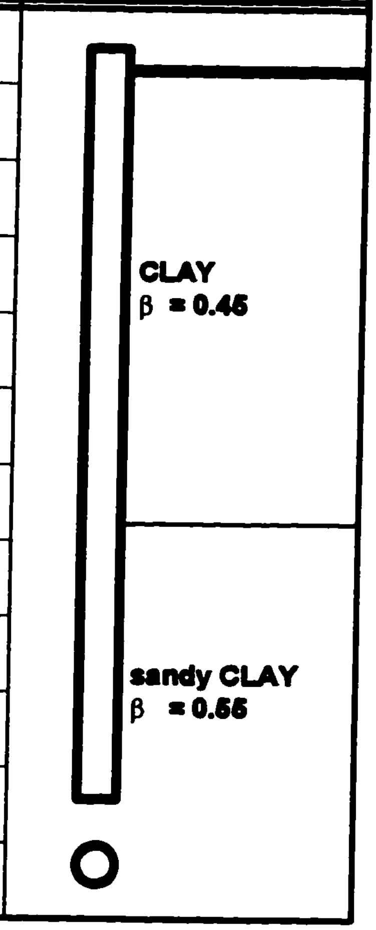

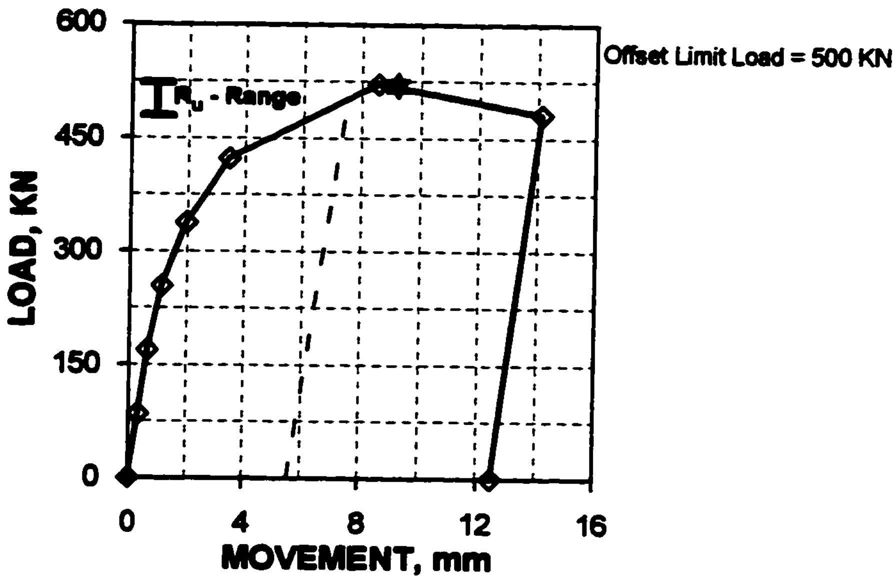

Case 85 PNTRA5
Sheet a CPT data

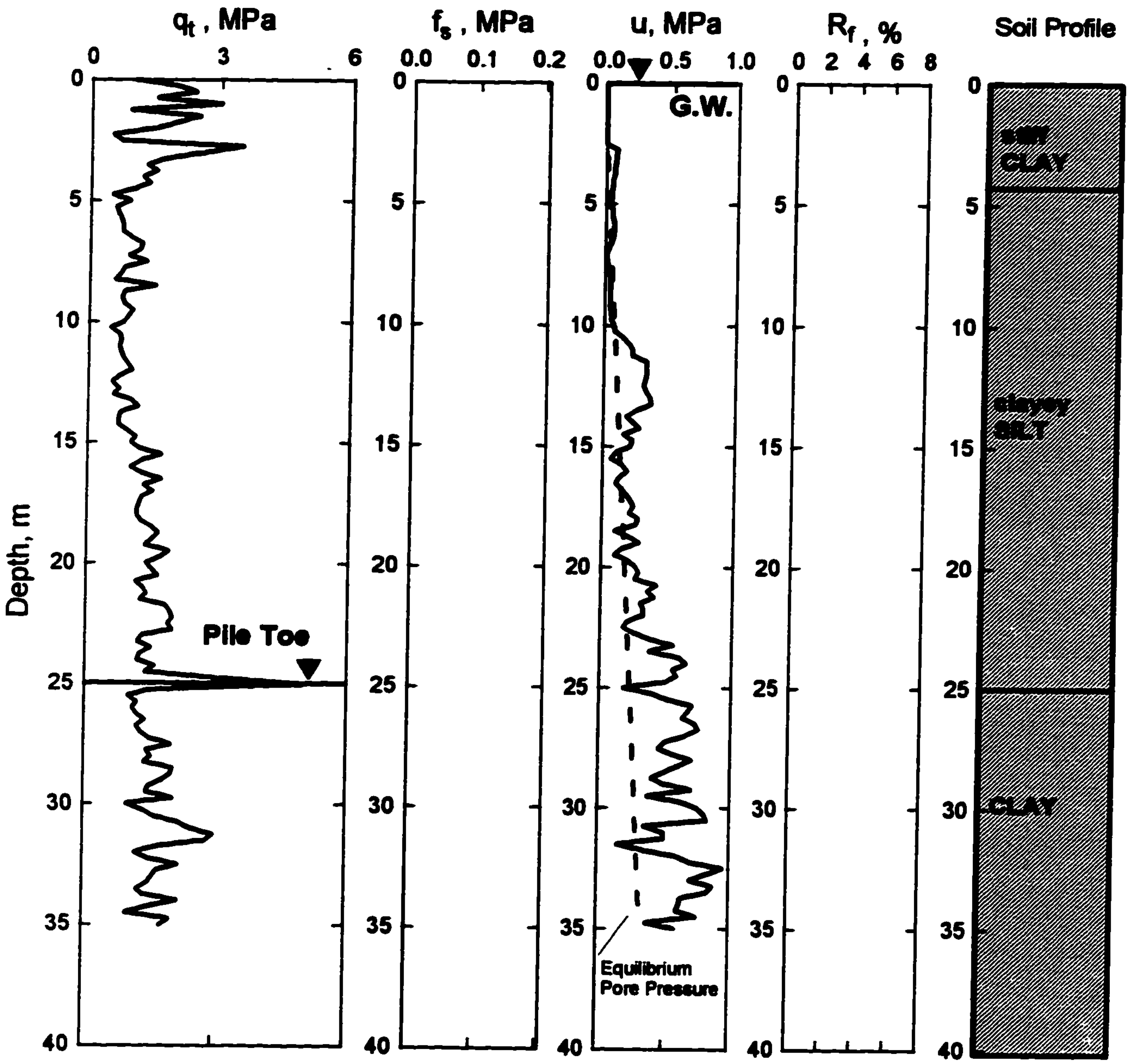

Case 85 PNTRA5
Sheet b Pile data

	DETAIL	DESCRIPTION
1	Site	Pentre, UK
2	Reference	Almeida et al., 1996
3	Shape, Material, and Installation	Pipe, Steel, Driven
4	Diameter, b, and Wall Thickness, t, mm	219
5	Embedment Length D, m	25
6	Cross Sectional Area A_t, m^2	0.038
7	Unit Circumferential Area, A_s, m^2/m	0.688
8	Toe, Closed or Open	Closed
9	Type of Test and Loading	Static Tension, SML
10	Toe Capacity, R_t, KN	
11	Shaft Capacity, R_s, KN	190
12	Capacity, R_u, KN	

SCHEMATIC PROFILE

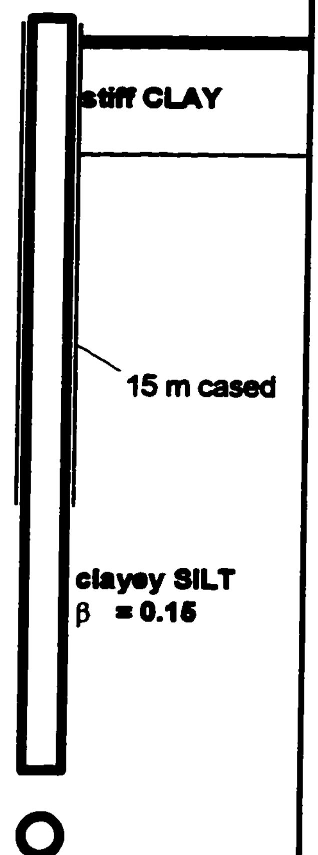

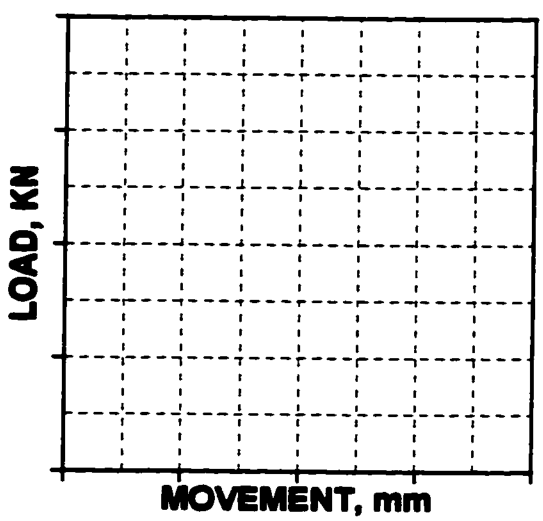

Case 86 PNTRA6
Sheet a CPT data

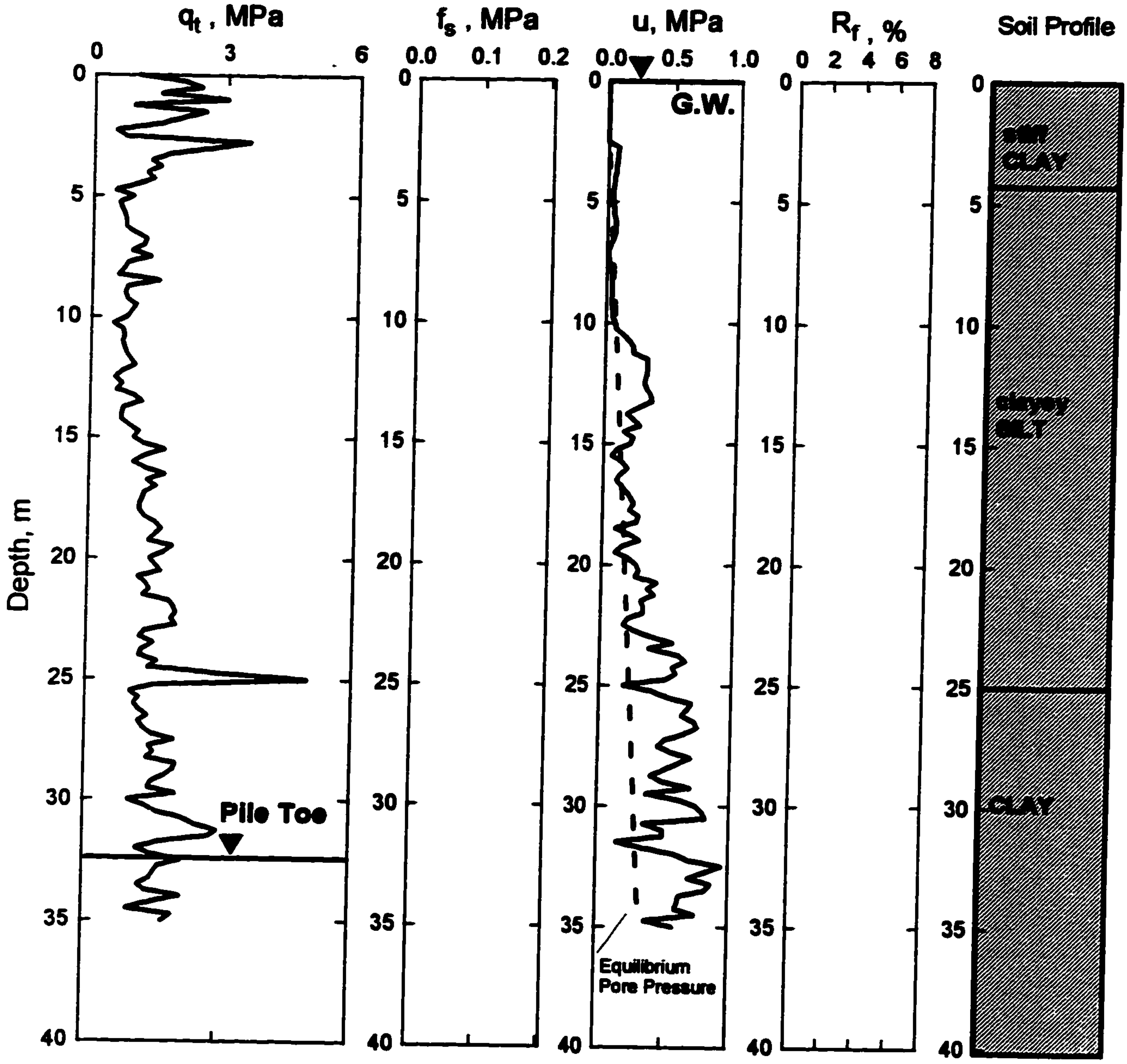

Case 86 PNTRA6
Sheet b Pile data

	DETAIL	DESCRIPTION
1	Site	Pentre, UK
2	Reference	Almeida et al., 1996
3	Shape, Material, and Installation	Pipe, Steel, Driven
4	Diameter, b, and Wall Thickness, t, mm	219
5	Embedment Length D, m	32.5
6	Cross Sectional Area A_t, m^2	0.038
7	Unit Circumferential Area, A_s, m^2/m	0.688
8	Toe, Closed or Open	Closed
9	Type of Test and Loading	Static Tension, SML
10	Toe Capacity, R_t, KN	
11	Shaft Capacity, R_s, KN	460
12	Capacity, R_u, KN	

SCHEMATIC PROFILE

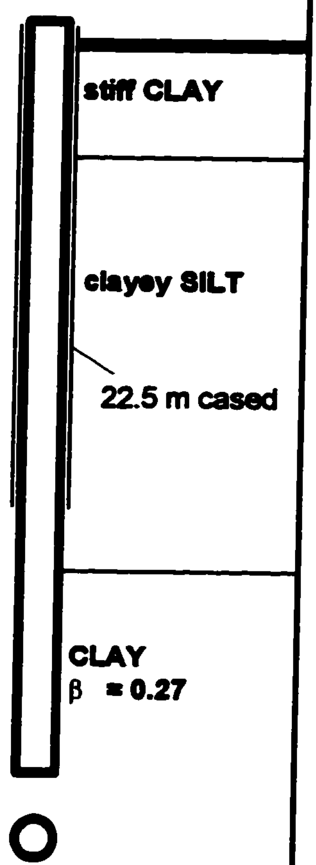

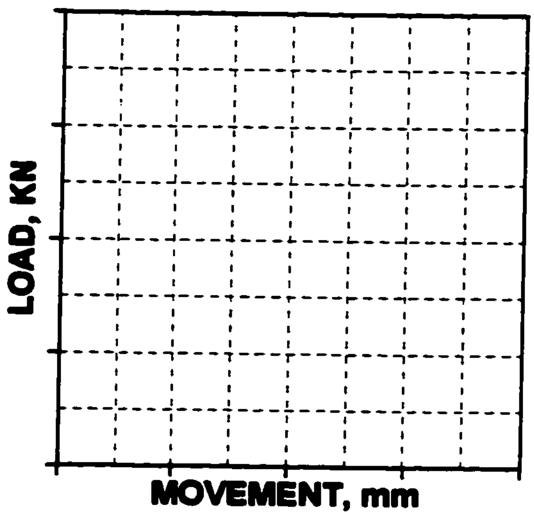

Case 87 CWDNC
Sheet a CPT data

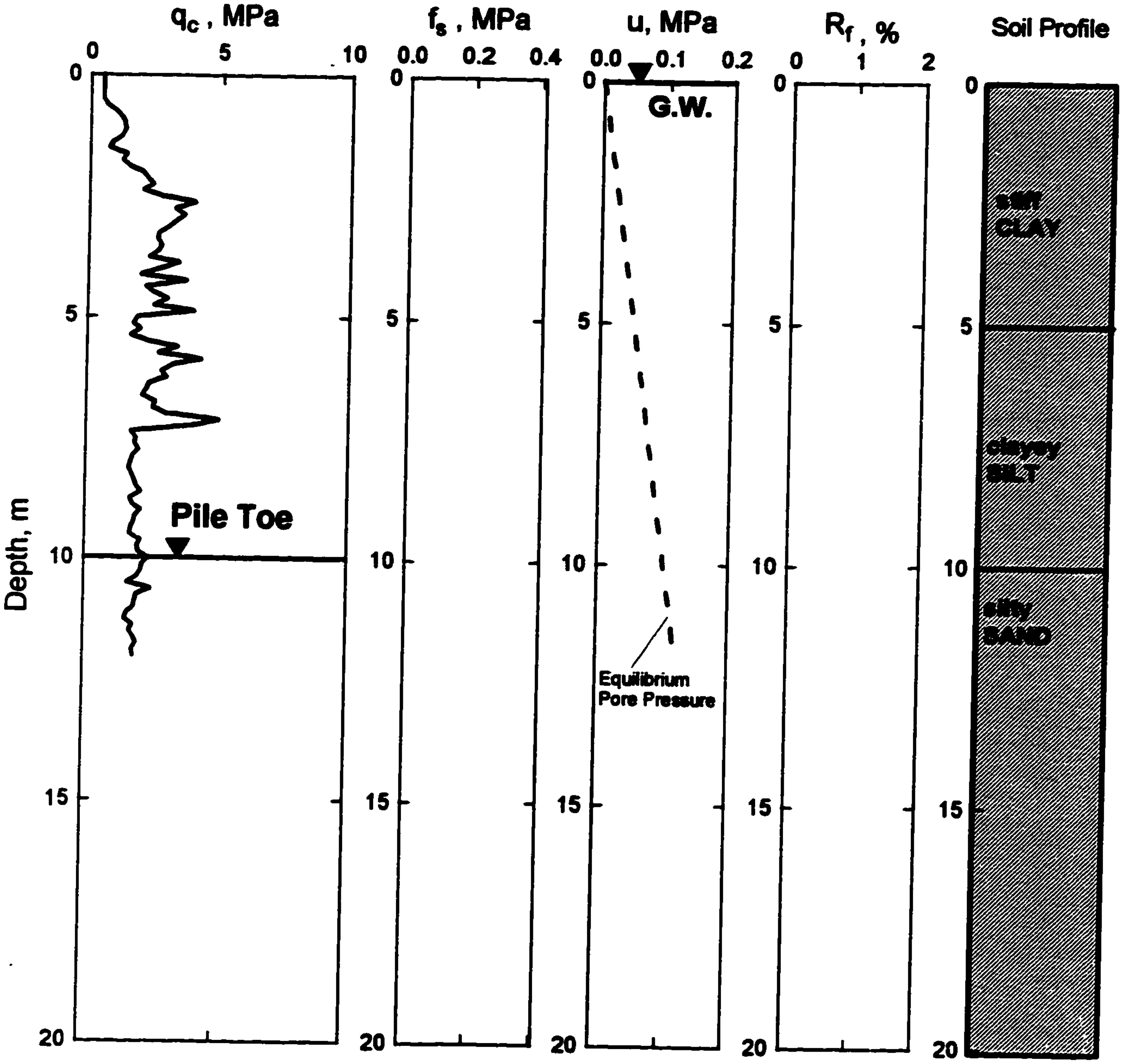

Case 87 CWDNC
Sheet b Pile data

	DETAIL	DESCRIPTION
1	Site	Cowden, UK
2	Reference	Almeida et al., 1996
3	Shape, Material, and Installation	Pipe, Steel, Driven
4	Diameter, b, and Wall Thickness, t, mm	305
5	Embedment Length D, m	10
6	Cross Sectional Area A_t, m^2	0.073
7	Unit Circumferential Area, A_s, m^2/m	0.958
8	Toe, Closed or Open	Open
9	Type of Test and Loading	Static Tension, SML
10	Toe Capacity, R_t, KN	
11	Shaft Capacity, R_s, KN	400
12	Capacity, R_u, KN	

SCHEMATIC PROFILE

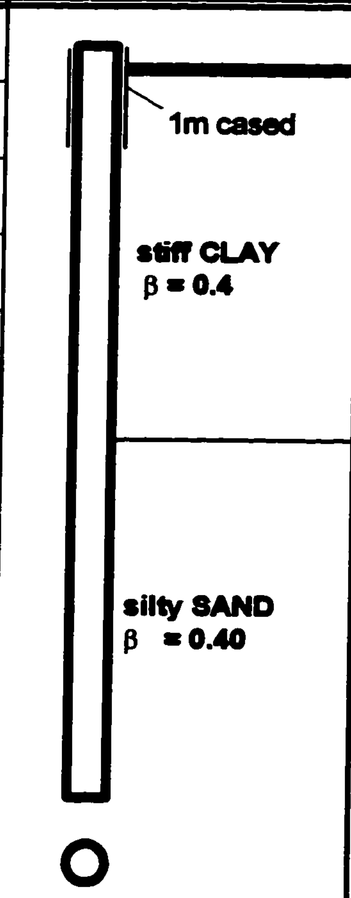

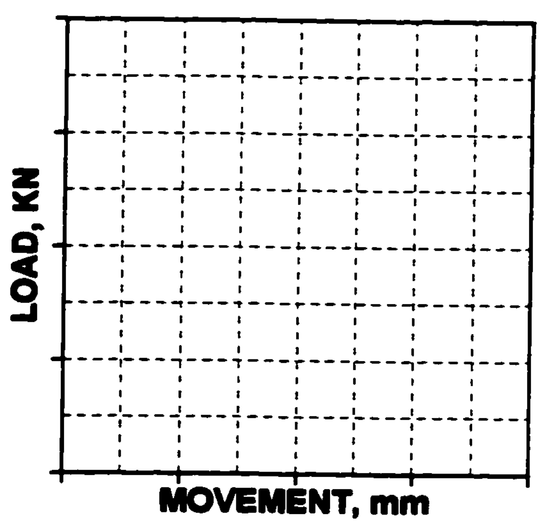

Case 88 CWDND
Sheet a CPT data

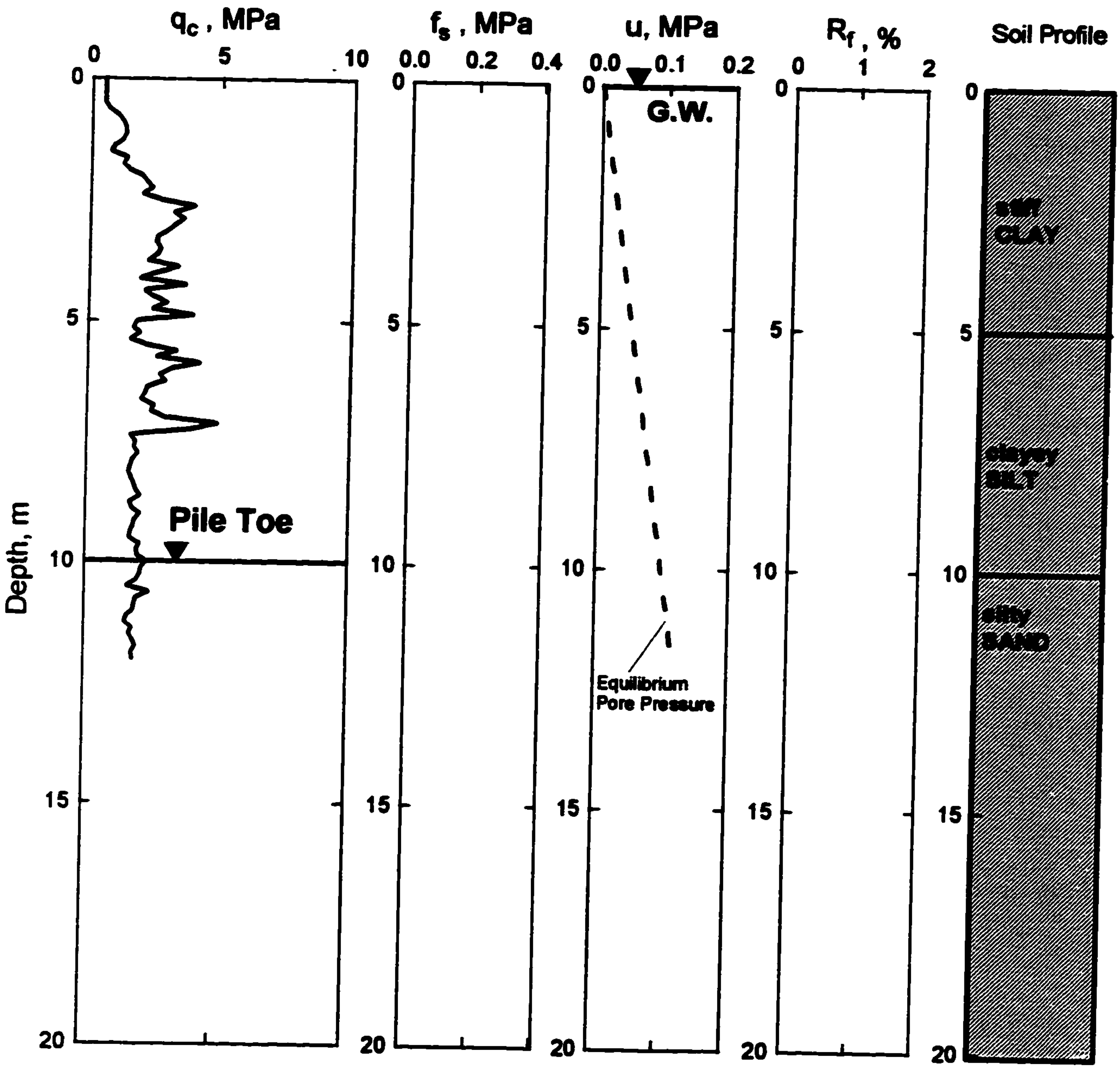

Case 88 CWDND
Sheet b Pile data

DETAIL		DESCRIPTION
1	Site	Cowden, UK
2	Reference	Almeida et al., 1996
3	Shape, Material, and Installation	Pipe, Steel, Driven
4	Diameter, b, and Wall Thickness, t, mm	305
5	Embedment Length D, m	10
6	Cross Sectional Area A_t, m^2	0.073
7	Unit Circumferential Area, A_s, m^2 /m	0.958
8	Toe, Closed or Open	Open
9	Type of Test and Loading	Static Tension, SML
10	Toe Capacity, R_t, KN	
11	Shaft Capacity, R_s, KN	404
12	Capacity, R_u, KN	

SCHEMATIC PROFILE

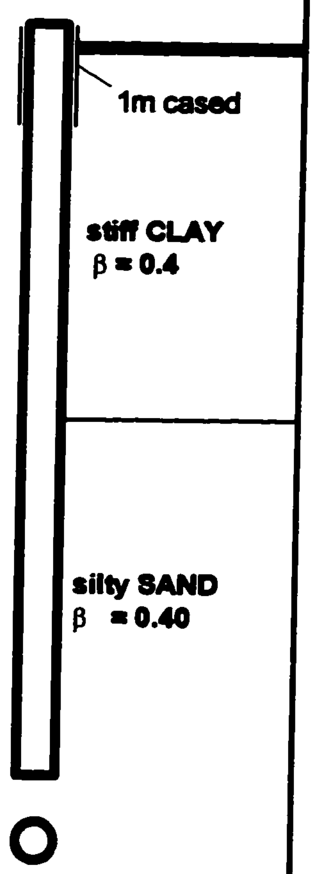

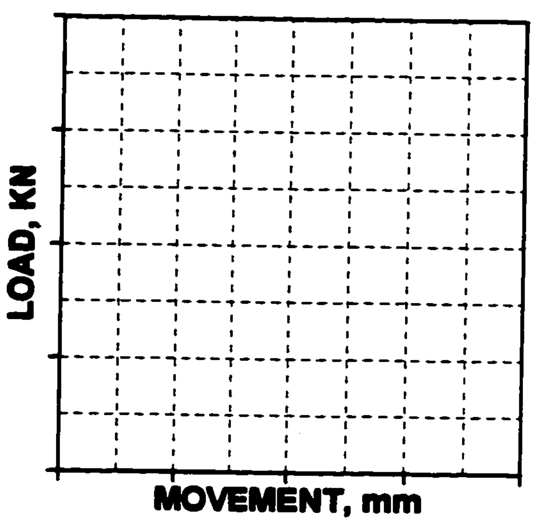

Case 89 CWDNE
Sheet a CPT data

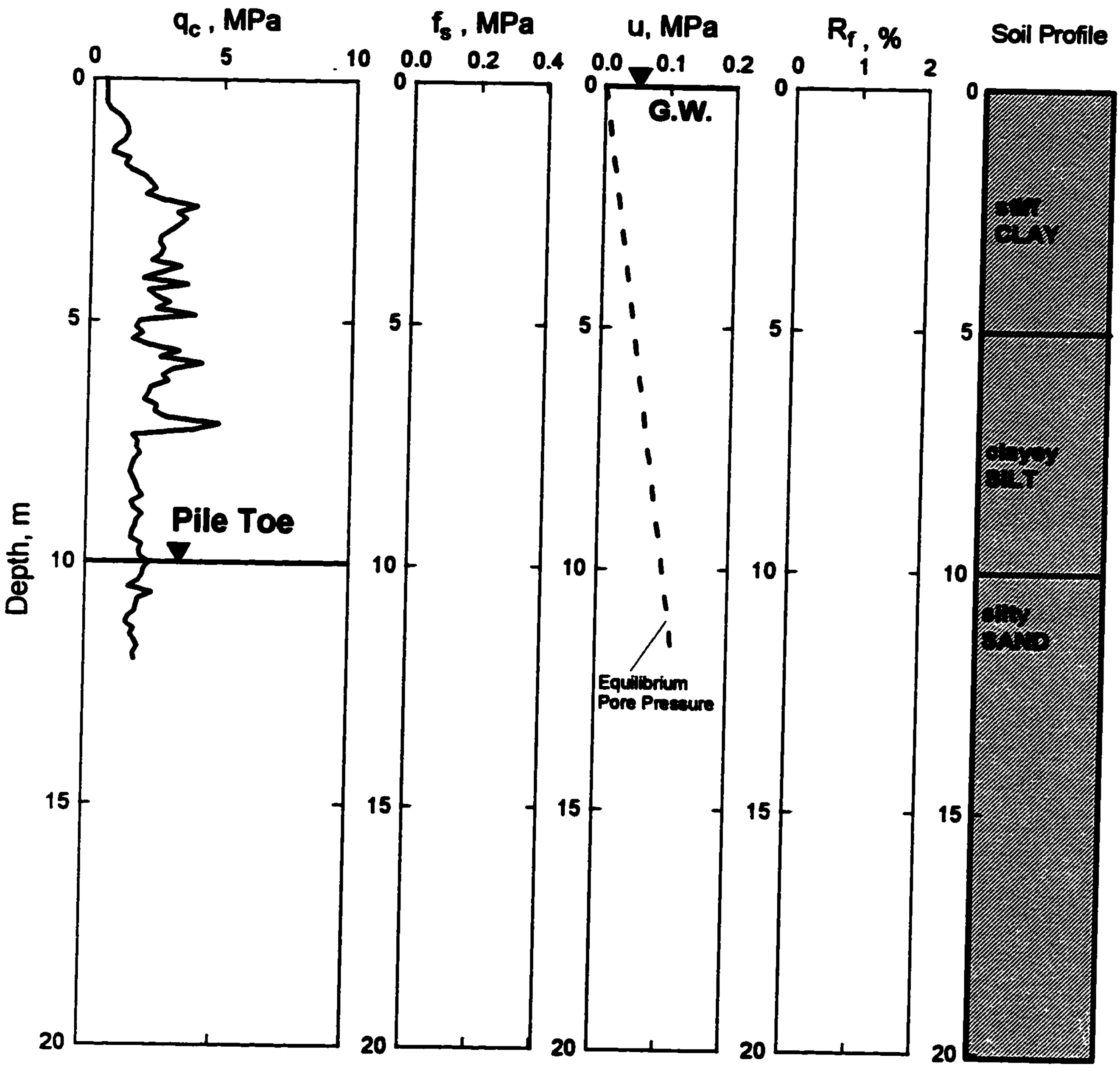

Case 89 CWDNE
Sheet b Pile data

	DETAIL	DESCRIPTION	SCHEMATIC PROFILE
1	Site	Cowden, UK	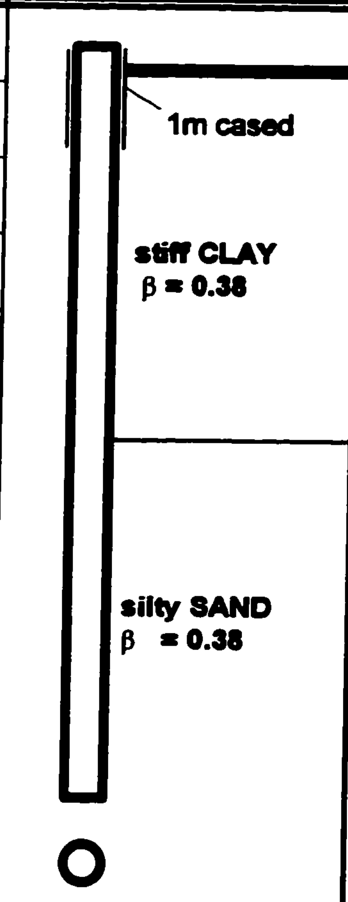
2	Reference	Almeida et al., 1996	
3	Shape, Material, and Installation	Pipe, Steel, Driven	
4	Diameter, b, and Wall Thickness, t, mm	305	
5	Embedment Length D, m	10	
6	Cross Sectional Area A_t, m^2	0.073	
7	Unit Circumferential Area, A_s, m^2/m	0.958	
8	Toe, Closed or Open	Open	
9	Type of Test and Loading	Static Tension, SML	
10	Toe Capacity, R_t, KN		
11	Shaft Capacity, R_s, KN	380	
12	Capacity, R_u, KN		

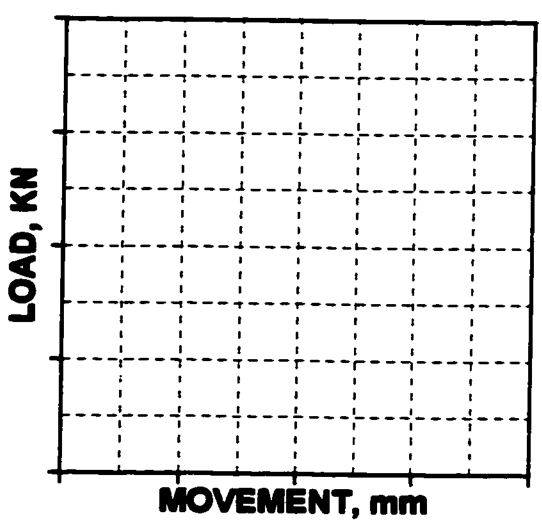

Case 90 CWDNF
Sheet a CPT data

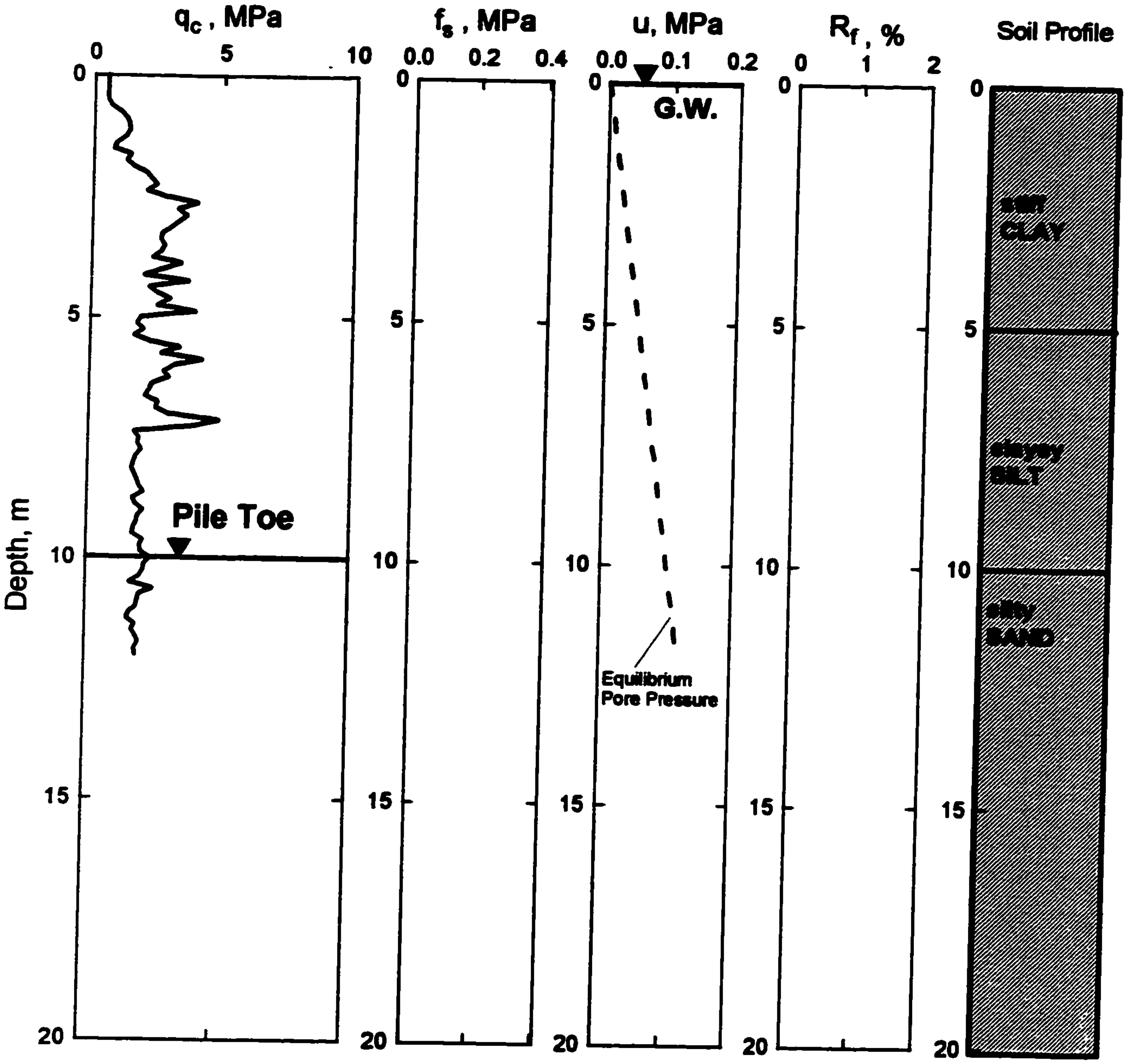

Case 90 CWDNF
Sheet b Pile data

	DETAIL	DESCRIPTION	SCHEMATIC PROFILE
1	Site	Cowden, UK	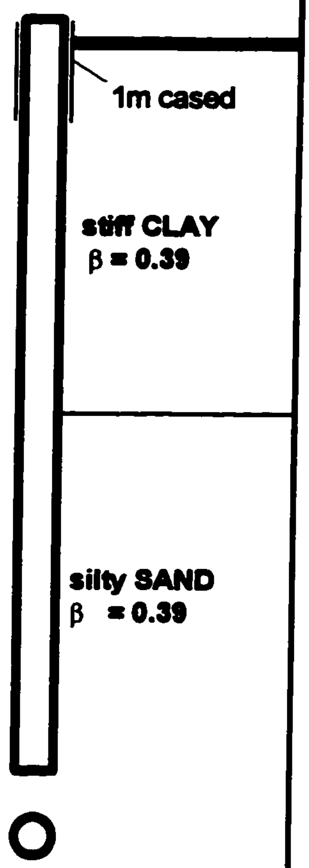
2	Reference	Almeida et al., 1996	
3	Shape, Material, and Installation	Pipe, Steel, Driven	
4	Diameter, b, and Wall Thickness, t, mm	305	
5	Embedment Length D, m	10	
6	Cross Sectional Area A_t , m^2	0.073	
7	Unit Circumferential Area, A_s , m^2 /m	0.958	
8	Toe, Closed or Open	Open	
9	Type of Test and Loading	Static Tension, SML	
10	Toe Capacity, R_t , KN		
11	Shaft Capacity, R_s , KN	390	
12	Capacity, R_u , KN		

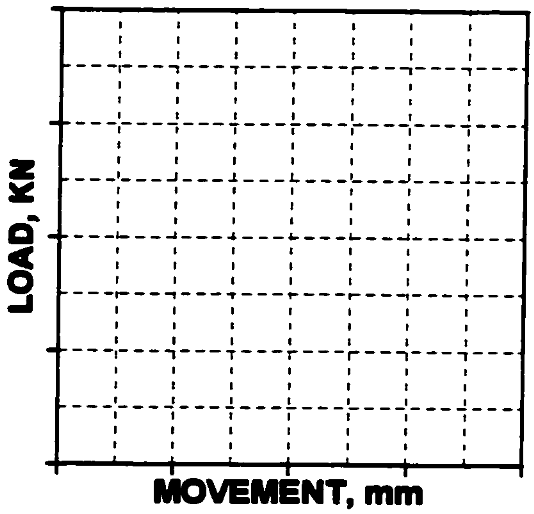

Case 91 CWDNG
Sheet a CPT data

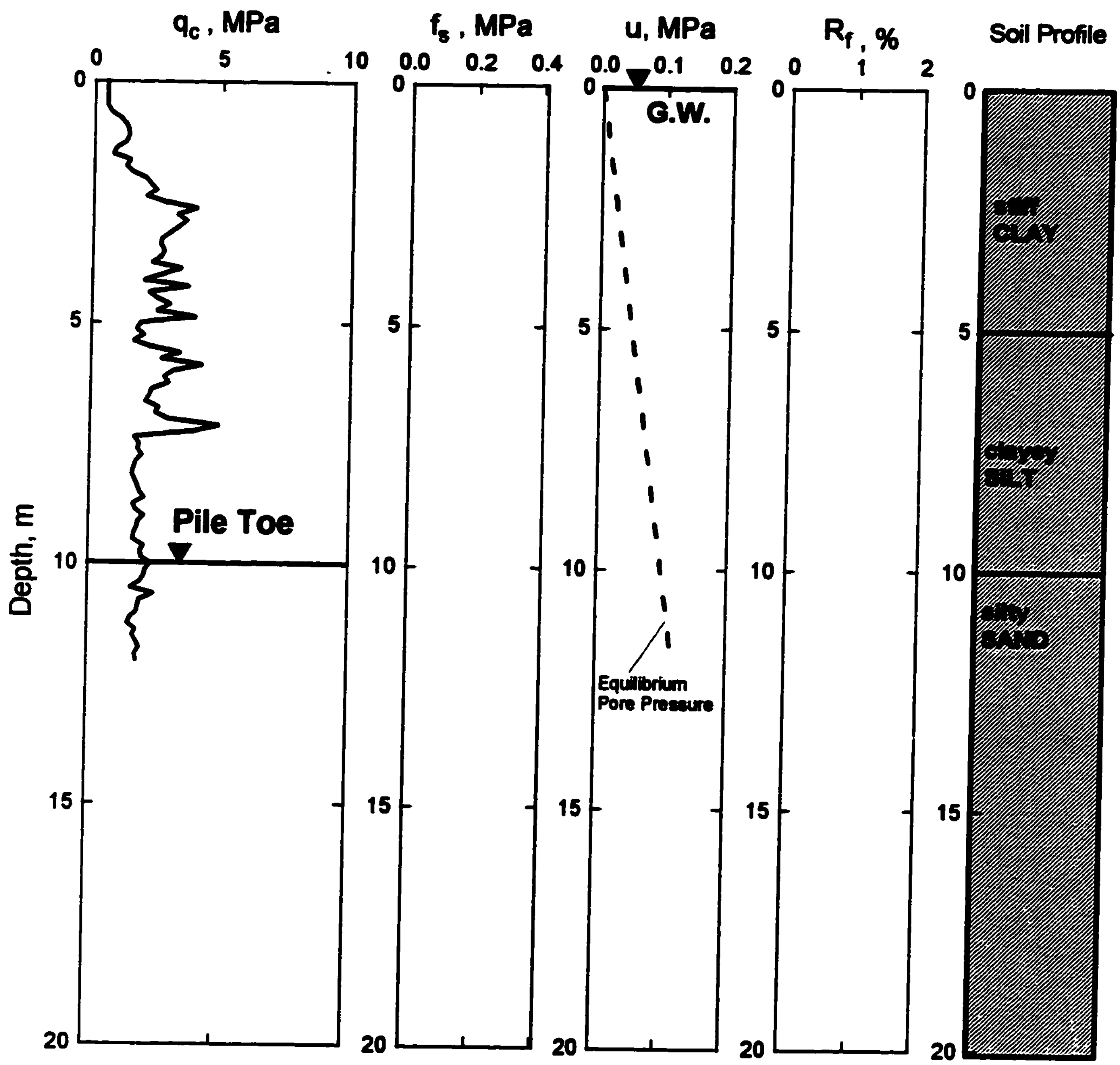

Case 91 CWDNG
Sheet b Pile data

	DETAIL	DESCRIPTION	SCHEMATIC PROFILE
1	Site	Cowden, UK	
2	Reference	Almeida et al., 1996	
3	Shape, Material, and Installation	Pipe, Steel, Driven	
4	Diameter, b, and Wall Thickness, t, mm	203	
5	Embedment Length D, m	10	
6	Cross Sectional Area A_t, m^2	0.032	
7	Unit Circumferential Area, A_s, m^2/m	0.638	
8	Toe, Closed or Open	Open	
9	Type of Test and Loading	Static Tension, SML	
10	Toe Capacity, R_t, KN		
11	Shaft Capacity, R_s, KN	311	
12	Capacity, R_u, KN		

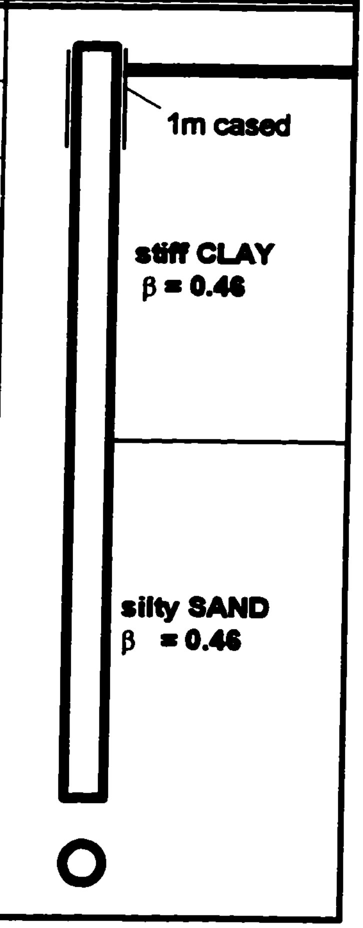

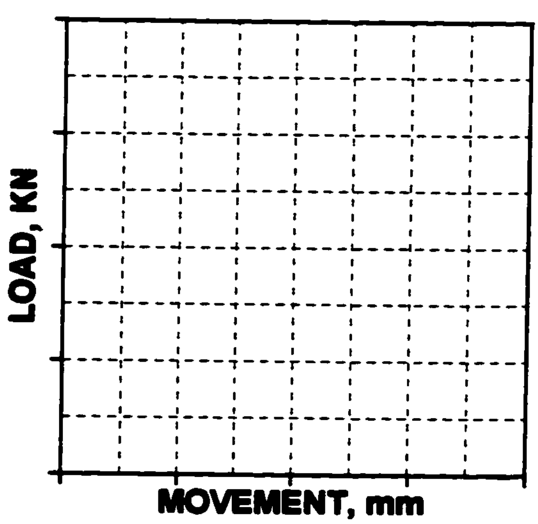

Case 92 CWDNH
Sheet a CPT data

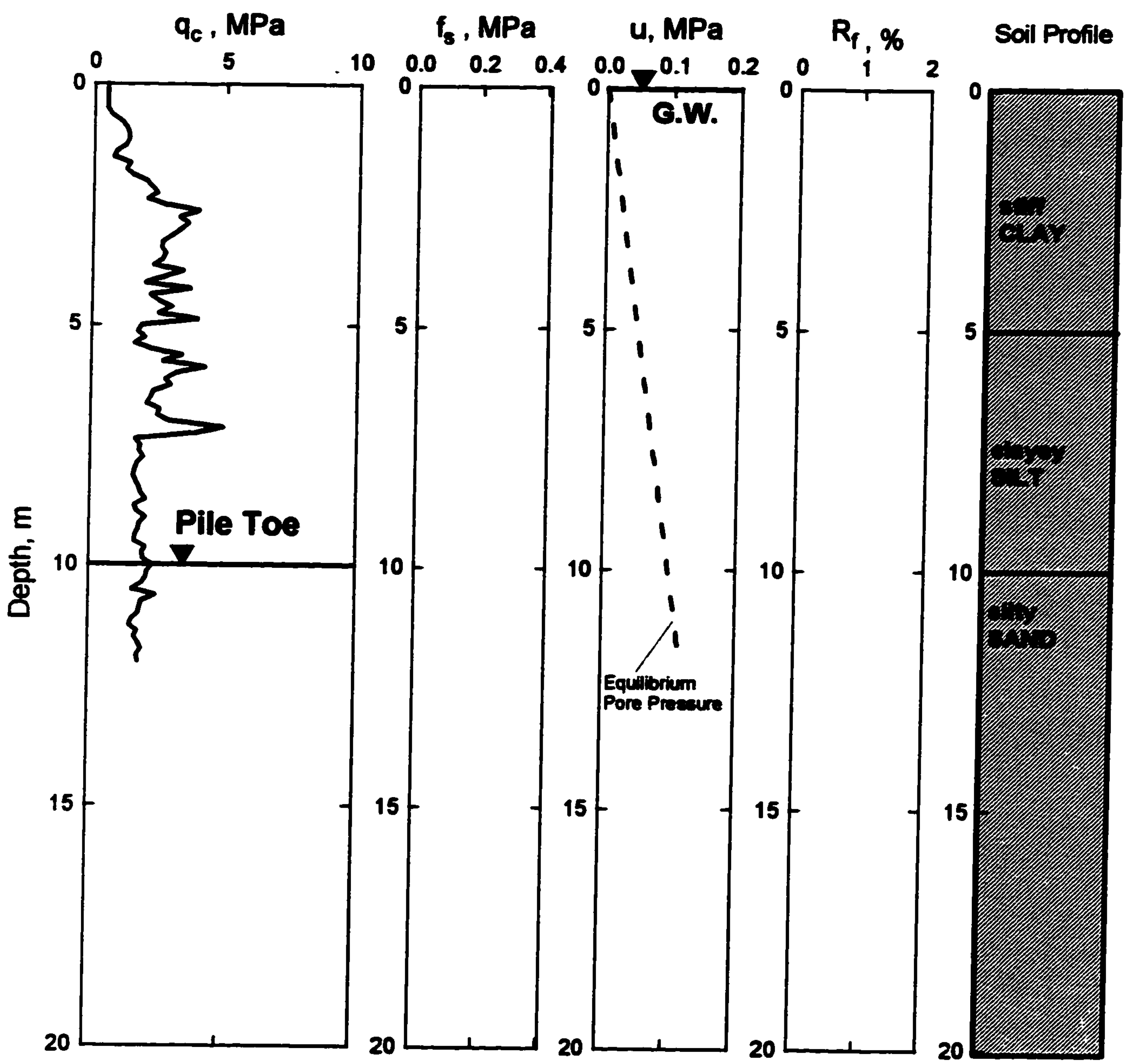

Case 92 CWDNH
Sheet b Pile data

	DETAIL	DESCRIPTION	SCHEMATIC PROFILE
1	Site	Cowden, UK	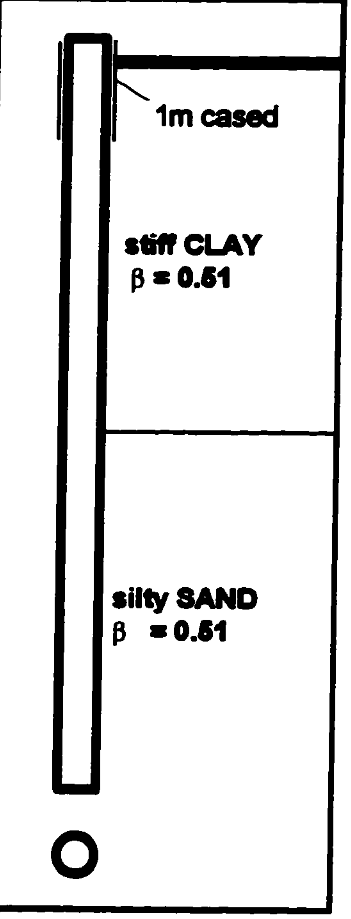
2	Reference	Almeida et al., 1996	
3	Shape, Material, and Installation	Pipe, Steel, Driven	
4	Diameter, b, and Wall Thickness, t, mm	203	
5	Embedment Length D, m	10	
6	Cross Sectional Area A_t, m²	0.032	
7	Unit Circumferential Area, A_s, m²/m	0.638	
8	Toe, Closed or Open	Open	
9	Type of Test and Loading	Static Tension, SML	
10	Toe Capacity, R_t, KN		
11	Shaft Capacity, R_s, KN	350	
12	Capacity, R_u, KN		

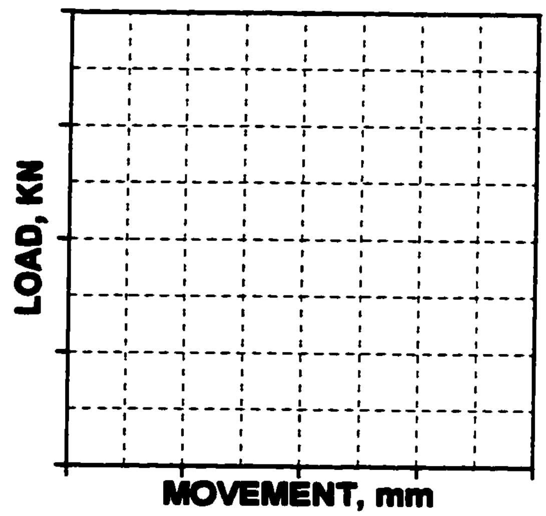

Case 93 CWDNI
Sheet a CPT data

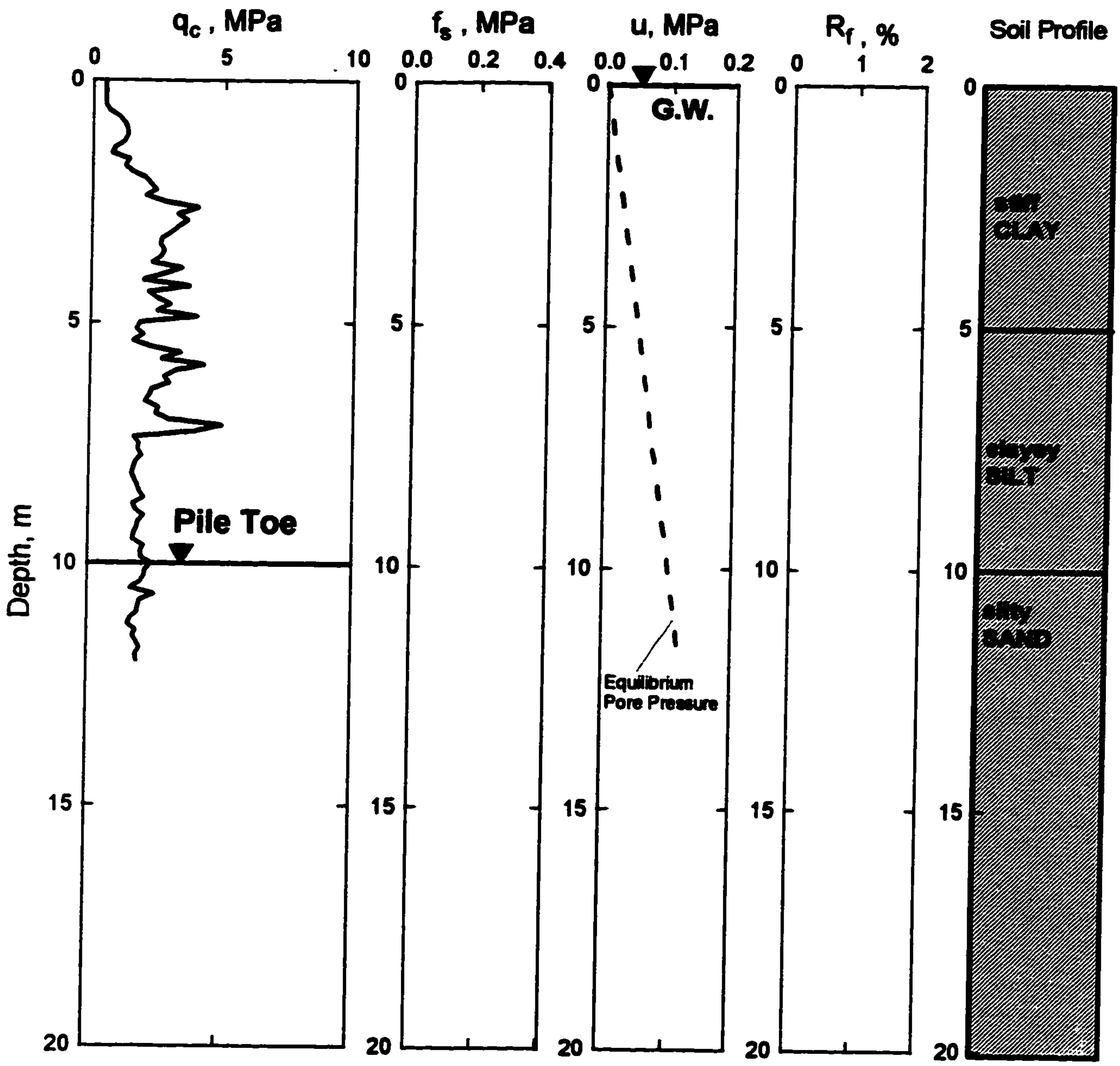

Case 93 CWDNI
Sheet b Pile data

	DETAIL	DESCRIPTION
1	Site	Cowden, UK
2	Reference	Almeida et al., 1996
3	Shape, Material, and Installation	Pipe, Steel, Driven
4	Diameter, b, and Wall Thickness, t, mm	203
5	Embedment Length D, m	10
6	Cross Sectional Area A_t, m^2	0.032
7	Unit Circumferential Area, A_s, m^2/m	0.638
8	Toe, Closed or Open	Open
9	Type of Test and Loading	Static Tension, SML
10	Toe Capacity, R_t, KN	
11	Shaft Capacity, R_s, KN	290
12	Capacity, R_u, KN	

SCHEMATIC PROFILE

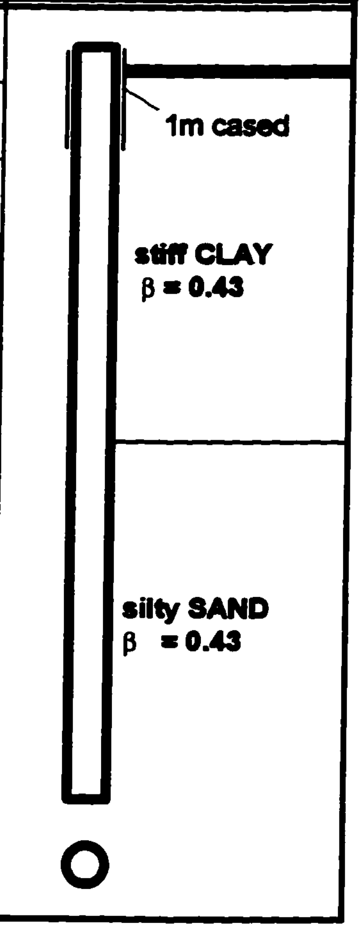

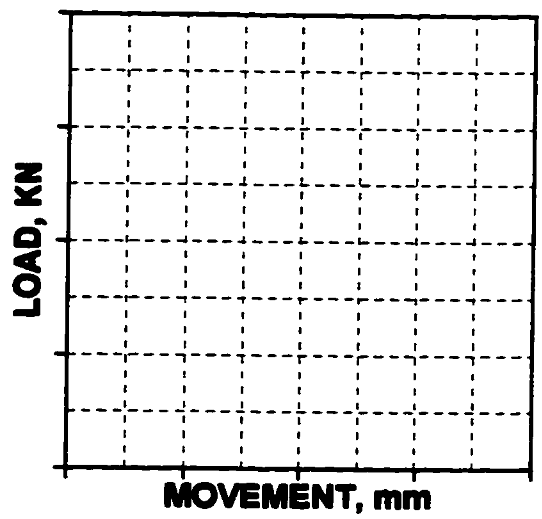

Case 94 CWDNJ
Sheet a CPT data

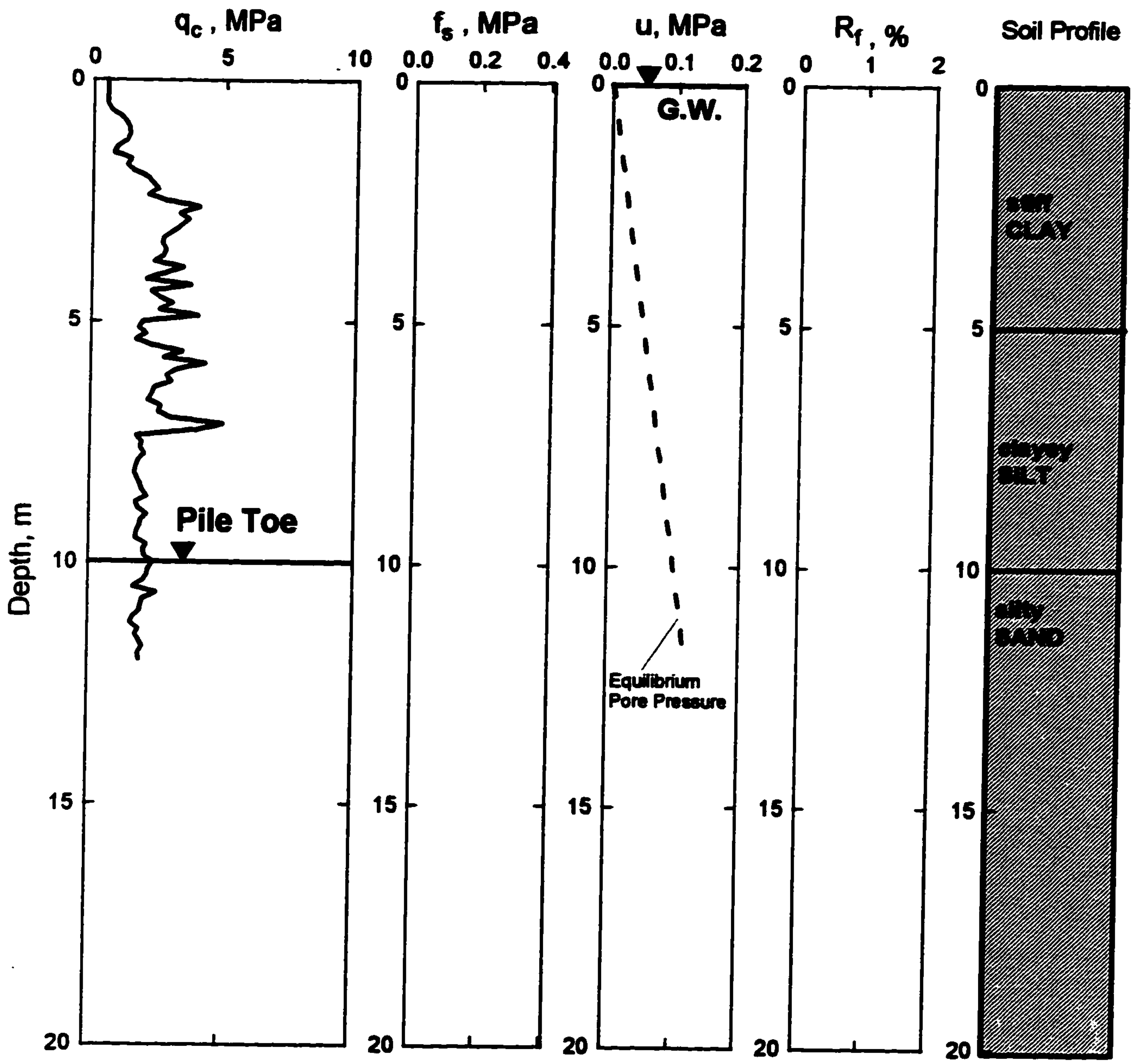

Case 94 CWDNJ
Sheet b Pile data

	DETAIL	DESCRIPTION
1	Site	Cowden, UK
2	Reference	Almeida et al., 1996
3	Shape, Material, and Installation	Pipe, Steel, Driven
4	Diameter, b, and Wall Thickness, t, mm	203
5	Embedment Length D, m	10
6	Cross Sectional Area A_t, m^2	0.032
7	Unit Circumferential Area, A_s, m^2/m	0.638
8	Toe, Closed or Open	Open
9	Type of Test and Loading	Static Tension, SML
10	Toe Capacity, R_t, KN	
11	Shaft Capacity, R_s, KN	280
12	Capacity, R_u, KN	

SCHEMATIC PROFILE

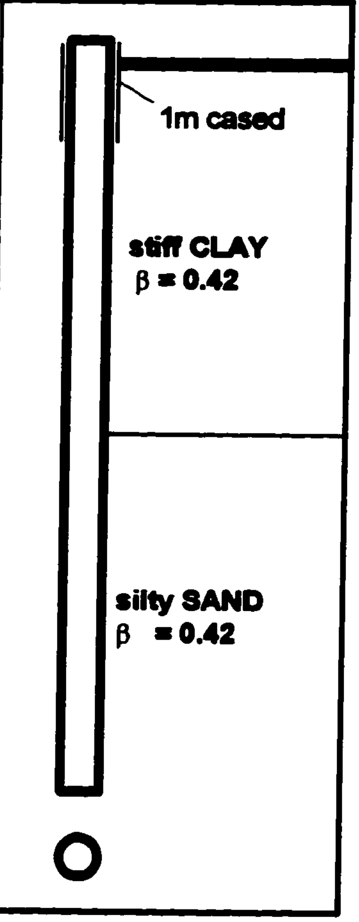

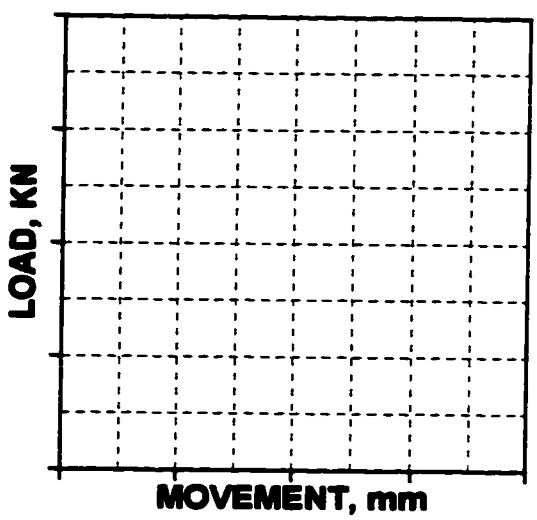

Case 95 CWDNK
Sheet a CPT data

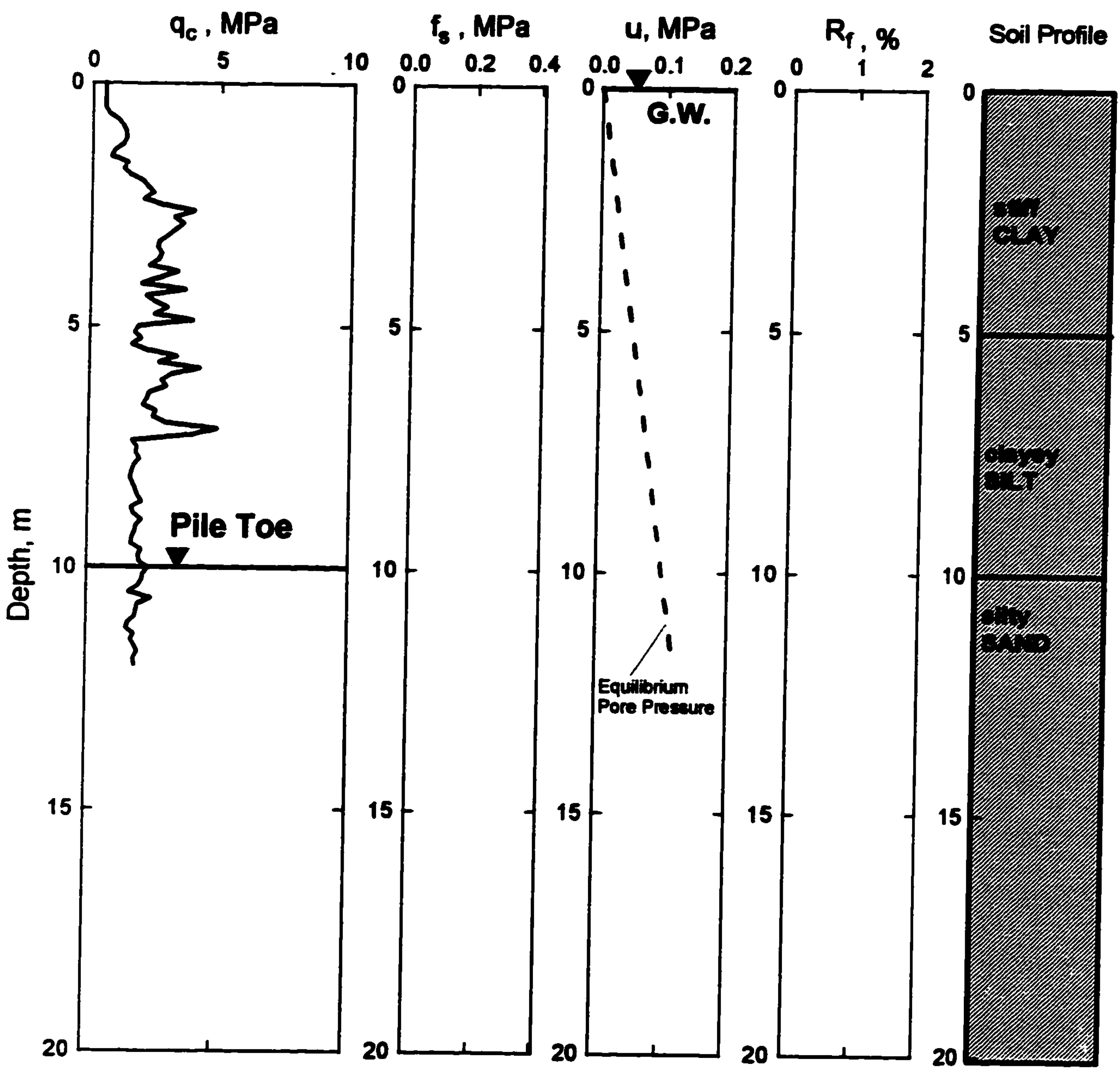

Case 95 CWDNK
Sheet b Pile data

	DETAIL	DESCRIPTION
1	Site	Cowden, UK
2	Reference	Almeida et al., 1996
3	Shape, Material, and Installation	Pipe, Steel, Driven
4	Diameter, b, and Wall Thickness, t, mm	203
5	Embedment Length D, m	10
6	Cross Sectional Area A_t, m^2	0.032
7	Unit Circumferential Area, A_s, m^2/m	0.638
8	Toe, Closed or Open	Open
9	Type of Test and Loading	Static Tension, SML
10	Toe Capacity, R_t, KN	
11	Shaft Capacity, R_s, KN	350
12	Capacity, R_u, KN	

SCHEMATIC PROFILE

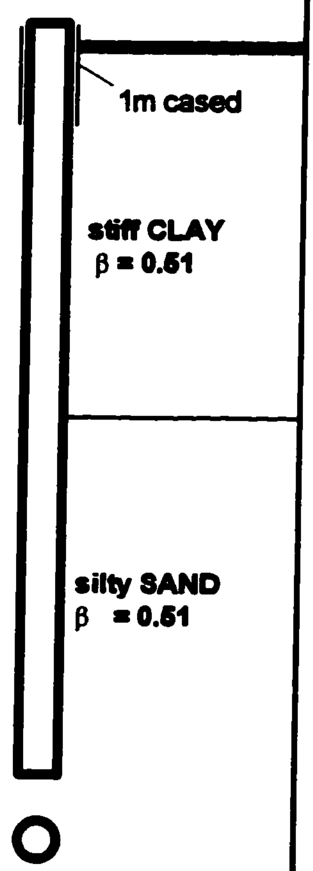

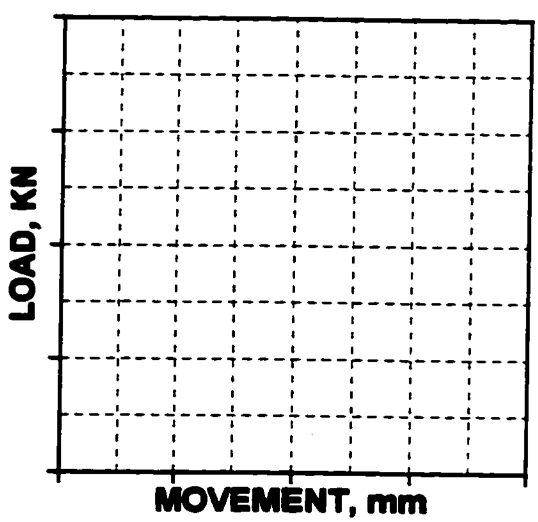

Case 96 ONSYA1
Sheet a CPT data

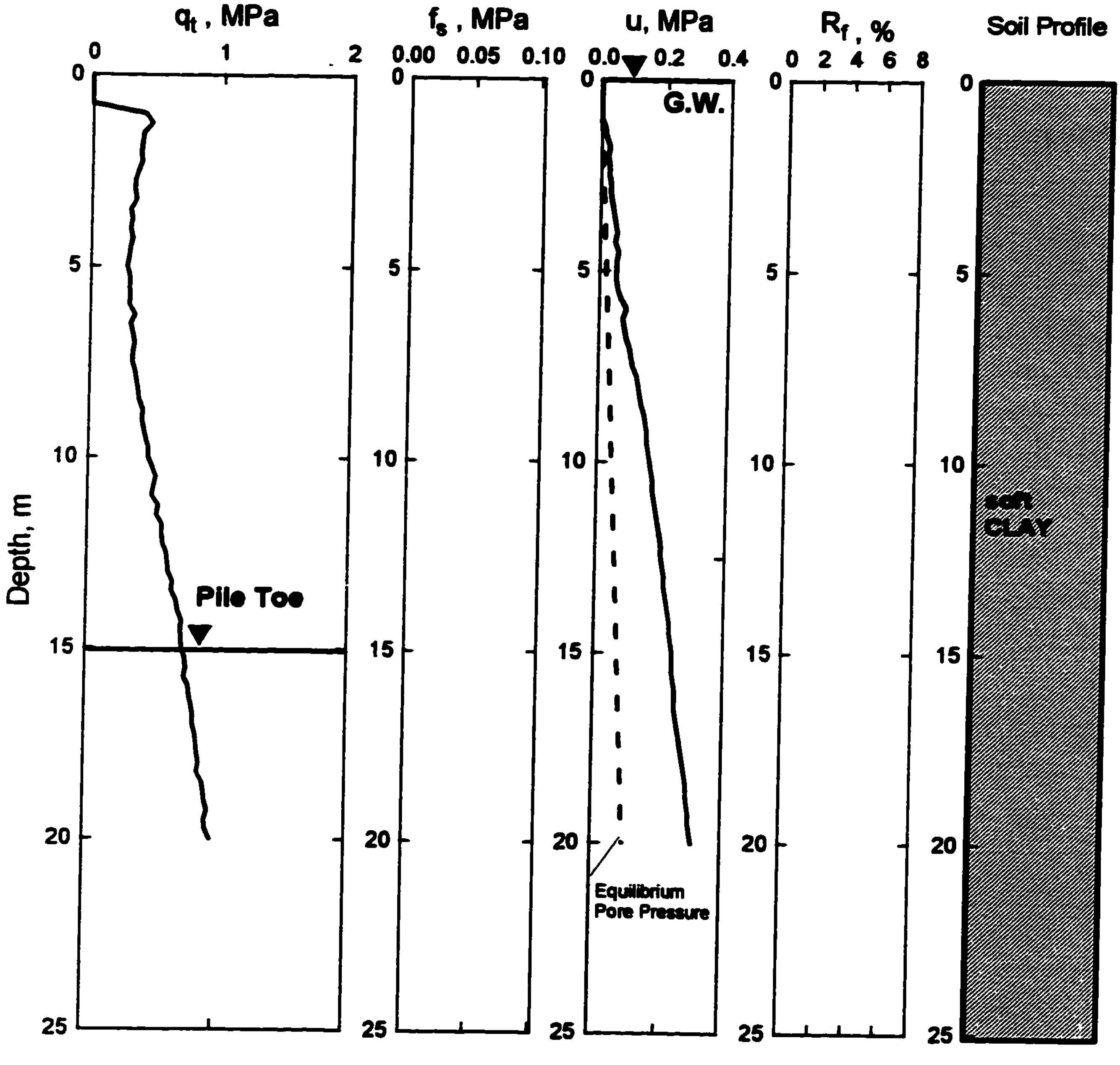

Case 96 ONSYA1
Sheet b Pile data

	DETAIL	DESCRIPTION	SCHEMATIC PROFILE
1	Site	Onsoy, Norway	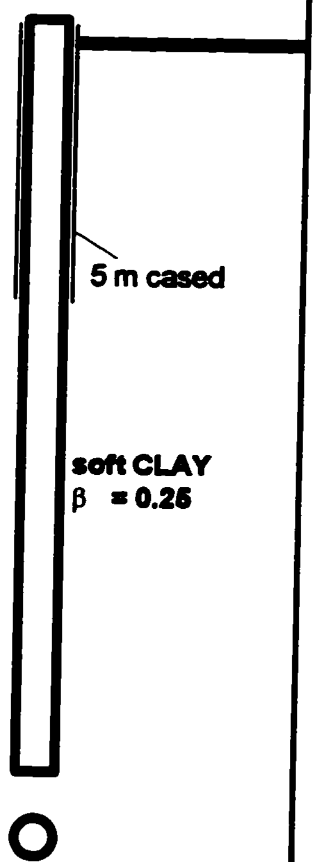
2	Reference	Almeida et al., 1996	
3	Shape, Material, and Installation	Pipe, Steel, Driven	
4	Diameter, b, and Wall Thickness, t, mm	219	
5	Embedment Length D, m	15	
6	Cross Sectional Area A_t, m^2	0.038	
7	Unit Circumferential Area, A_s, m^2 /m	0.688	
8	Toe, Closed or Open	Closed	
9	Type of Test and Loading	Static Tension, SML	
10	Toe Capacity, R_t, KN		
11	Shaft Capacity, R_s, KN	105	
12	Capacity, R_u, KN		

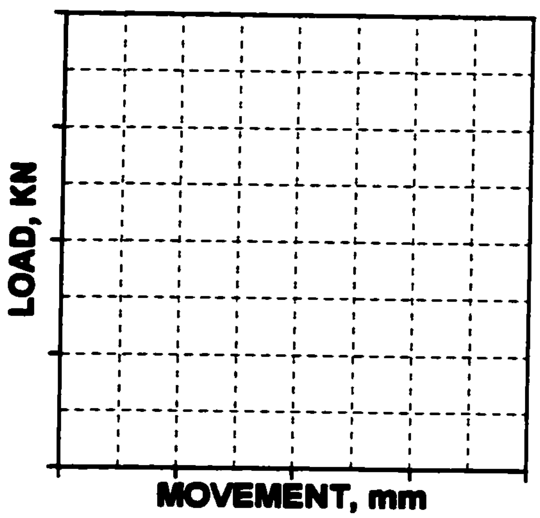

Case 97 ONSYB1
Sheet a CPT data

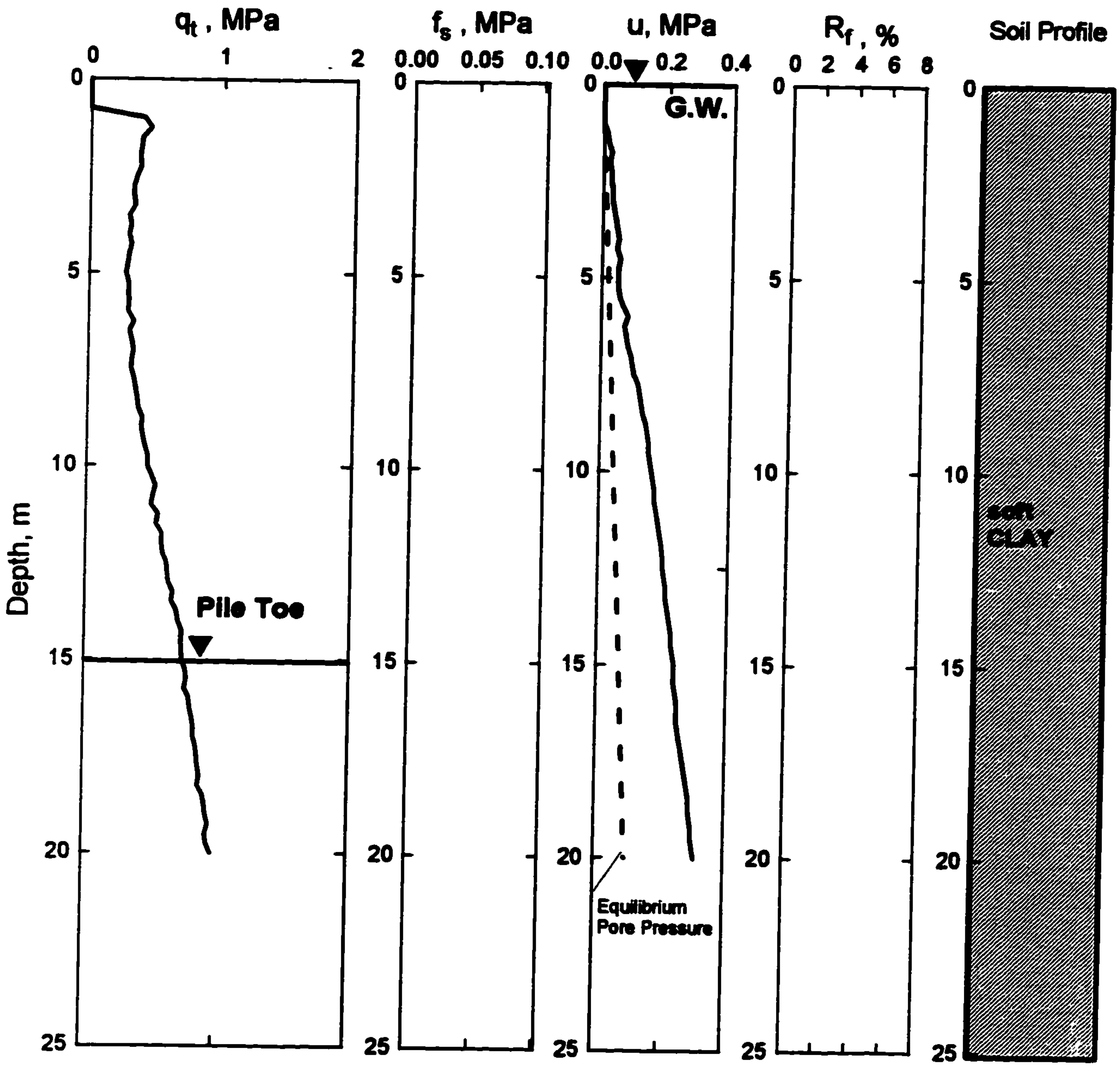

Case 97 ONSYB1
Sheet b Pile data

	DETAIL	DESCRIPTION	SCHEMATIC PROFILE
1	Site	Onsoy, Norway	
2	Reference	Almeida et al., 1996	
3	Shape, Material, and Installation	Pipe, Steel, Driven	
4	Diameter, b, and Wall Thickness, t, mm	812 9.5	
5	Embedment Length D, m	15	
6	Cross Sectional Area A_t, m^2	0.512	
7	Unit Circumferential Area, A_s, m^2/m	2.55	
8	Toe, Closed or Open	Closed	
9	Type of Test and Loading	Static Tension, SML	
10	Toe Capacity, R_t, KN		
11	Shaft Capacity, R_s, KN	374 (Reduced inside friction, 2 KPa per m)	
12	Capacity, R_u, KN		

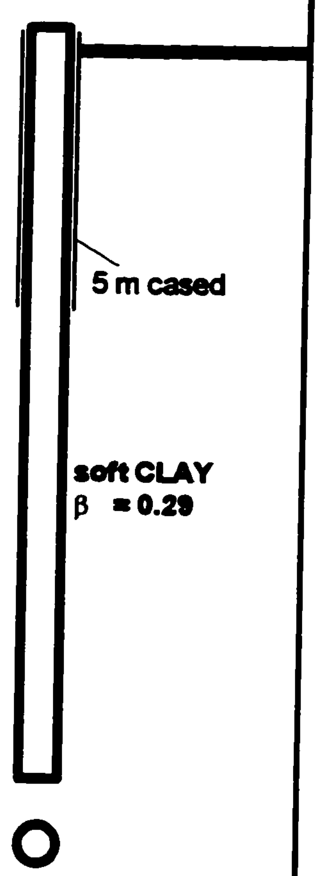

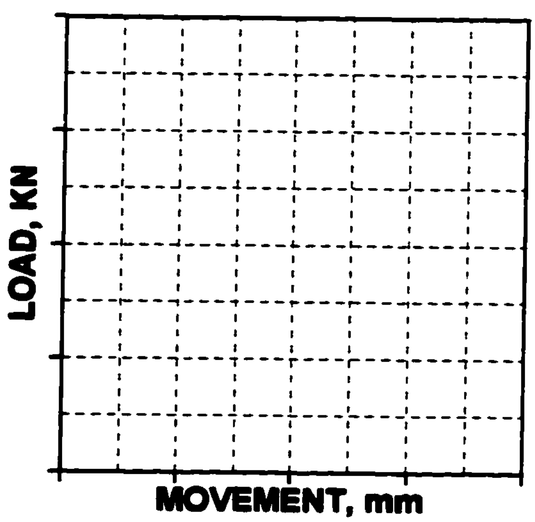

Case 98 LSTDA7
Sheet a CPT data

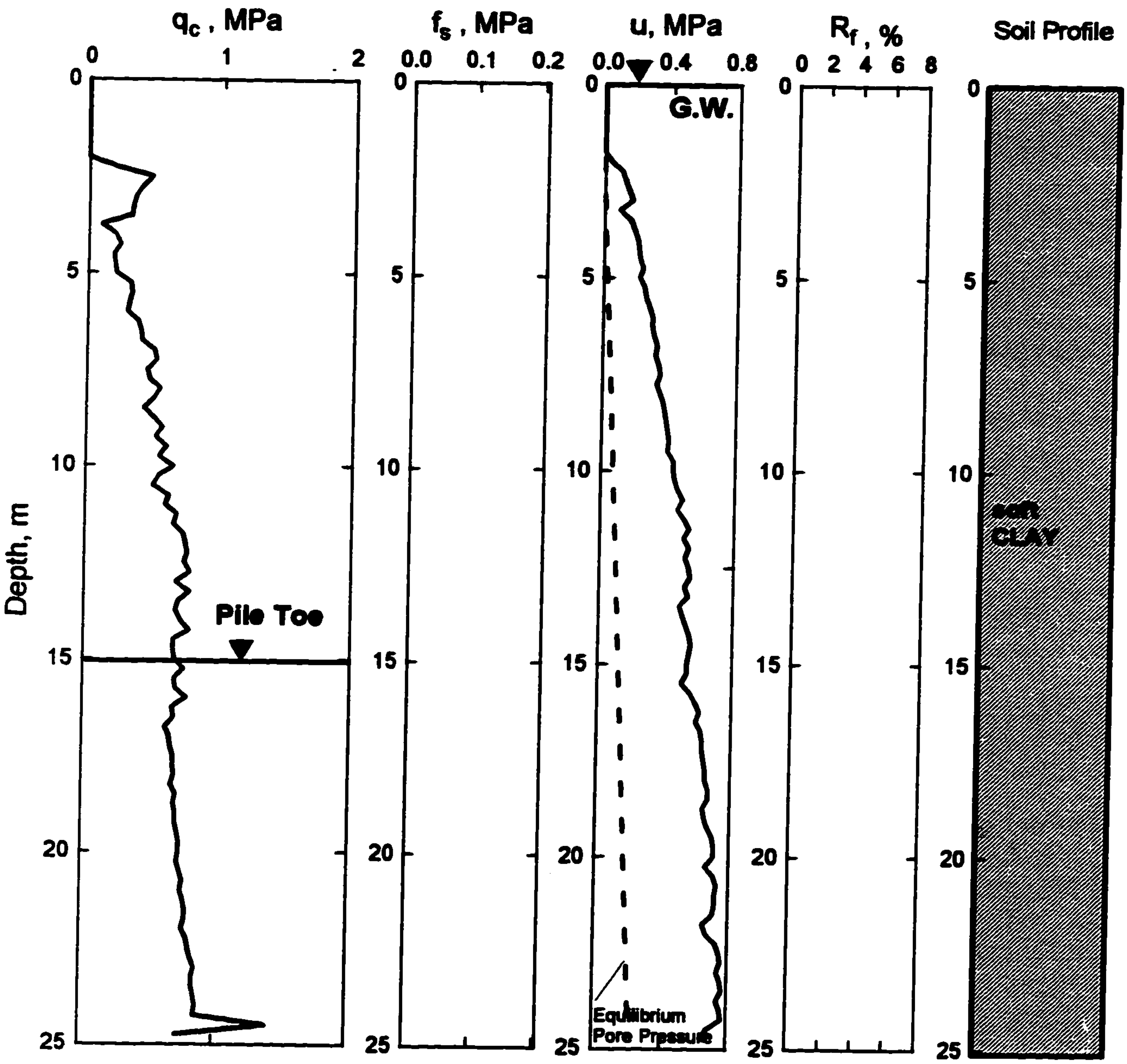

Case 98 LSTDA7
Sheet b Pile data

	DETAIL	DESCRIPTION	SCHEMATIC PROFILE
1	Site	Lierstranda, Norway	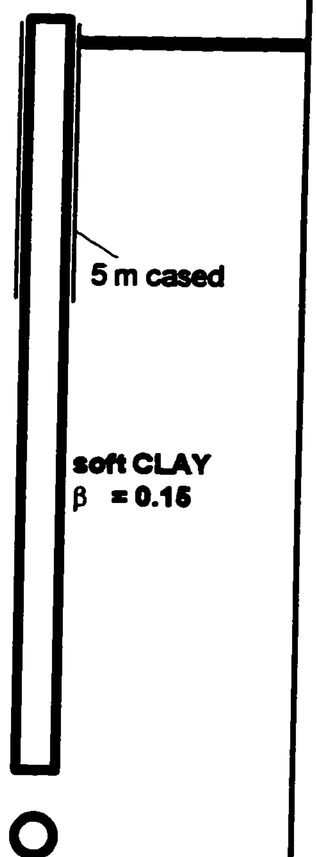
2	Reference	Almeida et al., 1996	
3	Shape, Material, and Installation	Pipe, Steel, Driven	
4	Diameter, b, and Wall Thickness, t, mm	219 8.2	
5	Embedment Length D, m	15	
6	Cross Sectional Area A_t, m^2	0.038	
7	Unit Circumferential Area, A_s, m^2/m	0.688	
8	Toe, Closed or Open	Closed	
9	Type of Test and Loading	Static Tension, SML	
10	Toe Capacity, R_t, KN		
11	Shaft Capacity, R_s, KN	78	
12	Capacity, R_u, KN		

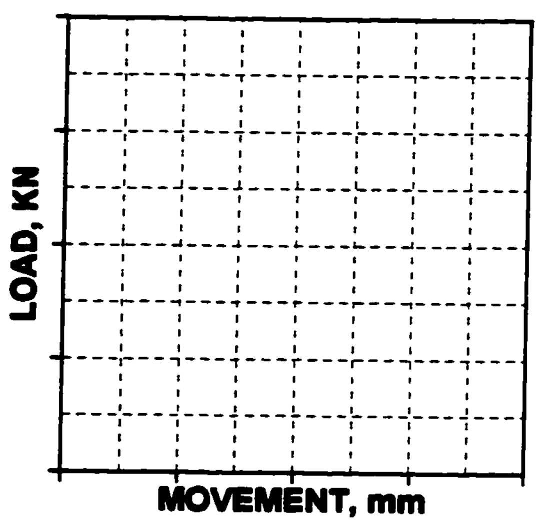

Case 99 LSTDA8
Sheet a CPT data

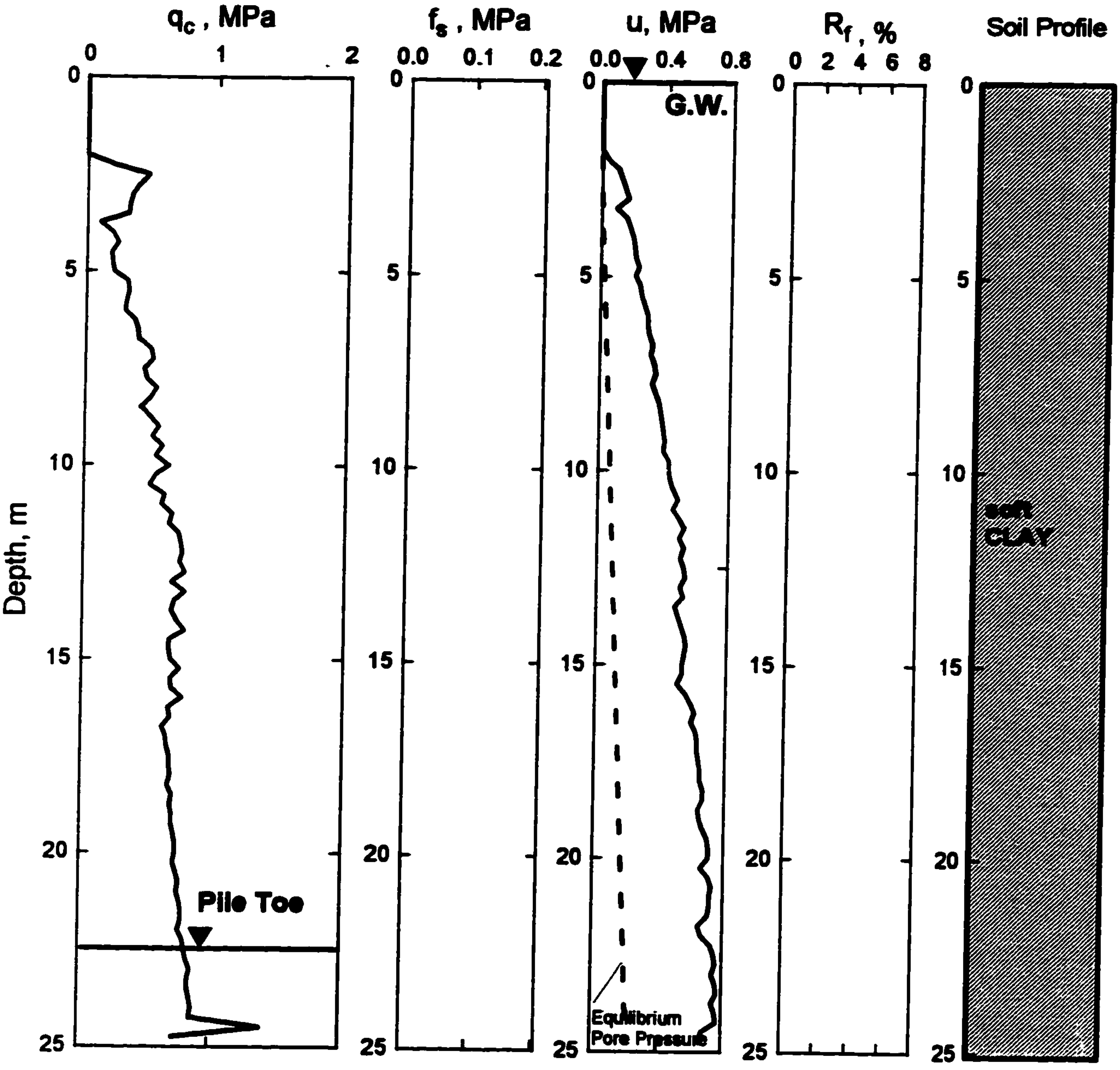

Case 99 LSTDA8
Sheet b Pile data

	DETAIL	DESCRIPTION
1	Site	Lierstranda, Norway
2	Reference	Almeida et al., 1996
3	Shape, Material, and Installation	Pipe, Steel, Driven
4	Diameter, b, and Wall Thickness, t, mm	219 8.2
5	Embedment Length D, m	22.5
6	Cross Sectional Area A_t, m^2	0.038
7	Unit Circumferential Area, A_s, m^2/m	0.688
8	Toe, Closed or Open	Closed
9	Type of Test and Loading	Static Tension, SML
10	Toe Capacity, R_t, KN	
11	Shaft Capacity, R_s, KN	86
12	Capacity, R_u, KN	

SCHEMATIC PROFILE

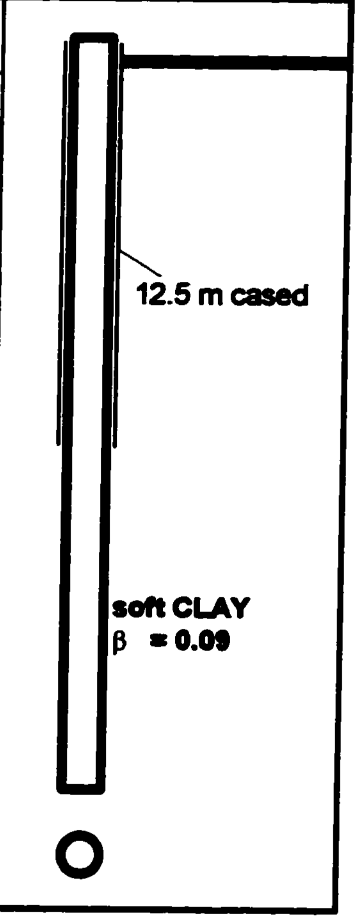

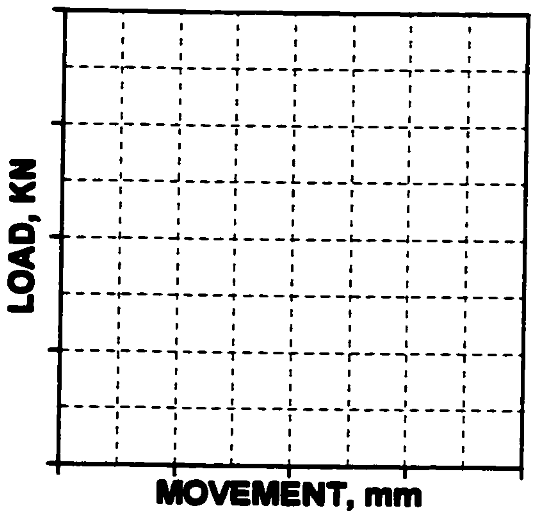

Case 100 LSTDB2
Sheet a CPT data

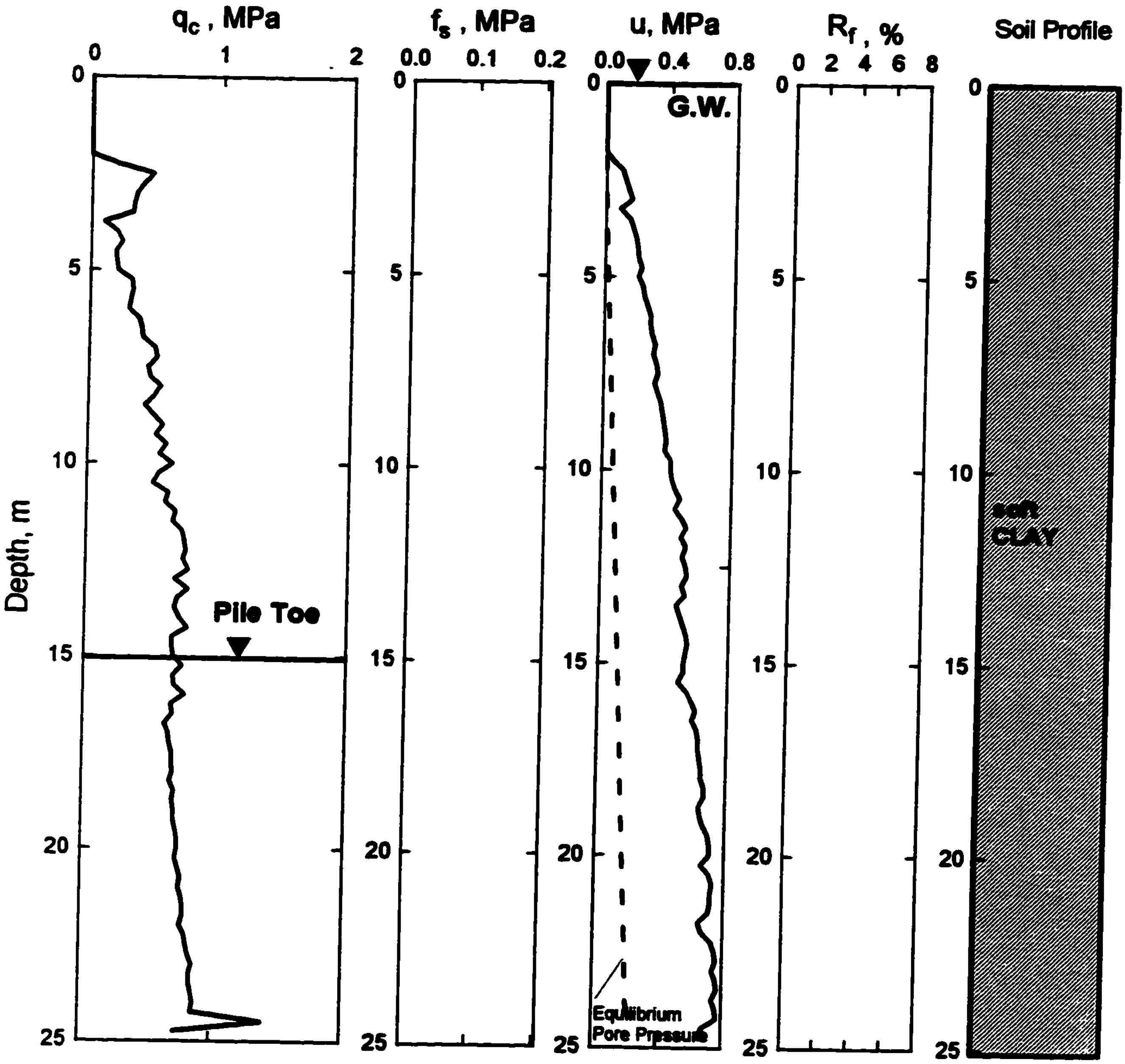

Case 100 LSTDB2
Sheet b Pile data

	DETAIL	DESCRIPTION	SCHEMATIC PROFILE
1	Site	Lierstranda, Norway	
2	Reference	Almeida et al., 1996	
3	Shape, Material, and Installation	Pipe, Steel, Driven	
4	Diameter, b, and Wall Thickness, t, mm	812 9.5	
5	Embedment Length D, m	15	
6	Cross Sectional Area A_t, m^2	0.512	
7	Unit Circumferential Area, A_s, m^2/m	2.55	
8	Toe, Closed or Open	Open	
9	Type of Test and Loading	Static Tension, SML	
10	Toe Capacity, R_t, KN		
11	Shaft Capacity, R_s, KN	444 (Reduced inside friction, 2 KPa per m)	
12	Capacity, R_u, KN		

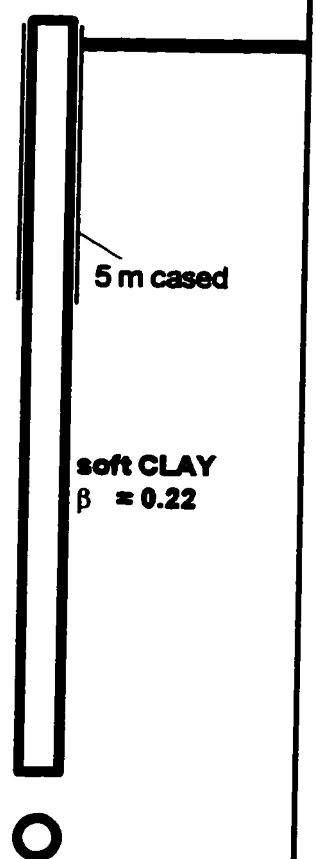

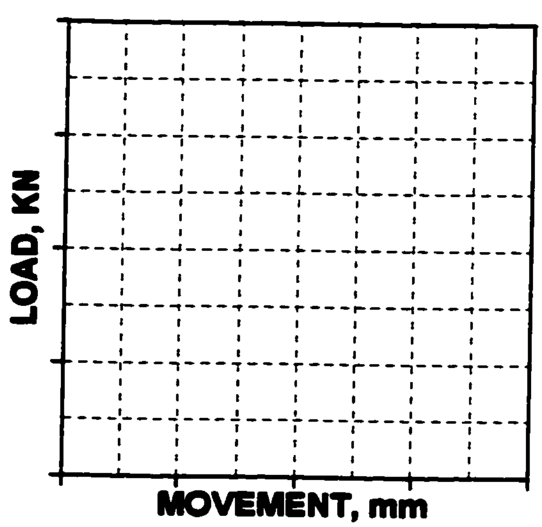

Case 101 PRS
Sheet a CPT data

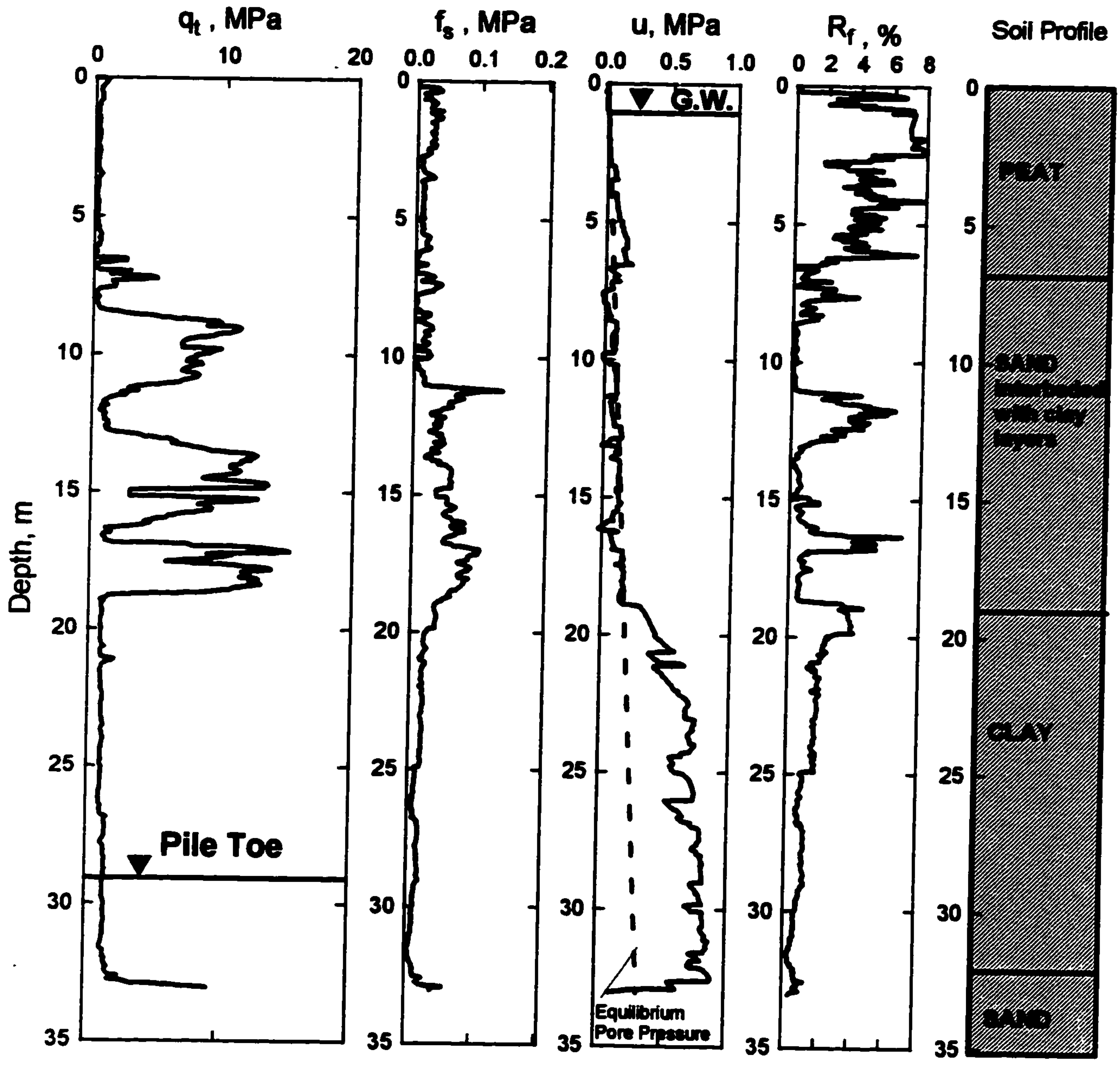

Case 101 PRS
Sheet b Pile data

	DETAIL	DESCRIPTION	SCHEMATIC PROFILE
1	Site	Puerto Rico, USA	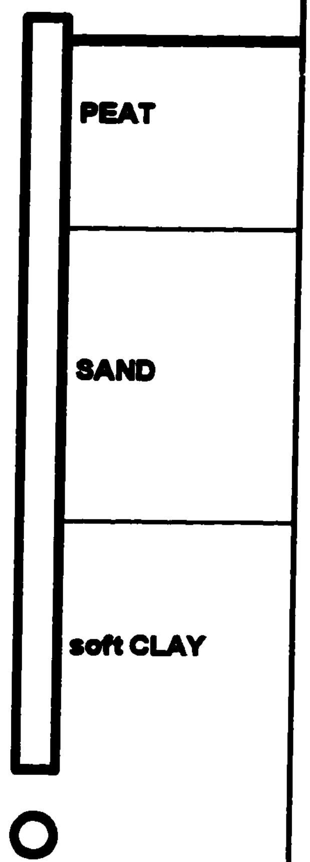
2	Reference	Urkkada Ltd., 1995	
3	Shape, Material, and Installation	Pipe, Steel, Driven	
4	Diameter, b, and Wall Thickness, t, mm	300	
5	Embedment Length D, m	28.4	
6	Cross Sectional Area A_t, m²	0.071	
7	Unit Circumferential Area, A_s, m²/m	0.942	
8	Toe, Closed or Open	Closed	
9	Type of Test and Loading	Static Compression, SML	
10	Toe Capacity, R_t, KN		
11	Shaft Capacity, R_s, KN		
12	*Capacity, R_u, KN	1,240	

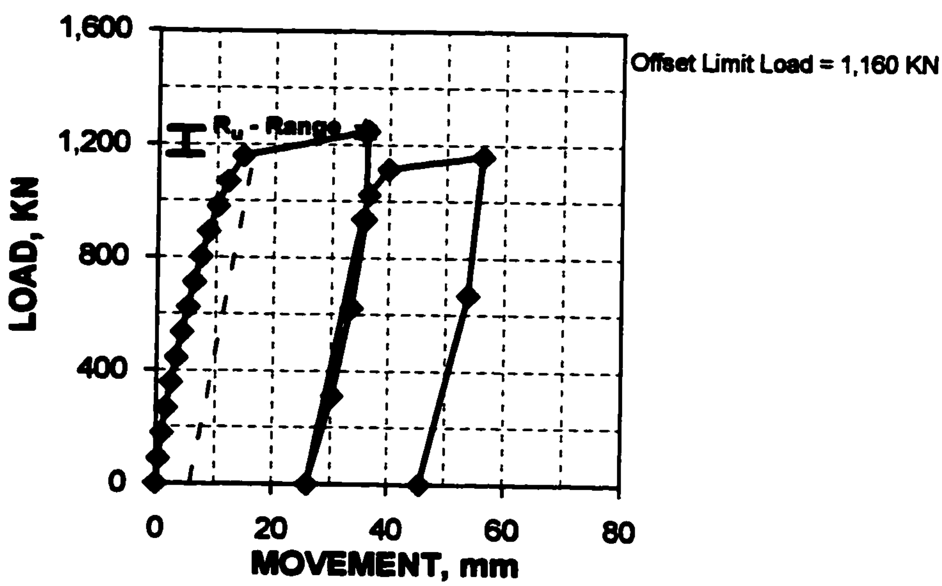

Case 102 PRL
Sheet a CPT data

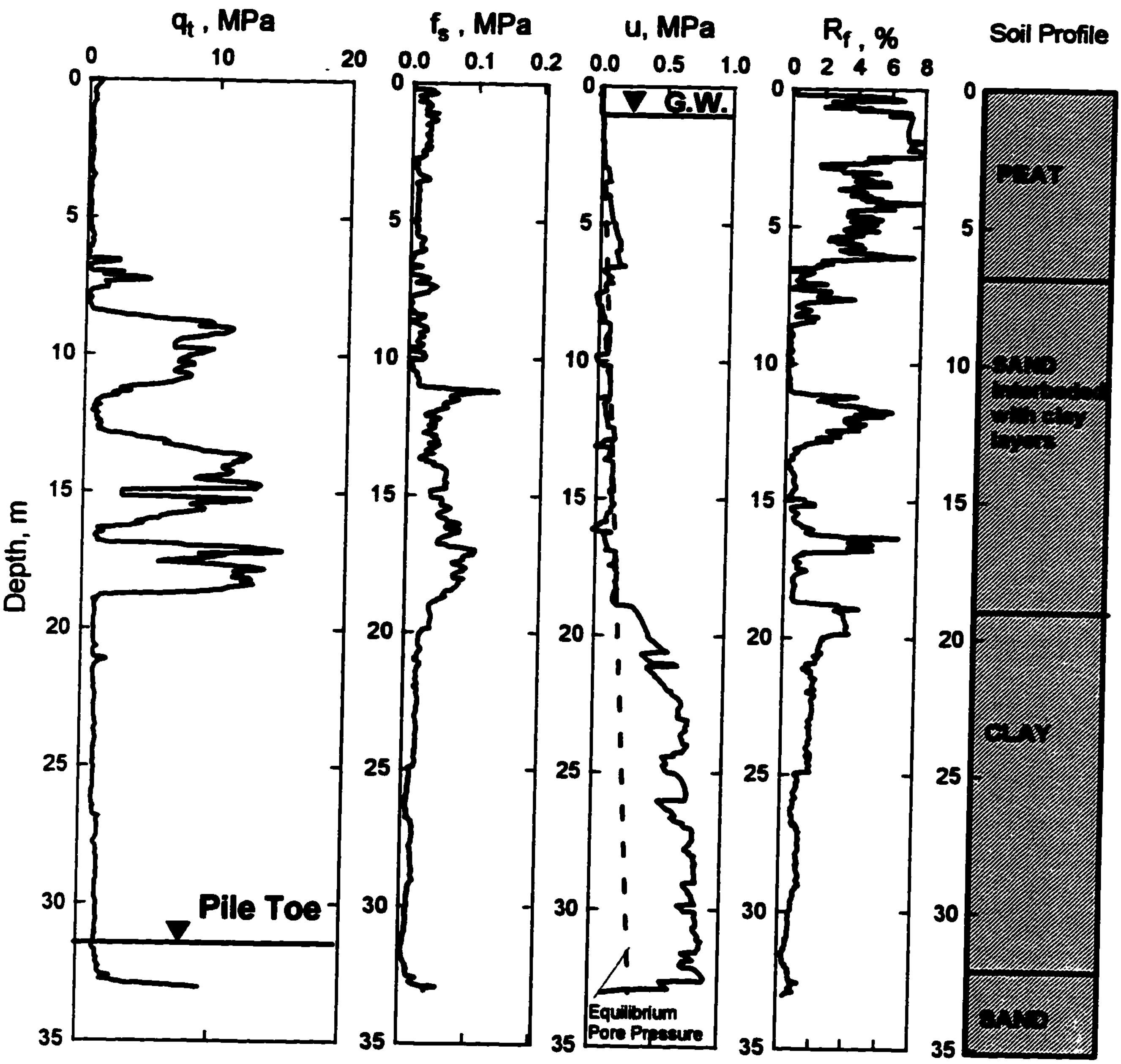

Case 102 PRL
Sheet b Pile data

	DETAIL	DESCRIPTION
1	Site	Puerto Rico, USA
2	Reference	Urkkada Ltd., 1995
3	Shape, Material, and Installation	Pipe, Steel, Driven
4	Diameter, b, and Wall Thickness, t, mm	300
5	Embedment Length D, m	31.4
6	Cross Sectional Area A_t, m^2	0.071
7	Unit Circumferential Area, A_s, m^2 /m	0.942
8	Toe, Closed or Open	Closed
9	Type of Test and Loading	Static Compression, SML
10	Toe Capacity, R_t, KN	
11	Shaft Capacity, R_s, KN	
12	*Capacity, R_u, KN	1,690

SCHEMATIC PROFILE

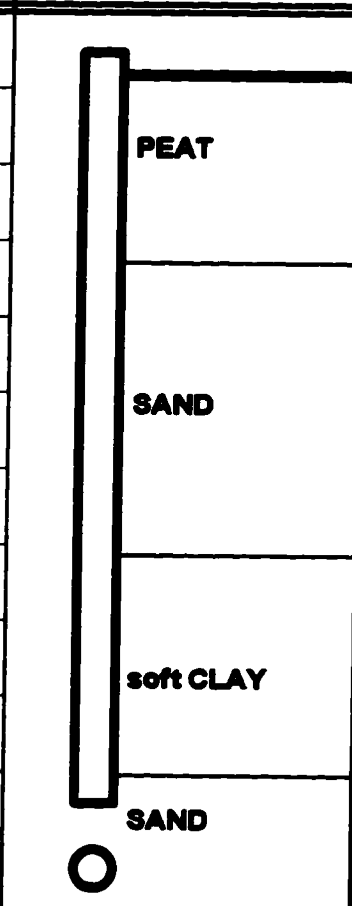

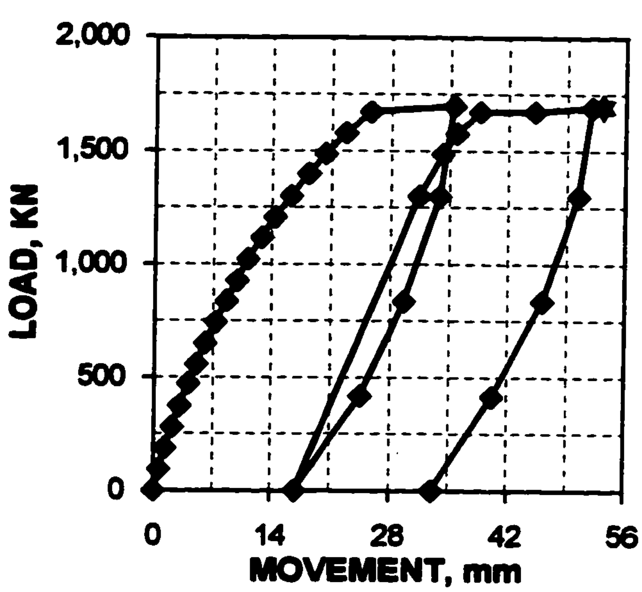

Case 103 A&M5
Sheet a CPT data

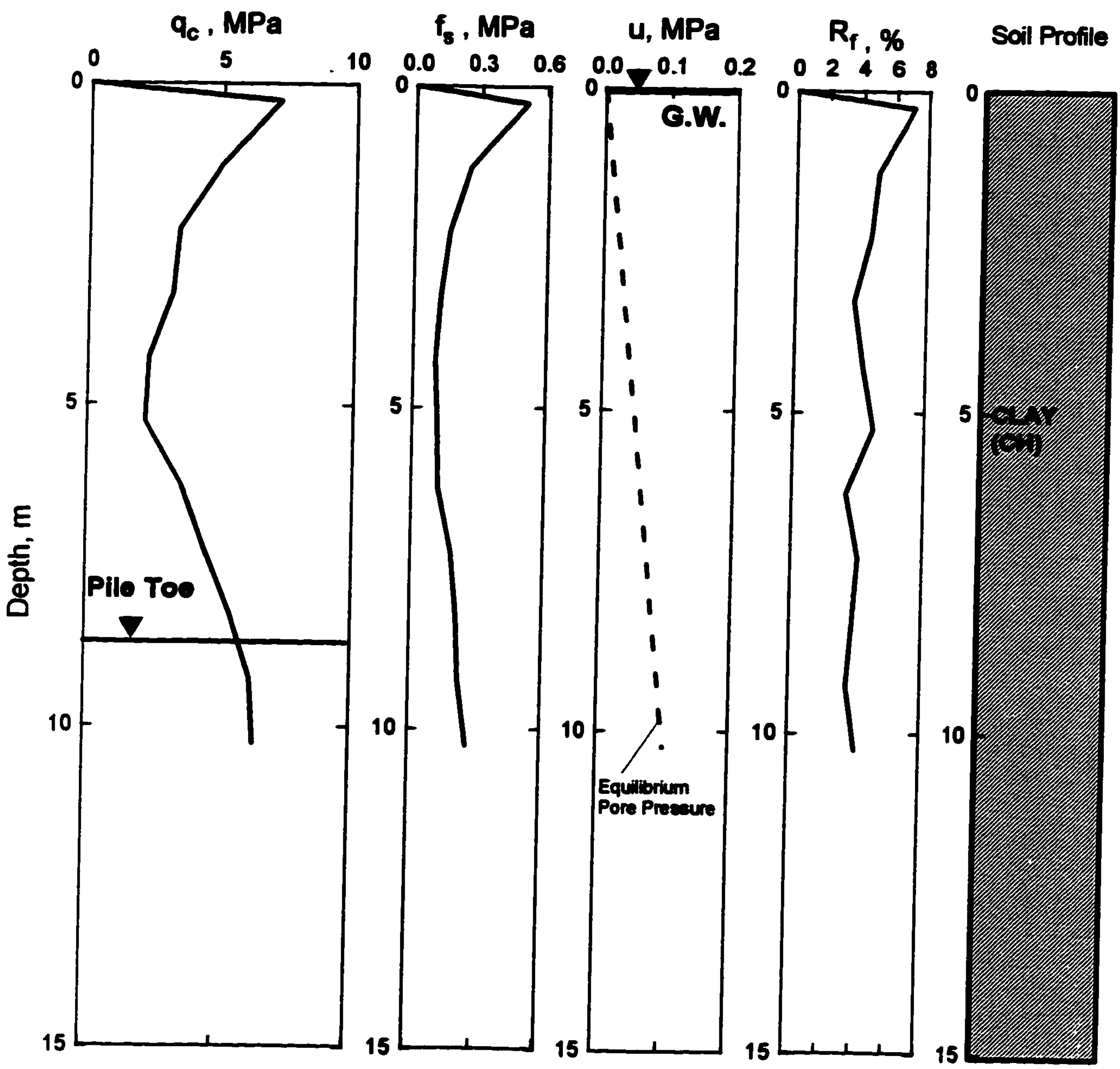

Case 103 A&M5
Sheet b Pile data

DETAIL		DESCRIPTION
1	Site	Hinds, MS, USA
2	Reference	Briaud et al., 1988
3	Shape, Material, and Installation	Square, Concrete, Driven
4	Diameter, b, and Wall Thickness, t, mm	450
5	Embedment Length D, m	8.5
6	Cross Sectional Area A_t, m^2	0.203
7	Unit Circumferential Area, A_s, m^2/m	1.8
8	Toe, Closed or Open	Closed
9	Type of Test and Loading	Static Compression, SML
10	Toe Capacity, R_t, KN	
11	Shaft Capacity, R_s, KN	
12	*Capacity, R_u, KN	1,330

SCHEMATIC PROFILE

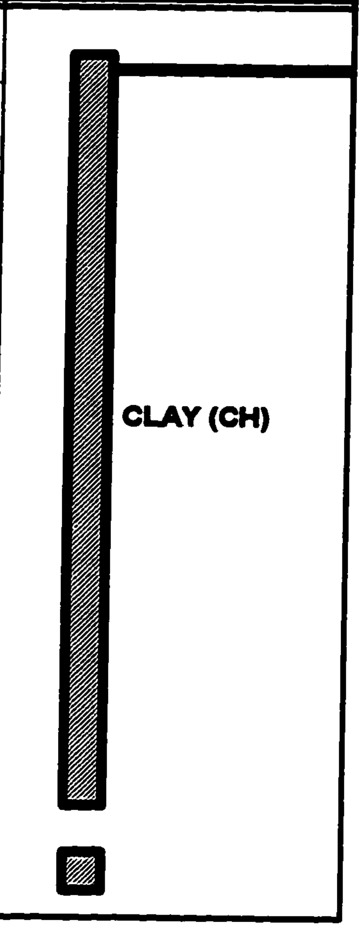

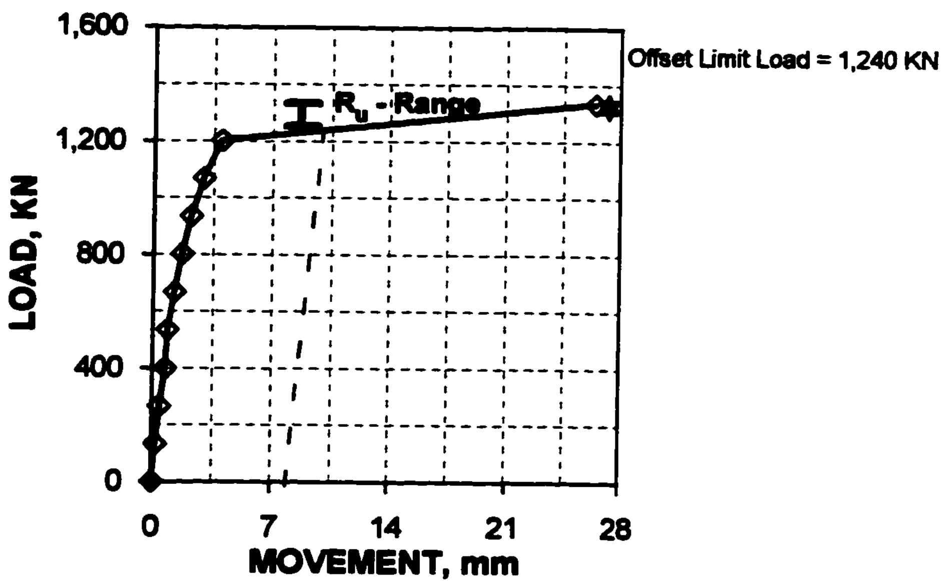

Case 104 A&M6
Sheet a CPT data

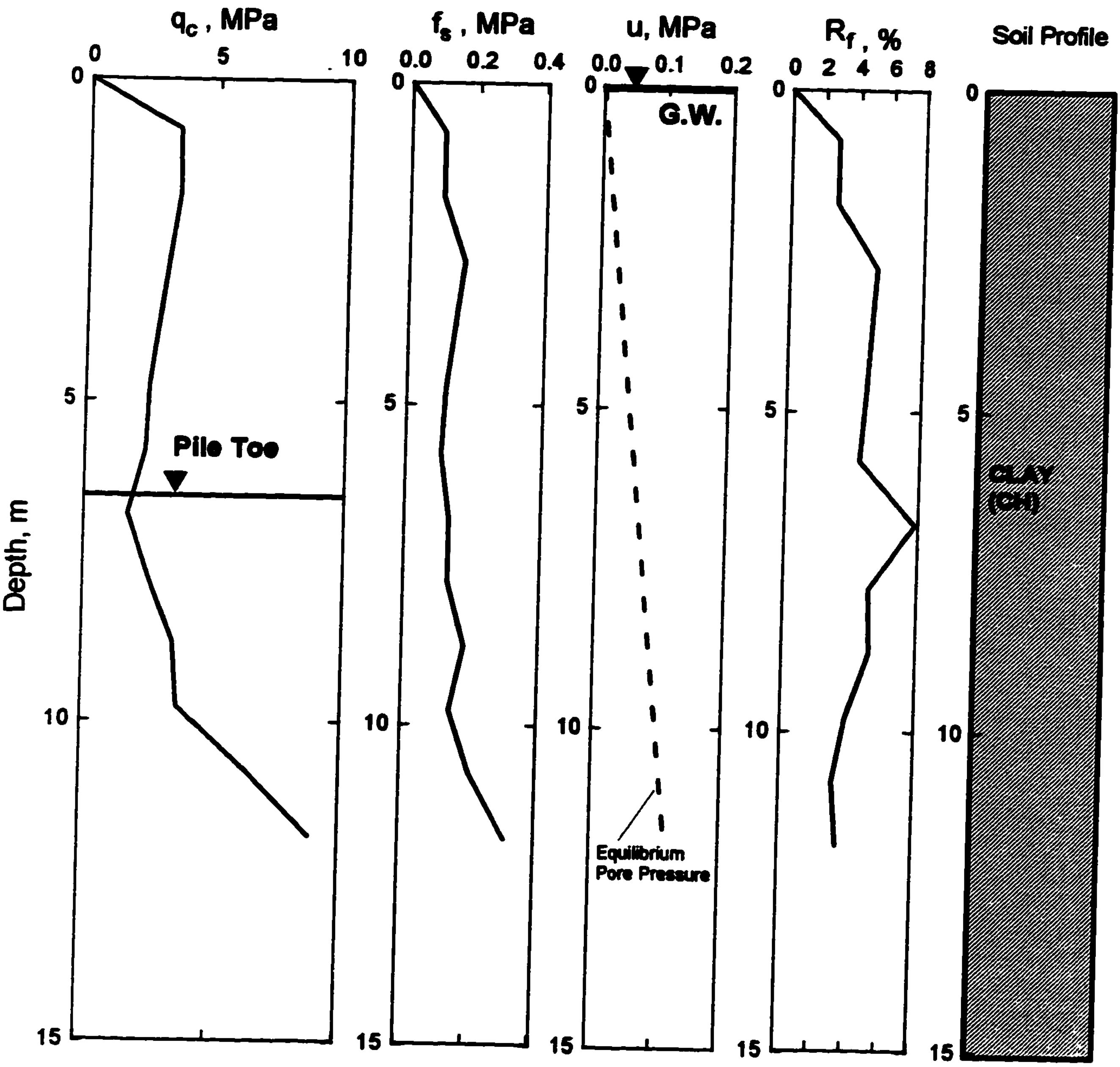

Case 104 A&M6
Sheet b Pile data

	DETAIL	DESCRIPTION
1	Site	Hinds, MS, USA
2	Reference	Briaud et al., 1988
3	Shape, Material, and Installation	Square, Concrete, Driven
4	Diameter, b, and Wall Thickness, t, mm	350
5	Embedment Length D, m	6.5
6	Cross Sectional Area A_t, m^2	0.123
7	Unit Circumferential Area, A_s, m^2/m	1.4
8	Toe, Closed or Open	Closed
9	Type of Test and Loading	Static Compression, SML
10	Toe Capacity, R_t, KN	
11	Shaft Capacity, R_s, KN	
12	*Capacity, R_u, KN	800

SCHEMATIC PROFILE

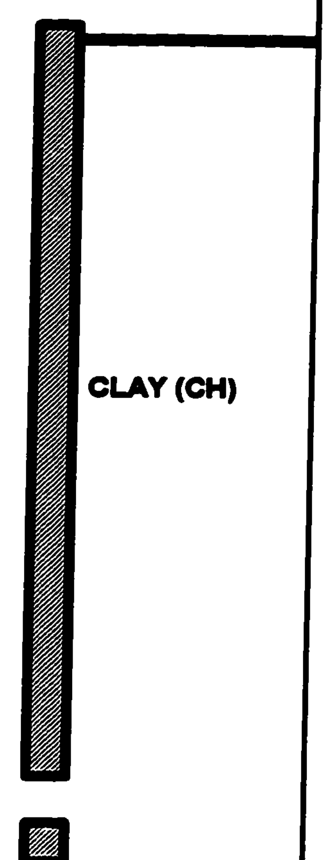

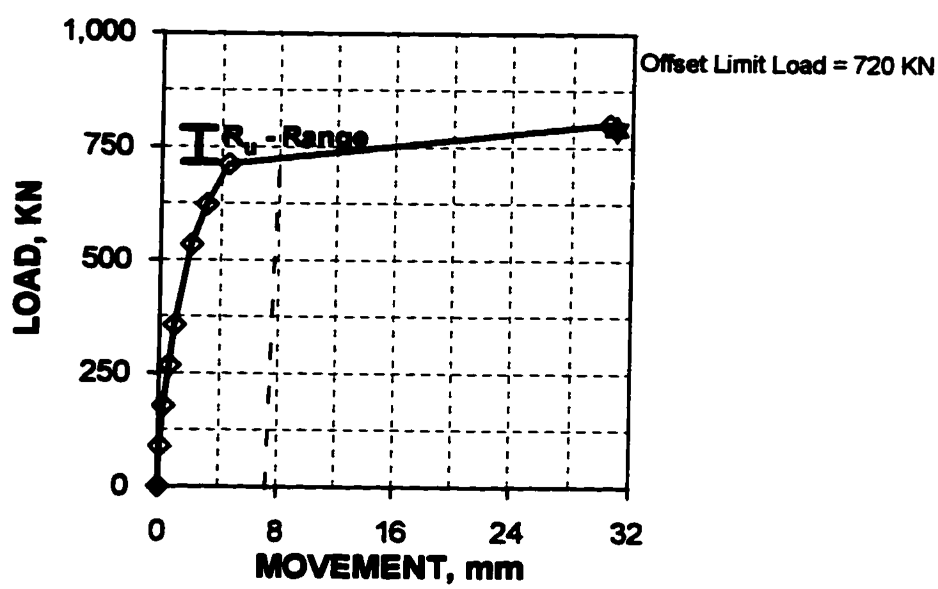

Case 105 A&M7
Sheet a CPT data

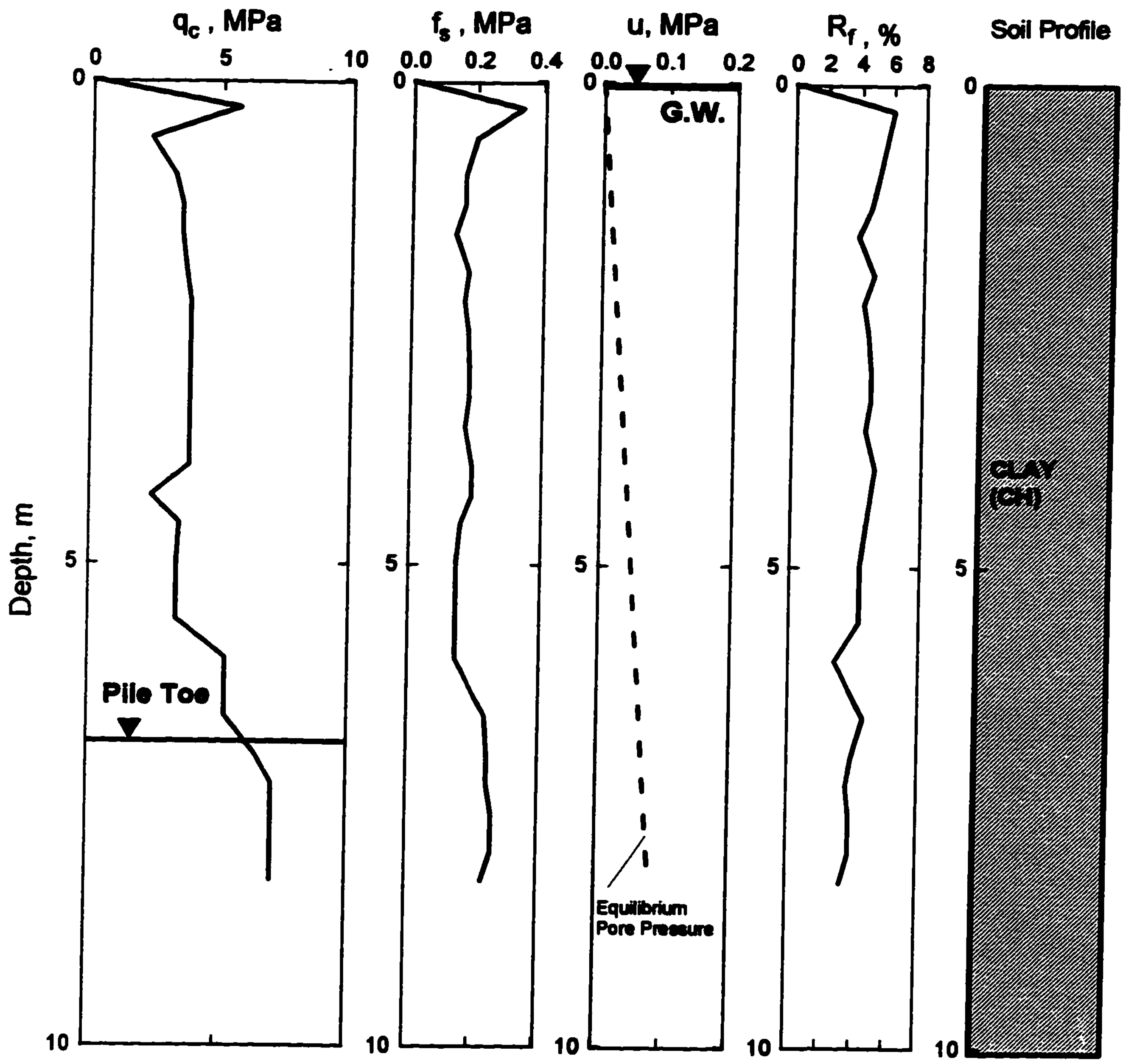

Case 105 A&M7
Sheet b Pile data

	DETAIL	DESCRIPTION
1	Site	Hinds, MS, USA
2	Reference	Briaud et al., 1988
3	Shape, Material, and Installation	Square, Concrete, Driven
4	Diameter, b, and Wall Thickness, t, mm	350
5	Embedment Length D, m	6.7
6	Cross Sectional Area A_t, m²	0.123
7	Unit Circumferential Area, A_s, m²/m	1.4
8	Toe, Closed or Open	Closed
9	Type of Test and Loading	Static Compression, SML
10	Toe Capacity, R_t, KN	
11	Shaft Capacity, R_s, KN	
12	*Capacity, R_u, KN	1,470

SCHEMATIC PROFILE

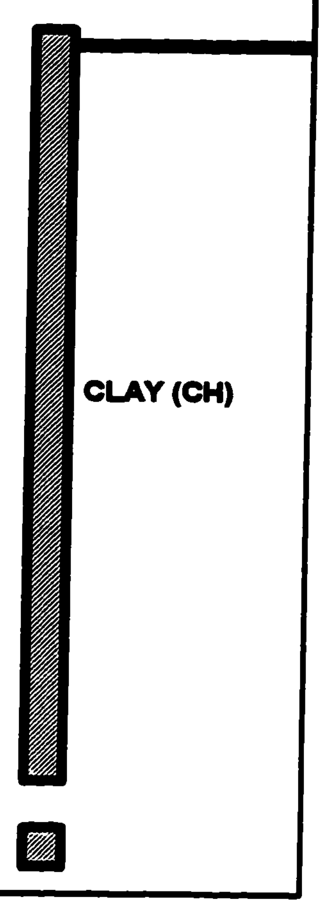

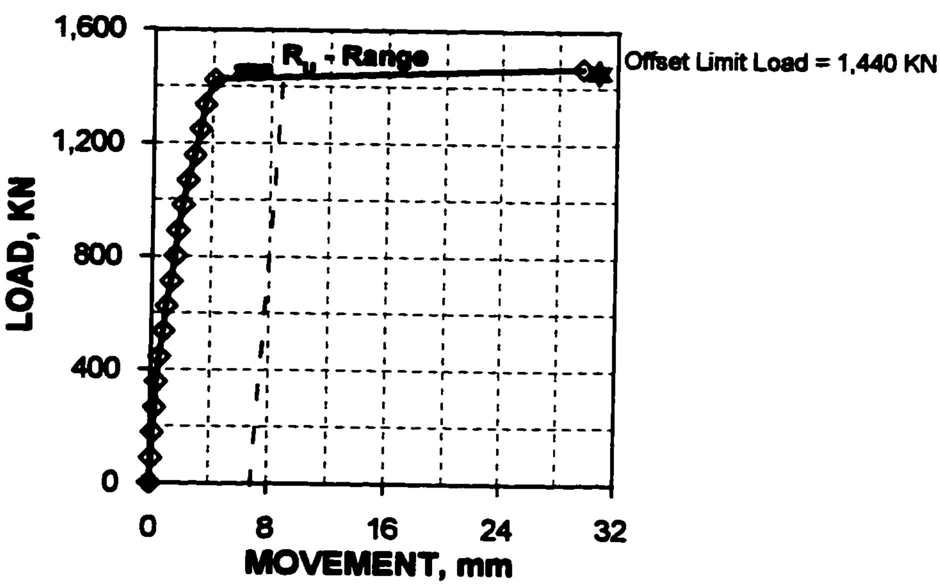

Case 106 A&M8
Sheet a CPT data

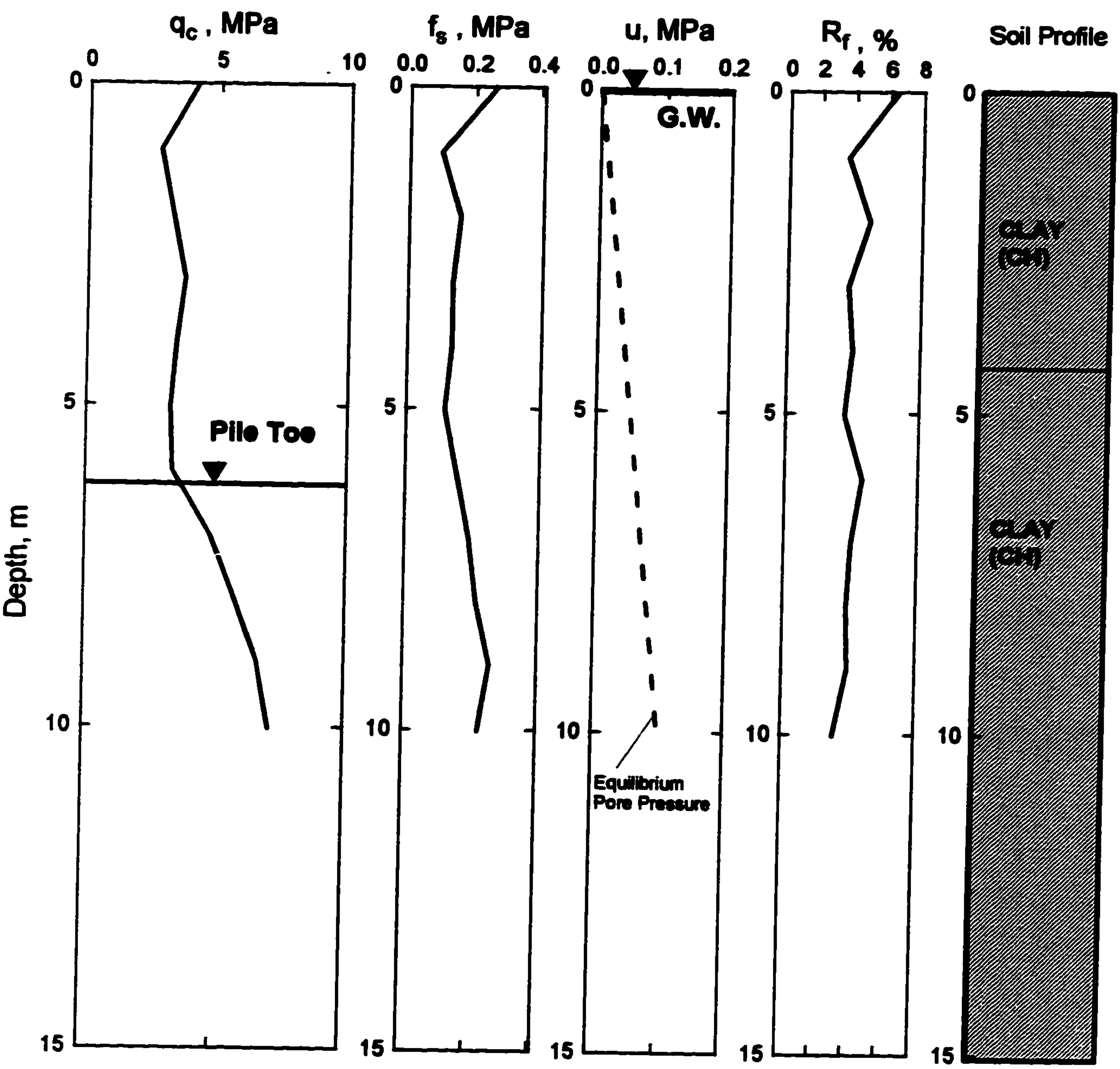

Case 106 A&M8
Sheet b Pile data

DETAIL		DESCRIPTION
1	Site	Hinds, MS, USA
2	Reference	Briaud et al., 1988
3	Shape, Material, and Installation	Square, Concrete, Driven
4	Diameter, b, and Wall Thickness, t, mm	450
5	Embedment Length D, m	7.6
6	Cross Sectional Area A_t, m^2	0.203
7	Unit Circumferential Area, A_s, m^2/m	1.8
8	Toe, Closed or Open	Closed
9	Type of Test and Loading	Static Compression, SML
10	Toe Capacity, R_t, KN	
11	Shaft Capacity, R_s, KN	
12	*Capacity, R_u, KN	1,070

SCHEMATIC PROFILE

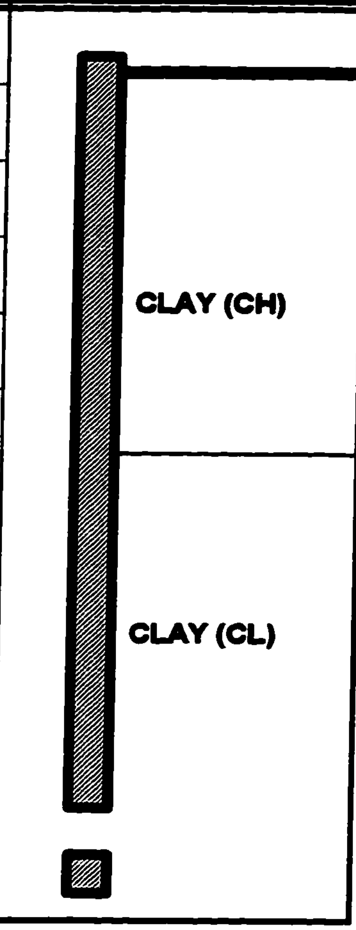

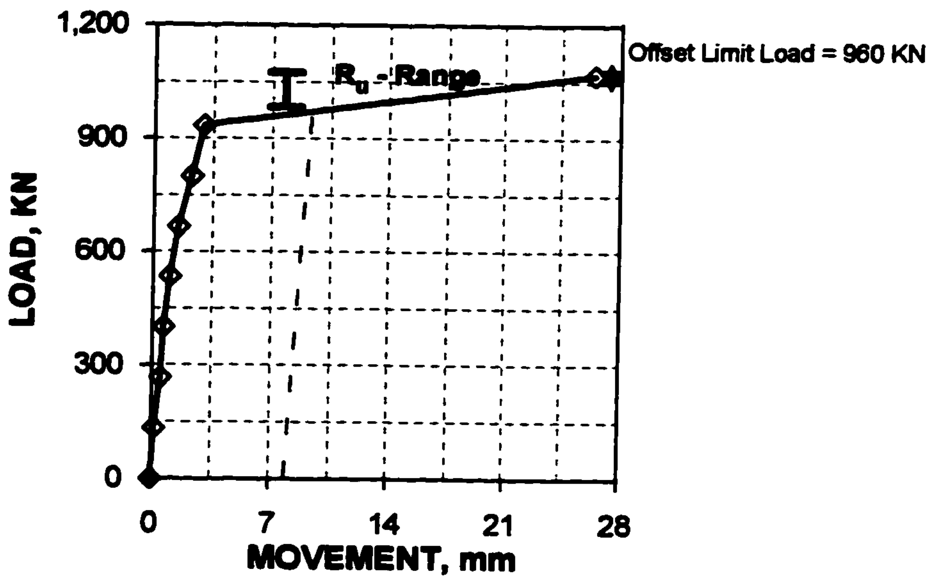

Case 107 A&M11
Sheet a CPT data

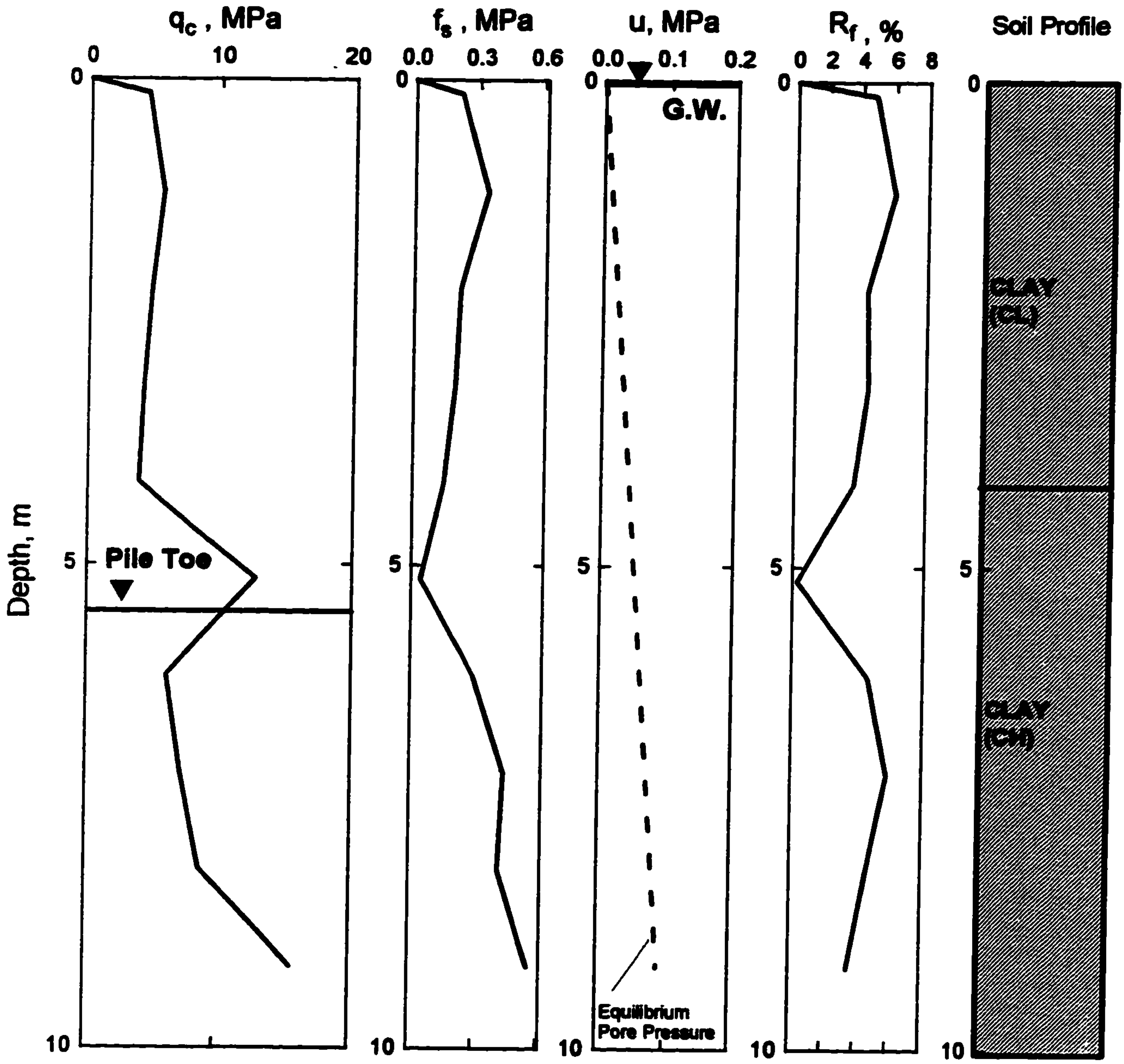

Case 107 A&M11
Sheet b Pile data

	DETAIL	DESCRIPTION	SCHEMATIC PROFILE
1	Site	Hinds, MS, USA	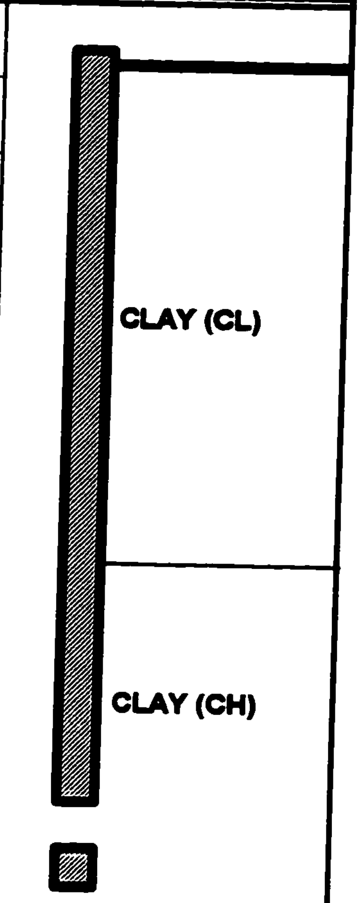
2	Reference	Briaud et al., 1988	
3	Shape, Material, and Installation	Square, Concrete, Driven	
4	Diameter, b, and Wall Thickness, t, mm	350	
5	Embedment Length D, m	5.5	
6	Cross Sectional Area A_t, m^2	0.123	
7	Unit Circumferential Area, A_s, m^2/m	1.4	
8	Toe, Closed or Open	Closed	
9	Type of Test and Loading	Static Compression, SML	
10	Toe Capacity, R_t, KN		
11	Shaft Capacity, R_s, KN		
12	*Capacity, R_u, KN	1,050	

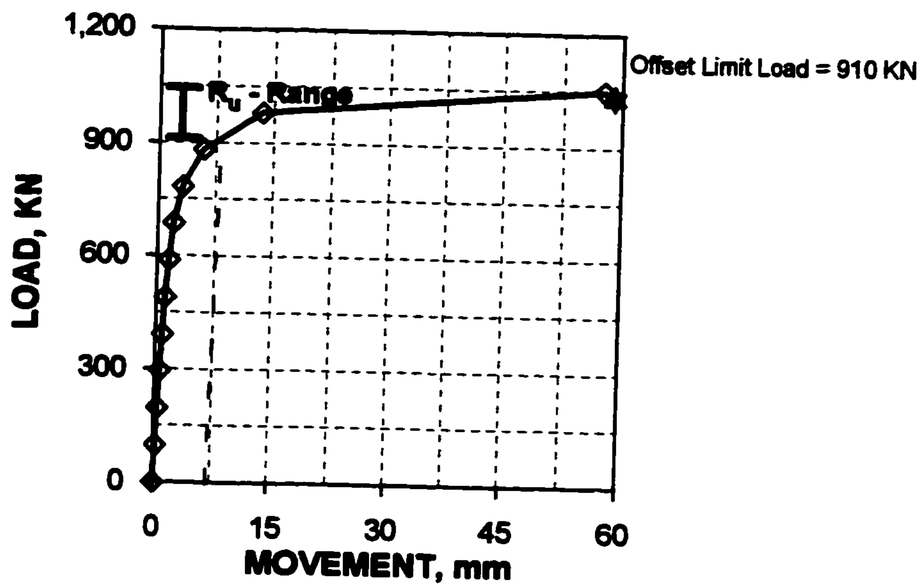

Case 108 A&M14
Sheet a CPT data

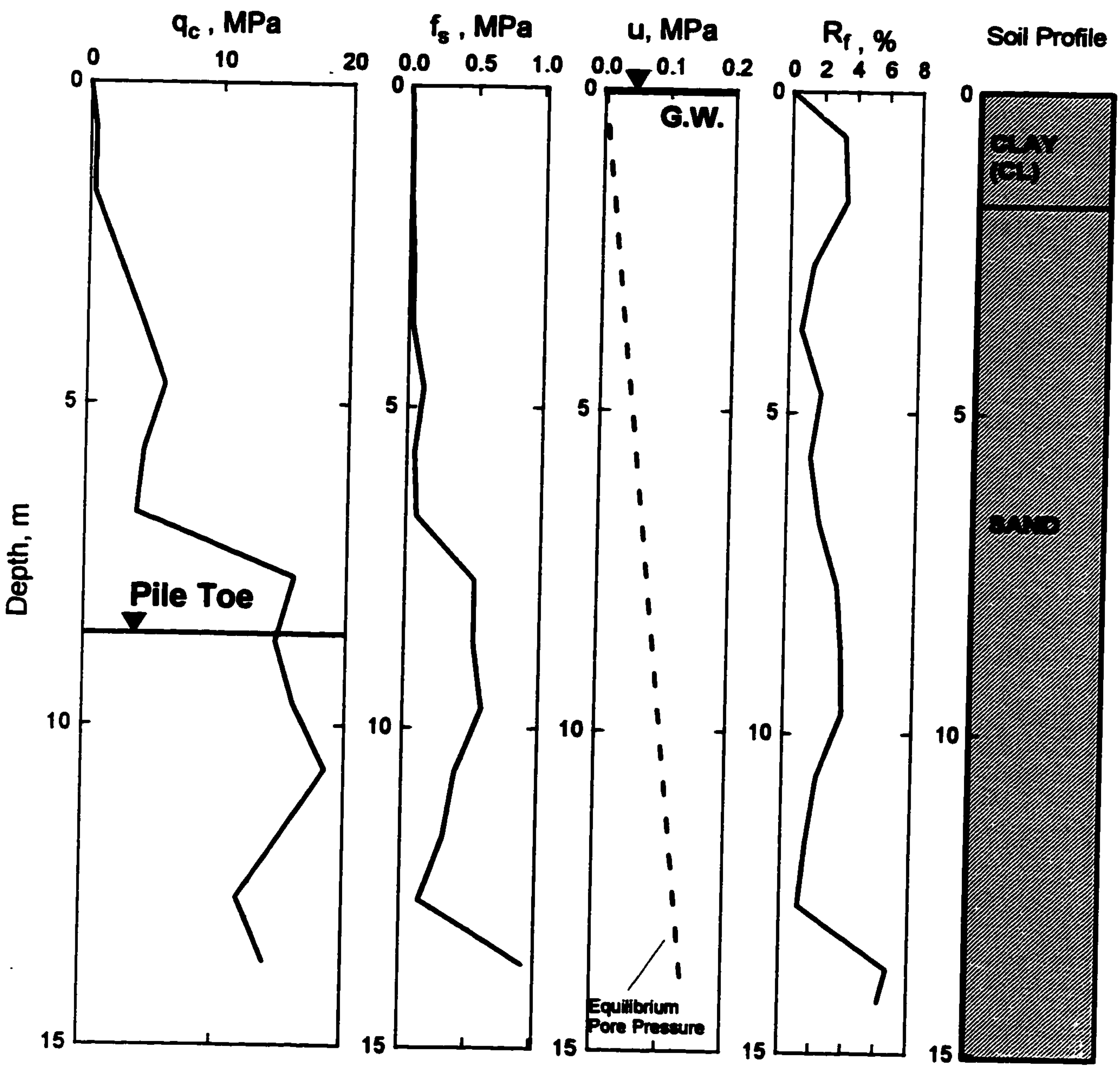

Case 108 A&M14
Sheet b Pile data

No.	CASE	DESCRIPTION	SCHEMATIC PROFILE
1	Site	Launderdale, MS, USA	
2	Reference	Briaud et al., 1988	
3	Shape, Material, and Installation	H-Pile, Steel, Driven	
4	Diameter, b, and Wall Thickness, t, mm	246*256	
5	Embedment Length D, m	8.5	
6	Cross Sectional Area A_t, m^2	0.008	
7	Unit Circumferential Area, A_s, m^2/m	1.01	
8	Toe, Closed or Open	Open	
9	Type of Test and Loading	Static Compression, SML	
10	Toe Capacity, R_t, KN		
11	Shaft Capacity, R_s, KN		
12	*Capacity, R_u, KN	590	

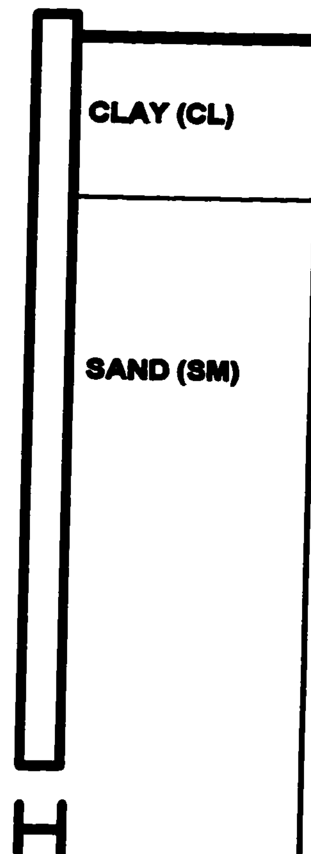

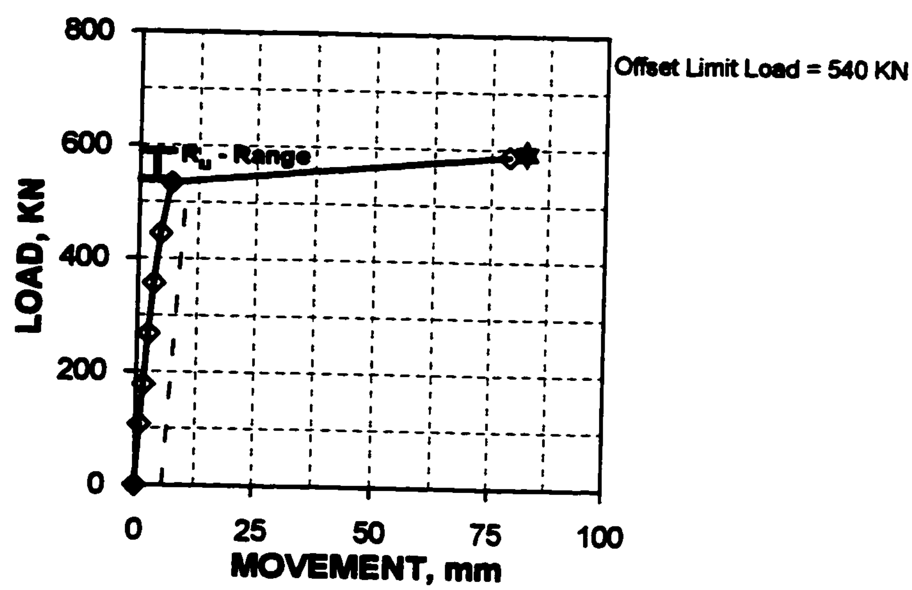

Case 109 A&M16
Sheet a CPT data

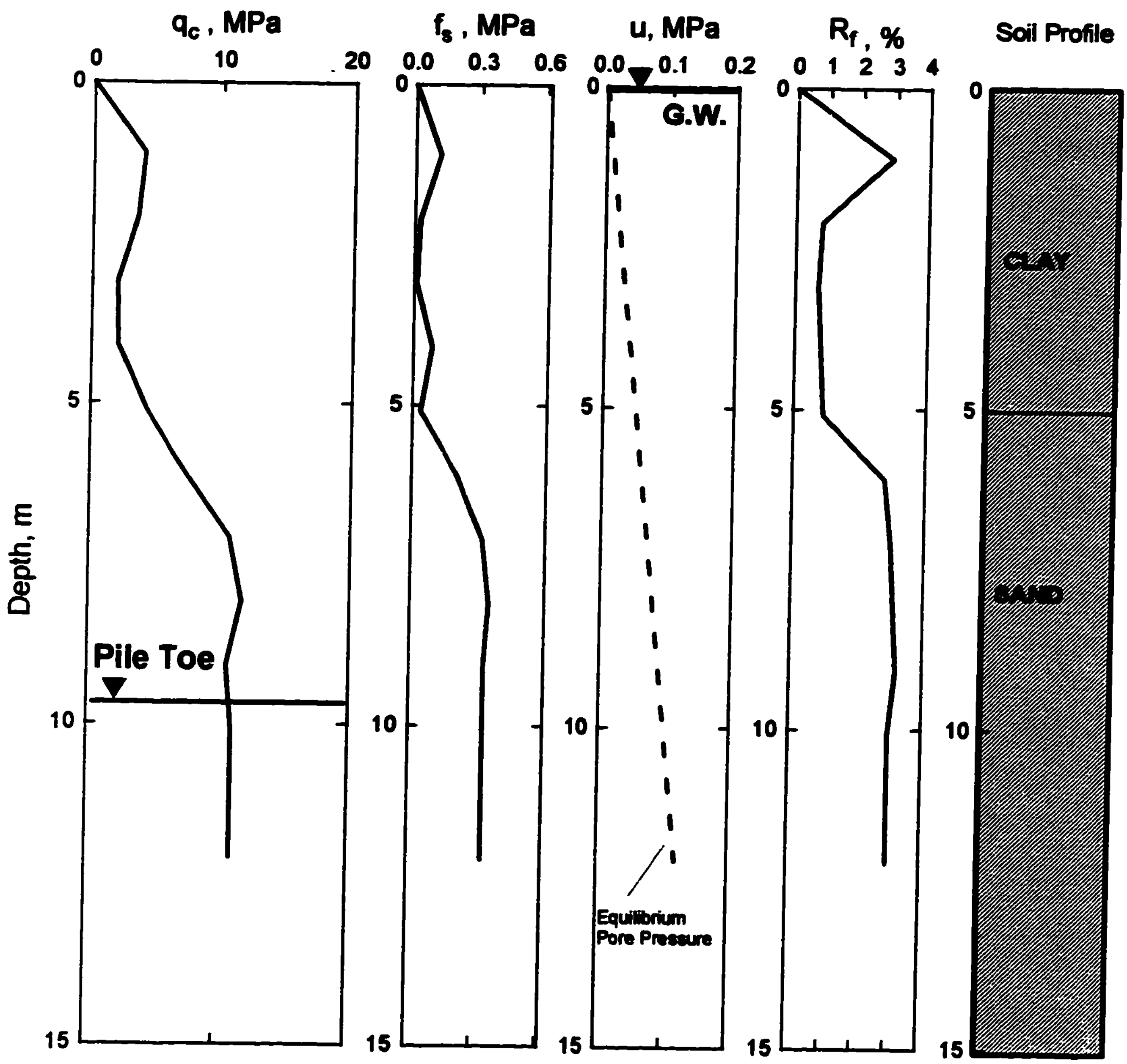

Case 109 A&M16
Sheet b Pile data

No.	CASE	DESCRIPTION
1	Site	Launderdale, MS, USA
2	Reference	Briaud et al., 1988
3	Shape, Material, and Installation	H-Pile, Steel, Driven
4	Diameter, b, and Wall Thickness, t, mm	246*256
5	Embedment Length D, m	9.7
6	Cross Sectional Area A_t, m²	0.008
7	Unit Circumferential Area, A_s, m² /m	1.01
8	Toe, Closed or Open	Open
9	Type of Test and Loading	Static Compression, SML
10	Toe Capacity, R_t, KN	
11	Shaft Capacity, R_s, KN	
12	*Capacity, R_u, KN	1,070

SCHEMATIC PROFILE

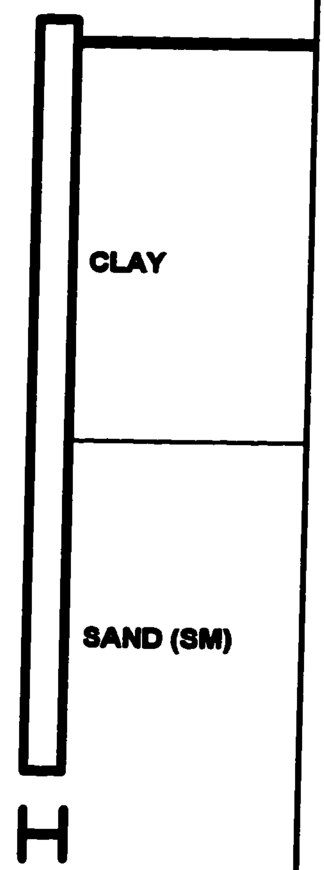

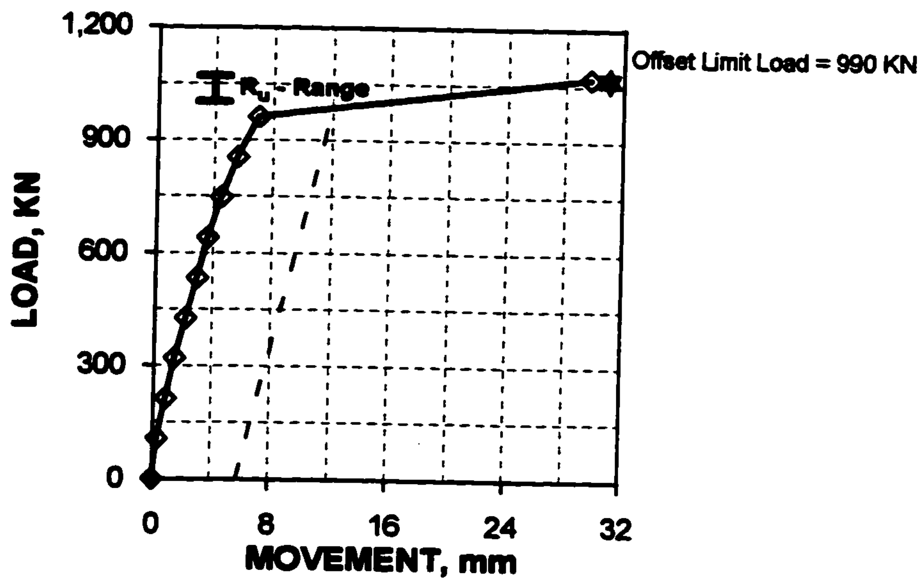

Case 110 A&M19
Sheet a CPT data

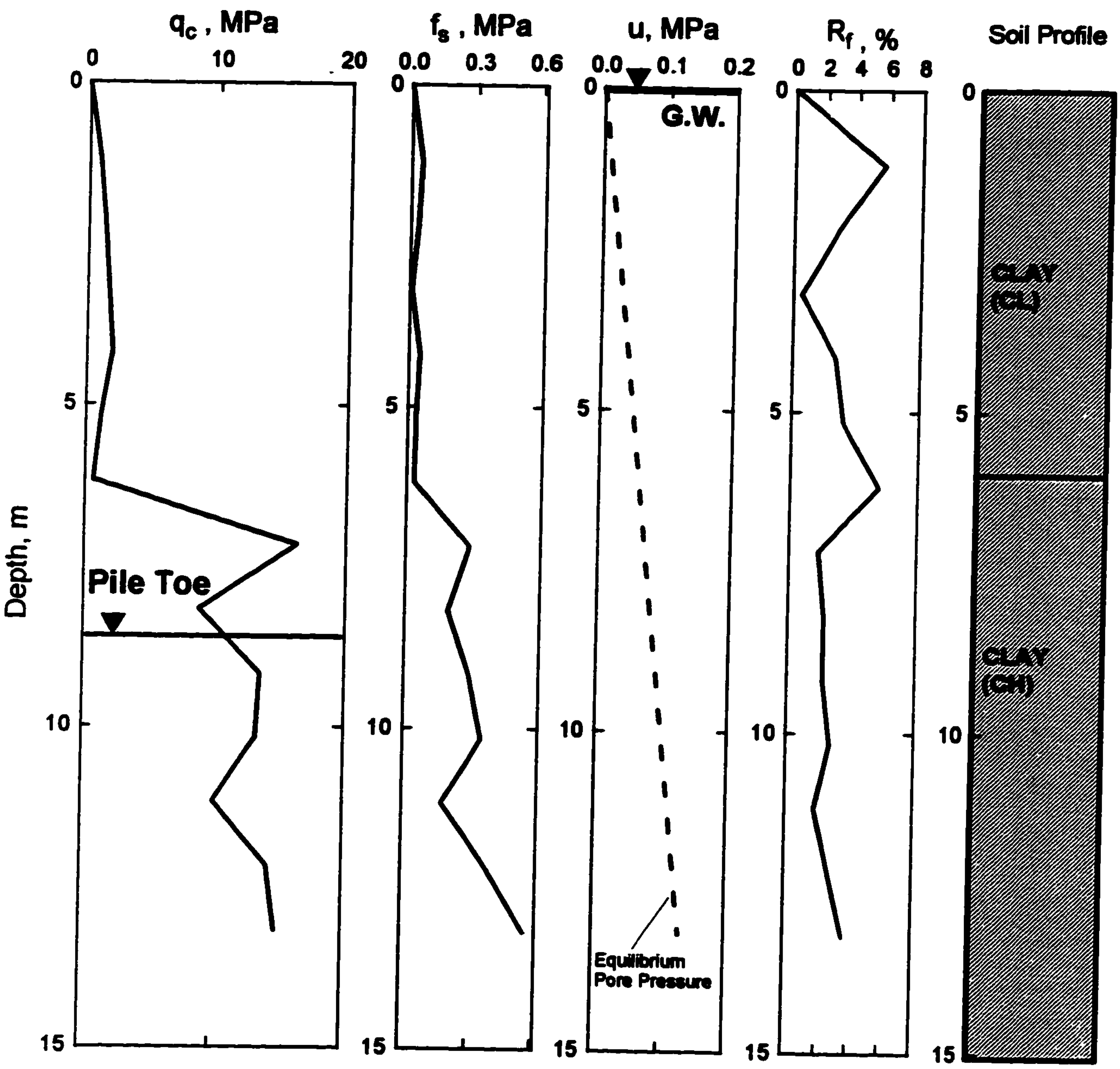

Case 110 A&M19
Sheet b Pile data

	DETAIL	DESCRIPTION
1	Site	Neshoba, MS, USA
2	Reference	Briaud et al., 1988
3	Shape, Material, and Installation	Square, Concrete, Driven
4	Diameter, b, and Wall Thickness, t, mm	400
5	Embedment Length D, m	8.4
6	Cross Sectional Area A_t, m^2	0.16
7	Unit Circumferential Area, A_s, m^2/m	1.6
8	Toe, Closed or Open	Closed
9	Type of Test and Loading	Static Compression, SML
10	Toe Capacity, R_t, KN	
11	Shaft Capacity, R_s, KN	
12	*Capacity, R_u, KN	1,240

SCHEMATIC PROFILE

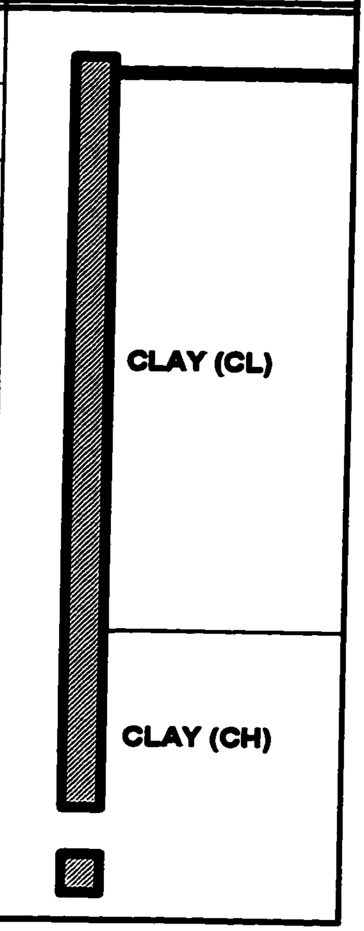

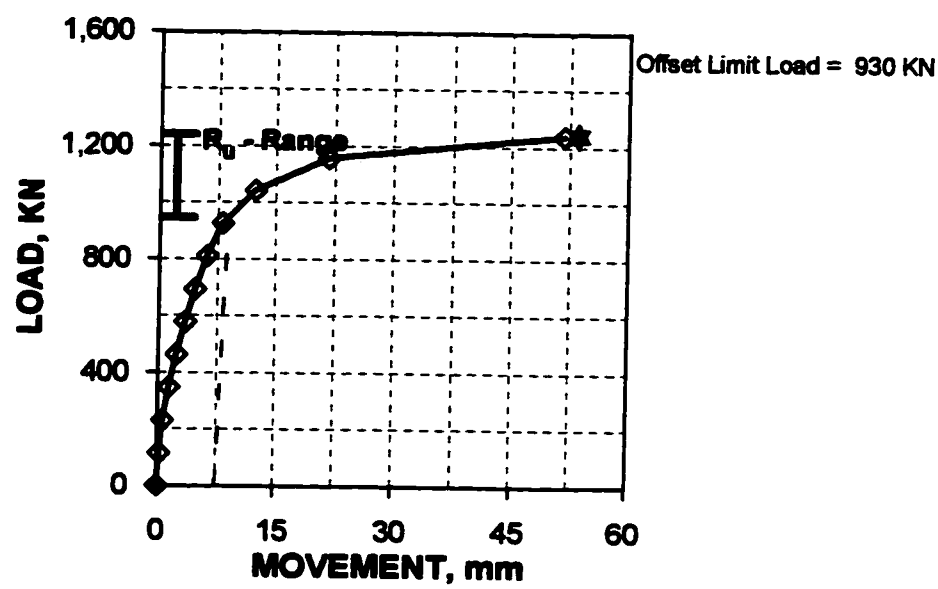

Case 111 A&M20
Sheet a CPT data

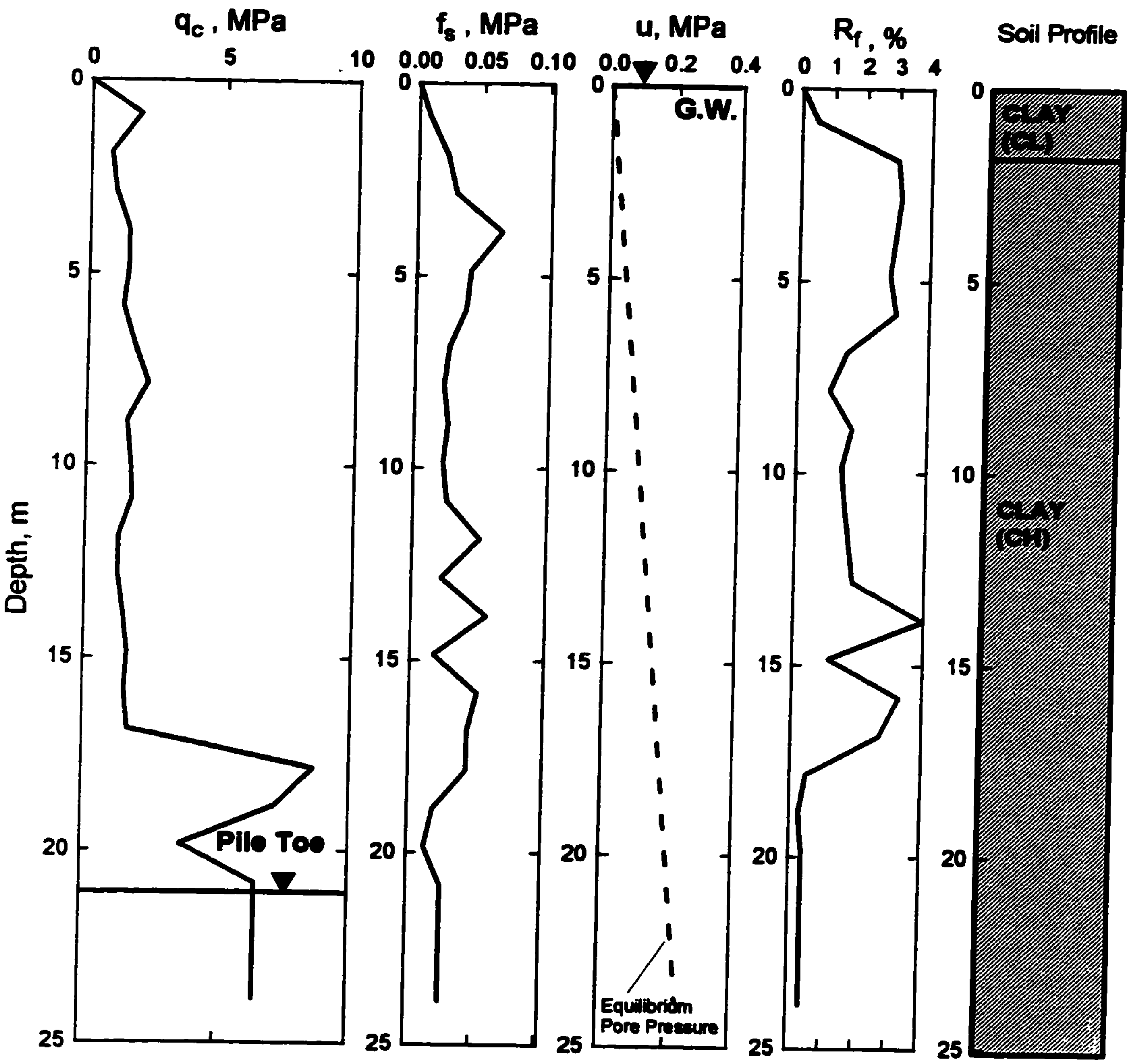

Case 111 A&M20
Sheet b Pile data

	DETAIL	DESCRIPTION
1	Site	Issaquena, MS, USA
2	Reference	Briaud et al., 1988
3	Shape, Material, and Installation	Square, Concrete, Driven
4	Diameter, b, and Wall Thickness, t, mm	400
5	Embedment Length D, m	21
6	Cross Sectional Area A_t, m^2	0.16
7	Unit Circumferential Area, A_s, m^2/m	1.6
8	Toe, Closed or Open	Closed
9	Type of Test and Loading	Static Compression, SML
10	Toe Capacity, R_t, KN	
11	Shaft Capacity, R_s, KN	
12	*Capacity, R_u, KN	1,330

SCHEMATIC PROFILE

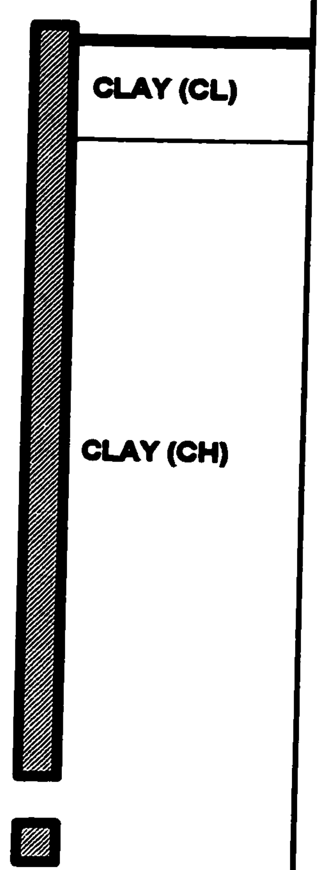

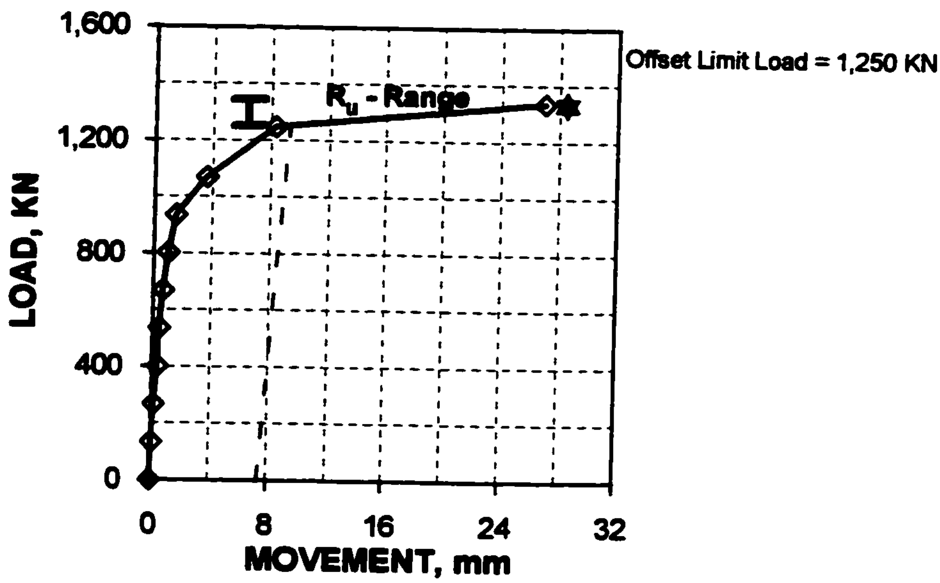

Case 112 A&M21
Sheet a CPT data

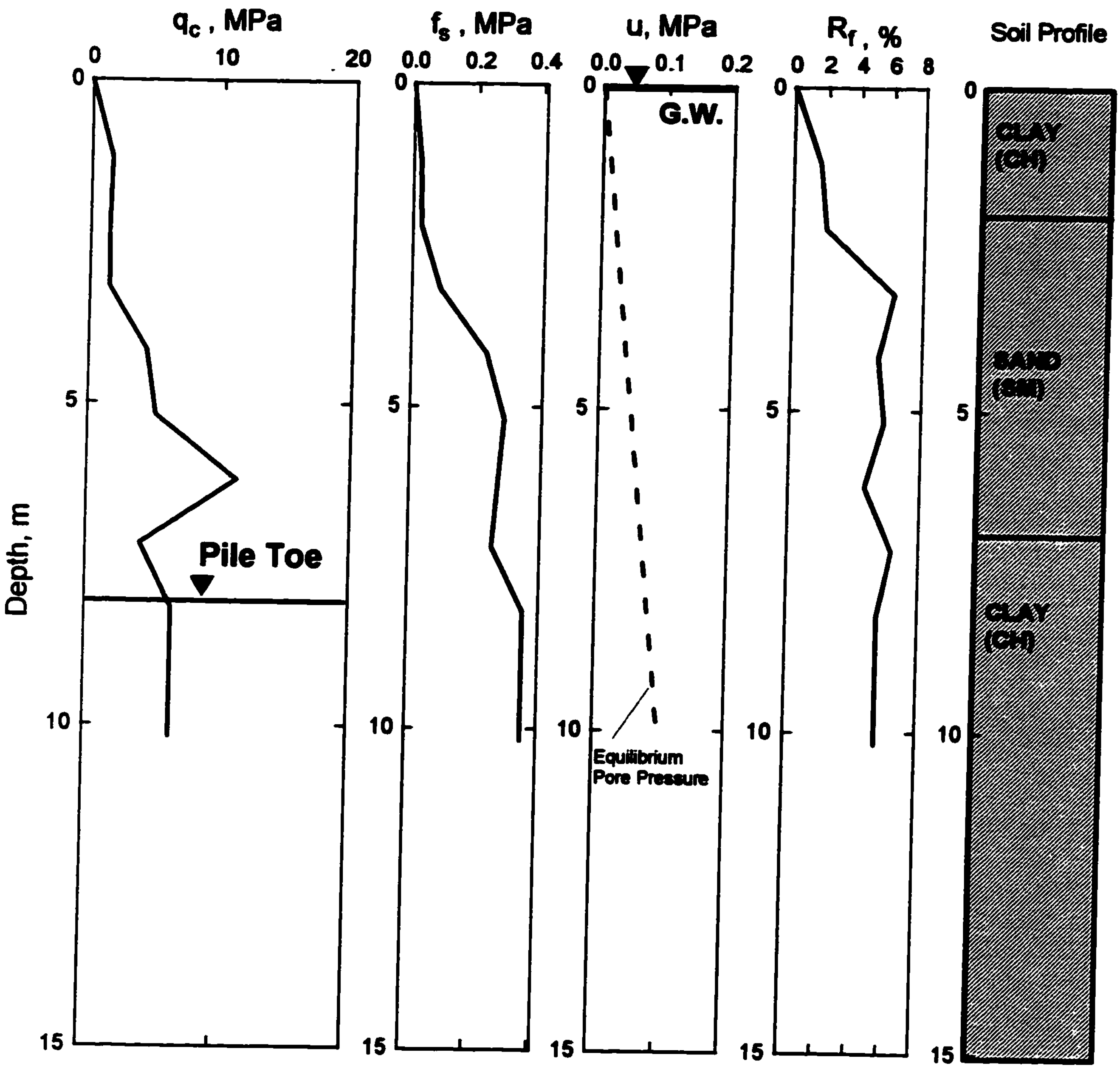

Case 112 A&M21
Sheet b Pile data

	DETAIL	DESCRIPTION	SCHEMATIC PROFILE
1	Site	Launderdale, MS, USA	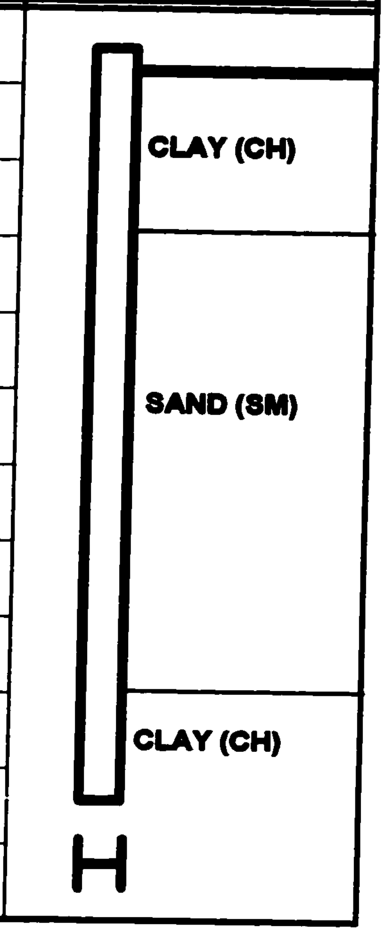
2	Reference	Briaud et al., 1988	
3	Shape, Material, and Installation	H-Pile, Steel, Driven	
4	Diameter, b, and Wall Thickness, t, mm	299*306	
5	Embedment Length D, m	8	
6	Cross Sectional Area A_t, m^2	0.01	
7	Unit Circumferential Area, A_s, m^2/m	1.21	
8	Toe, Closed or Open	Open	
9	Type of Test and Loading	Static Compression, SML	
10	Toe Capacity, R_t, KN		
11	Shaft Capacity, R_s, KN		
12	*Capacity, R_u, KN	470	

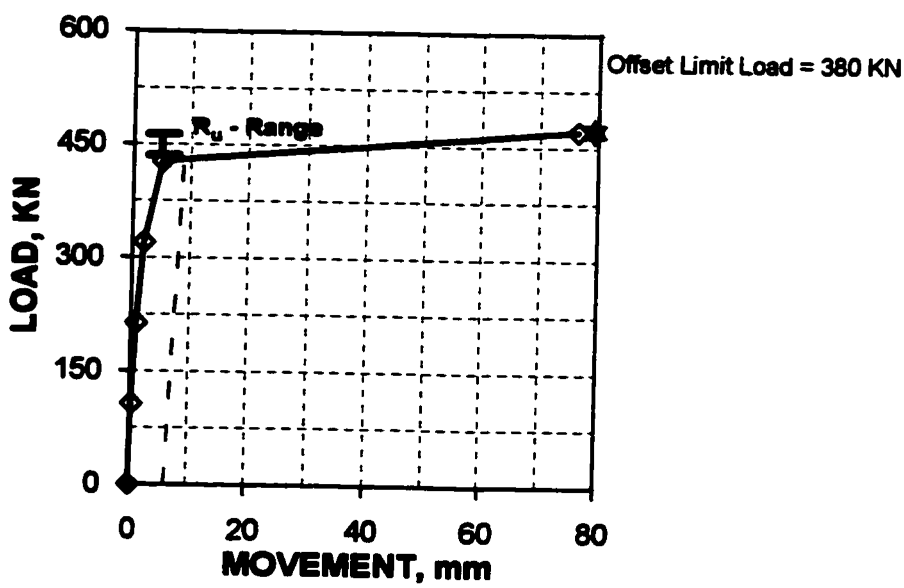

Case 113 A&M22
Sheet a CPT data

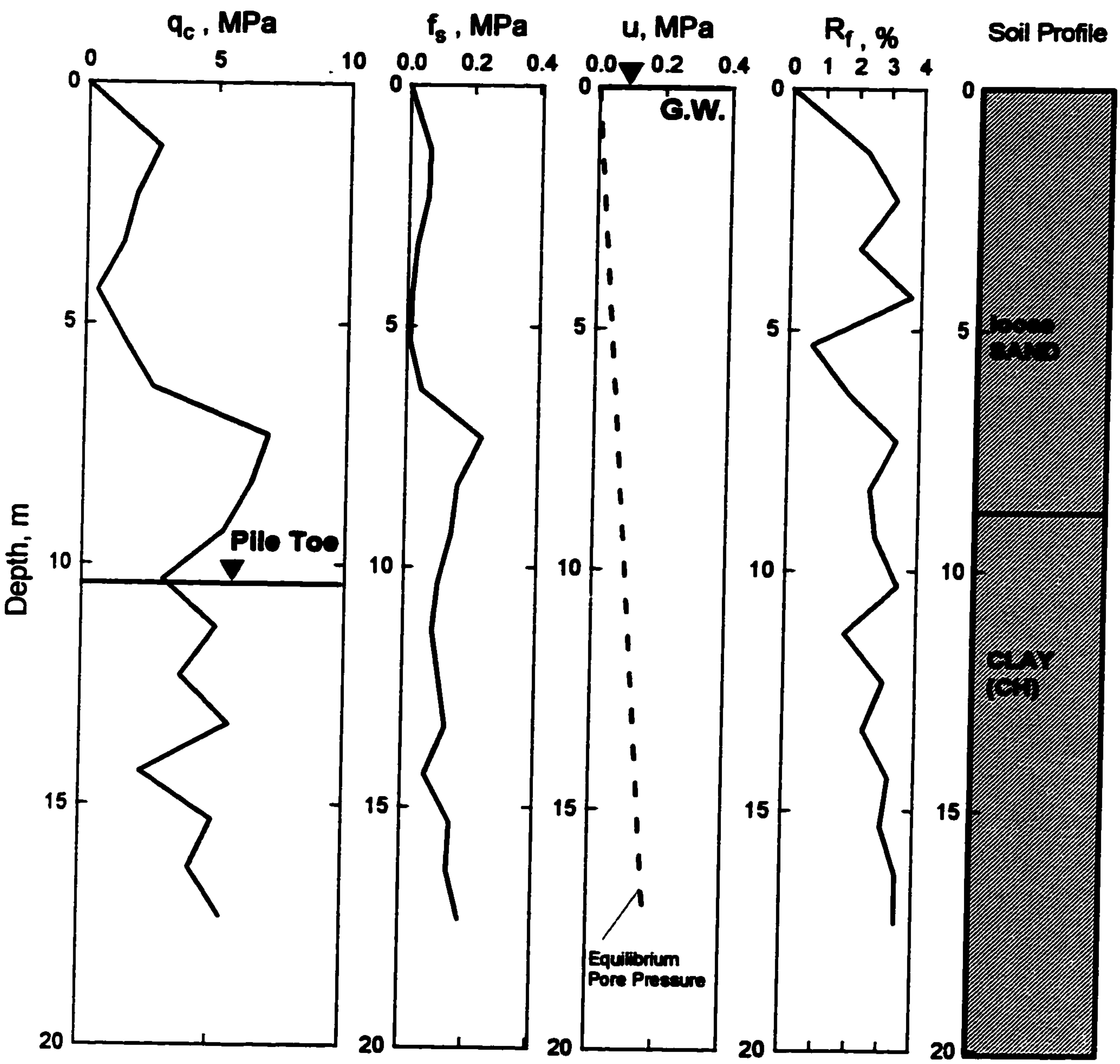

Case 113 A&M22
Sheet b Pile data

	DETAIL	DESCRIPTION	SCHEMATIC PROFILE
1	Site	Walthall, MS, USA	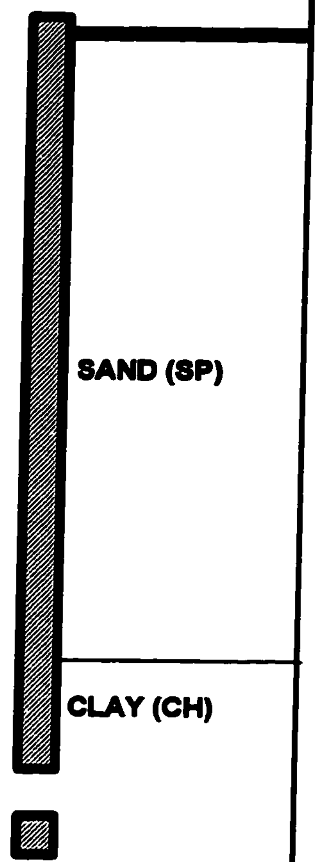
2	Reference	Briaud et al., 1988	
3	Shape, Material, and Installation	Square, Concrete, Driven	
4	Diameter, b, and Wall Thickness, t, mm	450	
5	Embedment Length D, m	10.3	
6	Cross Sectional Area A_t, m²	0.203	
7	Unit Circumferential Area, A_s, m² /m	1.8	
8	Toe, Closed or Open	Closed	
9	Type of Test and Loading	Static Compression, SML	
10	Toe Capacity, R_t, KN		
11	Shaft Capacity, R_s, KN		
12	*Capacity, R_u, KN	1,250	

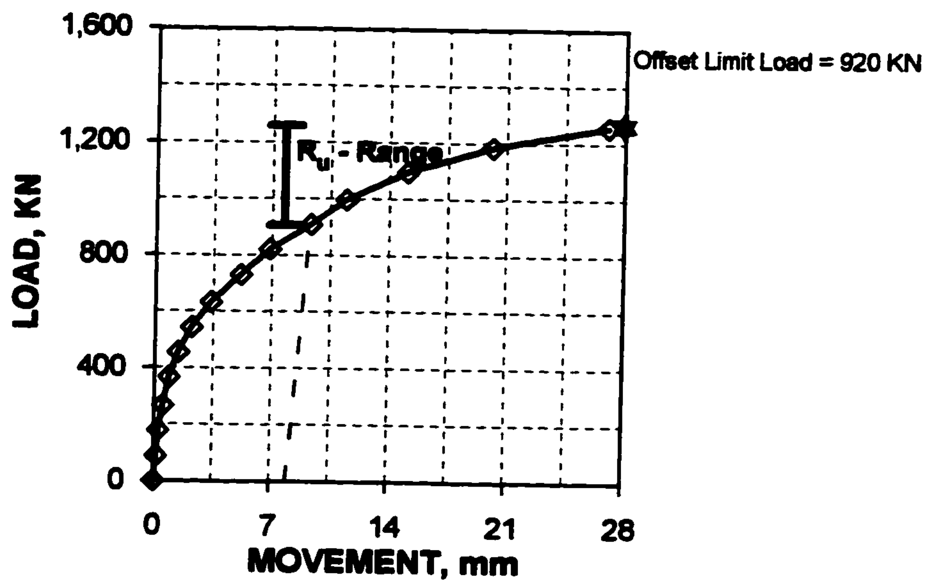

Case 114 A&M24
Sheet a CPT data

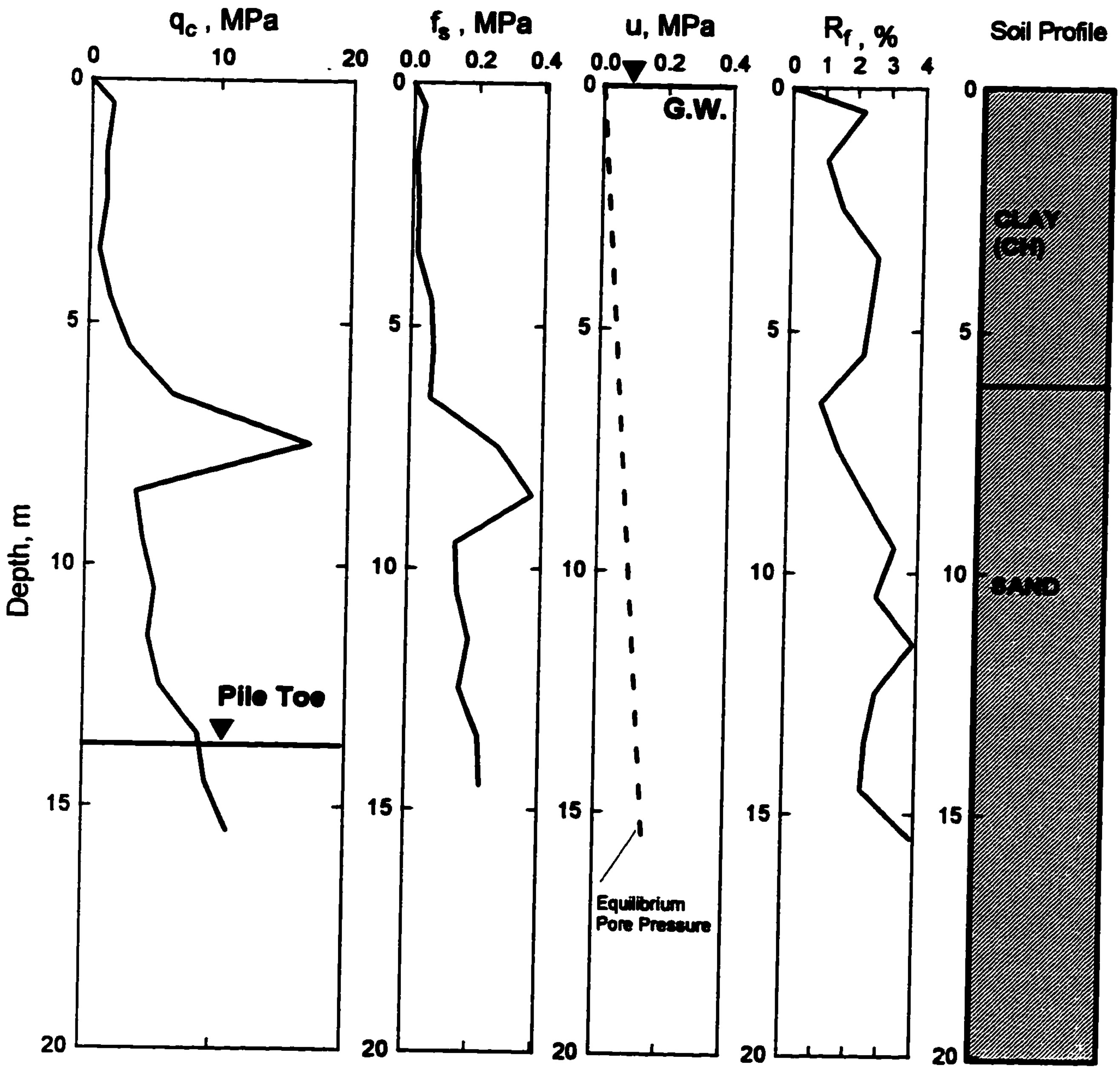

Case 114 A&M24
Sheet b Pile data

DETAIL		DESCRIPTION	SCHEMATIC PROFILE
1	Site	Yazoo, MS, USA	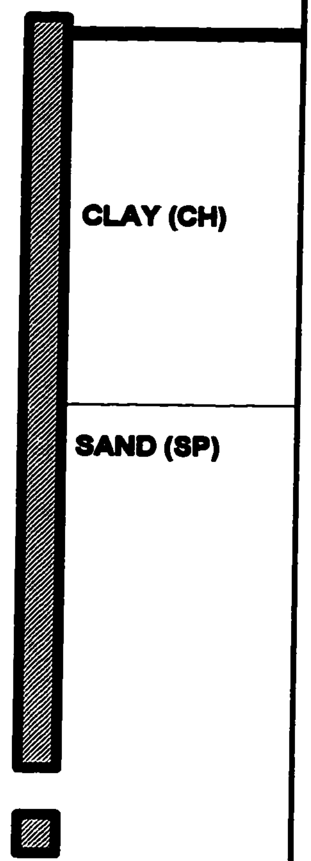
2	Reference	Briaud et al., 1988	
3	Shape, Material, and Installation	Square, Concrete, Driven	
4	Diameter, b, and Wall Thickness, t, mm	400	
5	Embedment Length D, m	13.4	
6	Cross Sectional Area A_t, m^2	0.16	
7	Unit Circumferential Area, A_s, m^2/m	1.6	
8	Toe, Closed or Open	Closed	
9	Type of Test and Loading	Static Compression, SML	
10	Toe Capacity, R_t, KN		
11	Shaft Capacity, R_s, KN		
12	*Capacity, R_u, KN	1,170	

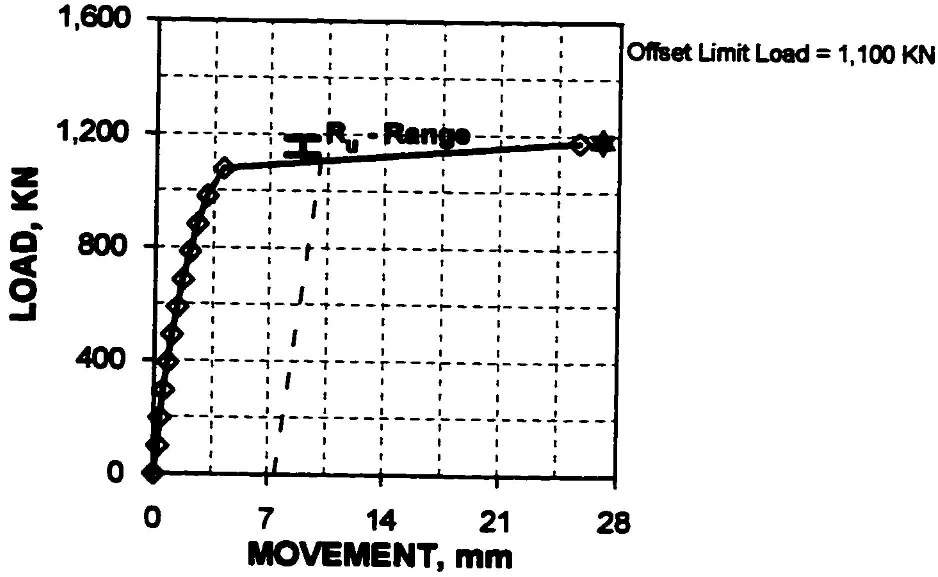

Case 115 A&M26
Sheet a CPT data

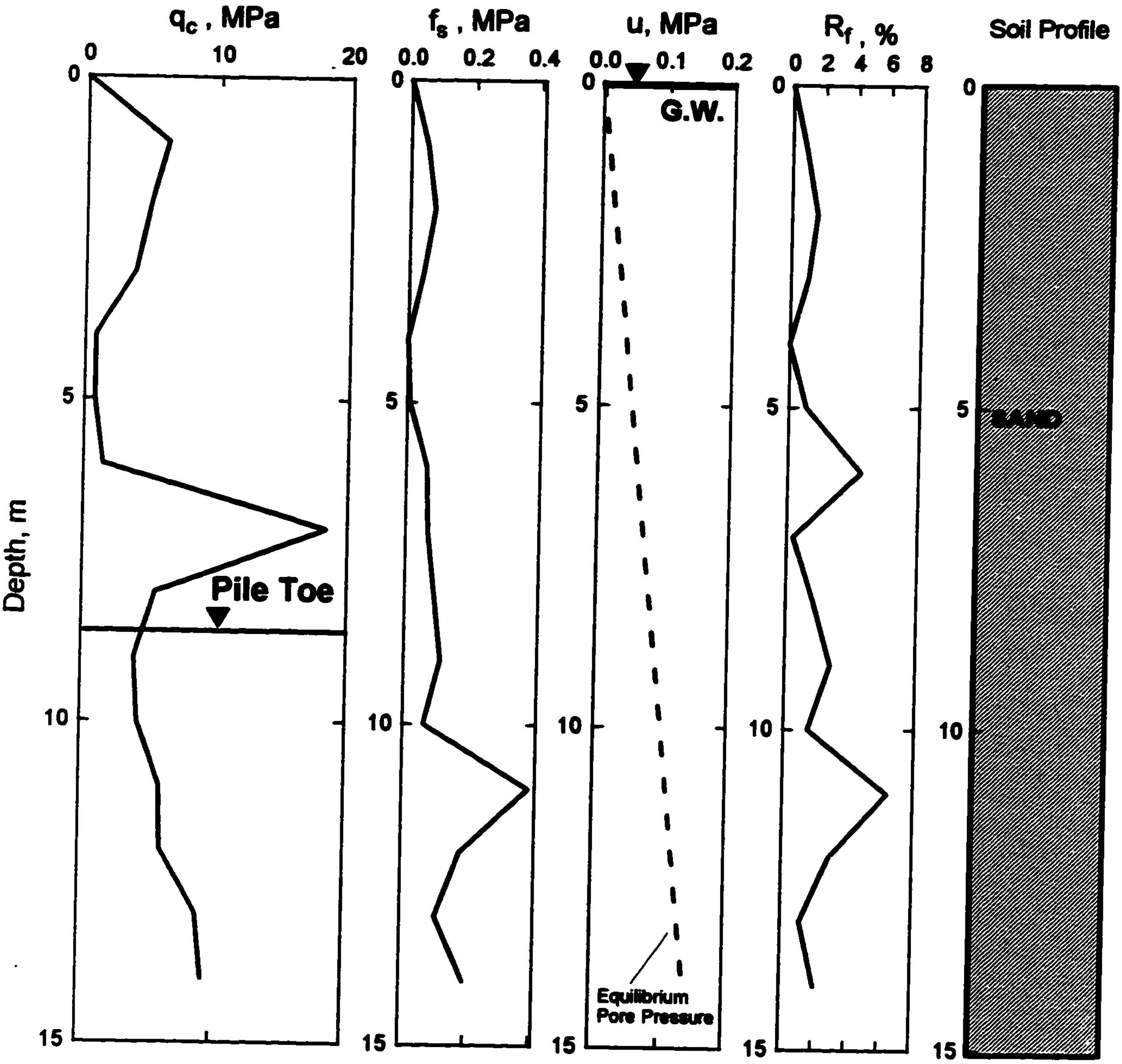

Case 115 A&M26
Sheet b Pile data

	DETAIL	DESCRIPTION
1	Site	Perry, MS, USA
2	Reference	Briaud et al., 1988
3	Shape, Material, and Installation	Square, Concrete, Driven
4	Diameter, b, and Wall Thickness, t, mm	350
5	Embedment Length D, m	8.6
6	Cross Sectional Area A_t, m^2	0.123
7	Unit Circumferential Area, A_s, m^2/m	1.4
8	Toe, Closed or Open	Closed
9	Type of Test and Loading	Static Compression, SML
10	Toe Capacity, R_t, KN	
11	Shaft Capacity, R_s, KN	
12	*Capacity, R_u, KN	600

SCHEMATIC PROFILE

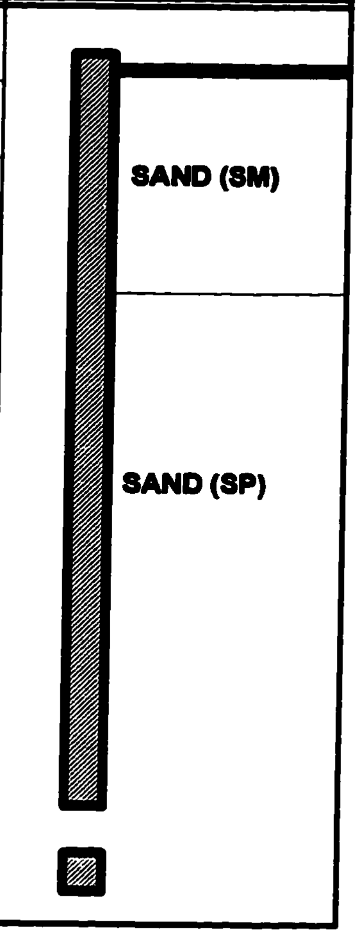

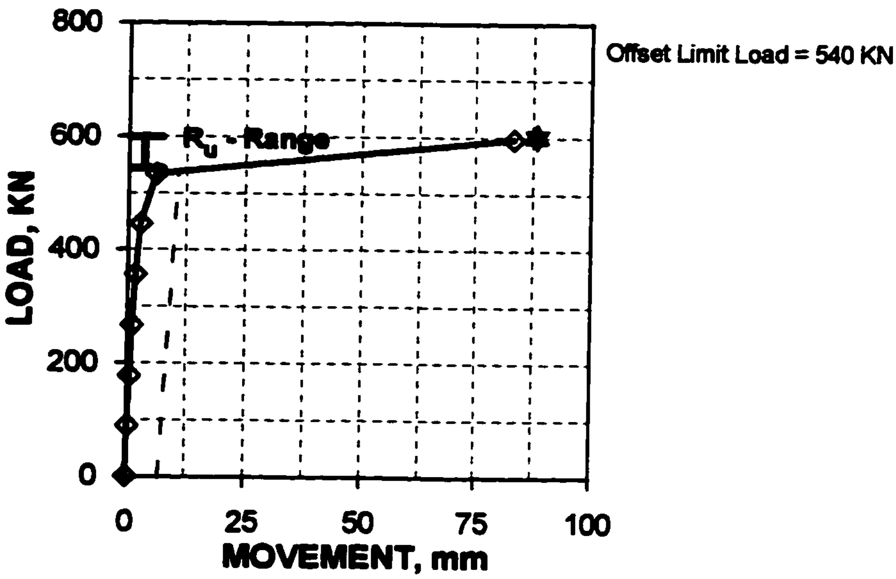

Case 116 A&M30
Sheet a CPT data

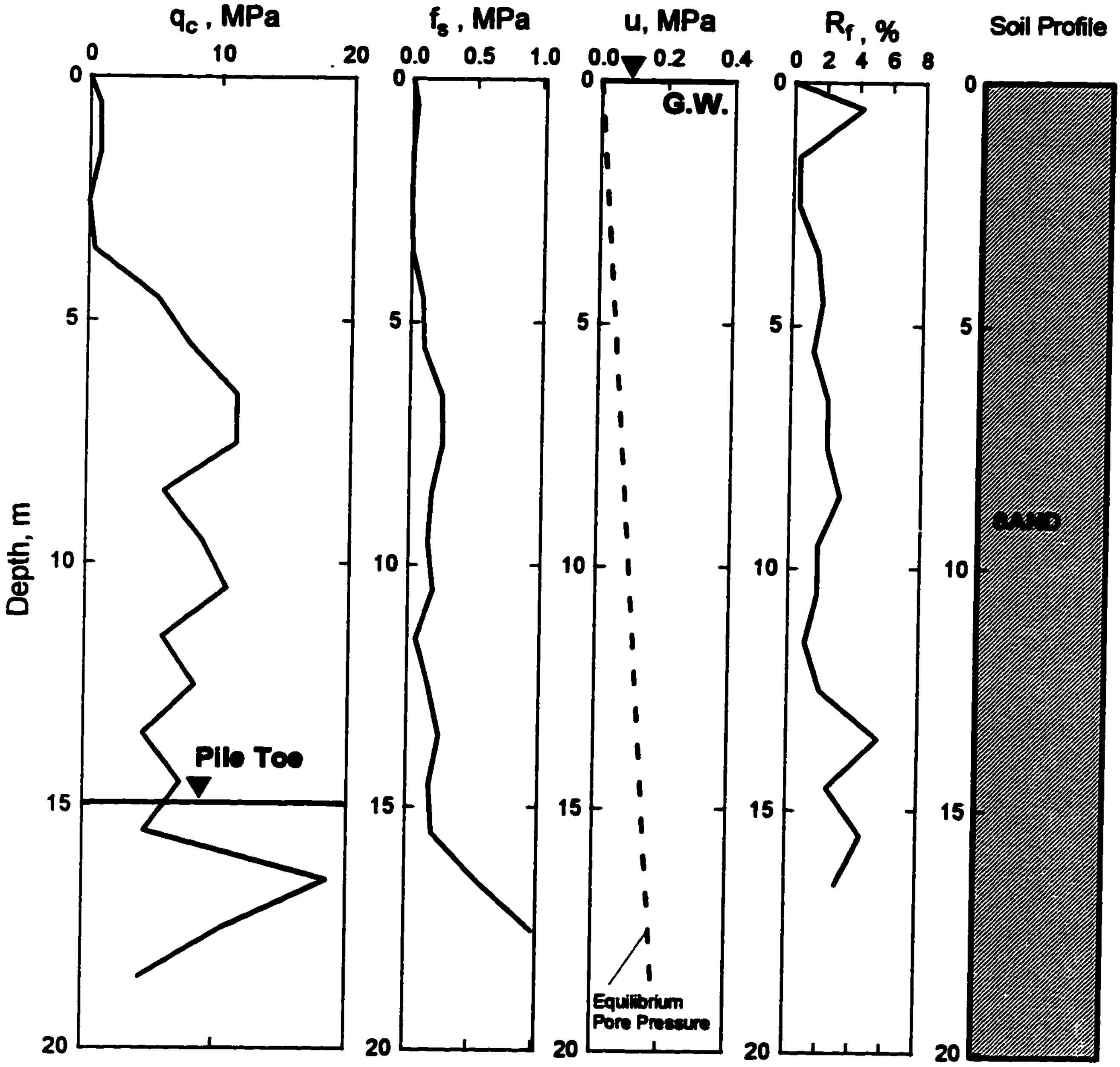

Case 116 A&M30
Sheet b Pile data

	DETAIL	DESCRIPTION
1	Site	Harrison, MS, USA
2	Reference	Briaud et al., 1988
3	Shape, Material, and Installation	Square, Concrete, Driven
4	Diameter, b, and Wall Thickness, t, mm	450
5	Embedment Length D, m	15
6	Cross Sectional Area A_t, m^2	0.203
7	Unit Circumferential Area, A_s, m^2/m	1.8
8	Toe, Closed or Open	Closed
9	Type of Test and Loading	Static Compression, SML
10	Toe Capacity, R_t, KN	
11	Shaft Capacity, R_s, KN	
12	*Capacity, R_u, KN	1,420

SCHEMATIC PROFILE

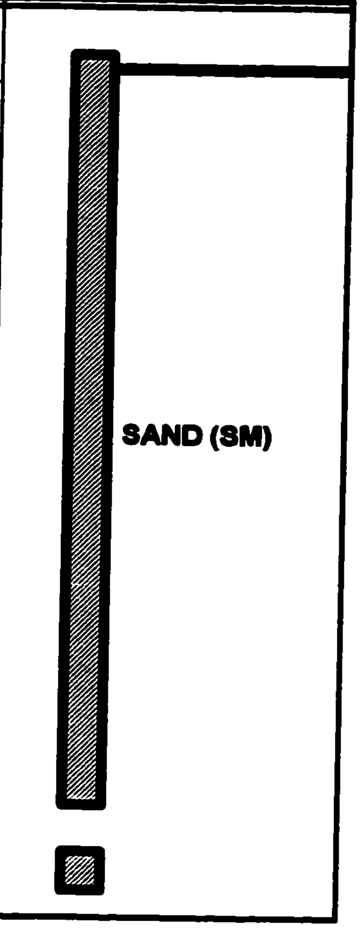

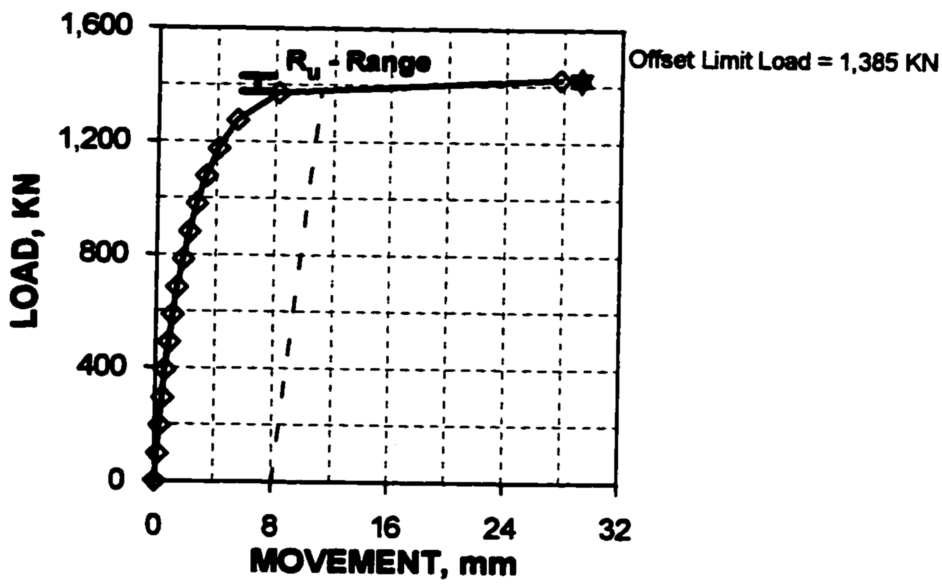

Case 117 A&M31
Sheet a CPT data

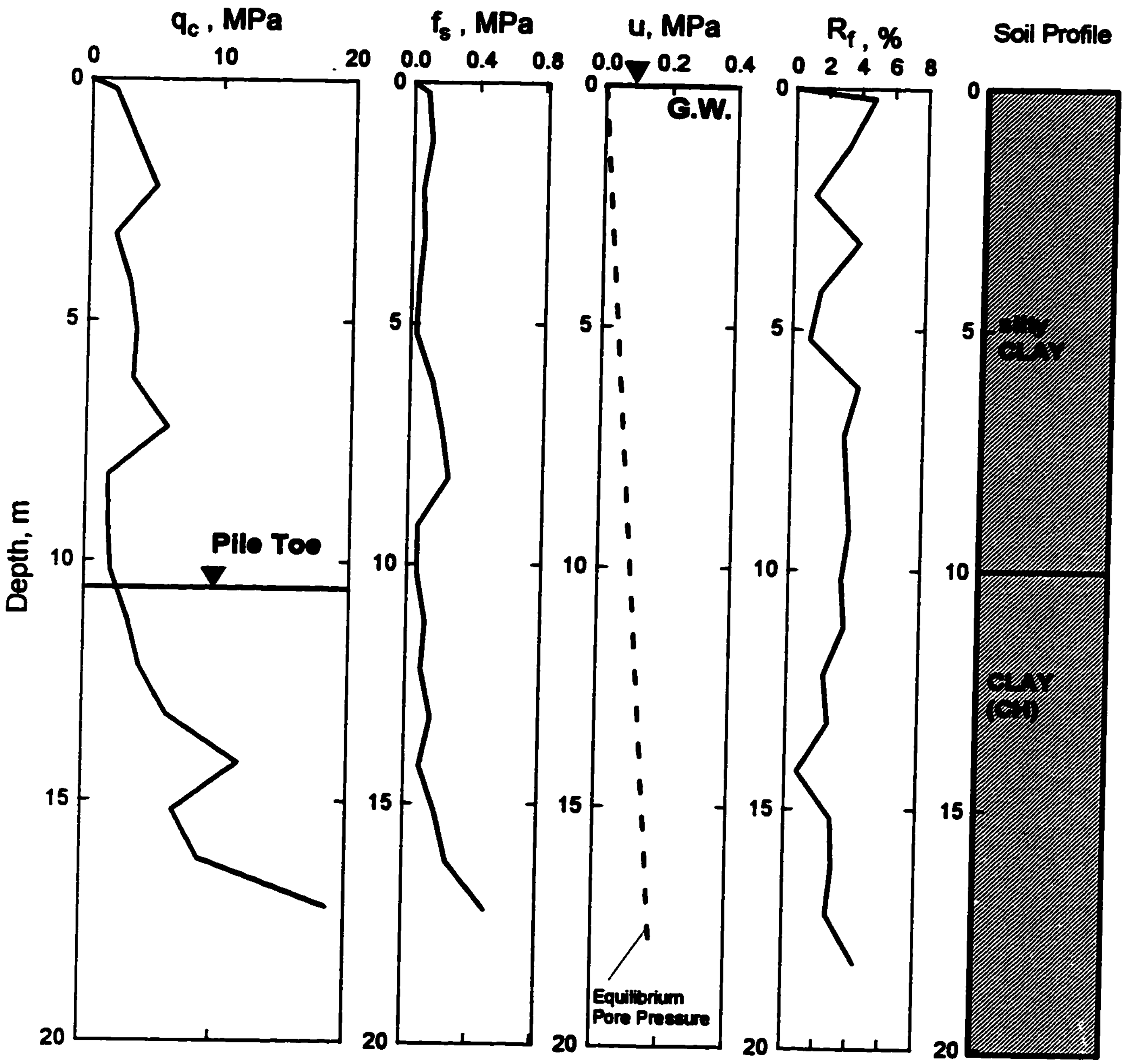

Case 117 A&M31
Sheet b Pile data

	DETAIL	DESCRIPTION	SCHEMATIC PROFILE
1	Site	Harrison, MS, USA	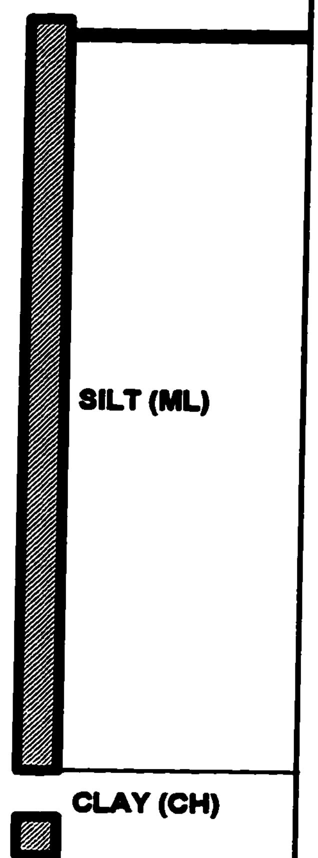
2	Reference	Briaud et al., 1988	
3	Shape, Material, and Installation	Square, Concrete, Driven	
4	Diameter, b, and Wall Thickness, t, mm	450	
5	Embedment Length D, m	10.4	
6	Cross Sectional Area A_t, m^2	0.203	
7	Unit Circumferential Area, A_s, m^2/m	1.8	
8	Toe, Closed or Open	Closed	
9	Type of Test and Loading	Static Compression, SML	
10	Toe Capacity, R_t, KN		
11	Shaft Capacity, R_s, KN		
12	*Capacity, R_u, KN	1,070	

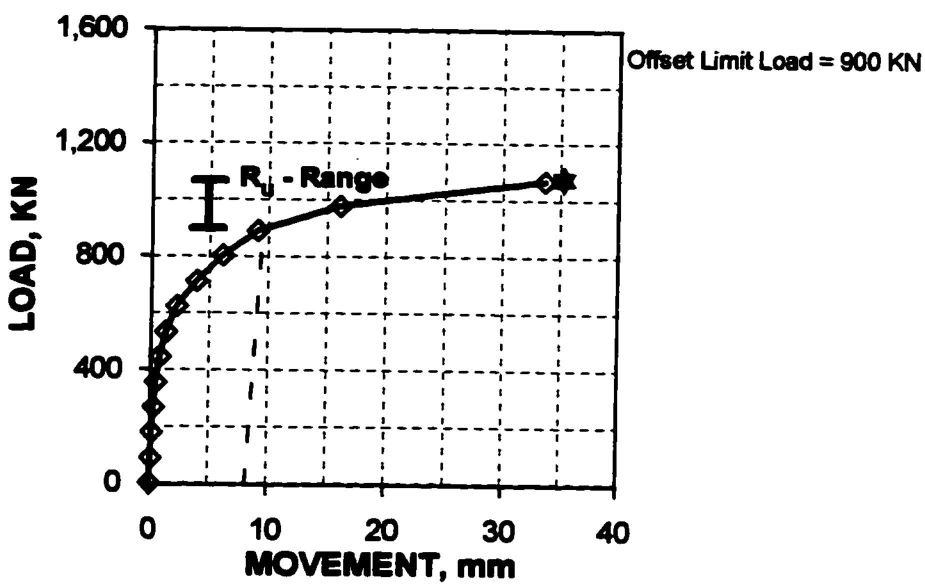

Case 118 A&M32
Sheet a CPT data

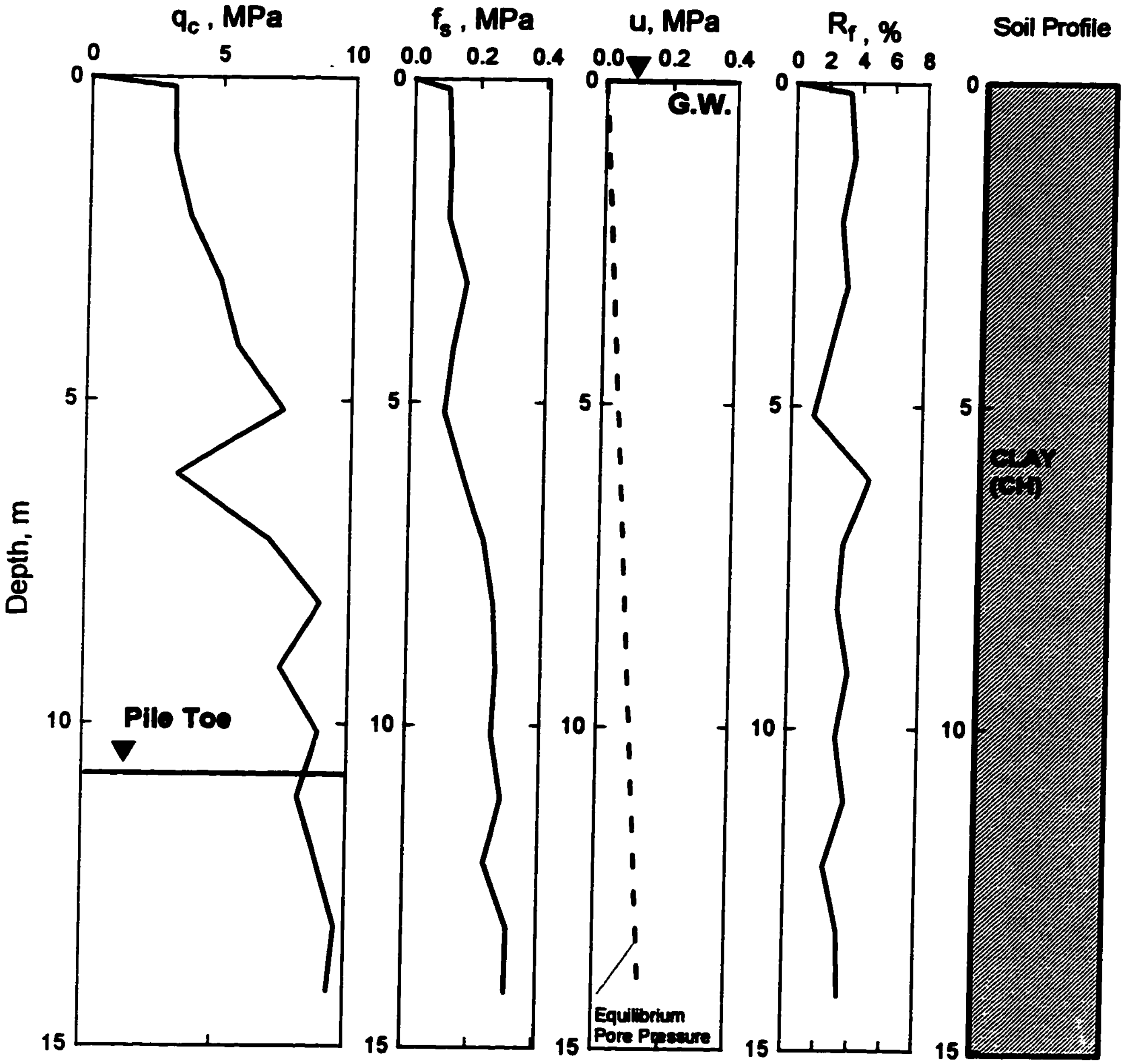

Case 118 A&M32
Sheet b Pile data

	DETAIL	DESCRIPTION	SCHEMATIC PROFILE
1	Site	Hinds, MS, USA	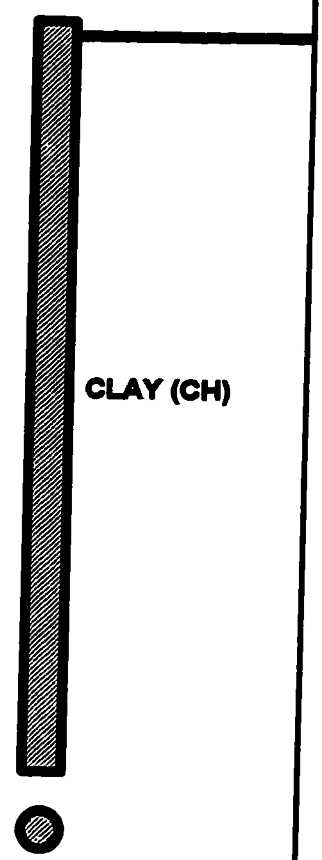
2	Reference	Briaud et al., 1988	
3	Shape, Material, and Installation	Round, Concrete, Bored	
4	Diameter, b, and Wall Thickness, t, mm	350	
5	Embedment Length D, m	10.6	
6	Cross Sectional Area A_t, m^2	0.096	
7	Unit Circumferential Area, A_s, m^2/m	1.1	
8	Toe, Closed or Open	Closed	
9	Type of Test and Loading	Static Compression, SML	
10	Toe Capacity, R_t, KN		
11	Shaft Capacity, R_s, KN		
12	*Capacity, R_u, KN	1,160	

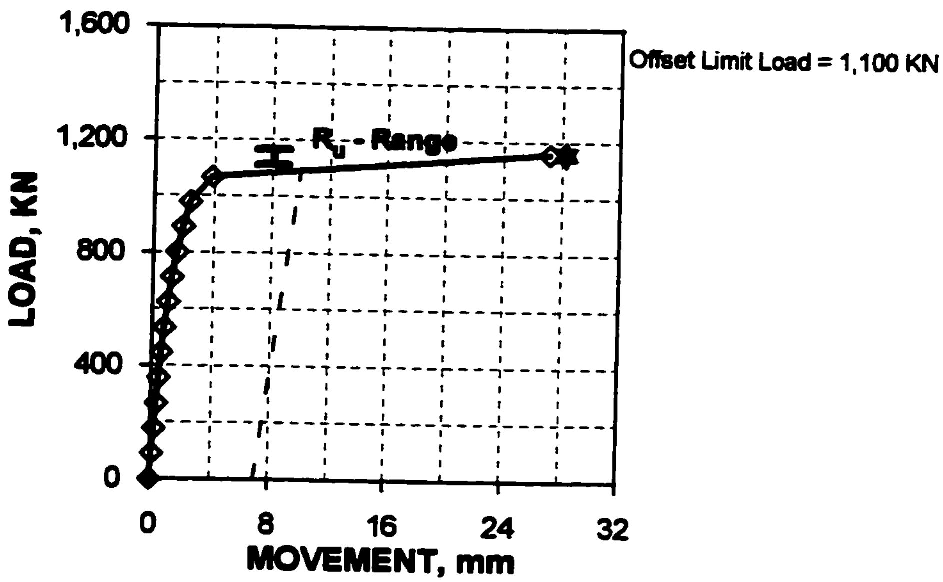

Case 119 A&M33
Sheet a CPT data

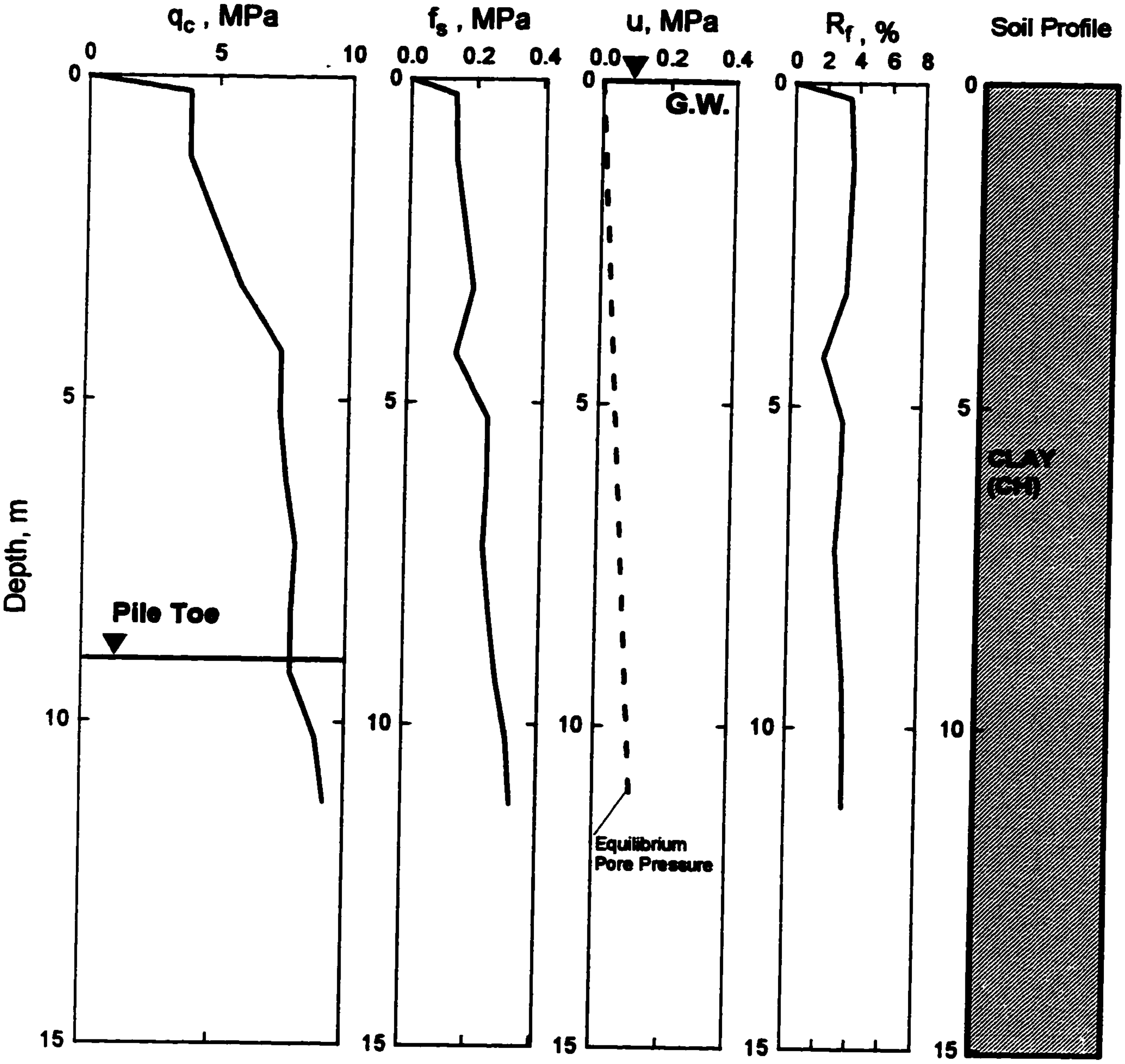

Case 119 A&M33
Sheet b Pile data

	DETAIL	DESCRIPTION	SCHEMATIC PROFILE
1	Site	Hinds, MS, USA	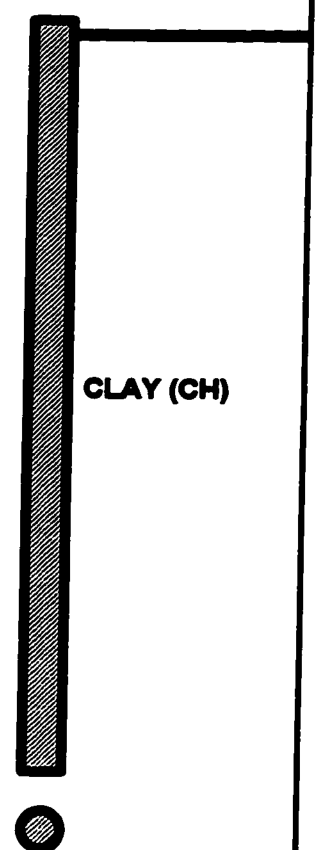
2	Reference	Briaud et al., 1988	
3	Shape, Material, and Installation	Round, Concrete, Bored	
4	Diameter, b, and Wall Thickness, t, mm	350	
5	Embedment Length D, m	8.9	
6	Cross Sectional Area A_t, m^2	0.096	CLAY (CH)
7	Unit Circumferential Area, A_s, m^2 /m	1.1	
8	Toe, Closed or Open	Closed	
9	Type of Test and Loading	Static Compression, SML	
10	Toe Capacity, R_t, KN		
11	Shaft Capacity, R_s, KN		
12	*Capacity, R_u, KN	1,170	

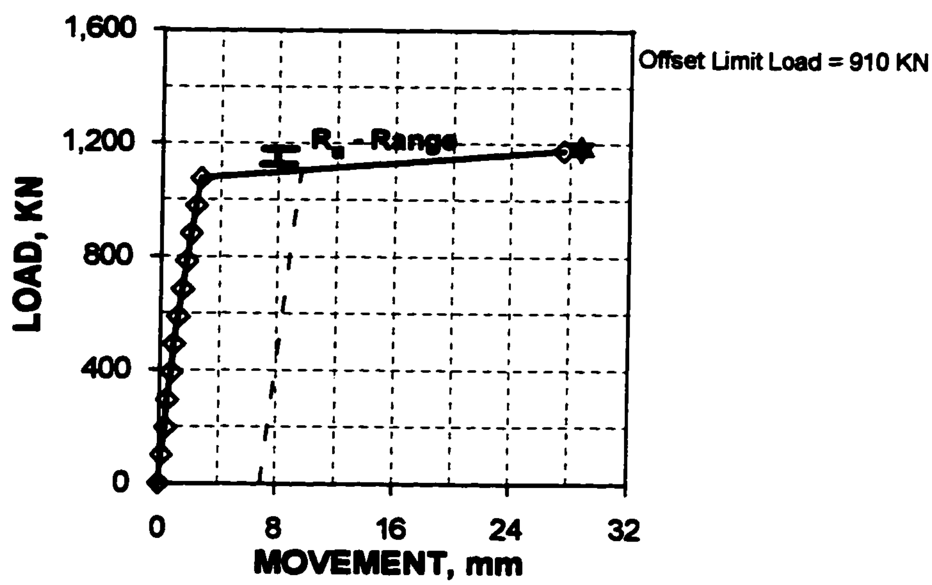

Case 120 A&M34
Sheet a CPT data

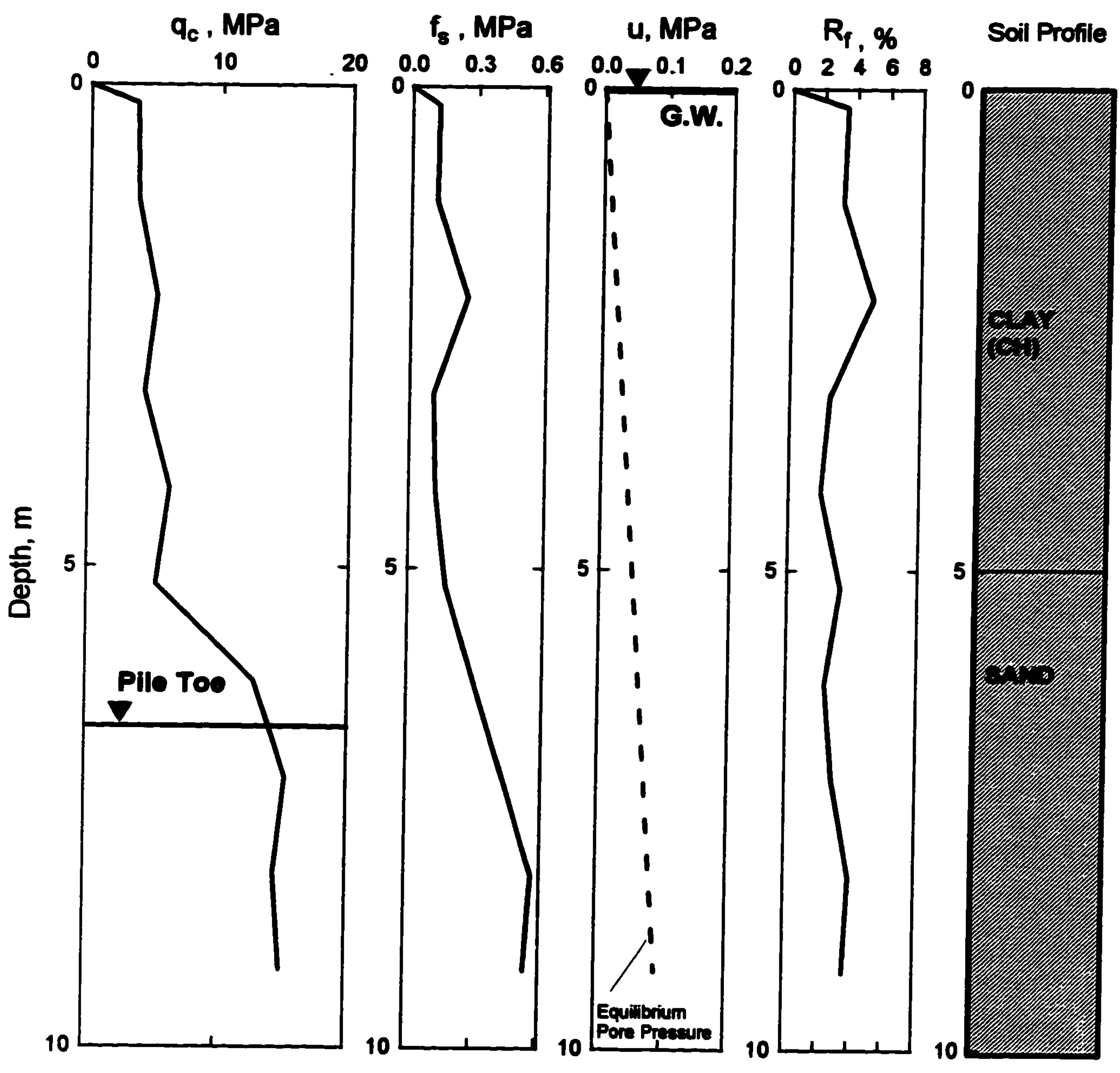

Case 120 A&M34
Sheet b Pile data

	DETAIL	DESCRIPTION
1	Site	Hinds, MS, USA
2	Reference	Briaud et al., 1988
3	Shape, Material, and Installation	Round, Concrete, Bored
4	Diameter, b, and Wall Thickness, t, mm	350
5	Embedment Length D, m	6.5
6	Cross Sectional Area A_t, m^2	0.096
7	Unit Circumferential Area, A_s, m^2/m	1.1
8	Toe, Closed or Open	Closed
9	Type of Test and Loading	Static Compression, SML
10	Toe Capacity, R_t, KN	
11	Shaft Capacity, R_s, KN	
12	*Capacity, R_u, KN	880

SCHEMATIC PROFILE

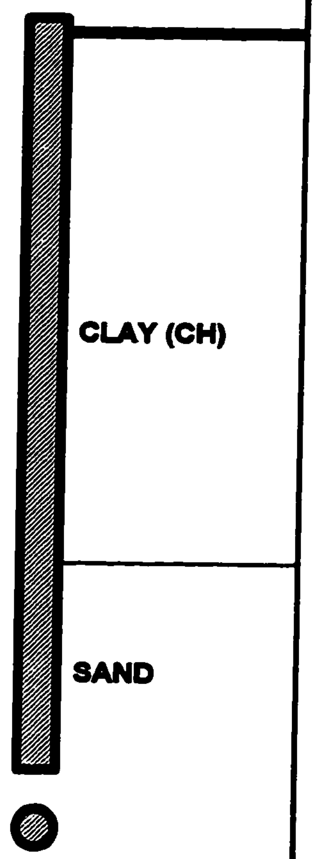

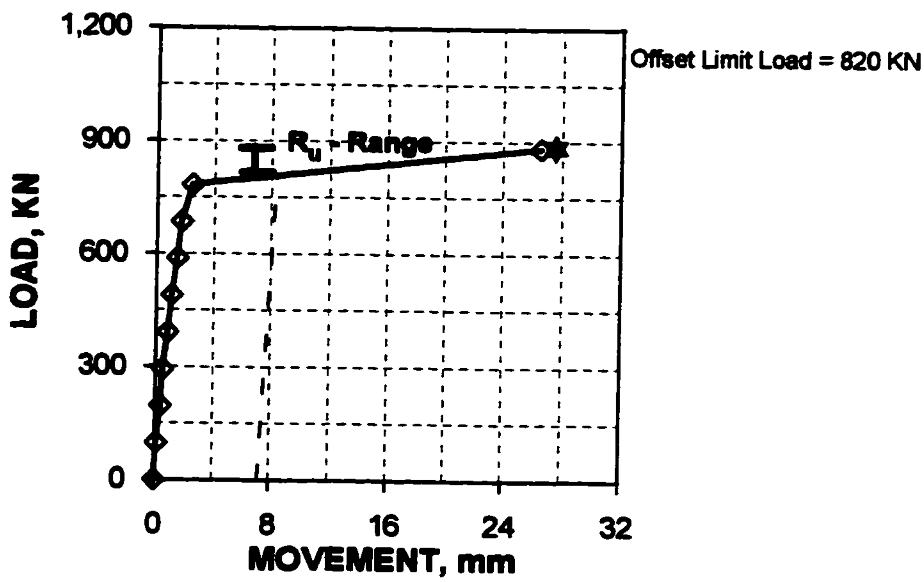

Case 121 A&M35
Sheet a CPT data

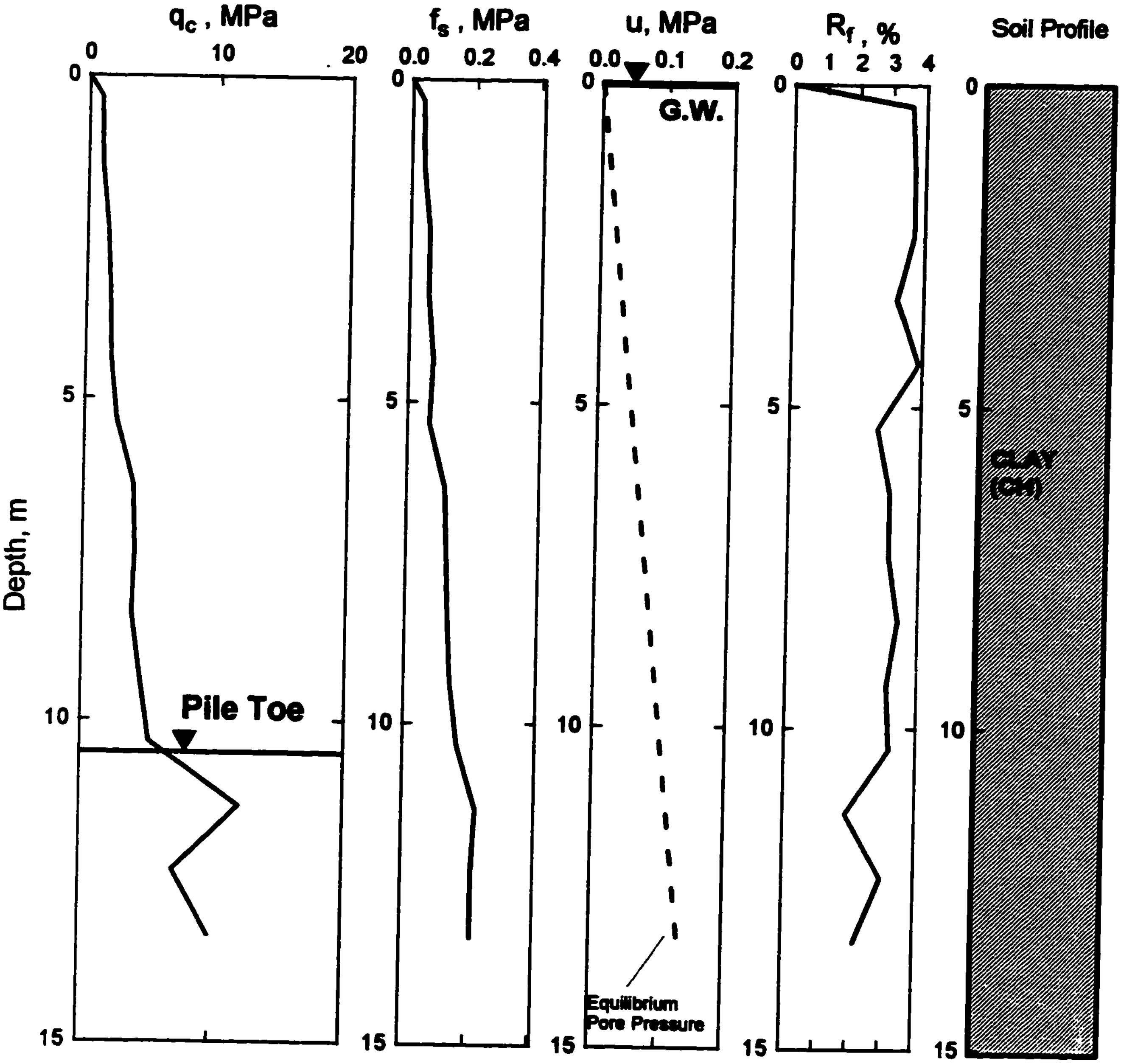

Case 121 A&M35
Sheet b Pile data

	DETAIL	DESCRIPTION	SCHEMATIC PROFILE
1	Site	Hinds, MS, USA	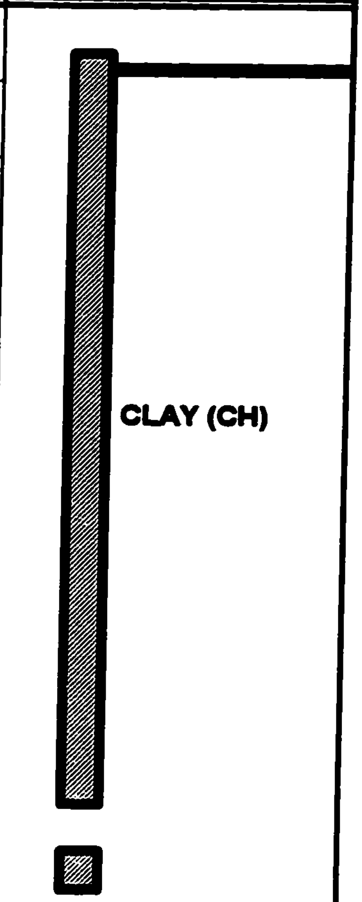
2	Reference	Briaud et al., 1988	
3	Shape, Material, and Installation	Square, Concrete, Driven	
4	Diameter, b, and Wall Thickness, t, mm	400	
5	Embedment Length D, m	10.4	
6	Cross Sectional Area A_t, m^2	0.16	
7	Unit Circumferential Area, A_s, m^2/m	1.6	
8	Toe, Closed or Open	Closed	
9	Type of Test and Loading	Static Compression, SML	
10	Toe Capacity, R_t, KN		
11	Shaft Capacity, R_s, KN		
12	*Capacity, R_u, KN	1,170	

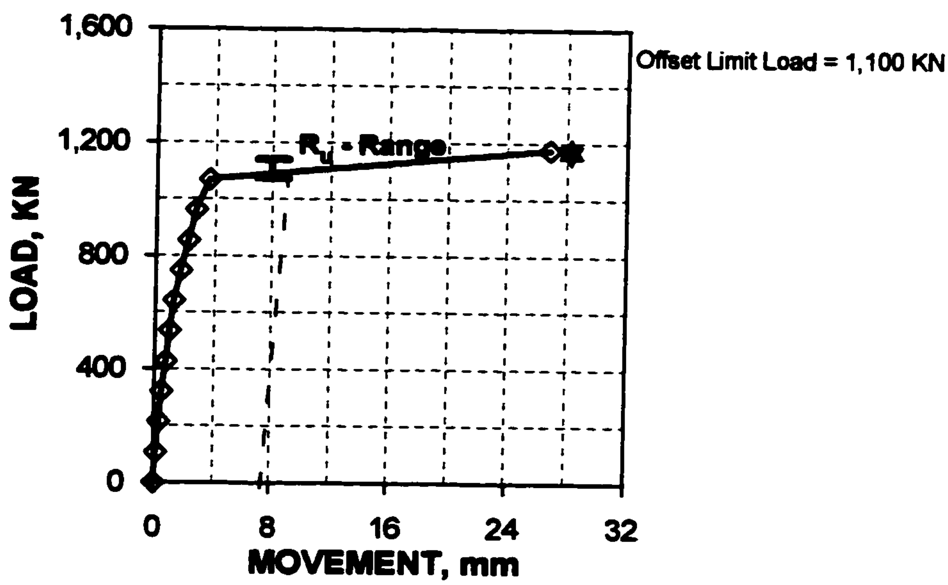

Case 122 A&M36
Sheet a CPT data

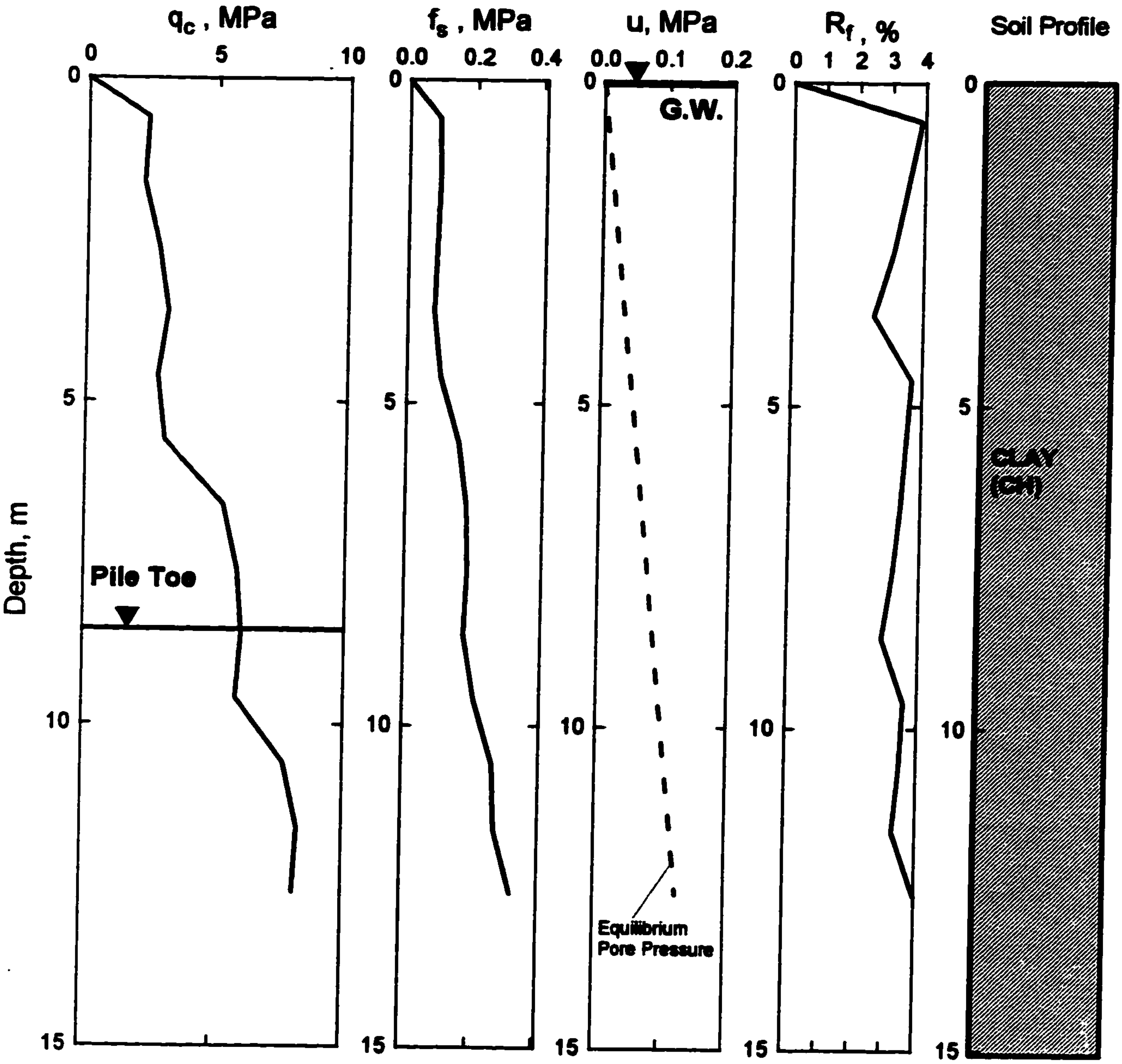

Case 122 A&M36
Sheet b Pile data

	DETAIL	DESCRIPTION
1	Site	Hinds, MS, USA
2	Reference	Briaud et al., 1988
3	Shape, Material, and Installation	Round, Concrete, Bored
4	Diameter, b, and Wall Thickness, t, mm	350
5	Embedment Length D, m	8.5
6	Cross Sectional Area A_t, m^2	0.096
7	Unit Circumferential Area, A_s, m^2/m	1.1
8	Toe, Closed or Open	Closed
9	Type of Test and Loading	Static Compression, SML
10	Toe Capacity, R_t, KN	
11	Shaft Capacity, R_s, KN	
12	*Capacity, R_u, KN	720

SCHEMATIC PROFILE

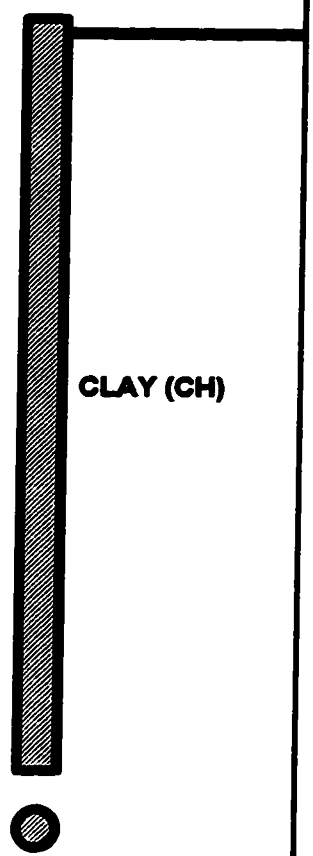

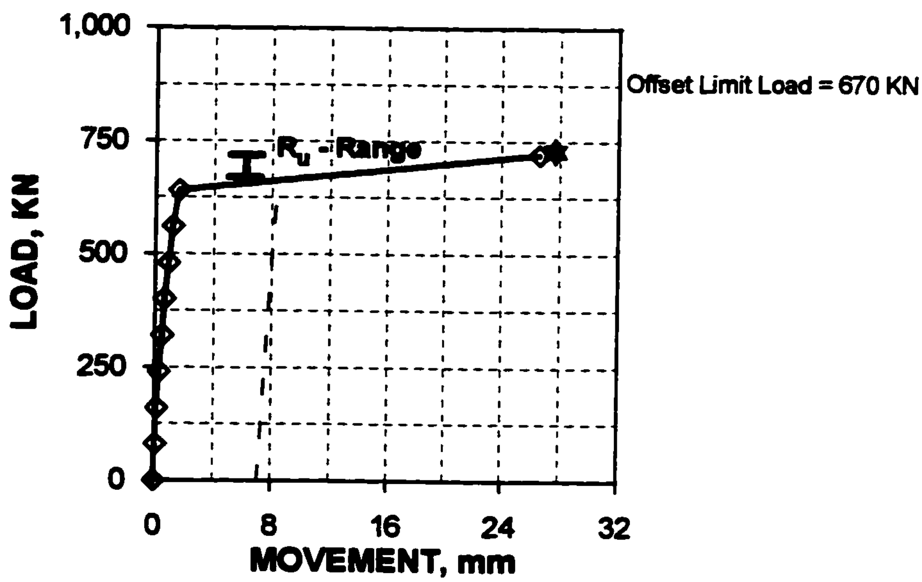

Case 123 A&M38
Sheet a CPT data

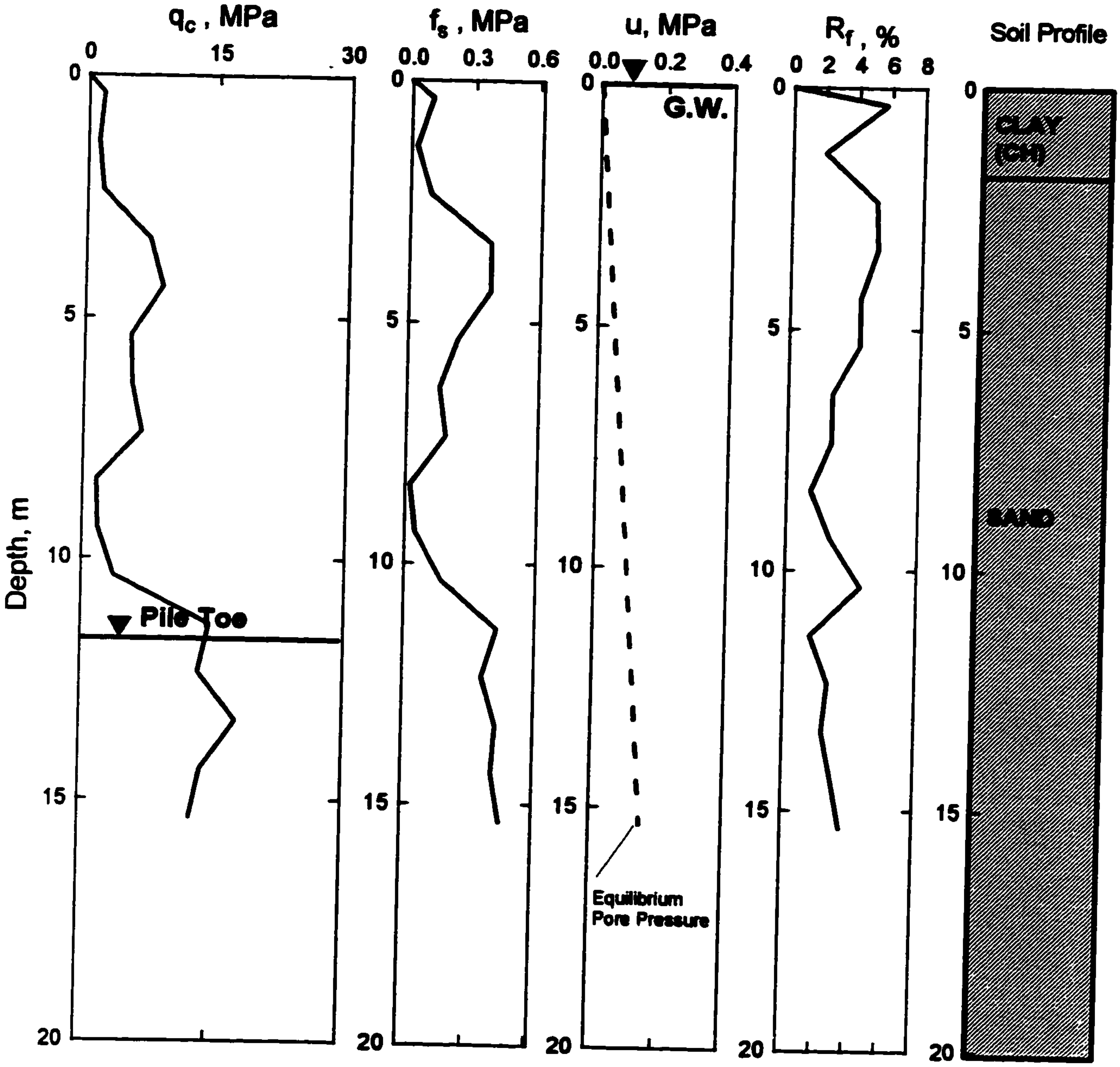

Case 123 A&M38
Sheet b Pile data

	DETAIL	DESCRIPTION	SCHEMATIC PROFILE
1	Site	Washington, MS, USA	
2	Reference	Briaud et al., 1988	CLAY (CH)
3	Shape, Material, and Installation	Square, Concrete, Driven	
4	Diameter, b, and Wall Thickness, t, mm	400	
5	Embedment Length D, m	11.3	
6	Cross Sectional Area A_t, m^2	0.16	
7	Unit Circumferential Area, A_s, m^2/m	1.6	
8	Toe, Closed or Open	Closed	SAND (SP)
9	Type of Test and Loading	Static Compression, SML	
10	Toe Capacity, R_t, KN		
11	Shaft Capacity, R_s, KN		
12	*Capacity, R_u, KN	870	

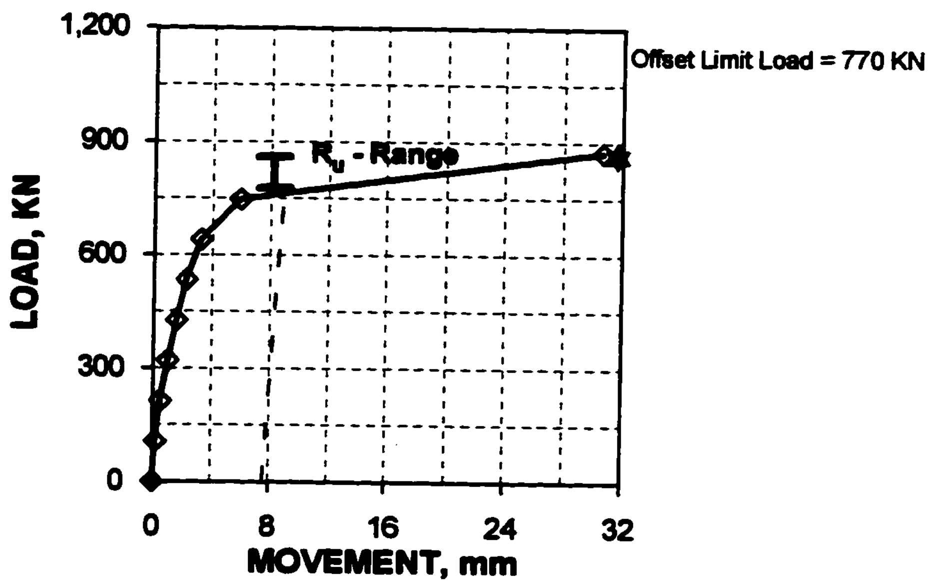

Case 124 A&M39
Sheet a CPT data

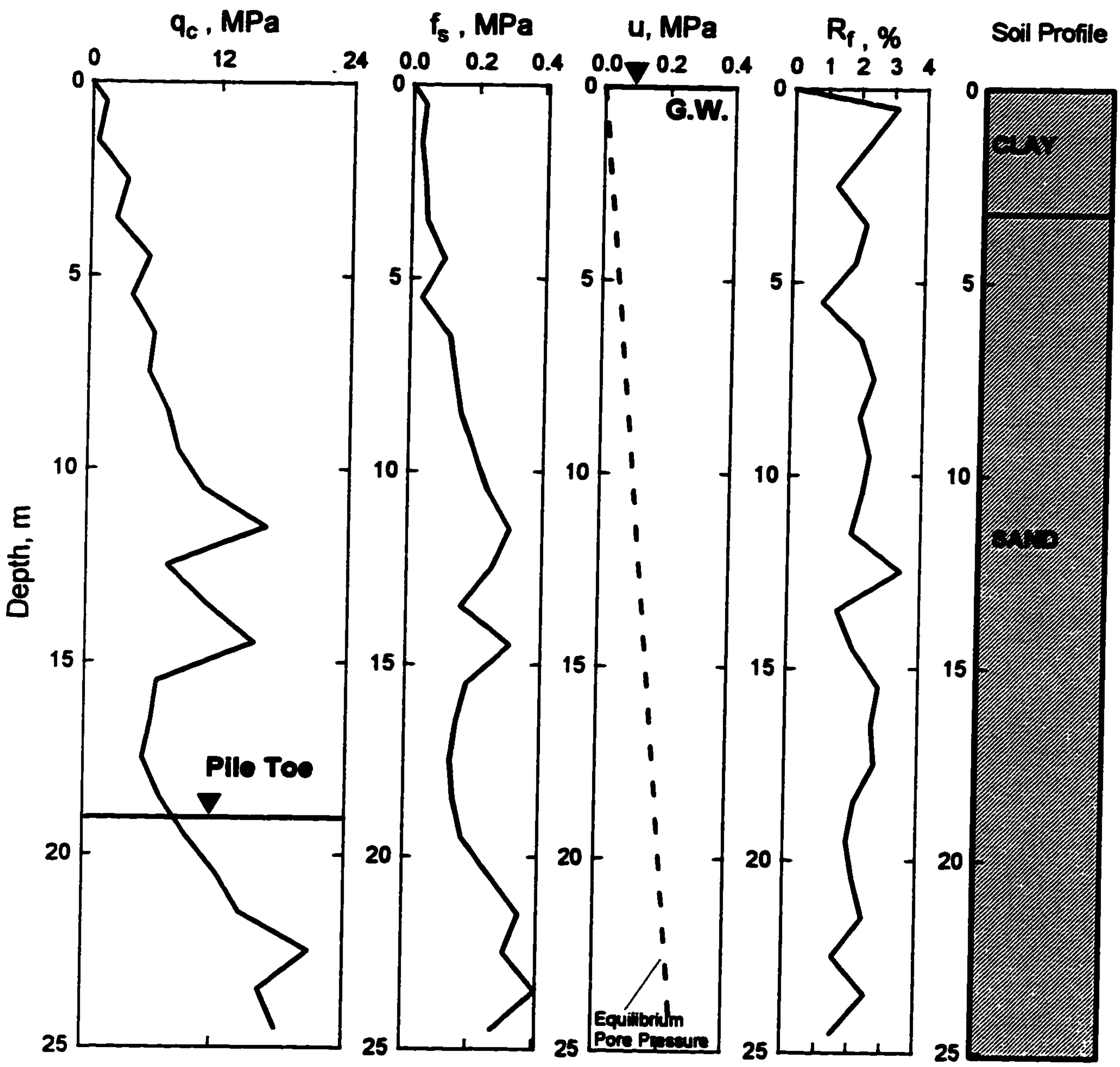

Case 124 A&M39
Sheet b Pile data

	DETAIL	DESCRIPTION	SCHEMATIC PROFILE
1	Site	Washington, MS, USA	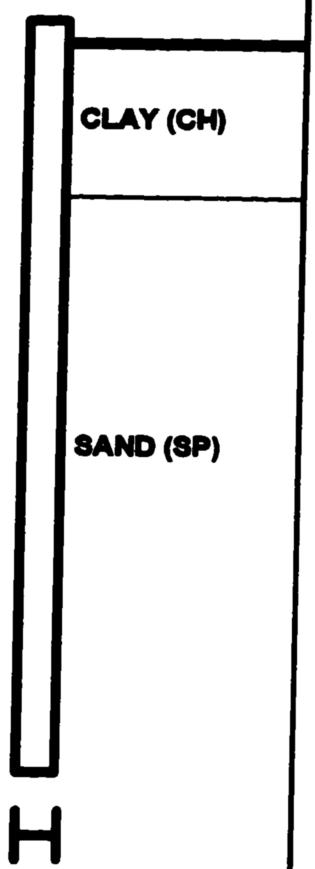
2	Reference	Briaud et al., 1988	
3	Shape, Material, and Installation	H-Pile, Steel, Driven	
4	Diameter, b, and Wall Thickness, t, mm	299*306	
5	Embedment Length D, m	19	
6	Cross Sectional Area A_t, m^2	0.01	
7	Unit Circumferential Area, A_s, m^2/m	1.21	
8	Toe, Closed or Open	Open	
9	Type of Test and Loading	Static Compression, SML	
10	Toe Capacity, R_t, KN		
11	Shaft Capacity, R_s, KN		
12	*Capacity, R_u, KN	1,370	

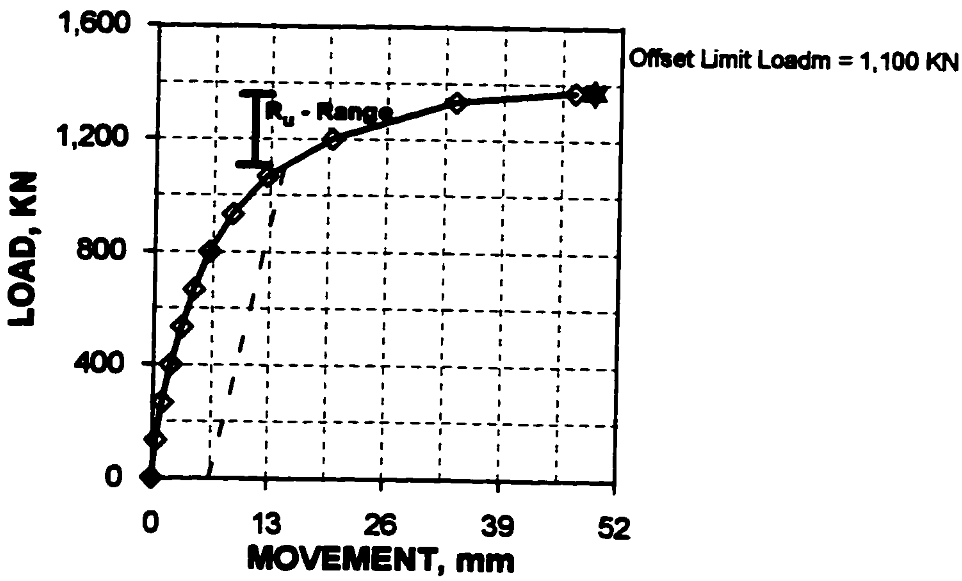

Case 125 A&M40
Sheet a CPT data

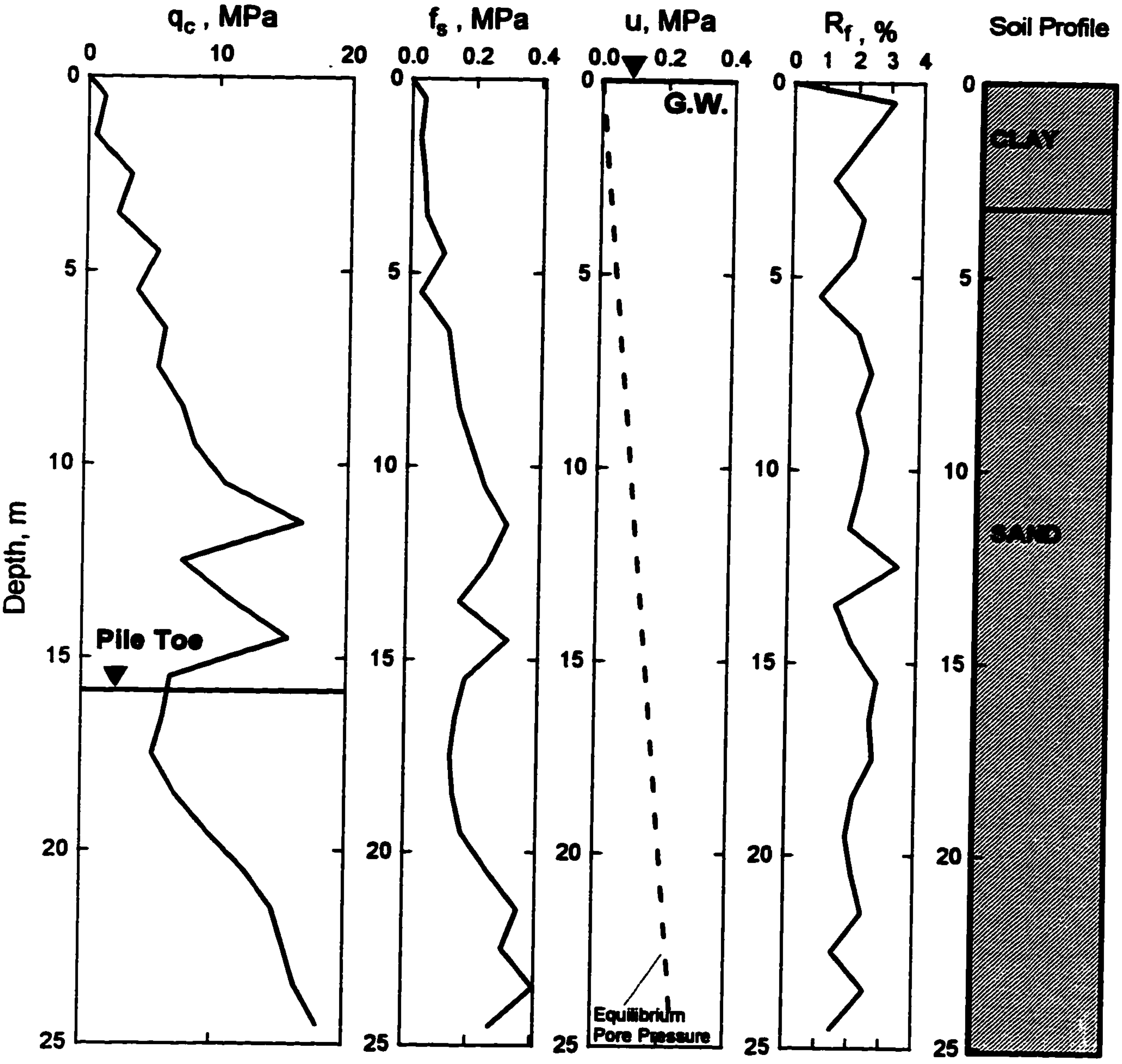

Case 125 A&M40
Sheet b Pile data

	DETAIL	DESCRIPTION
1	Site	Washington, MS, USA
2	Reference	Briaud et al., 1988
3	Shape, Material, and Installation	Square, Concrete, Driven
4	Diameter, b, and Wall Thickness, t, mm	350
5	Embedment Length D, m	16
6	Cross Sectional Area A_t, m^2	0.123
7	Unit Circumferential Area, A_s, m^2/m	1.4
8	Toe, Closed or Open	Closed
9	Type of Test and Loading	Static Compression, SML
10	Toe Capacity, R_t, KN	
11	Shaft Capacity, R_s, KN	
12	*Capacity, R_u, KN	1,070

SCHEMATIC PROFILE

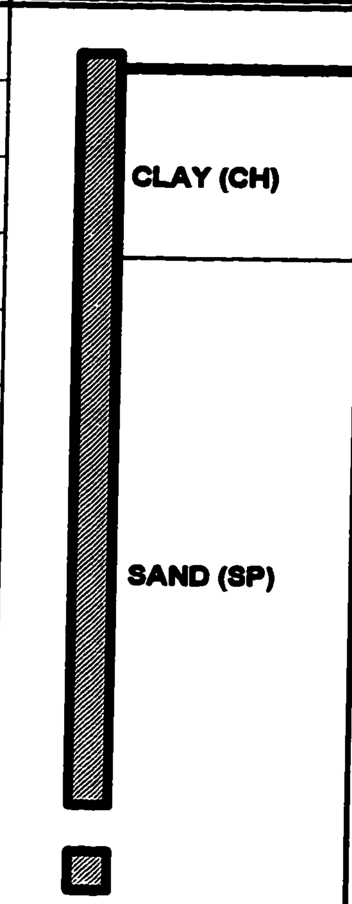

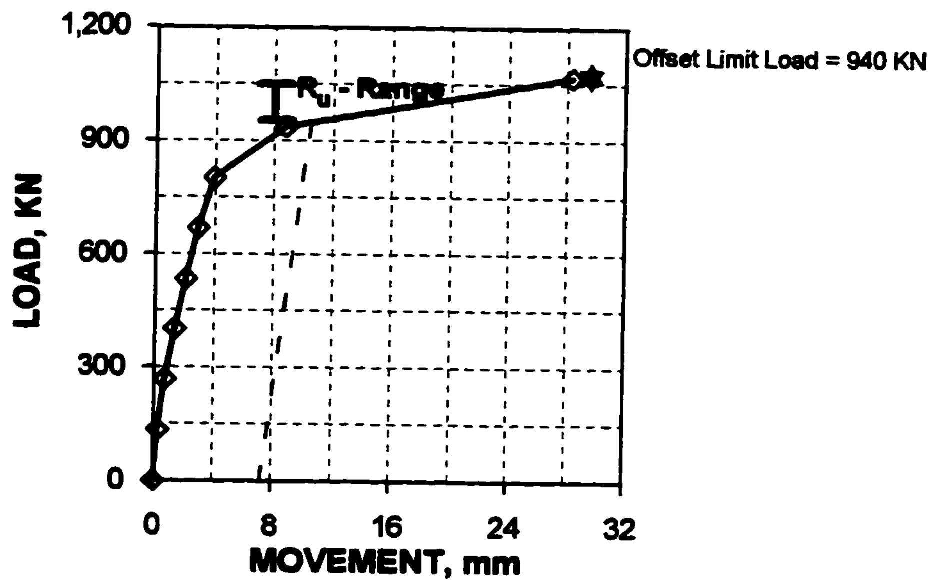

Case 126 A&M41
Sheet a CPT data

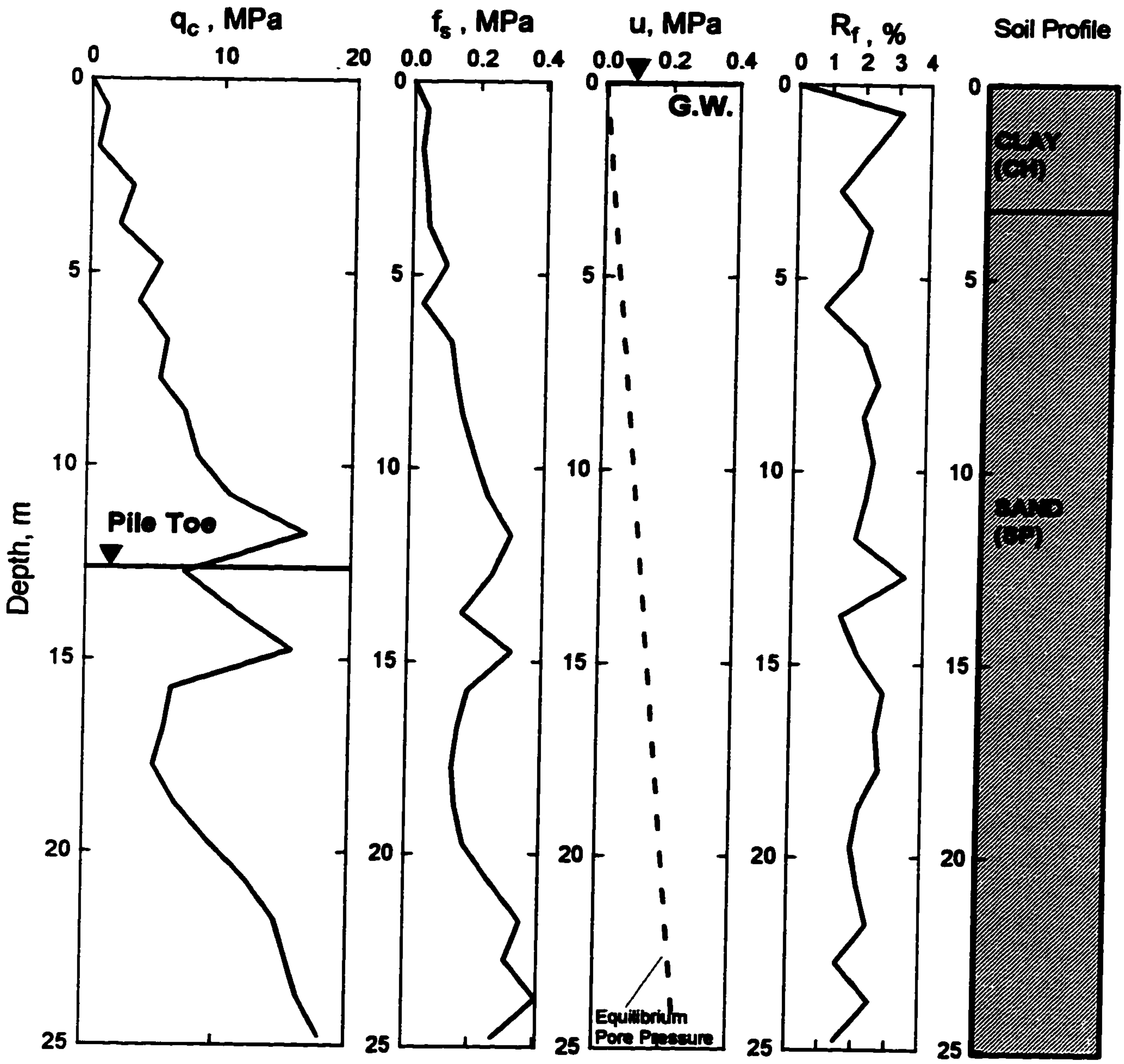

Case 126 A&M41
Sheet b Pile data

	DETAIL	DESCRIPTION	SCHEMATIC PROFILE
1	Site	Washington, MS, USA	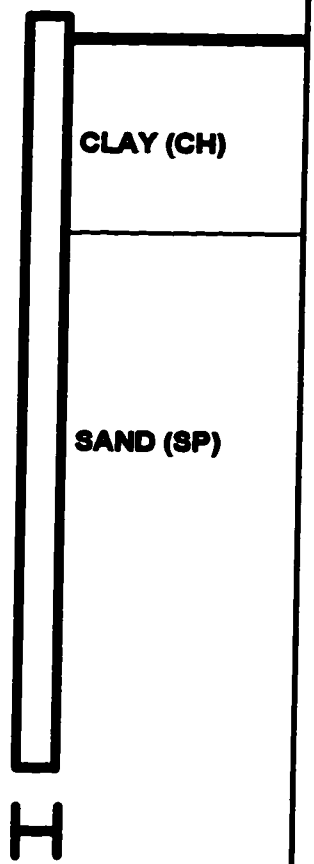
2	Reference	Briaud et al., 1988	
3	Shape, Material, and Installation	H-Pile, Steel, Driven	
4	Diameter, b, and Wall Thickness, t, mm	299*306	
5	Embedment Length D, m	12.4	
6	Cross Sectional Area A_t, m^2	0.01	
7	Unit Circumferential Area, A_s, m^2/m	1.21	
8	Toe, Closed or Open	Open	
9	Type of Test and Loading	Static Compression, SML	
10	Toe Capacity, R_t, KN		
11	Shaft Capacity, R_s, KN		
12	*Capacity, R_u, KN	520	

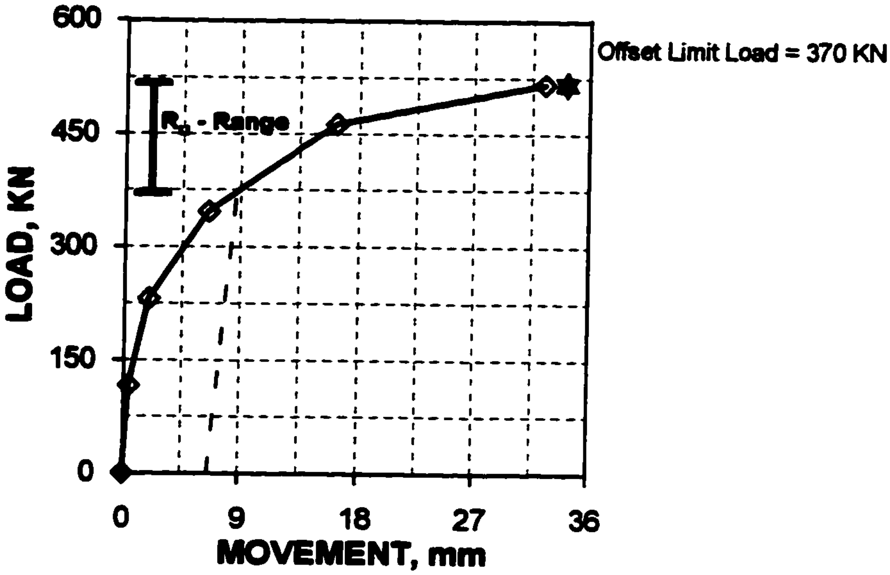

Case 127 A&M46
Sheet a CPT data

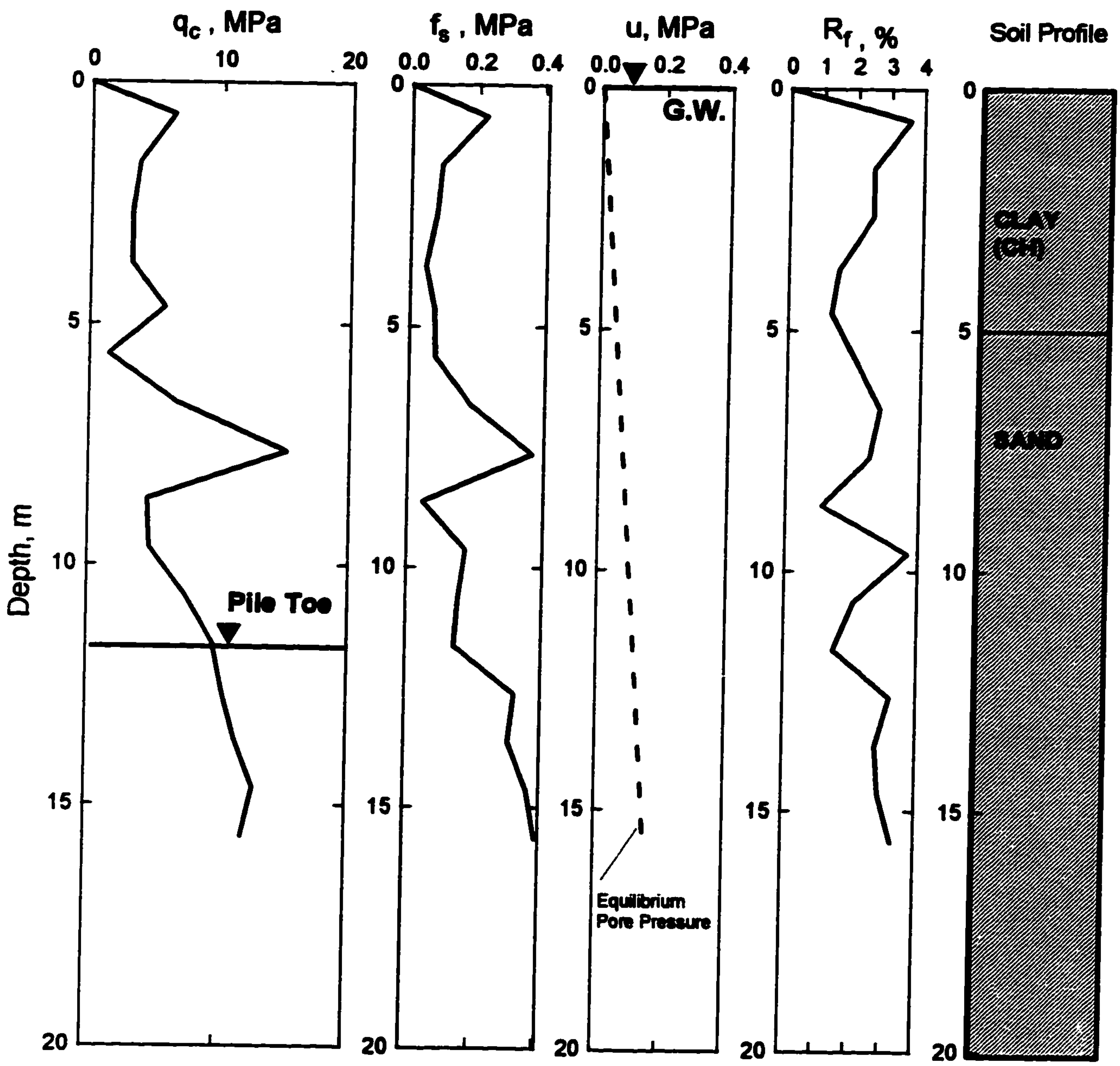

Case 127 A&M46
Sheet b Pile data

	DETAIL	DESCRIPTION	SCHEMATIC PROFILE
1	Site	Madison, MS, USA	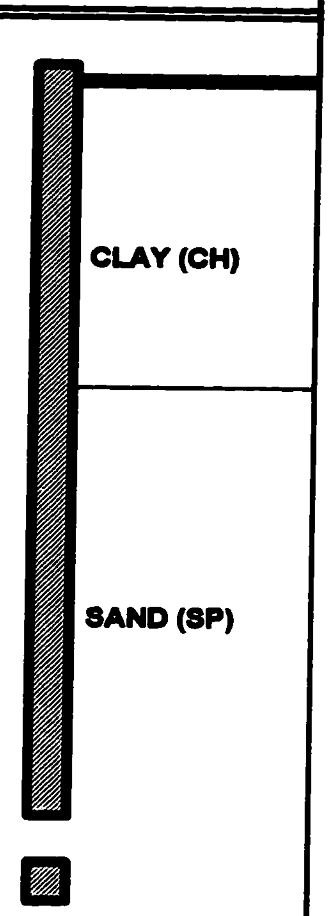
2	Reference	Briaud et al., 1988	
3	Shape, Material, and Installation	Square, Concrete, Driven	
4	Diameter, b, and Wall Thickness, t, mm	400	
5	Embedment Length D, m	11.4	
6	Cross Sectional Area A_t, m^2	0.16	
7	Unit Circumferential Area, A_s, m^2/m	1.6	
8	Toe, Closed or Open	Closed	
9	Type of Test and Loading	Static Compression, SML	
10	Toe Capacity, R_t, KN		
11	Shaft Capacity, R_s, KN		
12	*Capacity, R_u, KN	1,140	

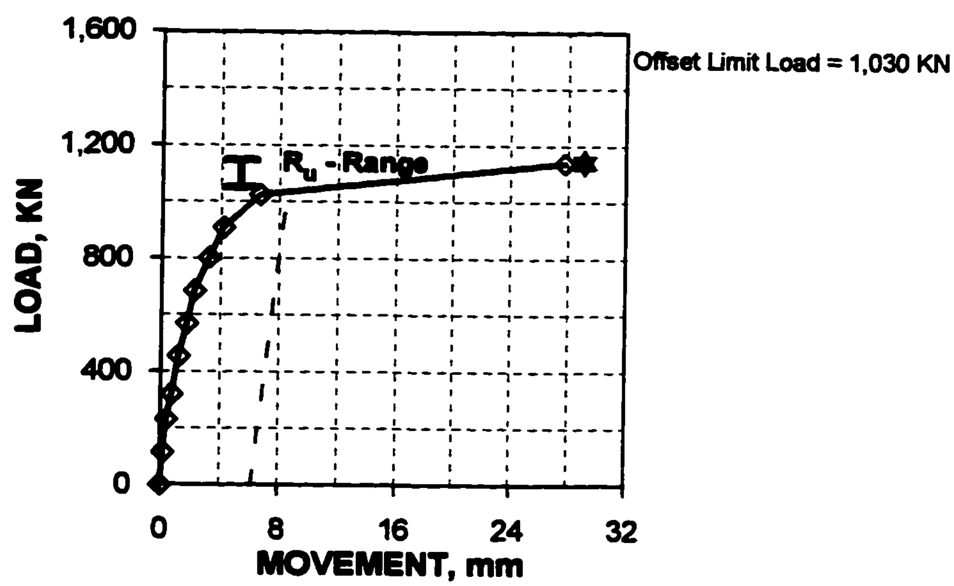

Case 128 A&M47
Sheet a CPT data

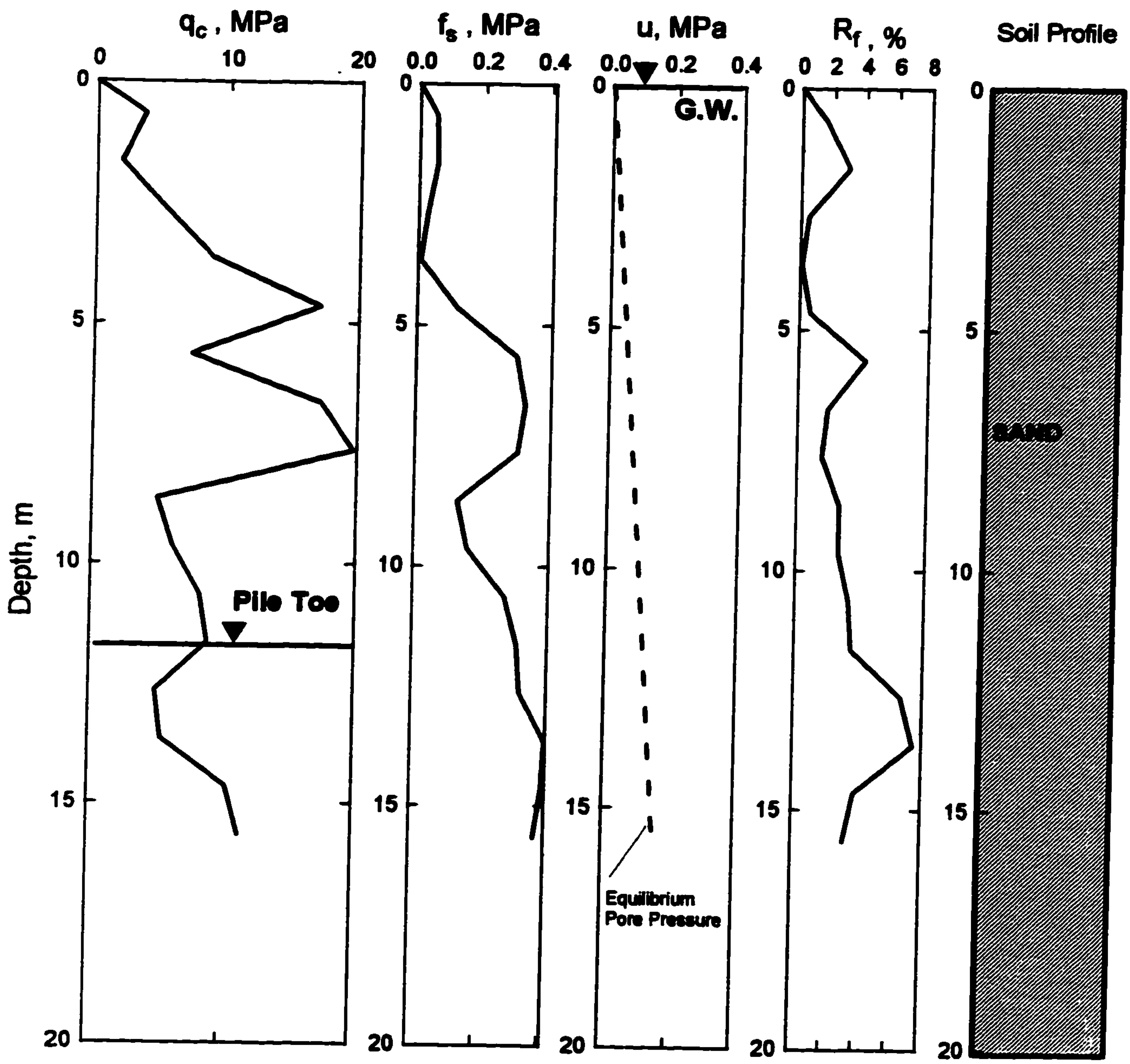

Case 128 A&M47
Sheet b Pile data

DETAIL		DESCRIPTION	SCHEMATIC PROFILE
1	Site	Madison, MS, USA	
2	Reference	Briaud et al., 1988	
3	Shape, Material, and Installation	Square, Concrete, Driven	
4	Diameter, b, and Wall Thickness, t, mm	400	
5	Embedment Length D, m	11.2	
6	Cross Sectional Area A_t, m^2	0.16	
7	Unit Circumferential Area, A_s, m^2/m	1.6	
8	Toe, Closed or Open	Closed	
9	Type of Test and Loading	Static Compression, SML	
10	Toe Capacity, R_t, KN		
11	Shaft Capacity, R_s, KN		
12	*Capacity, R_u, KN	1,020	

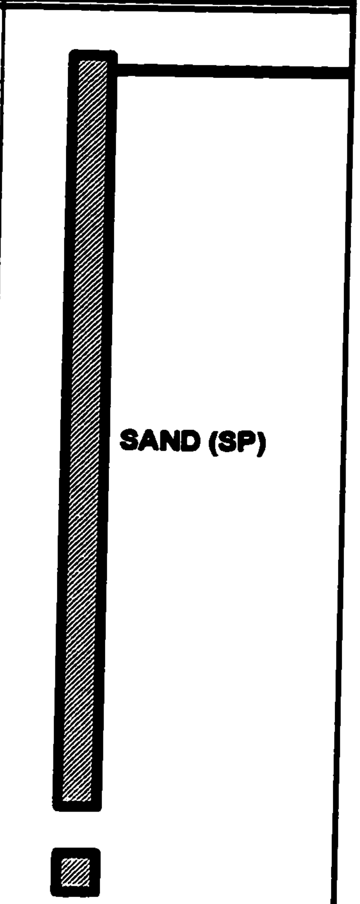

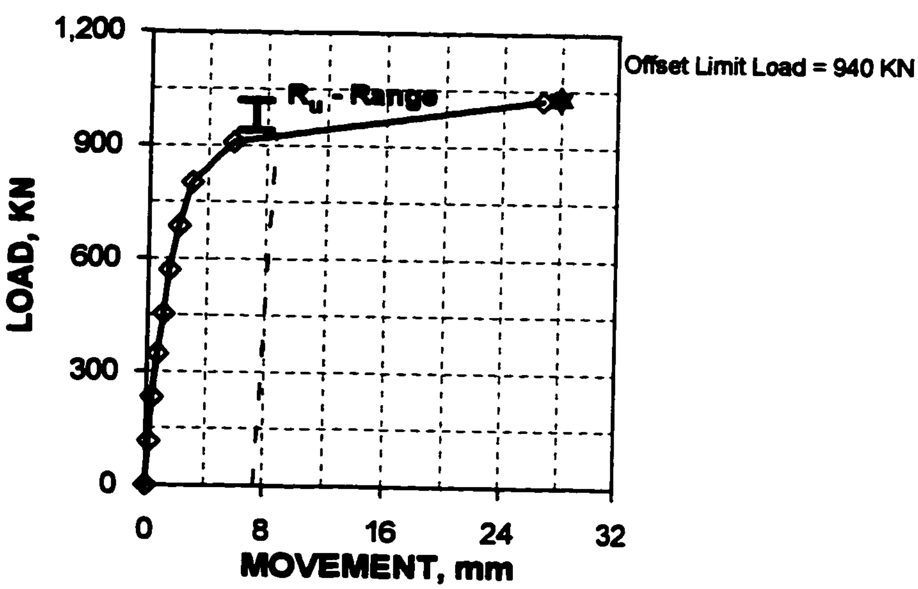

Case 129 A&M48
Sheet a CPT data

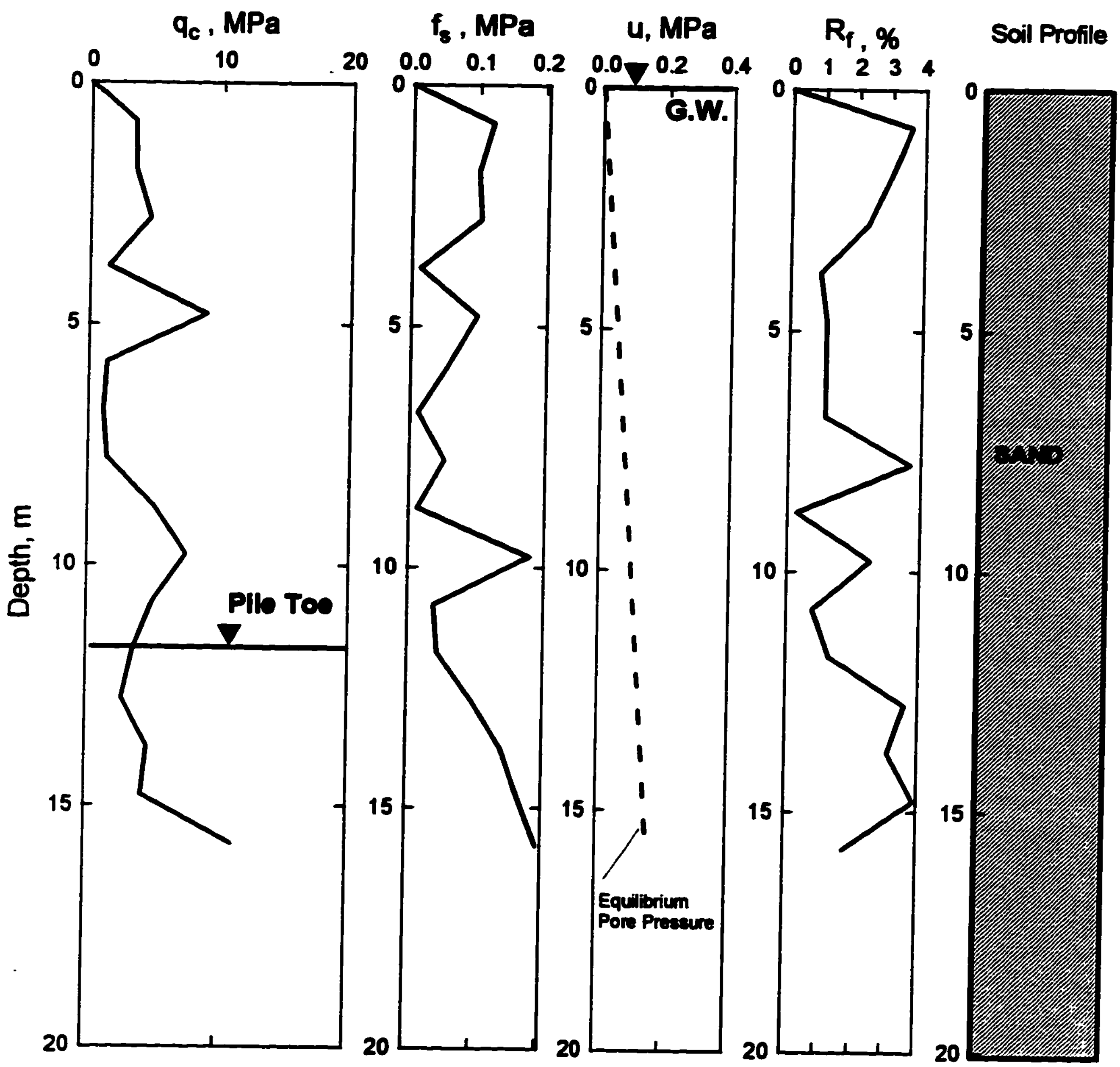

Case 129 A&M48
Sheet b Pile data

	DETAIL	DESCRIPTION
1	Site	Hinds, MS, USA
2	Reference	Briaud et al., 1988
3	Shape, Material, and Installation	Square, Concrete, Driven
4	Diameter, b, and Wall Thickness, t, mm	400
5	Embedment Length D, m	12.5
6	Cross Sectional Area A_t, m^2	0.16
7	Unit Circumferential Area, A_s, m^2/m	1.6
8	Toe, Closed or Open	Closed
9	Type of Test and Loading	Static Compression, SML
10	Toe Capacity, R_t, KN	
11	Shaft Capacity, R_s, KN	
12	*Capacity, R_u, KN	620

SCHEMATIC PROFILE

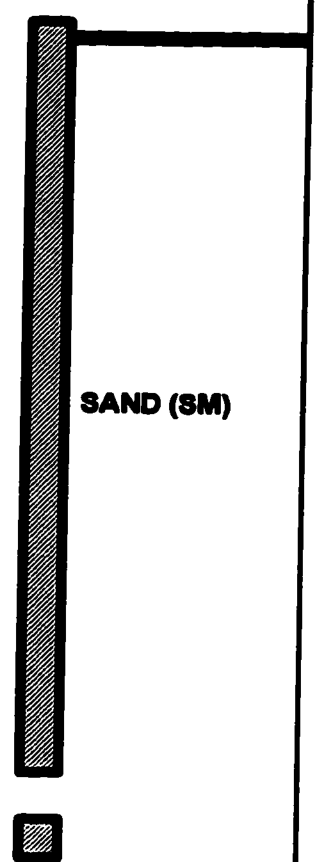

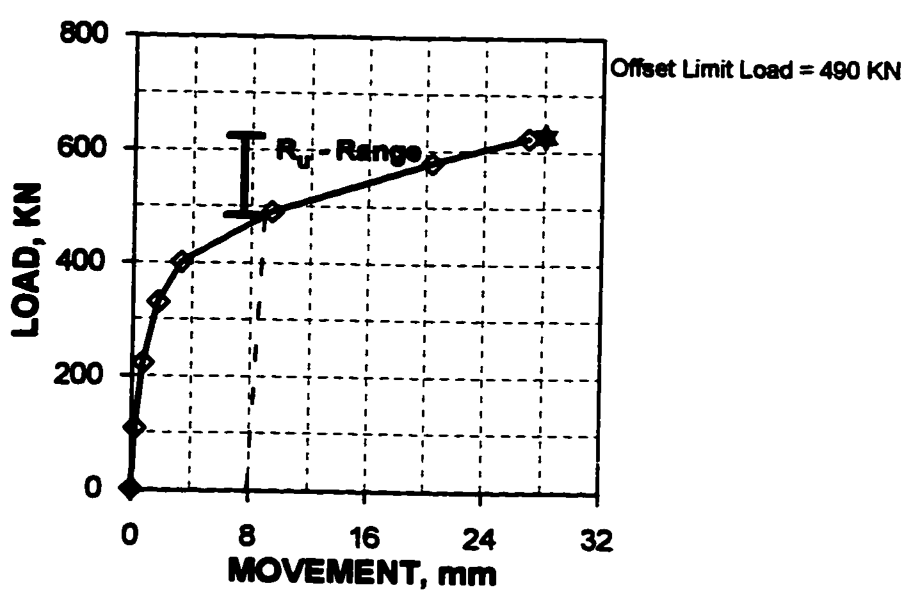

Case 130 A&M49
Sheet a CPT data

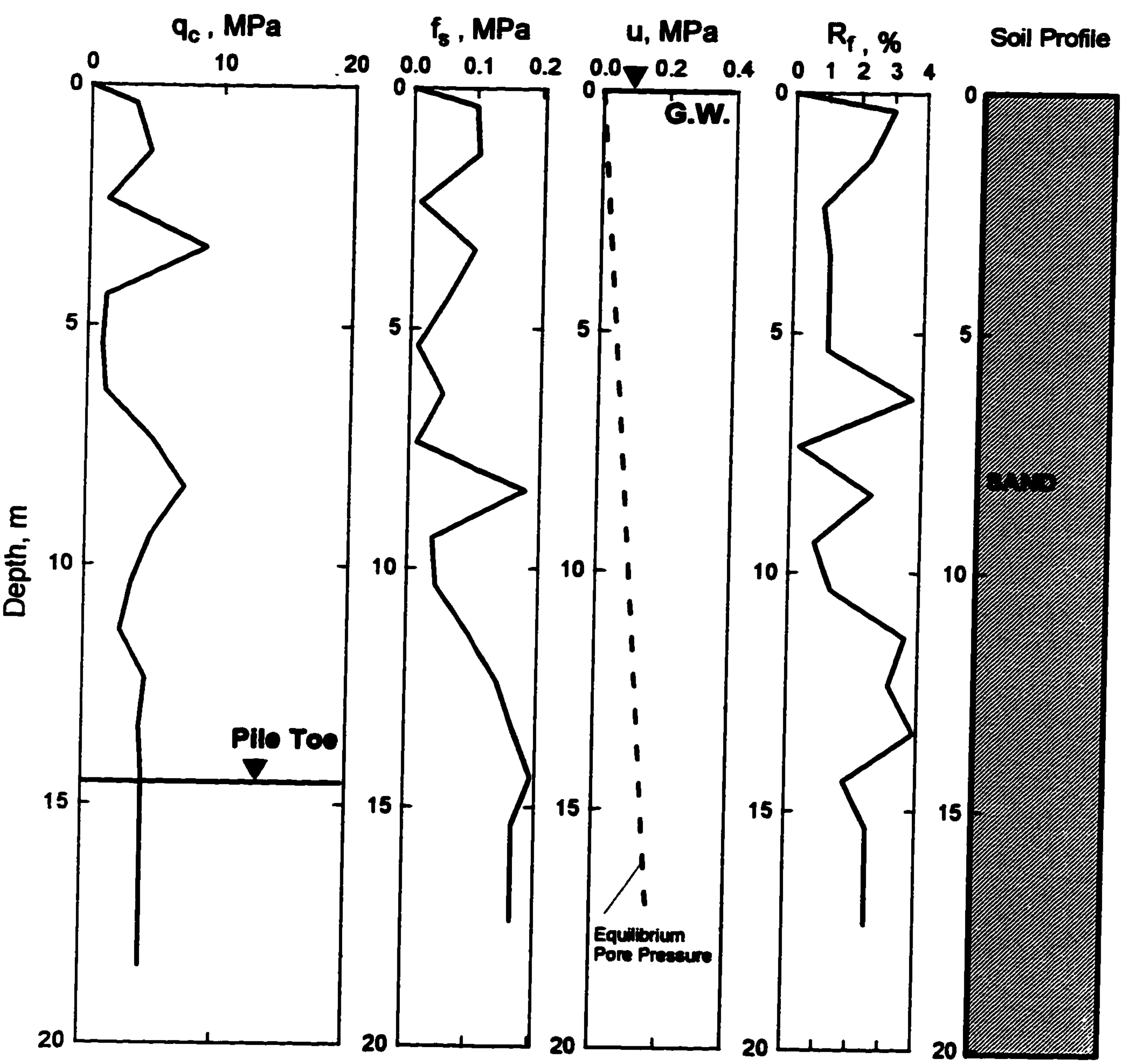

Case 130 A&M49
Sheet b Pile data

	DETAIL	DESCRIPTION	SCHEMATIC PROFILE
1	Site	Hinds, MS, USA	SAND (SM)
2	Reference	Briaud et al., 1988	
3	Shape, Material, and Installation	Square, Concrete, Driven	
4	Diameter, b, and Wall Thickness, t, mm	400	
5	Embedment Length D, m	12.5	
6	Cross Sectional Area A_t, m^2	0.16	
7	Unit Circumferential Area, A_s, m^2/m	1.6	
8	Toe, Closed or Open	Closed	
9	Type of Test and Loading	Static Compression, SML	
10	Toe Capacity, R_t, KN		
11	Shaft Capacity, R_s, KN		
12	*Capacity, R_u, KN	1,170	

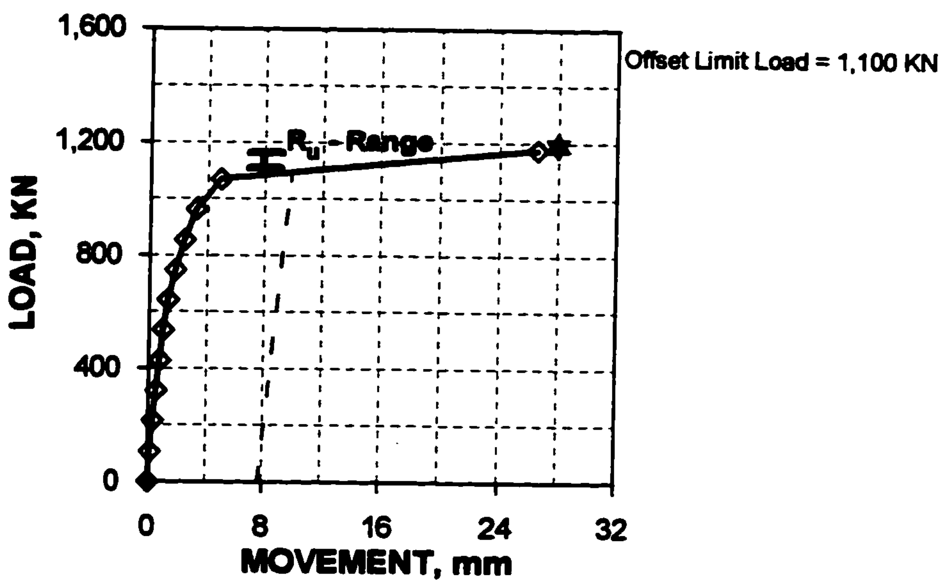

Case 131 A&M66
Sheet a CPT data

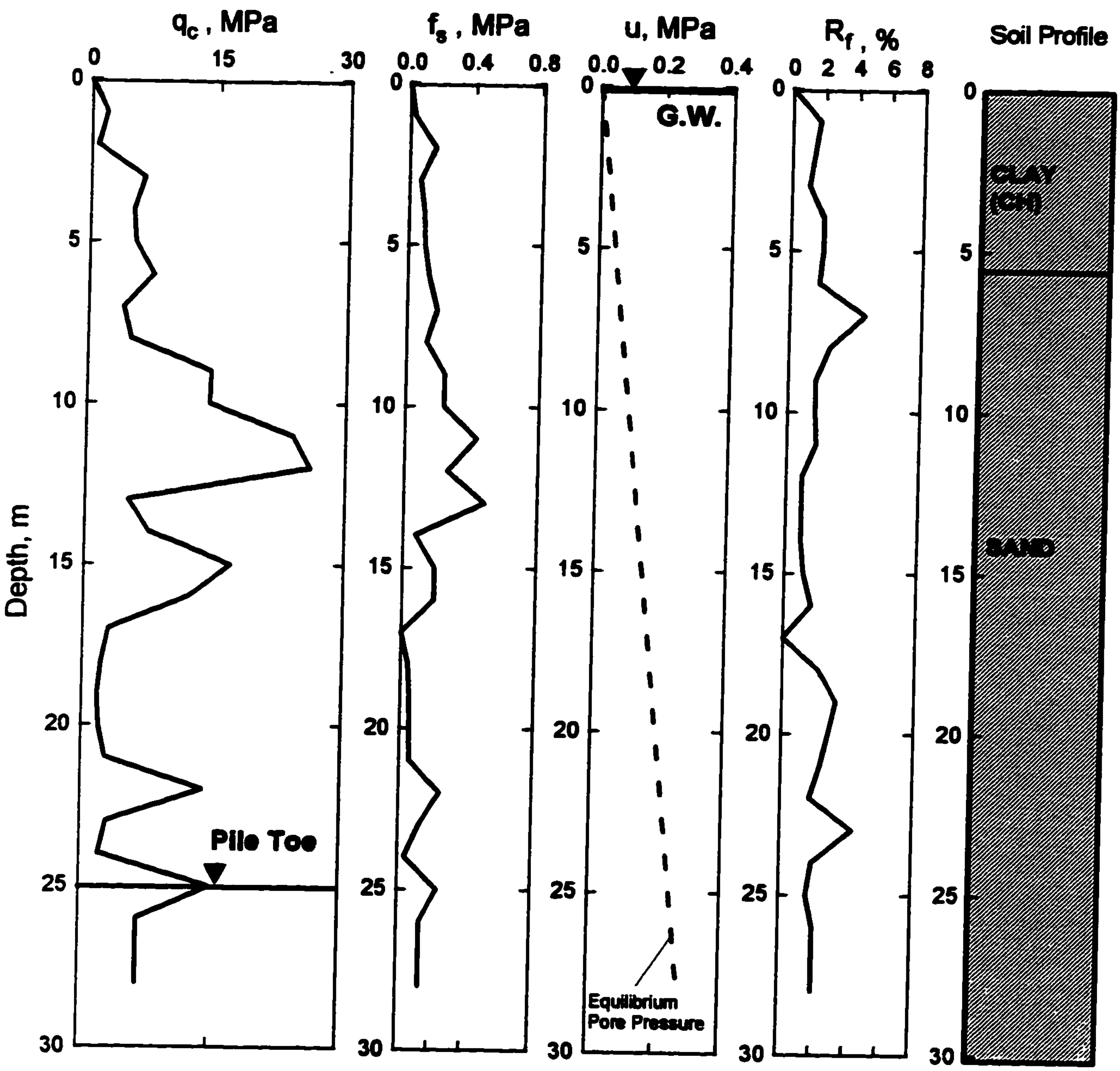

Case 131 A&M66
Sheet b Pile data

	DETAIL	DESCRIPTION
1	Site	Jackson, MS, USA
2	Reference	Briaud et al., 1988
3	Shape, Material, and Installation	Square, Concrete, Driven
4	Diameter, b, and Wall Thickness, t, mm	350
5	Embedment Length D, m	25
6	Cross Sectional Area A_t, m²	0.123
7	Unit Circumferential Area, A_s, m² /m	1.4
8	Toe, Closed or Open	Closed
9	Type of Test and Loading	Static Compression, SML
10	Toe Capacity, R_t, KN	
11	Shaft Capacity, R_s, KN	
12	*Capacity, R_u, KN	1,560

SCHEMATIC PROFILE

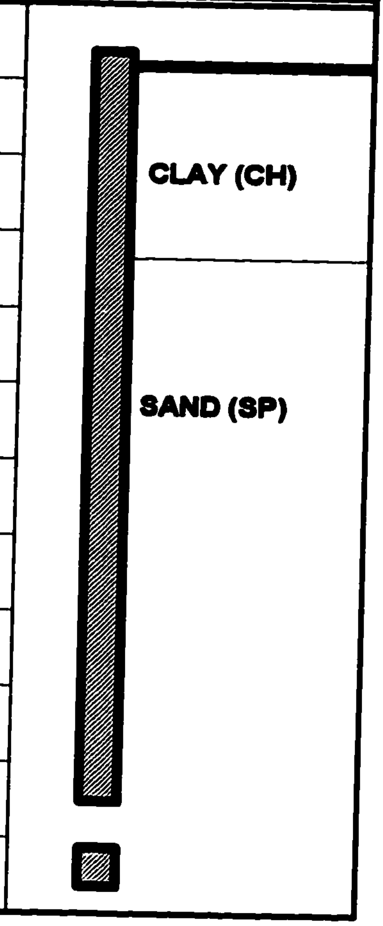

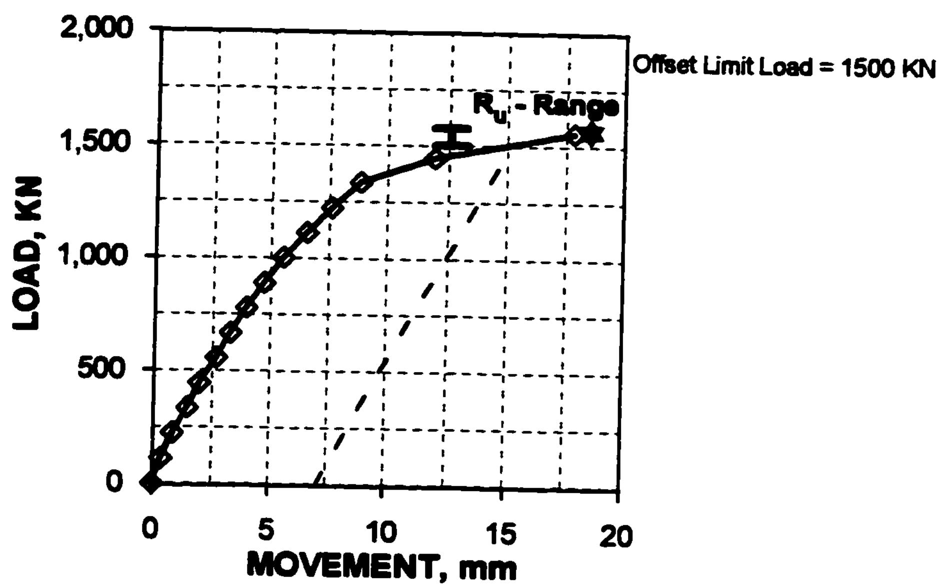

Case 132 A&M69
Sheet a CPT data

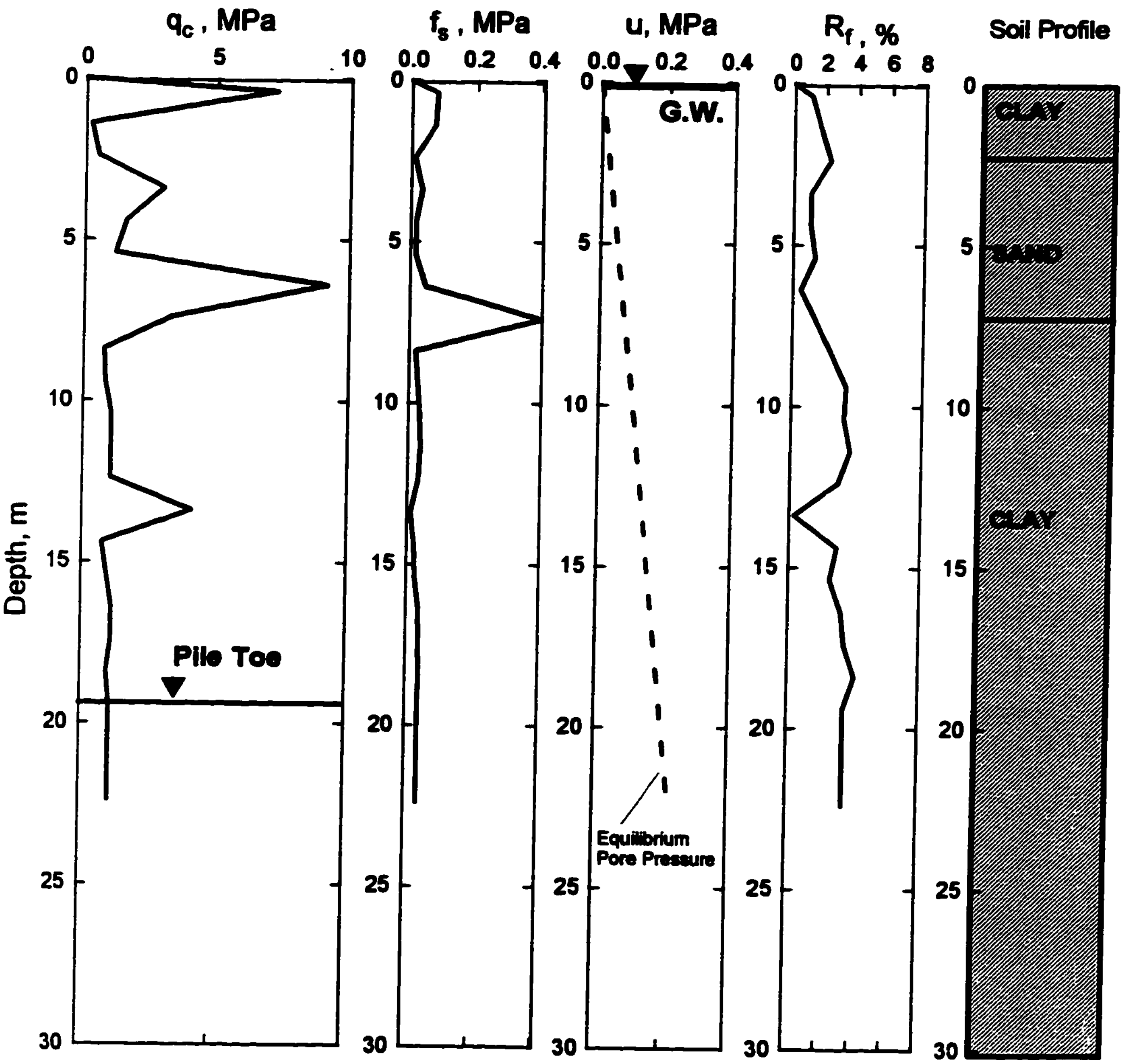

Case 132 A&M69
Sheet b Pile data

	DETAIL	DESCRIPTION
1	Site	Jackson, MS, USA
2	Reference	Briaud et al., 1988
3	Shape, Material, and Installation	Square, Concrete, Driven
4	Diameter, b, and Wall Thickness, t, mm	400
5	Embedment Length D, m	19.2
6	Cross Sectional Area A_t, m^2	0.16
7	Unit Circumferential Area, A_s, m^2/m	1.6
8	Toe, Closed or Open	Closed
9	Type of Test and Loading	Static Compression, SML
10	Toe Capacity, R_t, KN	
11	Shaft Capacity, R_s, KN	
12	*Capacity, R_u, KN	1,780

SCHEMATIC PROFILE

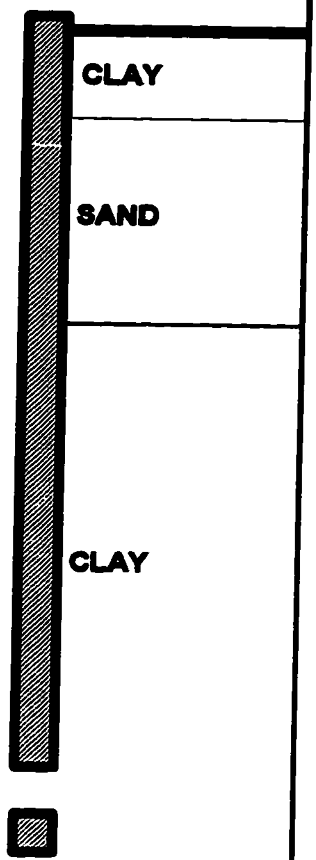

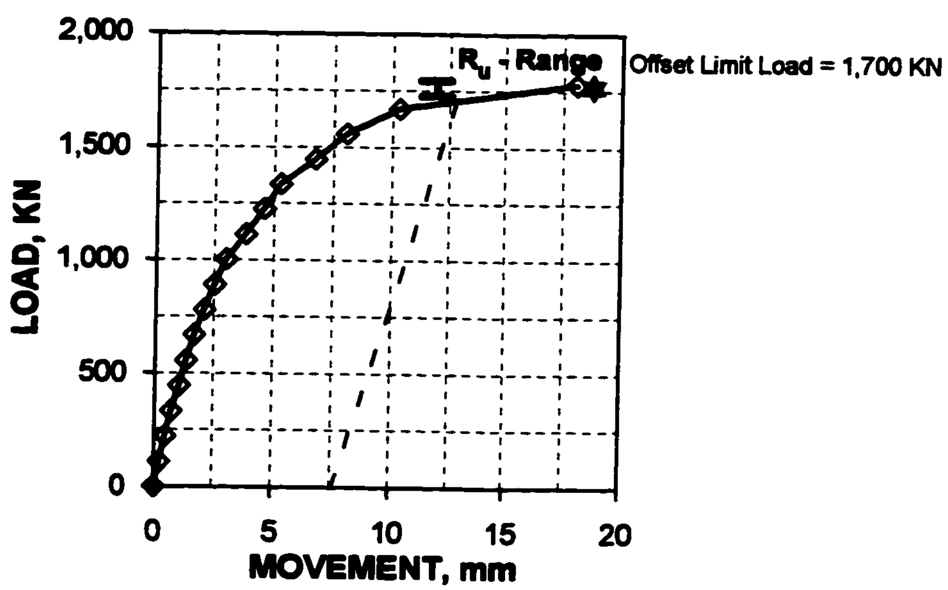

Case 133 A&M79
Sheet a CPT data

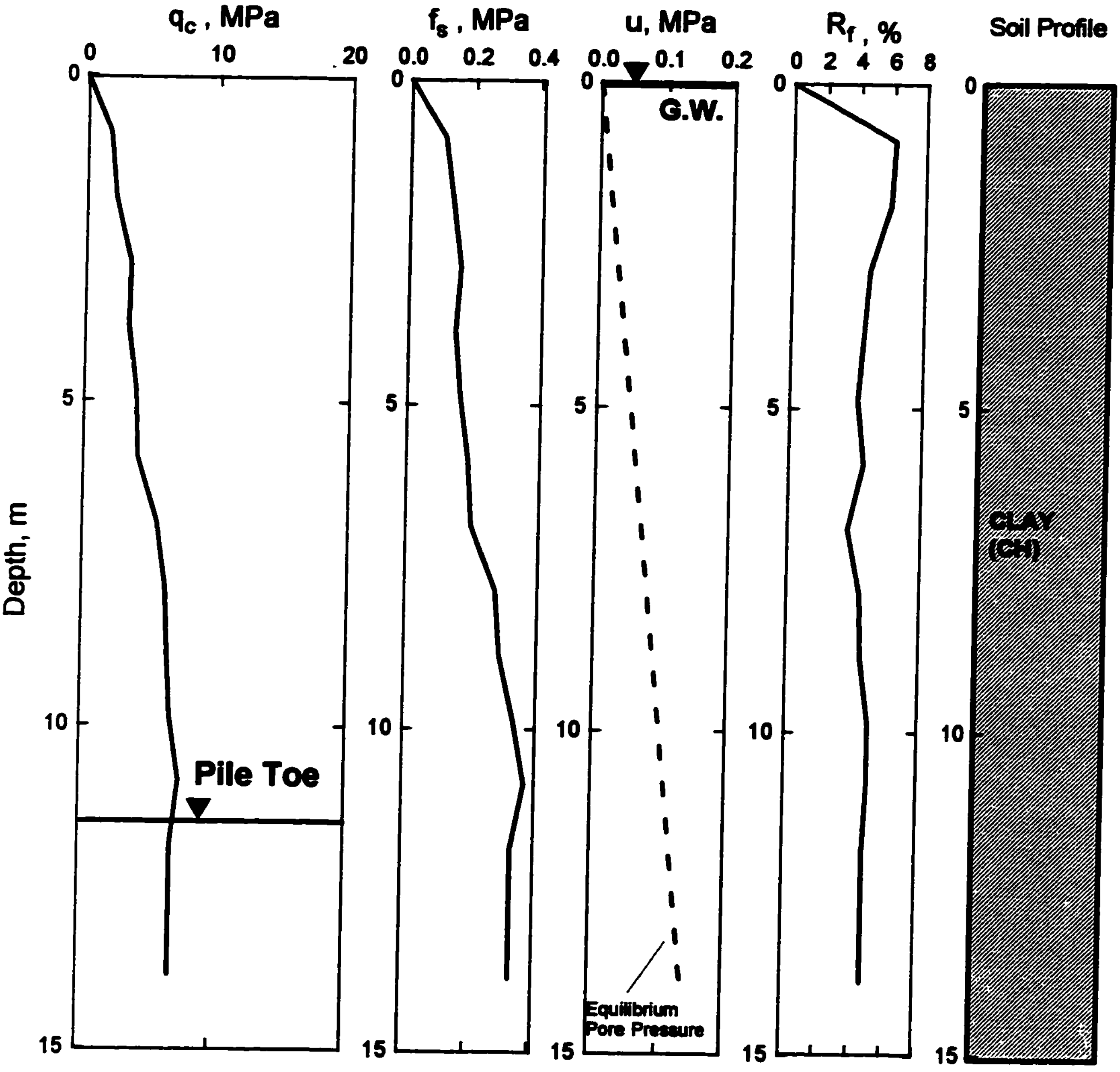

Case 133 A&M79
Sheet b Pile data

	DETAIL	DESCRIPTION
1	Site	Scott, MS, USA
2	Reference	Briaud et al., 1988
3	Shape, Material, and Installation	Round, Concrete, Bored
4	Diameter, b, and Wall Thickness, t, mm	300
5	Embedment Length D, m	11.5
6	Cross Sectional Area A_t, m^2	0.071
7	Unit Circumferential Area, A_s, m^2/m	0.942
8	Toe, Closed or Open	Closed
9	Type of Test and Loading	Static Compression, SML
10	Toe Capacity, R_t, KN	
11	Shaft Capacity, R_s, KN	
12	*Capacity, R_u, KN	1,320

SCHEMATIC PROFILE

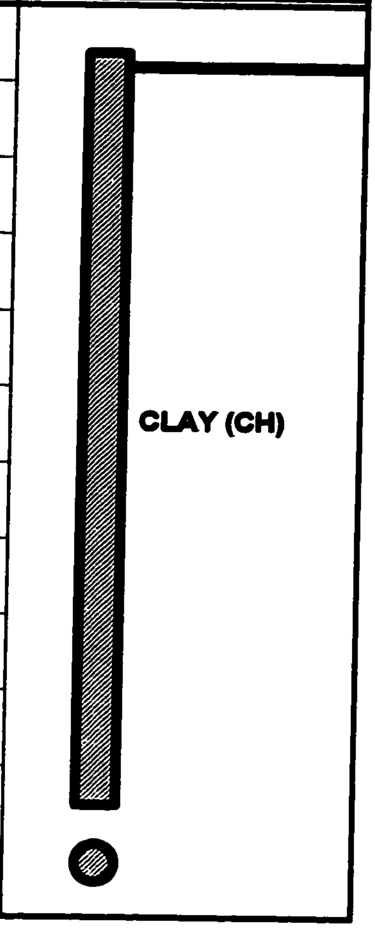

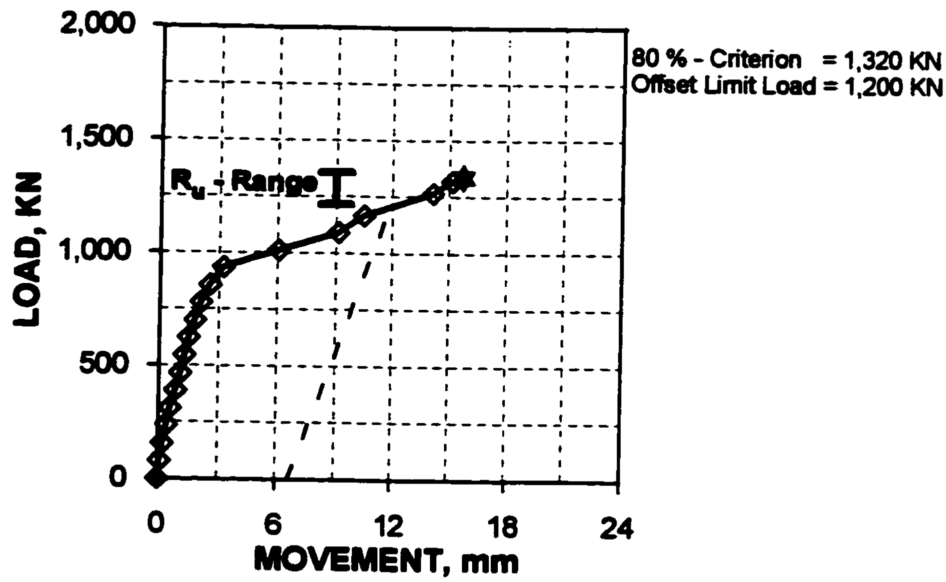

Case 134 A&M81
Sheet a CPT data

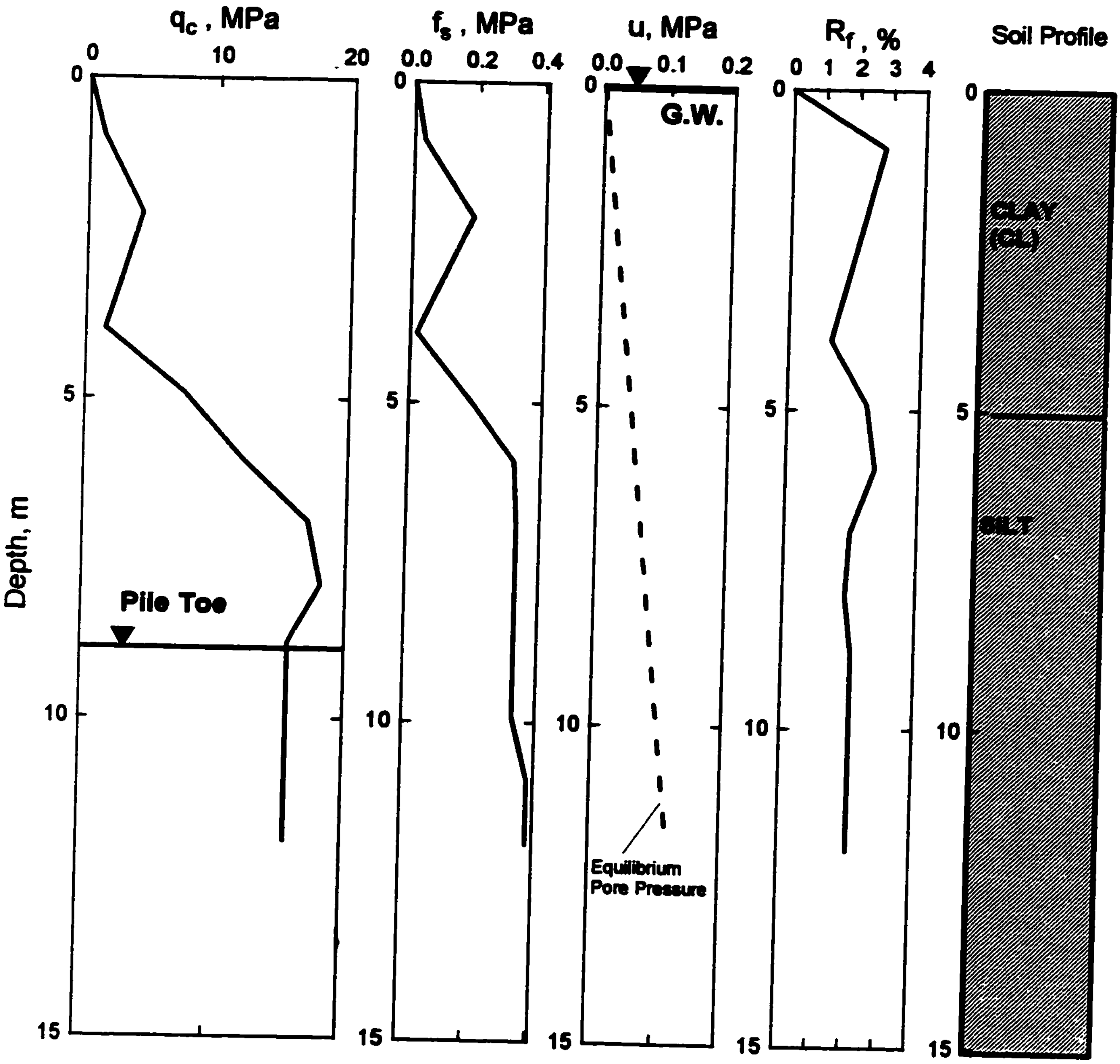

Case 134 A&M81
Sheet b Pile data

No.	CASE	DESCRIPTION
1	Site	Launderdale, MS, USA
2	Reference	Briaud et al., 1988
3	Shape, Material, and Installation	H-Pile, Steel, Driven
4	Diameter, b, and Wall Thickness, t, mm	299*306
5	Embedment Length D, m	9
6	Cross Sectional Area A_t, m^2	0.01
7	Unit Circumferential Area, A_s, m^2/m	1.21
8	Toe, Closed or Open	Open
9	Type of Test and Loading	Static Compression, SML
10	Toe Capacity, R_t, KN	
11	Shaft Capacity, R_s, KN	
12	*Capacity, R_u, KN	2,100

SCHEMATIC PROFILE

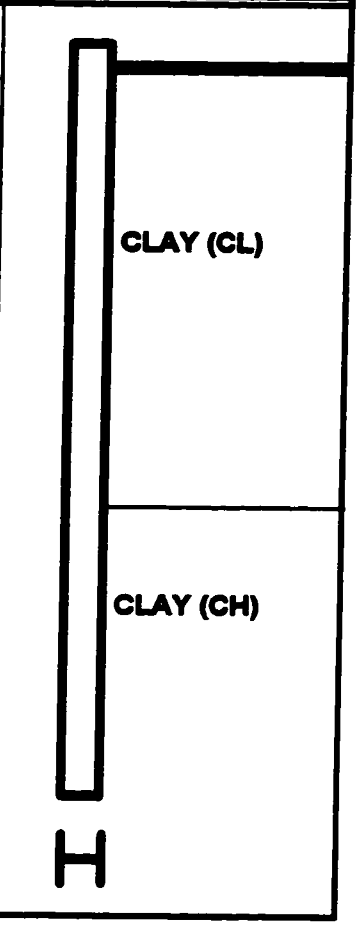

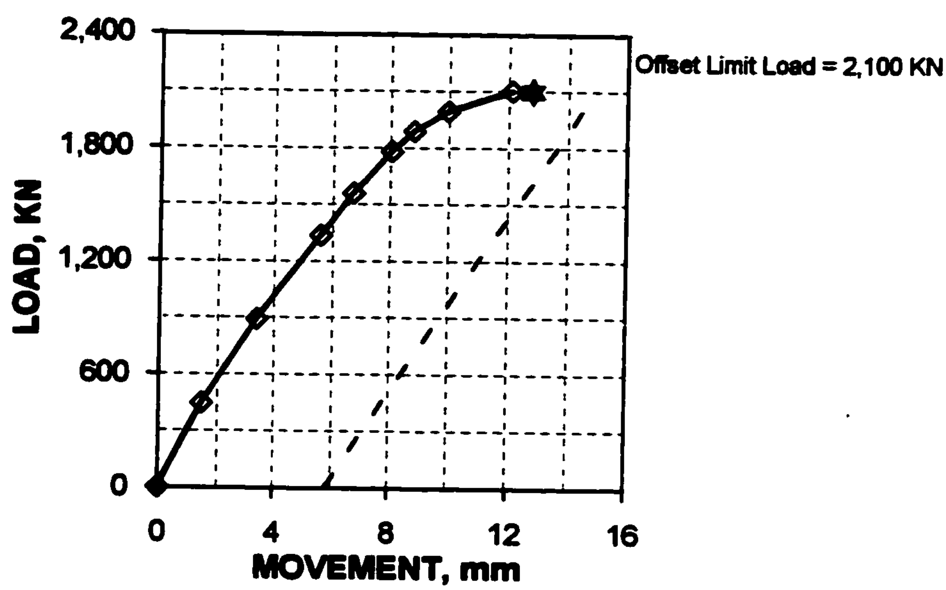

Case 135 A&M86
Sheet a CPT data

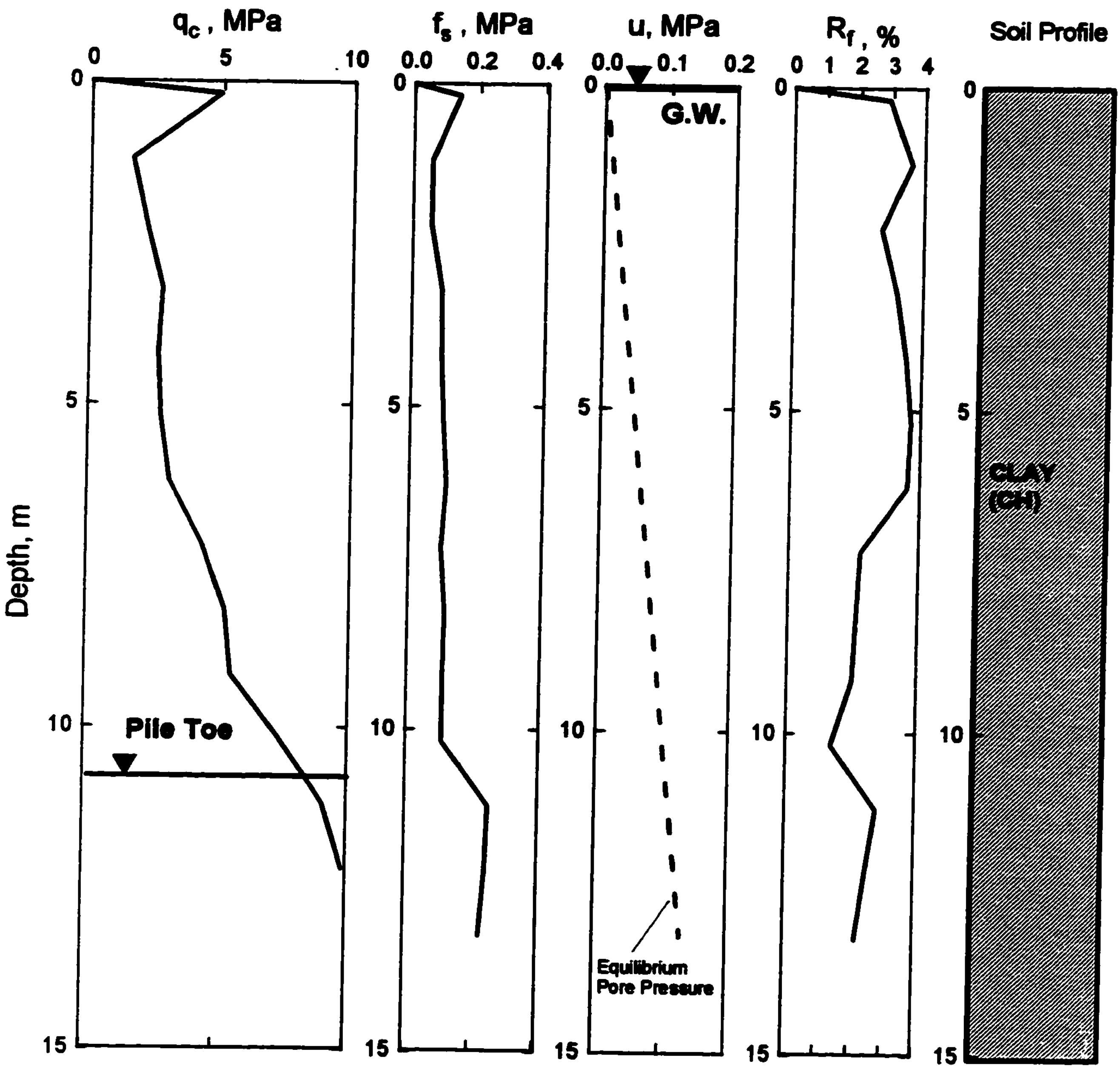

Case 135 A&M86
Sheet b Pile data

	DETAIL	DESCRIPTION
1	Site	Hinds, MS, USA
2	Reference	Briaud et al., 1988
3	Shape, Material, and Installation	Round, Concrete, Bored
4	Diameter, b, and Wall Thickness, t, mm	350
5	Embedment Length D, m	10.7
6	Cross Sectional Area A_t, m^2	0.096
7	Unit Circumferential Area, A_s, m^2/m	1.1
8	Toe, Closed or Open	Closed
9	Type of Test and Loading	Static Compression, SML
10	Toe Capacity, R_t, KN	
11	Shaft Capacity, R_s, KN	
12	*Capacity, R_u, KN	1,390

SCHEMATIC PROFILE

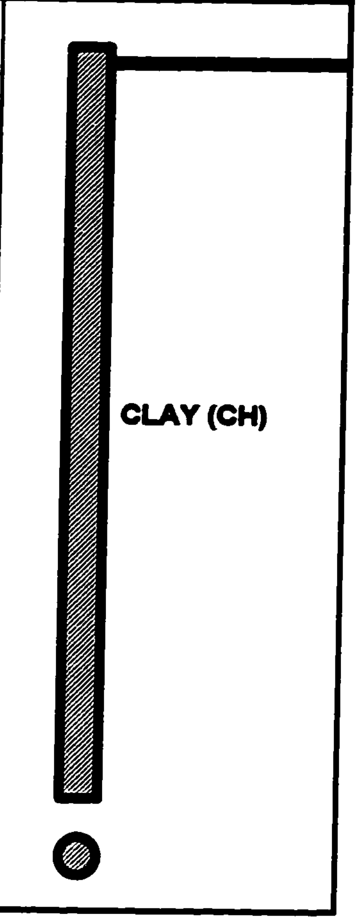

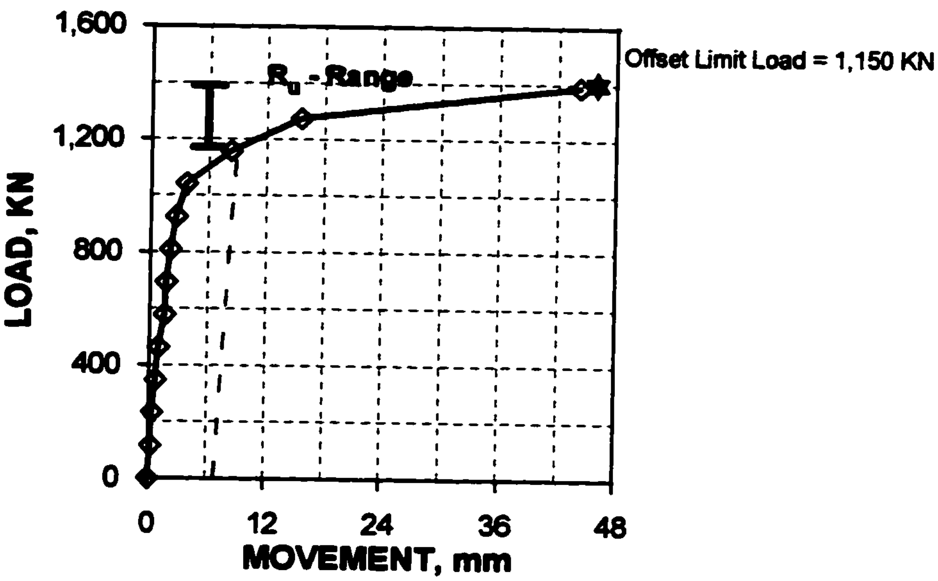

Case 136 A&M87
Sheet a CPT data

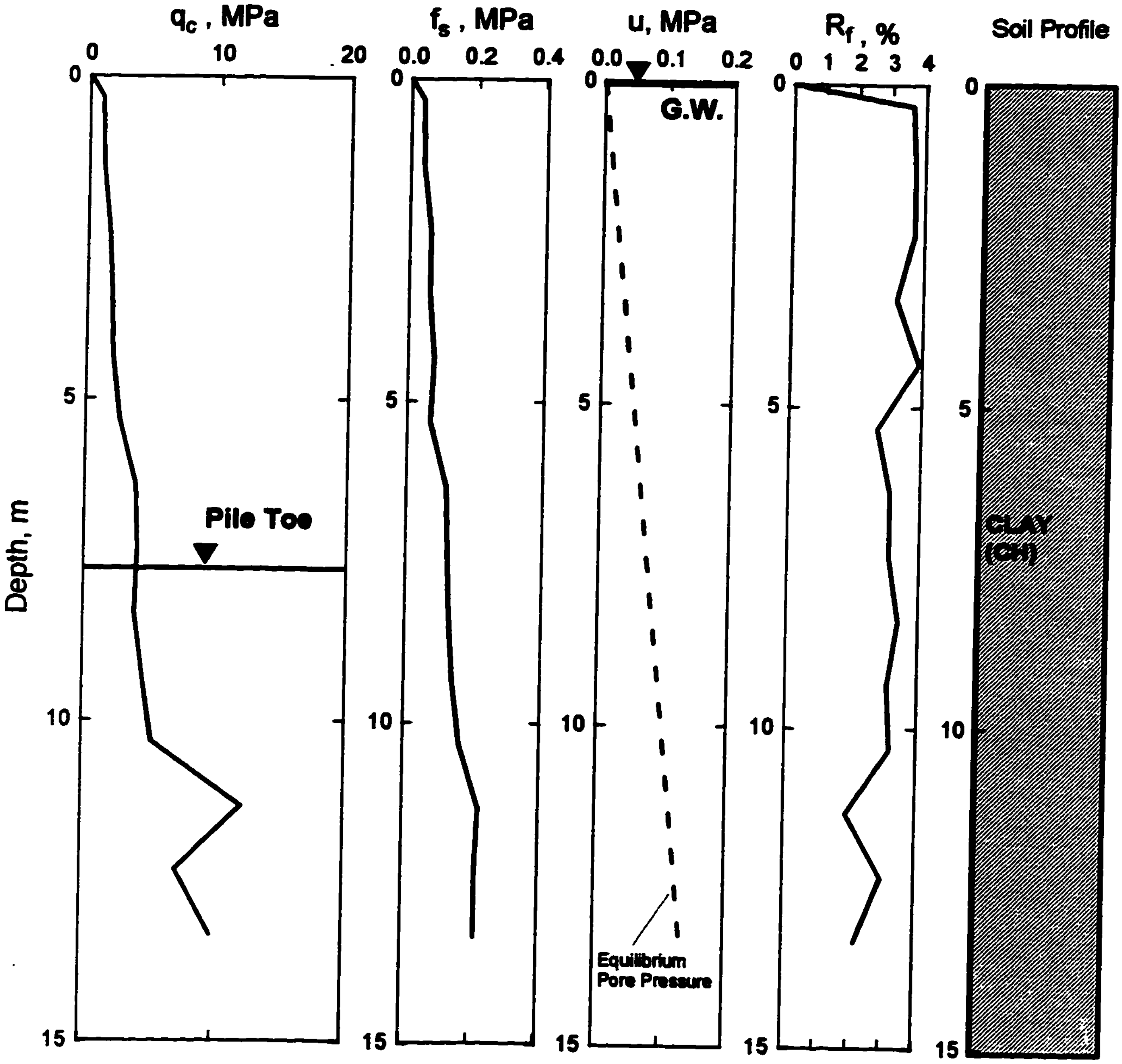

Case 136 A&M87
Sheet b Pile data

	DETAIL	DESCRIPTION	SCHEMATIC PROFILE
1	Site	Hinds, MS, USA	
2	Reference	Briaud et al., 1988	
3	Shape, Material, and Installation	Square, Concrete, Driven	
4	Diameter, b, and Wall Thickness, t, mm	400	
5	Embedment Length D, m	7.4	
6	Cross Sectional Area A_t, m^2	0.16	
7	Unit Circumferential Area, A_s, m^2 /m	1.6	
8	Toe, Closed or Open	Closed	
9	Type of Test and Loading	Static Compression, SML	
10	Toe Capacity, R_t, KN		
11	Shaft Capacity, R_s, KN		
12	*Capacity, R_u, KN	640	

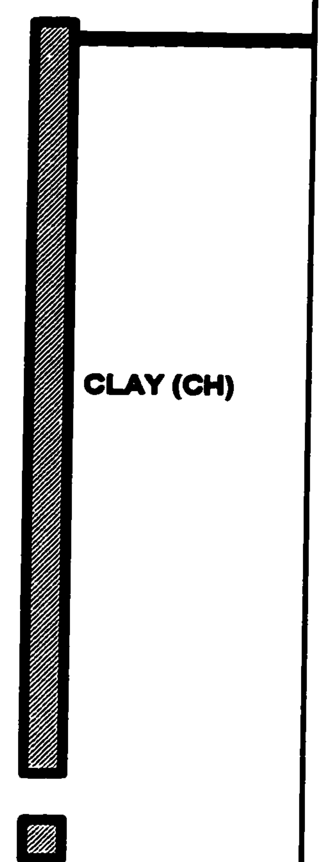

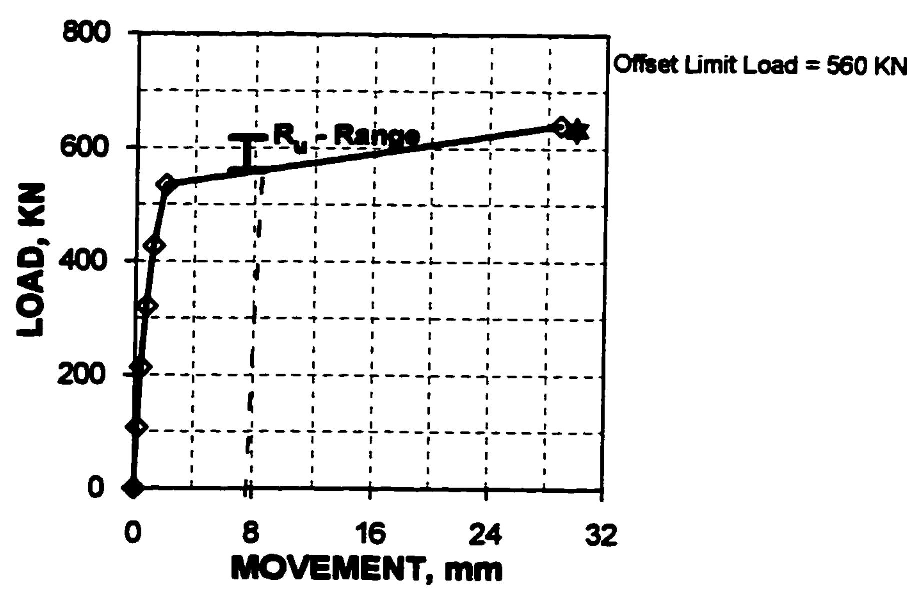

Case 137 A&M90
Sheet a CPT data

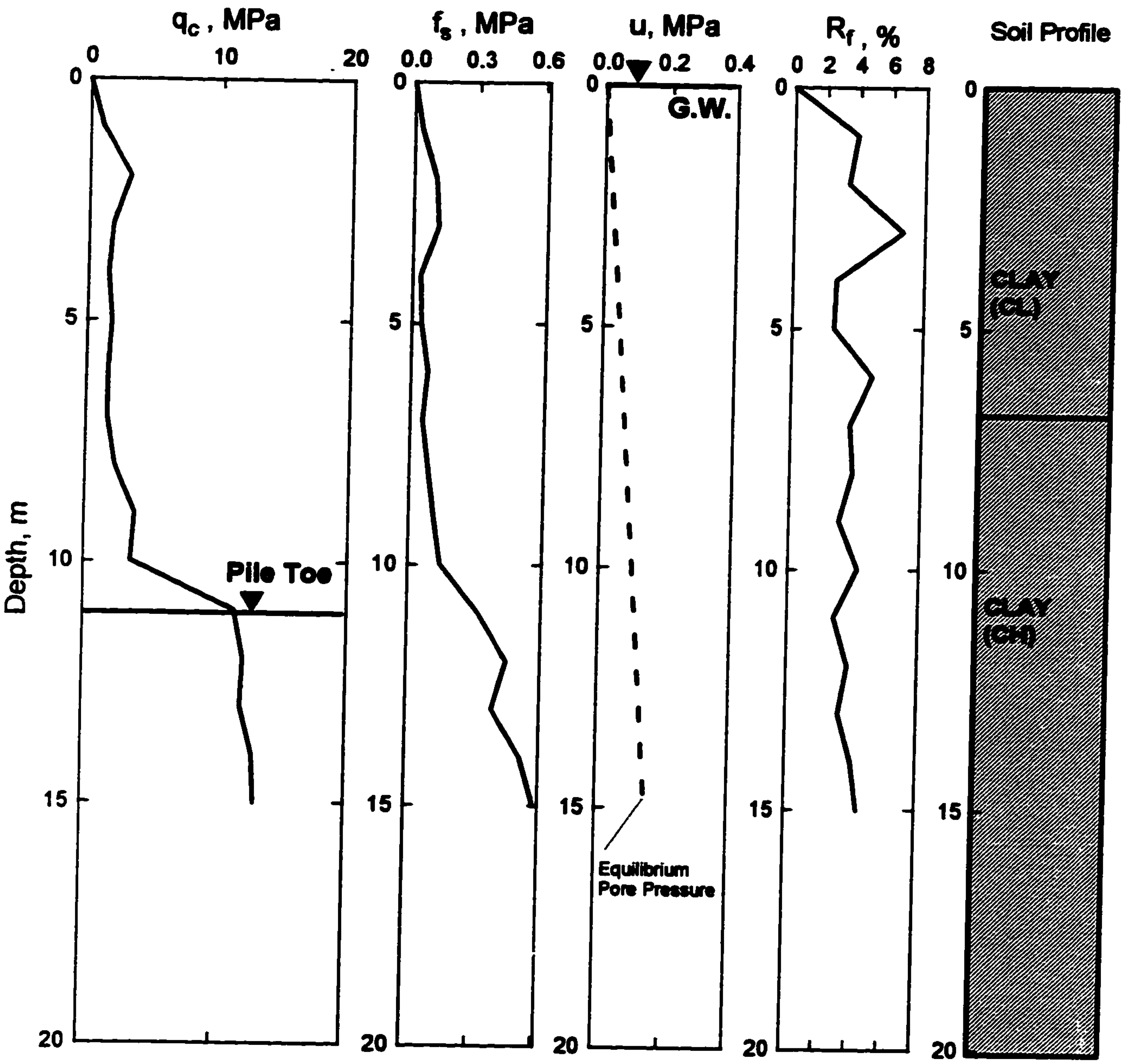

Case 137 A&M90
Sheet b Pile data

	DETAIL	DESCRIPTION	SCHEMATIC PROFILE
1	Site	Yazoo, MS, USA	
2	Reference	Briaud et al., 1988	
3	Shape, Material, and Installation	Square, Concrete, Driven	
4	Diameter, b, and Wall Thickness, t, mm	450	CLAY (CL)
5	Embedment Length D, m	10.7	
6	Cross Sectional Area A_t, m^2	0.203	
7	Unit Circumferential Area, A_s, m^2/m	1.8	
8	Toe, Closed or Open	Closed	
9	Type of Test and Loading	Static Compression, SML	
10	Toe Capacity, R_t, KN		CLAY (CH)
11	Shaft Capacity, R_s, KN		
12	*Capacity, R_u, KN	1,500	

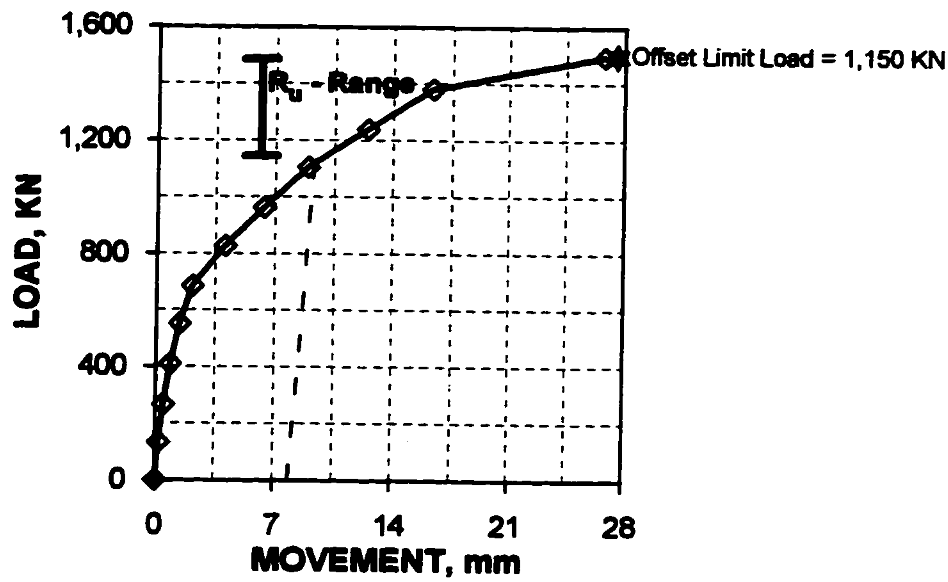

Case 138 A&M93
Sheet a CPT data

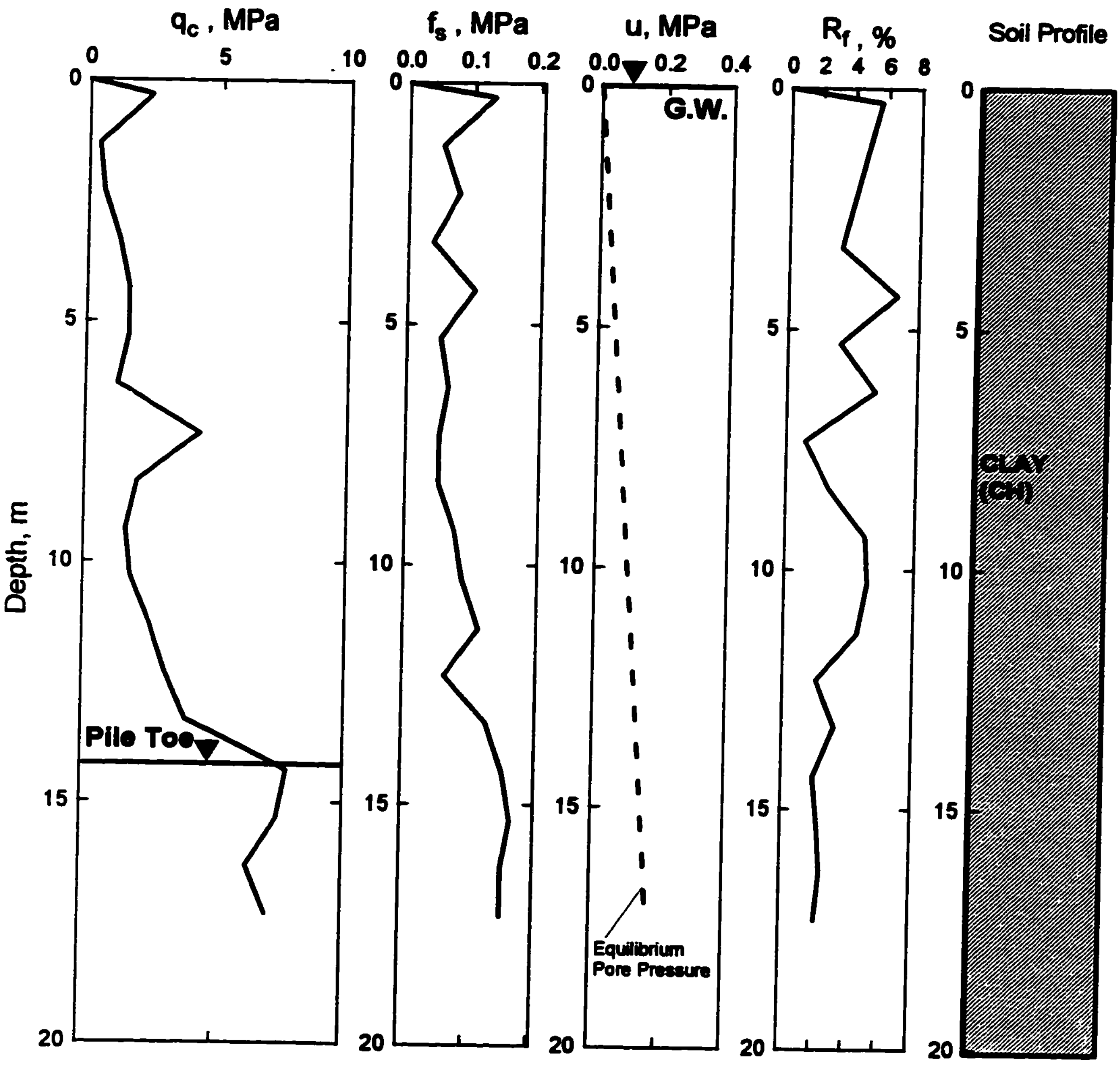

Case 138 A&M93
Sheet b Pile data

DETAIL		DESCRIPTION	SCHEMATIC PROFILE
1	Site	Hinds, MS, USA	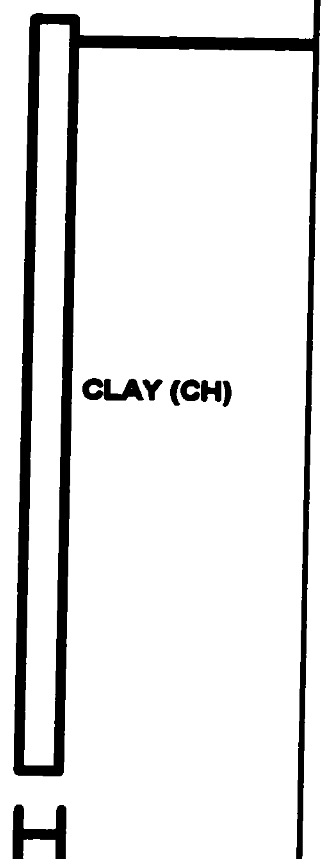
2	Reference	Briaud et al., 1988	
3	Shape, Material, and Installation	H-Pile, Steel, Driven	
4	Diameter, b, and Wall Thickness, t, mm	246*256	
5	Embedment Length D, m	14.5	
6	Cross Sectional Area A_t, m^2	0.008	
7	Unit Circumferential Area, A_s, m^2/m	1.01	
8	Toe, Closed or Open	Open	
9	Type of Test and Loading	Static Compression, SML	
10	Toe Capacity, R_t, KN		
11	Shaft Capacity, R_s, KN		
12	*Capacity, R_u, KN	1,240	

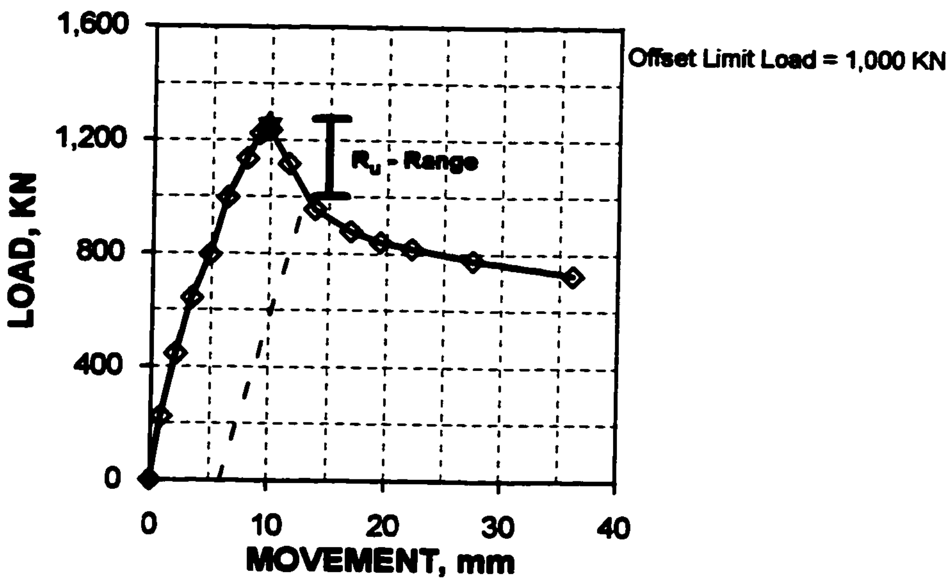

Case 139 A&M95
Sheet a CPT data

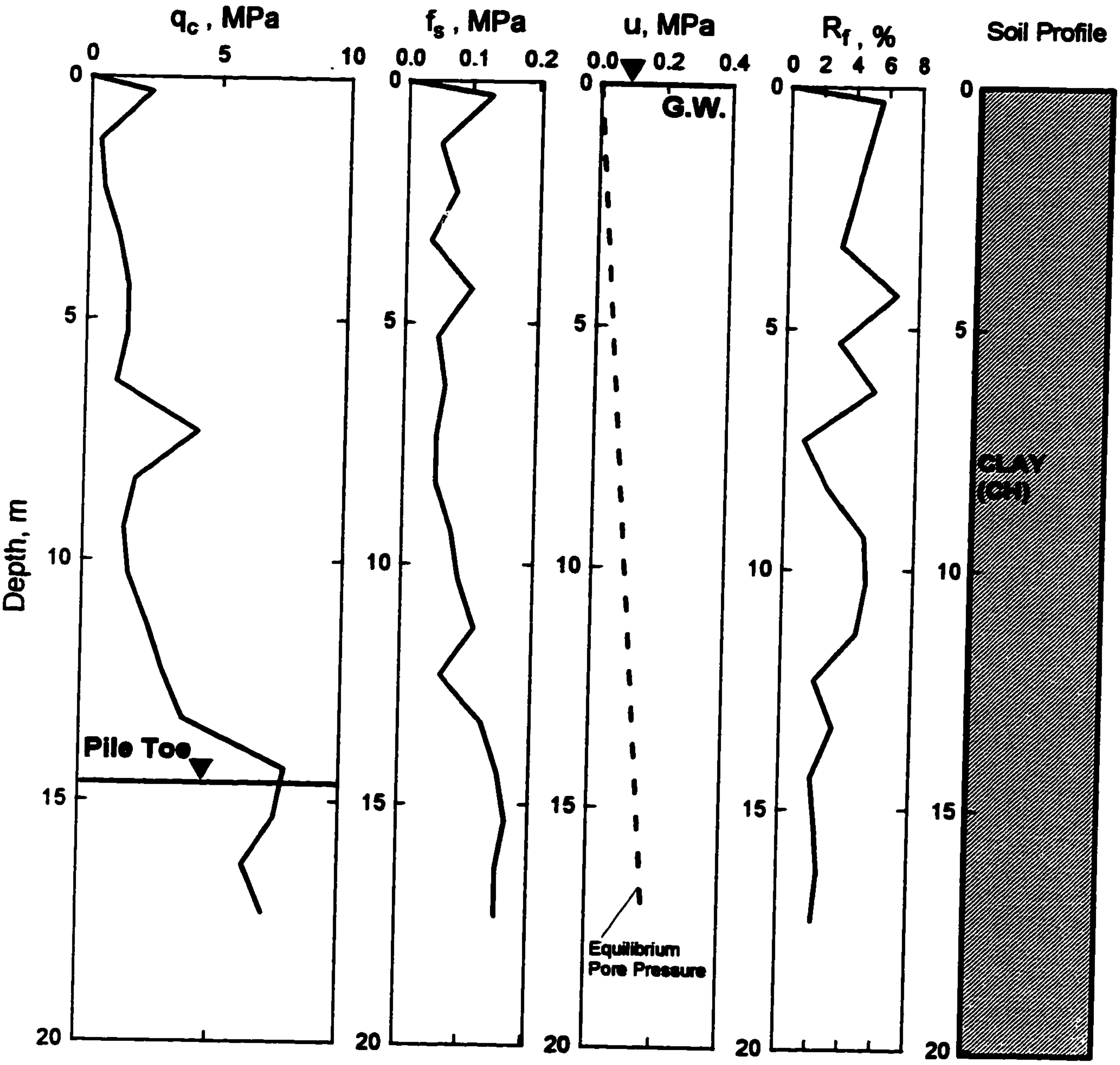

Case 139 A&M95
Sheet b Pile data

	DETAIL	DESCRIPTION	SCHEMATIC PROFILE
1	Site	Hinds, MS, USA	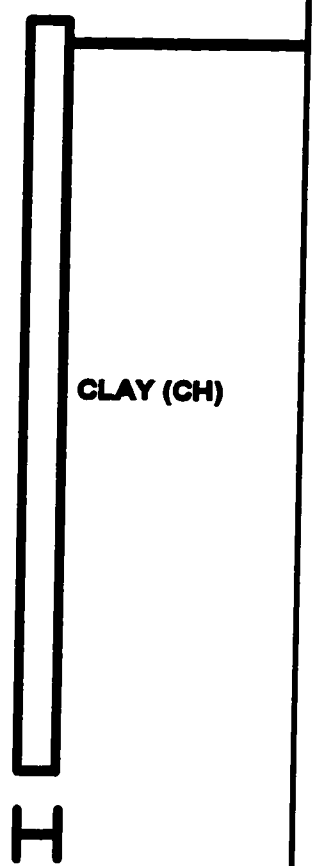
2	Reference	Briaud et al., 1988	
3	Shape, Material, and Installation	H-Pile, Steel, Driven	
4	Diameter, b, and Wall Thickness, t, mm	246*256	
5	Embedment Length D, m	14.7	
6	Cross Sectional Area A_t, m²	0.008	CLAY (CH)
7	Unit Circumferential Area, A_s, m² /m	1.01	
8	Toe, Closed or Open	Open	
9	Type of Test and Loading	Static Compression, SML	
10	Toe Capacity, R_t, KN		
11	Shaft Capacity, R_s, KN		
12	*Capacity, R_u, KN	1,260	

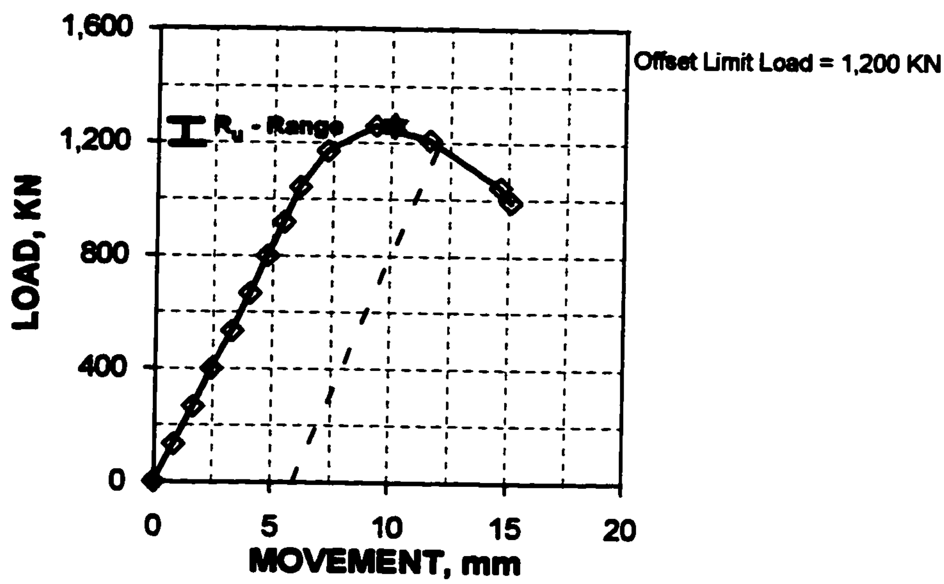

Case 140 A&M97
Sheet a CPT data

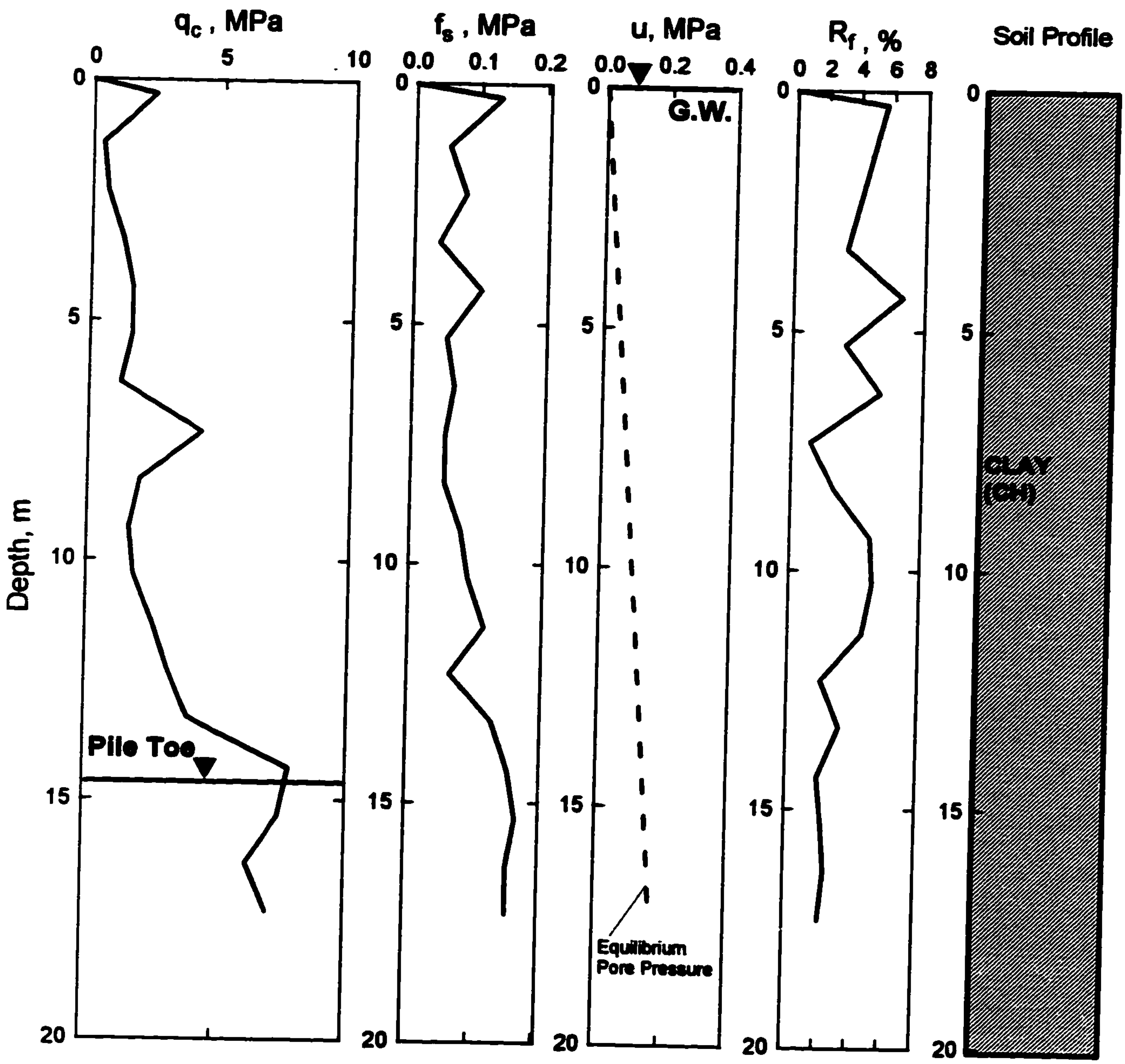

Case 140 A&M97
Sheet b Pile data

	DETAIL	DESCRIPTION
1	Site	Hinds, MS, USA
2	Reference	Briaud et al., 1988
3	Shape, Material, and Installation	H-Pile, Steel, Driven
4	Diameter, b, and Wall Thickness, t, mm	246*256
5	Embedment Length D, m	14.75
6	Cross Sectional Area A_t, m^2	0.008
7	Unit Circumferential Area, A_s, m^2/m	1.01
8	Toe, Closed or Open	Open
9	Type of Test and Loading	Static Compression, SML
10	Toe Capacity, R_t, KN	
11	Shaft Capacity, R_s, KN	
12	*Capacity, R_u, KN	1,201

SCHEMATIC PROFILE

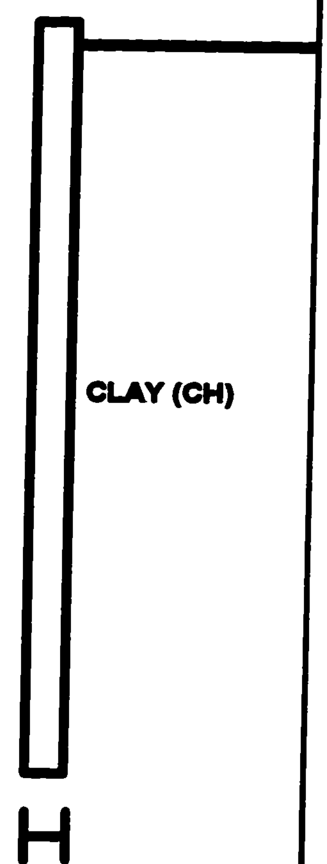

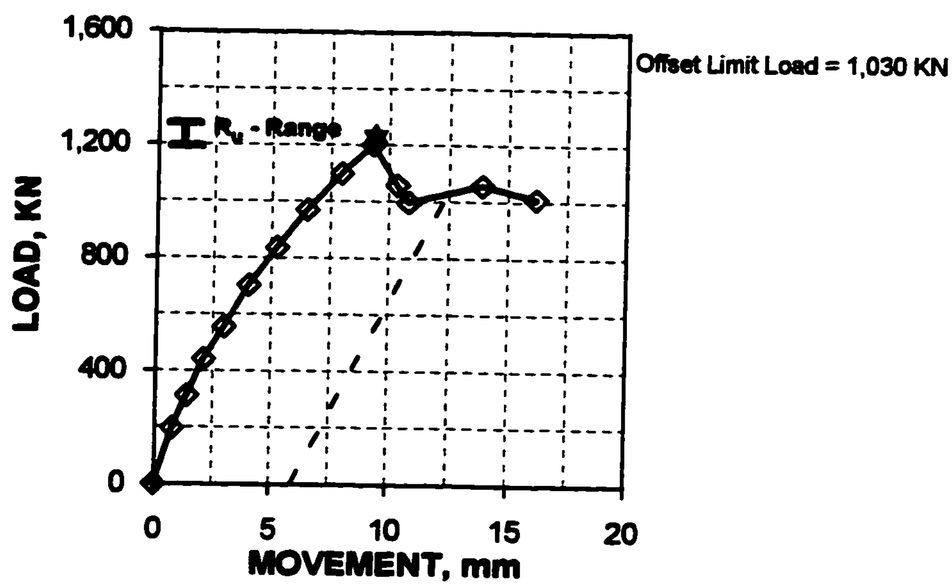

Case 141 A&M1
Sheet a CPT data

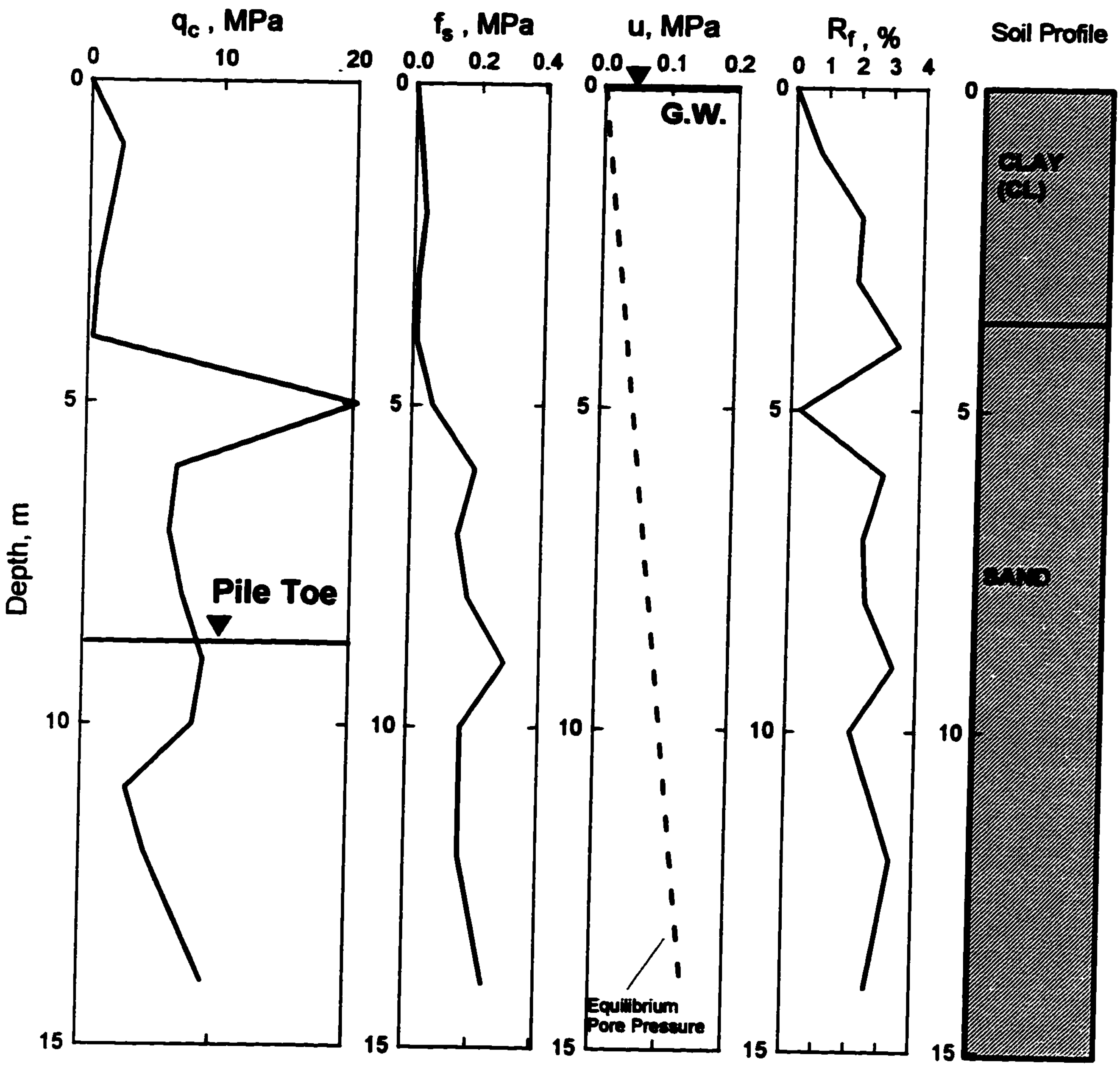

Case 141 A&M1
Sheet b Pile data

DETAIL		DESCRIPTION
1	Site	Smith, MS, USA
2	Reference	Briaud et al., 1988
3	Shape, Material, and Installation	Square, Concrete, Driven
4	Diameter, b, and Wall Thickness, t, mm	400
5	Embedment Length D, m	8.8
6	Cross Sectional Area A_t, m^2	0.16
7	Unit Circumferential Area, A_s, m^2/m	1.6
8	Toe, Closed or Open	Closed
9	Type of Test and Loading	Static Compression, SML
10	Toe Capacity, R_t, KN	
11	Shaft Capacity, R_s, KN	
12	*Capacity, R_u, KN	1,140

SCHEMATIC PROFILE

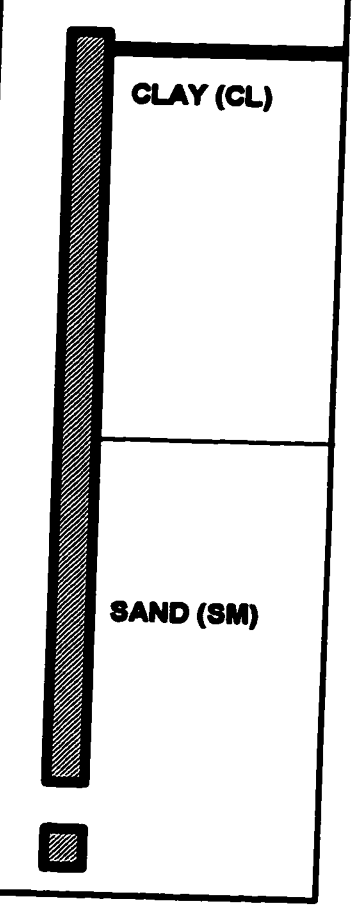

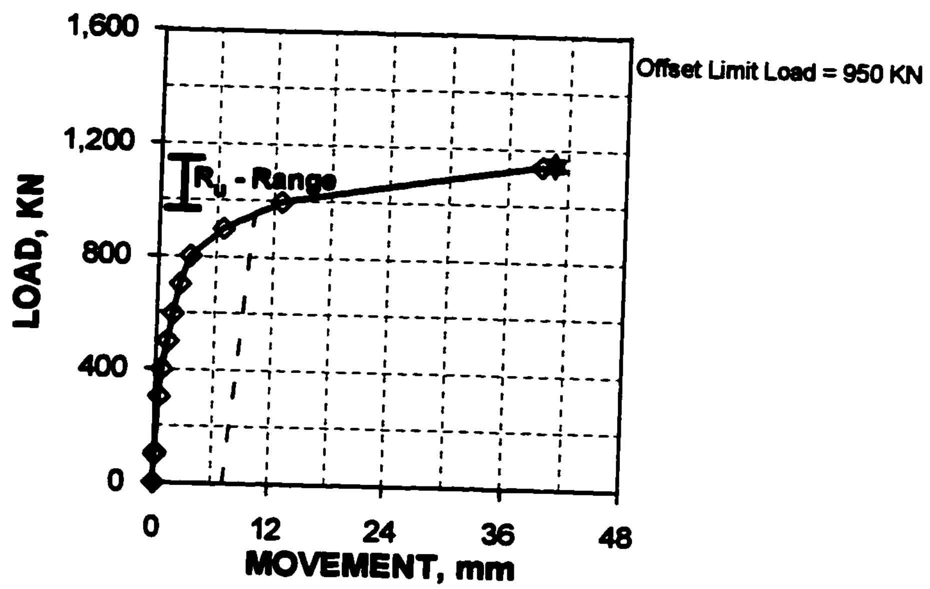

Case 142 A&M4
Sheet a CPT data

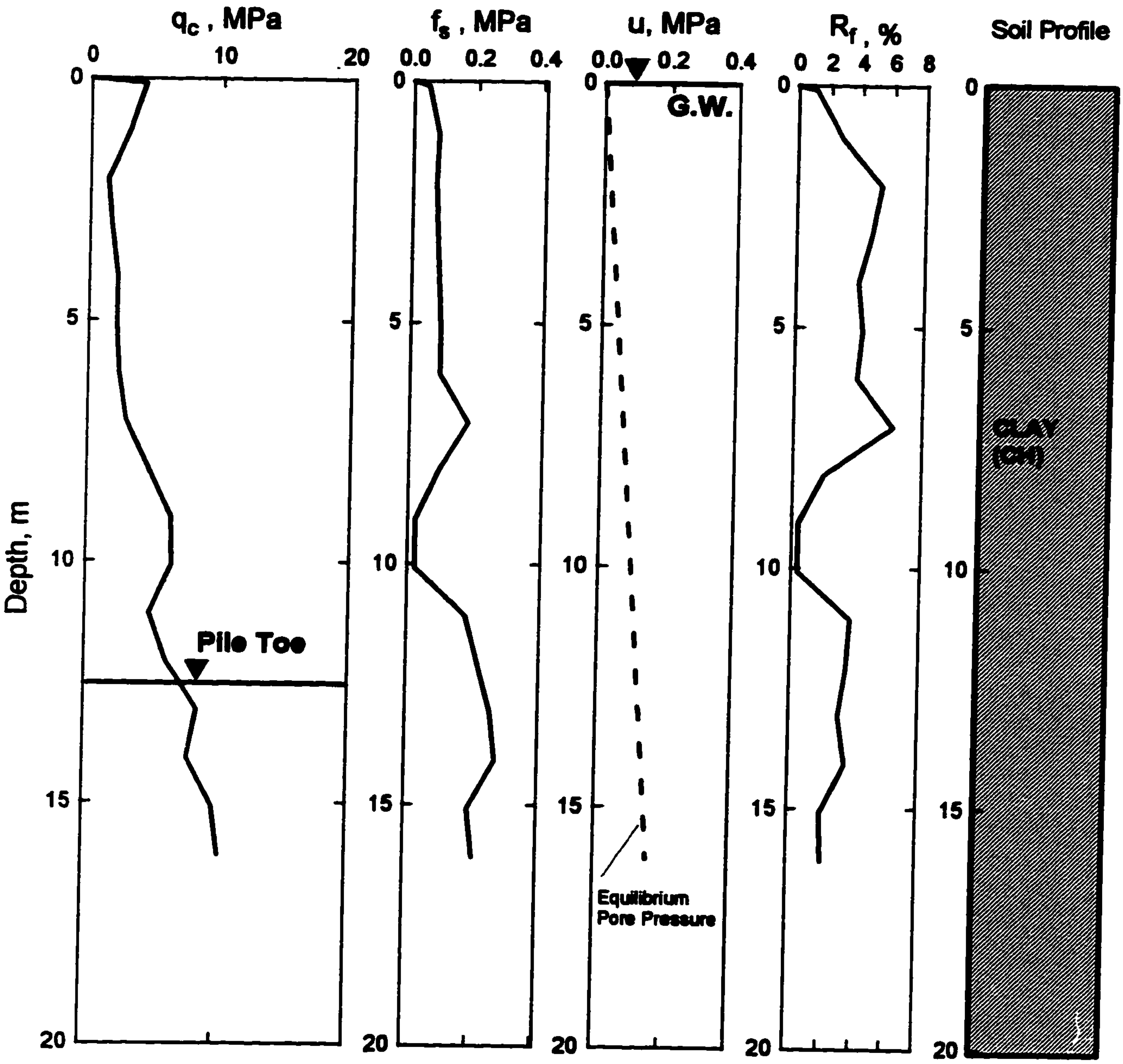

Case 142 A&M4
Sheet b Pile data

	DETAIL	DESCRIPTION
1	Site	Hinds, MS, USA
2	Reference	Briaud et al., 1988
3	Shape, Material, and Installation	Round, Concrete, Bored
4	Diameter, b, and Wall Thickness, t, mm	350
5	Embedment Length D, m	12.5
6	Cross Sectional Area A_t, m^2	0.096
7	Unit Circumferential Area, A_s, m^2/m	1.1
8	Toe, Closed or Open	Closed
9	Type of Test and Loading	Static Compression, SML
10	Toe Capacity, R_t, KN	
11	Shaft Capacity, R_s, KN	
12	*Capacity, R_u, KN	1,100

SCHEMATIC PROFILE